

GENERATION OF PHENOTYPIC DIVERSITY IN THE FUNGAL PATHOGEN  
*CANDIDA ALBICANS*

A DISSERTATION  
SUBMITTED TO THE FACULTY OF THE GRADUATE SCHOOL  
OF THE UNIVERSITY OF MINNESOTA  
BY

Lucía Florencia Zacchi

IN PARTIAL FULFILLMENT OF THE REQUIREMENTS  
FOR THE DEGREE OF  
DOCTOR OF PHILOSOPHY

Dana A. Davis, Ph.D., Advisor

September 2010

© Lucía Florencia Zacchi 2010

## Acknowledgements

I would first like to thank the many people who participated in the work presented in this dissertation and whom I was very lucky to be able to collaborate with, including Andy Kruse and Douglas Ohlendorf (Chapter 2); Eric Bensen, and Zhen Jin Tu (Chapter 3); Mingchun Li, Paul and Bebe Magee, Anna Selmecki, Helen Wang, and Judith Berman (Chapter 4 and Appendix B); and Tim Leonard (Appendix B). I would like to especially thank Mark T. Anderson, Matt J. Hamilton, Zubin Mukadam, Sean Sutton, and Margaret Dimond, who contributed to the identification of *MDS3* as a regulator of phenotypic switching and in the characterization of virulence traits expression and switching frequencies of the switched *mds3Δ/Δ* strains (Chapter 4). I would also like to especially thank Jonatan Gomez-Raja and Gabriela Vazquez-Benitez, both of them great friends and excellent researchers, for their invaluable contributions (Chapter 3). Last, but not least, I would like to thank the members of the scientific fungal community for their ideas and suggestions during the meetings and conferences I attended.

I am indebted to Aaron Mitchell, Ed Winter, Doreen Harcus, Joseph Heitman, Malcolm Whiteway, David Kirkpatrick, Paul and Bebe Magee, Maryam Gerami-Nejad, Judith Berman, Patrick Van Dijck, and Scott Filler for numerous strains and plasmids that I have used in these studies. I would also like to thank Steve Rice, Leslie Schiff, and Paul and Bebe Magee for many reagents that they kindly provided me. I am also grateful to Melanie Legrand, Robert Bastidas, and Laura Okagaki for technical advice.

I am very grateful to Judith Berman, Kirsten Nielsen, Timothy Brickman, Do-Hyung Kim, Thomas Neufeld, Ryan Kelly, Laura Diaz-Martinez, and the members of the Davis and Nielsen labs for numerous helpful discussions and critical reading of my manuscripts.

I would also like to thank the Fulbright Commission in Argentina for giving me the opportunity to pursue my Ph.D. in the United States. Further, the work presented here was supported by the Investigators in Pathogenesis of Infectious Disease Award from the Burroughs Wellcome Fund to D.A.D, and by the NIH National Institute of Allergy and Infectious Diseases award R01-AI064054 to D.A.D. I was also able to attend several conferences thanks to the generous help from the American Society for Microbiology, the Milne-Brandenburgh MICaB Student Travel Award, the Council of Graduate Students of the University of Minnesota, the Graduate and Professional Student Assembly of the University of Minnesota, and the Xi Chapter of Graduate Women in Science.

Finally, there have been a lot of people who, directly or indirectly, helped me walk this path. I would like to thank my advisor, Dana Davis, for his help and support, for his critical thinking and rigorous science, and, importantly, for putting up with me for all these years. I would also like to thank all my committee members for their help and suggestions, especially Judy Berman. I am very grateful to my colleagues of the MICaB program, both classmates and faculty, who led me by their example and always encouraged me throughout the inevitable difficult times in research. I would like to thank Bruce Boudia for his company, his teachings about American culture and history, and for making sure I was safe all those late nights in which I stayed working in the laboratory. I would also like to thank David Chmielewski, who helped to keep the lab running and organized even though he was already retired, thank you David!. I am deeply grateful to all my friends in Minnesota -they were my family here- and to my partner in life, Christoph, for his unconditional love and support. Finally, I would like to thank, and also dedicate this work, to my family in Argentina and Germany and to my grandparents (the ones who are still here and the ones who have already departed); they all tolerated the enormous distance because they knew that this was what I really wanted to do. None of these people may ever realize how important it is sometimes to have someone who believes that you can actually do it. Thank you very much, to all of you.

## **Dedication**

*To my grandparents*

*To my family*

*A mis abuelos*

*A mi familia*

## Abstract

Microbial organisms have a diverse array of mechanisms to obtain phenotypic variation. Phenotypic variation not only enhances population fitness and competitiveness for a specific niche but it is also critical for the survival of a population to unexpected environmental changes. Further, in pathogenic organisms, phenotypic variation is directly associated with virulence. Therefore, besides of the contribution to our understanding of microbial evolution, dissecting the mechanisms that lead to phenotypic variation in pathogenic organisms is very clinically relevant.

*Candida albicans* is the most successful opportunistic fungi that infect humans. *C. albicans* is an obligate diploid yeast with an almost exclusive clonal form of reproduction. In the absence of meiosis to introduce variation in the population, *C. albicans* needs alternative mechanisms to achieve variability, such as the colony morphology phenotypic switching (CMPS). CMPS is the formation of colonies that have an altered, heritable, and low frequency reversible morphology. CMPS is associated with pathogenesis in *C. albicans*: variant colony morphologies have been isolated during infections in humans and show an altered expression of diverse virulence factors, including the secretion of hydrolytic enzymes and resistance to antifungal drugs. Despite the potential role of CMPS in the pathogenesis of *C. albicans*, little is known about the mechanisms that regulate this phenomenon. In our lab, we serendipitously identified a negative regulator of CMPS in *C. albicans*: the Kelch protein Mds3. Mds3 had been previously associated with other morphogenetic processes in fungi, but the biological role of Mds3 in the cell was unknown. Therefore, my goals in this dissertation were to understand the function of Mds3 in the cell and to use this knowledge to gain insights into *C. albicans* CMPS mechanisms and regulation. Through a combination of bioinformatic, biochemical, and genetic analyses we found that Mds3 appears to be a large Kelch/BTB cytoplasmic scaffold protein that functions as a regulator of two major signaling cascades, the TOR and Ras pathways (Chapters 2, 3, and 5). With this information, I was able to identify more CMPS regulators that belong to these

pathways and environmental signals that regulate CMPS and which are all strongly associated with signaling through these pathways (Chapters 4 and 5). Analyses of morphologically switched *mds3Δ/Δ* strains indicated that the phenotypic switch is accompanied by an increase in the sensitivity to the TOR inhibitor rapamycin, which suggests an increased dependence on TOR function in the switched strains. Further, the phenotypic switch was also accompanied by increased sensitivity to genotoxic agents and sometimes also by karyotypic rearrangements and aneuploidies (Chapter 4). Increased DNA damage and genomic instability are mechanisms associated with phenotypic variation in several highly diverse organisms, and could also be mechanisms leading to the phenotypic switch in *C. albicans* (Chapter 4). Taken together, I propose a model for CMPS in *C. albicans* in which defects in the signaling through the TOR and Ras signal transduction pathways as cells become nutrient limited and stressed lead to the accumulation of genetic and epigenetic alterations that eventually cause the phenotypic switch.

## Table of Contents

<b>List of tables</b> .....	<b>Page viii</b>
<b>List of figures</b> .....	<b>Page x</b>
<b>Chapter 1:</b> .....	<b>Page 1</b>
<b>INTRODUCTION</b>	
<i>Candida albicans</i> , the pathogen .....	Page 2
Virulence traits of <i>C. albicans</i> .....	Page 2
Microbial phenotypic variation .....	Page 10
Mechanisms of phenotypic variation .....	Page 14
The Ras and TOR signal transduction pathways .....	Page 21
Using Mds3 as a tool to understand CMPS in <i>C. albicans</i> .....	Page 26
<b>Chapter 2:</b> .....	<b>Page 29</b>
<b>BIOINFORMATIC AND MUTATIONAL ANALYSIS OF MDS3</b>	
Summary .....	Page 30
Introduction .....	Page 31
Materials and methods .....	Page 33
Results .....	Page 38
Discussion .....	Page 51
Tables .....	Page 56
<b>Chapter 3:</b> .....	<b>Page 60</b>
<b>MDS3 REGULATES MORPHOGENESIS IN <i>CANDIDA ALBICANS</i> THROUGH THE TOR PATHWAY</b>	
Summary .....	Page 62
Introduction .....	Page 63
Materials and methods .....	Page 66
Results .....	Page 73
Discussion .....	Page 91
Tables .....	Page 98
Supplementary table .....	Page 106
<b>Chapter 4:</b> .....	<b>Page 116</b>
<b>COLONY MORPHOLOGY PHENOTYPIC SWITCHING IN <i>CANDIDA ALBICANS</i> IS ASSOCIATED WITH GENOMIC ALTERATIONS AND DEFECTS IN DNA DAMAGE RESPONSE AND TOR PATHWAY FUNCTION</b>	
Summary .....	Page 117
Introduction .....	Page 118
Materials and methods .....	Page 123
Results .....	Page 127
Discussion .....	Page 144
Tables .....	Page 155
<b>Chapter 5:</b> .....	<b>Page 159</b>
<b>MDS3, AT THE CROSSROADS OF THE PATHWAYS TO PHENOTYPIC SWITCHING</b>	
Summary .....	Page 160

Introduction	-----Page 161
Materials and methods	-----Page 167
Results	-----Page 172
Discussion	-----Page 198
Tables	-----Page 205

**Chapter 6: -----Page 208**

**CONCLUDING REMARKS**

The regulation of CMPS	-----Page 209
The mechanisms of CMPS, lessons from the mutants	-----Page 211
What is the role of CMPS in <i>C. albicans</i> ?	-----Page 213
CMPS in the host	-----Page 216
The importance of being Mds3	-----Page 219

**REFERENCES-----Page 224**

**Appendix A: -----Page 263**

***HOS2* AND *HDA1* ENCODE HISTONE DEACETYLASES WITH OPPOSING ROLES IN *CANDIDA ALBICANS* MORPHOGENESIS**

Summary	-----Page 264
Introduction	-----Page 265
Materials and methods	-----Page 266
Results	-----Page 268
Discussion	-----Page 270
Tables	-----Page 272
Figures	-----Page 275

**Appendix B: -----Page 277**

**LOW DOSAGE OF HISTONE H4 LEADS TO GROWTH DEFECTS AND MORPHOLOGICAL CHANGES IN *CANDIDA ALBICANS***

Summary	-----Page 278
Introduction	-----Page 279
Materials and methods	-----Page 281
Results and Discussion	-----Page 283
Tables	-----Page 290
Figures	-----Page 292

**Appendix C: -----Page 299**

**A FEW QUESTIONS AND SHORT PROJECTS**

## List of Tables

<b>Table 2.1</b>	-----	<b>Page 56</b>
<i>C. albicans</i> strains used in this study		
<b>Table 2.2</b>	-----	<b>Page 57</b>
Plasmids used in this study		
<b>Table 2.3</b>	-----	<b>Page 58</b>
Primers used in this study		
<b>Table 2.4</b>	-----	<b>Page 58</b>
Effects of mutations in Mds3s' second Kelch repeat on filamentation in M199 pH 8		
<b>Table 2.5</b>	-----	<b>Page 59</b>
<i>MDS3</i> Tn7 mutant alleles in pDDB408		
<b>Table 3.1</b>	-----	<b>Page 99</b>
<i>C. albicans</i> and <i>S. cerevisiae</i> strains used in this study		
<b>Table 3.2</b>	-----	<b>Page 101</b>
Primers used in this study		
<b>Table 3.3</b>	-----	<b>Page 102</b>
Results of the transcriptional profiling of the wild-type, the <i>mds3Δ/Δ</i> , and the <i>rim101Δ/Δ</i> <i>C. albicans</i> strains		
<b>Table 3.4</b>	-----	<b>Page 103</b>
GO categories of differentially expressed ORFs in the <i>mds3Δ/Δ</i> and <i>rim101Δ/Δ</i> mutants compared to wild type <i>C. albicans</i> .		
<b>Table 3.5</b>	-----	<b>Page 105</b>
Hyphal formation in M199 pH 8 in the presence and absence of 5nM rapamycin		
<b>Table 3.6</b>	-----	<b>Page 105</b>
Hyphal formation in M199 pH 8 in the presence and absence of 5nM rapamycin		
<b>Table S3.1</b>	-----	<b>Page 106</b>
ORFs differentially expressed ( $\geq 2$ ) in the <i>mds3Δ/Δ</i> mutant compared to the wild-type strain at pH 4 or at pH 8		
<b>Table 4.1</b>	-----	<b>Page 155</b>
<i>C. albicans</i> strains used in this study		
<b>Table 4.2</b>	-----	<b>Page 156</b>
Primers used in this study		
<b>Table 4.3</b>	-----	<b>Page 157</b>
Karyotypic rearrangements, aneuploidies, and resistance to rapamycin and DNA damage agents in switched <i>mds3Δ/Δ</i> strains		
<b>Table 5.1</b>	-----	<b>Page 205</b>
<i>C. albicans</i> strains used in this study		

<b>Table 5.2</b>	-----	<b>Page 206</b>
Plasmids used in this study		
<b>Table 5.3</b>	-----	<b>Page 207</b>
Primers used in this study		
<b>Table A.1</b>	-----	<b>Page 272</b>
List of mutants in histone deacetylases, the mutagenesis strategies, and corresponding TIGR CAG clones		
<b>Table A.2</b>	-----	<b>Page 272</b>
Germ tube formation delay of the <i>hda1</i> $\Delta/\Delta$ mutant in M199 pH 8 and Spider media		
<b>Table A.3</b>	-----	<b>Page 273</b>
<i>C. albicans</i> strains		
<b>Table A.4</b>	-----	<b>Page 274</b>
Primers used in this study		
<b>Table B.1</b>	-----	<b>Page 290</b>
Strains used in this study		
<b>Table B.2</b>	-----	<b>Page 291</b>
Primers used in this study		

## List of Figures

<b>Figure 1.1</b>	-----	<b>Page 9</b>
Example of colony morphology variations in the <i>C. albicans</i> strain 3513A		
<b>Figure 1.2</b>	-----	<b>Page 22</b>
Ras/PKA and Gpr1/Gpa2 circuits in <i>C. albicans</i>		
<b>Figure 1.3</b>	-----	<b>Page 25</b>
TOR signal transduction pathway (as it may be in <i>C. albicans</i> )		
<b>Figure 2.1</b>	-----	<b>Page 39</b>
CLUSTAL 2.0.12 multiple sequence alignment of Mds3, ScMds3, and Pmd1		
<b>Figure 2.2</b>	-----	<b>Page 40</b>
Bioinformatic and genetic analysis of Mds3		
<b>Figure 2.3</b>	-----	<b>Page 44</b>
Functional characterization of the only bioinformatically identified Kelch repeat in Mds3 by site-directed mutagenesis		
<b>Figure 2.4</b>	-----	<b>Page 45</b>
Functional characterization of the tagged Mds3 alleles		
<b>Figure 2.5</b>	-----	<b>Page 47</b>
Functional characterization of the <i>MDS3-Tn7</i> alleles		
<b>Figure 2.6</b>	-----	<b>Page 49</b>
Mds3 localizes in discrete cytoplasmic spots		
<b>Figure 2.7</b>	-----	<b>Page 50</b>
Functional characterization of the <i>MDS3-Kelch::V5</i> tagged alleles		
<b>Figure 3.1</b>	-----	<b>Page 74</b>
VENN diagram of wild-type, Mds3, and Rim101-dependent genes		
<b>Figure 3.2</b>	-----	<b>Page 77</b>
Microarray validation by Northern blot analysis		
<b>Figure 3.3</b>	-----	<b>Page 79</b>
Rapamycin rescues <i>mds3Δ/Δ</i> hyphal associated phenotypes		
<b>Figure 3.4</b>	-----	<b>Page 80</b>
Rapamycin rescues <i>mds3Δ/Δ</i> filamentation defects in nutrient poor medium but cycloheximide does not		
<b>Figure 3.5</b>	-----	<b>Page 82</b>
The effect of rapamycin on filamentation is TOR dependent		

<b>Figure 3.6</b>	-----	<b>Page 83</b>
The <i>TOR1-1</i> Δ <i>mds3</i> Δ/Δ mutant grows poorly		
<b>Figure 3.7</b>	-----	<b>Page 88</b>
Mds3 and TOR pathway members have altered rapamycin resistance		
<b>Figure 3.8</b>	-----	<b>Page 90</b>
Mds3 and Sit4 interact physically		
<b>Figure 3.9</b>	-----	<b>Page 92</b>
Models of Mds3 as a TOR pathway member		
<b>Figure 4.1</b>	-----	<b>Page 128</b>
Colony morphology and white-opaque phenotypic switching in the <i>mds3</i> Δ/Δ mutant		
<b>Figure 4.2</b>	-----	<b>Page 130</b>
Karyotypic rearrangements in switched <i>mds3</i> Δ/Δ strains observed through CHEF electrophoresis		
<b>Figure 4.3</b>	-----	<b>Page 132</b>
Aneuploidies are common in switched <i>mds3</i> Δ/Δ strains, but are not required for the phenotypic switch		
<b>Figure 4.4</b>	-----	<b>Page 135</b>
The phenotypic switch in the <i>mds3</i> Δ/Δ mutant is accompanied by alterations in the sensitivity to DNA damaging agents		
<b>Figure 4.5</b>	-----	<b>Page 137</b>
Phenotypic switching in the <i>mds3</i> Δ/Δ mutant is enhanced under glucose starvation and repressed under alkaline pH conditions		
<b>Figure 4.6</b>	-----	<b>Page 139</b>
Alkaline pH enhances rapamycin resistance in <i>C. albicans</i>		
<b>Figure 4.7</b>	-----	<b>Page 141</b>
The switch in the <i>mds3</i> Δ/Δ mutant is accompanied by enhanced rapamycin sensitivity		
<b>Figure 4.8</b>	-----	<b>Page 142</b>
Synergistic effect of the <i>TOR1-1</i> allele and <i>mds3</i> Δ/Δ deletion on papilli formation		
<b>Figure 4.9</b>	-----	<b>Page 148</b>
Summary model of CMPS in the <i>mds3</i> Δ/Δ mutant		
<b>Figure 5.1</b>	-----	<b>Page 163</b>
The Ras1 pathway in <i>C. albicans</i> . Figure adapted from Leberer et al (2001).		
<b>Figure 5.2</b>	-----	<b>Page 169</b>
<i>C. albicans</i> SC5314 has two <i>RAS1</i> alleles		

<b>Figure 5.3A</b>	-----	<b>Page 173</b>
<b>Figure 5.3B</b>	-----	<b>Page 175</b>
<b>Figure 5.3C</b>	-----	<b>Page 176</b>
Looking for <i>MDS3</i> -dependent phenotypes in mutants in the MAPK, PKA and TOR pathways		
<b>Figure 5.4A</b>	-----	<b>Page 178</b>
<b>Figure 5.4B</b>	-----	<b>Page 179</b>
<b>Figure 5.4C</b>	-----	<b>Page 180</b>
Genetic interaction between <i>MDS3</i> , <i>SIT4</i> , and <i>RAS1</i>		
<b>Figure 5.5</b>	-----	<b>Page 182</b>
The <i>mds3Δ/Δ</i> and <i>ras1Δ/Δ</i> mutant have a very similar gene expression profile, and <i>sit4Δ/Δ</i> mutation is dominant to both <i>mds3Δ/Δ</i> and <i>ras1Δ/Δ</i> mutations		
<b>Figure 5.6</b>	-----	<b>Page 186</b>
In the absence of <i>MDS3</i> , starvation responses are upregulated		
<b>Figure 5.7A</b>	-----	<b>Page 188</b>
<b>Figure 5.7B,C</b>	-----	<b>Page 189</b>
An overactive <i>RAS1<sup>GI3V</sup></i> allele rescues <i>mds3Δ/Δ</i> defects, but not <i>sit4Δ/Δ</i> defects		
<b>Figure 5.8A</b>	-----	<b>Page 191</b>
<b>Figure 5.8B</b>	-----	<b>Page 192</b>
<b>Figure 5.8C,D</b>	-----	<b>Page 193</b>
<i>CDC25</i> , <i>RAS1</i> , and <i>SCH9</i> are also negative regulators of CMPS		
<b>Figure 5.9</b>	-----	<b>Page 195</b>
Genetic interaction between <i>MDS3</i> , <i>SIT4</i> , and <i>RAS1</i> in resistance to genotoxic stress		
<b>Figure 5.10</b>	-----	<b>Page 202</b>
Model of Mds3, Ras1, and Sch9 regulation of CMPS in <i>C. albicans</i>		
<b>Figure 6.1</b>	-----	<b>Page 212</b>
Model of CMPS regulation in <i>C. albicans</i>		
<b>Figure A.1</b>	-----	<b>Page 275</b>
HDACs regulate filamentation on solid media		
<b>Figure A.2</b>	-----	<b>Page 276</b>
HDACs regulate filamentation in liquid media		
<b>Figure B.1</b>	-----	<b>Page 292</b>
Genomic organization of the histone H3 and H4 loci in <i>Candida albicans</i>		
<b>Figure B.2</b>	-----	<b>Page 293</b>
Amino acid sequence alignment of histone H3 and H4 genes		
<b>Figure B.3</b>	-----	<b>Page 294</b>
Growth of different histone mutants in YPD medium		
<b>Figure B.4</b>	-----	<b>Page 295</b>
Growth defect and phenotypic instability of mutants containing a single allele of histone H4		
<b>Figure B.5</b>	-----	<b>Page 296</b>

Histone deficit causes alterations in colony morphology

**Figure B.6** -----**Page 297**  
Quantitative Southern blot of histone H4 alleles

**Figure B.7** -----**Page 298**  
CGH analysis of a *hhf22-hht2Δ/Δ HHF1/hhf1Δ* (DAY1072) small colony (A) and a spontaneous large colony suppressor (B)

## **CHAPTER 1**

### **INTRODUCTION**

## ***Candida albicans*, the pathogen**

*Candida albicans* is a commensal of the skin and mucosae of most individuals and is also one of the most important fungal pathogens of humans (Calderone, 2002). Immunosuppression in the host or prolonged broad spectrum antibiotic treatment are risk factors for *C. albicans* infections (Samonis and Bafaloukos, 1992; Gullo, 2009; Hauman et al., 1993). The growing population of immunocompromised patients due to medical advances such as chemotherapy and organ transplantation, and the steady increase in the AIDS population has led to an increase in the incidence of opportunistic *C. albicans* infections during the last decades (Pfaller et al., 1999; Hazen, 1995). *C. albicans* can also cause infections in otherwise healthy individuals. For example, *C. albicans* is one of the major causes of single or recurrent infections in the female genital tract (Sobel, 1992). Most *C. albicans* infections are superficial and treatable with antifungal therapy. However, *C. albicans* is also the fourth leading cause of nosocomial bloodstream infections, which are associated with more than 40% mortality rate despite antifungal treatment (Pfaller et al., 2001). Thus, *C. albicans* is responsible for a diverse array of superficial and systemic infections in humans that are associated with a high morbidity and mortality.

### **Virulence traits of *C. albicans***

Given the relevance of *C. albicans* as a pathogen, the most well studied characteristics of this organism are its virulence traits. *C. albicans* virulence attributes include the secretion of hydrolytic enzymes, adhesion to human cells, antifungal drug resistance, morphogenetic transitions, and phenotypic variation.

### *Hydrolytic enzymes*

*C. albicans* secretes three different types of enzymes: secreted aspartic proteinases (SAPs), lipases, and phospholipases. The SAPs are a family of ten secreted aspartic proteinases, eight of them are secreted to the extracellular space and two of them are GPI-linked to the cell wall (Monod et al., 1994; Naglick et al., 2003). Mutations in selected *SAP* genes and inactivation of proteinase activity through the use of pepstatin A or anti-SAP antibodies led to reduced virulence in diverse models of infection, indicating the SAPs are important for *C. albicans* pathogenesis (Schaller et al., 2005). Further, the different *SAP* genes are transcribed under diverse environmental conditions *in vitro* and at different location or stages of infection in murine models and in the human host (Monod et al., 1998; Naglick et al., 1999; Cassone et al., 1987). The actual target of the SAPs in the host remains elusive, although SAPs have been proposed to act on host extracellular matrix and immune system components (Gropp et al., 2009; Schaller et al., 2005). Thus, there is a clear role for secreted aspartic proteinases in *C. albicans* pathogenesis.

*C. albicans* also secrete phospholipases and lipases into the extracellular space. Phospholipases hydrolyze ester linkages in glycerophospholipids, while lipases (and esterases) hydrolyze ester bonds of triacylglycerols. Two genes encode extracellular phospholipases: *PLB1* and *PLB2*. Phospholipases are synthesized *in vivo* during infection in the human host, and their role in pathogenesis has been associated with tissue penetration, adhesion to epithelial cells, and interaction with host signal transduction pathways (Pugh and Cawson, 1977; Leidich et al., 1998; Filler et al., 1991). Lipases are encoded by a lipase isoenzyme family, composed of ten *LIP* genes (Hube et al., 2000). Different *LIP* genes have been found to be induced under different growth conditions *in vitro*, and during infection in murine models of infection and in the human host, suggesting that they fulfill a role in pathogenesis (Tsuboi et al., 1996; Stehr et al., 2004; Schaller et al., 2005). However, the role of lipases in *C. albicans* virulence remains unclear.

Thus, *C. albicans* genome encodes a diverse array of extracellular hydrolytic enzymes which are mainly associated with tissue invasion and colonization. Expression of the genes encoding different hydrolytic enzymes is regulated according to the location and stage of the infection, suggesting a role in pathogenesis. Importantly, inhibition of SAPs activity can prevent tissue invasion in animal models and disease progression in AIDS patients. Further, phospholipases are also required for infection (Cauda et al., 1999; Hoegl et al., 1988; Leidich et al., 1998). Therefore, a better understanding of the function of *C. albicans* hydrolytic enzymes might provide targets for combinatory antifungal therapy.

#### *Adhesion to epithelial cells*

In order to colonize and invade tissue, *C. albicans* needs to adhere to the surface of the cells. *C. albicans* genome contains multiple adhesins, including Als proteins, Hwp1, Eap1, and Csh1 (Sundstrom, 2002; Hoyer et al., 2008). Similar to the hydrolytic enzyme families, the different genes in the adhesin families are expressed under different conditions and morphogenetic states (Cheng et al., 2005; Green et al., 2004, 2006; Argimon et al., 2007). The different adhesins also play different roles in *C. albicans* virulence. For example, Als proteins bind to diverse host substrates, including the surface of endothelial or epithelial cells, collagen, fibronectin, and laminin; Als5 can mediate self-binding, and Als3 also mediates invasion to endothelial cells by inducing host cell phagocytosis (Zhu and Filler, 2010; Phan et al., 2007; Hoyer et al., 2008). Several Als proteins are required for biofilm formation, and Hwp1, a hyphae-specific adhesin, is required for biofilm formation and mating (Ene and Bennett, 2009; Nobile et al., 2008). Adherence is a key step in fungal pathogenesis. Since adhesins are expressed on the cell surface they constitute potential antifungal targets, underscoring the relevance of identifying them and understanding their function. In this regard, a vaccine against Als3 has been developed and is currently under clinical trials (Lin et al., 2009).

### *Antifungal drug resistance*

Most antifungal drugs available for therapy target components of the fungal cell envelope, including the synthesis of ergosterol and  $\beta$ 1,3 glucans, and also ergosterol itself (Odds et al., 2003). Examples of these antifungals include azoles, polyenes, echinocandins, morphollines, and allylamines. Other targets for antifungal drugs include DNA and RNA synthesis (flucytosine), microtubule assembly (griseofulvin), and protein synthesis (sordarins) (Odds et al., 2003). *C. albicans* is not naturally resistant to any of these antifungal drugs, but it shows a remarkable ability to generate resistance during infection and *in vitro* (Cannon, et al., 2007; Cowen, 2008; White et al., 1998, 2002; White, 1997; Anderson, 2005; Selmecki et al., 2006, 2009; Kurtz et al., 1996).

The best studied mechanisms of antifungal drug resistance are against azoles, a family of drugs that target specific enzymes in the ergosterol biosynthetic pathway. Ergosterol is a lipid critical to ensure fluidity of the plasma membrane. Azoles prevent the formation of ergosterol, which is replaced by a toxic sterol as a consequence of the defective metabolism (Cowen, 2008). Antifungal resistance in *C. albicans* is mediated by several mechanisms involving transcriptional changes, point mutation, and genomic rearrangements that lead to the amplification of drug efflux pumps or alterations in drug targets (White et al., 1998; Cowen, 2008). For example, *C. albicans* can acquire azole resistance by upregulating the expression of drug transporters (*CDR1*, *CDR2*, and *MDR1*), by altering the target enzyme (*ERG11*) through point mutations followed by gene conversion mechanisms that amplify the more resistant *ERG11* allele, or by upregulation of *ERG11* transcription; and by altering the ergosterol biosynthetic pathway to reduce or eliminate the production of toxic sterols (MacPherson et al., 2005; Coste et al., 2004; Dunkel et al., 2008; Selmecki et al., 2006, 2008, 2009). Finally, *C. albicans* can also enhance antifungal drug resistance by forming biofilms (Sanglard et al., 2009; d'Enfert, 2006). Therefore, *C. albicans* has

many diverse mechanisms to acquire resistance to antifungal drugs, which makes this feature an important concern for clinicians and a critical area of research.

### *Morphogenetic transitions*

*C. albicans* can transition between different morphogenetic states, including the yeast-pseudohyphal-hyphal transition (Y-PH-H), and chlamyospore formation (Staib and Morschhauser, 2007; Biswas et al., 2007). The ability of *C. albicans* to switch between the yeast and hyphal morphologies is a critical virulence trait (Mitchell, 1998). Mutants locked in either morphology show reduced virulence in animal models of infections (Lo et al., 1997; Murad et al., 2001; Bastidas and Heitman, 2009; Saville et al., 2003, 2008; Carlisle et al., 2009). Further, the different morphologies are required for biofilm formation, trigger different immune responses in the host, and have different abilities to adhere to cells, to secrete hydrolytic enzymes, to invade tissues, and to disseminate in the host (Baillie and Douglas, 1999; Richard et al., 2005; Hawser and Douglas, 1995; Acosta-Rodriguez et al., 2007; Romani et al., 2003, 2004; Mitchell et al., 1998; Gow et al., 2002). Therefore, Y-PH-H morphogenetic transitions in *C. albicans* have pleiotropic effects on this fungus pathogenesis.

The Y-PH-H transition in *C. albicans* requires the induction of complex morphogenetic programs that respond to different environmental cues and that are regulated by several (sometimes overlapping) signaling pathways. For example, hyphal formation in *C. albicans* can be triggered by alkaline pH, body temperature, serum, high CO<sub>2</sub> pressure, N-acetyl-glucosamine, the embedment in a matrix, and starvation (Biswas et al., 2007). Several signal transduction pathways are required for the proper response to the different environmental signals, including the Rim101, cAMP/PKA, MAPK, and TOR pathways (Biswas et al., 2007; Davis, 2009; Monge et al., 2006; Cutler et al., 2001; Bastidas et al., 2009; Zacchi et al., 2010a). Y-PH-H in *C. albicans* is regulated by many signals and signal transduction pathways and is critical for pathogenesis.

*C. albicans* can also form chlamydozoospores. Chlamydozoospores are spherical cells with a thick wall that form at hyphal tips during growth in poor nutrient media. Chlamydozoospores can be found during *C. albicans* infections. However, the role of chlamydozoospores on *C. albicans* virulence is unclear (Staib and Morschhauser, 2007). Only a handful of genes have been identified as regulators of chlamydozoospore formation, including *SCH9* and *MDS3*, two genes that we will discuss later (Nobile et al., 2003; Bambach et al., 2009; Eisman et al., 2006; Staib and Morschhauser, 2005). Thus, chlamydozoospore formation is an intriguing and rather unexplored type of morphogenetic transition in *C. albicans*.

#### *Phenotypic switching*

Although *C. albicans* is able to mate at a low frequency, it does not appear to undergo meiosis, a major mechanism to introduce variation in a population (Forche et al., 2009; Soll, 2009). Since phenotypic variation is critical for the survival of any organism in a changing environment, *C. albicans* requires of alternative mechanisms to achieve variation. High-frequency phenotypic switching has been suggested to account for some of the variation observed in this fungus and is thus an important virulence trait (Soll, 1992). *C. albicans* undergoes two types of phenotypic switching: white-opaque switching and colony morphology phenotypic switching.

White-opaque switching (W-O) is the bi-stable switch between a white, hemispherical colony formed by round cells and a grey, flat colony formed by more elongated cells with pimples in their cell wall (Slutsky et al., 1987; Anderson et al., 1990). Opaque cells are the mating competent type, and the transition from white to opaque phase is required for mating in *C. albicans* (Miller et al., 2002). Pheromone signaling from opaque cells to white cells can trigger white cells biofilm formation, a phenomenon that has been proposed to help the mating process (Daniels et al., 2006; Soll, 2009). The white and opaque cells differ in their expression of several

virulence attributes, including antigenicity, adhesion to cells, Y-PH-H transitions, sensitivity to neutrophils, secretion of hydrolytic enzymes, antifungal drug susceptibility, and the ability to avoid macrophage phagocytosis or develop infections in different pathogenesis models (Lohse and Johnson, 2008; Anderson et al., 1989, 1990; Kennedy et al., 1988; Kolotila and Diamond, 1990; Morrow et al., 1992; Vargas et al., 2000; Kvaal et al., 1997, 1999). Thus, the W-O switching in *C. albicans* is involved in mating and leads to marked differences in pathogenesis.

The second type of phenotypic switching in *C. albicans* is colony morphology phenotypic switching (CMPS). CMPS, also known as the 3153A-type switching because it was re-discovered in this common laboratory *C. albicans* strain, refers to the generation of variant colony morphologies at a frequency of  $\sim 10^{-4}$  (Figure 1.1; Slutsky et al., 1985; Negroni, 1935). Variant colony phenotypes include, but are not limited to, star (Figure 1.1B), ring (Figure 1.1C), and irregular wrinkle (Figure 1.1D), while the normal colony morphology of *C. albicans* is smooth (Figure 1.1A). Several characteristics define CMPS. First, the switch only occurs in a small fraction of the population. Second, the colony morphology phenotypic switch is heritable. Third, the switch is only partially stable, and switched strains continue to give rise to colonies with a different morphology at a low frequency, including the possibility of reverting to the wild-type colony morphology. CMPS is associated with pathogenesis in *C. albicans*. Morphologically switched colonies that are genetically similar have been found in infected patients (Hellstein et al., 1993; Jones et al., 1994; Vargas et al., 2000; Soll et al., 1987, 1988, 1989). Further, phenotypic switching affects the expression of several virulence traits in *C. albicans*, including antifungal drug resistance, morphogenesis, secretion of hydrolytic enzymes, adhesion to cells, and virulence in murine models of infection (Gallagher et al., 1992; Vargas et al., 1994, 2004; Dutton and Penn, 1989). Thus, CMPS is a mechanism to achieve phenotypic variation in *C. albicans*, especially important due to its effects on the expression of virulence attributes in *C. albicans*.

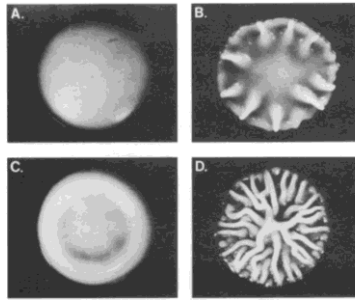


**Figure 1.1:** Example of colony morphology variations in the *C. albicans* strain 3513A (from Slutsky et al., 1985). A) Smooth, B) Star, C) Ring, D) Irregular-wrinkle.

Given the important role in pathogenesis of phenotypic switching, much effort has been devoted to understand their mechanisms of regulation. The great majority of the studies have focused on W-O switching, probably to its simpler bi-phasic characteristic. The W-O switch is regulated epigenetically by histone modifying enzymes and by feedback regulatory loops that involve several transcription factors, including Wor1, Efg1, Czf1, and Wor2 (Huang et al., 2006; Zordan et al., 2006, 2007; Srikantha et al., 2001; Hnisz et al., 2009; Klar et al., 2001). Further, several environmental signals also affect W-O switching, including temperature, CO<sub>2</sub> concentration, N-acetyl-glucosamine, and oxidative stress (Kolotila and Diamond, 1990; Ramirez-Zavala et al., 2008; Huang et al., 2010; Rikkerink et al., 1988; Lohse and Johnson, 2009; Alby and Bennett, 2009).

Unlike the W-O switch, very little is known about the environmental signals, mechanisms, and genetic factors that regulate CMPS in *C. albicans*. The only environmental signals known to contribute to CMPS are growth on low-zinc, amino acid rich medium and exposure to low doses of UV radiation (Slutsky et al., 1985; Pomes et al., 1985; Soll, 1992; Bedell and Soll; 1979). It is also known that CMPS is sometimes accompanied by karyotypic alterations. However, repeated efforts to determine a correlation between particular karyotypes and phenotypes have failed, suggesting that the karyotypic rearrangements are not the cause of

CMPS (Rutschenko et al., 1993, 1994; Rustchenko-Bulgac and Howard, 1993; Rustchenko, 2007; Ramsey et al., 1994; Barton and Scherer, 1994). Finally, two negative regulators of CMPS are known: Ssn6 and Mds3 (Garcia-Sanchez et al., 2005; Chapter 4). Ssn6 is a protein directly involved in transcription: it forms a co-repressor complex with Tup1. Ssn6 also regulates Y-PH-H morphogenetic transitions in *C. albicans* (Hwang et al., 2003). Deletion of *SSN6* leads to the formation of colonies with variant, unstable morphology, which include alterations in colony size and colony surface wrinklyness, and that are reminiscent of CMPS. Importantly, expression of *SSN6* in variant *ssn6*<sup>-</sup> colonies immediately restores wild-type colony morphology. The mechanism through which *SSN6* regulates CMPS is unclear, but it is likely through its direct effects on gene transcription (Garcia-Sanchez et al., 2005; Hwang et al., 2003). The second regulator of CMPS, Mds3, is a poorly characterized fungal-specific protein, and the focus of this dissertation (see below). Thus, although CMPS appears to be important for *C. albicans* pathogenesis and as a mechanism to generate variability in this fungus, there is very little known about the mechanisms and signals that govern CMPS.

### **Microbial phenotypic variation**

CMPS belongs to a larger class of phenomena that generate phenotypic variation. Here, I summarize the current knowledge on microbial phenotypic variation mechanisms, focusing mostly on human pathogenic fungi, but also on bacteria and protozoa.

#### *Phenotypic switching in fungi*

Besides *C. albicans*, phenotypic switching has been described in several fungal species, including *C. glabrata*, *C. lusitaniae*, *C. tropicalis*, *Trichosporon assahii*, *Pneumocystis* spp., *Histoplasma capsulatum*, *Paracoccidioides brasiliensis*, *Cryptococcus neoformans*, and *C. gattii* (Slutsky et al., 1985, 1987; Ichikawa et al., 2004; Goldman et al., 1998; Jain et al., 2006;

Srikantha et al., 2008; Jain et al., 2009; Macoris et al., 2006; Ichikawa et al., 2004; Stringer et al., 2007; Soll et al., 1988; Keely et al., 2003; Eissenberg et al., 1996). In all cases, phenotypic switching leads to alterations in the colony morphology which may be associated with differences in virulence trait expression.

*C. glabrata*, the second most prevalent *Candida* species in human infections, presents two types of switching: core switching, in which colonies with different brown coloration appear on agar supplemented with CuSO<sub>4</sub>; and irregular wrinkly switching (Lachke et al., 2000, 2002). *C. glabrata* core phenotypic switching occurs *in vivo* (Brockert et al., 2003). Further, most clinical *C. glabrata* isolates can switch between colony colors, although one type of color is predominant in natural isolates and it is also associated with increased virulence in murine models of infection. It is unclear what makes one colony type more virulent than the others (Srikantha et al., 2005). Thus, *C. glabrata* also undergoes phenotypic switching, and this switching appears to play a role in pathogenesis.

*C. lusitanae* is an emergent pathogenic yeast of medical concern due to its ability to readily acquire resistance *in vivo* to the antifungal drug amphotericin B. Similar to *C. glabrata*, *C. lusitanae* also undergoes core switching (Sterling and Merz, 1998; Blinkhorn et al., 1989; Miller et al., 2006). Core switching has been associated with the acquisition of resistance to amphotericin B (Yoon et al., 1999). Thus, core switching might be a common type of switching in certain pathogenic *Candida* species, which is of particular relevance given its strong association with virulence.

*H. capsulatum* is an intracellular fungal pathogen which causes primarily respiratory infections that can subsequently become systemic (Wheat et al., 2006). When plated on agar surfaces, this fungus gives rise to colony phenotypic variants. Cells from these colony variants adopt unusual morphologies inside macrophages. One of these *H. capsulatum* colony variants lacks  $\alpha$ -1,3-glucan, a major cell wall constituent and critical for virulence, which explains why

these variant cells have reduced macrophage toxicity (Klimpel and Goldman, 1987, 1988; Eissenberg et al., 1996; Holbrook and Rappleye, 2008). It has been suggested that one role of phenotypic variation in *H. capsulatum* is to enhance persistence in the host (Eissenberg et al., 1996). Therefore, in *H. capsulatum*, colony phenotypic variation is also associated with pathogenesis.

Perhaps the fungal phenotypic switching phenomenon that has been most studied (from the pathogenesis perspective) is that of *Cryptococcus*. *Cryptococcus* is one of the main causes of chronic respiratory diseases and meningitis in immunocompromised individuals. Phenotypic variation in *Cryptococcus* occurs *in vivo*, and the variants display altered virulence *in vivo* and differential expression of virulence traits *in vitro* (Goldman et al., 1998; Fries et al., 1999, 2005; Franzot et al., 1998; Guerrero et al., 2006, 2010). The colony variants include smooth, mucoid, wrinkled, serrated, and pseudohyphal morphologies (Jain et al., 2008). Phenotypic switching in *Cryptococcus* has been proposed to be a mechanism of microevolution, which generates fungal variants during acute and chronic infections that allow the persistence of infection (Guerrero et al., 2006). The mechanisms leading to the switch in *Cryptococcus* remain poorly understood. Karyotypic instability has been observed in certain switched *Cryptococcus* strains, but it has not been possible to correlate karyotypic alterations with particular phenotypes (Fries et al., 1999). *Cryptococcus* generates phenotypic variants *in vivo*, which appear to have an important role in determining the outcome of the infection.

To sum up, phenotypic switching of colony morphologies is common in diverse fungal pathogens and in many cases a direct role for the phenotypic switch in pathogenesis has been demonstrated. Despite extensive research in many different fungi, the underlying mechanisms of CMPS are unknown. Importantly, CMPS is not an effect of *in vitro* culture of laboratory strains. CMPS happens *in vivo* during commensalism and during infection. CMPS has been proposed to be a mechanism to generate variation and of microevolution in fungal pathogens. It may be

interesting to understand what mechanisms regulate CMPS in the different fungi, not only from an evolutionary perspective, but also because of their relevant role in fungal pathogenesis.

#### *Phenotypic variation in bacteria and protozoa*

Bacteria and protozoan parasites have also developed strategies to alter their phenotypes and antigenic composition of their cellular surface. Phenotypic variation in bacteria is important to generate phenotypic diversity and for niche adaptation. Two types of phenotypic variation in bacteria are phase and antigenic variation. Both phenomena are generated through genetic, epigenetic, and post-translational mechanisms that lead to the synthesis of different enzymes and secondary metabolites, and to the expression of different surface antigens (such as pili, fimbriae, and outer polysaccharides) (Zieg et al., 1977; Yamamoto and Kutsukake, 2006; Bayliss et al., 2001; van de Broek et al., 2005). Phenotypic variation can be enhanced in certain environments. For example, growth in a biofilm triggers the formation of phenotypic variants in *Streptococcus pneumoniae* and *Pseudomonas aeruginosa*. These biofilm variant strains enhance the resistance to stress in the biofilm, and also have a different ability to disseminate or accelerate biofilm formation, contributing to the survival of the biofilm community (Allegrucci and Sauer, 2007; Boles et al., 2004). Similarly, protozoan parasites such as *Trypanosoma brucei* and *Plasmodium falciparum* have evolved sophisticated mechanisms to alter their surface antigens and, thus, successfully evade the pressure of the immune system (Morrison et al., 2009; Ralph and Scherf, 2005). In both organisms, antigenic variation leads to the formation of subpopulations expressing different surface antigens (VSG or PfEMP1) that arise stochastically (see below). These subpopulations are able to continue the infection once the rest of the population is eliminated by the immune system. Therefore, phenotypic variation is a common feature of diverse microorganisms that thrive in different ecosystems, and it serves the common purpose of enhancing the population fitness and ensuring population survival.

## Mechanisms of phenotypic variation

### *Genetic (mutation, genomic rearrangements) and epigenetic mechanisms*

To achieve phenotypic variation, microbes often combine genetic variation with epigenetic mechanisms. One good example of combined genetic and epigenetic mechanisms to generate variation is *P. falciparum*. *P. falciparum* expresses an outer membrane protein, PfEMP1, which is one of the main antigens recognized by the immune system and, thus, a useful substrate for immune evasion (Baruch et al, 1995; Smith et al., 1995; Su et al., 1995). The PfEMP1 family can be encoded by 60-70 *var* genes, located near the telomeric regions of *P. falciparum* chromosomes (Gardner et al., 2002). These *var* genes are subject to a high frequency of ectopic recombination and give rise to novel variants of PfEMP1 (Freitas-Junior et al., 2000). Each *P. falciparum* strain encodes in its genome a large number of PfEMP1 variants, but epigenetic mechanisms operating at the subtelomeric and telomeric regions restrict expression to only one *var* gene at a given time, while simultaneously allowing for a high frequency of *var* switching (Duraisingh et al., 2005; Verstrepen and Fink, 2009; Ralph and Scherf, 2005). This system allows for the temporary expression of unique PfEMP1 versions, thereby providing constant substrate for immune evasion and ensuring the establishment of a chronic infection.

*T. brucei* also employs a combination of mechanisms to generate surface variation in its main antigen VSG. *T. brucei* contains ~ 1600 VSG genes and pseudogenes, located mostly at subtelomeric regions (Marcello and Barry, 2007; Wickstead et al, 2004). There are ~20-45 VSG expression sites (ES), and VSG genes are recombined into them by gene conversion, reciprocal telomeric VSG exchange, and recombination of VSG pseudogenes to generate VSG mosaics (Thon et al., 1999; Pays et al., 1985; Morrison et al., 2009). Only one ES is active at a time, and it is unclear how this happens. It has been proposed that activity of only one ES is achieved through the localization of ES in ES bodies (a specialized nuclear compartment), which can apparently

only accommodate and allow transcription of one ES at a time (Navarro and Gulk, 2001). Given the necessity to evade the immune system in order to ensure a successful chronic infection, *T. brucei* has evolved a successful mechanism to generate a wide range of surface phenotypic variation through the combination of several genetic and cellular approaches.

The *var* and VSG genes belong to a group of genes called contingency genes. Contingency genes are present in virus, bacteria, fungi, and protozoa. These genes are subject to higher mutation rate than the rest of the genome because their function is to provide phenotypic variation (Moxon et al., 1994; Deistch et al., 1997). Noticeably, an increasing number of examples indicate that contingency loci are usually placed nearby the telomeres, including the above mentioned *P. falciparum* and *T. brucei*, and also the fungus *Pneumocystis*, and the bacteria *Borrelia*. Telomeric and subtelomeric regions are subject to epigenetic silencing mechanisms, higher frequency of recombination, and tend to cluster at the nuclear periphery, providing an ideal location for genes that need to be mutated, recombined, or silenced (Barry et al., 2003). For example, the fungus *Pneumocystis carinii* has ~ 100 genes per haploid genome encoding the major surface glycoprotein (MSG), which are located in 2-4 gene clusters at subtelomeric regions (Stringer and Keely, 2001). Similar to *T. brucei*'s VSG, MSGs can only be transcribed from a unique expression site in *P. carinii*. These arrangements are also observed in bacteria containing linear chromosomes, like *Borrelia burgdoferi* and *Haemophilus influenzae* (Barbour and Restrepo, 2000; Moxon et al., 2006). The presence of contingency loci in fundamentally different organisms is an indication of the efficiency of these mechanisms to provide phenotypic variation.

Besides *P. carinii*, other fungi also have gene families located near telomeric regions. For example, *Saccharomyces cerevisiae* can obtain surface phenotypic variation by regulating the expression of the *FLO* gene family located nearby the telomeres, which encode flocculins. *S. cerevisiae* can genetically and epigenetically regulate the expression of the *FLO* genes. At a frequency of  $\sim 10^{-3}$ , *S. cerevisiae* gives rise to wrinkly colonies with increased flocculation due to

*FLO10* mis-expression. *FLO10* mis-expression occurs due to mutations in *IRA1* and *IRA2*, the Ras GTPase activators. The mutations in *IRA1/2* are frameshift mutations or transversions, and occur at a higher frequency than in the rest of the genome. Thus, the effect of *Ira* on *S. cerevisiae* colony switching appears to be dependent on Ras overactivation (Halme et al., 2004). Another example is *C. glabrata*. *C. glabrata* can alter its ability to adhere to a surface by modifying the expression of adhesins encoded by the subtelomeric *EPA* gene family. This fungus has evolved an exquisite system to induce *EPA6* expression only during urinary tract infections. *C. glabrata* is auxotrophic for nicotinic acid, which is a precursor of NAD<sup>+</sup>, the cofactor of the Sir silencing enzymes. Nicotinic acid is low in the urinary tract. This leads to low intracellular NAD<sup>+</sup> levels, improper Sir protein function, and, thus, *EPA6* derepression. The expression of *EPA6* allows *C. glabrata* to adhere to the epithelial cells in the urinary tract (Domergue et al, 2005). Unlike *C. glabrata* and *S. cerevisiae*, *C. albicans* does not encode genes involved in adhesion to surfaces near the telomeres, and epigenetic mechanisms governing subtelomeric gene expression in *C. albicans* have not been defined yet. However, *C. albicans* harbors the *TLO* gene family at subtelomeric regions, and although some of the *TLO* genes are known to be expressed, the function and regulation of these genes is unknown (van het Hoog et al., 2007). Given the relevance of subtelomeric genes in the other organisms discussed here, it is possible that *TLO* genes in *C. albicans* also fulfill a role in this fungus survival and pathogenesis.

Bacteria have developed other mechanisms to achieve phenotypic variation, including phase variation and bistability. Phase variation requires genetic alterations, whereas bistability is an epigenetic switch (Dubnau and Losick, 2006). Phase variation is common in bacteria, and involves the ability to express only one member of a gene family at any given time. Some mechanisms of phase variation include DNA conversion, genomic rearrangements, accumulation of mutations due to DNA repair/replication errors, and differential methylation (epigenetic) (van den Broek et al., 2005). For example, *Salmonella typhimurium* expresses one of two flagelin

genes, and the expression is controlled by a reversible chromosomal inversion in the promoter region (Zieg et al., 1977; Silverman et al., 1979). Phase variation is regulated by environmental cues, including temperature, the composition of the media, and stress. On the other hand, bistability refers to a clonal population that can switch between two distinguishable states (Veening et al., 2008). Some common bistable phenomena in bacteria include: the persister effect, in which bacteria like *Staphylococcus aureus* survives antibiotic treatment by a stochastic decrease in growth rate and metabolism (Bigger, 1944; Keren et al., 2004); entry into genetic competence or sporulation; and the swimming and chaining phenomenon in *Bacillus subtilis* and *Caulobacter crescentus* (Kearns and Losick, 2005; Skerker and Laub, 2004). Phase variation and bistability allow for the generation of heterogeneous bacterial subpopulations, and are regulated or stochastic processes achieved through a myriad of genetic and epigenetic mechanisms.

One process to generate variation during environmental stress is stress-induced mutagenesis, which has been very well characterized in bacteria (Rosenberg, 2001; Galhardo et al., 2007; Foster, 2007). In a stressful environment that has halted the growth of the population, mutagenesis may provide the cells with a growth advantage. The mutations can be caused by defects in recombination and DNA repair, the induction of the error prone DNA polymerase (Pol IV), or by the SOS and catabolite repression systems (Taddei et al., 1995; Kivisaar, 2003). Transient or long term inactivation of DNA repair mechanisms or the activity of DNA polymerases defective in the proofreading subunit cause the “mutator” phenotype (Funchain et al., 2000; Giraud et al., 2001; Aersten and Michiels, 2004). “Mutator” phenotypes also exist in eukaryotes. For example, “mutator” phenotypes have been implicated in cancer development, they can be induced in yeast, and occur naturally in lymphocytes during somatic hypermutation (Drotschmann et al., 2000; Harris et al., 1999; Loeb et al., 2008). Thus, environmental stress is a potent inducer of variation in highly diverse organisms.

### *Codon usage*

Most living organisms share a common genetic code. However, throughout evolution there has been several codon reassignments (Moura et al., 2009). In *C. albicans*, the codon CUG that is normally translated as leucine has been replaced with serine, an amino acid that is structurally different (Santos and Tuite, 1995). The tRNA that recognizes CUG codons in *C. albicans* can be aminoacylated with serine (with a 97% frequency) but also with leucine (with a 3% frequency), indicating that a percentage of the proteins that contain CUG codons will have intrinsic structural and functional variations (Suzuki et al., 1997). Experimental increase of the frequency at which CUG codons are recognized by leucine and not serine generated a burst of phenotypic variation in *C. albicans*, including alterations in cellular and colony morphology, adhesive properties, and gene expression; and in some cases the changes were accompanied by karyotypic alterations (Miranda et al., 2007). Thus, CUG ambiguity has the potential to generate variability *in vivo* in *C. albicans*. It is possible that, under certain conditions or simply stochastically, *C. albicans* might be able to alter the frequency at which the tRNA<sub>CAG</sub> is aminoacylated with leucine or serine, thereby generating phenotypic and genetic variability.

### *Transcriptional noise, translation error, and Hsp90*

One mechanism that is responsible for the generation of phenotypic diversity in otherwise identical individuals is transcriptional noise. Transcriptional noise is the stochastic variability in gene expression (Ozbudak et al., 2002). The effect of transcriptional noise on a phenotype depends on the strength of the promoter, i.e. phenotypic differences due to transcriptional noise are most observable in genes that have low transcription (Kaern et al., 2005). Stochasticity in gene expression can have beneficial effects on population fitness and survival (Freed et al., 2008). Further, if alterations in gene expression are part of feedback regulatory loops, these alterations may become epigenetically fixed and allow for the maintenance of a particular phenotype (Raser

and O'Shea, 2005; Sriram et al., 2009). Thus, transcriptional noise is an important mechanism that allows rapid adaptation to environmental change, but it is also involved in more long-term adaptation strategies.

Another mechanism of variation is translational errors. Precision during protein synthesis is critical to ensure the proper function of any polypeptide and to avoid protein mis-folding and aggregation. However, protein synthesis is error prone: ~15% of average length proteins contain a minimum of one mis-incorporated amino acid (Parker, 1989; Ogle and Ramakrishnan, 2005). Although organisms have developed mechanisms to enhance the fidelity of protein synthesis, synthesis error can have some benefits (Drummond and Wilke, 2009). For example, allowing a certain level of translation or folding mistakes increases the phenotypic diversity without impacting the genetic sequence. Microorganisms take advantage of mechanisms that induce ribosomal mistakes, such as programmed frame-shifting (ribosomes shift to a different open reading frame) and ribosome skipping. Ribosomal mistakes can increase the diversity of polypeptides that can be produced with the same mRNA, allow for the synthesis of polypeptides that carry otherwise deleterious mutations (e.g. an early stop codon), and produce proteins with novel phenotypes (Farabaugh, 1996; Pleiss et al., 2007; Engelberg-Kulka et al., 1979; Drummond and Wilke, 2009). Thus, alterations in protein synthesis can lead to phenotypic diversity and genome evolution.

Besides protein translation efficiency, organisms need to ensure protein stability and folding. Improperly folded proteins have a modified function or are non-functional and can aggregate, which has severe consequences on cellular function (Ecroyd and Carver, 2008). To aid in protein folding cells have molecular chaperones. One example of a highly conserved chaperone is Hsp90 (Taipale et al., 2010). However, Hsp90 is a specialized chaperone that not only functions in protein folding, it also has the ability to buffer cryptic mutations, allowing for the normal function of proteins that otherwise would show an altered function (Yahara et al., 1999).

When Hsp90 function is compromised or Hsp90 is less available (e.g. due to stress), the phenotypic variability that Hsp90 had masked is displayed. Thus, Hsp90 allows for the evolution of genes under non-selective pressure. Hsp90 is associated with many signal transduction pathways, including the PKA and TOR pathways (see below), and functions in several morphogenetic processes in yeast, flies, and plants (Sollars et al., 2003; Queistch et al., 2002; Shapiro et al., 2009; Rutheford and Lindquist, 1998; Delgoffe et al., 2009). Thus, modulation of Hsp90 function allows for the acquisition and display of phenotypic variation.

Finally, there are other mechanisms to generate variation that I have not discussed here, such as the movement of transposable elements. All organisms need to generate variation, and it is likely that some of the mechanisms cells employ to generate variation are more common among highly diverse organisms than previously expected.

Phenotypic variation is a way organisms have to cope with environmental changes. Thus, it is logical that many of the mechanisms that lead to the generation of phenotypic variation function in response to the environment. In order to sense environmental changes, cells use an array of signal transduction pathways. Alterations in the function of these pathways are directly linked with the generation of phenotypic variation in highly diverse organisms, including yeast and mammals. Two major signal transduction cascades that regulate cell growth in response to the environment and that are also directly involved in phenotypic variation are the Ras/protein kinase A (PKA) and the Target of Rapamycin (TOR) signal transduction pathways (Mennon and Manning, 2009; Bjornsti and Houghton, 2004; Prasad et al., 2003; Taddei et al., 1995; Weeks, 2000; Fuchs et al., 2010; Horinouchi et al., 2001; Janion et al., 2002; Menon and Manning, 2008). Interestingly, the protein that is the focus of study in this dissertation, Mds3, functions as a regulator of both of these signal transduction pathways (Chapters 3, 5 and 6). Therefore, below I summarize the current knowledge on the structure and function of this signal cascades in fungi.

## **The Ras and TOR signal transduction pathways**

Two critically important signal transduction pathways in eukaryotic organisms are the Ras and TOR pathways. Both pathways are responsible for regulating cellular growth in response to environmental nutrients. During active growth and in nutrient replete conditions, the Ras and TOR pathways promote protein synthesis and cellular division. Entry to stationary phase or starvation requires Ras and TOR pathways inactivation, which leads to induction of stress responses, autophagy, and cell cycle arrest (Thevelein and de Winde, 1999; Wullschleger et al., 2006; Rohde et al., 2001; Zaman et al., 2008). Inactivation of the TOR pathway also leads to the activation of the nitrogen catabolite repression response, which allows for the metabolism of poor nitrogen sources (Cardenas et al., 1999). Since the Ras and TOR pathways regulate many similar processes they share some downstream effectors, but the actual level of crosstalk between the pathways in yeast is not fully understood (Zaman et al., 2008; Lempiainen et al., 2009; Schmelzle et al., 2004; Zurita-Martinez and Cardenas, 2005; Soulard et al., 2010).

### *The Ras pathway*

In *S. cerevisiae* and *C. albicans* Ras functions upstream of both the cAMP/PKA and MAPK pathways (Thevelein and de Winde, 1999; Biswas et al., 2007) (Figures 1.2 and 5.1). Ras is a small G protein that is active when bound to GTP and inactive when bound to GDP (Broach, 1991). The GTP-GDP exchange factor of Ras is Cdc25 (and Sdc25 in *S. cerevisiae*), an upstream activator of Ras1. GTP-bound Ras activates adenylate cyclase (Cyr1/Cdc35) (Thevelein and de Winde, 1999). This activation is facilitated by Srv2 (or Cap1) (Bahn and Sundstrom, 2001; Fedor-Chaiken et al., 1990). Adenylate cyclase is also activated by the Gpr1-Gpa2 parallel circuit (Maidan et al., 2005; Miwa et al., 2004; Xue et al., 1998). Active adenylate cyclase produces cAMP, which activates PKA by binding to its regulatory subunit, Bcy1, and causing the

dissociation of Bcy1 from the PKA catalytic subunits, the Tpk1 and Tpk2 (Toda et al., 1987). *C. albicans* has two PKA catalytic subunits: Tpk1 and Tpk2, which have both redundant and independent functions (Bockmuhl et al., 2001; Giacommetti et al., 2009; Souto et al., 2006). *S. cerevisiae* has three PKA subunits (Toda et al., 1987b). Thus, PKA is activated by Ras and Gpr1/Gpa2 via adenylate cyclase. In addition, Ras also activates the MAPK pathway in both *S. cerevisiae* and *C. albicans*, and Gpa2 functions in a cAMP-independent pathway (Monge et al., 2006; Leberer et al., 2001; Wilson et al., 2010).

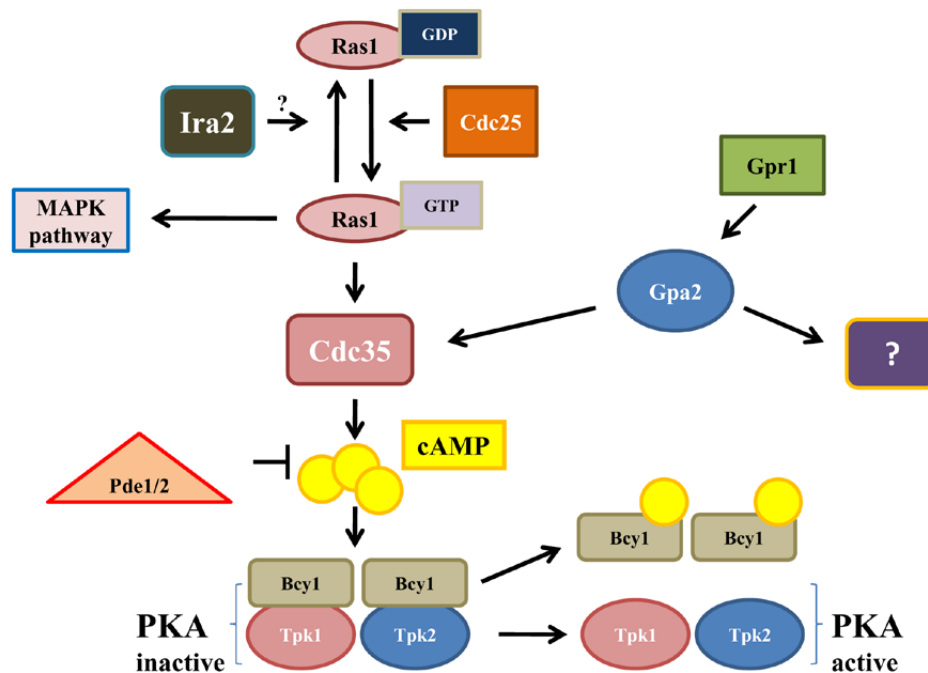


**Figure 1.2:** Ras/PKA and Gpr1/Gpa2 circuits in *C. albicans*. ? on arrow indicates that function is inferred from *S. cerevisiae* studies.

Since overactivation of the Ras/PKA pathway has several negative consequences for cell survival, signaling through this pathway needs to be fine-tuned and downregulated when necessary. Downregulation of the Ras/PKA pathway can be achieved in several of its steps. Ras can be inactivated by the GTPase Ira2 (and Ira1 in *S. cerevisiae*). Gpa2 activity is antagonized by the Kelch proteins Gpb1/Gpb2, which are also inducers of Ira1/Ira2 activity (Harashima et al., 2006). It is to note that *C. albicans* does not appear to have Gpb1/Gpb2 homologs. Finally,

adenylate cyclase function is antagonized by Pde1 and Pde2, two phosphodiesterases that degrade cAMP and promote PKA inactivation (Ma et al., 1999; Jung and Stateva, 2003).

In sum, the structure of the Ras/PKA signal cascade is conserved between *S. cerevisiae* and *C. albicans*, although *C. albicans* appears to lack some pathway members like Scd25, Gbp1/2, and Ira1 that are present in *S. cerevisiae*. Further, there are functional differences between these pathways in both organisms. In *S. cerevisiae*, the *cdc25Δ* and *ras1Δ ras2Δ* mutants are inviable (Broek et al., 1987). However, in *C. albicans* the mutant in *CDC25* grows similar to wild-type, and the double *ras1Δ/Δ ras2Δ/Δ* mutant is still viable (Zhu et al., 2009; Enloe et al., 2000; Leberer et al., 2001). Further, in *S. cerevisiae* the *cyr1Δ* mutant is inviable, while the *C. albicans cdc35Δ/Δ* mutant is viable (Leberer et al., 2001). In *S. cerevisiae*, the Gpr1-Gpa2 circuit is required for glucose sensing (Thevelein and de Winde, 1999). However in *C. albicans* there is conflicting evidence that either support the *S. cerevisiae* model, or suggest that glucose sensing is mediated by Cdc25 while the ligand of Gpr1 is unknown (Zaman et al., 2008; Maidan et al., 2005; Miwa et al., 2004). Therefore, although there is high conservation in the molecular architecture of the Ras/PKA signaling cascade between *S. cerevisiae* and *C. albicans*, there also appear to be major differences between the function of Ras or of Ras downstream effectors in these fungi.

Ras has a critical role in the activation of different signal cascades in eukaryotes and, thus, has been intensively studied. In *S. cerevisiae*, the Ras/PKA pathway is a positive regulator of ribosomal protein synthesis, ribosome biogenesis, and translation; and a negative regulator of the Rim15 dependent activation of stationary phase program, and of Msn2/4 dependent stress responses (Figure 1.2; Zaman et al., 2008; Thevelein and de Winde, 1999). Besides glucose and CO<sub>2</sub>, the upstream environmental signals that feed into PKA are unclear (Klengel et al., 2005; Zaman et al., 2008). In *C. albicans*, the function of the Ras/MAPK/PKA pathway is critical for pathogenesis (Hogan and Sundstrom, 2009). For example, the Ras/MAPK/PKA pathways are

required for several morphogenetic processes, including the yeast-hyphal transition and the white-opaque switching, and for virulence in murine models of infection (Leberer et al., 2001; Bahn et al., 2007; Huang et al., 2010). However, despite the efforts to dissect the Ras pathway in *S. cerevisiae*, it is still not fully understood how Ras receives signals from upstream effectors, what types of signals feed into Ras, and what other roles Ras plays in the cell besides of the activation of the MAPK and PKA pathways (Zaman et al., 2008).

### *The TOR pathway*

A second major signal transduction pathway in eukaryotes is the TOR pathway. TOR is a kinase that functions as a member of a large multiprotein complex (Loewith et al., 2002). The most direct upstream activator of TOR is Rhb1 (or RHEB, in mammals), whose function is antagonized by Tsc1 and Tsc2 (Figure 1.3). TOR phosphorylates several downstream effectors, although the only ones that have been clearly shown to be substrates of TOR are Tap42 and the kinase Sch9 (Urban et al., 2007; Duvel et al., 2003). In *S. cerevisiae*, Tap42 binds the type 2A phosphatases Pph21/22/3 and the type 2A like phosphatase Sit4 and has a dual function on the activation of these phosphatases (Duvel and Broach, 2004; Wang et al., 2003). While phosphorylated, Tap42 is bound to the phosphatases and keeps them inactive within the TOR multiprotein complex. Upon TOR inactivation, the Tap42-phosphatase complex is released, and the phosphatases exert their TOR dependent function until they dissociate from Tap42 (Yan et al., 2006; Di Como and Jiang, 2006). Studies in flies and mammals have uncovered many more upstream members and downstream effectors of the TOR pathway, as well as several feedback regulatory loops in which TOR participates (Wullschleger et al., 2006). However, the dissection of the TOR pathway in *S. cerevisiae* has been slower, perhaps complicated by the fact that *S. cerevisiae* has two TOR kinases, Tor1 and Tor2, which are found in two different (although

sometimes interchangeable complexes) (Loewith et al., 2002), while mammals and *C. albicans* have only one TOR kinase (Figure 1.3; Helliwell et al., 1994).

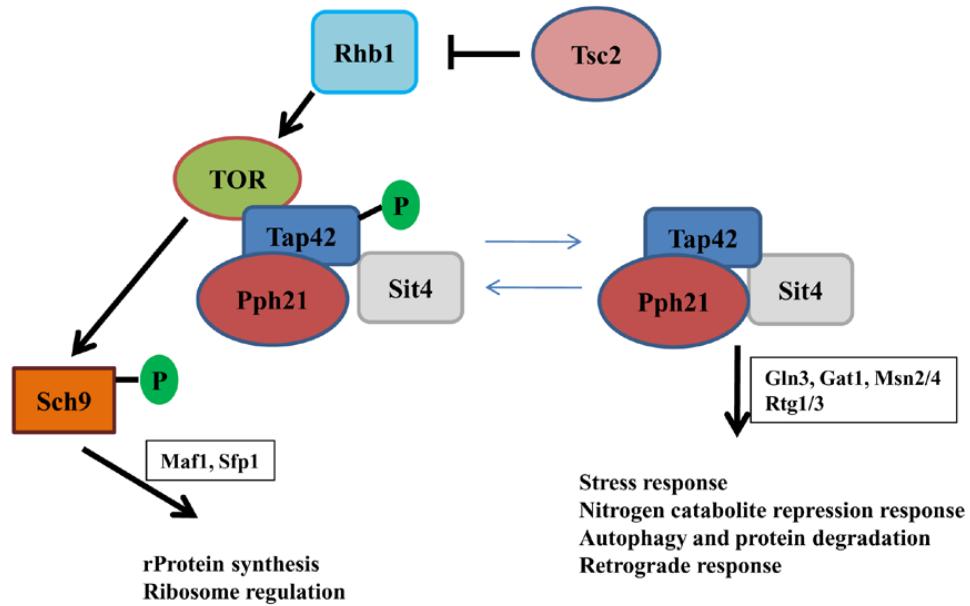


**Figure 1.3:** TOR signal transduction pathway (as it may be in *C. albicans*). P: indicates phosphorylation. In boxes: TOR regulated transcription factors.

Besides the number of TOR kinases, there are other differences between *S. cerevisiae* and *C. albicans* TOR pathways. *S. cerevisiae* has a gene encoding Rhb1, but its role in the TOR pathway is unclear (Urano et al., 2000). Further, *S. cerevisiae* does not encode homologs of *TSC1/2*. On the contrary, *C. albicans* has both Rhb1 and Tsc2, and an *rhb1Δ/Δ* mutant is more sensitive to rapamycin, indicating that at least Rhb1 is likely functioning in the TOR pathway in *C. albicans* (Tsao et al., 2009). Finally, *C. albicans* only appears to have Pph21 and Sit4. Notably, the structure of the TOR pathway in *C. albicans* appears more similar to the mammalian mTOR pathway than to the structure of the TOR pathway in *S. cerevisiae*.

The TOR pathway shares functional similarities with the PKA pathway. TOR activation leads to enhanced protein synthesis, ribosome synthesis, and protein translation, while simultaneously repressing processes required to survive stress and starvation, like the STRE response, the retrograde response, the nitrogen catabolite repression response, and autophagy

(Rohde and Cardenas, 2004; Schmelzle and Hall, 2000). TOR also regulates actin filaments and cytoskeleton dynamics (Loewith et al., 2002). It is unclear what signals activate/inactivate the TOR pathway, although TOR has been shown to respond to environmental nitrogen and carbon sources (Di Como and Arndt, 1996; Jacinto, 2008). The TOR pathway in *C. albicans* is required for several morphogenetic processes, including the yeast-hyphal transition and chlamyospore formation (Cutler et al., 2001, Bastidas et al., 2009; Lee et al., 2004; Nobile et al., 2003; Zacchi et al., 2010a). Given the myriad of processes that the TOR pathway is involved in, TOR is likely to be required for the expression of other virulence traits in *C. albicans* as well. In fact, I show here that both the Ras and TOR pathways are also regulators of CMPS in *C. albicans* (Chapters 4,5).

The Ras and TOR pathways are critical signal transduction pathways that regulate cellular growth in response to environmental nutrients. These pathways share the control of several downstream effectors. The intimate connection between the Ras and TOR pathways is clear in mammalian cells, where Ras is an upstream activator of TOR. However, in *S. cerevisiae* the level of crosstalk between Ras and TOR and the interdependence of the pathways is still controversial. Besides their role in nutrient sensing, these pathways are required for proper control of morphogenetic processes, they are involved in aging, DNA damage responses, and in mammals they are also directly involved in cancer development. Therefore, it is important to understand the function of the Ras and TOR pathways and the consequences of their de-regulation in cellular growth and survival.

### **Using Mds3 as a tool to understand CMPS in *C. albicans***

The fungal pathogen *C. albicans*, an asexual diploid yeast, is able to obtain phenotypic variation by the colony morphology phenotypic switching (CMPS) (see above for more information on this). CMPS occurs *in vivo* and is associated with alterations in the expression of virulence factors, which strongly suggest an important role for CMPS during *C. albicans*

infection. Despite the role of CMPS in pathogenesis in *C. albicans*, very little is known about the mechanisms that regulate CMPS in this fungus. In our laboratory, we serendipitously found that the protein Mds3 is a negative regulator of CMPS in *C. albicans*. After prolonged incubation of *mds3Δ/Δ* colonies in rich medium we observed the formation of extensions and blebs on the colony surface, which we call papilli (Figure 4.1A). Cells isolated from these *mds3Δ/Δ* papilli gave rise to colonies with altered, heritable, and low frequency reversible colony morphologies, all characteristics that perfectly match the definition of CMPS (Figure 4.1B; Soll, 1992). Thus, the *mds3Δ/Δ* papilli contain morphologically switched cells, and Mds3 acts as a negative regulator of CMPS. We had discovered a new genetic tool to gain insights on CMPS mechanisms and regulation: *MDS3*.

The mechanism(s) through which Mds3 and the second known CMPS regulator Ssn6 effect CMPS in *C. albicans* likely differ. The *ssn6Δ/Δ* mutant is highly unstable and gives rise to switched colonies rapidly, whereas in the *mds3Δ/Δ* mutant the initial switch likely occurs when cells have entered stationary phase. Further, the switch in the *ssn6Δ/Δ* mutant involves the whole colony indicating that the switch occurred in the colony-founder cell. On the contrary, the *mds3Δ/Δ* mutant requires the intermediate step of papilli formation to give rise to morphologically switched colonies, indicating that the switch occurred within the colony during the prolonged incubation (Chapter 4; Garcia-Sanchez et al., 2005). It is to note that once the *mds3Δ/Δ* mutant has switched, it continues to produce colonies with variant morphologies at a frequency of  $10^{-2}$ , without the need of an intermediary papilli (our unpublished results). Thus, Ssn6 and Mds3 represent two distinct tools to study CMPS, although it is also possible that Ssn6 functions downstream of Mds3.

Little was known about Mds3 when I began this work. *MDS3* encodes a 1383 amino acid protein with putative N-terminal Kelch-domains (Chapter 2, Davis et al., 2002). Mds3 was initially shown to be a negative regulator of meiosis and sporulation in *S. cerevisiae* and was

proposed to function upstream or in parallel to the Ras/PKA pathway (Benni and Neigeborn, 1997; McDonalds et al., 2009). In *C. albicans*, *MDS3* was found to be required for growth and morphogenesis at alkaline pH, growth on LiCl, and biofilm and chlamyospore formation (Davis et al., 2002; Nobile et al., 2005; Richards et al., 2005). Despite the role of Mds3 in important morphogenetic and developmental processes in *S. cerevisiae* and *C. albicans*, the biological function of Mds3 was unknown.

In this dissertation I aimed to study the mechanisms of CMPS in *C. albicans* using the mutant in *MDS3* as our genetic tool. My goal was to understand the biological role of Mds3 in *C. albicans* cells and the role of Mds3 in the generation of phenotypic diversity in this human pathogen. I found that Mds3 appears to be a Kelch/BTB protein localized in cytoplasmic spots that functions as a regulator of both the TOR and the Ras pathways in *C. albicans* (Chapter 2, 3 and 5). Consequently, I found that both the TOR and Ras pathways are involved in the regulation of CMPS, and I identified additional negative regulators of CMPS, including Ras1 and the TOR effector Sch9 (Chapter 5). Through the characterization of the phenotypic variants from the *mds3Δ/Δ* mutant, I conclude that there is likely more than one mechanism associated with the phenotypic switch, including genomic instability and DNA repair defects (Chapters 4, 5). I also found environmental conditions that effect CMPS in *C. albicans*, such as glucose starvation, amino acids, and environmental pH, all conditions that are known to directly influence the function of the TOR, Ras/PKA and Sch9 pathways (Chapter 4, 5). Taken together, I have elaborated a model of CMPS in *C. albicans* that shares many similarities with the model of stress-induced mutagenesis in bacteria. I propose that CMPS in *C. albicans* is a regulated process, triggered during stationary phase, in which defects in the signaling through the TOR and Ras pathways lead to the stepwise accumulation of genetic and epigenetic alterations that eventually cause the phenotypic switch.

## **CHAPTER 2**

### **BIOINFORMATIC AND MUTATIONAL ANALYSIS OF *MDS3***

## SUMMARY

In order to get insights into the function of Mds3, I performed bioinformatic, mutational, and localization studies of Mds3. The bioinformatic analysis of the open reading frame (ORF) of *MDS3* suggested that Mds3 contains six N-terminal Kelch domains, followed by a serine rich bridge, and a C-terminal region with low homology to a BTB/POZ domain that is highly conserved among Mds3's orthologs in *Candida* and *Saccharomyces cerevisiae*. Several disordered regions are distributed throughout the ORF of Mds3, suggesting that Mds3 is a modular Kelch/BTB protein. The functional relevance of the Kelch and BTB domains were determined by point and insertional mutagenesis in the domains. A Tn7 insertional mutagenesis of Mds3's ORF was performed in order to find a region that would tolerate the insertion of an epitope tag. Twenty-one *MDS3-Tn7* alleles were generated that did not cause a truncated protein, but only one out of 13 alleles analyzed allowed the insertion of a V5-HIS6 tag without affecting Mds3 function. Mds3-V5 localized in cytoplasmic spots. Thus, based on the studies performed Mds3 appears to be a cytoplasmic modular Kelch/BTB protein. It would be interesting to further dissect the localization, molecular interactions, and posttranslational modifications of Mds3. To this end, many tools have been generated and several of them are described in this chapter.

## INTRODUCTION

Mds3 is associated with several morphogenetic and growth-related processes in fungi. In *S. cerevisiae*, Mds3 (hereafter referred to as ScMds3) and its paralog Pmd1 function as negative regulators of meiosis (Benni and Neigeborn, 1997; McDonald et al., 2009). In *C. albicans*, Mds3 is required for chlamydospore formation, for filamentation, and for biofilm formation (Davis et al., 2002; Nobile et al., 2003; Richard et al., 2005), and it is also a negative regulator of colony morphology phenotypic switching in *C. albicans* (Chapter 4). Mds3 is required for growth and filamentation at alkaline pH and for growth in the presence of LiCl (Davis et al., 2002). Mutants in *MDS3* also show a slight growth defect in YPD. Thus, Mds3 is involved in diverse morphogenetic processes in fungi, including some that are critical for *C. albicans* virulence, and for proper pH responses.

Mds3 is a fungal specific protein, with putative uncharacterized orthologs in diverse fungal genera, including *Debaryomyces*, *Ashbya*, and *Schizosaccharomyces*. In *S. pombe* the ortholog of *MDS3* is *RAL2*, a gene encoding a 611 amino acids protein involved in mating and proposed to function as a Ras1 guanyl-exchange factor (Fukui et al., 1989). However, the homology between Mds3 and Ral2 is limited to the Kelch domains (e-value:  $9e^{-08}$  from BLASTp sequence alignment). ScMds3 has also been associated with the Ras pathway in *S. cerevisiae*, although it remains unclear whether ScMds3 is a member of the Ras pathway or if it functions in parallel (Benni and Neigeborn, 1997; McDonald et al., 2009). Thus, Mds3 is conserved in fungi and might be a member of a signal transduction pathway.

To begin to gain insights into Mds3 function, I performed a bioinformatic analysis of *MDS3*'s open reading frame (ORF) in order to identify potential functional domains. Furthermore, I performed mutational analysis of *MDS3* in order to corroborate the biological relevance of the bioinformatic predictions and to identify a benign location within *MDS3* that would tolerate an epitope tag. Finally, I epitope tagged Mds3 and used it for indirect

immunofluorescence localization experiments. Our results suggest that Mds3 functions as a cytoplasmic scaffold protein.

## MATERIALS AND METHODS

### Bioinformatic analysis

The amino acid sequence alignments were performed using BLASTp available at NCBI <http://blast.ncbi.nlm.nih.gov/Blast.cgi> and Clustal 2.0.12 Multiple Sequence alignment <http://www.ebi.ac.uk/Tools/clustalw2/index.html>. Programs available on-line through the ExPASy server from the Swiss Institute of Bioinformatics <http://www.expasy.ch/tools/> were used to analyze Mds3, ScMds3, and Pmd1 ORFs from *C. albicans* and *S. cerevisiae*, including MyHits [http://myhits.isb-sib.ch/cgi-bin/motif\\_scan](http://myhits.isb-sib.ch/cgi-bin/motif_scan), PreDisorder (<http://casp.rnet.missouri.edu/predisorder.html>), Signal IP 3.0 <http://www.cbs.dtu.dk/services/SignalP/>, COILS [http://www.ch.embnet.org/software/COILS\\_form.html](http://www.ch.embnet.org/software/COILS_form.html), ePESTfind <http://emboss.bioinformatics.nl/cgi-bin/emboss/epestfind>, MITOPROT <http://ihg2.helmholtz-muenchen.de/ihg/mitoprot.html>, and PTS1 <http://mendel.imp.ac.at/mendeljsp/sat/pts1/PTS1predictor.jsp>. Further, ProtComp (<http://linux1.softberry.com/berry.phtml?topic=protcompan&group=programs&subgroup=proloc>) and WoLFPSORT (<http://wolfsort.org/>) were used to predict protein localization.

The N-terminal region of Mds3 was modeled by Andy Kruse and Douglas Ohlendorf (Department of Biochemistry, University of Minnesota) as follows. To model Mds3, predictions of disorder, secondary structure, and folding were determined using the Phyre server (<http://www.sbg.bio.ic.ac.uk/~phyre/>). The structural models were prepared with Modeller (<http://www.salilab.org/modeller/>), using a structure-guided sequence alignment, followed by manual adjustments based on the Kelch repeat motifs that could be readily identified. The final structure was generated using the best scoring model available. Due to the lack of closely homologous structures, the disordered regions and the loops inter Kelch motifs were not possible to model. The 3-D images presented here were made with PyMol (<http://pymol.org/rel/099/>).

### ***C. albicans* strains and plasmid construction**

All *C. albicans* strains used in this study are listed in Table 2.1. All strains were constructed by chemical transformation (Wilson et al., 1999) with PmeI or NheI linearized vectors. Integration of *MDS3* containing vectors was verified by genomic DNA PCR using primers MDS3 Seq 2 and MDS3 NruI Seq 3' (Table 2.3).

The *MDS3::V5* tagged vectors pLZ38, pLZ39, and pLZ86 were constructed as follows. To construct plasmid pLZ38 and pLZ39, the *V5-HIS6* tag was PCR amplified from plasmid pTRACER-EF (Invitrogen) using primers Mds3 HpaI V5His6 5' and Mds3 HpaI V5His6 3' or Mds3 BstBI V5His6 5' and Mds3 BstBI V5His6 3' (Table 2.3) and *in vivo* recombined into HpaI or BstBI digested plasmid pDDB353 (Zacchi et al., 2010, see Chapter 3), respectively, using *S. cerevisiae* L40 strain. HpaI and BstBI are unique restriction sites in *MDS3* ORF located at nucleotide position 4131 and 3129 from the START codon (Figure 2.2A). To construct plasmid pLZ86, the *V5-HIS6* tag was PCR amplified from pTRACER-EF (Invitrogen) using primers 56-V5 5' and 56-V5 3' (Table 2.3) and *in vivo* recombined into PmeI digested pDDB500 (Zacchi et al., 2010, see Chapter 3) to give pLZ86 (the V5 tag was placed at position 1056 because insertion at 1051 disrupted *MDS3* function (data not shown)). pLZ86 rescued an *mds3Δ/Δ* mutant, indicating that Mds3 tolerated the addition of the 23 amino acids of the V5-His6 tag at amino acid position 1056; pLZ38 and pLZ39 only partially rescued an *mds3Δ/Δ* mutant. pLZ86 was linearized with NheI for integration into DAY938 to generate strain LUZ379. pLZ38 and pLZ39 were linearized with PmeI for integration in to DAY956 to generate strains LUZ14 and LUZ20.

The strain containing an *MDS3::HA* C-terminal tagged allele (LUZ23) was constructed by transforming strain DAY415 with a 3xHA::ADH1term::URA3 cassette PCR amplified from plasmid pDDB367 (pGM1874, Gerami-Nejad et al., 2009) using primers MDS3 HA C-ter 5' and MDS3 URA3 c-ter 3' (Table 2.3).

The *MDS3* vectors pLZ78-83 were constructed as follows. Plasmid pDDB353 was used as template to PCR amplify (Pfu Turbo DNA polymerase, Stratagene) two overlapping segments that spanned the N-terminal region of *MDS3* using primers MDS3 Seq 1 combined with any of the second-Kelch-repeat mutational 3' primers, and MDS3 NruI Seq 3' combined with the corresponding second-Kelch-repeat mutational 5' primer (Tables 2.3). Both PCR products were transformed with AflIII-digested pDDB353 or pLZ38 into *trp-* *S. cerevisiae* strain L40 to produce pLZ78-83 through *in vivo* recombination (Table 2.2). The mutated *MDS3* ORF of each plasmid was verified by sequencing. Plasmids were linearized with PmeI for transformation into DAY938, to generate strains LUZ397, LUZ399, LUZ400, and LUZ402, and into DAY956 to generate LUZ316.

The mutations in pLZ78-82 were subcloned into pLZ86 by ligating the ~3.8kb XhoI/NruI gel purified band from pLZ78-82 to the ~9.8kb XhoI/NruI gel purified fragment from pLZ86 to give pLZ122-125 (Table 2.2). Plasmids were verified by sequencing, and the presence of the V5 tag was verified by MluI digestion. pLZ122-125 were linearized with NheI for integration into DAY938, to generate strains LUZ461, 462, 464, and 466.

Vector construction and random Tn7 mutagenesis protocols have been described (Zacchi et al., 2010; see Methods Chapter 3). After Tn7 excision, religated *Mds3* alleles were subcloned into pDDB409 as previously described, to construct pLZ87-101 and pLZ107-111 (Table 2.2 and 2.5). pLZ118-120 containing clones 35.1, 104.1, and 108.1 were also prepared, although they were not phenotypically assessed. Plasmids were linearized with NheI for transformation into DAY938 to generate strains LUZ426-458. Independently transformed mutants with pLZ93, pLZ100, and pLZ101 gave conflicting results upon re-testing, and therefore have been excluded from the analysis.

### **Media and growth conditions**

*C. albicans* was routinely grown at 30°C in YPD (2% Bacto-peptone, 2% dextrose, 1% yeast extract). For selection of His<sup>+</sup> or Trp<sup>+</sup> transformants, synthetic medium without histidine or tryptophan was used (0.17% yeast nitrogen base without ammonium sulfate (Q-BioGene), 0.5% ammonium sulfate, 2% dextrose, and supplemented with a dropout mix containing amino and nucleic acids except those necessary for the selection (Adams et al., 1997)). Media were buffered at the indicated pH using 150mM HEPES. Filamentation assays were performed in M199 medium (Gibco BRL) buffered at pH 8 and incubated at 37°C. For solid media filamentation assays, strains were pre-grown in liquid YPD at 30°C, 3ul were spotted onto M199 pH 8 medium, and incubated at 37°C for 5 days. For liquid assays of filamentation, strains were pre-grown in liquid YPD at 30°C and diluted 1:100 in M199 pH 8. Samples were incubated for 2 hrs. To determine the % of hyphae producing cells samples were quantified under the microscope. The values reported are representative of two independent experiments, in which every strain was tested at least in duplicate. For growth assays in YPD, YPD + 150mM LiCl, and YPD pH 9, strains were pre-grown in liquid YPD at 30°C, streaked onto the media or serially 5-fold diluted and plated, and incubated at 30°C for 2 days. All media were supplemented with 80 µg/ml uridine. For solid media, 2% Bacto-agar was added.

### **Protein extraction and Western Blot analysis**

Overnight cultures of *C. albicans* were diluted 40-fold into YPD medium and grown for 4 hours at 30°C. Cells were pelleted and resuspended in ice-cold RIPA buffer (50mM Tris pH 8, 150mM NaCl, 1% NP-40, 3mM EDTA, 0.5% deoxycholate, 0.1% SDS) containing 1µg/ml leupeptin, 2µg/ml aprotinin, 1µg/ml pepstatin, 0.1mM phenylmethylsulfonyl fluoride, and 10 mM dithiothreitol and lysed by vortexing with acid-washed glass beads 4X 2 min at 4 °C, with 2 min resting in ice in between. Cell lysates were pelleted and supernatants stored at -80°C. For Western

blot assays 50  $\mu$ L of total protein was resuspended in 2X SDS gel-loading buffer (100mM Tris-Cl, pH 6.8; 200mM dithiothreitol; 4% SDS; 0.1% bromophenol blue; 20% glycerol), boiled at 95-100°C for 5 minutes and run in 6% SDS-PAGE gel. Proteins were transferred to nitrocellulose and blocked in 5 % nonfat milk in TBS-T (50mM Tris, pH 7.6, 150mM NaCl, 0.1% Tween 20). Blots were incubated with 1:5000  $\alpha$ V5 (Invitrogen) or 1:1000  $\alpha$ HA (F-7 probe, Santa Cruz) in 5% non-fat milk TBS-T, washed in TBS-T, and incubated with 1:10,000  $\alpha$ mouseIgG-horseradish peroxidase antibody (GE Healthcare) in 5% nonfat milk in TBS-T. Blots were washed in TBS-T, incubated with ECL reagent (GE Healthcare), and exposed to film.

### **Immunofluorescence**

YPD overnight cultures were diluted 1:200 in 12.5 ml M199 pH 8 and incubated at 30°C for 4 hours in agitation. Cells were fixed 1 hr at room temperature (~23°C) in gentle agitation (80 rpm) with 3.7% formaldehyde, washed with 2 ml Solution B (100mM pH 7.5 phosphate buffer, 1.2M sorbitol) (Pringles et al., 1989), resuspended in 1ml Solution B containing 0.5mg/ml Yeast Lytic Enzyme (MPBio) and 2  $\mu$ l  $\beta$ -mercaptoethanol, and spheroplasted at 37°C for no longer than 30 min. Cells were washed twice by pelleting 5 min at 0.5 rcf and resuspending in 1ml Solution B. Cells were resuspended in 1ml Solution B and spotted on polylysine coated microscope slides. Samples were blocked with 5% bovine serum albumin (BSA) in TBS for 10 min, incubated 1 hr with 1:50  $\alpha$ V5 antibody (Invitrogen), washed 10X with TBS-T, incubated 1 hr with 1:500  $\alpha$ mouseIgG-AlexaFluor555 SFX (Invitrogen), washed 10X with TBS-T, and coated with Gel Mount Aqueous Mounting media (Sigma) containing 1:1000 DAPI. Images were captured using a Zeiss Axio camera, Axiovision 4.6.3 software (Zeiss), and a Zeiss AxioImager fluorescence microscope. All images were processed with Adobe Photoshop 7.0 software. All the antibody procedures were done at room temperature in a humid chamber and in the dark once the fluorescent antibody was applied.

## RESULTS

### Bioinformatic analysis

To begin to elucidate Mds3 function, I performed several bioinformatic analyses on the ORF of *MDS3* and its orthologs in *S. cerevisiae* *ScMDS3* and *PMD1*, including domain searches, prediction of disorder, coils, and PEST domains. The amino acid sequence alignment of Mds3 with ScMds3 and Pmd1 obtained through BLASTp at NCBI showed that these proteins share higher similarity within the first 600 N-terminal residues [27% and 32% identity, E values of  $1e^{-60}$  or  $3e^{-36}$ , respectively], and ~150 residues between amino acids 900 and 1,050 from Mds3 [37% and 35%, E values of  $4e^{-25}$  and  $2e^{-24}$ , respectively] (Figure 2.1). Domain searches using several databases only identified one putative Kelch domain in the N-terminal region of Mds3 between amino acids 112-166 ( $4.9e^{-06}$ ) (Figure 2.1, underlined) and a serine rich region between amino acids 630-885 ( $2.7e^{-09}$ ) (e values from MyHits) (Figure 2.2A). Similarly, ScMds3 is predicted to encode two Kelch motifs between amino acids 159-211 ( $3.2e^{-10}$ ) and 232-268 ( $1.1e^{-05}$ ), and a serine rich region between amino acids 660 and 851 ( $3.1e^{-05}$ ). Pmd1 is predicted to encode a Kelch domain between amino acids 131-183 ( $1.7e^{-08}$ ) and a serine rich region between amino acids 638 and 1009 ( $3.9e^{-08}$ ). Interestingly, the InterProScan program (version 7.1) predicted a BTB/POZ domain between amino acids 1014 and 1067 of ScMds3. Although this prediction is not extensive to Mds3 or Pmd1, the putative BTB/POZ domain in ScMds3 falls within the highly conserved internal region between the three proteins (Figure 2.2A). Thus, it appears that all three proteins share sequence similarity in two distinct regions in their ORFs: at the N-terminus, where they encode at least one Kelch domain, and closer to the C-terminus, where they possibly encode a BTB/POZ domain.

**Figure 2.1:** CLUSTAL 2.0.12 multiple sequence alignment of Mds3, ScMds3, and Pmd1. Only the alignment for the 600 N-terminal residues (A) and the residues between ~900-1050 (B) in Mds3 are shown. Underlined is the only Kelch repeat detected bioinformatically. Sc=*S. cerevisiae*, Ca=*C. albicans*.



Mds3, ScMds3, and Pmd1 contain several regions that were predicted to be highly disordered by the program PreDisorder (Deng et al., 2009). In the three proteins, the disordered regions fell between two ordered regions spanning the predicted Kelch domain region and the putative BTB/POZ domain, and included the serine-rich region and the C-terminal portion (Figure 2.2B and data not shown). In Mds3 the program predicted a third ordered region of ~ 50 amino acids that lies right before the serine-rich region, and a fourth ordered region of 136 amino acids between amino acids 1109 and 1245 that did not show any homology to any functional domain in database searches; and BLASTp searches only identified putative uncharacterized *MDS3* orthologs in other fungal species.

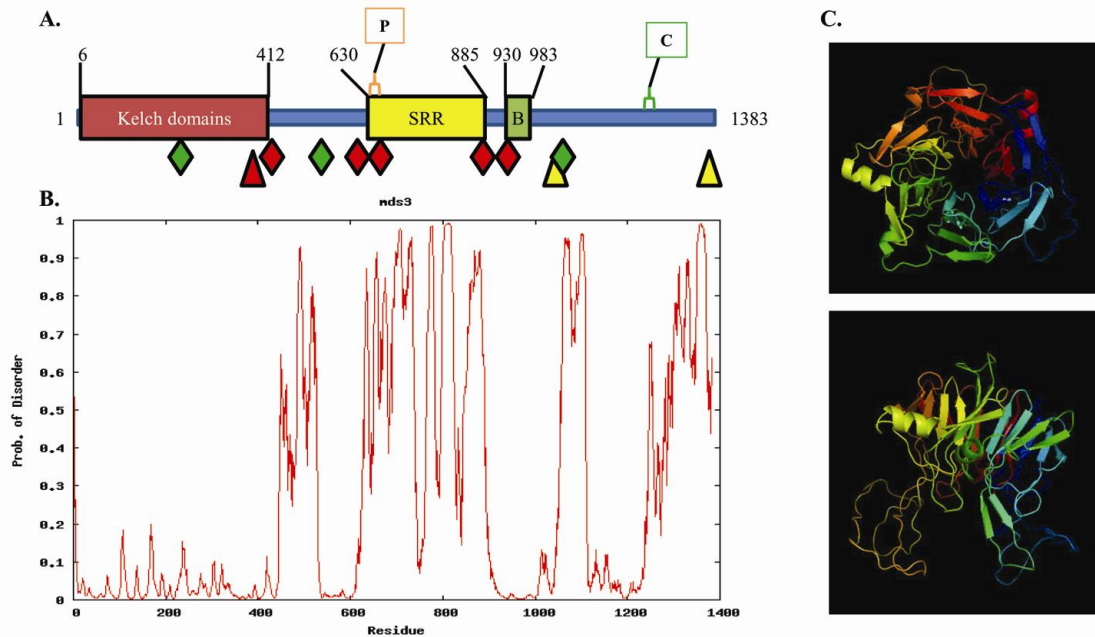


**Figure 2.2:** Bioinformatic and genetic analysis of Mds3. A) Representation of the putative functional domains in Mds3 identified bioinformatically, including sites of mutagenesis with Tn7 and epitope tags. SRR = serine rich region; B= BTB/POZ; P=PEST; C=coils. Triangle: V5 tags in unique restriction sites. Rhombus: 5 amino acid insertions obtained through Tn7 random mutagenesis. Red, yellow, and green colors indicate if the insertion is functional, partially functional, or non-functional, respectively. B) Prediction of ordered and disordered regions in Mds3. C) Hypothetical 3-D folding of the first 400 amino acids of Mds3 N-terminus into a six-bladed Kelch propeller.

I further characterized Mds3 and its orthologs using programs that predict signal peptides, coils, and PEST domains. While neither Mds3 nor Pmd1 were predicted to contain a signal peptide in their N-termini, Signal IP 3.0 predicted that ScMds3 contains a signal peptide (cut-off 0.48) at amino acid positions 1-11. The program COILS predicted that Mds3 contains coils between amino acids 1218 and 1237 (Figure 2.2A), while ScMds3 is predicted to have coils between amino acids 738-758, 1108-1125, 1267-1298, 1326-1351, and 1456-1476; and Pmd1 has a similar distribution as ScMds3. Other coils predictive programs produced similar results for Mds3 (data not shown). Finally, the program ePESTfind predicted that Mds3 contains a potential PEST domain between amino acids 631-644 (PEST Score: 12.76) (Figure 2.2A); while ScMds3 was predicted to have potential PEST domains between amino acids 654-678 (PEST Score: 18.91), 681-695 (PEST Score:20.61), 870-899 (PEST Score: 10.99), and 917-932 (PEST Score: 9.16); and Pmd1 was predicted to have PEST domains between amino acids 707-723 (PEST Score: 6.42), 1026-1046 (PEST Score: 5.82), 1323-1346 (PEST Score: 15.09), and 1353-1367 (PEST Score: 12.74). Thus, although there are differences between ScMds3, Pmd1, and Mds3, the programs identified three common features among these proteins: that they contain highly disordered regions in their ORFs that are similarly aligned, PEST domains, and a C-terminal region with coils.

From the combination of all the bioinformatic data, the following picture of Mds3 emerges (Figure 2.2). Mds3 appears to have at least one Kelch domain in the N-terminus, followed by a serine-rich region that contains a putative PEST domain, a ~150 amino acid segment highly conserved between *C. albicans* and *S. cerevisiae* with low homology to BTB/POZ domains, and a third ordered region close to the C-terminus, of unknown function, which ends in putative coil structural motifs. Furthermore, Mds3 contains highly disordered regions that span the serine rich and C-terminal regions.

## Uncovering more Kelch domains

Kelch domains are 44-56 amino acids long, and consist of a four-stranded antiparallel  $\beta$ -sheet. Only 8 (generally) conserved residues are required to form a Kelch domain: 4 hydrophobic residues followed by 2 glycines constitute the second strand of the  $\beta$ -sheet, and are separated from 2 aromatic residues which are located each in the third and fourth strand of the  $\beta$ -sheet (usually W and Y). Kelch domains fold into a tertiary structure called the  $\beta$ -propeller, in which each Kelch domain constitutes a blade of the propeller (Adams et al., 2000). The sequence conservation between Kelch repeats is low, and the sequences that separate each strand and each  $\beta$ -sheet (loops) are variable in length. For these reasons, motif databases are often unable to identify the Kelch repeats. Manual alignment is sometimes required to uncover Kelch domains, as was the case of the Kelch proteins Gpb1/Krh2 and Gpb2/Krh1 (Harashima et al., 2002; Peeters et al., 2006). Because the Kelch  $\beta$ -propeller requires a minimum of four Kelch domains in order to fold properly but only one was found bioinformatically in Mds3, I manually searched for more Kelch domains in Mds3 and was able to model the N-terminus of Mds3 into a Kelch  $\beta$ -propeller, in collaboration with Douglas Ohlendorf and Andy Kruse (Department of Biochemistry, University of Minnesota). Using as a template other Kelch containing proteins, the N-terminus of Mds3 was modeled into a six-bladed Kelch propeller (Figure 2.2C). The first 4 Kelch domains were largely contiguous, except that the first strand of the first Kelch domain was at the C-terminus of the protein (a common arrangement in other Kelch proteins (Prag and Adams, 2003)). However, the fifth and sixth Kelch domains appeared to be separated from the other Kelch domains by a longer stretch of amino acids. Loops of diverse lengths protruded from Mds3's Kelch propeller, which could serve as platforms for protein-protein interactions. Therefore, even though domain prediction algorithms only recognized one Kelch repeat, Mds3 N-terminal region appears to fold into a 6-bladed Kelch propeller.

To further assess the functional relevance of the Kelch domains in the N-terminus of Mds3, I generated point mutations in the only Kelch domain detected bioinformatically (Figure 2.1, underlined) and tested the alleles for *mds3Δ/Δ* complementation in YPD, LiCl, pH 9, and M199 pH 8. Following a previously published Kelch mutational strategy (Gomez et al., 2000), I constructed *MDS3* alleles containing single or double amino acid substitutions in the second strand of the second Kelch repeat. I made conserved (L→I) and non-conserved substitutions (Y, I, G→A) (Figure 3.2 and Table 2.2), and tested the ability of the alleles to rescue an *mds3Δ/Δ* mutant. I also generated a Y→F mutation, which is moderately conservative change considering that F and Y are structurally similar and that F is more hydrophobic than Y (high hydrophobicity being the “conserved” characteristic of the amino acids in this location). As expected, strains carrying plasmids with conserved mutations (L→I and Y→F) behaved like the wild-type and *mds3Δ/Δ* + *MDS3* strains for growth in YPD, YPD + LiCl, YPD pH 9, and filamentation in solid and liquid M199 pH 8 (Figure 2.3B and 2.3C and Table 2.4). Strains carrying plasmids with non conserved mutations (Y, I, G→A) behaved like the *mds3Δ/Δ* strain for growth in YPD, YPD + LiCl, YPD pH 9 and filamentation in solid and liquid M199 pH 8 (Figures 2.3B and 2.3C and Table 2.4). There was no observable difference between the two alleles that rescued the *mds3Δ/Δ* mutation and between the two alleles that did not rescue the *mds3Δ/Δ* mutation. Thus, these results indicate that the integrity of the predicted second Kelch domain is critical for Mds3 function. It is important to note that the non-conserved mutations might affect folding/stability of Mds3. However, Western blot analysis of an *mds3Δ/Δ* + *MDS3*<sup>G129A L131S</sup>::V5 strain (LUZ83) showed Mds3-V5 expression at the expected size and no indication of degradation (data not shown). Overall, these results support the model that Mds3 contains a six bladed Kelch propeller in its N-terminus.

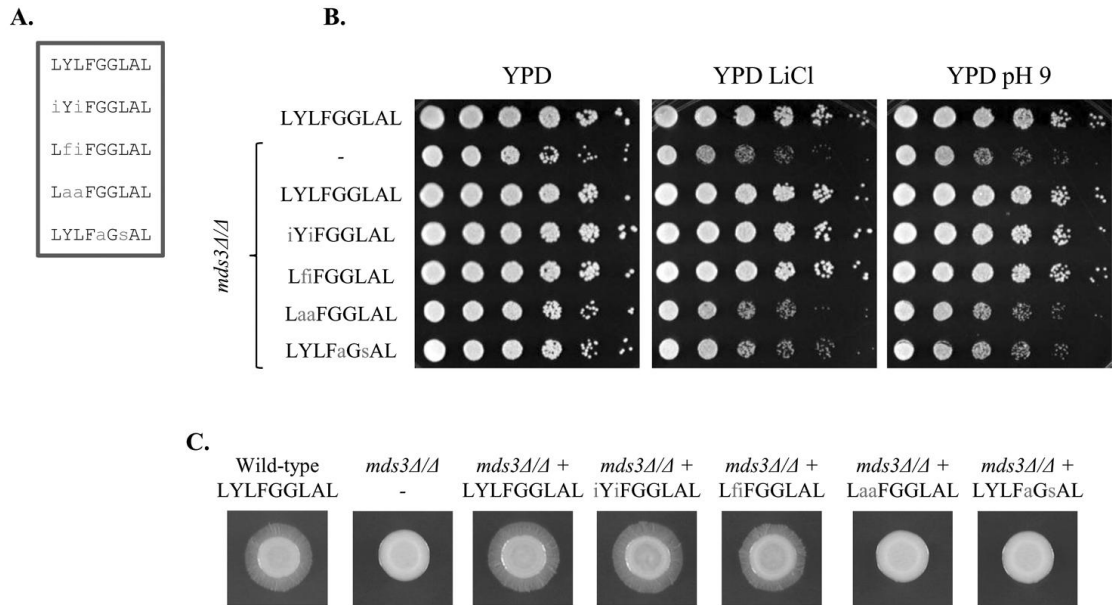


**Figure 2.3:** Functional characterization of the only bioinformatically identified Kelch repeat in Mds3 by site-directed mutagenesis. A) Description of the alleles constructed in the second blade of the second Kelch Repeat. Mutated amino acids are shown in red lowercase. B, C) Growth in YPD, YPD+150mM LiCl, and YPD pH 9, and filamentation in solid M199 pH 8 of the wild-type strain (DAY185), *mds3Δ/Δ* (DAY1118), and *mds3Δ/Δ* strains carrying wild-type (DAY1119) or mutated versions of *MDS3*: *MDS3*<sup>Y126A L127A</sup> (LUZ397), *MDS3*<sup>G129AL131S</sup> (LUZ399), *MDS3*<sup>Y126F L127I</sup> (LUZ400), and *MDS3*<sup>Y125I L127I</sup> (LUZ402).

### Random Tn7 mutagenesis: looking for a benign spot in *MDS3* ORF

Since there are no commercially available antibodies against Mds3, it was necessary to tag Mds3 with an epitope or with GFP in order to detect it. I first tried to tag Mds3 at unique internal restriction sites or at the C- or N-termini of the protein. Internal V5-His6 tagging of the Mds3 ORF at unique restriction sites (HpaI, BstBI, and NruI) (Figure 2.2A, red/yellow triangles) yielded Mds3-V5 versions that were partially or non-functional (Figure 2.4). The HpaI and BstBI-V5-His6 tagged alleles were partially functional (Figure 2.4A and 2.4B). This result was unexpected, since both restriction sites are predicted to lie within disordered regions which are generally more permissive to mutations (HpaI is ~ at amino acid 1377, and BstBI is ~ at amino acid 1043). The NruI-V5-His6 tag was located ~ at amino acid 382, within the predicted Kelch

domains, and was non-functional (Figure 2.4A and 2.4B). Further, addition of GFP to the N-terminus or C-terminus of Mds3, or addition of a 3xHA tag at the C-terminus of Mds3 also yielded non-functional proteins (Figure 2.4 and data not shown). Since both the N- and C-terminal portions of Mds3 were predicted to fold into Kelch repeats (see above) it was not surprising that Mds3 did not tolerate insertions at any of these terminal regions. It became clear that finding a benign site in Mds3 that tolerated the epitope tag would require a more extensive functional analysis of Mds3's ORF.

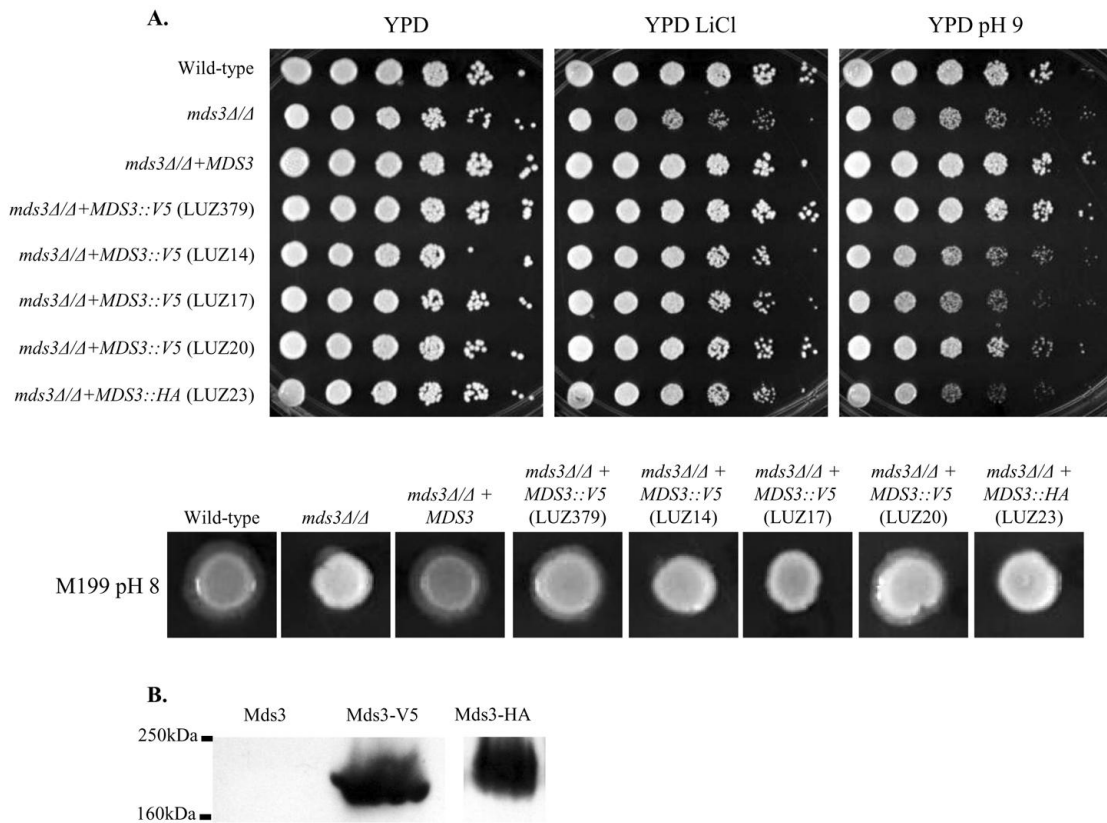


**Figure 2.4:** Functional characterization of the tagged Mds3 alleles. A) Growth in YPD, YPD+150mM LiCl, and YPD pH 9, and filamentation in solid M199 pH 8 of the wild-type strain (DAY185), *mds3Δ/Δ* (DAY1118), *mds3Δ/Δ+MDS3* (DAY1119) and the following tagged alleles: *MDS3::V5* [V5 at amino acid position 1056] (LUZ379), *MDS3::V5* [V5 at unique HpaI site] (LUZ14), *MDS3::V5* [V5 at unique NruI site] (LUZ17), *MDS3::V5* [V5 at unique BstBI site] (LUZ20), and *MDS3::HA* [HA at C-terminus] (LUZ23). C) Western blot of tagged Mds3 alleles. Overnights of *MDS3::V5* (LUZ379) and *MDS3::HA* (LUZ23) were diluted 1:40 in YPD, and incubated for 4 hrs at 30°C before protein extraction.

In order to find regions within Mds3 that tolerated small insertions without significantly affecting Mds3 function, we performed random mutagenesis of Mds3's ORF using the GPS-LS Linker Scanning System. In this system, a Tn7 transposon is randomly inserted within the ORF of Mds3, and after excision the transposon leaves a 5 amino acid (15 nt) mutagenic insertion. We generated 34 *MDS3* alleles with Tn7 insertions throughout the ORF (Table 2.5). Approximately one third of the insertions generated a stop codon (10/34 insertions) and 3/34 insertions had defective sequence runs making it impossible to determine precisely the location of the insertion or the mutation caused by the insertion. The remaining 21/34 insertions generated full length *MDS3* alleles with 15 nucleotides (or 5 amino acids) insertions that spanned the Mds3 ORF, although most of the alleles were concentrated around the serine-rich region, between amino acids 470 and 950 (Figure 2.2A and Table 2.5). 13/21 alleles were successfully subcloned into a shuttle vector for integration into the *HIS1* locus of *Candida*. Most of these alleles were tested for their ability to rescue the *mds3Δ/Δ* phenotypes for growth in YPD, YPD+LiCl, YPD pH 9, and for filamentation in solid and liquid M199 pH 8 (Figure 2.5 and Davis et al., 2002). Alleles 55.1, 67.1, 12.1, 33.1, 36.1, and 82.1 behaved like the *mds3Δ/Δ* mutant in all media tested, indicating that the 15 nt insertions disrupted Mds3 function (Figure 2.5). Most *MDS3-Tn7* alleles with a functional defect had insertions between amino acids 528 and 935, with the exception of allele *MDS3-12.1* whose insertion was at amino acid position 1361 (Figure 2.5, Table 2.5). The null phenotype of allele *MDS3-55.1*, which carries an insertion at the region of Mds3 predicted to be a BTB/POZ region, indicates that indeed this region is required for Mds3 function (Figures 2.2 and 2.5). On the other hand, alleles 4.2, 41.1, 56.1, and 20.1 behaved like the wild-type and *mds3Δ/Δ+MDS3* strains in all media, indicating that their 15 nt insertions were not affecting Mds3 function (Figure 2.5). These *MDS3-Tn7* alleles with a wild-type function had insertions either at the C-terminal region (amino acids position 1051, or 1378) or within or near the Kelch domains (amino acids position 226 and 526) (Figure 2.5 and Table 2.5). Therefore, the behavior

of the different alleles suggests that the middle region of Mds3 is less tolerant to insertions than the C-terminal region of Mds3, and that the region of the Kelch domains can tolerate small insertions (especially if they fall in the loops between the propeller blades). I noted that in all cases the alleles showed a homogeneous response in all media, i.e. they either showed a null phenotype or a wild-type phenotype in all conditions tested. It is also important to point out that the null phenotype of some of the Mds3-Tn7 alleles might be caused by misfolding or lower stability of the allele, and not because the insertions affect specific functional domains in Mds3. Overall, I found 4 *MDS3* alleles that tolerated 15 nt insertions (Table 2.5).

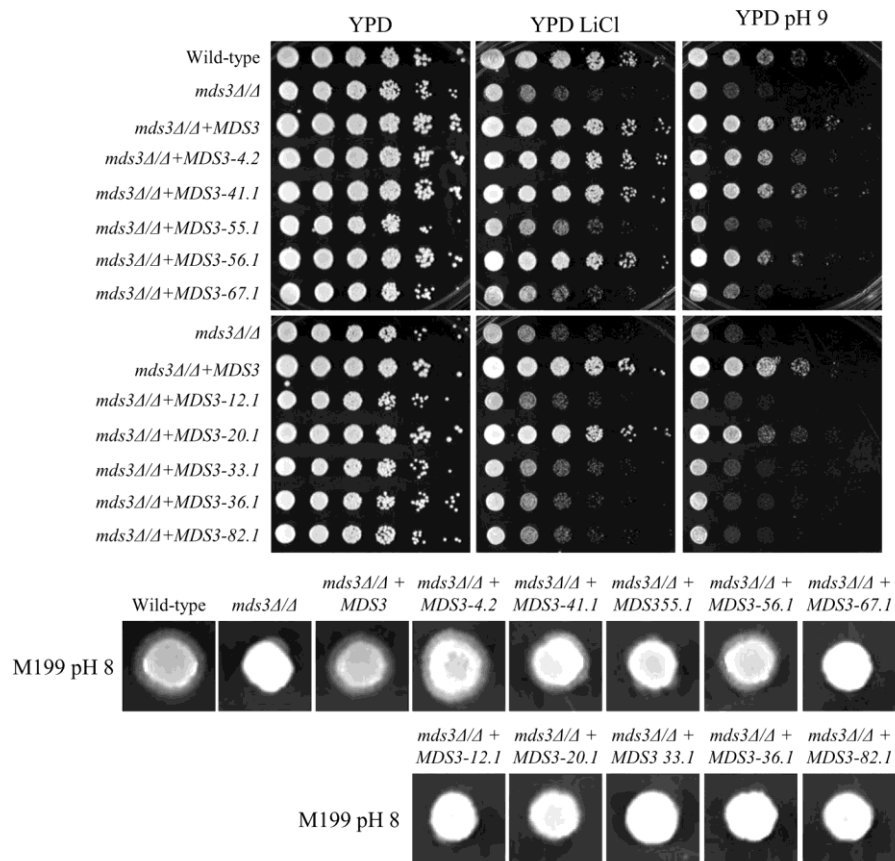


**Figure 2.5:** Functional characterization of the *MDS3*-Tn7 alleles. Growth in YPD, YPD+150mM LiCl, and YPD pH 9, and filamentation in solid M199 pH 8 of the wild-type strain (DAY185), *mds3Δ/Δ* (DAY1118), *mds3Δ/Δ*+MDS3 (DAY1119) and the following alleles: *MDS3*-4.2 (LUZ426), *MDS3*-41.1 (LUZ427), *MDS3*-55.1 (LUZ431), *MDS3*-56.1 (LUZ433), *MDS3*-67.1 (LUZ436), *MDS3*-12.1 (LUZ441), *MDS3*-20.1 (LUZ444), *MDS3*-33.1 (LUZ446), *MDS3*-36.1 (LUZ448), *MDS3*-82.1 (LUZ450).

### **Mds3 localization**

The subcellular localization of a protein is intimately connected with its function. Thus, finding where Mds3 localizes in *Candida* cells should aid in understanding Mds3 function. From bioinformatic analyses, neither ScMds3 nor Mds3 were predicted to be targeted to the peroxisome or the mitochondria (MITOPROT and PTS1), and Mds3 was predicted to be nuclear by ProtComp Version 6 and WoLFPSORT. However, large scale analysis of protein subcellular localization in yeast identified ScMds3 in the mitochondria (Sickmann et al., 2003, Reinders et al., 2006; Huh et al., 2003) and in the cytoplasm (Kumar et al.2002; Horton et al., 2007). Thus, to experimentally determine Mds3 localization in *C. albicans*, we constructed an epitope tagged version of Mds3 using the locations that tolerated small insertions discovered by the Tn7 mutagenesis strategy (see above), and performed indirect immunofluorescence studies.

Three *MDS3::V5::HIS6* alleles were generated that contained the V5 epitope tag at either one of the three sites that tolerated the 5 amino acids insertion: amino acids positions 226, 526 and 1051 (alleles 41.1, 4.2, and 56.1) [the fourth location: allele 20.1, was found after Mds3 had been successfully tagged and was therefore not used for tagging]. Replacing the 5 amino acids insertion with the 23 amino acids of the V5-His6 tag in the three sites generated non-functional alleles (data not shown). The lack of function of the tagged allele at position 226 can be explained by a disruption in the conformation of the Kelch domains in that area, similar to the NruI-V5-His6 tag defect (see above). The insertions at amino acid positions 526 and 1051 fell in regions that were predicted to be ordered (Figure 2.2A), which might explain why these regions can tolerate a small insertion but not the insertion of the tag. The insertion at amino acid position 1051 fell near a predicted disordered region. Therefore, we generated a construct in which the tag was placed at position 1056, within the predicted disordered region. This V5-His6 tagged allele at position 1056 was fully functional (strain LUZ379) (Figures 2.4 and 2.7) and produced a protein of the expected size (Figure 2.4C). The *mds3Δ/Δ* strain carrying a functional *MDS3::V5::HIS6*

tagged allele was grown in M199 pH 8 for 4 hours, fixed with formaldehyde, and used in indirect immunofluorescence studies to localize Mds3. Mds3 localized in discrete spots throughout the yeast cytoplasm (Figure 2.6).

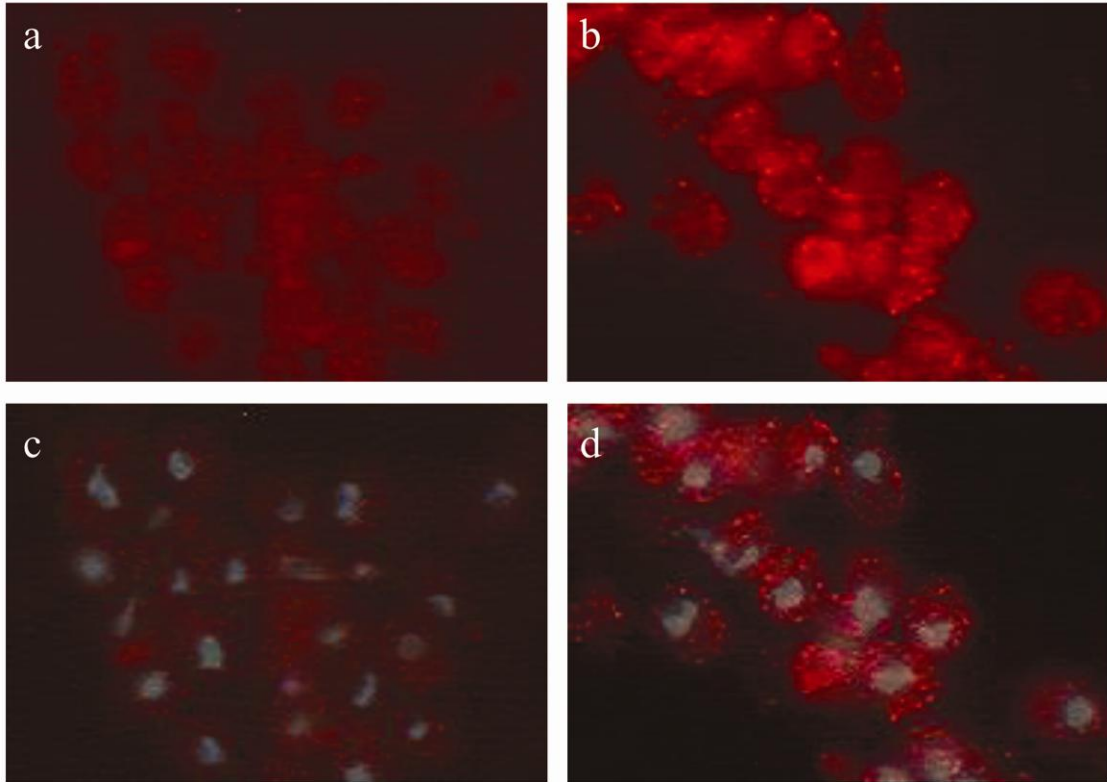


**Figure 2.6:** Mds3 localizes in discrete cytoplasmic spots. Indirect immunofluorescence of an untagged wild-type (a,c) and *mds3Δ/Δ* + *MDS3-V5* (LUZ379) (b,d) strains. Red: Mds3-V5, Blue: DAPI.

It would be interesting to determine if the localization of Mds3 is influenced by the function of the Kelch or putative BTB/POZ domains. For this purpose the Kelch domain alleles tested above (Figure 2.3 and Table 2.4) were tagged with a *V5::HIS6* tag in the benign location identified above. The tagged Kelch alleles were tested for growth in YPD, YPD+LiCl, and for filamentation in solid M199 pH 8 to determine if there was an additive effect of the *V5::HIS6* tag and the Kelch mutations in the function of Mds3. We did not observe any additive effect of both mutations on the function of Mds3 (Figure 2.7). Thus, the alleles are ready to be used to

determine protein stability and localization of the Kelch alleles. A similar process should be carried out with the Tn7 allele *MDS3*-55.1 which fell within the predicted BTB/POZ domain.

Therefore, from these bioinformatics, genetic, and localization studies, Mds3 appears to be a cytoplasmic Kelch/BTB protein, which contains a serine rich region bridging the N- and C-terminus of the protein, two other ordered regions of unknown function, and several highly disordered regions that span the ORF.

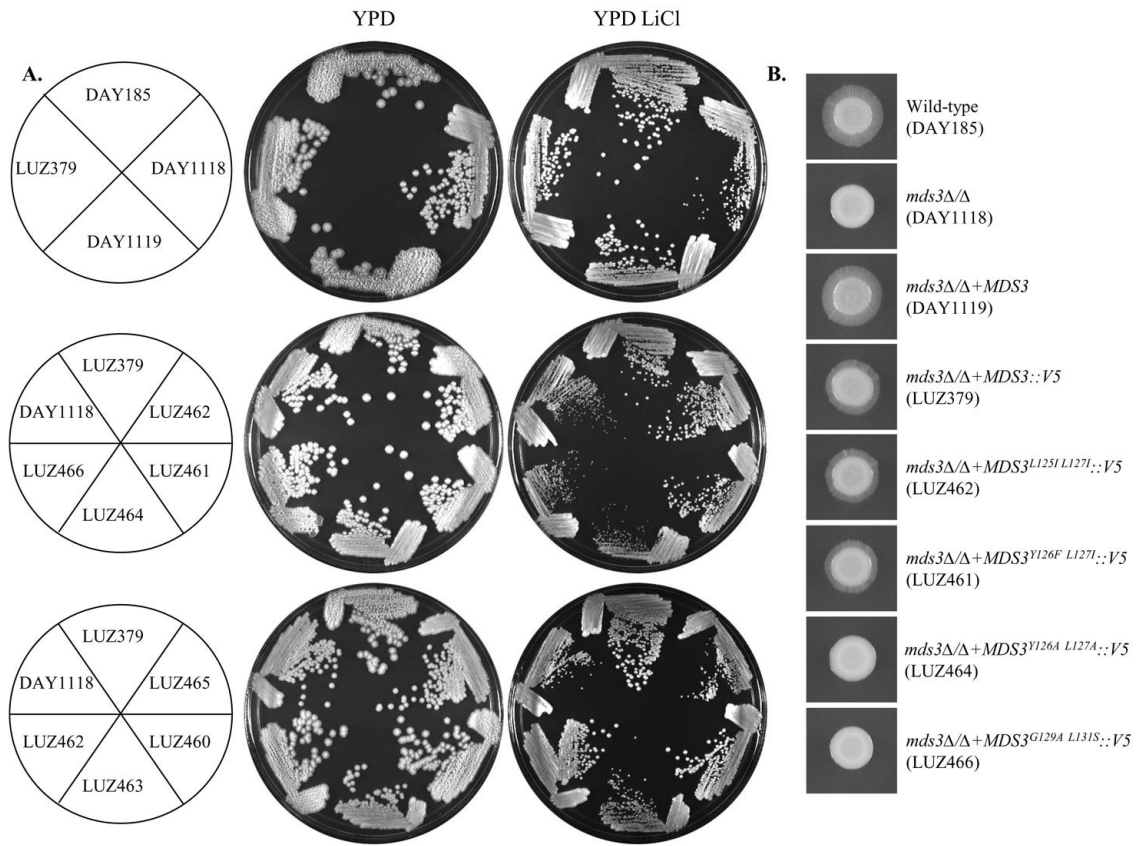


**Figure 2.7:** Functional characterization of the *MDS3-Kelch::V5* tagged alleles. A,B) Growth in YPD and YPD+150mM LiCl, and filamentation in solid M199 pH 8 of the wild-type strain (DAY185), *mds3Δ/Δ* (DAY1118), *mds3Δ/Δ+MDS3* (DAY1119), *mds3Δ/Δ+MDS3::V5* (LUZ379) and the following Kelch::V5 tagged alleles: *MDS3<sup>Y1251 L1271::V5</sup>* (LUZ462), *MDS3<sup>Y126F L1271::V5</sup>* (LUZ461), *MDS3<sup>Y126A L127A::V5</sup>* (LUZ464), and *MDS3<sup>G129A L131S::V5</sup>* (LUZ466).

## DISCUSSION

Bioinformatic analyses are a useful first step to predict potential functions of uncharacterized proteins. The combination of bioinformatic domain searches and protein modeling showed that Mds3 likely contains a six-bladed Kelch propeller in its N-terminus, followed by a serine rich region that contains a PEST domain, and two ordered regions in the C-terminal half, one of which has low homology to BTB/POZ domains. Thus, Mds3 appears to be a modular protein: a multidomain protein with flexible, disordered linker regions (Dyson and Wright, 2005).

The most prominent functional domain in Mds3 is the N-terminal Kelch propeller. Although the first crystallized Kelch  $\beta$ -propeller belongs to the enzyme galactose oxidase, the Kelch propellers are generally considered to function as protein-protein interaction domains (Adams et al., 2000). Kelch motifs have very low sequence conservation. However, alterations in key residues such as the glycines and the hydrophobic residues in the second  $\beta$ -strand of a Kelch domain (the most conserved of the strands) can render the protein non-functional (Gomez et al., 2000). Accordingly, we found that site-directed mutagenesis to non-conserved residues in the second  $\beta$ -strand of the bioinformatically predicted Kelch domain of Mds3 had significant effects on protein function (Figure 2.2A and 2.3). The loops that protrude from the propeller, which are variable in length, can also function as sites for protein interactions. This might explain why several 5 amino acid insertions and most 23 amino acids insertions in the Kelch domain areas rendered a non-functional protein (Figure 2.2A, 2.4, and data not shown). It remains possible that the lack of function of Mds3 alleles carrying non-conserved point mutations or insertions is due to an increased instability of the protein. However, similar point mutations in Rag2 Kelch domains did not alter protein stability (Gomez et al., 2000), and we also detected expression of non-complementing Mds3<sup>G129A L131S</sup>-V5 tagged and Mds3-C-terminal-HA tagged strains by Western blot, with no obvious evidence of protein degradation (Figure 2.4B and data not shown).

Thus, it is likely that the different mutations within the Kelch domains are affecting Mds3 function by limiting its ability to interact with other proteins, and not by causing protein degradation. Overall, the four approaches: two bioinformatic and two mutational, independently support the conclusion that the first ~400 amino acids of the Mds3 N-terminal region fold into a six-bladed Kelch  $\beta$ -propeller whose integrity is required for Mds3 to fulfill its role in growth, resistance to LiCl and pH 9, and filamentation in *C. albicans*.

The second domain predicted in ScMds3 was the BTB domain (Figure 2.2A). Similar to Kelch domains, BTB domains have a low degree of sequence conservation. However, the secondary structure and overall arrangement of the domain is conserved: 5  $\alpha$ -helices with a 3-stranded  $\beta$ -sheet at one end (Perez-Torrado et al., 2006). Even though the BTB domain was identified in ScMds3 only with low homology, there is high sequence similarity between ScMds3, Mds3, and Pmd1 in that region of the proteins. Further, secondary structure predictions using Phyre indicate that the “BTB” region in Mds3 folds into  $\alpha$ -helices, and that there is a potential 2-stranded  $\beta$ -sheet N-terminal to the domain (data not shown), which supports the existence of a poorly conserved BTB domain in Mds3 as well. Independent evidence suggests that this region is critical for function. First, insertional mutations in the “BTB” region caused Mds3 to lose functionality (Figure 2.5, allele *MDS3-55.1*). Second, overexpression of the C-terminal region of ScMds3 has a dominant negative effect, suggesting titration of an interacting factor (Benni and Neugeborn, 1997). BTB domains can homo-, hetero-, or oligo-dimerize, depending on the sequence and structure of the domain; and they are usually involved in transcription and protein degradation (Perez-Torrado et al., 2006). BTB domains are usually associated with Kelch domains in metazoans (Prag and Adams, 2003). The function of most Kelch/BTB proteins remains unknown, but they have been suggested to function in multi-protein complexes (Prag and Adams, 2003). Overall, our results suggest that Mds3 is a Kelch/BTB protein.

Mds3 contains a ~250 amino acids long serine rich region in the middle of the protein, which is predicted to have a PEST domain. PEST domains are segments of low sequence conservation rich in proline (P), glutamic acid (E), serine (S), threonine (T), and aspartic acid that are flanked by arginine or lysine residues. The presence of PEST domains often correlates with short half life of proteins, and they are thought to be cleavage sites that promote protein degradation by proteosomes (Rogers et al., 1986; Rechsteiner and Roggers, 1996). In fact, PEST-like regions are cleaved by calpains (Tompa et al., 2004) and caspases (Garay-Malpartida et al., 2005). Many of the proteins with caspase cleavage domains are involved in signal transduction pathways, such as mTOR, MAPK, and PI3K/Akt (Belizario et al., 2008). Furthermore, PEST regions often contain consensus sites for several kinases, and it has been shown that many PEST-containing proteins are regulated by phosphorylation. While Mds3 was predicted by a stringent evolutionary proteomics approach to be a substrate for PKA (amino acid position 754 in ScMds3 and 518 in Mds3), the predicted phosphorylation sites do not fall within the predicted PEST domains (Budovskaya et al., 2005 and Figure 2.2A). However, it is possible that Mds3 is a substrate for other kinases, such as PKC and TOR. Therefore, the presence of putative PEST domains and phosphorylation sites in Mds3 suggests that Mds3 function is controlled posttranslationally through different mechanisms.

One interesting aspect of Mds3 that became evident from the bioinformatic analysis was the presence of several highly disordered regions across the ORF (Figure 2.2B). Intrinsically disordered proteins are common in eukaryotes, and fulfill diverse functions including transcriptional and translational regulation and signal transduction (Dyson and Wright, 2005; Garza et al., 2009). Proteins vary in the distribution and extent of their disordered regions, ranging from highly unstructured to modular (multidomains joined by linkers) to highly folded structures. Posttranslational modifications such as phosphorylation, or the binding to a substrate can alter the conformation and function of an unstructured region and cause it to fold into a

secondary or tertiary defined structure. The flexibility of the disordered regions allows proteins to adopt different conformations, increasing the type and number of targets they can interact with. Thus, many modular proteins function as scaffolds in multiple signal transduction pathways and are part of multi-protein complexes (Iakoucheva et al., 2002; Dyson and Wright, 2005). The modular characteristics and length of the Mds3 ORF, and the presence of two potential protein-protein interaction domains, suggest that indeed Mds3 could function as a molecular scaffold.

Another bioinformatic prediction for ScMds3, but not Mds3, was the presence of a signal peptide. Signal peptides target the nascent amino acid chain to the endoplasmic reticulum, where it is re-directed for secretion to the extracellular space or to organelles such as the mitochondria or the chloroplasts (Martoglio and Dobberstein, 1998; Hedge and Bernstein, 2006). Interestingly, ScMds3, but not Pmd1, was predicted to contain a signal peptide, suggesting localization and/or functional differences between the paralogs. In support of this, large scale proteomic analyses found ScMds3 (but not Pmd1) in the mitochondria (Sickmann et al., 2003; Reinders et al., 2006; Huh et al., 2003). Our results and those of others also localize Mds3 in the cytoplasm (Figure 2.5, Kumar et al., 2002; Horton et al., 2007), where Mds3 appears to localize to discrete spots randomly dispersed in the cytoplasm (Figure 2.5). While some of these spots could indeed be the mitochondria, another appealing hypothesis is that they constitute vesicles or endosomes. Besides a role in vesicle trafficking, endosomes provide a surface for the convergence of multiple signaling pathways, including the Rim101 pathway, the mating response pathway, and the TOR dependent and independent nitrogen starvation response pathway (Mitchell, 2008; Hancock, 2003; Zurita-Martinez et al., 2007; Sturgill et al., 2008; Aronova et al., 2007; Slessareva et al., 2006; Puria et al., 2008; Xu et al., 2004). A second appealing hypothesis is that the cytoplasmic spots are plasma membrane microdomains. Plasma membrane microdomains, such as the Ras nanoclusters, are involved in the regulation of signal transduction (Hancock and Parton, 2005; Tian et al., 2007). Since we hypothesize that Mds3 functions as a scaffold in signal transduction

pathways, its localization on the surface of endosomes or at plasma membrane microdomains would be ideal to fulfill this role.

In sum, our bioinformatic, mutational, and localization studies support a model in which Mds3 is a cytoplasmic, modular, Kelch-BTB protein that functions as a scaffold and participates in the regulation of signal transduction cascades.

Plenty of work is still required to better understand the function of Mds3. However, I have presented here preliminary data and have constructed molecular tools that should aid in answering some of the questions regarding localization, structure, posttranslational modifications, and molecular interactions of Mds3. For example, the availability of tagged Mds3 alleles under the control of its own promoter or overexpressed (data not shown) are ideal for large scale experiments to find Mds3 binding partners and determine Mds3 putative posttranslational modifications. Studies of co-localization of Mds3 with endosomal and other organelle markers (such as Mitotracker, etc) using immunofluorescence and confocal microscopy or subcellular fractionation should contribute to define the localization of Mds3 in the cell. Further, it would be interesting to determine whether the Kelch and/or putative BTB domains are required for proper Mds3 protein interactions or localization. Finally, if Mds3 is indeed a phospho-protein, it would be interesting to find the kinase(s) and phosphatases responsible for the phosphorylation/de-phosphorylation of Mds3; to determine what residues in Mds3 are important for phosphorylation; to determine what role the phosphorylation plays on Mds3 function, localization, interactions, stability, and structural conformation; and to find the signals (if any) that lead to changes in the phosphorylation status of Mds3. A similar analysis can be performed for any other posttranslational modification that Mds3 is shown to undergo.

TABLES

Table 2.1. *C. albicans* strains used in this study

Strain	Parent	Genotype	Reference
<b>DAY1 (BPW17)</b>	SC5314	<i>ura3::λimm434/ura3::λimm434 his1::hisG/his1::hisG arg4::hisG/arg4::hisG</i>	Wilson et al., 1999
<b>DAY185</b>	DAY286	<i>ura3::λimm434/ura3::λimm434 pHIS1::his1::hisG/his1::hisG ARG4::URA3::arg4::hisG/arg4::hisG</i>	Davis et al., 2000
<b>DAY938</b>	BWP17	<i>ura3::λimm434/ura3::λimm434 his1::hisG/his1::hisG arg4::hisG/arg4::hisG mds3::ARG4/mds3::URA3dpl200</i>	Zacchi et al., 2010
<b>DAY1118</b>	DAY938	<i>ura3::λimm434/ura3::λimm434 HIS1::his1::hisG/his1::hisG arg4::hisG/arg4::hisG mds3::ARG4/mds3::URA3dpl200</i>	Zacchi et al., 2010
<b>DAY1119</b>	DAY938	<i>ura3::λimm434/ura3::λimm434 HIS1::MDS3::his1::hisG/his1::hisG arg4::hisG/arg4::hisG_mds3::ARG4/mds3::URA3dpl200</i>	Zacchi et al., 2010
<b>LUZ14</b>	DAY956	<i>ura3::λimm434/ura3::λimm434 HIS1::MDS3::V5::his1::hisG/his1::hisG arg4::hisG/arg4::hisG_mds3::ARG4/mds3::dpl200</i>	This study
<b>LUZ17</b>	DAY956	<i>ura3::λimm434/ura3::λimm434 HIS1::MDS3::V5::his1::hisG/his1::hisG arg4::hisG/arg4::hisG_mds3::ARG4/mds3::dpl200</i>	This study
<b>LUZ20</b>	DAY956	<i>ura3::λimm434/ura3::λimm434 HIS1::MDS3::V5::his1::hisG/his1::hisG arg4::hisG/arg4::hisG_mds3::ARG4/mds3::dpl200</i>	This study
<b>LUZ23</b>	DAY415	<i>ura3::λimm434/ura3::λimm434 his1::hisG/his1::hisG arg4::hisG/arg4::hisG_mds3::ARG4/MDS3::HA::URA3</i>	
<b>LUZ316</b>	DAY956	<i>ura3::λimm434/ura3::λimm434 HIS1::MDS3<sup>G129A</sup><sub>L131S</sub>::V5::his1::hisG/his1::hisG arg4::hisG/arg4::hisG mds3::ARG4/mds3::dpl200</i>	This study
<b>LUZ379</b>	DAY938	<i>ura3::λimm434/ura3::λimm434 HIS1::MDS3::V5::his1::hisG/his1::hisG arg4::hisG/arg4::hisG_mds3::ARG4/mds3::URA3dpl200</i>	This study
<b>LUZ397</b>	DAY938	<i>ura3::λimm434/ura3::λimm434 HIS1::MDS3<sup>Y126A L127A</sup>::his1::hisG/his1::hisG arg4::hisG/arg4::hisG_mds3::ARG4/mds3::URA3dpl200</i>	This study
<b>LUZ399</b>	DAY938	<i>ura3::λimm434/ura3::λimm434 HIS1::MDS3<sup>G129A</sup><sub>L131S</sub>::his1::hisG/his1::hisG arg4::hisG/arg4::hisG mds3::ARG4/mds3::URA3dpl200</i>	This study
<b>LUZ400</b>	DAY938	<i>ura3::λimm434/ura3::λimm434 HIS1::MDS3<sup>Y126F</sup><sub>L127I</sub>::his1::hisG/his1::hisG arg4::hisG/arg4::hisG mds3::ARG4/mds3::URA3dpl200</i>	This study
<b>LUZ402</b>	DAY938	<i>ura3::λimm434/ura3::λimm434 HIS1::MDS3<sup>L125I L127I</sup>::his1::hisG/his1::hisG arg4::hisG/arg4::hisG_mds3::ARG4/mds3::URA3dpl200</i>	This study
<b>LUZ426</b>	DAY938	<i>ura3::λimm434/ura3::λimm434 HIS1::MDS3-4.2::his1::hisG/his1::hisG arg4::hisG/arg4::hisG mds3::ARG4/mds3::URA3dpl200</i>	This study
<b>LUZ427</b>	DAY938	<i>ura3::λimm434/ura3::λimm434 HIS1::MDS3-41.1::his1::hisG/his1::hisG arg4::hisG/arg4::hisG_mds3::ARG4/mds3::URA3dpl200</i>	This study
<b>LUZ431</b>	DAY938	<i>ura3::λimm434/ura3::λimm434 HIS1::MDS3-55.1::his1::hisG/his1::hisG arg4::hisG/arg4::hisG_mds3::ARG4/mds3::URA3dpl200</i>	This study
<b>LUZ433</b>	DAY938	<i>ura3::λimm434/ura3::λimm434 HIS1::MDS3-56.1::his1::hisG/his1::hisG arg4::hisG/arg4::hisG_mds3::ARG4/mds3::URA3dpl200</i>	This study
<b>LUZ436</b>	DAY938	<i>ura3::λimm434/ura3::λimm434 HIS1::MDS3-67.1::his1::hisG/his1::hisG arg4::hisG/arg4::hisG_mds3::ARG4/mds3::URA3dpl200</i>	This study
<b>LUZ441</b>	DAY938	<i>ura3::λimm434/ura3::λimm434 HIS1::MDS3-12.1::his1::hisG/his1::hisG arg4::hisG/arg4::hisG_mds3::ARG4/mds3::URA3dpl200</i>	This study
<b>LUZ444</b>	DAY938	<i>ura3::λimm434/ura3::λimm434 HIS1::MDS3-20.1::his1::hisG/his1::hisG arg4::hisG/arg4::hisG_mds3::ARG4/mds3::URA3dpl200</i>	This study
<b>LUZ446</b>	DAY938	<i>ura3::λimm434/ura3::λimm434 HIS1::MDS3-33.1::his1::hisG/his1::hisG arg4::hisG/arg4::hisG_mds3::ARG4/mds3::URA3dpl200</i>	This study
<b>LUZ448</b>	DAY938	<i>ura3::λimm434/ura3::λimm434 HIS1::MDS3-36.1::his1::hisG/his1::hisG arg4::hisG/arg4::hisG_mds3::ARG4/mds3::URA3dpl200</i>	This study
<b>LUZ450</b>	DAY938	<i>ura3::λimm434/ura3::λimm434 HIS1::MDS3-82.1::his1::hisG/his1::hisG arg4::hisG/arg4::hisG_mds3::ARG4/mds3::URA3dpl200</i>	This study

<b>LUZ451/3</b>	DAY938	<i>ura3::λimm434/ura3::λimm434 HIS1::MDS3-35.1::his1::hisG/his1::hisG arg4::hisG/arg4::hisG_mds3::ARG4/mds3::URA3dpl200</i>	This study
<b>LUZ455/7</b>	DAY938	<i>ura3::λimm434/ura3::λimm434 HIS1::MDS3-104.1::his1::hisG/his1::hisG arg4::hisG/arg4::hisG_mds3::ARG4/mds3::URA3dpl200</i>	This study
<b>LUZ458</b>	DAY938	<i>ura3::λimm434/ura3::λimm434 HIS1::MDS3108.1::his1::hisG/his1::hisG arg4::hisG/arg4::hisG_mds3::ARG4/mds3::URA3dpl200</i>	This study
<b>LUZ461</b>	DAY938	<i>ura3::λimm434/ura3::λimm434 HIS1::MDS3<sup>Y126F</sup><sub>L1271</sub>::V5::his1::hisG/his1::hisG arg4::hisG/arg4::hisG_mds3::ARG4/mds3::URA3dpl200</i>	This study
<b>LUZ462</b>	DAY938	<i>ura3::λimm434/ura3::λimm434 HIS1::MDS3<sup>L125I</sup><sub>L1271</sub>::V5::his1::hisG/his1::hisG arg4::hisG/arg4::hisG_mds3::ARG4/mds3::URA3dpl200</i>	This study
<b>LUZ464</b>	DAY938	<i>ura3::λimm434/ura3::λimm434 HIS1::MDS3<sup>Y126A</sup><sub>L127A</sub>::V5::his1::hisG/his1::hisG arg4::hisG/arg4::hisG_mds3::ARG4/mds3::URA3dpl200</i>	This study
<b>LUZ466</b>	DAY938	<i>ura3::λimm434/ura3::λimm434 HIS1::MDS3<sup>G129A</sup><sub>L131S</sub>::V5::his1::hisG/his1::hisG arg4::hisG/arg4::hisG_mds3::ARG4/mds3::URA3dpl200</i>	This study
<b>DAY414 (L40)</b>	<i>S. cerevisiae</i>	<i>MATα his3Δ200 trp1-901 leu2-3,-112 ade2 LYS2::(lexAop)<sub>4</sub>-HIS3 URA3::(lexAop)<sub>8</sub>-lacZ GAL4</i>	Vojtek et al., 1993

**Table 2.2.** Plasmids used in this study

Plasmid	Description	Reference
<b>pDDB353</b>	<i>HIS1- MDS3</i> complementation vector	Zacchi et al., 2010
<b>pDDB408</b>	pGEM-T- <i>MDS3</i> for Tn7 mutagenesis	Zacchi et al., 2010
<b>pLZ38</b>	<i>HIS1- MDS3::V5HIS6</i> vector, V5 in unique HpaI site	This study
<b>pLZ39</b>	<i>HIS1- MDS3::V5HIS6</i> vector, V5 in unique BstBI site	This study
<b>pLZ78</b>	<i>HIS1- MDS3<sup>L125I L127I</sup></i> vector	This study
<b>pLZ79</b>	<i>HIS1- MDS3<sup>Y126A L127A</sup></i> vector	This study
<b>pLZ81</b>	<i>HIS1- MDS3<sup>G129A L131S</sup></i> vector	This study
<b>pLZ82</b>	<i>HIS1- MDS3<sup>Y126F L127I</sup></i> vector	This study
<b>pLZ83</b>	<i>HIS1- MDS3<sup>G129A L131S</sup>::V5HIS6</i> vector	This study
<b>pLZ86</b>	<i>HIS1-MDS3::V5HIS6</i> vector	This study
<b>pLZ87</b>	<i>HIS1-MDS3-4.2</i> vector	This study
<b>pLZ92</b>	<i>HIS1-MDS3-41.1</i> vector	This study
<b>pLZ93</b>	<i>HIS1-MDS3-42.1</i> vector	This study
<b>pLZ96</b>	<i>HIS1-MDS3-55.1</i> vector	This study
<b>pLZ97</b>	<i>HIS1-MDS3-56.1</i> vector	This study
<b>pLZ99</b>	<i>HIS1-MDS3-67.1</i> vector	This study
<b>pLZ100</b>	<i>HIS1-MDS3-91.1</i> vector	This study
<b>pLZ101</b>	<i>HIS1-MDS3-95.1</i> vector	This study
<b>pLZ107</b>	<i>HIS1-MDS3-12.1</i> vector	This study
<b>pLZ108</b>	<i>HIS1-MDS3-20.1</i> vector	This study
<b>pLZ109</b>	<i>HIS1-MDS3-33.1</i> vector	This study
<b>pLZ110</b>	<i>HIS1-MDS3-36.1</i> vector	This study
<b>pLZ111</b>	<i>HIS1-MDS3-82.1</i> vector	This study
<b>pLZ118</b>	<i>HIS1-MDS3-35.1</i> vector	This study
<b>pLZ119</b>	<i>HIS1-MDS3-104.1</i> vector	This study
<b>pLZ120</b>	<i>HIS1-MDS3-108.1</i> vector	This study
<b>pLZ122</b>	<i>HIS1- MDS3<sup>Y126F L127I</sup>::V5HIS6</i> vector	This study
<b>pLZ123</b>	<i>HIS1- MDS3<sup>L125I L127I</sup>::V5HIS6</i> vector	This study
<b>pLZ124</b>	<i>HIS1- MDS3<sup>Y126A L127A</sup>::V5HIS6</i> vector	This study
<b>pLZ125</b>	<i>HIS1- MDS3<sup>G129A L131S</sup>::V5HIS6</i> vector	This study

**Table 2.3.** Primers used in this study

Primer	Sequence	Reference
MDS3 Seq 1	TGTTTTCACCCCTCACGCC	This study
MDS3 Seq 2	TGGTGGATTGGCTCTACTGC	This study
MDS3 Nru1 Seq 3'	TTATGATGAGATTGCCATGC	This study
MDS3 L125I L127I 5'	GTGCATTCAACAATTGTattTATattTTTGGTGGATTGGCTC	This study
MDS3 L125I L127I 3'	GAGCCAATCCACCAAAaatATAaatACAATTGTTGAATGCAC	This study
MDS3 Y126A L127A 5'	GTGCATTCAACAATTGTCTAgetgctTTTGGTGGATTGGCTC	This study
MDS3 Y126A L127A 3'	GAGCCAATCCACCAAAagcagcTAGACAATTGTTGAATGCAC	This study
MDS3 G129A L131S 5'	GTCTATATCTATTTgctGGAtcaGCTCTACTGCAAGAAAATGACG	This study
MDS3 G129A L131S 3'	CGTCATTTTCTTGCAGTAGAGCtgaTCCagcAAATAGATATAGAC	This study
MDS3 Y126F L127I 5'	GTGCATTCAACAATTGTCTAttattTTTGGTGGATTGGCTC	This study
MDS3 Y126F L127I 3'	GAGCCAATCCACCAAAaataaaTAGACAATTGTTGAATGCAC	This study
56-V5 5'	AGCTTCGAAAATTCATGCAGATAGTGTGCGCAATGTCTTTGGGT AAGCCTATCCCTAACCC	This study
56-V5 3'	AAGCATTTTCGAGATTATTACTTGTAAACCGATTTCTTTTTATGG TGATGGTGATGATGAC	This study
MDS3 HpaI V5His6 5'	TATTAATCTAGTAGTAAAAAGCGTGAATATTTGGATTGGGT AAGCCTATCCCTAACCC	This study
MDS3 HpaI V5His6 3'	AATATACCCCCTATATTATTATCTTTTTAATCCTGTAAATGG TGATGGTGATGATGAC	This study
MDS3 BstBI V5His6 3'	CGATGATGGCTACCTTGATATTACATTGTTGAAAAAAGCTGGT AAGCCTATCCCTAACCC	This study
MDS3 BstBI V5His6 3'	CTTTTCAAAGACATTGCGACACTATCTGCATGAATTTTCGAA TGGTGTGATGATGATGAC	This study
MDS3 HA C-ter 5'	TCTATTAATCTAGTAGTAAAAAGCGTGAATATTTGGATTGT TAACAGGATTA AAAAGACGGATCCCCGGGTAAATTA	This study
MDS3 URA3 C-ter 3'	CATATAATTAGCCTATTCAACCAATATAACGTGAATATACACC CCTATATTATTAGAATTCCGGAATATTTATGAGAAAC	This study

**Table 2.4.** Effects of mutations in Mds3s' second Kelch repeat on filamentation in M199 pH 8

Strain	Genotype	Average +/- SD
DAY185	<i>MDS3/MDS3</i>	45.8 ± 6.2
DAY1118	<i>mds3Δ/Δ</i>	8.2 ± 4.2
DAY1119	<i>mds3Δ/Δ</i> + <i>LYLFGGLAL</i>	52.3 ± 14.8
LUZ402	<i>mds3Δ/Δ</i> + <i>iYiFGGLAL</i>	35.5 ± 6.7
LUZ400	<i>mds3Δ/Δ</i> + <i>LfiFGGLAL</i>	49.6 ± 5.6
LUZ397	<i>mds3Δ/Δ</i> + <i>LaaFGGLAL</i>	9.5 ± 2.2
LUZ399	<i>mds3Δ/Δ</i> + <i>LYLFaGsAL</i>	8.0 ± 2.1

SD= standard deviation

**Table 2.5.** *MDS3* Tn7 mutant alleles in pDDB408

Allele name	Amino acid position	Stop codon	Wild-type sequence with insertions	Subcloned	Phenotype
4.2	526	NO	SDKlfk <del>h</del> kSP	YES	Wild-type
8.2	999	YES	LKA <del>v</del> .tk <del>a</del> RY	YES	ND
12.1	1361	NO	SSSc <del>l</del> nssASS	YES	Null
13.1	714	YES	ST <del>v</del> .tstAI	YES	ND
15.1	733	NO	SFQlfk <del>h</del> qSN	NO	ND
20.1	1378	NO	FGLlfk <del>q</del> LLT	YES	Wild-type
26.1	379	NO	RPT <del>c</del> ln <del>t</del> tGK	NO	ND
32.1	446	YES	SSEF <del>v</del> .telS	YES	ND
33.1	676	NO	KPQ <del>c</del> ln <del>t</del> qKD	YES	Null
35.1	620	NO	DQA <del>l</del> fk <del>q</del> aLGL	NO	ND
36.1	528	NO	KSPT <del>c</del> ln <del>t</del> tAV	YES	Null
40.1	384	YES	KWS <del>r</del> v. <del>t</del> sRLN	NO	ND
41.1	226	NO	KRY <del>c</del> ln <del>r</del> yVG	YES	Wild-type
42.1	424	NO	TSS <del>c</del> ln <del>s</del> sVR	YES	ND
43.1	293	YES	HES <del>i</del> v. <del>t</del> sIV	NO	ND
47.1	34	YES	TGS <del>a</del> v <del>t</del> . <del>t</del> sAS	YES	ND
48.1	123	NO	FNN <del>c</del> ln <del>n</del> nCL	NO	ND
51.3	344	NO	IPY <del>n</del> fk <del>h</del> yNLR	NO	ND
52.1	440	YES	PIT <del>n</del> v. <del>t</del> tNI	YES	ND
54.1	425	YES	TSS <del>e</del> v. <del>t</del> sVRF	NO	ND
55.1	935	NO	TVK <del>c</del> ln <del>s</del> kAF	YES	Null
56.1	1051	NO	DSV <del>c</del> ln <del>s</del> vAM	YES	Wild-type
57.1	?	?	?	YES	ND
60.1	1183	YES	DAP <del>s</del> v. <del>t</del> pSDY	NO	ND
67.1	607	NO	AKG <del>l</del> fk <del>q</del> gYI	YES	Null
69.1	?	?	?	NO	ND
82.1	732	NO	SSF <del>l</del> fk <del>h</del> fQSN	YES	Null
91.1	656	NO	LSS <del>c</del> ln <del>t</del> sSSG	YES	ND
93	856	YES	IES <del>v</del> . <del>t</del> esSLD	NO	ND
95.1	876	NO	VPG <del>c</del> ln <del>t</del> gEN	YES	ND
97	?	?	?	NO	ND
104.1	658	NO	SSS <del>v</del> fk <del>q</del> sGE	NO	ND
108.1	1266	NO	IIP <del>n</del> fk <del>q</del> pTVS	NO	ND
109	873	NO	KVS <del>m</del> fk <del>q</del> sSSV	NO	ND

? Indicates defective sequence run. (.) Indicates a STOP codon

ND= not determined

## CHAPTER 3

### MDS3 REGULATES MORPHOGENESIS IN *CANDIDA ALBICANS* THROUGH THE TOR PATHWAY

**Zacchi, L.F.**, Gomez Raja, J., Davis, D.A. (2010). Mds3 regulates morphogenesis in *Candida albicans* through the TOR pathway. *Molecular and Cellular Biology*. 30(14):3695-3710.

**Luckey, Adar**

---

**From:** Lucia F Zacchi [zacch002@umn.edu]  
**Sent:** Saturday, April 24, 2010 3:03 PM  
**To:** ASM Journals  
**Subject:** Question about permission to use copyrighted material

To whom it may concern,

A manuscript of mine has been recently accepted for publication in the journal Molecular and Cellular Biology. I would like to include the contents of this manuscript in my Ph.D. dissertation, which I am about to submit for review before my graduation. I would like to know if I need a letter from MCB allowing me to use this material, and if so whom I should contact to obtain this permit.

Thank you very much in advance for your help.

Best regards,

Lucia

--

Lucia F. Zacchi  
Microbiology, Immunology and Cancer Biology (MICaB) Graduate Program  
University of Minnesota  
Department of Microbiology  
Room 1360 Mayo Building  
420 Delaware St SE  
Minneapolis, MN 55455  
USA  
Email: zacch002@umn.edu  
Web: www.micab.umn.edu  
Lab Phone: (612) 624-7994

**PERMISSION GRANTED**  
**CONTINGENT ON AUTHOR PERMISSION (which you must obtain)**  
**AND APPROPRIATE CREDIT**

**American Society for Microbiology**  
**Journals Department**

*Barbara M. Gilman* Date 4/27/10

## SUMMARY

The success of *Candida albicans* as a major human fungal pathogen is dependent on its ability to colonize and survive as a commensal on diverse mucosal surfaces. One trait required for survival and virulence in the host is the morphogenetic yeast-to-hyphal transition. Mds3 was identified as a regulator of pH-dependent morphogenesis that functions in parallel with the classic Rim101 pH sensing pathway. Microarray analyses revealed that *mds3* $\Delta/\Delta$  cells had an expression profile indicative of a hyperactive TOR pathway, including the preferential expression of genes encoding ribosomal proteins and a decreased expression of genes involved in nitrogen source utilization. The transcriptional and morphological defects of the *mds3* $\Delta/\Delta$  mutant were rescued by rapamycin, an inhibitor of TOR, and this rescue was lost in strains carrying the rapamycin resistant *TOR1-1* allele or an *rbp1* $\Delta/\Delta$  deletion. Rapamycin also rescued the transcriptional and morphological defects associated with loss of Sit4, a TOR pathway effector, but not loss of Rim101 or Ras1. The *sit4* $\Delta/\Delta$  and *mds3* $\Delta/\Delta$  mutants had additional phenotypic similarities suggesting that Sit4 and Mds3 function similarly in the TOR pathway. Finally, we found that Mds3 and Sit4 co-immunoprecipitate. Thus, Mds3 is a new member of the TOR pathway that contributes to morphogenesis in *C. albicans* as a regulator of this key morphogenetic pathway.

## INTRODUCTION

Eukaryotic cell growth and morphogenesis is effected by numerous environmental signals. These environmental signals are integrated by highly conserved regulators, including Ras, PKC, and the target of rapamycin (TOR). These regulators govern the activity of signal transduction pathways, which generally promote changes in gene expression affecting an appropriate cellular response to the environmental signal. TOR is an essential kinase conserved throughout eukaryotic evolution. In mammalian systems, mTOR is required for embryogenesis (Hwang et al., 2008) and for cellular morphogenesis in neurons (Han et al., 2008), vacuolar smooth muscle cells (Martin et al., 2004), and T-cells (Delgoffe et al., 2009). In the model yeast *S. cerevisiae*, TOR plays a fundamental role in morphogenesis being required for pseudohyphal growth and sporulation (Cutler et al., 2001; Zheng and Schreiber, 1997). TOR governs morphogenesis by regulating numerous biological processes including, autophagy, translation, and ribosome biogenesis (Wullschleger et al., 2006). Thus, in eukaryotic cells, TOR responds to environmental signals to promote growth and morphogenetic changes.

In the fungal opportunistic pathogen *Candida albicans*, the most well studied morphogenetic transition is the yeast-hyphal switch. The switch between the yeast and hyphal growth forms plays a critical role in *C. albicans* ability to colonize as a commensal and cause disease as a pathogen. Yeast cells are small, non-adherent, less immunogenic and divide rapidly, which may allow *C. albicans* to successfully outcompete the faster growing bacterial flora and the immune responses as well as pass through capillary beds during disseminated disease. Hyphal cells are long, extremely adherent, promote profound immune responses, and divide more slowly. Further hyphal cells secrete numerous degradative enzymes and are invasive (Gow et al., 2002; Mitchell, 1998). Hyphal cells may allow *C. albicans* to maintain itself on mucosal surfaces and in immunocompromised hosts, enter the bloodstream. Both yeast and hyphal cells are observed in commensally colonized and diseased sites, demonstrating the relevance of this morphogenetic

switch for *C. albicans* survival in the host. This idea is further supported by genetic analyses demonstrating that *C. albicans* mutants locked in a yeast or filamentous form are unable to cause disease (Lo et al., 1997; Murad et al., 2001). Thus, the yeast-hyphal morphogenetic switch is critical for pathogenesis.

Because the yeast-hyphal transition is critical for pathogenicity, much work has been devoted to identifying the environmental sensors and signal transduction pathways that respond to these signals. The yeast-hyphal morphogenetic switch is governed by a plethora of environmental cues, including pH, nutrient availability, temperature, and host factors (Alonso-Monge et al., 2009; Cottier and Muhlschlegel, 2009; Davis, 2009; Mitchell, 1998). For example, neutral-alkaline environmental pH is sensed by the Rim101 signal transduction pathway resulting in proteolytic activation of the Rim101 transcription factor, which promotes hyphal formation (Davis et al., 2000b; Porta et al., 1999; Ramon et al., 1999). Loss-of-function mutants in the Rim101 pathway do not form hyphae in response to neutral-alkaline environmental pH and show reduced virulence in animal models of infection (Davis et al., 2000a, Nobile et al., 2008). Similarly, nutrient levels are sensed by the TOR pathway, which also promotes hyphal formation and is required for pathogenesis (Bastidas et al., 2009; Cutler et al., 2001; Lee et al., 2004). These studies highlight the profound link between morphogenesis and virulence in the host in response to environmental signals, such as pH and starvation.

In order to gain further insights in *C. albicans* adaptation to environmental pH, we identified additional signal transduction pathways that contribute to adaptation to environmental pH. For example, calcineurin and its associated transcription factor Crz1 were found to act in parallel with Rim101 for adaptation to alkaline pH in *C. albicans* (Kullas et al., 2007). Further, using a forward genetics approach, *MDS3* was identified as a positive regulator of alkaline pH responses in *C. albicans* (Davis et al., 2002). Like calcineurin, Mds3 was shown to act in parallel to Rim101 to promote neutral-alkaline pH responses. Mds3 also governs adaptation to neutral-

alkaline pH response in *S. cerevisiae*, however this function was originally masked by the presence of the redundant Mds3 paralog, Pmd1. While the well studied Rim101 pathway is required for adaptation to environmental pH, Mds3 plays a key role in adaptation to environmental pH.

*MDS3* was originally identified in *S. cerevisiae* as a positive regulator of meiosis, a morphogenetic process that requires an alkaline environment (Benni and Neigeborn, 1997; Esposito and Klapholz, 1981). In *C. albicans*, Mds3 is involved in a variety of morphogenetic processes, including the yeast-hyphal transition, chlamydospore formation, and biofilm formation (Davis et al., 2002; Nobile et al., 2003; Richard et al., 2005). Despite a clear role for Mds3 in diverse morphogenetic processes in fungi, how Mds3 promotes morphogenesis is unknown. Work done in *S. cerevisiae* suggested that Mds3 may transmit starvation signals to Ras (Benni and Neigeborn, 1997; McDonald et al., 2009). However, we demonstrate that Mds3 contributes to morphogenesis in *C. albicans* through the negative regulation of the TOR pathway. We find that an *mds3* $\Delta/\Delta$  mutant has transcriptional defects indicative of a hyper-active TOR pathway and that these transcriptional defects are rescued by rapamycin, a TOR pathway inhibitor. Further, the filamentation defects associated with the *mds3* $\Delta/\Delta$  mutant are rescued by rapamycin. We also demonstrate that loss of Sit4, a downstream effector of TOR, mimics loss of Mds3. In *C. albicans* loss of Sit4 or Mds3 results in resistance to rapamycin, whereas in *S. cerevisiae* this loss results in sensitivity to rapamycin, suggesting that TOR functions are distinct in these two species. Finally, we demonstrate that Mds3 and Sit4 interact suggesting a mechanism of TOR pathway regulation. In total, our results establish that Mds3 is a member of the TOR pathway and suggest that Mds3 regulates *C. albicans* development and morphogenesis through the TOR pathway.

## MATERIALS AND METHODS

### *C. albicans* strains and plasmids

All yeast strains used in this study are listed in Table 3.1. DAY938 was constructed by deleting the second copy of *MDS3* from VIC1, the *MDS3/mds3::ARG4* parent of strain VIC3 (Davis et al., 2002), using an *mds3::URA3-dpl200* disruption cassette amplified with primers MDS3 5DR and MDS3 3DR (Table 3.2). Strains DAY1122 and DAY1123 were constructed by transforming strains DAY938 and DAY286 respectively with the *tor1::HIS1* disruption cassette, which was amplified using primers TOR1 5DR and TOR1 3DR (Table 3.2). All deletions are from the start to the stop codon and were generated by chemical transformation (Wilson et al., 1999). Correct integration of the disruption cassettes was verified by the PCR using the Mds3null 5-detect and Mds3null 3-detect primers or TOR1 5'detect-2 and TOR1 3'detect primers (Table 3.2). DAY1118 and DAY1119 were generated by transforming DAY938 with the PmeI-digested plasmids pDDB343 and pDDB353, respectively.

Strains DAY1120, DAY1121, DAY1124, DAY1125, and DAY1321 that contain the *TOR1-1* allele were generated as previously described with minor modifications (Cruz et al., 2001). Briefly, primers TOR1 A-C and TOR1 A-C Rev (Table 3.2) were annealed and used for transformation. Transformants were selected on YPD supplemented with 100nM rapamycin. Rapamycin resistant clones were screened by NheI digestion of a PCR product amplified with primers JOHE6247 and JOHE6248 and were verified by sequencing (Cruz et al., 2001). DAY1255 was then generated by transforming DAY1120 with PmeI-digested pDDB343. The correct genotype of all the mutants carrying *TOR1-1* and/or *tor1::HIS1* alleles was verified by Southern blot of NheI/NcoI or NheI/PvuII digestions of genomic DNA (data not shown), and using PCR products amplified with primers TOR1 probe 5' and TOR1 probe 3' or TOR1 probe5'-2 and TOR1 probe 3' as probes (Table 3.2). The probes were radiolabelled with [ $\alpha$ -<sup>32</sup>P]-dCTP using the Prime-a-Gene labeling system (Promega).

The *mds3* $\Delta/\Delta$  *sit4* $\Delta/\Delta$  mutant DAY1233 was constructed by sequentially deleting both *MDS3* alleles from the *sit4* $\Delta/\Delta$  strain DAY972, using the *mds3::URA3-dpl200* disruption cassette amplified with primers MDS3 5DR and MDS3 3DR described above. The *URA3-dpl200* marker was recycled by growing the cells in SC medium supplemented with 5-fluoroorotic acid (5-FOA).

The *mds3* $\Delta/\Delta$  *rbp1* $\Delta/\Delta$  mutant DAY1239 was constructed by sequentially deleting both *MDS3* alleles from the *rbp1* $\Delta/\Delta$  strain DAY1230. Strain DAY1230 was generated by recycling the *MX3::URA3R::MX3* marker in strain DAY1223 (Cruz et al., 2001) in 5-FOA. The *mds3::URA3-dpl200* disruption cassette was amplified with primers MDS3 5DR and MDS3 3DR described above and the *URA3-dpl200* marker was recycled by growing the cells in 5-FOA.

DAY1234, which contains a functional *SIT4-cMyc* allele was constructed by introducing a C-terminal MYC-T<sub>ADHI</sub>-*URA3* cassette. The MYC-T<sub>ADHI</sub>-*URA3* cassette was PCR amplified with primers Sit4 MYC Nter 5' and Sit4 MYC URA3 Nter 3', from plasmid pDDB372 (pMG1095 (Gerami-Nejad et al., 2009)) (Table 3.2). Correct integration of the cassette was verified by the PCR using primers 5' Myc detect and Sit4 3' detect (Table 3.2) and by Western Blot, using anti-Myc antibody (R950-25, Invitrogen).

To construct the strains for the co-immunoprecipitation studies, DAY1234 was transformed with *NheI* digested pDDB499 (*MDS3-HA*) to generate strain DAY1236. DAY1234 was also transformed with *PmeI* digested pDDB353 (untagged *MDS3* vector) to generate the control strain DAY1235.

The *MDS3* complementation vector pDDB353 was constructed as follows. Plasmid pDDB343 was generated by replacing the *NruI* restriction site in pDDB78 with a *PmeI* site. Primers DDB78 *PmeI*x*NruI* 5' and DDB78 *PmeI*x*NruI* 3' were annealed and used for gap repair of the *NruI* digested pDDB78 through *in vivo* recombination in *trp-* *S. cerevisiae* strain L40 to generate plasmid pDDB343. Wild-type *MDS3* sequence with flanking promoter and terminator sequences was amplified in two high fidelity PCRs (*Pfu Turbo DNA* polymerase, Stratagene)

using primer pairs MDS3 5comp new and MDS3 5-2 comp new, and MDS3 3comp new-2 and MDS3 3-2comp new-2 from strain BWP17 genomic DNA (Table 3.2). Both PCR products were transformed with EcoRI/NotI-double digested pDDB343 into strain L40 to produce plasmid pDDB353 through *in vivo* recombination. The complete ORF of *MDS3* was verified by sequencing.

The *MDS3-HA* tagged vector DDB499 was constructed as follows. In order to find a location in *MDS3*'s ORF that could be tagged without affecting Mds3 function, we performed random mutagenesis of *MDS3* using the GPS-LS Linker Scanning System (New England BioLabs). A NheI/AhdI fragment from plasmid DDB353 containing *MDS3* and its flanking regions was cloned into a NheI/AhdI digested pGEM-T Easy vector (Promega) pDDB407, to generate plasmid pDDB408. pDDB408 was used as substrate for random Tn7 insertion mutagenesis. Plasmids carrying Tn7 integrations within *MDS3*'s ORF were screened by the PCR using primer S and primer N (Promega), MDS3null 5-detect, and MDS3null 3-detect (Table 3.2). The Tn7 transposon was excised and plasmids were religated, leaving a 15bp insertion that contains a PmeI site. Plasmids containing mutated versions of *MDS3*'s ORF were AhdI/NdeI digested, subcloned into a NotI/EcoRI digested pDDB409 by *in vivo* recombination and tested for complementation of an *mds3Δ/Δ* mutant. Plasmid pDDB500, containing a 5 amino acid insertion at amino acid 1051, was selected for HA tagging. The HA tag was PCR amplified from plasmid pDDB369 (pMG1921 (Gerami-Nejad et al., 2009)) using primers MDS3-HA 56 5' and MDS3-HA 56 3' (Table 3.2) and *in vivo* recombined into the PmeI digested plasmid pDDB500 using *S. cerevisiae* L40 strain, to generate pDDB499, which inserts HA after residue 1056. pDDB499 rescued the *mds3Δ/Δ* mutant, indicating that Mds3 tolerated the addition of the 29 amino acids of the 3xHA tag.

Plasmid pDDB409 was constructed by replacing the unique NruI site in pDDB78 with a 26 bp linker containing NgoMIV-KpnI-NheI restriction sites. The 26 bp primers NgoMIV KpnI

NheI x NruI 5' and NgoMIV KpnI NheI x NruI 3' were annealed, and ligated in NruI digested pDDB78 to give pDDB409.

### **Media and growth conditions**

*C. albicans* was routinely grown at 30°C in YPD (2% Bacto-peptone, 2% dextrose, 1% yeast extract). For selection of Ura<sup>+</sup>, His<sup>+</sup> or Trp<sup>+</sup> transformants, synthetic medium without uridine, histidine or tryptophan was used (0.17% yeast nitrogen base without ammonium sulfate (Q-BioGene), 0.5% ammonium sulfate, 2% dextrose, and supplemented with a dropout mix containing amino and nucleic acids except those necessary for the selection (Adams et al., 1997)). Media were buffered at the indicated pH using 150mM HEPES. The assays for filamentation in the presence of rapamycin were performed in M199 medium (Gibco BRL) buffered at pH 8, and SLAD (0.17% yeast nitrogen base without ammonium sulfate (Q-BioGene), 50µM ammonium sulfate, 2% dextrose). Filamentation assays were conducted at 37°C except as indicated. Rapamycin (LC Laboratories) was added to the media at the indicated concentrations from a stock solution in 90% ethanol-10% Tween-20. For liquid assays of filamentation in the presence of rapamycin, strains were pre-grown in liquid YPD at 30°C, pelleted, resuspended in an equal volume of PBS and diluted 1:100 in M199 pH 8 supplemented with rapamycin or solvent alone. Samples were incubated for 6 hrs. To determine the % of hyphae producing cells, samples were gently sonicated and quantified under the microscope. The values reported represent the average of at least two independent experiments, in which every strain was tested at least in duplicate. For filamentation in serum, strains were pre-grown in liquid YPD at 30°C, diluted 1:100 in liquid YPD supplemented with 10% fetal bovine serum (Gibco) and incubated at 37°C for 5.5 hrs. For growth assays in the presence of rapamycin, strains were pre-grown in liquid YPD at 30°C, diluted in PBS to an OD 600nm of 1.6, then serially diluted 5-fold in PBS, spotted on YPD or Spider medium (1% mannitol, 1% nutrient broth, 0.2% K<sub>2</sub>HPO<sub>4</sub>, pH 7.2 before autoclaving (Liu

et al., 1994)) supplemented with rapamycin or solvent alone and incubated at 30°C for 2 or 3 days. All media except that for selection of Ura<sup>+</sup> transformants were supplemented with 80 µg/ml uridine. For solid media, 2% Bacto-agar was added, except for Spider medium which used 1.35% Bacto-agar.

### **Microarray analysis**

Strains were pre-grown in YPD at 30°C, pelleted, washed with M199 pH 4 or pH 8 medium, diluted 40-fold in pre-warmed M199 pH 4 or pH 8 and incubated for 4 hrs at 37°C with agitation. Procedures for RNA extraction, microarray construction and analysis have been previously described (Bensen et al., 2004). Corrected *P* values for the Gene Ontology (GO) categories were obtained using the GO Term Finder algorithms available through the Candida Genome Database website ([www.candidagenome.org](http://www.candidagenome.org)) on February 2009.

### **Northern blot analysis**

Cells were grown overnight in YPD at 30°C. The following day, cells were washed with M199 medium at either pH4 or pH8 and diluted 40-fold into fresh M199 pH4 or pH8 medium containing solvent or 5nM rapamycin and incubated for 4 hours at 37°C with agitation. For Spider medium experiments, cells were diluted 1:40 in Spider medium containing solvent or 5nM rapamycin and incubated for 4 hours at 37°C with agitation. For YPD medium experiments, cells were grown as described previously (Bastidas et al., 2009). Briefly, YPD overnights were inoculated into YPD at an OD ~0.1. Cells were grown 5 hours at 30°C, followed by 1 hour at 30°C with solvent or 20nM rapamycin. Cells were then harvested and frozen in a dry ice-EtOH bath. RNA extraction and Northern blot procedures were previously described (Bensen et al., 2004), except that the PCR products for the probes were purified with a PCR purification kit

(Qiagen). RNA concentration was measured using a NanoDrop Spectrophotometer ND-1000. Probes for *ECE1* and *HWPI* were described previously (Davis et al., 2002).

### **Statistical analysis**

Statistical analysis for data in Table 5 was performed using the software SAS 9.13 (SAS Institute Inc. 2004). We used repeated ANCOVA analysis (assuming different variances for each strain) and included “day of experiment” as covariate. We tested for strain-treatment interaction, and compared specific strain treatment effects after adjusting for multiple comparisons using Bonferroni correction (14 comparisons were made, significant *P* values < 0.05/14=0.0036).

### **Microscopy**

Pictures of colonies were taken using a Canon Powershot A560 digital camera on a Zeiss Opton microscope. Images of liquid cultures were captured using a Zeiss Axio camera, Axiovision 4.6.3 software (Zeiss), and a Zeiss AxioImager fluorescence microscope. All images were processed with Adobe Photoshop 7.0 software.

### **Protein purification and Western blot analysis**

Overnight cultures of *C. albicans* were diluted 200-fold into M199 pH 8 or YPD medium and grown for 4-5 hours at 30°C. Cells were pelleted and resuspended in ice-cold RIPA buffer (50mM Tris pH 8, 150mM NaCl, 1% NP-40, 3mM EDTA, 0.5% deoxycholate, 0.1% SDS) containing 1µg/ml leupeptin, 2µg/ml aprotinin, 1µg/ml pepstatin, 0.1mM phenylmethylsulfonyl fluoride, and 10 mM dithiothreitol and lysed by vortexing with acid-washed glass beads for 1 hour at 4 °C. Cell lysates were pelleted and supernatants stored at -80°C. For Western blot assays of input, ~1.25 mg of total protein was resuspended in 2X SDS gel-loading buffer (100mM Tris-Cl, pH 6.8; 200mM dithiothreitol; 4% SDS; 0.1% bromophenol blue; 20% glycerol), boiled at 95-

100°C for 3 minutes and run in 8% SDS-PAGE gel. Proteins were transferred to nitrocellulose and blocked in 6 % nonfat milk in TBS-T (50mM Tris, pH 7.6, 150mM NaCl, 0.1% Tween 20). Blots were incubated with anti-HA (F-7 probe, Santa Cruz) or anti-Myc (Invitrogen) at 1:1000 dilution or 1:5000 respectively in 6% non-fat milk TBS-T, washed in TBS-T, and incubated with anti-mouse–horseradish peroxidase antibody (GE Healthcare) at 1:5000 in 6% nonfat milk in TBS-T. Blots were washed in TBS-T, incubated with ECL reagent (GE Healthcare), and exposed to film.

### **Co-Immunoprecipitations**

Mds3-HA was immunoprecipitated as follows. ~18mg of total protein was incubated overnight at 4°C with 20µl of slurry anti-HA agarose beads (Sigma-Aldrich). Beads were washed four times with Tris-buffered saline (25 mM Tris, 0.15 M NaCl, pH 7.2, 0.05% Tween). Protein was eluted from the beads by resuspension in 50µl 2x SDS gel loading buffer and boiling for 5 minutes. The products of two immunoprecipitations were combined, separated by SDS-PAGE, and analyzed by Western blot.

## RESULTS

### Mds3 affects TOR-dependent gene expression

Mds3 acts in parallel to the Rim101 pathway to promote the yeast-to-hyphal morphogenetic switch in response to neutral-alkaline pH (Davis et al., 2002). To gain insights into how Mds3 contributes to pH responses, we determined the transcriptional profiles of wild-type, *rim101Δ/Δ*, and *mds3Δ/Δ* strains grown at pH 8 and pH 4 (Supplemental Table S3.1). The microarray experiments for all three strains were performed concomitantly, but the results for the wild-type and *rim101Δ/Δ* strains, including the microarray methodology and validation, have been reported previously (Bensen et al., 2004).

Since Mds3 and Rim101 are required for growth and morphogenesis at alkaline pH, we expected that most transcriptional differences observed between the mutant strains and wild-type would occur at pH 8. Indeed, ~80% (287) and ~95% (180) of all differentially expressed ORFs in the *mds3Δ/Δ* and *rim101Δ/Δ* mutants, respectively, occurred at pH 8 (Table 3.3 and (Bensen et al., 2004)). Further, because the *mds3Δ/Δ* and *rim101Δ/Δ* mutants are defective for filamentation at alkaline pH, we expected to find common changes in the expression of hyphal associated genes. In fact, the expression of genes associated with cell wall/filamentation were decreased in the *mds3Δ/Δ* and *rim101Δ/Δ* mutants relative to the wild-type strain (Table 3.4 and (Bensen et al., 2004)). Thus, *mds3Δ/Δ* and *rim101Δ/Δ* mutants share similar transcriptional defects, as predicted based on their similar phenotypes at alkaline pH.

However, as Mds3 and Rim101 act in parallel, we also expected to find differences between the transcriptional profiles of these mutants relative to the wild-type strain. Indeed several fundamental differences were observed. First, the *mds3Δ/Δ* mutant affected the expression of twice as many genes as did the *rim101Δ/Δ* mutant (363 total ORFs vs. 187 total ORFs, respectively) (Table 3.3). ~60% (229) of the genes affected by the *mds3Δ/Δ* mutant were not pH-regulated in wild-type cells, compared to ~38% (72) genes in the *rim101Δ/Δ* mutant (Figure 3.1).

Second, the *mds3* $\Delta/\Delta$  mutant affected the expression of more genes at pH 4 than the *rim101* $\Delta/\Delta$  mutant (76 vs. 7 genes respectively) (Table 3.3). Third, in the *rim101* $\Delta/\Delta$  mutant, ~70% of the differentially expressed genes showed reduced expression, suggesting that Rim101 primarily functions as a positive regulator (Table 3.3). However, in the *mds3* $\Delta/\Delta$  mutant, the differentially expressed genes showed increased and reduced expression at an ~50:50 ratio, demonstrating that Mds3 functions as both a positive and negative regulator (Table 3.3). Overall, these results suggest that Mds3 has broader effects on gene expression than Rim101 and that Mds3 has roles in addition to adaptation to environmental pH.

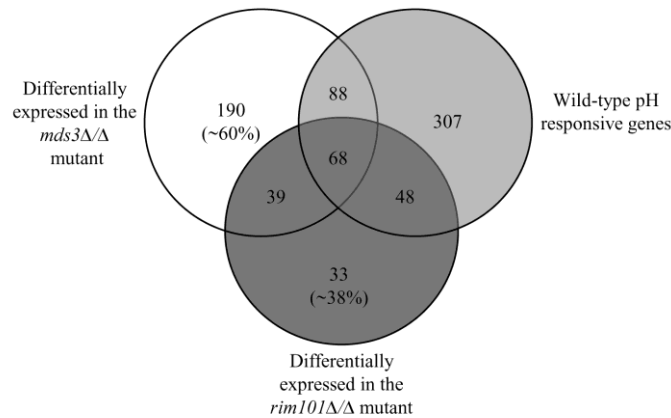


**Figure 3.1:** VENN diagram of wild-type, Mds3, and Rim101-dependent genes. Differentially expressed genes in the *mds3* $\Delta/\Delta$  (white circle) or *rim101* $\Delta/\Delta$  (dark grey circle) mutants vs. the wild-type strain were separated into pH-dependent and pH-independent depending on whether these ORFs were differentially expressed in wild-type cells in response to pH (light grey circle). Genes that were differentially regulated in the *mds3* $\Delta/\Delta$  or *rim101* $\Delta/\Delta$  mutant vs. the wild-type strain at both pH 8 and pH 4 were only included once in this analysis. Numbers in parentheses represent the % ORFs that are pH-independent.

To identify potential biological functions for Mds3, we analyzed the Mds3-dependent genes by gene ontology (GO). Of the genes up-regulated in the *mds3* $\Delta/\Delta$  mutant compared to the wild-type strain, the GO categories of “Glycolysis” and “Translation” were significantly over-represented ( $P < 1.1E-04$  and  $P < 5.3E-15$  respectively) (Table 3.4 and Supplemental Table S3.1). In wild-type cells, most of the ORFs in “Translation” were expressed preferentially at pH 8

compared to pH 4 (Bensen et al., 2004). This suggests that loss of Mds3 enhances these gene expression changes observed in wild-type cells at alkaline pH. Of the genes down-regulated in the *mds3Δ/Δ* mutant compared to the wild-type strain, the GO categories of “Amino acid transport” and “Vacuolar protein catabolic activity” ( $P < 4.7E-04$  and  $P < 1.6E-03$  respectively) were significantly overrepresented (Table 3.4). Further, the categories of “Amine transport,” “Lytic vacuole,” “Glycolysis,” and “Translation” were also overrepresented when this analysis was done in the *mds3Δ/Δ* mutant exclusively for genes that are pH-independent (data not shown). These results show that Mds3 affects a variety of distinct processes, including growth and starvation responses, and supports the idea that Mds3 has functions in pH-independent processes.

In order to corroborate the microarray results, we analyzed the expression of several *MDS3*-dependent ORFs by Northern blot (Figure 3.2A). In M199 pH 8 medium, the glycolysis gene *CDC19* and the translation genes *RPS26A* and *TEF1* were expressed ~2 - 4-fold more in the *mds3Δ/Δ* mutant than the wild-type or the complemented *mds3Δ/Δ +MDS3* strains (Figure 3.2A, lanes 6-8). Increased expression of *CDC19*, *RPS26A*, and *TEF1* in the *mds3Δ/Δ* mutant was also observed at pH 4 (Figure 3.2A, lanes 1-3), suggesting that Mds3 governs expression of these genes in a pH-independent manner. *GAP2*, an amino acid transport gene, was reduced > 2-fold in the *mds3Δ/Δ* mutant compared to the wild-type or the *mds3Δ/Δ +MDS3* complemented strains at both pH 4 and pH 8 (Figure 3.2A, compare lanes 2 and 7 with lanes 1, 3, 6, and 8). These results establish the veracity of the microarray data and support the idea that Mds3 has pH-independent functions.

The GO categories affected by the *mds3Δ/Δ* mutant reflect processes that are transcriptionally regulated by the TOR pathway. During conditions of active growth, TOR positively regulates expression of genes involved in ribosomal biogenesis, translation initiation and elongation, rRNA and tRNA synthesis, and glycolysis (Wullschleger et al., 2006) and negatively regulates expression of genes involved in protein degradation and nitrogen catabolite

repression (NCR) (Bastidas et al., 2009; Cardenas et al., 1999; Hardwick et al., 1999; Shamji et al., 2000). During starvation conditions, TOR is inactive and genes involved in translation and glycolysis are repressed while genes involved in amino acid transport and vacuolar degradation are induced (Bastidas et al., 2009; Cardenas et al., 1999; Hardwick et al., 1999; Shamji et al., 2000). Since the *mds3Δ/Δ* mutant shows gene expression differences that reflect TOR activation, we hypothesized that Mds3 functions as a negative regulator of TOR.

To address the idea that Mds3 is a negative regulator of TOR, we predicted that rapamycin, a TOR inhibitor (Heitman et al., 1991), would rescue the transcriptional defects associated with the *mds3Δ/Δ* mutant. Indeed, 5nM rapamycin reduced expression of *CDC19*, *RPS26A*, and *TEF1* and restored expression of *GAP2* in *mds3Δ/Δ* mutant cells compared to solvent alone (Figure 3.2A, compare lanes 6-8 and 11-13). Rapamycin did not appear to affect expression of *RPS26A*, *TEF1*, and *GAP2* in the wild-type or *mds3Δ/Δ+MDS3* complemented strains; however expression of *CDC19* was increased ~2-fold compared to solvent alone. Regardless, in the presence of rapamycin expression of *CDC19*, *RPS26A*, *TEF1*, and *GAP2* was quantitatively similar in wild-type, *mds3Δ/Δ*, and *mds3Δ/Δ +MDS3* cells. These results demonstrate that rapamycin restores the transcriptional defects due to loss of Mds3 and corroborates the idea that Mds3 acts as a negative regulator of TOR.

In nutrient poor Spider medium, we observed similar transcriptional results (Figure 3.2B). Expression of *CDC19*, *RPS26A*, and *TEF1* was increased in the *mds3Δ/Δ* mutant compared to wild-type (Figure 3.2B, compare lanes 1 and 2). Further, addition of rapamycin reduced *CDC19*, *RPS26A*, and *TEF1* expression in the *mds3Δ/Δ* mutant, wild-type, and *mds3Δ/Δ +MDS3* complemented strains. We noted that in Spider medium this rapamycin-dependent restoration of gene expression in the *mds3Δ/Δ* mutant was less than that observed in M199 pH 8 medium. We also found that in Spider medium, *GAP2* was expressed poorly in wild-type cells and expressed at greater levels in the absence of *MDS3*. Addition of rapamycin increased *GAP2*

expression in all strains tested (Figure 3.2B, compare lanes 1-5 with 6-10). These results support the idea that Mds3 acts in the TOR pathway, and suggests that, not surprisingly, growth medium differences cause distinct effects.

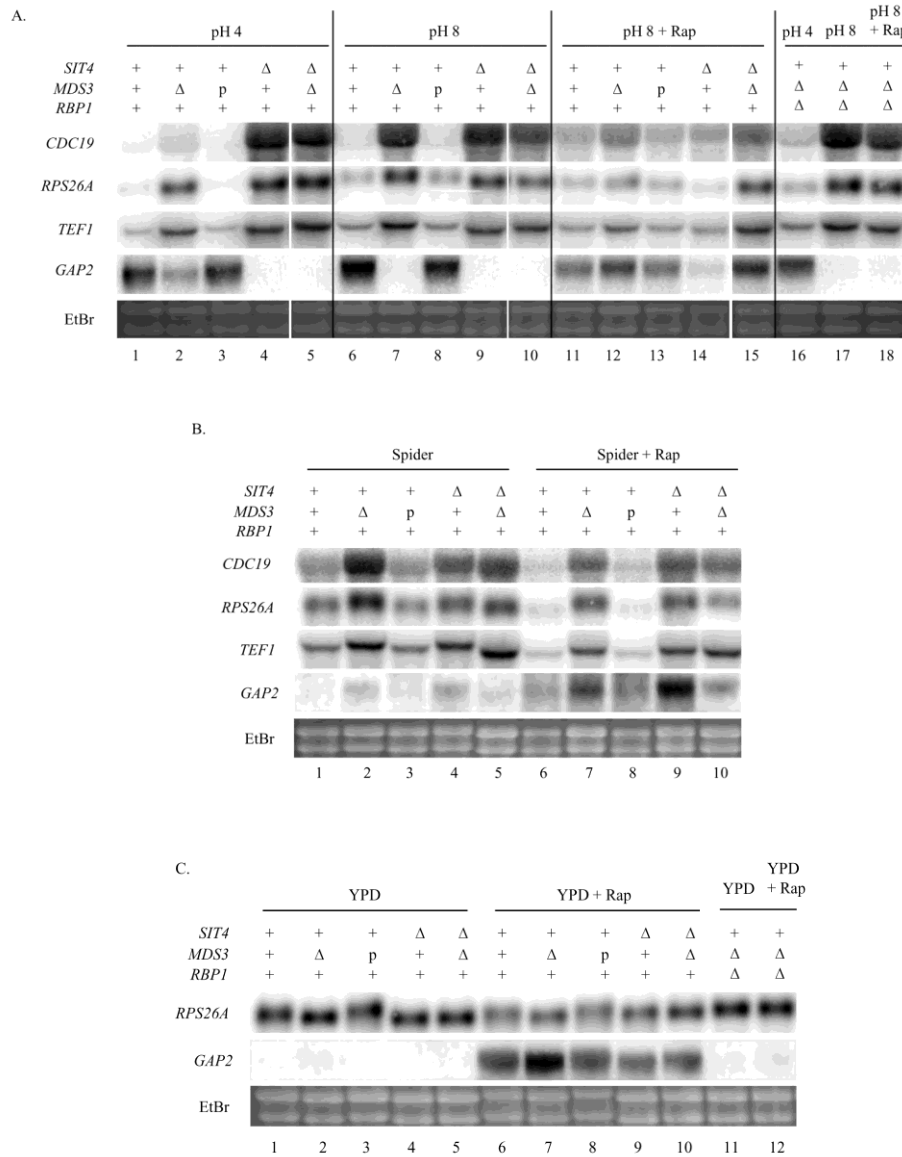


**Figure 3.2:** Microarray validation by Northern blot analysis. Overnight YPD cultures of the wild-type (DAY185), *mds3* $\Delta/\Delta$  (DAY1118), *mds3* $\Delta/\Delta$ +*MDS3* (DAY1119), *sit4* $\Delta/\Delta$  (DAY972), *sit4* $\Delta/\Delta$  *mds3* $\Delta/\Delta$  (DAY1233), and *mds3* $\Delta/\Delta$  *rbp1* $\Delta/\Delta$  (DAY1239) strains were diluted in pre-warmed M199 pH 8 (A), Spider medium (B), or YPD (C) with or without rapamycin. Ethidium bromide staining was used as a loading control because commonly used loading controls (*TEF1*, *ACT1* or *TDH3*) varied in expression due to the mutations, the growth conditions and/or the addition of the rapamycin. *MDS3*, *SIT4*, and *RBP1* genotypes are noted above the samples: wild-type (+), deletion ( $\Delta$ ), or complemented (p).

### **Rapamycin rescues the *mds3Δ/Δ* mutant filamentation defect**

The TOR pathway regulates fungal morphogenesis (Cutler et al., 2001), and rapamycin triggers the expression of hyphal associated genes in *C. albicans* (Bastidas et al., 2009). Since Mds3 also regulates morphogenesis and is required for the expression of hyphal associated genes (Davis et al., 2002), we asked if rapamycin also rescues expression of these genes in the *mds3Δ/Δ* mutant (Figure 3.3A). Wild-type, *mds3Δ/Δ*, and *mds3Δ/Δ +MDS3* cells were incubated in M199 pH 8 medium at 37°C, which promotes hyphal formation, with and without 5nM rapamycin and analyzed for expression of the hyphal associated genes *HWP1* and *ECE1* (Figure 3.3A). While the *mds3Δ/Δ* mutant showed little *HWP1* and *ECE1* expression, addition of rapamycin completely restored this expression (Figure 3.3A, compare lanes 2 and 5). We noted that rapamycin also led to increased expression of *HWP1* and *ECE1* in both wild-type and *mds3Δ/Δ +MDS3* strains compared to solvent alone. Thus, rapamycin promotes expression of hyphal associated genes and rescues the *mds3Δ/Δ* mutant defects in *HWP1* and *ECE1* expression.

Since rapamycin rescued the transcriptional defects associated with loss of Mds3, we asked if rapamycin could also rescue the hyphal formation defect of the *mds3Δ/Δ* mutant. In liquid M199 pH 8 medium at 37°C, >90% of wild-type cells germinated to form hyphae; <5% of *mds3Δ/Δ* mutant cells germinated to form hyphae (Table 3.5 and Figure 3.3B). However, addition of 5nM rapamycin partially restored hyphal formation in the *mds3Δ/Δ* mutant to 45% ( $P < 0.0001$  compared to *mds3Δ/Δ* in solvent) (Figure 3.3B and Table 3.5). Rapamycin also promoted hyphal formation in wild-type cells compared to the solvent control ( $P < 0.001$ ) (Table 3.5), and we noted that the hyphae formed in the wild-type, *mds3Δ/Δ*, and *mds3Δ/Δ +MDS3* strains in the presence of rapamycin appeared less branched than in solvent alone. Similar results were observed in liquid SLAD medium, a nutrient poor medium, indicating that the effect of rapamycin is not specific to M199 medium (Figure 3.4A). These results demonstrate that rapamycin rescues the morphogenetic defect of the *mds3Δ/Δ* mutant.

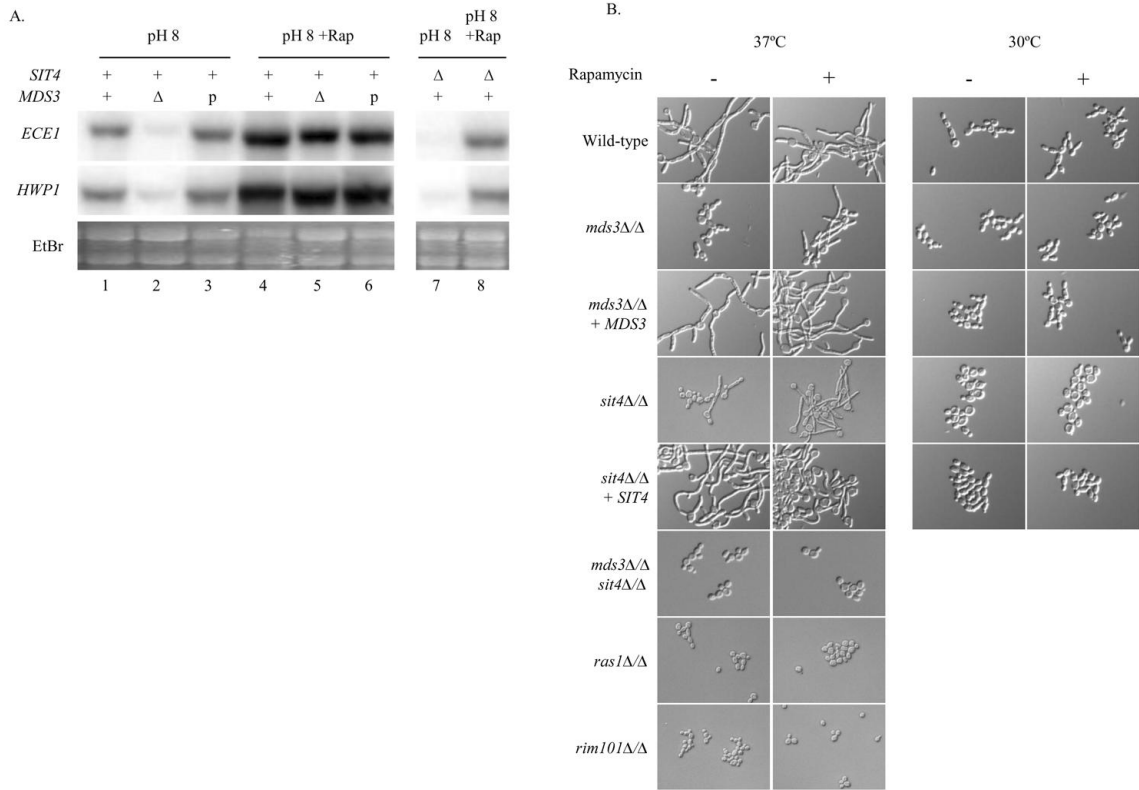


**Figure 3.3:** Rapamycin rescues *mds3Δ/Δ* hyphal associated phenotypes. A) Northern blots of hyphae associated genes performed on the wild-type (DAY185), *mds3Δ/Δ* (DAY1118), *mds3Δ/Δ+MDS3* (DAY1119), and *sit4Δ/Δ* (DAY972) strains grown for 4 hrs in M199 pH 8 supplemented with solvent or 5nM rapamycin. *MDS3* and *SIT4* genotypes are noted above the samples: wild-type (+), deletion (Δ), or complemented (p). B) Overnight YPD cultures of the wild-type (DAY185), *mds3Δ/Δ* (DAY1118), *mds3Δ/Δ+MDS3* (DAY1119), *sit4Δ/Δ* (DAY972), *sit4Δ/Δ+SIT4* (DAY973), *mds3Δ/Δ sit4Δ/Δ* (DAY1233), *rim101Δ/Δ* (DAY25), and *ras1Δ/Δ* (DAY1109) strains were washed in PBS and diluted 1:100 in M199 pH 8 liquid medium with and without 5nM rapamycin. Cells were visualized under the microscope (40X) after 6 hrs of incubation at 30°C or at 37°C.

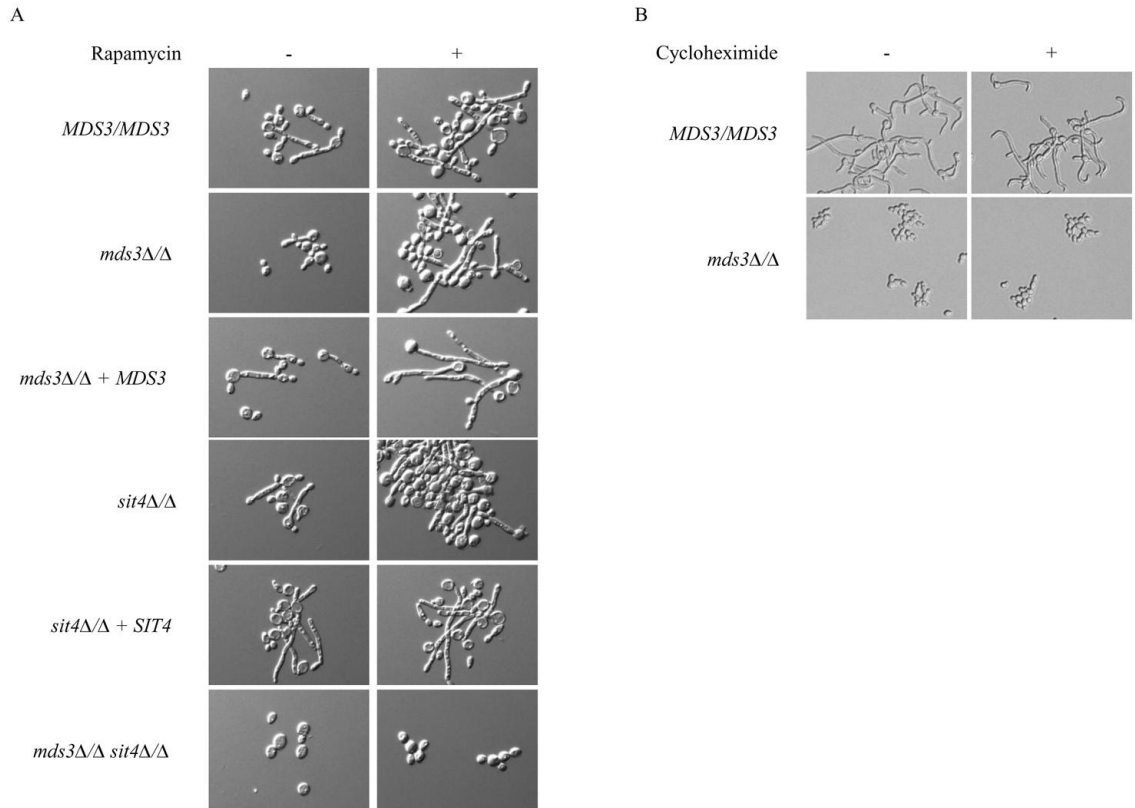


**Figure 3.4:** Rapamycin rescues *mds3Δ/Δ* filamentation defects in nutrient poor medium but cycloheximide does not. (A) Wild-type (DAY185), *mds3Δ/Δ* (DAY1118), *mds3Δ/Δ+MDS3* (DAY1119), *sit4Δ/Δ* (DAY971), *sit4Δ/Δ+SIT4* (DAY973), and *mds3Δ/Δ sit4Δ/Δ* (DAY1233) cells were grown for 6 hrs in SLAD liquid medium at 37°C with or without 10nM rapamycin. (B) Wild-type (DAY185) and *mds3Δ/Δ* (DAY1118) cells were grown for 6 hrs in M199 pH 8 liquid medium at 37°C with or without 100μM cycloheximide. Similar results were observed with 150μM and 250μM cycloheximide but higher concentrations inhibited growth of all strains tested.

We found that the effect of rapamycin on hyphal formation was not due to translational inhibition, because cycloheximide did not rescue the filamentation defect of the *mds3Δ/Δ* mutant (Figure 3.4B). Further rapamycin is not a constitutive inducer of hyphal formation, because rapamycin did not rescue the *mds3Δ/Δ* hyphal formation defect in M199 pH 8 medium at 30°C (Figure 3.3B). These results demonstrate that rapamycin is not a constitutive inducer of hyphal formation and further support a link between Mds3 and TOR.

To determine if the effect of rapamycin was actually dependent on TOR, we introduced the rapamycin resistant *TOR1-1* allele into the wild-type and *mds3Δ/Δ* strains and determined if rapamycin still promoted hyphal formation (Cafferkey et al., 1993; Cruz et al., 2001). As expected, strains carrying a *TOR1-1* allele were resistant to rapamycin (Figure 3.5A). In the absence of rapamycin, the *TOR1-1* allele did not affect hyphal formation in either the *MDS3/MDS3* or *mds3Δ/Δ* backgrounds (Figure 3.5B and Table 3.5). However, in the presence of rapamycin, the *TOR1-1* allele prevented the rapamycin-induced hyphal formation observed in *MDS3/MDS3* cells (Table 3.5), and the hypha formed showed a branching pattern similar to the wild-type strain without rapamycin (Figure 3.5B). Thus, in the *MDS3/MDS3* background rapamycin-mediated phenotypes are TOR-dependent. In the presence of rapamycin, the *TOR1-1* allele reduced the rapamycin-induced hyphal formation observed in *mds3Δ/Δ* cells by ~50% (Table 3.5). We hypothesized that the semi-responsive effect of rapamycin in the *mds3Δ/Δ TOR1-1/TOR1* mutant was an attribute of the remaining wild-type *TOR1* allele. To address this possibility, we constructed *TOR1-1/Δ* strains in the *MDS3/MDS3* and *mds3Δ/Δ* backgrounds. Deletion of one copy of *TOR1* in either background had no significant effect on hyphal formation (Figure 3.5B and Table 3.5), demonstrating that *TOR1* is not haploinsufficient. While the *MDS3/MDS3 TOR1-1/Δ* strain filamented similarly to the *MDS3/MDS3 TOR1-1/TOR1* strain in the presence or absence of rapamycin, the *mds3Δ/Δ TOR1-1/Δ* strain failed to filament in the presence or absence of rapamycin (Figure 3.5B and Table 3.5). The *mds3Δ/Δ TOR1-1/Δ* mutant did form hyphae in serum, an *MDS3*-independent inducer of hyphal formation (data not shown and (Davis et al., 2002)), demonstrating that the *mds3Δ/Δ TOR1-1/Δ* strain did not have an absolute block in hyphal formation. These results demonstrate that rapamycin rescues *mds3Δ/Δ* phenotypes through TOR.

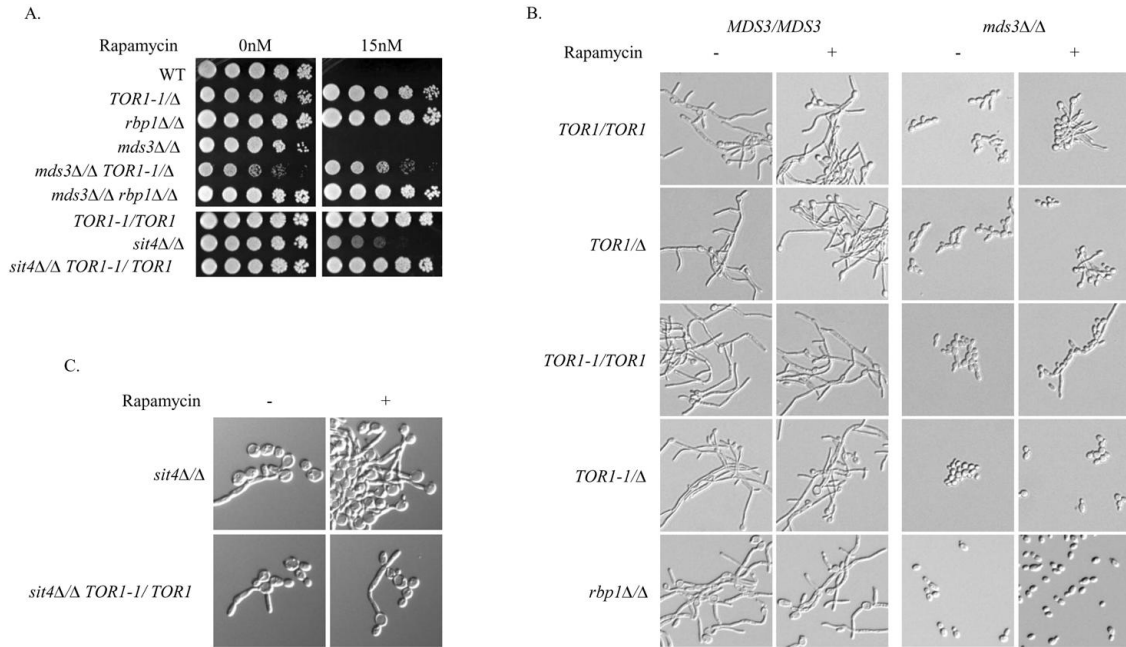


**Figure 3.5:** The effect of rapamycin on filamentation is TOR dependent. (A) Wild-type (DAY185), *TOR1-1/tor1*Δ (DAY1125), *rbp1*Δ/Δ (DAY1223), *mds3*Δ/Δ (DAY1118), *mds3*Δ/Δ *TOR1-1/tor1*Δ (DAY1124), *mds3*Δ/Δ *rbp1*Δ/Δ (DAY1239), *TOR1-1/TOR1* (DAY1121), *sit4*Δ/Δ (DAY972), and *sit4*Δ/Δ *TOR1-1/TOR1* (DAY1321) strains were grown overnight in YPD and serial dilutions spotted onto YPD with or without 15nM rapamycin. (B) Overnight YPD cultures of the wild-type and the *mds3*Δ/Δ backgrounds carrying *TOR1/TOR1* (DAY185 and DAY1118), *TOR1*Δ (DAY1123 and DAY1122), *TOR1-1/TOR1* (DAY1121 and DAY1255), *TOR1-1*Δ alleles (DAY1125 and DAY1124) or *rbp1*Δ/Δ deletion (DAY1223 and DAY1239); and (C) *sit4*Δ/Δ *TOR1/TOR1* (DAY972) and *sit4*Δ/Δ *TOR1-1/TOR1* (DAY1321) were washed in PBS and diluted 1:100 in M199 pH 8 liquid medium with and without 5nM rapamycin.

We noted that in the absence of a wild-type copy of *TOR1*, the *TOR1-1* allele conferred growth defects in both the wild-type and *mds3*Δ/Δ backgrounds (Figure 3.5A and 3.6), demonstrating that the *TOR1-1* allele is not completely functional. Thus, we considered that this growth defect could influence our hyphal formation data. To address this, we constructed an *mds3*Δ/Δ *rbp1*Δ/Δ double mutant, which did not have a growth defect (Figure 3.5A). Rapamycin inhibits the TOR kinase as a complex with Rbp1 (FKBP12 in mammals), and *rbp1*Δ/Δ mutants are rapamycin resistant (Figure 3.5A and (Cruz et al., 2001)). While *rbp1*Δ/Δ mutants did not have a defect in hyphal formation, loss of Rbp1 in the *mds3*Δ/Δ background completely blocked the ability of rapamycin to rescue the *mds3*Δ/Δ hyphal formation defects (Figure 3.5B and Table

3.6). Loss of Rbp1 also prevented the transcriptional effects of rapamycin in the *mds3Δ/Δ* mutant (Figures 3.2A lanes 16-18, and 3.2C lanes 11-12). In total, these results clearly demonstrate that the transcriptional effects of the *mds3Δ/Δ* mutant have biological consequences that are associated with inappropriate activation of the TOR pathway.

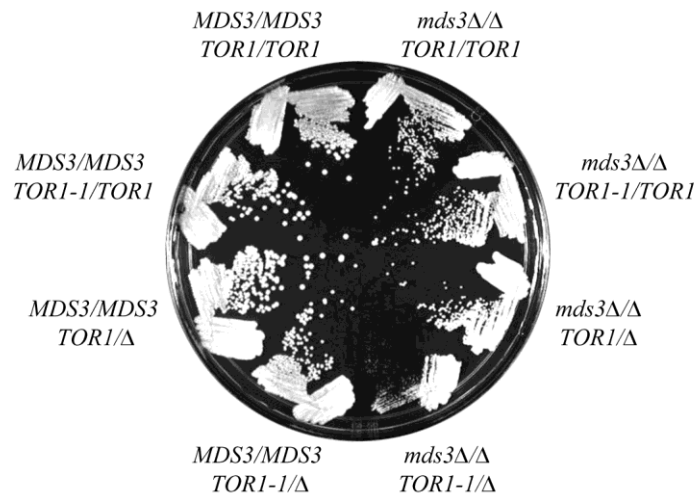


**Figure 3.6:** The *TOR1-1/Δ mds3Δ/Δ* mutant grows poorly. (A) Overnight YPD cultures of the wild-type and the *mds3Δ/Δ* backgrounds carrying *TOR1/TOR1* (DAY185 and DAY1118), *TOR1/Δ* (DAY1123 and DAY1122), *TOR1-1/TOR1* (DAY1121 and DAY1255), or *TOR1-1/Δ* alleles (DAY1125 and DAY1124) or *rbp1Δ/Δ* deletion (DAY1223 and DAY1239) were streaked onto YPD medium at 30°C for 2 days.

### Mds3 and the TOR effector Sit4 act similarly

One downstream effector of the TOR pathway is the type 2A-like phosphatase Sit4 (Duvel and Broach, 2004; Duvel et al., 2003; Rohde and Cardenas, 2004). Sit4 promotes starvation responses and is inhibited by TOR-dependent phosphorylation during periods of active growth (DiComo and Jiang, 2006; Jiang and Broach, 1999). Thus, in the absence of Sit4, TOR-dependent starvation responses are defective. Since the *mds3Δ/Δ* mutant is also defective for TOR-dependent starvation responses and promotes TOR activation (Table 3.4 and Figure 3.2), we predicted that a *sit4Δ/Δ* mutant may have similar transcriptional defects as the *mds3Δ/Δ* mutant. Indeed, in the *sit4Δ/Δ* mutant, *CDC19*, *RPS26A*, and *TEF1* were expressed at higher

levels when compared to the wild-type strain at both pH 4 and pH 8 (Figure 3.2A, compare lanes 4 and 9 with lanes 1 and 6) and in nutrient poor Spider medium (Figure 3.2B). We noted that at pH 4 *CDC19* expression in the *sit4Δ/Δ* mutant was ~4-fold higher than in the *mds3Δ/Δ* mutant. Further, in the *sit4Δ/Δ* mutant, *GAP2* was not expressed at either pH 4 or pH 8, although it was expressed more in Spider medium similar to the *mds3Δ/Δ* mutant. Thus, loss of Sit4 has similar transcriptional effects as loss of Mds3.

Addition of rapamycin to *sit4Δ/Δ* cells reduced expression of *CDC19*, *RPS26A*, and *TEF1* to approximately wild-type levels in M199 pH 8 medium (Figure 3.2A, compare lanes 9 and 14), but had a more modest effect on Spider medium (Figure 3.2B). Rapamycin also promoted expression of *GAP2* in *sit4Δ/Δ* cells. However in M199 pH 8 medium, *GAP2* expression was still ~2-fold lower than wild-type cells, indicating that Sit4 is required for full induction of *GAP2*. These results demonstrate that loss of Sit4 promotes activation of the TOR pathway similar to the loss of Mds3 and provides independent support for the idea that Mds3 acts in the TOR pathway.

Sit4 is also required for hyphal formation in *C. albicans* ((Lee et al., 2004) and Figure 3.3B). We found that *sit4Δ/Δ* mutant cells expressed little *HWPI* and *ECE1* in M199 pH 8 medium and that this defect was partially rescued by addition of rapamycin (Figure 3.3A, lanes 7 and 8). Similar to the *mds3Δ/Δ* mutant, rapamycin rescued the *sit4Δ/Δ* hyphal formation defect in M199 pH 8 (12.9±0.1% in solvent vs 60.5±2.6% in rapamycin) and SLAD media (9.2±1.0% in solvent vs 19.2±0.5% in rapamycin) (Figure 3.3B and 3.4A), and this rescue was prevented by the *TOR1-1* rapamycin resistant allele (Figure 3.5A and 3.5C). Importantly, rapamycin did not rescue the filamentation defects associated with loss of Ras1 or Rim101, which are not associated with the TOR pathway (Figure 3.3B). In total, these results suggest a functional association between Mds3 and Sit4.

To determine if Mds3 and Sit4 act in the same pathway or parallel pathways, we constructed an *mds3Δ/Δ sit4Δ/Δ* double mutant. If Mds3 and Sit4 function in the same pathway, then the *mds3Δ/Δ sit4Δ/Δ* double mutant should have similar phenotypes as either single mutant; if Mds3 and Sit4 function in parallel pathways then the *mds3Δ/Δ sit4Δ/Δ* double mutant should have more severe phenotypes than either single mutant. The *mds3Δ/Δ sit4Δ/Δ* double mutant expressed *CDC19*, *RPS26A*, *TEF1*, and *GAP2* similarly to the *mds3Δ/Δ* and *sit4Δ/Δ* single mutants in M199 pH 8 and Spider media (Figure 3.2A, compare lanes 7, 9, and 10). In M199 pH 4 medium, the *mds3Δ/Δ sit4Δ/Δ* double mutant behaved similarly to the *sit4Δ/Δ* single mutant, which had a more severe phenotype than the *mds3Δ/Δ* mutant (Figure 3.2A, compare lanes 2, 4, and 5). In Spider medium, the *mds3Δ/Δ sit4Δ/Δ* double mutant also behaved similarly to the *sit4Δ/Δ* single mutant. However, the *mds3Δ/Δ* single mutant had a more severe phenotype, indicating a dominant effect of the *sit4Δ/Δ* mutation (Figure 3.2B, compare lanes 2, 4, and 5). These results demonstrate that the *mds3Δ/Δ sit4Δ/Δ* mutant does not have transcriptional defects beyond that of the single mutants, suggesting Mds3 and Sit4 act in the same pathway. However, addition of rapamycin did not restore *CDC19*, *RPS26A*, and *TEF1* expression in the *mds3Δ/Δ sit4Δ/Δ* double mutant (Figures 3.2A, lanes 12, 14-15 and 3.2B, lanes 7, 9-10), although it did restore *GAP2* expression (Figure 3.2A, lanes 10 and 15). Rapamycin also did not rescue the hyphal formation defect associated with the *mds3Δ/Δ sit4Δ/Δ* double mutant (Figures 3.3 and 3.4A), which suggests that Mds3 and/or Sit4 may have additional parallel functions.

We noted that regardless of pH, wild-type cells grown in M199 medium express relatively little *RPS26A* and robust levels of *GAP2*, suggesting that this medium may be a nutrient poor medium (Figure 3.2A, lane 1). Since TOR responds to nutrient availability, we asked if Mds3 and Sit4 effect gene expression in a nutrient rich environment. Thus, we determined *RPS26A* and *GAP2* expression in rich YPD medium with or without rapamycin. Unlike the results obtained for M199 pH 8 and Spider medium (Figure 3.2A and B), we observed robust

expression of *RPS26A* and no expression of *GAP2* in wild-type cells, and cells lacking Mds3 and/or Sit4 behaved similarly (Figure 3.2C, compare lane 1 with lanes 2, 4, and 5). Addition of rapamycin reduced expression of *RPS26A* and promoted expression of *GAP2* in wild-type cells, as expected if TOR is inhibited (Figure 3.2C, lane 6). Addition of rapamycin had a similar effect on *mds3Δ/Δ*, *sit4Δ/Δ*, and *mds3Δ/Δ sit4Δ/Δ* mutants (Figure 3.2C, lanes 7, 9, and 10). Further, this effect is clearly due to TOR inhibition as *RPS26A* and *GAP2* expression was similar in the *mds3Δ/Δ rbp1Δ/Δ* double mutant with and without rapamycin (Figure 3.2C, lanes 11 and 12). We noted that *GAP2* expression in the presence of rapamycin was consistently higher in the *mds3Δ/Δ* mutant and that this increase was *SIT4*-dependent. This is in contrast to the results observed in M199 pH 8 medium, where *GAP2* expression in the *mds3Δ/Δ* mutant in the presence of rapamycin appears to be Sit4-independent. These results suggest that M199 medium is a more nutrient poor medium than YPD and suggest that Mds3 and Sit4 contribute to the regulation of TOR-dependent targets in nutrient poor conditions.

### **Mds3 promotes rapamycin sensitivity**

Since rapamycin rescued the filamentation defects of the *mds3Δ/Δ* and the *sit4Δ/Δ* mutants, we wanted to determine if these mutations affected rapamycin sensitivity in *C. albicans*. On YPD medium, the wild-type, *mds3Δ/Δ*, and *mds3Δ/Δ + MDS3* strains showed similar rapamycin sensitivities, but the *sit4Δ/Δ* mutant was resistant to rapamycin (Figure 3.7A). Complementation of the *sit4Δ/Δ* mutant restored rapamycin sensitivity to wild-type levels. This result for the *sit4Δ/Δ* mutant is in sharp contrast to the situation in *S. cerevisiae* where the *sit4Δ* mutant is sensitive to rapamycin and this sensitivity can be rescued by *C. albicans SIT4*, suggesting Sit4 is functioning similarly in the two organisms (Cutler et al., 2001; Lee et al., 2004). These results indicate that *MDS3* does not affect rapamycin sensitivity in rich medium,

and that unlike the case in *S. cerevisiae* Sit4 function promotes rapamycin sensitivity in *C. albicans*.

Since Mds3 appears to promote TOR-dependent responses in nutrient poor conditions, we considered that Mds3 may affect rapamycin sensitivity on nutrient poor medium. Indeed, while wild-type cells were sensitive to 5nM rapamycin on nutrient poor Spider medium, the *mds3Δ/Δ* mutant was resistant (Figure 3.7A). Similar results were also observed for the *sit4Δ/Δ* mutant. The *mds3Δ/Δ sit4Δ/Δ* double mutant behaved like the *sit4Δ/Δ* single mutant on both media, suggesting that Sit4 and Mds3 do not make independent contributions to rapamycin sensitivity. These results demonstrate that Mds3 and Sit4 promote rapamycin sensitivity in *C. albicans*, and support the idea that different nutrient conditions have distinct constraints on the TOR pathway and the function of Mds3 and Sit4 in the TOR pathway.

Since the function of Sit4 in *S. cerevisiae* promotes rapamycin resistance (Cutler et al., 2001), we predicted that the function of Mds3 in *S. cerevisiae* would be similar. To test this hypothesis, we determined the rapamycin sensitivity of congenic wild-type, *mds3Δ*, *pmd1Δ* (an *MDS3* paralog), and *mds3Δ pmd1Δ S. cerevisiae* strains (Figure 3.7B). On rich medium, the wild-type and *pmd1Δ* mutant grew similarly in the presence of rapamycin, and the *mds3Δ* and *mds3Δ pmd1Δ* mutants were more sensitive to rapamycin. Similar results were observed in nutrient poor Spider medium, however we noted that the *mds3Δ pmd1Δ* double mutant grew extremely poorly on this medium (Figure 3.7B). Since the rapamycin sensitivities of the *mds3Δ* and *mds3Δ pmd1Δ* mutants were similar and since the *pmd1Δ* mutant did not confer rapamycin sensitivity, we conclude that Mds3, but not Pmd1 functions in the TOR pathway. Cells lacking Sit4 or Mds3 have similar phenotypes in relation to rapamycin sensitivity, however these phenotypes are disparate between *S. cerevisiae* and *C. albicans*. Thus, we conclude that Mds3 and Sit4 function similarly in *C. albicans* and *S. cerevisiae* but that the effect of these functions has changed since *C. albicans* and *S. cerevisiae* split evolutionarily.

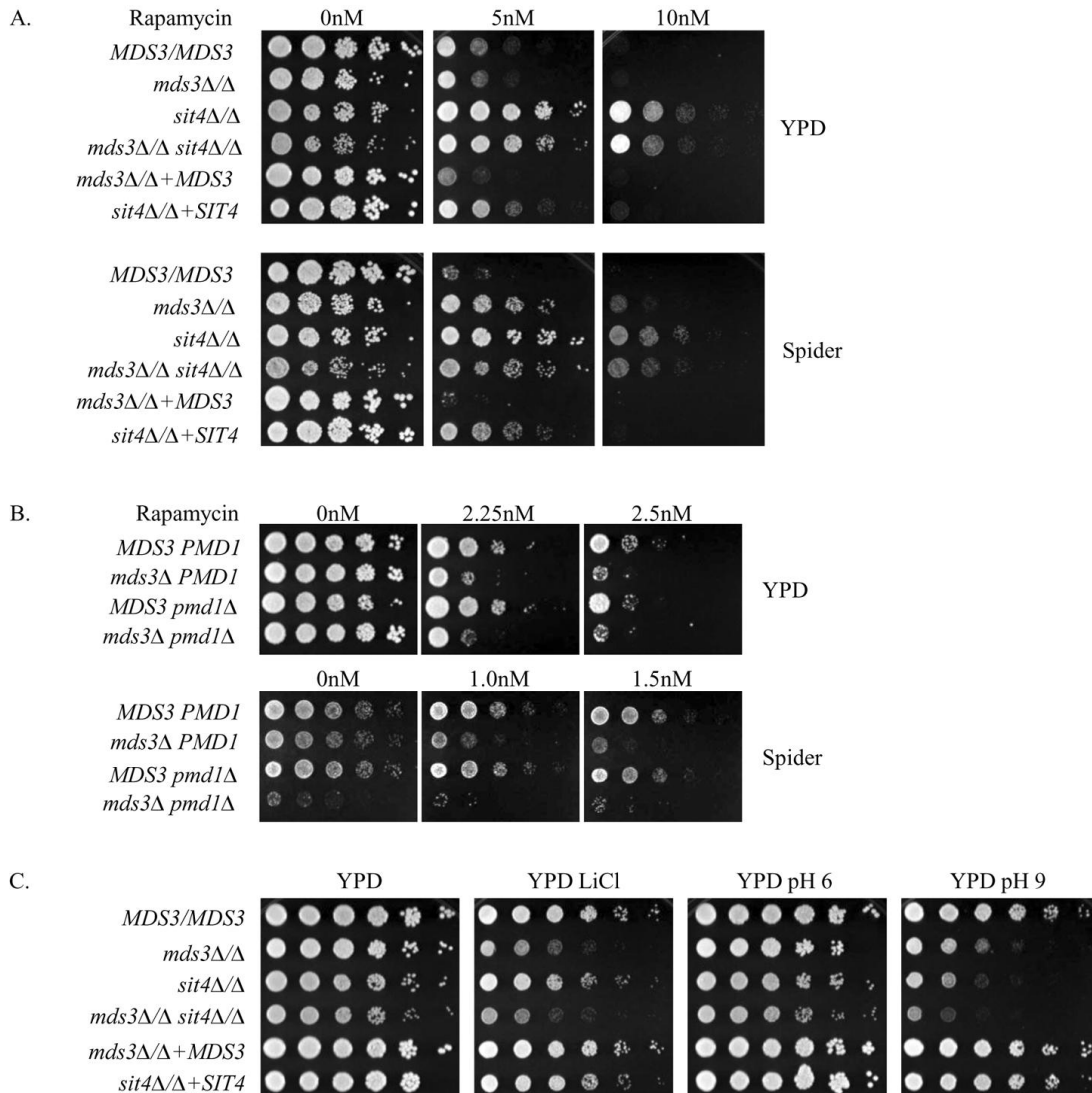


**Figure 3.7:** Mds3 and TOR pathway members have altered rapamycin resistance. (A) *C. albicans* wild-type (DAY185), *mds3Δ/Δ* (DAY1118), *sit4Δ/Δ* (DAY972), *sit4Δ/Δ +SIT4* (DAY973), *mds3Δ/Δ+MDS3* (DAY1119), and *mds3Δ/Δ sit4Δ/Δ* (DAY1233) strains were serially diluted in PBS and spotted onto YPD or Spider media with or without rapamycin. (B) *S. cerevisiae* wild-type (DAY1208), *mds3Δ PMD1* (DAY1209), *MDS3 pmd1Δ* (DAY1210), and *mds3Δ pmd1Δ* (DAY1211) strains were serially diluted in PBS and spotted onto YPD or Spider media supplemented with or without rapamycin. Plates were photographed after 48 or 72 hrs growth at 30°C. (C.) *C. albicans* strains, above, were serially diluted in PBS and spotted onto YPD, YPD supplemented with 150mM LiCl or buffered at pH 6 or pH 9. Growth was scored after 48 hrs of incubation at 30°C.

Because the *mds3* $\Delta/\Delta$  and *sit4* $\Delta/\Delta$  mutants share a number of phenotypic traits, we wanted to determine if the *sit4* $\Delta/\Delta$  mutant had other *mds3* $\Delta/\Delta$ -dependent phenotypes (Davis et al., 2002). While the *sit4* $\Delta/\Delta$  mutant has a slight growth defect on YPD, YPD +LiCl, or YPD pH 6 medium, the *sit4* $\Delta/\Delta$  mutant had a severe growth defect on YPD pH 9 medium that was rescued by reintroduction of a wild-type copy of *SIT4* (Figure 3.7C). The *mds3* $\Delta/\Delta$  *sit4* $\Delta/\Delta$  double mutant grew worse on both YPD and YPD pH 9 medium than either single mutant (Figure 3.7C), supporting the idea that Mds3 and Sit4 have some independent functions. The *mds3* $\Delta/\Delta$  *sit4* $\Delta/\Delta$  double mutant grew similarly to the *mds3* $\Delta/\Delta$  mutant on LiCl medium, suggesting that Sit4 does not play a role in response to this stress medium. These results support a model in which Mds3 and Sit4 function similarly in the TOR pathway, but are not completely dependent.

### **Mds3 and Sit4 physically interact**

Mds3 was identified as a protein that interacts with Sit4 in a *S. cerevisiae* proteomic screen (Gavin et al., 2002, 2006). Since we have demonstrated a strong genetic interaction between Mds3 and Sit4, we tested whether Mds3 and Sit4 can indeed physically interact. Thus, we generated a strain carrying a functional C-terminal 13xMyc tagged *SIT4* allele and then introduced a functional *MDS3* allele containing the 3xHA epitope. Whole cell extracts of cells grown in M199 pH 8 medium were immunoprecipitated with  $\alpha$ -HA and separated by SDS PAGE. Sit4-Myc was detected in similar amounts in whole cell extracts from strains with and without Mds3-HA (Figure 3.8). In  $\alpha$ -HA immunoprecipitates from cells containing Mds3-HA, Sit4-Myc was pulled down. Sit4-Myc was not detected in  $\alpha$ -HA immunoprecipitates in the absence of Mds3-HA, demonstrating that Sit4-Myc is specifically associating with Mds3-HA. Similar results were observed in whole cell extracts from cells grown in YPD, indicating that this interaction is not dependent on nutrient availability (Figure 3.8). Thus, Mds3 and Sit4 physically interact, demonstrating that Mds3 is a member of the TOR pathway.

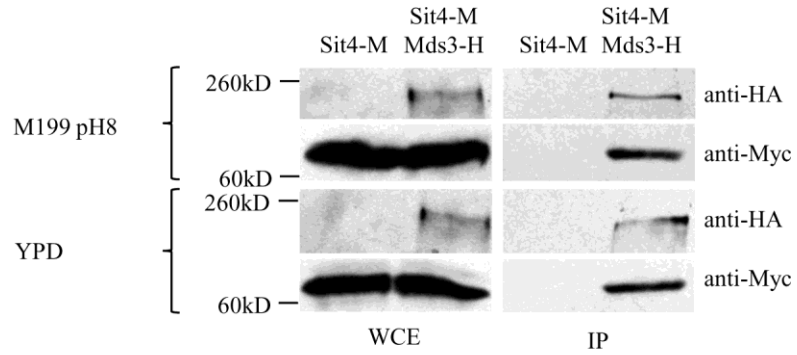


**Figure 3.8:** Mds3 and Sit4 interact physically. *C. albicans* Sit4-Myc tagged (Sit4-M) strains with and without Mds3-HA (Mds3-H) (DAY1236 and DAY1235 respectively) were grown in M199 pH 8 and YPD. An aliquot of the whole cell extracts (WCE) were separated by SDS-PAGE and an aliquot was incubated with  $\alpha$ -HA beads, centrifuged, washed, and eluted (IP) prior to SDS-PAGE. Blots were probed with  $\alpha$ -HA first, stripped, and then probed with  $\alpha$ -Myc.

## DISCUSSION

Growth and morphogenesis is controlled by numerous signal transduction pathways which respond to diverse environmental cues. The TOR pathway is a key regulator of growth and morphogenesis in eukaryotes, and in *C. albicans*, the TOR pathway governs the yeast-to-hyphal morphogenetic transition, which is critical for pathogenesis (Cutler et al., 2001; Whiteway and Oberholzer, 2004). Microarray analyses suggested that *MDS3* is a member of the TOR pathway in *C. albicans* and this idea was supported by genetic, pharmacological, and biochemical approaches. Thus, Mds3 represents a new member of the TOR morphogenetic pathway.

### **How does Mds3 contribute to the TOR pathway?**

Mds3 is a 1383 amino acid protein with predicted Kelch repeats in the N-terminal region but no other obvious motifs and functional domains (Davis et al., 2002). Kelch repeats form a  $\beta$ -propeller structure that functions as a protein-protein interaction domain, and is found in an array of proteins, including cytoskeletal proteins and signal transduction proteins (Adams et al., 2000; Feierbach et al., 2004; Harashima and Heitman, 2002; Lu and Hirsch, 2005). To the best of our knowledge Mds3 represents the first Kelch repeat protein associated with the TOR pathway. However, two components of the TOR complex, Lst8 and Kog1 (G $\beta$ L and Raptor in mammalian systems), contain WD-40 domains, which also fold into  $\beta$ -propeller structures (Chen and Kaiser, 2003; Gettemans et al., 2003; Kim et al., 2002, 2003; Loewith et al., 2002). Thus, we propose that Mds3 may act as a scaffold to facilitate interactions between TOR pathway members to control morphogenetic processes in *C. albicans*.

Based on our results, which include the transcriptional and morphological similarities between the *mds3 $\Delta$ / $\Delta$*  and *sit4 $\Delta$ / $\Delta$*  mutants that are rescued by rapamycin and the interaction between Mds3 and Sit4, we propose two models to explain how Mds3 acts in the TOR pathway (Figure 3.9). First, Mds3 may act upstream of TOR potentially as a member of a nutrient sensitive

complex such as the one composed by Raptor, GβL, and mTOR (Kim et al., 2002, 2003). Support for this model comes from the fact that rapamycin, which inhibits TOR kinase activity, rescues the transcriptional defects and morphogenetic defects associated with the *mds3Δ/Δ* mutant (Figures 3.2-3.4). Further, rapamycin-mediated rescue of the *mds3Δ/Δ* mutant is lost with the introduction of a *TOR1-1* allele or loss of Rbp1 (Figures 3.2 and 3.5). Based on this data Mds3 appears to act upstream of TOR. However, for this model to be accurate, Mds3 interacts indirectly with Sit4.

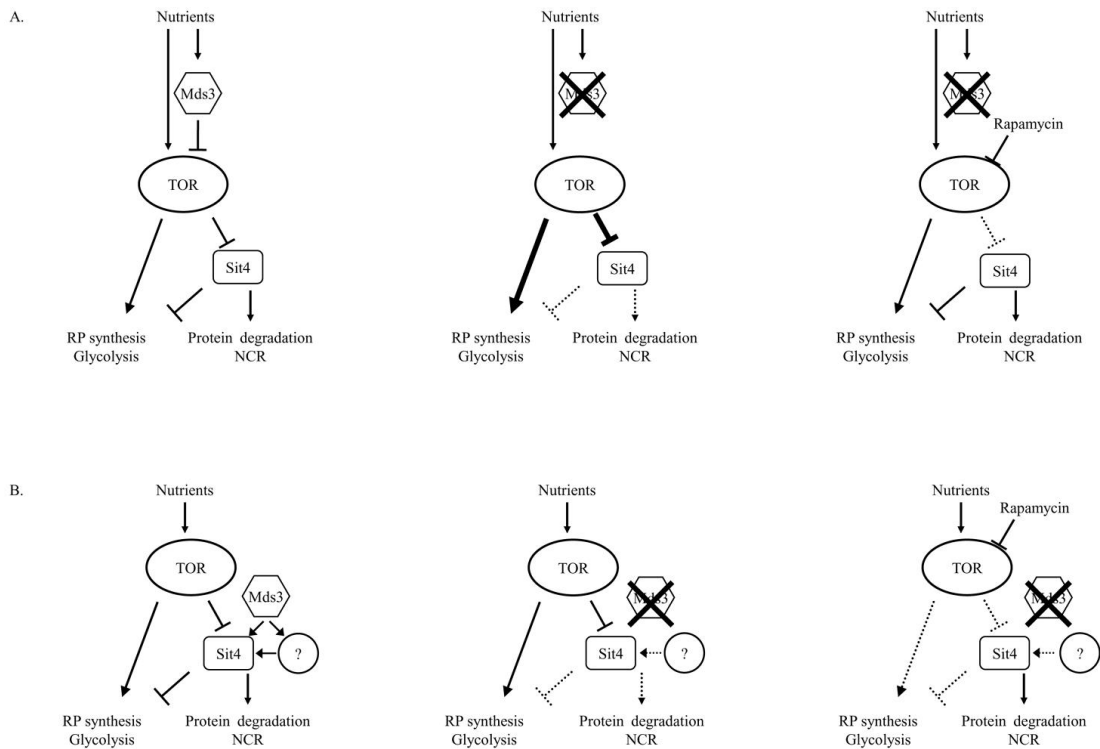


**Figure 3.9:** Models of Mds3 as a TOR pathway member. (A) Mds3 as an upstream negative regulator of TOR (left). Loss of Mds3 leads to increased expression of genes involved in translation and increased repression of Sit4 and less expression of the NCR genes (middle). This loss of negative regulation can be restored with rapamycin (right). (B) Mds3 as a downstream member of the Sit4-dependent pathway inhibited by TOR. This Sit4-dependent pathway inhibits expression of RP synthesis genes and promotes expression of NCR genes (left). Loss of Mds3 (or Sit4) leads to increased expression of genes involved in translation and decreased expression of the NCR genes (middle). Rapamycin inhibits TOR activation, restoring RP synthesis expression by reduced TOR kinase function. NCR expression is also restored, although this mechanism is not yet understood (right).

How could Mds3 function upstream of TOR? One possibility is that Mds3 modulates the interaction of Kog1 and Lst8, Raptor and GβL in mammalian systems, with TOR. GβL promotes TOR kinase activity, and Raptor-GβL constitutively interacts with mTOR. However, Raptor-GβL-mTOR interaction is effected by nutrient signals (Kim et al., 2002). Under nutrient poor conditions Raptor-mTOR interaction is stabilized, which interferes with GβL-stimulation of mTOR (Kim et al., 2003). In yeast, Kog1-Lst8 interaction with Tor1 does not appear to be effected by nutrient status (Loewith et al., 2002). This led to the hypothesis that an additional factor, such as Mds3, may be involved that affects the activity of Kog1 and/or Lst8 on Tor1.

An alternative model is that Mds3 acts downstream of Tor1 to promote starvation responses when Tor1 is inactive (Figure 3.9). Support for this model comes from the fact that the *sit4Δ/Δ* mutant has similar transcriptional and morphological defects as the *mds3Δ/Δ* mutant, and that these defects are rescued by rapamycin (Figures 3.2-3.5). Additionally both *mds3Δ/Δ* and *sit4Δ/Δ* mutants are sensitive to alkaline pH (Figure 3.7C). Since rapamycin inhibits TOR kinase activity, these results suggest that the transcriptional and morphogenetic defects associated with the *mds3Δ/Δ* and *sit4Δ/Δ* mutants are due to an increase in TOR kinase activity or TOR kinase-dependent activities, and that reduced kinase activity by rapamycin is sufficient to rescue the *sit4Δ/Δ* and *mds3Δ/Δ* mutants. Finally the fact that Mds3 and Sit4 coimmunoprecipitate suggests that these proteins interact within the same complex either directly or indirectly. One potential problem for this model is the restoration of *GAP2* expression by rapamycin in the *mds3Δ/Δ* mutant (Figure 3.2). However, *GAP2* expression is also rescued by rapamycin in the *sit4Δ/Δ* mutant. Thus, additional PP2As, which are activated by rapamycin treatment, may promote expression of *GAP2* independent of Mds3 or Sit4. A similar phenomenon has been described in *S. cerevisiae* (Cox et al., 2004; Georis et al., 2009; Tate et al., 2009). Finally, we noted that the *TOR1-1* allele and *mds3Δ/Δ* mutation had a synergistic effect, which generally suggests parallel pathways. However, the *TOR1-1* allele and similar alleles, have altered functions in both *S.*

*pombe* and mammalian systems (McMahon et al., 2002; Vilella-Bach et al., 1999; Weisman and Choder, 2001) and we find that *TOR1-1* confers growth defects in the absence of a wild-type *TOR1* allele (Figures 3.5A and 3.6B). Thus, we propose that the *TOR1-1 mds3Δ/Δ* synergism reflects defective kinase function in Tor1-1, which exacerbates the TOR pathway defects associated with the *mds3Δ/Δ* mutant.

How could Mds3 function downstream of TOR? One possibility is that Mds3 acts as a scaffold bridging TOR activity to its effectors. For example, Sit4 activity is dependent upon its association with Tap42 and several Sit4 associated proteins (SAPs), and Mds3 may govern these associations (DiComo and Arndt, 1996; Duvel and Broach, 2004; Luke et al., 1996). Mds3 may facilitate or stabilize these interactions to promote Sit4 activity. Support for this idea comes from large scale protein-protein interaction analyses that identified Sap185, a Sit4 regulatory protein, as an Mds3 binding partner (DiComo and Arndt, 1996; Gavin et al., 2002, 2006; Luke et al., 1996).

### **Mds3, TOR, and nutrient sensing**

TOR kinase activity is controlled by nutrient availability (Crespo et al., 2002; DiComo and Arndt, 1996; Kim et al., 2002; Rohde and Cardenas, 2004). In nutrient rich conditions, TOR kinase activity is stimulated leading to activation of growth processes and inactivation of starvation responses. In starvation conditions, TOR kinase activity is inhibited preventing the activation of growth responses and leading to activation of starvation responses. Here, we found that wild-type cells promote expression of *RPS26A* and repression of *GAP2* when grown in YPD, but promote expression of *RPS26A*, although to reduced levels compared to YPD, and *GAP2* when grown in M199 (Figure 3.2). This suggests that M199 is nutrient poor when compared to YPD. Further, wild-type cells divide slower in M199 pH 8 medium compared to M199 pH 4 medium suggesting that M199 pH 8 is more poor than M199 pH 4 medium. This latter growth

difference can be explained by the inhibition of plasma membrane transporters and the dependence on endocytic uptake of nutrients in alkali environments (Munn and Riezman, 1994; van der Rest et al., 1995; Weissman et al., 2008). Thus, YPD > M199 pH 4 > M199 pH 8 in nutrient availability, and cells grown in these media may require different levels of TOR kinase activity.

We found that the *mds3* $\Delta/\Delta$  and *sit4* $\Delta/\Delta$  mutants did not affect expression of TOR-dependent genes when grown in YPD, as expected if Mds3 and Sit4 promote TOR-dependent starvation responses (Figure 3.2). In M199 pH 8 medium and Spider medium, the *mds3* $\Delta/\Delta$  and *sit4* $\Delta/\Delta$  mutants had similar defects suggesting that both media are nutrient poor and require TOR-dependent starvation responses. In M199 pH 4 medium, the *mds3* $\Delta/\Delta$  and *sit4* $\Delta/\Delta$  mutants did not repress *CDC19*, *RPS26A*, or *TEF1* nor did they induce *GAP2* to wild-type levels, supporting the idea that M199 pH 4 medium is a semi-starvation medium that requires some level of the TOR-dependent starvation response. In M199 pH 4 medium, the *sit4* $\Delta/\Delta$  mutant clearly had a more severe defect in repression of *CDC19* and *RPS26A* and induction of *GAP2* than the *mds3* $\Delta/\Delta$  mutant. This represents the first demonstration that Sit4 negatively regulates RP synthesis and is in contrast with work from *S. cerevisiae*, which suggests that Sit4 does not govern RP synthesis (Duvel et al., 2003; Schmelzle et al., 2004). However, these results suggest that Sit4 plays a more general role in promoting TOR-dependent starvation responses than Mds3. For example, Sit4 may be required under both semi-starvation and starvation conditions, whereas Mds3 may only function under starvation conditions. This idea is supported by the fact that the *mds3* $\Delta/\Delta$  mutant was resistant to rapamycin in nutrient poor medium, but not in rich medium, whereas the *sit4* $\Delta/\Delta$  mutant was resistant to rapamycin in both media (Figure 3.7A).

### **Mds3 function in *C. albicans* and *S. cerevisiae***

*MDS3* was first identified in *S. cerevisiae* as a multicopy suppressor of the  $\Delta mck1$  sporulation defect and was subsequently identified as a regulator of the *C. albicans* yeast-to-hyphal transition (Benni and Neigeborn, 1997; Davis et al., 2002). These morphogenetic processes are promoted by neutral-alkaline environmental pH, which led to the idea that Mds3 is a pH response regulator similar to Rim101. This idea was supported by the fact that Mds3 is required for wild-type growth at alkaline pH (Davis et al., 2002). However, Mds3 is also required for chlamydospore and biofilm formation in *C. albicans*, neither of which require neutral-alkaline pH (Nobile et al., 2003; Richard et al., 2005). We also found that the *mds3* $\Delta/\Delta$  mutant has a slight growth defect on rich medium, which is acidic, and our microarray studies demonstrated that the *mds3* $\Delta/\Delta$  mutant showed transcriptional changes at both acidic and alkaline pH (Figures 3.1-3.3A, 3.6 and Tables 3.3, 3.4, and S3.1). Thus, Mds3 clearly plays a broader role than neutral-alkaline pH regulation in *C. albicans*, and we propose that the morphogenetic defects observed in the *mds3* $\Delta/\Delta$  mutant reflect defects in general cellular processes that are also required for growth and filamentation at alkaline pH.

In *S. cerevisiae*, Mds3 and Pmd1 are proposed to act upstream or in parallel to the Ras/PKA pathway (Benni and Neigeborn, 1997; McDonald et al., 2009), because the sporulation defect of the *mds3* $\Delta$  *pmd1* $\Delta$  double mutant was rescued by the hyperactive *RAS2*<sup>V19</sup> allele (Benni and Neigeborn, 1997). However, several lines of evidence suggest that Mds3 is unlikely to function upstream of Ras, independent of TOR. First, the hyperactive *RAS2*<sup>V19</sup> allele rescues TOR pathway mutants in *S. cerevisiae* suggesting that Ras2 acts in parallel or downstream of the TOR pathway (Cutler et al., 2001; Schmelzle et al., 2004; Zurita-Martinez and Cardenas, 2005). Second, the filamentation defect of the *ras1* $\Delta/\Delta$  mutant is not rescued by rapamycin, unlike the *mds3* $\Delta/\Delta$  mutant (Figures 3.7 and (Feng et al., 1999; Leberer et al., 2001)). Third, we found that both the  $\Delta sit4$  and  $\Delta mds3$  mutants are sensitive to rapamycin in *S. cerevisiae*. Thus, we propose

that Mds3 acts in the TOR pathway in both *S. cerevisiae* and *C. albicans*, but that the hyperactive *RAS2*<sup>V19</sup> allele is able to bypass this by acting either in parallel or downstream of TOR.

Why does *S. cerevisiae* encode two *MDS3* paralogs? In *S. cerevisiae*, phenotypes associated with the  $\Delta mds3$  mutant are masked by the functionally redundant *PMD1* (Benni and Neigeborn, 1997; Davis et al., 2002). However, we found that the *S. cerevisiae*  $\Delta mds3$  mutant, like the  $\Delta sit4$  mutant but not the  $\Delta pmd1$  mutant, was sensitive to rapamycin, which is the first demonstration that Mds3 and Pmd1 are not completely redundant in *S. cerevisiae*. In *C. albicans*, the  $mds3\Delta/\Delta$  and  $sit4\Delta/\Delta$  mutants behave similarly, however our results suggest that Mds3 has Sit4-independent functions. First, the  $mds3\Delta/\Delta$  mutant is sensitive to high concentration of LiCl, whereas the  $sit4\Delta/\Delta$  mutant is not (Figure 3.7C and (Davis et al., 2002)). Second, the  $mds3\Delta/\Delta sit4\Delta/\Delta$  double mutant has more severe growth defects on YPD and at alkaline pH than either single mutant (Figure 3.7C). Third, the filamentation defect of the  $mds3\Delta/\Delta sit4\Delta/\Delta$  double mutant is not rescued by rapamycin (Figures 3.3 and 3.4). Thus, in *C. albicans*, Mds3 has Sit4-dependent and -independent function. This raises the interesting possibility that in *S. cerevisiae*, Mds3 governs the Sit4-dependent functions, rapamycin sensitivity, and Pmd1 governs the Sit4-independent functions. It is not yet known if Sit4-independent functions of Mds3 in *C. albicans* occur through the TOR pathway or completely independent of the TOR pathway.

While Mds3 appears to act in the TOR pathway in both *C. albicans* and *S. cerevisiae*, our results have demonstrated that the role of TOR pathway in these organisms has diverged. In *S. cerevisiae*, sporulation requires both nitrogen and carbon starvation and is negatively regulated by Mds3. This suggests that Mds3 functions as a positive regulator of the TOR pathway (Benni and Neigeborn, 1997; McDonald et al., 2009). However, we have clearly shown that Mds3 functions as a negative regulator of the TOR pathway in *C. albicans* during starvation conditions. Thus, while the TOR pathway is mechanistically similar in *C. albicans* and *S. cerevisiae*, the signals coming in to and/or responses coming out of the TOR pathway appear to be distinct. This idea is

supported by the rapamycin resistance observed for the *mds3* $\Delta/\Delta$  and *sit4* $\Delta/\Delta$  mutants in *C. albicans* compared to the sensitivity observed for these mutants in *S. cerevisiae* (Figure 3.7B and (Cutler et al., 2001; Lee et al., 2004). Regardless, several signal transduction pathways have been identified that while mechanistically similar lead to distinct responses in *C. albicans* and *S. cerevisiae*, which is not surprising given the ~300 million years of evolutionary distance between these organisms (Hogues et al., 2008; Ihmels et al., 2005; Martchenko et al., 2007; Tsong et al., 2006).

Despite the fact that rapamycin initially triggered interest because of its antifungal properties against *C. albicans* (Vezina et al., 1975), the TOR pathway has received relatively little attention in this organism. In fact, most work has focused on the role of TOR in multicellular organisms in processes as diverse as angiogenesis and embryogenesis. However, TOR appears to have conserved functions in growth and stress responses in both multicellular and unicellular eukaryotes (Reiling and Sabatini, 2006; Wullschleger et al., 2006). Our studies demonstrate that the kelch repeat protein Mds3, which promotes morphogenetic processes critical for pathogenesis, such as the yeast-to-hyphal transition and biofilm formation, is a new member of the TOR pathway (Davis et al., 2000a; Kumamoto and Vences, 2005; Nobile et al., 2006). Our study represents the first example in which a kelch repeat protein has been implicated in the TOR pathway and raises the possibility that an Mds3-like protein may exist in mammalian systems to promote TOR-dependent responses.

**TABLES**

**Table 3.1.** *C. albicans* and *S. cerevisiae* strains used in this study

<b>Strain</b>	<b>Parent</b>	<b>Genotype</b>	<b>Reference</b>
<b>DAY1 (BWP17)</b>	SC5314	<i>ura3::λimm434/ura3::λimm434 his1::hisG/his1::hisG arg4::hisG/arg4::hisG</i>	Wilson et al., 1999
<b>DAY25</b>	BWP17	<i>ura3::λimm434/ura3::λimm434 HIS1::his1::hisG/his1::hisG arg4::hisG/arg4::hisG rim101::ARG4/rim101::URA3</i>	Davis et al., 2000a
<b>DAY185</b>	DAY286	<i>ura3::λimm434/ura3::λimm434 HIS1::his1::hisG/his1::hisG ARG4::URA3::arg4::hisG/arg4::hisG</i>	Davis et al., 2000a
<b>DAY286</b>	BWP17	<i>ura3::λimm434/ura3::λimm434 his1::hisG/his1::hisG ARG4::URA3::arg4::hisG/arg4::hisG</i>	Wilson et al., 1999
<b>DAY414 (L40)</b>	<i>S. cerevisiae</i>	<i>MATa his3Δ200 trp1-901 leu2-3,-112 ade2 LYS2::(lexAop)<sub>4</sub>-HIS3 URA3::(lexAop)<sub>8</sub>-lacZ GAL4</i>	Vojtek et al., 1993
<b>DAY415 (VIC1)<sup>1</sup></b>	BWP17	<i>ura3::λimm434/ura3::λimm434 his1::hisG/his1::hisG arg4::hisG/arg4::hisG_mds3::ARG4/MDS3</i>	Davis et al., 2002
<b>DAY439 (VIC25)</b>	BWP17	<i>ura3::λimm434/ura3::λimm434 HIS1::his1::hisG/his1::hisG arg4::hisG/arg4::hisG mds3::Tn7::URA3/mds3::Tn7::UAU1</i>	Davis et al., 2002
<b>DAY938</b>	BWP17	<i>ura3::λimm434/ura3::λimm434 his1::hisG/his1::hisG arg4::hisG/arg4::hisG_mds3::ARG4/mds3::URA3-dpl200</i>	This study
<b>DAY956</b>	DAY938	<i>ura3::λimm434/ura3::λimm434 his1::hisG/his1::hisG arg4::hisG/arg4::hisG_mds3::ARG4/mds3::dpl200</i>	This study
<b>DAY971 (CM02)</b>	RM1000	<i>ura3::λimm434/ura3::λimm434 his1::hisG/his1::hisG sit4::HIS1/sit4::URA3</i>	Lee et al., 2004
<b>DAY972 (CM20)</b>	RM1000	<i>ura3::λimm434/ura3::λimm434 his1::hisG/his1::hisG sit4::HIS1/sit4::dpl200</i>	Lee et al., 2004
<b>DAY973 (CM22)</b>	RM1000	<i>ura3::λimm434/ura3::λimm434 his1::hisG/his1::hisG sit4::HIS1/sit4::dpl200 [pVEC1::SIT4]</i>	Lee et al., 2004
<b>DAY1109 (CDH107)</b>	CAI4	<i>ura3::λimm434/ura3::λimm434 ras1::hisG-URA3-hisG/ras1::hisG</i>	Leberer et al., 2001
<b>DAY1118</b>	DAY938	<i>ura3::λimm434/ura3::λimm434 HIS1::his1::hisG/his1::hisG arg4::hisG/arg4::hisG mds3::ARG4/mds3::URA3-dpl200</i>	This study
<b>DAY1119</b>	DAY938	<i>ura3::λimm434/ura3::λimm434 HIS1::MDS3::his1::hisG/his1::hisG arg4::hisG/arg4::hisG mds3::ARG4/mds3::URA3-dpl200</i>	This study
<b>DAY1120</b>	DAY938	<i>ura3::λimm434/ura3::λimm434 his1::hisG/his1::hisG arg4::hisG/arg4::hisG mds3:: ARG4/mds3::URA3-dpl200 TOR1-1/TOR1</i>	This study
<b>DAY1121</b>	DAY185	<i>ura3::λimm434/ura3::λimm434 HIS1::his1::hisG/his1::hisG ARG4::URA3::arg4::hisG/arg4::hisG TOR1-1/TOR1</i>	This study
<b>DAY1122</b>	DAY938	<i>ura3::λimm434/ura3::λimm434 his1::hisG/his1::hisG arg4::hisG/arg4::hisG mds3::ARG4/mds3::URA3-dpl200 TOR1/tor1::HIS1</i>	This study
<b>DAY1123</b>	DAY286	<i>ura3::λimm434/ura3::λimm434 his1::hisG/his1::hisG ARG4::URA3::arg4::hisG/arg4::hisG TOR1/tor1::HIS1</i>	This study
<b>DAY1124</b>	DAY1122	<i>ura3::λimm434/ ura3::λimm434 his1::hisG / his1::hisG arg4::hisG/ arg4::hisG mds3::ARG4/mds3::URA3-dpl200 TOR1-1/tor1::HIS1</i>	This study
<b>DAY1125</b>	DAY1123	<i>ura3::λimm434/ura3::λimm434 his1::hisG/his1::hisG ARG4::URA3::arg4::hisG/arg4::hisG TOR1-1/tor1::HIS1</i>	This study
<b>DAY1208</b>	SK1	<i>MATa/MAT□ his3/his3 leu2::hisG/leu2::hisG trp1::hisG/trp1::hisG lys2/lys2 ura3/ura3 ho::LYS2/ho::LYS2</i>	McDonald et al., 2009

<b>(MWY64)</b>			
<b>DAY1209</b>	SK1	<i>MATa/MAT</i> <sup>□</sup> <i>mds3::URA3/mds3::URA3 his3/his3 leu2::hisG/leu2::hisG trp1::hisG/trp1::hisG lys2/lys2 ura3/ura3 ho::LYS2/ho::LYS2</i>	McDonald et al., 2009
<b>(CMY164)</b>			
<b>DAY1210</b>	SK1	<i>MATa/MAT</i> <sup>□</sup> <i>pmd1::LEU2/pmd1::LEU2 his3/his3 leu2::hisG/leu2::hisG trp1::hisG/trp1::hisG lys2/lys2 ura3/ura3 ho::LYS2/ho::LYS2</i>	McDonald et al., 2009
<b>(CMY165)</b>			
<b>DAY1211</b>	SK1	<i>MATa/MAT</i> <sup>□</sup> <i>mds3::URA3/mds3::URA3 pmd1::LEU2/pmd1::LEU2 his3/his3 leu2::hisG/leu2::hisG trp1::hisG/trp1::hisG lys2/lys2 ura3/ura3 ho::LYS2/ho::LYS2</i>	McDonald et al., 2009
<b>(CMY166)</b>			
<b>DAY1223</b>	CAI4	<i>ura3::λimm434/ura3::λimm434 rbp1::MX3/rbp1::CaURA3MX3R</i>	Cruz et al., 2001
<b>DAY1230</b>	DAY1223	<i>ura3::λimm434/ura3::λimm434 rbp1::MX3/rbp1::MX3</i>	This study
<b>DAY1231</b>	DAY972	<i>ura3::λimm434/ura3::λimm434 his1::hisG/his1::hisG sit4::HIS1/sit4::dpl200 MDS3/mds3::URA3-dpl200</i>	This study
<b>DAY1232</b>	DAY1231	<i>ura3::λimm434/ura3::λimm434 his1::hisG/his1::hisG sit4::HIS1/sit4::dpl200 MDS3/mds3::dpl200</i>	This study
<b>DAY1233</b>	DAY1232	<i>ura3::λimm434/ura3::λimm434 his1::hisG/his1::hisG sit4::HIS1/sit4::dpl200 mds3::URA3-dpl200/mds3::dpl200</i>	This study
<b>DAY1234</b>	DAY1	<i>ura3::λimm434/ura3::λimm434 his1::hisG/his1::hisG arg4::hisG/arg4::hisG SIT4/SIT4-Myc-URA3</i>	This study
<b>DAY1235</b>	DAY1234	<i>ura3::λimm434/ura3::λimm434 HIS1::MDS3::his1::hisG/his1::hisG arg4::hisG/arg4::hisG SIT4/SIT4-Myc-URA3</i>	This study
<b>DAY1236</b>	DAY1234	<i>ura3::λimm434/ura3::λimm434 HIS1::MDS3-HA::his1::hisG/his1::hisG arg4::hisG/arg4::hisG SIT4/SIT4-Myc-URA3</i>	This study
<b>DAY1237</b>	DAY1230	<i>ura3::λimm434/ura3::λimm434 rbp1::MX3/rbp1::MX3 MDS3/mds3::URA3dpl200</i>	This study
<b>DAY1238</b>	DAY1237	<i>ura3::λimm434/ura3::λimm434 rbp1::MX3/rbp1::MX3 MDS3/mds3::dpl200</i>	This study
<b>DAY1239</b>	DAY1238	<i>ura3::λimm434/ura3::λimm434 rbp1::MX3/rbp1::MX3 mds3::dpl200/mds3::URA3dpl200</i>	This study
<b>DAY1255</b>	DAY1120	<i>ura3::λimm434/ura3::λimm434 HIS1::his1::hisG/his1::hisG arg4::hisG/arg4::hisG mds3:: ARG4/mds3::URA3-dpl200 TOR1-1/TOR1</i>	This study
<b>DAY1321</b>	DAY972	<i>ura3::λimm434/ura3::λimm434 his1::hisG/his1::hisG sit4::HIS1/sit4::dpl200 TOR1-1/TOR1</i>	This study

<sup>1</sup>Parent of VIC3 (*mds3::ARG4/mds3::URA3*). VIC1 was not described in Davis et al. (2002).

**Table 3.2.** Primers used in this study

Name	Sequence (5' to 3')	Reference
<b>MDS3 5DR</b>	TCTTAAGGCACAAGTTATTGGCTTGACGTAGAAGTTT GCAAAGATTTTCACAATATCATGTTTCCCAGTCACGA CGTT	Davis et al., 2002
<b>MDS3 3DR</b>	ACCAATATAACGTGAATATACACCCCTATATTATTAT CTTTTAATCCTGTTAACAATCCGTGGAATTGTGAGCG GATA	Davis et al., 2002
<b>MDS3null 5-detect</b>	GTGTCCCAATTTTGTCTAGC	This study
<b>MDS3null 3-detect</b>	TGCGGAAGAAGCTGTAAACCC	This study
<b>TOR1 5DR</b>	AGTAGATAAATACTTCTAACTTTGATAGTAACATTAAC GAAGAAAAACAAATCATTAATCATTTCCCAGTCACG ACGTT	This study
<b>TOR1 3DR</b>	TATTTCCCTTTATAAAATAGTTACACATACCATACTT AACGACACATGACGATACTCAACGTGGAATTGTGAG CGGATA	This study
<b>TOR1 5' detect-2</b>	TCTCTTAGTTGTTGAGTGGC	This study
<b>TOR1 3' detect</b>	AAATTTCTTCCAAACCTGC	This study
<b>TOR1 A-C</b>	GTTTTATGGCACGAACAATGGCACGATGCTTTGGAAG ATGCTCGCAGGTTTTTCTTTGGTGAACACAACACAGA AAAGATG	This study
<b>TOR1 A-C Rev</b>	CATCTTTTCTGTGTTGTGTTACCAAAGAAAAACCTG CGAGCATCTTCCAAAGCATCGTGCCATTGTTCTGTGCC ATAAAAC	This study
<b>JOHE6247</b>	GGCAAGGTGTTTCTTGAAGC	Cruz et al., 2001
<b>JOHE6248</b>	TACTTCTTGATTTCGCGATAGC	Cruz et al., 2001
<b>DDB78 PmeI x NruI 5'</b>	ATAATCAAAATGAGTCAATTCTCACAACCGCTCGGTT TAAACCGACACGTTTCAACGAAATGGCCTCCCCTACC A	This study
<b>DDB78 PmeI x NruI 3'</b>	TGGTAGGGGAGGCCATTTTCGTTGAAACGTGTGCGGTTT AAACCGAGCGGTTGTGAGAATTGACTCATTTTGATTA T	This study
<b>MDS3 5comp new</b>	AAGCTCGGAATTAACCCTCACTAAAGGGAACAAAAAG CTGGTGGTCTTTAATTGGGCGGAC	This study
<b>MDS3 3comp new-2</b>	ACGACGGCCAGTGAATTGTAATACGACTCACTATAG GGCGGTTCTCGATTAGTCCATTGACCTGCC	This study
<b>MDS3 5-2comp new</b>	GATGGAGAGATGGGGACAGC	This study
<b>MDS3 3-2comp new-2</b>	TTTGTCATGTTACCCGACG	This study
<b>TOR1 probe 5'</b>	ATGAAATAGTGAGTCGCTCC	This study
<b>TOR1 probe 5'-2</b>	CTTTTGTTGCAAATGGCACC	This study
<b>TOR1 probe 3'</b>	CTACCAAGCATAATGGGGTC	This study
<b>RPS26A 5'</b>	CAAGAAAGGTAGAGGTCACG	This study
<b>RPS26A 3'</b>	TTTAGCAGCATCTTGTGGAG	This study
<b>CDC19 5' a</b>	CTTCAATGTTGAAACTGTTCC	This study
<b>CDC19 3' b</b>	AACAGTGTTAGAGTGACCAG	This study
<b>GAP2 5'</b>	TTATTGTACAGTTATGTCCC	This study
<b>GAP2 3'</b>	CCAGCGAAAGCAAAGGCAGC	This study
<b>TEF1-5'</b>	ATAGTCATAATCAATCATGGGT	Davis et al., 2000b
<b>TEF1-3'</b>	CTTACATAATATTCAACTAGC	Davis et al., 2000b
<b>Sit4 MYC N-ter 5'</b>	GATGGTGACTTATCAGTCAAGAACAATGCCAACAAA CAACAAAGAAGTGATTATTTTTTGGCGATCCCCGGGT TAATTAA	This study
<b>Sit4 MYC URA3 N- ter 3'</b>	GCATCATTAAGGGATTTGAAAAAAAAGATATAAAT ATAAAAAATCATTCATCATTCGTTATCTAGAAGGACCA CCTTTGATTG	This study
<b>5' Myc detect</b>	GAACAAAAATTAATTTCTGAAGAAGATTTA	This study
<b>Sit4 3' detect</b>	TGGTTTGTATGTGTAAGTCC	This study
<b>NgoMIV KpnI NheI x NruI 5'</b>	TAGCCGGCTGGGTACCCGGCTAGCCA	This study

<b><u>NgoMIV KpnI NheI</u></b> <b><u>x NruI 3'</u></b>	TGGCTAGCCGGGTACCCAGCCGGCTA	This study
<b>MDS3-HA-56 5'</b>	AGCTTCGAAAATTCATGCAGATAGTGTGCGCAATGTCT TTGTACCCATACGATGTTCTGAC	This study
<b>MDS3-HA-56 3'</b>	AAGCATTTTCGAGATTATTACTTGTAACCGATTTCTTT TTGTAATCTGGAACGTCATATGG	This study

The sequences underlined indicate the restriction site created. Sequences in bold and underlined indicate point mutation.

**Table 3.3.** Results of the transcriptional profiling of the wild-type, the *mds3Δ/Δ*, and the *rim101Δ/Δ* *C. albicans* strains.

<b>Condition</b>	# of ORFs with ≥ 2-fold difference		# of ORFs expressed more in the mutant		# of ORFs expressed less in the mutant	
	<i>mds3Δ/Δ</i>	<i>rim101Δ/Δ</i> <sup>1</sup>	<i>mds3Δ/Δ</i>	<i>rim101Δ/Δ</i> <sup>1</sup>	<i>mds3Δ/Δ</i>	<i>rim101Δ/Δ</i> <sup>1</sup>
<b>WT pH 8 vs. mutant pH 8</b>	337	186	146	55	191	131
<b>WT pH 4 vs. mutant pH 4</b>	76	7	37	1	39	6
<b>ORFs ≥ 2-fold difference at pH 8 and pH 4</b>	50	6				
<b>Total</b>	363	187				

<sup>1</sup>Data from (Bensen et al., 2004)

**Table 3.4.** GO categories of differentially expressed ORFs in the *mds3* $\Delta/\Delta$  and *rim101* $\Delta/\Delta$  mutants compared to wild type *C. albicans*.

GO categories	Expressed more at pH 8		Expressed less at pH 8		Expressed more at pH 4		Expressed less at pH 4	
	<i>mds3</i> $\Delta/\Delta$	<i>rim101</i> $\Delta/\Delta$						
<b>Amino acid biosynthesis</b>	11	1	8	4	6	0	3	3
<b>Carbohydrate metabolism</b>	15	3	8	3	8	0	0	0
<b>Glycolysis</b>	6	0	0	0	5	0	0	0
<b>Translation</b>	50	0	1	1	0	0	0	0
<b>Initiation/Elongation</b>	6	0	0	0	0	0	0	0
<b>rRNA/tRNA processing</b>	5	0	0	0	0	0	0	0
<b>Ribosome</b>	37	0	1	0	0	0	0	0
<b>Mitochondrial</b>	2	0	0	1	0	0	0	0
<b>Protein synthesis/folding</b>	15	2	1	2	2	0	0	0
<b>Protein degradation/autophagy</b>	2	0	11	0	0	0	1	1
<b>Vacuolar protein catabolic activity</b>	0	0	5	0	0	0	0	1
<b>Amino acid degrad/proteosome</b>	2	0	3	0	0	0	1	0
<b>Others</b>	0	0	3	0	0	0	0	0
<b>Lipid Metabolism</b>	4	1	10	4	1	0	0	0
<b>Permeases/transport</b>	9	9	33	25	2	0	13	0
<b>Amino acid transport</b>	0	2	12	5	0	0	4	0
<b>Hexose transport</b>	4	0	4	1	1	0	1	0
<b>Other transport</b>	5	7	17	19	1	0	8	0
<b>DNA replication/transcription</b>	7	1	2	0	1	0	2	0
<b>Transcript. factor/Signal transduction</b>	2	2	13	4	3	0	5	0

---

<b>Electron transport</b>	2	0	3	0	1	0	0	0
<b>Cell wall/filamentation</b>	4	2	22	17	1	1	3	2
<b>Other</b>	10	7	19	23	4	0	4	0
<b>Unknown/Novel</b>	15	27	60	48	8	0	8	0
<b>Total ORFs</b>	146	55	191	131	37	1	39	6

---

**Table 3.5.** Hyphal formation in M199 pH 8 in the presence and absence of 5nM rapamycin.

Strain	Genotype	% of hyphae $\pm$ SEM <sup>1</sup>	
		Solvent	Rapamycin
<b>DAY185</b>	<i>MDS3/MDS3 TOR1/TOR1</i>	88.5 $\pm$ 2.0	98.3 $\pm$ 2.0
<b>DAY1121</b>	<i>MDS3/MDS3 TOR1-1/TOR1</i>	85.0 $\pm$ 2.2	89.6 $\pm$ 2.2
<b>DAY1123</b>	<i>MDS3/MDS3 TOR1/<math>\Delta</math></i>	94.3 $\pm$ 0.7	98.5 $\pm$ 0.7
<b>DAY1125</b>	<i>MDS3/MDS3 TOR1-1/<math>\Delta</math></i>	90.6 $\pm$ 1.6	93.3 $\pm$ 1.6
<b>DAY1118</b>	<i>mds3<math>\Delta</math>/<math>\Delta</math> TOR1/TOR1</i>	2.9 $\pm$ 3.2	44.5 $\pm$ 3.2
<b>DAY1120</b>	<i>mds3<math>\Delta</math>/<math>\Delta</math> TOR1-1/TOR1</i>	5.0 $\pm$ 3.2	23.4 $\pm$ 3.2
<b>DAY1122</b>	<i>mds3<math>\Delta</math>/<math>\Delta</math> TOR1/<math>\Delta</math></i>	5.1 $\pm$ 1.8	37.3 $\pm$ 1.8
<b>DAY1124</b>	<i>mds3<math>\Delta</math>/<math>\Delta</math> TOR1-1/<math>\Delta</math></i>	0.9 $\pm$ 0.3	0.8 $\pm$ 0.3

**Table 3.6.** Hyphal formation in M199 pH 8 in the presence and absence of 5nM rapamycin

Strain	Genotype	% of hyphae $\pm$ SEM <sup>1</sup>	
		Solvent	Rapamycin
<b>DAY185</b>	<i>MDS3/MDS3 RBP1/RBP1</i>	75.6 $\pm$ 2.9	84.9 $\pm$ 4.0
<b>DAY1233</b>	<i>MDS3/MDS3 rbp1<math>\Delta</math>/rbp1<math>\Delta</math></i>	91.4 $\pm$ 1.1	91.1 $\pm$ 1.7
<b>DAY1118</b>	<i>mds3<math>\Delta</math>/<math>\Delta</math> RBP1/RBP1</i>	4.4 $\pm$ 1.7	30.4 $\pm$ 3.5
<b>DAY1239</b>	<i>mds3<math>\Delta</math>/<math>\Delta</math> rbp1<math>\Delta</math>/rbp1<math>\Delta</math></i>	3.0 $\pm$ 0.9	3.5 $\pm$ 1.0

<sup>1</sup> SEM, standard error of the mean

**Table S3.1** ORFs differentially expressed ( $\geq 2$ ) in the *mds3Δ/Δ* mutant compared to the wild-type strain at pH 4 or at pH 8.

ORFs expressed less in the *mds3Δ/Δ* mutant than in the wild-type strain at pH 4

Orf19.	Locus name	<i>S. cerevisiae</i> ortholog or best hit	log 2 ratio	Function/Process
orf19.4274	PUT1	PUT1	-1.02	Amino acid biosynthesis
orf19.986	GLY1	GLY1	-1.17	Amino acid biosynthesis
orf19.4026	HIS1	HIS1	-4.17	Amino acid biosynthesis
orf19.7631	SLD5	SLD5	-1.31	DNA replication
orf19.5634	FRP1	FRE5	-1.38	Fe utilization
orf19.5674	PGA10	FIT1	-1.57	Fe utilization/cell wall
orf19.4025	PRE1	PRE1	-3.47	Protein degradation/proteasome
orf19.6586	orf19.6586	NAB3	-1.66	RNA transcription
orf19.5045	orf19.5045	PTP2	-1.14	Signal transduction
orf19.4593	RGA2	RGA1, RGA2	-1.10	Signal transduction
orf19.5635	PGA7	TIR1	-1.52	Structural
orf19.5636	RBT5		-1.29	Structural
orf19.909	STP4	STP4	-1.43	Transcription factor
orf19.1837	TBP1	SPT15	-1.04	Transcription factor
orf19.1255	ZCF5	HAP1	-1.18	Transcription factor
orf19.4118	CNT		-1.39	Transport
orf19.4779	orf19.4779	VBA5	-1.06	Transport
orf19.2751	orf19.2751	MCH4	-1.26	Transport
orf19.918	CDR11	PDR5	-1.55	Transport
orf19.1979	GIT1	GIT1	-1.21	Transport (Carbon)
orf19.4784	CRP1	CCC2	-1.54	Transport (Copper)
orf19.3668	HGT2	RGT2	-1.96	Transport (glucose)
orf19.3440	FRP5	ATO2	-1.09	Transport (Nitrogen)
orf19.6937	PTR2	PTR2	-1.08	Transport (Nitrogen)
orf19.6993	GAP2	GAP1	-1.14	Transport (Nitrogen)
orf19.84	CAN3	CAN1	-1.01	Transport (Nitrogen)
orf19.111	CAN2	CAN1	-1.21	Transport (Nitrogen)
orf19.4063	GPT1	UGA4	-1.70	Transport (Nitrogen)
orf19.7058	orf19.7058	RMD8	-1.15	Unknown function
orf19.3973	orf19.3973	HUA1	-1.03	Unknown function
orf19.1523	orf19.1523		-1.08	Unknown function
orf19.2724	orf19.2724	MOT3	-1.14	Unknown function
orf19.3369	MOH1	MOH1	-1.11	Unknown function
orf19.5037	orf19.5037		-1.54	Unknown function
orf19.1500	orf19.1500	YBL010C	-1.07	Unknown function
orf19.4873	orf19.4873		-1.30	Unknown function
orf19.822	orf19.822		-1.50	Unknown function
orf19.3117	CSA2		-1.60	Unknown function
orf19.5282	orf19.5282		-1.15	Unknown function

ORFs expressed more in the *mds3Δ/Δ* mutant than in the wild-type strain at pH 4

<b>Orf19.</b>	<b>Locus name</b>	<b><i>S. cerevisiae</i> ortholog or best hit</b>	<b>log 2 ratio</b>	<b>Function/Process</b>
orf19.2551	MET6	MET6	1.07	amino acid biosynthesis
orf19.5650	PRO3	PRO3	1.08	amino acid biosynthesis
orf19.3554	AAT1	AAT1	1.50	amino acid biosynthesis
orf19.3911	SAH1	SAH1	1.09	amino acid biosynthesis
orf19.7448	LYS9	LYS9	1.39	amino acid biosynthesis
orf19.88	ILV5	ILV5	1.38	amino acid biosynthesis
orf19.2608	ADH5	ADH2	1.33	Carbon metabolism/Ethanol catabolism
orf19.7514	PCK1	PCK1	2.69	Carbon metabolism/Gluconeogenesis
orf19.3651	PGK1	PGK1	1.60	Carbon metabolism/Glycolisys
orf19.3575	CDC19	CDC19	1.17	Carbon metabolism/Glycolisys
orf19.395	ENO1	ENO1	1.61	Carbon metabolism/Glycolisys
orf19.542	HXK2	HXK2	1.09	Carbon metabolism/Glycolisys
orf19.6814	TDH3	TDH3	1.48	Carbon metabolism/Glycolisys
orf19.3358	LSC1	LSC1	1.24	Carbon metabolism/TCA
orf19.5614	orf19.5614	RNH1	1.21	DNA replication
orf19.5117	OLE1	OLE1	2.09	Fatty acid biosynthesis
orf19.6882	OSM1	OSM1	1.06	NADH biogenesis
orf19.4311	YNK1	YNK1	1.37	precursor biosynthesis
orf19.7446	OPI3	OPI3	1.11	precursor biosynthesis
orf19.7585	INO1	INO1	4.07	Precursor biosynthesis
orf19.1154	EGD1	EGD1	1.28	Protein synthesis/folding
orf19.5858	EGD2	EGD2	1.02	Protein synthesis/folding
orf19.3707	YHB1	YHB1	1.65	Response to stress
orf19.3669	SHA3	SKS1	3.52	Signal transduction
orf19.535	RBR1		1.11	Structural
orf19.5334	orf19.5334	TIS11	1.78	Transcription
orf19.4941	TYE7	TYE7	2.42	Transcription/Carbon metabolism
orf19.6327	HET1		1.00	Transport
orf19.2021	HGT8	HXT6	1.06	Transport (Glucose)
orf19.6078	POL93	YGR109W-B	1.33	Unknown function
orf19.1344	orf19.1344		1.25	Unknown function
orf19.2460	orf19.2460		1.15	Unknown function
orf19.4503	orf19.4503	YGR169C-A	1.05	Unknown function
orf19.1186	orf19.1186		1.22	Unknown function
orf19.6329	orf19.6329	HPF1	1.18	Unknown function
orf19.320	orf19.320	YOR246C	1.62	Unknown function
orf19.7328	orf19.7328		1.01	Unknown function

ORFs expressed less in the *mds3Δ/Δ* mutant than in the wild-type strain at pH 8

<b>Orf19.</b>	<b>Locus name</b>	<b><i>S. cerevisiae</i> ortholog or best hit</b>	<b>log 2 ratio</b>	<b>Function/Process</b>
orf19.4716	GDH3	GDH3	-2.22	Amino acid biosynthesis
orf19.5519	GCV1	GCV1	-2.21	Amino acid biosynthesis
orf19.4788	ARG5,6	ARG5,6	-1.08	Amino acid biosynthesis
orf19.5610	ARG3	ARG3	-1.89	Amino acid biosynthesis
orf19.385	GCV2	GCV2	-2.32	Amino acid biosynthesis
orf19.1996	CHA1	CHA1	-2.37	Amino acid biosynthesis
orf19.4026	HIS1	HIS1	-3.64	Amino acid biosynthesis
orf19.7469	ARG1	ARG1	-2.40	Amino acid biosynthesis
orf19.7668	MAL2	YGR287C	-1.19	Carbon metabolism
orf19.5806	ALD5	ALD5	-1.66	Carbon metabolism/Acetate
orf19.4287	orf19.4287	XYL2	-1.21	Carbon metabolism/Ethanol
orf19.789	PYC2	PYC2	-1.06	Carbon metabolism/gluconeogenesis
orf19.6844	ICL1	ICL1	-2.37	Carbon metabolism/glyoxylate pathway
orf19.4883	MLS1	MLS1	-1.85	Carbon metabolism/glyoxylate pathway
orf19.1719	SGA1	SGA1	-1.50	Carbon metabolism
orf19.4393	CIT1	CIT1	-2.53	Carbon metabolism/TCA cycle
orf19.1743	ACS1	ACS1	-2.40	Chromatin modification
orf19.3264	CCE1	CCE1	-1.62	DNA recombination
orf19.3029	orf19.3029	EHD3	-1.70	Endocytosis
orf19.7288	orf19.7288	YBR047W	-1.95	Fatty acid Boxidation/Respiration
orf19.1288	FOX2	FOX2	-1.48	Fatty-acid Boxidation
orf19.1655	PXP2	POX1	-2.05	Fatty-acid Boxidation
orf19.4121	orf19.4121	TES1	-1.13	Fatty-acid Boxidation
orf19.5215	orf19.5215	TES1	-1.61	Fatty-acid Boxidation
orf19.2809	CTN3	YAT2	-2.37	Fatty-acid Boxidation
orf19.4551	CTN1	YAT1	-2.20	Fatty-acid Boxidation
orf19.3684	orf19.3684	SPS19	-1.62	Fatty-acid Boxidation
orf19.2896	SOU1	SPS19	-1.00	Fatty-acid Boxidation
orf19.4041	orf19.4041	PEX4	-1.10	Fatty-acid/Precursor biosynthesis/peroxisome
orf19.3538	FRE9	FRE3	-1.07	Fe metabolism
orf19.5634	FRP1	FRE5	-2.41	Fe metabolism
orf19.6548	ISU1	ISU1	-1.00	Fe metabolism
orf19.1264	CFL2	FRE4	-1.50	Fe metabolism
orf19.6073	HMX1	HMX1	-2.40	Fe metabolism
orf19.7112	FRP2	FRE5	-3.00	Fe metabolism
orf19.1325	ECM38	ECM38	-2.27	Glutathione metabolism
orf19.1774	orf19.1774	FDH1	-2.68	NAD biogenesis
orf19.1117	orf19.1117	FDH1	-3.03	NAD biogenesis
orf19.638	FDH1	FDH1	-2.73	NAD biogenesis
orf19.2114	orf19.2114	PRM10	-1.38	Nitrogen metabolism
orf19.4736	orf19.4736	PHO8	-1.29	Phosphate metabolism
orf19.7118	orf19.7118	ADK2	-1.13	Precursor biosynthesis

orf19.3567	BIO32	BIO3	-1.34	Precursor biosynthesis/Biotin
orf19.2242	PRB1	PRB1	-2.57	Protein degradation
orf19.1339	CPY1	PRC1	-1.31	Protein degradation
orf19.4743	AFG1	AFG1	-1.61	Protein degradation
orf19.4135	PRC2	PRC1	-1.42	Protein degradation
orf19.1847	ARO10	ARO10	-2.17	Protein degradation
orf19.539	LAP3	LAP3	-2.78	Protein degradation
orf19.1891	APR1	PEP4	-1.04	Protein degradation
orf19.7196	orf19.7196	PRB1	-2.37	Protein degradation
orf19.7445	orf19.7445	VID24	-1.33	Protein degradation
orf19.2480.1	AUT7	ATG8	-1.92	Protein degradation/autophagy
orf19.4025	PRE1	PRE1	-3.21	Protein degradation/proteasome
orf19.3682	CWH8	CAX4	-2.11	Protein synthesis
orf19.2062	SOD4	SOD1	-2.21	Response to stress
orf19.2781	orf19.2781	RCK1	-1.36	Response to stress
orf19.791	RIM11	RIM11	-1.08	Signal transduction
orf19.1943	orf19.1943	SDS22	-1.09	Signal transduction
orf19.5962	SNF3	SNF3	-1.11	Signal transduction
orf19.3415	PTK2	PTK1	-1.11	Signal transduction/transport
orf19.3924	orf19.3924	SAY1	-2.22	Sterol biosynthesis
orf19.1397	orf19.1397	CYB5	-1.05	Sterol biosynthesis
orf19.2706	CRH11	CRH1	-1.18	Structural/Cell wall
orf19.4072	IFF6	YBL113C	-1.12	Structural/Cell wall
orf19.3374	ECE1		-1.84	Structural/Cell wall
orf19.175	orf19.175	MUC1	-2.10	Structural/Cell wall
orf19.1327	RBT1		-1.06	Structural/Cell wall
orf19.4975	HYR1		-2.04	Structural/Cell wall
orf19.5302	PGA31		-1.35	Structural/Cell wall
orf19.2941	SCW4	SCW4	-1.65	Structural/Cell wall
orf19.1690	TOS1	TOS1	-1.27	Structural/Cell wall
orf19.5635	PGA7		-2.63	Structural/Cell wall
orf19.5636	RBT5		-1.59	Structural/Cell wall
orf19.1321	HWP1		-1.12	Structural/Cell wall
orf19.6336	PGA25		-1.95	Structural/Cell wall
orf19.5760	IHD1	SRP40	-2.33	Structural/Cell wall
orf19.3117	CSA2		-2.27	Structural/Cell wall
orf19.3111	PRA1	ZPS1	-3.62	Structural/Cell wall
orf19.876	PGA33		-1.07	Structural/Cell wall
orf19.642	PGA13		-1.36	Structural/Cell wall
orf19.7114	CSA1	MUC1	-4.46	Structural/Cell wall
orf19.7363	KRE6	KRE6	-1.29	Structural/Cell wall
orf19.5674	PGA10	FIT1	-2.17	Structural/Cell wall/Fe metabolism
orf19.1632	orf19.1632	DCW1	-1.09	Structural/Cell wall/Precursor biosynthesis
orf19.3353	orf19.3353		-2.03	Structural/Mitochondria
orf19.2667	RPF1	RPF1	-1.06	Structural/Ribosome
orf19.4590	RFX2	MTL1	-1.13	Transcription
orf19.1150	orf19.1150	GLN3	-1.19	Transcription
orf19.4647	HAP3	HAP3	-2.48	Transcription

orf19.2752	ADR1	ADR1	-1.57	Transcription
orf19.909	STP4	STP4	-1.10	Transcription
orf19.2736	orf19.2736	BUR6	-1.35	Transcription
orf19.610	EFG1	SOK2	-1.15	Transcription
orf19.5026	orf19.5026	YML081W	-1.04	Transcription
orf19.7381	ZCF37	LYS14	-1.02	Transcription
orf19.918	CDR11	PDR5	-2.04	Transport
orf19.3931	SFC1	SFC1	-1.02	Transport
orf19.3526	ITR1	ITR2	-1.42	Transport
orf19.6168	orf19.6168	USO1	-2.57	Transport
orf19.1027	PDR16	PDR16	-1.20	Transport
orf19.2751	orf19.2751	MCH4	-1.90	Transport
orf19.2496	orf19.2496	ADY2	-2.44	Transport (Acetate)
orf19.3981	MAL31	MAL31	-2.22	Transport (carbon)
orf19.3646	CTR1	CTR1	-2.78	Transport (Copper)
orf19.4356	HGT3	YDL199C	-1.54	Transport (Glucose)
orf19.2425	HGT18	YBR241C	-1.29	Transport (Glucose)
orf19.6141	HGT16	HXT1	-1.45	Transport (Glucose)
orf19.6005	HGT5	STL1	-1.25	Transport (Glucose)
orf19.4546	HOL4	HOL1	-1.93	Transport (ion)
orf19.2179	SIT1	ARN1	-1.39	Transport (iron)
orf19.7231	FTR2	FTR1	-2.79	Transport (Iron)
orf19.6169	orf19.6169	ADY2	-2.63	Transport (Nitrogen and acetate)
orf19.1224	FRP3	ATO2	-2.74	Transport (Nitrogen)
orf19.84	CAN3	CAN1	-1.91	Transport (Nitrogen)
orf19.1142	orf19.1142	AVT4	-1.08	Transport (Nitrogen)
orf19.111	CAN2	CAN1	-2.68	Transport (Nitrogen)
orf19.4059	orf19.4059	YHC3	-1.01	Transport (Nitrogen)
orf19.97	CAN1	CAN1	-1.15	Transport (Nitrogen)
orf19.2942	DIP5	DIP5	-2.36	Transport (Nitrogen)
orf19.176	OPT4	OPT2	-2.55	Transport (Nitrogen)
orf19.2810	AAP1	GAP1	-1.02	Transport (Nitrogen)
orf19.528	MUP1	MUP1	-1.20	Transport (Nitrogen)
orf19.6993	GAP2	GAP1	-3.13	Transport (Nitrogen)
orf19.1210	orf19.1210	AVT5	-1.08	Transport (Nitrogen)
orf19.7566	orf19.7566	GPN1	-1.66	Transport (Nitrogen)
orf19.1585	ZRT2	ZRT2	-2.76	Transport (Zinc)
orf19.3112	ZRT1	ZRT2	-3.20	Transport (Zinc)
orf19.1534	ZRT3	ZRT3	-1.53	Transport (Zinc)
orf19.4167	orf19.4167		-1.22	Unknown function
orf19.1301	orf19.1301		-1.04	Unknown function
orf19.2724	orf19.2724		-1.66	Unknown function
orf19.411	orf19.411		-1.91	Unknown function
orf19.4069	orf19.4069		-1.17	Unknown function
orf19.4873	orf19.4873		-1.56	Unknown function
orf19.4482	IFI3		-1.06	Unknown function
orf19.3499	orf19.3499		-1.72	Unknown function
orf19.1239	orf19.1239		-1.30	Unknown function
orf19.3902	orf19.3902		-1.52	Unknown function

orf19.6329	orf19.6329		-1.82	Unknown function
orf19.873	orf19.873		-1.87	Unknown function
orf19.7608	orf19.7608		-1.53	Unknown function
orf19.1152	orf19.1152		-1.25	Unknown function
orf19.1461	orf19.1461		-1.28	Unknown function
orf19.4445	orf19.4445		-1.44	Unknown function
orf19.5799	orf19.5799	CAF120	-1.30	Unknown function
orf19.1523	orf19.1523		-1.63	Unknown function
orf19.1350	orf19.1350		-2.25	Unknown function
orf19.4780	orf19.4780	YJR124C	-1.11	Unknown function
orf19.6017	orf19.6017		-1.93	Unknown function
orf19.4795	orf19.4795		-1.08	Unknown function
orf19.5063	orf19.5063		-2.29	Unknown function
orf19.1675	orf19.1675	YDL133W	-1.13	Unknown function
orf19.376	orf19.376		-2.09	Unknown function
orf19.3351	orf19.3351		-1.12	Unknown function
orf19.3936	orf19.3936	GDE1	-1.22	Unknown function
orf19.113	CIP1		-1.88	Unknown function
orf19.715	orf19.715		-2.34	Unknown function
orf19.716	orf19.716		-3.18	Unknown function
orf19.3369	MOH1	MOH1	-1.27	Unknown function
orf19.1107	orf19.1107	YDL173W	-2.16	Unknown function
orf19.5037	orf19.5037		-1.02	Unknown function
orf19.5125	orf19.5125	YLR149C	-1.46	Unknown function
orf19.4269	orf19.4269	YLR253W	-1.30	Unknown function
orf19.1505	orf19.1505		-1.20	Unknown function
orf19.2460	orf19.2460		-2.09	Unknown function
orf19.419	orf19.419		-2.29	Unknown function
orf19.1764	orf19.1764		-1.03	Unknown function
orf19.6469	orf19.6469	YIL082W-A	-1.14	Unknown function
orf19.4792	orf19.4792		-1.26	Unknown function
orf19.4210	orf19.4210	YGR110W	-1.12	Unknown function
orf19.1588	orf19.1588	FMP21	-1.10	Unknown function
orf19.2701	orf19.2701		-1.88	Unknown function
orf19.1258	orf19.1258		-1.10	Unknown function
orf19.5138	IFA21		-1.34	Unknown function
orf19.1562	orf19.1562		-1.96	Unknown function
orf19.4246	orf19.4246	YKR070W	-1.31	Unknown function
orf19.822	orf19.822		-1.93	Unknown function
orf19.6864	orf19.6864		-2.23	Unknown function
orf19.334	orf19.334		-1.44	Unknown function
orf19.2059	orf19.2059		-1.55	Unknown function
orf19.6556	orf19.6556		-1.72	Unknown function
orf19.5238	orf19.5238		-1.12	Unknown function
orf19.3016	orf19.3016		-1.16	Unknown function
orf19.4575	orf19.4575	YPL109C	-1.19	Unknown function
orf19.935	AGA1		-1.33	Unknown function
orf19.7296	orf19.7296		-1.72	Unknown function
orf19.7323	CBP1	FMS1	-1.48	Unknown function

orf19.7370	orf19.7370	YOL092W	-1.06	Unknown function
orf19.5952	orf19.5952		-2.48	Unknown function
orf19.1350	orf19.1350		-2.62	Unknown function

ORFs expressed more in the *mds3Δ/Δ* mutant than in the wild-type strain at pH 8

<b>Orf19.</b>	<b>Locus name</b>	<b><i>S. cerevisiae</i> ortholog or best hit</b>	<b>log 2 ratio</b>	<b>Function/Process</b>
orf19.2551	MET6	MET6	1.06	amino acid biosynthesis
orf19.4060	ARO4	ARO4	1.64	amino acid biosynthesis
orf19.4650	ILV6	ILV6	1.07	amino acid biosynthesis
orf19.1517	ARO3	ARO3	1.16	amino acid biosynthesis
orf19.5650	PRO3	PRO3	1.39	amino acid biosynthesis
orf19.3554	AAT1	AAT1	1.92	amino acid biosynthesis
orf19.3911	SAH1	SAH1	1.50	amino acid biosynthesis
orf19.3419	MAE1	MAE1	1.32	amino acid biosynthesis
orf19.2951	HOM6	HOM6	1.64	amino acid biosynthesis
orf19.7080	LEU2	LEU2	1.27	amino acid biosynthesis
orf19.88	ILV5	ILV5	1.83	amino acid biosynthesis/mitochondrial DNA
orf19.2244	orf19.2244	YJR096W	2.34	Carbon metabolism
orf19.5294	PDB1	PDB1	1.29	carbon metabolism
orf19.2608	ADH5	ADH2	1.92	Carbon metabolism
orf19.3133	GUT2	GUT2	1.38	carbon metabolism
orf19.3097	PDA1	PDA1	1.16	Carbon metabolism
orf19.5021	PDX1	PDX1	1.29	carbon metabolism
orf19.7514	PCK1	PCK1	2.03	Carbon metabolism (gluconeogenesis)
orf19.3651	PGK1	PGK1	1.46	Carbon metabolism/Glycolisys
orf19.3967	PFK1	PFK1	1.18	Carbon metabolism/Glycolisys
orf19.6540	PFK2	PFK2	1.10	Carbon metabolism/Glycolisys
orf19.3575	CDC19	CDC19	2.15	Carbon metabolism/Glycolisys
orf19.395	ENO1	ENO1	2.22	Carbon metabolism/Glycolisys
orf19.542	HXK2	HXK2	1.54	Carbon metabolism/Glycolisys
orf19.5024	GND1	GND1	1.14	Carbon metabolism/NADPH regeneration
orf19.3358	LSC1	LSC1	1.70	Carbon metabolism/TCA
orf19.1059	HHF1	HHF1	1.60	Chromatin component
orf19.6924	HTA1	HTA1	1.40	Chromatin component
orf19.6925	HTB1	HTB1	1.20	Chromatin component
orf19.5614	orf19.5614	RNH1	1.06	DNA replication
orf19.5117	OLE1	OLE1	1.42	Fatty acid biosynthesis
orf19.979	FAS1	FAS1	1.83	Fatty acid biosynthesis
orf19.7466	ACC1	ACC1	2.38	Fatty acid biosynthesis
orf19.5949	FAS2	FAS2	2.23	Fatty acid biosynthesis
orf19.7076	orf19.7076	GBP2	1.07	mRNA translocation
orf19.6882	OSM1	OSM1	1.41	NADH biogenesis
orf19.7522	orf19.7522	BNA3	1.70	NADH biogenesis
orf19.5228	RIB3	RIB3	1.02	FAD biogenesis
orf19.18	IMH3	IMD4	1.21	precursor biosynthesis

orf19.3331	ABC1	ABC1	1.43	precursor biosynthesis
orf19.4311	YNK1	YNK1	1.16	precursor biosynthesis
orf19.5630	APA2	APA1	1.04	Precursor biosynthesis
orf19.7446	OPI3	OPI3	1.26	precursor biosynthesis
orf19.7585	INO1	INO1	2.09	Precursor biosynthesis
orf19.754	orf19.754	OLA1	1.03	Protein degradation/proteosome
orf19.6582	PRE10	PRE10	1.02	Protein degradation/proteosome
orf19.641	orf19.641	ERJ5	1.14	Protein folding
orf19.4871	ERO1	ERO1	1.01	Protein folding
orf19.6176	SEC61	SEC61	1.22	Protein folding
orf19.717	HSP60	HSP60	1.01	Protein folding/mitoch integrity
orf19.2013	KAR2	KAR2	1.84	Protein folding/synthesis
orf19.4279	MNN1	MNN1	2.08	Protein synthesis
orf19.5130	PDI1	PDI1	1.57	Protein synthesis
orf19.5081	FUN12	FUN12	1.35	Protein synthesis
orf19.5073	DPM1	DPM1	1.74	Protein synthesis
orf19.3438	orf19.3438	SCJ1	1.18	Protein synthesis
orf19.2965	orf19.2965	GET3	1.03	Protein synthesis
orf19.1478	orf19.1478	STT3	1.06	Protein synthesis
orf19.6988	orf19.6988	OST1	1.07	Protein synthesis
orf19.1154	EGD1	EGD1	1.89	Protein synthesis/folding
orf19.5858	EGD2	EGD2	1.83	Protein synthesis/folding
orf19.3243	SRP54	SRP54	1.12	RNA
orf19.7655	RPO21	RPO21	1.55	RNA synthesis
orf19.7569	orf19.7569	SIK1	1.08	rRNA synthesis
orf19.2762	AHP1	AHP1	1.21	Stress response
orf19.4657	orf19.4657	NEM1	1.13	Structural
orf19.30	orf19.30	SPF1	2.25	Structural
orf19.1097	ALS2	FLO1	3.27	Structural/Cell wall
orf19.4555	ALS4	FLO9	3.17	Structural/Cell wall
orf19.1911	PGA52	YJL171C	1.72	Structural/Cell wall
orf19.4109	PMT4	PMT4	1.37	Structural/Cell wall/precursor biosynthesis
orf19.5334	orf19.5334	TIS11	2.20	Transcription
orf19.4941	TYE7	TYE7	2.36	Transcription/Carbon metabolism
orf19.1435	TEF1	TEF1	1.12	Translation elongation
orf19.2651	CAM1-1	TEF4	1.07	Translation elongation
orf19.382	TEF2	TEF2	1.11	Translation elongation
orf19.3838	EFB1	EFB1	1.65	Translation elongation
orf19.7382	CAM1	CAM1	1.84	Translation elongation
orf19.407	GCD6	GCD6	1.11	Translation initiation
orf19.3532	MRPL10	MRPL10	1.22	Translation/structural component of ribosome
orf19.3559	MRPS35	MRPS35	1.23	Translation/structural component of ribosome
orf19.1601	RPL3	RPL3	1.94	Translation/structural component of ribosome
orf19.4336	RPS5	RPS5	1.79	Translation/structural component of ribosome
orf19.4632	RPL20B	RPL20A	1.38	Translation/structural component of

orf19.2232	RPL11	RPL11B	1.50	ribosome Translation/structural component of ribosome
orf19.4490	RPL17B	RPL17B	1.29	Translation/structural component of ribosome
orf19.1700	RPS7A	RPS7A	1.36	Translation/structural component of ribosome
orf19.3789	RPL24A	RPL24A	1.20	Translation/structural component of ribosome
orf19.3334	RPS21	RPS2	1.69	Translation/structural component of ribosome
orf19.3465	RPL10A	RPL1A/RPL1B	1.73	Translation/structural component of ribosome
orf19.840	RPL21A	RPL21A	1.95	Translation/structural component of ribosome
orf19.2935	RPL10	RPL10	1.65	Translation/structural component of ribosome
orf19.3504	RPL23A	RPL23A/RPL23B	1.68	Translation/structural component of ribosome
orf19.4660	RPS6A	RPS6A/RPS6B	2.04	Translation/structural component of ribosome
orf19.2994	RPL13	RPL13A	1.42	Translation/structural component of ribosome
orf19.2992	RPP1A	RPP1A	1.28	Translation/structural component of ribosome
orf19.2478.1	orf19.2478.1	RPL7A	2.24	Translation/structural component of ribosome
orf19.6541	RPL5	RPL5	2.08	Translation/structural component of ribosome
orf19.6312	RPS3	RPS3	1.75	Translation/structural component of ribosome
orf19.6375	RPS20	RPS20	2.06	Translation/structural component of ribosome
orf19.6265	RPS22A	RPS22A	1.04	Translation/structural component of ribosome
orf19.6085	RPL16A	RPL16A	1.43	Translation/structural component of ribosome
orf19.1635	RPL12	RPL12A	1.36	Translation/structural component of ribosome
orf19.493	RPL15A	RPL15B	1.93	Translation/structural component of ribosome
orf19.1470	RPS26A	RPS26A	1.82	Translation/structural component of ribosome
orf19.6873	RPS8A	RPS8A/RPS8B	1.62	Translation/structural component of ribosome
orf19.6975	YST1	RPS0A	1.66	Translation/structural component of ribosome
orf19.7015	RPP0	RPP0	1.81	Translation/structural component of ribosome
orf19.7018	RPS18	RPS18A/RPS18B	1.57	Translation/structural component of ribosome
orf19.7217	RPL4B	RPL4B	2.23	Translation/structural component of ribosome
orf19.3268	TMA19	TMA19	1.52	Translation/structural component of

orf19.5341	RPS4A	RPS4B/RPS4A	1.52	ribosome Translation/structural component of ribosome
orf19.6785	RPS12	RPS12	2.29	Translation/structural component of ribosome
orf19.6002	RPL8B	RPL8B	2.13	Translation/structural component of ribosome
orf19.5982	RPL18	RPL18A/RPL18B	2.27	Translation/structural component of ribosome
orf19.5927	RPS15	RPS15	1.66	Translation/structural component of ribosome
orf19.236	RPL9B	RPL9B	1.74	Translation/structural component of ribosome
orf19.6906	ASC1	ASC1	1.38	Translation/structural component of ribosome/signal transduction
orf19.2023	HGT7	HXT6	1.20	Transport
orf19.2021	HGT8	HXT6	1.61	Transport
orf19.2020	HGT6	HXT4	1.37	Transport
orf19.4784	CRP1	CCC2	2.54	Transport
orf19.3669	SHA3	SKS1	3.02	Transport
orf19.4599	PHO89	PHO89	1.02	Transport
orf19.7327	PHO88	PHO88	1.08	Transport
orf19.3496	orf19.3496	CHC1	1.10	Transport/Intracellular vesicle transport
orf19.4732	SEC24	SEC24	1.11	Transport/Intracellular vesicle transport
orf19.2560	CDC60	CDC60	1.21	t-RNA
orf19.2422	ARC1	ARC1	1.26	t-RNA
orf19.2960	FRS2	FRS2	1.30	t-RNA
orf19.6749	KRS1	KRS1	1.15	t-RNA
orf19.4698	PTC8	PTC7	1.37	Signal transduction
orf19.1782	orf19.1782	IRC22	1.46	Unknown function
orf19.1344	orf19.1344		2.11	Unknown function
orf19.4220	orf19.4220	YLR456W	1.00	Unknown function
orf19.5293	orf19.5293		1.22	Unknown function
orf19.2212	orf19.2212		1.38	Unknown function
orf19.5525	orf19.5525	YMR315W	1.43	Unknown function
orf19.1186	orf19.1186		1.08	Unknown function
orf19.4149	orf19.4149		1.80	Unknown function
orf19.1368	orf19.1368		1.17	Unknown function
orf19.2775	orf19.2775	YNR021W	1.10	Unknown function
orf19.4247	orf19.4247		1.03	Unknown function
orf19.3318	orf19.3318	YBR255W	2.16	Unknown function
orf19.4831	orf19.4831		1.16	Unknown function
orf19.7328	orf19.7328		1.39	Unknown function

## **CHAPTER 4**

**COLONY MORPHOLOGY PHENOTYPIC SWITCHING IN *CANDIDA ALBICANS* IS ASSOCIATED WITH GENOMIC ALTERATIONS AND DEFECTS IN DNA DAMAGE RESPONSE AND TOR PATHWAY FUNCTION**

## SUMMARY

Variability is essential for adaptation to a constantly changing environment, and adaptation is critical for the success of any pathogen. In the absence of sexual reproduction (a major mechanism to generate variability in eukaryotes), the opportunistic pathogen *Candida albicans* can generate phenotypic variation by the colony morphology phenotypic switching (CMPS) process. CMPS is accompanied by changes in the expression of virulence factors and is thus associated with pathogenesis. Mds3, a member of the TOR pathway, is a poorly characterized negative regulator of CMPS. In this chapter, we aimed to characterize CMPS in the *C. albicans mds3Δ/Δ* strain, with the objective of identifying potential mechanisms of CMPS. We found that the phenotypic switch in the *mds3Δ/Δ* mutant is often accompanied by karyotypic rearrangements and aneuploidies, although these genomic alterations are not required for the switch to occur. CMPS in the *mds3Δ/Δ* mutant is also accompanied by changes in sensitivity to the TOR inhibitor rapamycin and to DNA damage agents (especially to the genotoxic oxidizing agent TBHP). Further, I found environmental conditions that can enhance (glucose starvation and glutamine) or inhibit (alkaline pH) CMPS in the *mds3Δ/Δ* mutant; and I began to explore whether *MDS3* might also be involved in white-opaque switching. The results presented here provide intriguing evidence that suggest that switching in the *mds3Δ/Δ* mutant is associated with defects in TOR pathway function.

## INTRODUCTION

Phenotypic heterogeneity is strongly associated with increased population fitness. In pathogenic organisms, phenotypic variation can enhance virulence attributes such as antibiotic resistance, motility, adherence, and immune evasion (Avery 2006; Morrison et al., 2009). Pathogenic bacteria, protozoa, and fungi benefit from phenotypic variation during infection. For example, phenotypic variation aids in immune evasion by altering the expression of enzymes and surface antigens, such as bacterial pili, fimbriae, and outer polysaccharides, and fungal and protozoan surface glycoproteins, including the major surface glycoprotein MSG from *Pneumocystis* and the well studied variable surface glycoprotein VSG and PfEMP1 surface antigens from *Trypanosoma* spp. and *Plasmodium* spp. (Zieg et al., 1977; Yamamoto and Kutsukake, 2006; Bayliss et al., 2001; van de Broek et al., 2005; Wada et al., 1995; Brockert et al., 2003; Morrison et al., 2009; Ralph and Scherf, 2005). Thus, phenotypic variation is critical for the success of pathogens in their host.

Phenotypic variation is a common phenomenon in diverse human pathogenic fungi, including *Candida albicans*, *C. glabrata*, *C. lusitaniae*, *Trichosporon assahii*, *Pneumocystis* spp., *Histoplasma capsulatum*, *Paracoccidioides brasiliensis*, *Cryptococcus neoformans*, and *C. gattii* (Slutsky et al., 1985, 1987; Ichikawa et al., 2004; Goldman et al., 1998; Jain et al., 2006; Srikantha et al., 2008; Jain et al., 2009; Macoris et al., 2006; Ichikawa et al., 2004; Stringer et al., 2007; Keely et al., 2003; Eissenberg et al., 1996). Phenotypic variation in pathogenic fungi happens during infection, and is associated with alterations in virulence (Slutsky et al., 1985, 1987; Goldman et al., 1998; Jain et al., 2006; Srikantha et al., 2008; Jain et al., 2009). Establishing the real impact of fungal phenotypic switching on disease progression in humans and finding the mechanisms that lead to the formation of phenotypic variants in the highly diverse pathogenic fungi are future challenges for mycologists.

Several phenotypic alterations observed in fungi are associated with changes in colony morphology (including size, texture, and color). For example, *C. glabrata* switches between different colony colors in plates supplemented with copper sulfate and reversibly switches between smooth and wrinkled colonies (Brockert et al., 2003; Lachke et al., 2002). Although the role of the different colony variants in *C. glabrata* remains unclear, they appear to have differential colonization abilities in distinct parts of the human body (Brockert et al., 2003). *H. capsulatum* gives rise to colony variants that have a differential ability to survive within and kill macrophages (Eissenberg et al., 1996; Kugler et al., 2000). *Cryptococcus* spp. also produces colonies with altered morphologies which display different infectivity in murine models of infection (Currie et al., 1995; Fries and Casadevall, 1998; Sukroongreung et al., 2001; Fries et al., 1996, 1999, 2001, 2002, 2005; Guerrero et al., 2006). Thus, alterations in colony morphology are common expressions of phenotypic variation in diverse fungal pathogens and are associated with altered virulence. Despite its role in pathogenesis, the molecular mechanisms that lead to colony morphology changes in the different fungi are not known.

*C. albicans*, the major fungal pathogen of humans, achieves phenotypic variation through two different morphogenetic processes that also involve changes in colony morphology: the white-opaque phenotypic switch (W-O) and the colony morphology phenotypic switch (CMPS) (Pfaller et al., 2001; Soll, 1992; Whiteway and Oberholzer, 2004). The W-O switch is a bi-stable, epigenetically determined switch between two different cellular and colonial morphologies: round cells that produce smooth and white colonies (white phase), and elongated cells with cell wall pimples that produce flat and grey colonies (opaque phase) (Huang et al., 2006; Zordan et al., 2006; Srikantha et al., 2001, 2006; Slutsky et al., 1987; Anderson et al., 1990; Hnisz et al., 2009). CMPS, also known as the 3153A-type switching, refers to the appearance of colonies with altered, heritable colony morphologies at a frequency of  $\sim 10^{-4}$  (Slutsky et al., 1985; Negroni 1935). The altered colony morphologies are interconvertible and can also revert to the wild-type

phenotype. Colonies with different morphologies have been isolated from infected patients, suggesting that morphologically switched variants have a role during infection (Jones et al., 1994; Vargas et al., 2000; Soll et al., 1987, 1988, 1989). Further, phenotypic switching affects the expression of several virulence traits in *C. albicans*, including antifungal resistance, morphogenesis, secretion of hydrolytic enzymes, adhesion to epithelial cell, susceptibility to neutrophils, and virulence in murine models of infection (Gallagher et al., 1992; Kennedy et al., 1998; Kolotila and Diamond, 1990; Vargas et al., 1994, 2004; Kvaal et al., 1997, 1999; Anderson et al., 1989; Lan et al., 2002). Therefore, phenotypic switching is an important mechanism to generate variation in *C. albicans* with direct implications in the pathogenesis of this fungus.

Only the white-opaque phenotypic switch has been well studied in *C. albicans*. The differences between the white and opaque phases on fungal physiology and pathogenesis have been explored (Lan et al., 2002; Kvaal et al., 1997, 1999). Further, the biological role of the W-O switch in mating and several genetic and epigenetic mechanisms, environmental signals and signaling cascades that regulate the W-O switch are well understood (Soll et al., 2009; Lohse and Johnson, 2009; Morschhauser, 2010).

On the contrary, very little is known about the mechanisms and environmental signals that regulate CMPS in *C. albicans*. Several processes have been already associated with alterations in colony morphology in *C. albicans*, including karyotypic rearrangements, aneuploidies, loss of heterozygosity, and CUG codon ambiguity (Zacchi et al., 2010b (Appendix B); Forche et al., 2009; Rustchenko et al., 1994; Uhl et al., 2003; Miranda et al., 2007). Further, the molecular chaperone Hsp90 and epigenetic mechanisms, which are involved in the generation of morphogenetic and surface variation in *C. albicans* and other organisms, might constitute yet undefined CMPS mechanisms (Cowen, 2008; Cowen et al., 2005; Shapiro et al., 2009; Sollars et al., 2002; Queitsch et al., 2002; Verstrepen and Fink, 2009; Lohse and Johnson, 2009; Domergue et al., 2005). The only environmental condition known to affect CMPS is the concentration of

zinc in the medium: CMPS in *C. albicans* strain 3153A was observed on zinc-limited medium (rich in amino acids) but was inhibited with higher zinc concentrations (Bedell and Soll, 1979; L.F.Z. unpublished observation). However, the molecular mechanism by which zinc affects CMPS remains unclear. Given the relevance of CMPS on *C. albicans* lifestyle, it is important to understand the mechanisms that control it.

While studying the role of Mds3 as a regulator of pH responses in *C. albicans* (Davis et al., 2002), we serendipitously found that Mds3 is a negative regulator of CMPS. The alterations in colony morphology of the switched *mds3Δ/Δ* strains are accompanied by changes in expression of several virulence traits, including antifungal drug resistance, adhesion to mammalian cells, protease secretion, and filamentation (M.J.H., S.S., Z.M., D.D. unpublished data). The heritability and reversibility of the colony morphology alteration in the switched *mds3Δ/Δ* strains fits the characteristics that define CMPS (Slutsky et al., 1985; Soll, 1992). Thus, Mds3 regulates CMPS in *C. albicans*, and constitutes a genetic tool to uncover the mechanism(s) of CMPS in this fungus.

Mds3 appears to function as a cytoplasmic scaffold that regulates the TOR pathway and possibly other signal transduction cascades (Chapters 2, 5, and Zacchi et al., 2010a (Chapter 3)). Here, we expanded the characterization of the original *mds3Δ/Δ* mutant and of the switched *mds3Δ/Δ* strains by testing potential processes associated with CMPS, including karyotypic rearrangements, aneuploidies, and sensitivity to the TOR inhibitor rapamycin and DNA damage agents. I also constructed *MTLa/a* strains to test if *MDS3* is involved in W-O switching. Further, I found environmental conditions that exacerbate (glucose starvation, glutamine) or inhibit (alkaline pH) the phenotypic switch, and found that alkaline pH appears to reduce cellular dependence on the TOR pathway. In line with this result, I found that most switched strains regained rapamycin sensitivity and are thus more dependent on TOR for growth. Even more, the *TOR1-1* allele, a partial-function *TOR1* allele, synergizes with the *mds3Δ/Δ* mutation to induce

CMPS. Our results suggest that phenotypic switching in the *mds3Δ/Δ* mutant is associated with the stepwise acquisition of alterations that lead to TOR signaling dependence during stationary phase.

## MATERIALS AND METHODS

### Strain construction

All strains used in this study are listed in Table 4.1. The SSY switched strains (Table 4.3) were obtained by isolating papilli from *mds3Δ/Δ* colonies; while the SSY parental strains were obtained by re-isolating the colony where papilli appeared (see Results and Figure 4.1). All SSY switched-parental strains are in pairs. The parental SSY strain constitutes the “aged-non-switched” control.

The mating type locus (*MTLa/a*) homozygous strains LUZ127 and LUZ145 were constructed by plating YPD overnights of the *mds3Δ/Δ* (DAY417) and wild-type (DAY286) strains on synthetic medium (SC) supplemented with 2% L-sorbose (Fluka) as carbon source. The loss of the *MTLa* allele and the presence of the *MTLa* allele were verified by genomic DNA PCR using primer pairs a1 ORF F and a1 ORF R, and MTLalpha2 5 detect and MTLalpha2 3 detect (Table 4.2). *MTLa/Δ* colonies were plated on YPD, and faster growing colonies (which reduplicated Chromosome 5 and are thus *MTLa/a*) were selected for further experiments.

Strain LUZ166, which carries a deletion in the centromere of one Chromosome 5 (*CEN5*) was constructed as previously described (Ketel et al., 2009) using the primers listed in Table 4.2. Briefly, Helen Wang, from Judith Berman’s lab at the University of Minnesota, transformed the *mds3Δ/Δ* strain DAY956 with an *icci::URA3* cassette PCR amplified from pGEM-URA3 with primers 2211 and 2212 (Table 4.2). Transformant screening and correct integration of the *URA3* cassette at *CEN5* was performed in our laboratory by genomic DNA PCR, using primer sets: 2003-945-1961 and 1915-944-1901 (Table 4.2). LUZ225-226 and LUZ227-228 were constructed by transforming LUZ166 with *PmeI* linearized plasmids pDDB343 and pDDB353, respectively (Chapter 3).

Strains LUZ796 and LUZ798 were generated by transformation of SSY194 and SSY210 with *NruI* digested pGEM-HIS1 (pDDB249). Strains LUZ797 and LUZ799 were generated by

transformation of SSY194 and SSY210 with NotI digested pVIN103 (pGEM-*HIS1::MDS3*, pDDB344) (Davis et al., 2002) (Table 4.1). Correct integration of pVIN103 was verified by genomic DNA PCR using primers MDS3 5-detect and MDS3 3-detect (Table 4.2).

### **Media and growth conditions**

*C. albicans* was routinely grown at 30°C in YPD (2% Bacto-peptone, 2% dextrose, 1% yeast extract). For *MTL* homozygosis and white-opaque switching experiments cells were plated on SC medium (0.17% yeast nitrogen base without ammonium sulfate (Q-BioGene), 0.5% ammonium sulfate, and supplemented with a dropout mix containing amino and nucleic acids (Adams et al., 1997)). Media were buffered at the indicated pH using 150mM HEPES. Rapamycin (LC Laboratories) was added to the media at the indicated concentrations from a stock solution in 90% ethanol-10% Tween-20. For growth assays in the presence of rapamycin, strains were pre-grown in liquid YPD at 30°C, diluted in PBS to an OD 600nm of 1.6, then serially diluted 5-fold in PBS, spotted on YPD or Spider medium (1% mannitol, 1% nutrient broth, 0.2% K<sub>2</sub>HPO<sub>4</sub>, pH 7.2 before autoclaving (Liu et al., 1994)) supplemented with rapamycin or solvent alone and incubated at 30°C for 2 or 3 days. For DNA damage experiments strains were pre-grown in liquid YPD at 30°C, diluted in PBS to an OD 600nm of 1.6, then serially diluted 5-fold in PBS and spotted on YPD supplemented with methyl methanesulfonate (MMS, Sigma), hydroxyurea (HU, Sigma), or tert-butyl hydroxyperoxide (TBHP, Sigma); plates were incubated at 30°C in a plastic bag. All media were supplemented with 80 µg/ml uridine. For solid media, 2% Bacto-agar was added, except for Spider medium which required 1.35% Bacto-agar.

## **Comparative genomic hybridizations and contour-clamped homogeneous electric field (CHEF) electrophoresis**

The protocol for comparative genomic hybridizations (CGH) is explained in Appendix B-Materials and Methods. Contour-clamped homogeneous electric field (CHEF) electrophoresis was done using a CHEF DRIII System (Bio-Rad). Sample preparation for electrophoresis was performed as previously described (Chu et al., 1993) with minor modifications. Briefly,  $\sim 5 \times 10^7$  cells/ml from YPD overnights were harvested, washed twice in 0.05M EDTA pH 7.5, resuspended in 130  $\mu$ l SCE (1M sorbitol, 0.1M sodium citrate [pH 5.8], 0.01M EDTA [pH 8.0]) containing lysing enzyme and then 250  $\mu$ l of warm (45°C) 2% low-melting point agarose in 0.125M EDTA pH 7.5 were added. Aliquots were transferred to molds for solidification. Solid agarose blocks were incubated 6 hrs at 37°C in 3 ml LET (0.1M EDTA, 0.01M Tris-HCl, pH 7.5, 5%  $\beta$ -mercaptoethanol) for spheroplasting. LET was replaced with 1.5 ml NDS (0.1M EDTA, 0.01M Tris-HCl, pH 7.5, 1% N-lauroyl sarcosine, 2 mg/mL proteinase K) and samples were incubated 24-48 hrs at 50°C for protein digestion. NDS was removed and plugs were washed 5-6X with 0.05M EDTA and stored at 4°C. Whole chromosomes were separated in 0.6% agarose (PFGE grade) in 0.5X TBE buffer using the program: 60-120 sec switch ramp, 6 V/cm, 120° angle,  $\sim 100$  mAmp, for  $\sim 24$  hrs; followed by 720-900 sec ramp, 2.0 V/cm, 106° angle, for 12hr.

## **Phenotypic switching assay**

Strains were grown overnight (>16 hrs) in YPD at 30°C, diluted to  $10^{-6}$  in PBS, and 100  $\mu$ l plated on YP plates with 2% or 0.2% glucose, YPD plates buffered at pH 6 or pH 8, or YNB plates (0.17% yeast nitrogen base without amino acids) supplemented with 2% glycerol and 5mM glutamine, ammonium sulfate, or proline as sole carbon and nitrogen sources, respectively. Plates were incubated at 30°C for 48 hrs, and then at room temperature ( $\sim 23$ -25°C) for three weeks,

wrapped in parafilm to prevent agar desiccation. The % of colonies showing papilli on the colony surface was scored every 2-3 days beginning at day 6 of incubation.

### **White-opaque switching assay**

For white-opaque experiments, the protocol described in Alby and Bennet (2009) was followed. Briefly, overnights were started in 3 ml YPD and incubated in a shaker at RT (~25°C) for 24 hrs. Cultures were checked for purity of white cells (>99%) under the microscope. Dilutions were made in PBS, plated in SC medium, and incubated at room temperature for 3 weeks. The presence of opaque sectors were readily visualized without the need for Phloxine B; however I noticed that addition of 1:10 Lugol's solution (5% iodine, 10% potassium iodine) to the plates markedly aided in visualization, as it did not stain efficiently opaque colonies (Figure 4.1C). Lugol solution stains stored carbohydrates. The difference observed in opaque *vs.* white cells might be an indication of differences in their metabolisms, as previously observed (Lan et al., 2002). The presence of opaque cells in opaque sectors was verified by microscopy.

### **Photography and microscopy**

Pictures of colonies were taken using a Canon Powershot A560 digital camera. Images of liquid cultures were captured using a Zeiss Axio camera, Axiovision 4.6.3 software (Zeiss), and a Zeiss AxioImager fluorescence microscope. All images were processed with Adobe Photoshop 7.0 software.

## RESULTS

Prolonged incubation of *mds3Δ/Δ* colonies leads to the formation of extensions and blebs on the colony surface, usually characterized by a change in color and/or morphology [hereafter called papilli (Figure 4.1A, white arrow)]. The formation of papilli is the first manifestation of the phenotypic switch in the *mds3Δ/Δ* mutant. Cells isolated from *mds3Δ/Δ* papilli give rise to colonies with an altered, heritable morphology that is reversible at low frequency (M.T.A., M.J.H., Z.M., and S.S. unpublished data). These strains are referred to as “switched” strains (Figure 4.1B and data not shown). To control for changes that occurred during prolonged incubation, cells from the colony in which the papilli originated were also isolated, and are called “parental” (Figure 4.1A, green arrow). Parental strains always maintained the original *mds3Δ/Δ* colony morphology (Figures 4.4, 4.7, and data not shown). Re-introduction of a wild-type *MDS3* copy in the original *mds3Δ/Δ* strain prevented the formation of papilli, indicating that papilli formation is an *MDS3*-dependent phenotype (D.D. unpublished data). However, re-introduction of a wild-type *MDS3* copy in the switched *mds3Δ/Δ* strains did not restore wild-type colony morphology nor did it alter the switching frequency, indicating that the events post-switching in the *mds3Δ/Δ* mutant are *MDS3*-independent (Figure 4.1C and L.F.Z. and M. D. unpublished results). In order to begin to understand the nature of the phenotypic switch, I constructed strains to determine if Mds3 is involved in white-opaque switching and searched for environmental conditions that affect the frequency of the switch. Further, we characterized the switched strains with the objective of finding common responses that might allow for a better understanding of the mechanisms behind the switch in the *mds3Δ/Δ* mutant.

### **Effect of *MDS3* deletion on white-opaque phenotypic switching**

The W-O phenotypic switch in *C. albicans* is a bi-stable switch between a white, dome-shaped, creamy colony formed by round cells and a darker, flat colony formed by elongated cells

(Figure 4.1D). The switch from white to opaque is required for mating in *C. albicans* (Miller and Johnson, 2002). The W-O switch has been well studied and many environmental and genetic factors that regulate this switch are known (Morschhauser, 2010). If Mds3 was also involved in white-opaque switching, we would have identified a protein involved in the two major mechanisms to generate variability in *C. albicans*. Further, given the extensive knowledge on the mechanisms to generate variability in *C. albicans*. Further, given the extensive knowledge on the mechanisms of W-O switching, finding that Mds3 is also a regulator of this phenomenon would provide us with information and genetic tools to understand Mds3 function and CMPS.

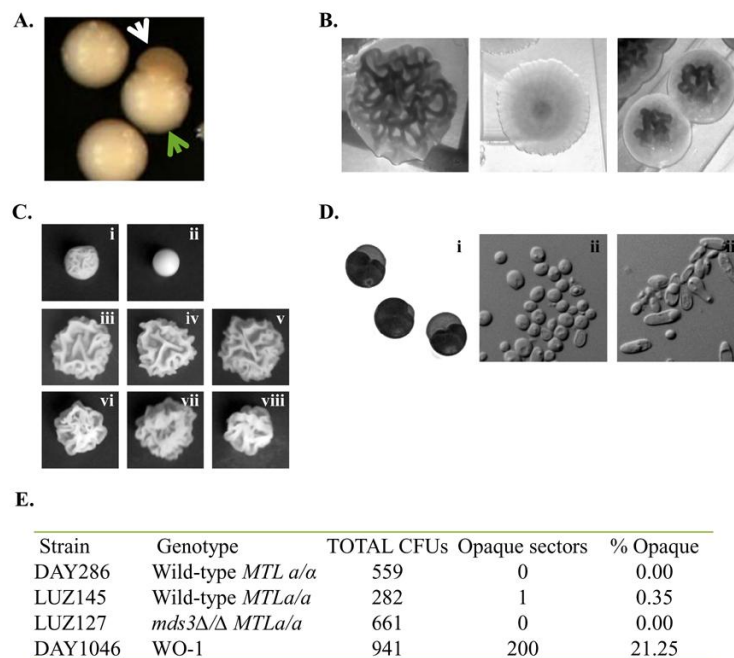


**Figure 4.1:** Colony morphology and white-opaque phenotypic switching in the *mds3Δ/Δ* mutant (A) Example of papilli formation on an *mds3Δ/Δ* colony. The white arrow points to a “papilli” from which a switched strain was isolated; the green arrow points to the colony from which a “parental” strain was isolated; (B) Examples of switched *mds3Δ/Δ* strains displaying alterations in colony morphology; (C) Re-introduction of *MDS3* into switched *mds3/mds3* strains does not restore colony morphology to the wild-type phenotype. (i) Wild-type (DAY185), (ii) *mds3/mds3* (GK09), (iii) SSY194, (iv) SSY194+*MDS3-HIS1* (LUZ797), (v) SSY194+*HIS1* (LUZ796), (vi) SSY210, (vii) SSY210+*MDS3-HIS1* (LUZ799), (viii) SSY210+*HIS1* (LUZ798). Picture taken after incubation in YPD at 37°C for 48 hrs; (D) Example of WO-1 (DAY1046) colonies with opaque sectors stained with lugol (i), and white (ii) and opaque (iii) cells under the microscope isolated from white and opaque sectors from WO-1 colonies. (E) Wild-type *MTL a/a* (DAY286) and *MTL a/a* strains (LUZ145), and *mds3Δ/Δ MTL a/a* (LUZ127) and WO-1 (DAY1046) strains were plated on SC medium and incubated at room temperature. Plates were scored for the formation of opaque sectors. The table shows the results at 10 days of incubation.

Homozygosis of the mating locus (*MTL*) in *C. albicans* is a pre-requisite for switching to the opaque phase (except in the case of an *HBR1* $\Delta$  strain (Pendrak et al., 2004)). To test if Mds3 regulates white-opaque switching, I constructed strains homozygous for the *MTL* locus in the wild-type and *mds3* $\Delta$  $\Delta$  backgrounds and determined the frequency at which these strains produced opaque sectors/colonies when plated on synthetic medium. The WO-1 hyper-switching *C. albicans* strain was used as a control (Slutsky et al., 1987, Figure 4.1D). There was no difference in white-opaque switching between the wild-type *MTL**a/a* and *mds3* $\Delta$  $\Delta$  *MTL**a/a* strains (Figure 4.1E). However, the frequency of white-opaque switching in the BWP17 background was considerably lower than in the WO-1 strain (Figure 4.1E, compare the wild-type BWP17 with the WO-1 strain). Thus, in order to determine if Mds3 is involved in W-O switching, this experiment needs to be repeated plating a minimum of 6000 colonies/strain in order to obtain more reliable data. Alternatively, an *mds3* $\Delta$  $\Delta$  mutant should be constructed in the WO-1 background and the switching frequency of the *mds3* $\Delta$  $\Delta$  WO-1 mutant should be compared with the wild-type WO-1 strain. Further, since *MTL* locus homozygosis is required for white-opaque switching, it would be interesting to determine if *MTL* homozygosis has any effect on the rate of CMPS as well.

### **Karyotypic rearrangements and aneuploidies are present in switched *mds3* $\Delta$ $\Delta$ strains**

One mechanism associated with phenotypic variation in *C. albicans* is genomic rearrangements (Rustchenko et al., 1993, 1994; Arbour et al., 2009; Selmecki et al., 2006; Forche et al., 2009). Thus, we predicted that switched *mds3* $\Delta$  $\Delta$  strains would carry aneuploidies or other genomic rearrangements. To test this idea, we performed CHEF gels and CGH analyses on different switched *mds3* $\Delta$  $\Delta$  strains (in collaboration with Mingchun Li, Paul and Bebe Magee, Anna Selmecki, and Judith Berman, at the University of Minnesota). CHEF and CGH assays are useful for the visualization of genomic alterations, but they differ in their sensitivity and on the

type of rearrangements that are readily observable in each of them. For example, CGH cannot distinguish a normal/diploid *C. albicans* DNA content from a genome with balanced chromosomal rearrangements (which do not alter the overall DNA content) or from tetraploid strains. Conversely, CHEF analyses do not allow for the simple detection of changes in copy number of chromosomes, or of rearrangements in which the new chromosomal fragments migrate similarly to other normal size chromosomal bands. Thus, CHEF and CGH are complementary assays.

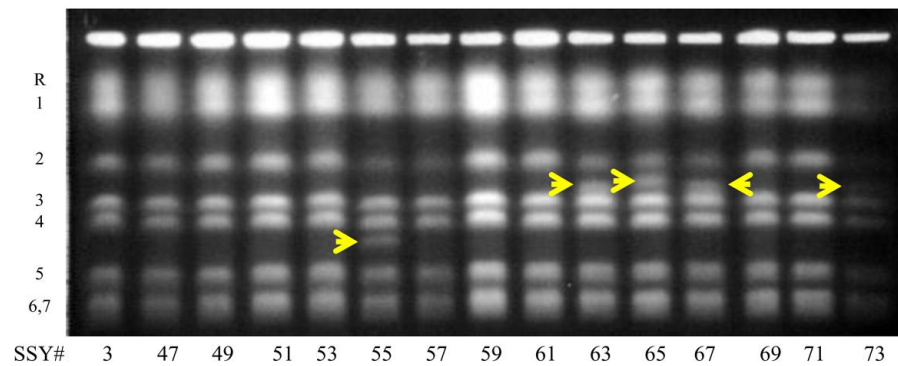


**Figure 4.2:** Karyotypic rearrangements in switched *mds3Δ/Δ* strains observed through CHEF electrophoresis. Chromosomes R to 7 are listed on the left. The yellow arrows point to new chromosomal fragments.

Gross karyotypic rearrangements can be detected by alterations in the band pattern obtained by CHEF analysis. We compared the karyotypes of 35 switched *mds3Δ/Δ* strains with the standard karyotype of *C. albicans* strain BWP17, and observed that nine strains (~26%) consistently showed a different karyotypic profile (Figure 4.2, Table 4.3). Of the nine strains with an aberrant karyotype, seven strains showed an extra band between Chromosomes 2 and 3, one (SSY16) showed an extra band between Chromosomes 1 and 2 and another between Chromosomes 2 and 3, and one strain (SSY55) showed an extra band between Chromosomes 4 and 5 (Figure 4.2, Table 4.3). Notably, almost all the strains with altered karyotype (eight out of nine) showed an extra band between Chromosomes 2 and 3. Although the size of the extra band

between Chromosomes 2 and 3 varied among isolates, it may indicate a common type of karyotypic aberration associated with the switch. Overall, CHEF analyses showed that chromosomal rearrangements occur in the switched strains, but that most switched *mds3Δ/Δ* strains appear to have a normal karyotype.

To complement the CHEF analyses, we performed CGH analyses in a smaller set of parental-switched *mds3Δ/Δ* strains. Three sets of matching parental-switched strains and one set of unmatched parental-switched strains (i.e. the parental strain pairs with a different switched strain) were analyzed by CGH (Figure 4.3, Table 4.3). While three out of four parental strains contained a normal diploid genome, the parental strain SSY209 showed a trisomy in Chromosome 6 and a loss of the Chromosome 5 monosomy at the *HIS1* locus, a characteristic of BWP17 strains (Selmecki et al., 2005) (Figure 4.3A,C,E,G). Chromosome 5 of strain SSY209 was only partially homozygous, because the MTL locus in this chromosome remained heterozygote, indicating that the event at Chromosome 5 likely involved a break induced recombination event or a single crossover (data not shown) (Forche et al., 2009). Three out of four switched strains showed aneuploidies (SSY34 showed a diploid genome): SSY73 and SSY75 showed partial Chromosome 2 aneuploidies, and SSY210 was trisomic for Chromosome 6 (Figure 4.3B,D,F,H). Interestingly, SSY210 still contained a Chromosome 5 monosomy at the *HIS1* locus. Since this Chromosome 5 monosomy is highly unlikely to occur randomly, these results suggest that the event that caused the partial homozygosis of Chromosome 5 in SSY209 occurred after the switched SSY210 was generated (Figure 4.3E,F). SSY73 was monosomic for the left 1/5<sup>th</sup> of Chromosome 2, while SSY75 was trisomic (or tetrasomic) for the right 4/5<sup>th</sup> of Chromosome 2 (Figure 4.3B,D). The 20% shorter Chromosome 2 defined by CGH analysis could be the extra band observed between Chromosomes 2 and 3 in SSY73 by CHEF (Figure 4.2, Table 4.3). However, CHEF analyses did not detect an extra band for strain SSY75 (data not shown), suggesting that the different results are either a property of variations in the colonies used for

each assay, or that the sensitivity of CHEF analyses is too low to consistently observe certain smaller karyotypic variations. Interestingly, the break point in Chromosome 2 at which SSY73 and SSY75 became aneuploid is similar (Figure 4.3B,D). Thus, both CHEF and CGH analyses

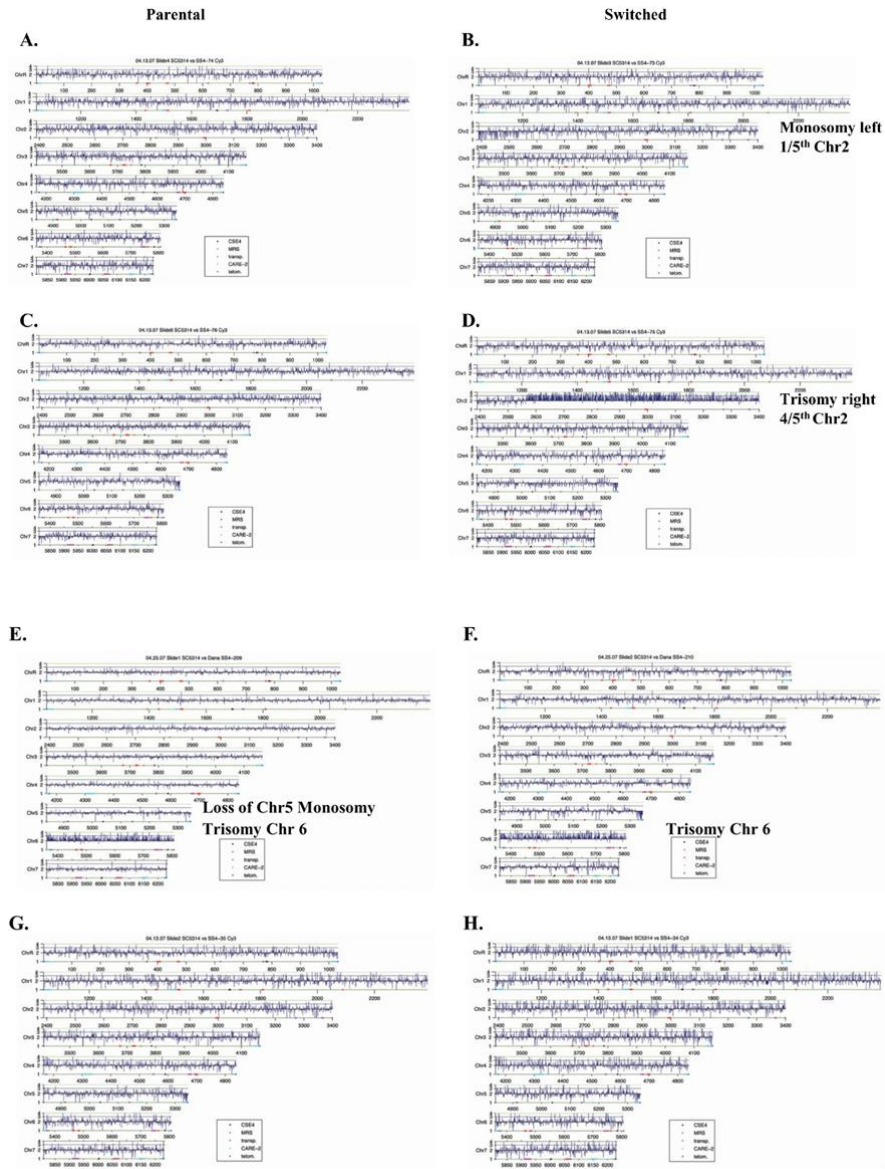


**Figure 4.3:** Aneuploidies are common in switched *mds3Δ/Δ* strains, but are not required for the phenotypic switch. The chromosomal content from three pairs of parental-switched *mds3Δ/Δ* strains (SSY74 (A) - SSY73 (B); SSY76 (C) - SSY75 (D)); SSY209 (E) - SSY210 (F)), and an unpaired set of a parental (SSY35 (G)) and a switched (SSY34 (H)) *mds3Δ/Δ* strains was compared to *C. albicans* strain SC5314 by CGH.

detect a higher frequency of karyotypic alterations in switched strains compared to the parental pairs that (may) involve Chromosome 2. Overall, CHEF and CGH results indicate that aneuploidies/karyotypic rearrangements occur in both switched and parental strains with a moderate frequency, and that they are not required for the switch to occur.

### **Switched *mds3Δ/Δ* strains show increased DNA damage sensitivity**

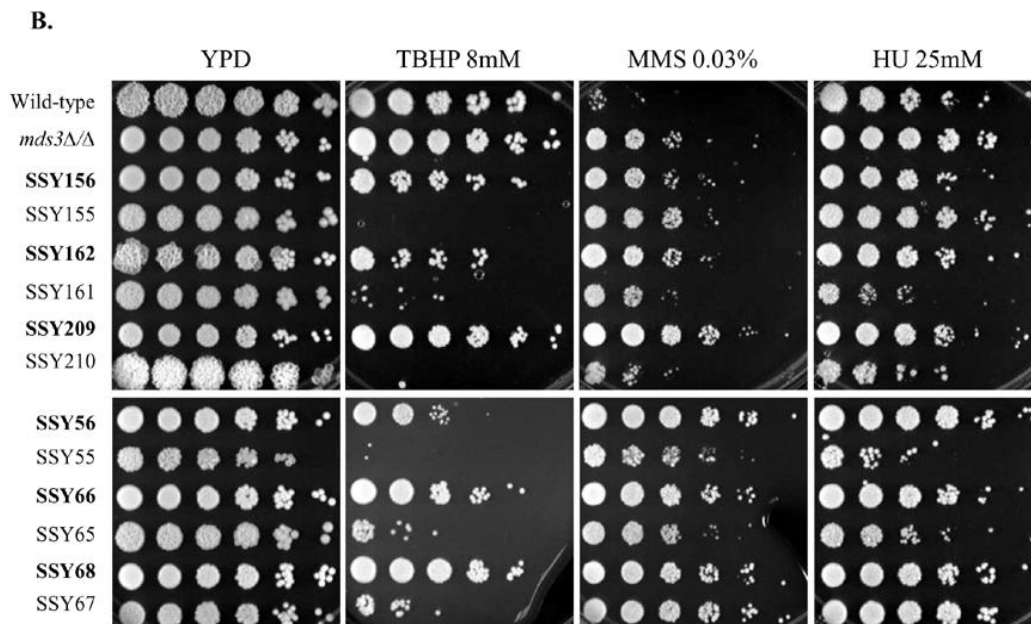
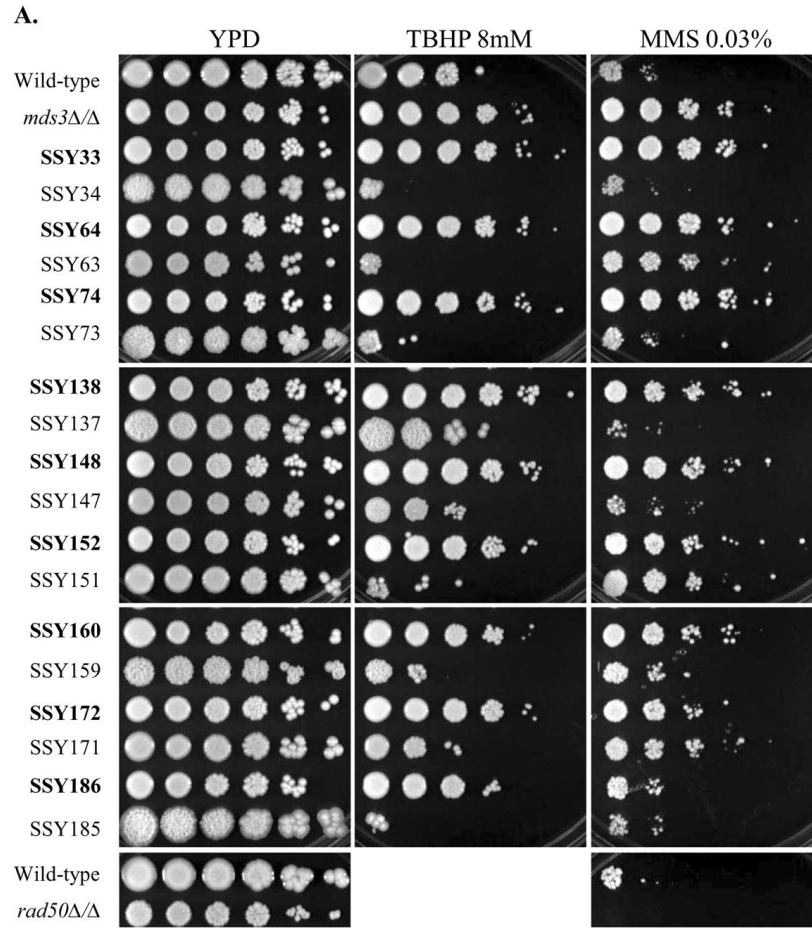
One mechanism to generate phenotypic diversity is by increasing the rate of genetic mutation (Loeb et al., 2008; Drotschmman et al., 2000; Funchain et al., 2000). One way to increase the rate of mutation is by relaxing the function of DNA repair mechanisms, which leads to an altered sensitivity to DNA damaging agents. Thus, I tested if the *mds3Δ/Δ* mutant showed an increased sensitivity to several DNA damaging agents: TBHP (an oxidizing agent), MMS (which indirectly causes double strand DNA breaks in cells deficient for homologous recombination), and HU (which inhibits DNA replication by depleting dNTP pools). As a control I used the *rad50Δ/Δ C. albicans* mutant which is hypersensitive to all these chemical stresses (Legrand et al., 2007). There was no difference in the sensitivity to TBHP or HU between the wild-type and *mds3Δ/Δ* strains (Figure 4.4). However, the *mds3Δ/Δ* mutant was more resistant to MMS than the wild-type strain (Figure 4.4). This result supports the idea that defective responses to genotoxic agents could lead to the phenotypic switch in the *mds3Δ/Δ* mutant.

The phenotypic switch in the *mds3Δ/Δ* mutant occurs after prolonged incubation. Thus, I wished to test if there was an effect of the aging of the colony on the sensitivity to genotoxic agents. Except SSY56, all the other fourteen *mds3Δ/Δ* parental strains tested showed similar TBHP sensitivity as the wild-type and original *mds3Δ/Δ* strains (Figure 4.4 and Table 4.3). Similarly, except SSY186, all other *mds3Δ/Δ* parental strains showed similar MMS sensitivity as the original *mds3Δ/Δ* strain (Figure 4.4 and Table 4.3). Finally, all six *mds3Δ/Δ* parental strains tested showed similar HU sensitivity as the the original *mds3Δ/Δ* strain (Figure 4.4 and Table

4.3). These results indicate that aging of the *mds3Δ/Δ* colony was generally not accompanied by any heritable alteration in the response to genotoxic stress.

Finally, I wished to determine if the phenotypic switch was associated with an alteration in the response to genotoxic agents. When I compared the sensitivity of switched vs. parental *mds3Δ/Δ* strains to DNA damage agents, I found that the phenotypic switch was generally accompanied by changes in the sensitivity to all genotoxic agents tested (Figure 4.4, Table 4.3). All fifteen switched *mds3Δ/Δ* strains tested showed increased sensitivity to TBHP. Eleven out of fifteen switched isolates showed enhanced MMS sensitivity compared to their parental *mds3Δ/Δ* counterparts; while four of the switched isolates showed similar MMS sensitivity as their parental *mds3Δ/Δ* counterparts (Figure 4.4, Table 4.3). Finally, four of the six switched *mds3Δ/Δ* strains were more sensitive to HU, one (SSY155) was equally sensitive as its parental counterpart, and one (SSY67) was highly resistant to HU (>50mM) (Figure 4.4). The degree of sensitivity to TBHP, MMS, or HU varied between the different isolates (Figure 4.4). Overall, these results indicate that the absence of *MDS3* enhances resistance to the genotoxic agent MMS, but not TBHP or HU. Further, the results show that the phenotypic switch in the *mds3Δ/Δ* mutant is accompanied by changes in the ability of cells to tolerate the presence of TBHP, MMS, and HU in the medium, and that these changes are not simply due to the aging of the colony. In particular, the switched *mds3Δ/Δ* strains showed a reproducible increase in sensitivity to the oxidizing agent TBHP.

**Figure 4.4:** The phenotypic switch in the *mds3Δ/Δ* mutant is accompanied by alterations in the sensitivity to DNA damaging agents. YPD overnights of the wild-type (DAY286), *mds3Δ/Δ* (DAY439 or DAY417), *rad50Δ/Δ* (DAY1063), and different *mds3Δ/Δ* switched-parental strains (SSY strains) were diluted in PBS to an ~OD<sub>600nm</sub> of 1.6, further diluted 1:5 in PBS and plated on YPD supplemented with TBHP, MMS (A,B) and HU (B). Plates were incubated at 30°C. Pictures were taken after 72 hrs incubation. Parental strains are in **bold**, and plated always above its corresponding switched pair.



### **Effects of glucose starvation and alkaline pH on *mds3Δ/Δ* mutant papilli formation**

Papilli formation in the *mds3Δ/Δ* mutant occurs only after prolonged incubation, a condition in which the colonies are starved for nutrients and have entered stationary phase. I reasoned that increasing the starvation signal might contribute to enhance papilli formation. To test this idea, I reduced the concentration of supplemented glucose in YPD to 0.2%, instead of the regular 2%. Indeed, I observed that while starving cells for glucose had no effect on wild-type cells, the % of colonies that showed papilli in the *mds3Δ/Δ* mutant (and the number of papilli/colony (data not shown)) increased significantly with time when compared with growth on 2% glucose (Figure 4.5). However, I did not observe an earlier onset of papilli formation in the *mds3Δ/Δ* mutant in YPD with 0.2% glucose compared to 2% glucose, which suggests that other nutrients need to become limiting as well, perhaps the nitrogen source. In this regard, I observed that papilli formation in the *mds3Δ/Δ* mutant was enhanced in the presence of the amino acid glutamine as the only nitrogen source in the media, but not in the presence of ammonium or of the amino acid proline (data not shown). In fact, addition of proline appeared to inhibit papilli formation (data not shown). Alternatively, a secondary metabolite might need to build up in the medium to induce papilli formation. Importantly, the presence of glucose is not required for papilli formation as we can also observe papilli in medium supplemented with glycerol as carbon source (data not shown). Overall, these results indicate that papilli formation can be exacerbated by glucose starvation in the absence of *MDS3*, and that it is likely the overall nutritional composition of the medium, including the availability of particular nitrogen sources, which play a critical role in the regulation of CMPS.

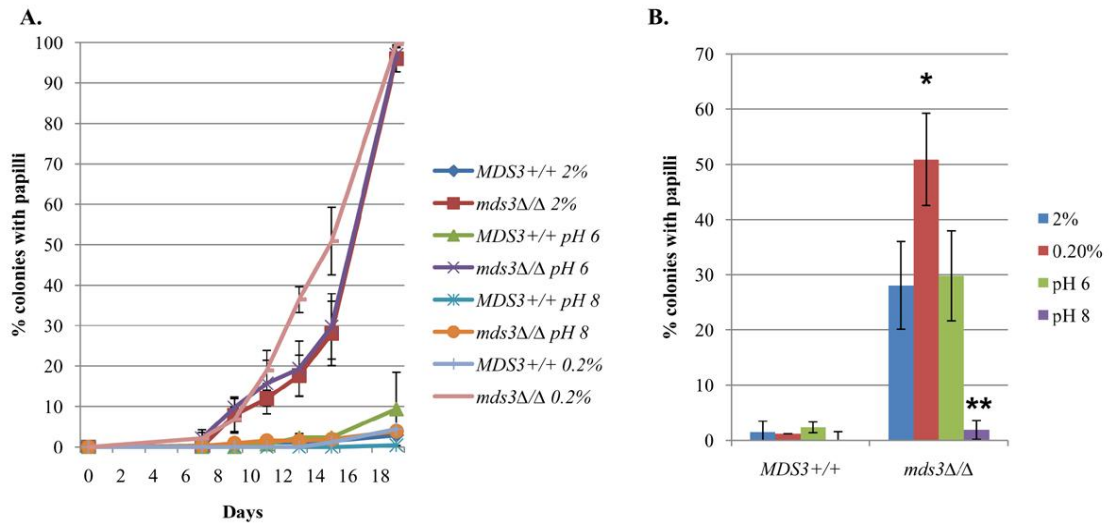


**Figure 4.5:** Phenotypic switching in the *mds3Δ/Δ* mutant is enhanced under glucose starvation and repressed under alkaline pH conditions. YPD overnights from the wild-type (DAY185) and *mds3Δ/Δ* (DAY1118) strains were diluted in PBS and plated in YP with 2% or 0.2% glucose, or YPD buffered at pH 6 or pH 8. Plates were incubated 48 hrs at 30°C and then at room temperature for over two weeks. (A) The graph shows the progressive accumulation of papilli in the *mds3Δ/Δ* mutant. (B) Papilli at day 15 of incubation. Results are representative of multiple independent experiments. \* p value <0.05; \*\* p value < 0.005, using one-tailed paired Student test (comparisons against *mds3Δ/Δ* grown with 2% glucose).

In *C. albicans*, Mds3 is required for growth and filamentation at alkaline pH, and Mds3 also regulates the expression of several alkaline responsive genes (Davis et al., 2002; Zacchi et al., 2010a). Thus, I wished to test if alkaline pH would have an effect on the ability of the *mds3Δ/Δ* mutant to produce papilli. While buffering YPD at alkaline pH had no effect on the wild-type strain, it significantly inhibited papilli formation in the *mds3Δ/Δ* mutant (Figure 4.5). The inhibition of papilli formation was not due to the buffer in the medium, because the *mds3Δ/Δ* mutant formed papilli in unbuffered YPD and YPD buffered at pH 6 at the same rate (Figure 4.5). Thus, alkaline pH inhibits papilli formation in the *mds3Δ/Δ* mutant.

### **Alkaline pH induces rapamycin resistance in *C. albicans***

We recently identified Mds3 as a regulator of the TOR pathway (Zacchi et al., 2010a). Mds3 is also required for proper alkaline pH responses (Davis et al., 2002; Zacchi et al., 2010a (Chapter 3)). Thus, I reasoned that alkaline pH might have an effect on TOR pathway function. To test this, I plated wild-type, *mds3Δ/Δ*, and *mds3Δ/Δ+MDS3* cells in unbuffered YPD and YPD buffered at pH 6 or pH 8 supplemented with solvent or with the TOR kinase inhibitor rapamycin. As a control, I plated a *sit4Δ/Δ* mutant, which is resistant to rapamycin (Zacchi et al., 2010a). While buffering the media at pH 6 had no effect on rapamycin resistance compared to unbuffered YPD medium, buffering YPD at pH 8 caused a marked increase in rapamycin resistance for all strains (Figure 4.6). It is possible that rapamycin resistance at alkaline pH was caused by a decrease in rapamycin intake or stability. However, rapamycin has a transcriptional effect in M199 pH 8 at 6 hrs of incubation, and is able to delay wild-type filamentation in M199 pH 8 solid medium after 48 hrs of incubation, indicating that at alkaline pH rapamycin is being incorporated into the cells and is exerting an effect (Zacchi et al., 2010a; Bastidas et al., 2009; and data not shown). A similar increase in rapamycin resistance was observed when cells were plated in SLAD medium supplemented with rapamycin (data not shown). The result observed in SLAD medium was not unexpected, since the low concentration of nitrogen sources in SLAD should already inactivate TOR function, making the cells less sensitive to further inactivation by rapamycin. Thus, alkaline pH is likely directly or indirectly reducing TOR function and/or the cellular dependence on TOR function, allowing for continued growth in the presence of normally inhibitory concentrations of rapamycin.

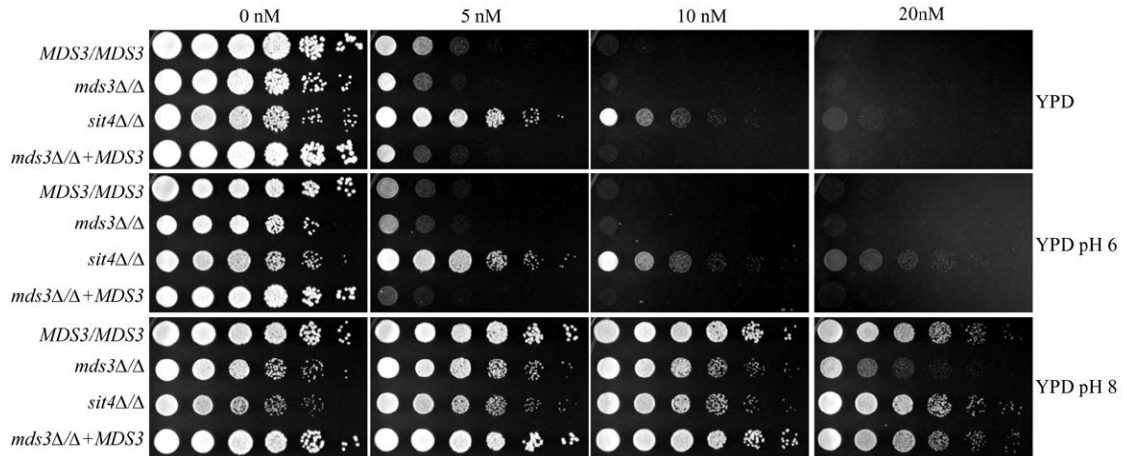


**Figure 4.6:** Alkaline pH enhances rapamycin resistance in *C. albicans*. YPD overnights of the wild-type (DAY185), *mds3Δ/Δ* (DAY1118), *mds3Δ/Δ+MDS3* (DAY1119), and *sit4Δ/Δ* (DAY972) were diluted in PBS to an  $\sim$ OD<sub>600nm</sub> of 1.6, further diluted 1:5 in PBS and plated on YPD supplemented with rapamycin. Plates were incubated at 30°C. Pictures were taken after 72 hrs incubation.

### Switched *mds3Δ/Δ* strains show increased rapamycin sensitivity

I reasoned that if the growth defects of the *mds3Δ/Δ* mutant were caused by a defective TOR pathway, then the appearance of the switched strains might reflect the formation of strains that are able to bypass and/or restore TOR function. To test the function of the TOR pathway in the *mds3Δ/Δ* switched strains I compared the growth of *mds3Δ/Δ* switched strains with their corresponding parental counterparts in media supplemented with rapamycin. In nutrient poor conditions, such as growth in Spider medium, the *mds3Δ/Δ* mutant is more resistant to rapamycin than the wild-type strain (Zacchi et al., 2010a). Thus, I hypothesized that the switched *mds3Δ/Δ* strains would have regained rapamycin sensitivity in nutrient poor medium. I also performed this experiment in nutrient rich YPD medium, to determine if the switch would alter the response to rapamycin in the *mds3Δ/Δ* strain in a condition in which this mutant does not normally have a phenotype.

Nineteen switched-parental *mds3Δ/Δ* strain pairs were plated on Spider and YPD media supplemented with rapamycin and their growth was compared to the wild-type and original

*mds3Δ/Δ* strains. In Spider medium, eighteen out of the nineteen parental strains behaved similarly to the original *mds3Δ/Δ* mutant, while one was more sensitive (SSY186, Table 4.3). Fifteen out of the nineteen switched *mds3Δ/Δ* pairs were more sensitive to rapamycin compared to the corresponding parental strains (including SSY186/5), and the remaining four were as resistant to rapamycin as their parental pair (Figure 4.7, Table 4.3). In YPD medium supplemented with rapamycin, fifteen of the nineteen parental strains grew similar to the original *mds3Δ/Δ* and wild-type strains; ten of their corresponding switched *mds3Δ/Δ* pairs were more sensitive to rapamycin, four were equally resistant, and one was more resistant than the corresponding parental *mds3Δ/Δ* pair (Figure 4.7, Table 4.3). The four remaining parental strains out of the nineteen pairs tested in YPD showed different rapamycin sensitivity when compared to the original *mds3Δ/Δ* strain: one was more resistant (SSY209) and three were more sensitive (SSY42, SSY76, SSY186). Of these four strains, the corresponding switched pairs SSY210 and SSY185 were more resistant to rapamycin compared to their parental *mds3Δ/Δ* pair, while SSY41 and SSY75 were more sensitive. I noted that those switched-parental pairs that were equally resistant to rapamycin in Spider medium were also equally resistant to rapamycin in YPD medium. Further, the degree at which each switched strain was more sensitive to rapamycin was variable, suggesting differences in the mechanisms that lead to rapamycin sensitivity. Since the *mds3Δ/Δ* mutant does not have a phenotype in YPD supplemented with rapamycin (Zacchi et al., 2010a) I was not expecting to see growth differences in the switched *mds3Δ/Δ* strains in YPD. However, most switched strains did show increased rapamycin sensitivity in YPD compared to their parental counterparts, although the phenotypic reversion in YPD medium was often more subtle than in Spider medium (Figure 4.7). Overall, these results indicate that the switch in the *mds3Δ/Δ* mutant is accompanied by an increase in rapamycin sensitivity in both poor and rich nutrient conditions. These results suggest that an alteration in the function of the TOR pathway is associated with the morphological switch in the *mds3Δ/Δ* mutant. Further, as observed previously

in the DNA damaging assays (Figure 4.4), most of the parental strains did not show an altered response to rapamycin, indicating that the processes that led to increased rapamycin sensitivity in the switched strains are not solely occurring due to the aging of the colony.

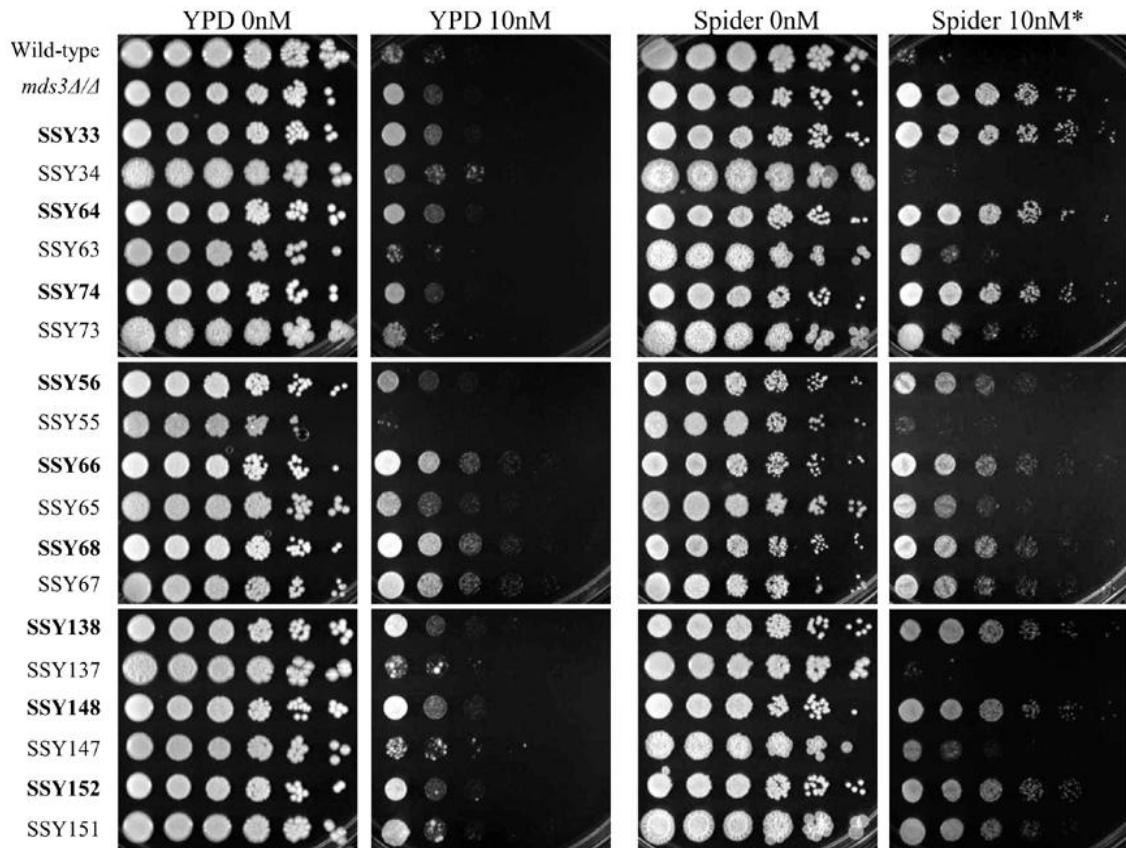


**Figure 4.7:** The switch in the *mds3Δ/Δ* mutant is accompanied by enhanced rapamycin sensitivity. YPD overnights of the wild-type (DAY286), *mds3Δ/Δ* (DAY439 or DAY417) and different *mds3Δ/Δ* switched-parental strains (SSY strains) were diluted in PBS to an  $\sim$ OD<sub>600nm</sub> of 1.6, further diluted 1:5 in PBS and plated on YPD and Spider media supplemented with rapamycin. Plates were incubated at 30°C. Pictures were taken after 72 hrs incubation. Parental strains are in **bold**, and plated always above its corresponding switched pair. \* The Spider plate shown here for SSY55-68 contains 15nM Rapamycin.

### The *TOR1-1* allele and *mds3Δ* have a synergism in papilli formation

The role of Mds3 as a regulator of the TOR pathway, the effect of alkaline pH on papilli formation and on rapamycin resistance, and the increased sensitivity to rapamycin of the switched strains suggest that defects in the signaling through the TOR pathway is involved in the

phenotypic switch (Figures 4.5-4.7). Previously, we found that the *TOR1-1* allele and *MDS3* deletion showed a synergistic growth defect, potentially caused by a partial or altered function of *TOR1-1* (Zacchi et al., 2010a (Chapter 3)). If alterations in TOR signaling are indeed associated with papilli formation then I might also see a synergism between the *TOR1-1* allele and the *mds3Δ* mutation on papilli formation.

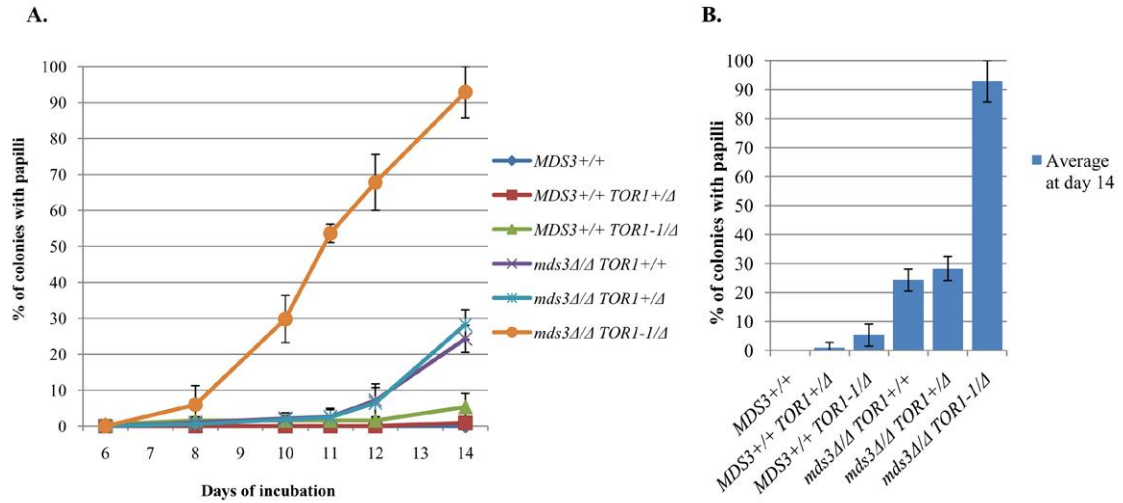


**Figure 4.8:** Synergistic effect of the *TOR1-1* allele and *mds3Δ/Δ* deletion on papilli formation. YPD overnights from the wild-type (DAY185), *TOR1Δ* (DAY1123), *TOR1-1Δ* (DAY1125), *mds3Δ/Δ* (DAY1118), *mds3Δ/Δ TOR1Δ* (DAY1122), and *mds3Δ/Δ TOR1-1Δ* (DAY1124) strains were diluted in PBS and plated in YPD. Plates were incubated 48 hrs at 30°C and then at room temperature for over two weeks. The results graphed are representative of two independent experiments (A). Results at day 14 (B).

To test this idea, I determined papilli formation in wild-type and *mds3Δ/Δ* strains with a *TOR1*<sup>+/+</sup>, *TOR1Δ*, and *TOR1-1Δ* genetic background. There was no difference in papilli formation among the *TOR1*<sup>+/+</sup>, *TOR1Δ*, and *TOR1-1Δ* wild-type strains (except for a small increase in the *TOR1-1Δ* strain), or between the *mds3Δ/Δ TOR1*<sup>+/+</sup> and *mds3Δ/Δ TOR1Δ* strains (Figure 4.8). However, the *mds3Δ/Δ TOR1-1Δ* mutant showed a marked exacerbation in papilli formation compared with the *mds3Δ/Δ TOR1*<sup>+/+</sup> and *mds3Δ/Δ TOR1Δ* strains (Figure 4.8). The presence of the single *TOR1-1* allele in the *mds3Δ/Δ* background increased both the % of colonies with papilli and the number of papilli/colony (Figure 4.8 and data not shown). Further, papilli

formation in the *mds3Δ/Δ TOR1-1/Δ* strain was observed 2-4 days before papilli appeared in the *TOR1/Δ* or *TOR1+/+ mds3Δ/Δ* strains, suggesting that defects in TOR pathway signaling accelerate the formation of papilli (Figure 4.8A). Since the TOR pathway is considered to respond primarily to nitrogen environmental sources, these results supports the hypothesis that besides glucose, nitrogen also needs to become limiting for papilli to appear (see above, Figure 4.5) (Crespo et al., 2002; Wullschleger et al., 2006; Dann and Thomas, 2006). Overall, these results support a role for TOR pathway signaling in papilli formation in the *mds3Δ/Δ* mutant.

Taken together, we have continued to uncover the vast diversity of phenotypes associated with the alteration in colony morphology of the *mds3Δ/Δ* mutant, including expression of virulence traits (M.T.A., M.J.H., Z.M., S.J.M unpublished results), genomic rearrangements and sensitivity to DNA damage agents and rapamycin (Figures 4.2-4 and 4.7). I have also found environmental conditions that enhance (glucose starvation) and inhibit (alkaline pH) the phenotypic switch in the *mds3Δ/Δ* mutant. Overall, our results support a model in which papilli appear in the *mds3Δ/Δ* mutant during stationary phase due to the accumulation of genetic and epigenetic defects caused by a de-regulated TOR pathway.

## DISCUSSION

Despite the strong association between CMPS and pathogenesis in *C. albicans* there is very little known about the mechanisms that regulate CMPS in this fungus. Mds3 is a fungal specific protein that is a negative regulator of CMPS in *C. albicans*. Mds3 is also involved in other morphogenetic processes in *C. albicans* and *S. cerevisiae*, including filamentation, chlamyospore formation, and meiosis (Davis et al., 2002; Nobile et al., 2003; Benni and Neugeborn, 1997; McDonald et al., 2008). Bioinformatic, genetic, and biochemical analyses suggest that Mds3 is a cytoplasmic Kelch/BTB protein that functions as a regulator of the TOR pathway (Zacchi et al, 2010a; Chapters 2 and 3). Indeed, our results support a role for the TOR pathway on papilli formation in the *mds3Δ/Δ* mutant, and suggest that the switching in this strain renders the colony morphology switching phenotype *MDS3*-independent and TOR-dependent (Figure 4.9).

*What is the evidence that the switch in the *mds3Δ/Δ* mutant is associated with an alteration in the function of the TOR pathway?*

Since Mds3 is a member of the TOR pathway (Chapter 3) it was reasonable to propose that TOR pathway function was associated with phenotypic switching. Four independent results support this idea. First, alkaline pH allows cells to grow in the presence of normally inhibitory concentrations of rapamycin (Figure 4.6). This suggests that alkaline pH could either contribute to TOR pathway inhibition, or, more likely, could activate mechanisms that bypass the need for an active TOR pathway. For example, similar to *S. cerevisiae*, alkaline pH could affect the function of the PKA pathway, a pathway which shares many downstream effectors with TOR (Dechant et al., 2010; Thevelein and de Winde, 1999; Soulard et al., 2010). Thus, the observation that alkaline pH significantly inhibits the switch in the *mds3Δ/Δ* mutant supports a role for TOR activation in the switching process (Figure 4.5). Second, there is a synergism in papilli formation

between the *mds3Δ* mutation and the *TOR1-1* allele, a partial function allele that carries a point mutation in the rapamycin binding domain of *TOR1* (Figure 4.8, Chapter 3). Third, the presence of glutamine –a TOR activator (Crespo et al., 2002; Dann and Thomas, 2006)-as the sole nitrogen source in the medium increased papilli formation in the *mds3Δ/Δ* mutant compared with the presence of ammonium, while the presence of the amino acid proline –which activates NCR mimicking TOR inhibition (Tate et al., 2008; Cox et al., 2000)- inhibited papilli formation (data not shown). Finally, and more importantly, the switch in the *mds3Δ/Δ* cells strongly correlates with increased rapamycin sensitivity, suggesting that these switched cells have become dependent on TOR pathway function (Figure 4.7). An analogous phenomenon to this last point, denominated “oncogene addiction”, occurs when certain mammalian tumor cells become dependent on the pathways that are upregulated. Tumors caused by an overactivation of the TOR pathway or of upstream TOR effectors become hypersensitive to, and thus treatable with, rapamycin (Menon and Maning, 2008; Weinstein, 2002; Strimpakos et al., 2009). Similarly, certain tumors develop and addiction to glutamine due to the TOR activating characteristics of this amino acid (Wise and Thompson, 2010). Thus, independent evidence suggests a role for the TOR pathway in phenotypic switching in the *mds3Δ/Δ* mutant. However, more direct evidence is needed to verify this hypothesis. To this end, strains in which several TOR pathway members are epitope tagged have been constructed, including Tap42-HA, and the transcription factors Npr1-HA and Gln3-Myc (Wang et al., 2003; Beck and Hall, 1999; Schmidt et al., 1998), and are ready to be tested for alterations in protein expression, and for TOR dependent and independent phosphorylation patterns and molecular interactions (data not shown).

#### *How does the switch occur in the mds3Δ/Δ mutant?*

The first manifestation of the switch in the *mds3Δ/Δ* mutant is the formation of papilli on the colony surface. Papilli become visible only after prolonged incubation (Figures 4.5 and

4.8), a condition in which nutrients become limited, toxic metabolites accumulate, stress responses are induced, and cell growth is inhibited: cells enter stationary phase, a state of quiescence. However, in order to enter stationary phase, cells need to inhibit TOR activity [TOR activity promotes cellular growth and cell division (Wullschleger et al., 2006)]. Cells that are unable to properly regulate the TOR pathway, such as *mds3Δ/Δ* cells, are likely to encounter difficulties in properly establishing the stationary phase program (Zacchi et al., 2010a). The switch in the *mds3Δ/Δ* cells is accompanied by karyotypic changes, by defects in the response to DNA damage agents, and by hypersensitivity to rapamycin (Figures 4.2-4 and 4.7). Karyotypic changes and the altered DNA damage response could function as mechanisms leading to the switch, while increased rapamycin sensitivity suggests alterations in TOR pathway function. Therefore, I propose a model in which the switch occurs due to the accumulation of genetic and epigenetic alterations that happen as *mds3Δ/Δ* cells try to enter stationary phase with a deregulated TOR pathway (Figure 4.9). The deletion of *MDS3* would predispose cells to undergo the phenotypic switch, but secondary events appear to be required for the switch to occur.

*Why do the switched mds3Δ/Δ mutant cells form papilli?*

In a nutrient poor medium, the switch might give cells the ability to scavenge alternative nutrient sources. Metabolic adaptation is associated with phenotypic switching in other organisms, such as tumor formation and progression in mammalian organism (Furuta et al., 2010). Further, the appearance of mutants with an altered metabolism that can outgrow an otherwise nutrient-limited population has been previously observed in evolution studies in yeast (Gresham et al., 2009; Dunham et al., 2002). Interestingly, a mutation in *MDS3*, likely a dominant gain of function mutation, led to increased fitness during *S. cerevisiae* evolution studies in glucose-limiting conditions, indicating that, similar to *C. albicans*, *Mds3* also controls nutrient adaptation processes in yeast (Anderson et al., 2010). Different mechanisms are associated with

the increased fitness of evolving cells, including chromosomal rearrangements, aneuploidies, point mutations, and gene amplifications/deletions (Pavelka et al, 2010; Gresham et al., 2009; Dunham et al., 2002). In *C. albicans* aneuploidy is also associated with altered nutrient assimilation (Rustchenko, 2007; Janbon et al., 1998). Thus, similar to the models for tumor progression in mammalian organisms (Merlo et al., 2006; Hanahan and Weinberg et al., 2000), papilli may form in the *mds3Δ/Δ* cells because of the acquisition of genetic (and epigenetic) alterations that provide these cells with a fitness advantage in a nutrient poor medium and/or that allow them to bypass cell cycle checkpoints and continue to divide under sub-optimal environmental conditions. (According to this model, the switched strains should be unable to enter stationary phase and should die of starvation faster than the original *mds3Δ/Δ* mutant. This idea awaits further experimentation).

The model in which the switch happens through a stepwise accumulation of changes helps to explain several characteristics of the *mds3Δ/Δ* switch. First, this model explains why switched *mds3Δ/Δ* cells do not revert to the original colony phenotype after a wild-type *MDS3* copy is incorporated back into them (Figure 4.1C and data not shown). Second, it explains why some parental colonies (which have aged, but not switched) retain the *mds3Δ/Δ* original colony morphology but carry genomic rearrangements and show altered resistance to DNA damage agents and rapamycin compared to the original *mds3Δ/Δ* mutant (Figures 4.3, 4.4 and 4.7, Table 4.3). Third, this model explains why each switched strain displays different phenotypes: each strain has a diverse, (semi) independent set of alterations that lead to different phenotypic outputs. Importantly, since the switch is reversible, these alterations need to allow for “phenotypic reversion” (see below).

In summary, my current model to explain CMPS in the *mds3Δ/Δ* mutant is the following: increased stress due at least partially to starvation, together with other environmental signals like acidic pH and glutamine, contribute to the formation of switched *mds3Δ/Δ* strains

through a stepwise accumulation of (reversible) genetic and epigenetic alterations that increase TOR dependence and *MDS3* independence (Figure 4.9).

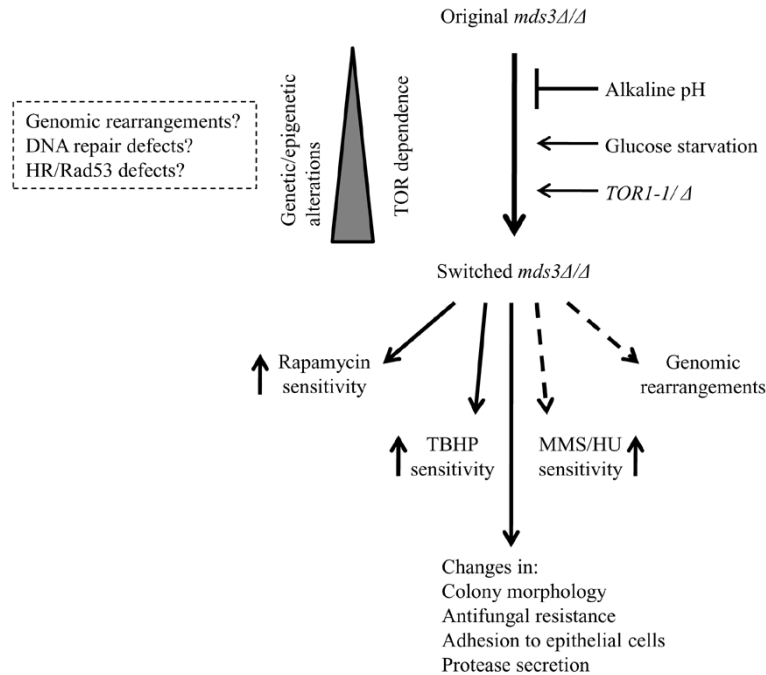


**Figure 4.9:** Summary model of CMPS in the *mds3Δ/Δ* mutant. See details in the text. HR: homologous recombination. The dashed arrows indicate that the phenotype is only seen in some switched strains, while solid arrow indicates >80% penetrance.

### Putative mechanisms leading to CMPS in the *mds3Δ/Δ* mutant

Several mechanisms can generate variability in *C. albicans*, including karyotypic rearrangements, aneuploidies, and increased mutation rate. Formation of aneuploidies are one appealing mechanism to explain a reversible phenotypic phenomenon like CMPS in *C. albicans* for two reasons: first, aneuploidy formation is common in *C. albicans*; and second, certain types of rearrangements can be randomly gained and subsequently randomly lost, as observed for the association between Chromosome 5 aneuploidies and the acquisition of antifungal resistance or the ability to grow in sorbose (Bouchonville et al., 2009; Arbour et al., 2009; Selmecki et al., 2005, 2006, 2008, 2009; Janbon et al., 1998). Our CHEF and CGH studies indicate that

karyotypic rearrangements and aneuploidies are present in *mds3Δ/Δ* switched strains, which is well in agreement with previous reports (Figures 4.2, and 4.3, Table 4.3) (Forche et al., 2009; Rustchenko et al., 1994; Rustchenko, 2007). However, not all switched strains appear to carry genomic rearrangements, and genomic rearrangements also occur in parental strains (Figure 4.3, Table 4.3). These results indicate that although karyotypic changes and aneuploidies are associated with the switch, they are not the cause of the switch nor they are required for the switch to occur (Barton and Scherer, 1994). We noted that one strain analyzed by CGH (SSY75) showed an aneuploidy that was not predicted by CHEF analysis (Figure 4.3, Table 4.3). These results suggest that CGH analyses are more sensitive than CHEF analyses in the detection of certain types of genomic changes, and that from our CHEF results we might be underestimating the actual level of genomic rearrangements in the switched *mds3Δ/Δ* strains.

Loss of heterozygosity (LOH) and aneuploidies of Chromosome 2 have been previously associated with changes in colony morphology in *C. albicans* (Forche et al., 2009). Interestingly, aneuploidies of Chromosome 2 appear to be one common feature in switched *mds3Δ/Δ* strains observed by CGH and suggested by CHEF analyses (Figure 4.3, Table 4.3). The CGH analyses suggest that there is a common breakpoint in Chromosome 2 where aneuploidies occur in the switched strains (Figure 4.3B, D). This common breakpoint could be a chromosomal fragile site (Arlt et al., 2006). One interpretation of the CGH data is that the Chromosome 2 aneuploidies might be causing a gene dosage effect: the ratio of the left 1/5<sup>th</sup> to the right 4/5<sup>th</sup> of Chromosome 2 is 1:2 (SSY73) or 2:3 (SSY75) (Figure 4.3B, D, Table 4.3). Chromosome 2 is one of the largest chromosomes in *C. albicans* genome. Therefore, speculating what genes or regions in Chromosome 2 might be involved in the putative dosage effect is difficult. However, we noted that *BCY1*, which encodes the protein kinase A (PKA) regulatory subunit, and *TPK2*, which encodes the major PKA catalytic subunit, are located in opposite sides of Chromosome 2 and would be subject to a dosage effect in these aneuploid strains (Figure 4.3, Candida Genome

Database, Souto et al., 2006; Tamaki, 2007; Giacometti et al., 2006). Given the haploinsufficiency of *BCY1*, these results suggest that these two aneuploid strains carry an overactive PKA pathway (Giacometti et al., 2006). Other genes that might be amplified in the trisomic strain include *RAS1*, an upstream positive regulator of PKA; the TOR pathway members *TOR1*, *SCH9*, *URE2*, *FHL1* (which requires *TBF1* for function, also amplified in the trisomy); the stress responsive elements *HOG1* and *HSP78*; and the zinc transporter *ZRT2*. Interestingly, Zrt1, a high-affinity zinc transporter, has been associated with a blebbing phenotype in *S. cerevisiae* strains caused by microsatellite rearrangements during stationary phase (Kelly et al., 2007). Further, zinc was identified as an environmental negative regulator of CMPS, suggesting a connection between zinc, Chromosome 2 aneuploidies, *ZRT2*, and CMPS (Bedell and Soll, 1979). Thus, it would be interesting to determine the frequency of Chromosome 2 aneuploidies in switched *mds3Δ/Δ* strains, and if the amplification or haploinsufficiency in particular genes in this chromosome are associated with the switch in the *mds3Δ/Δ* mutant.

DNA damage response defects could be a mechanism leading to CMPS in *C. albicans* (Figure 4.9). DNA damage response defects lead to increase frequency of point mutations, defects in cell cycle checkpoints, and genomic instability, which can all lead to phenotypic alterations (Negri et al., 2010; Drotschmann et al., 2000). Further, *C. albicans* mutants with defects in homologous recombination give rise to colonies with altered morphologies (Legrand et al., 2007). In line with this, the increased sensitivity to genotoxic agents observed in the switched strains would suggest that defective DNA damage response is contributing to CMPS in *C. albicans* (Figure 4.4, 4.9). The rate of phenotypic switching in the *mds3Δ/Δ* mutant is  $\sim 10^{-2}$  (not the frequency of papilli formation, but the frequency at which switched *mds3Δ/Δ* strains switch again to a different morphology), significantly above the normal rate of random point mutation in eukaryotes:  $10^{-8}$ . Such an increase in the mutagenic frequency would most certainly be lethal to any organism. Therefore, increased mutagenesis cannot solely account for CMPS in the *mds3Δ/Δ*

mutant. However, a combination of an increased point mutation rate with an increased rate of chromosomal rearrangements (chromosomal loss, or LOH events) could be one way through which *C. albicans* can achieve variability and retain reversibility. (We must keep in mind that phenotypic reversibility does not imply genetic reversibility, i.e., we can achieve similar phenotypes by compensating a mutation in X with a mutation in Y, not necessarily with a reversion of X). Further, the increased resistance to MMS observed in the original *mds3Δ/Δ* mutant suggests that this mutant might be able to tolerate and, therefore, accumulate DNA damage, which could eventually lead to the switch (Figure 4.9). Increased MMS resistance has been associated in yeast to low levels of the checkpoint protein Rad53 (Cordon-Preciado et al., 2006; Aguilera and Gomez-Gonzalez, 2008). Further, *S. cerevisiae rad53Δ* mutants show high instability of repetitive DNA, which is often associated with chromosomal fragile sites (Lahiri et al., 2004). Thus, defects in Rad53 function could also explain the Chromosome 2 aneuploidies observed in the *mds3Δ/Δ* switched strains (Figure 4.3). Thus, it would be interesting to determine if Mds3 plays a role in Rad53 regulation or stability, and if Rad53 function is altered in the switched strains. Further, defects in nutrient signaling pathways like PKA and TOR are associated with DNA damage response [and Rad53 function] (Searle et al., 2004; Shen et al., 2007; Budanov and Karin, 2008; Chapter 5), which supports the hypothesis that switched *mds3Δ/Δ* variants arise due to mechanisms that suppress TOR pathway defects.

LOH events and epigenetic mechanisms are also associated with phenotypic variation. We did not determine LOH levels in the switched *mds3Δ/Δ* strains and only began to explore the role of epigenetic mechanisms in CMPS, thus we cannot discard a role for these processes in CMPS. We took several approaches to look at the role of epigenetic mechanisms in CMPS. First, we constructed mutants in histone deacetylases (HDACs) and determined their ability to produce colonies with altered morphology and/or papilli (Appendix A and data not shown). Second, in collaboration with Helen Wang and Judith Berman (University of Minnesota) we constructed

*mds3Δ/Δ* and *mds3Δ/Δ+MDS3* strains with a *URA3* marker replacing the Chromosome 5 centromeric region in order to test if the absence of *MDS3* had an effect on the ability of cells to express and/or silence *URA3* at centromeres (see Methods, Table 4.1, Ketel et al., 2009). Third, since silencing requires different mechanisms at different chromosomal locations (Perrod and Gasser, 2003) I also tried to construct strains containing a *URA3* cassette near the telomeres to look for differences in telomeric silencing; while I obtained recombinants at the correct location, the *URA3* gene appeared to be lost instead of silenced (data not shown). We did not detect an increased frequency of switching in the HDACs mutants (data not shown), but we have not yet fully determined the role of *MDS3* in gene silencing at the centromeres. Importantly, even though the original *mds3Δ/Δ* mutant might not show a gene silencing defect, alterations in silencing might arise stepwise and eventually contribute to the switch. Thus, it would be interesting to isolate switched variants from the *mds3Δ/Δ cen5::URA3/CEN5* strains and determine their ability to silence *URA3*.

### **Environmental signals affecting CMPS in the *mds3Δ/Δ* mutant**

Why does glucose starvation enhance papilli formation and alkaline pH inhibits it? Glucose levels are sensed by several signaling pathways, including the PKA and TOR pathways. The PKA pathway receives signals from the Ras and Gpr1/Gpa2 parallel circuits, and low glucose concentration correlates with low PKA activity (Thevelein and de Winder, 1999). How the glucose signal feeds into the TOR pathway is still unclear. It is likely that the glucose signal feeds into downstream effectors of the TOR pathway, instead of upstream the TOR kinase (Bertram et al., 2002; Gerner et al., 2002; Di Como and Arndt, 1996; Kuruvilla et al., 2001). On the other hand, environmental alkaline pH activates the Rim101 pathway in fungi, which does not appear to have any connection with the TOR pathway (Davis, 2009). However, there is evidence that adaptation to alkaline pH also requires the activity of the cAMP/PKA pathway in both *C.*

*albicans* and *C. neoformans*, and the inhibition of TOR activity (Figure 4.6, O'Meara et al., 2009; Zacchi et al., 2010a (Chapter 3), Chapter 5). Thus, one possibility to explain the effect of glucose starvation and alkaline pH on the switch is that they may affect signaling pathways, such as PKA, that may regulate TOR or TOR downstream effectors. Alternatively, low glucose induces the phenomenon of caloric restriction involved in aging, a process regulated by the TOR and PKA pathways (Wei et al., 2008; Blagosklonny, 2009). The process of aging is associated with the accumulation of deleterious mutations (Gonzalo, 2010; Bitterman et al., 2003). It may be possible that *mds3Δ/Δ* cells cannot enter the aging program properly due to a TOR pathway deregulation, but that they still accumulate mutations. In this regard, overactivation of the TOR pathway by the amino acid glutamine might also contribute to deregulate the aging process, enhancing CMPS in *C. albicans* (data not shown) (Powers et al., 2006). Finally, alkaline pH might be neutralizing or preventing the accumulation of a particular metabolite that is required for papilli formation, as it occurs while yeast age (Burtner et al., 2009; Fabrizio et al., 2004). Regardless of the mechanism, environmental and nutritional signals undoubtedly play a key role in the regulation of the switch in the *mds3Δ/Δ* mutant.

The studies presented here begin to uncover the complexity of the phenotypes associated with the phenotypic switch in the *mds3Δ/Δ* mutant. Not only the switched strains display different colony morphologies and expression of a set of critical virulence traits, but they also show diverse genomic rearrangements and a differential response to genotoxic agents such as MMS and HU. These variable characteristics expose the inherent noise in the switching system and the diversity of responses associated with the switch. However, we have also found two generally unifying phenotypes of the switched *mds3Δ/Δ* strains: enhanced sensitivity to rapamycin and to the oxidizing agent TBHP. I propose that the increased rapamycin sensitivity of switched strains is a reflection of an increased TOR dependence (Figure 4.9). A deeper understanding of the processes that lead to rapamycin resistance and TBHP sensitivity in *C.*

*albicans* will likely contribute to uncover the mechanisms behind the phenotypic switching in the *mds3Δ/Δ* mutant. Defects in TOR pathway regulation are strongly associated with the generation of phenotypic diversity and tumor progression in mammalian organisms. If indeed TOR pathway defects are also causally associated with the generation of phenotypic diversity in *C. albicans*, we may have found a more malleable model than mammalian organisms to study these processes.

**TABLES**

**Table 4.1.** *C. albicans* strains used in this study

<b>Strain</b>	<b>Parent</b>	<b>Genotype</b>	<b>References</b>
<b>DAY1 (BPW17)</b>	SC5314	<i>ura3::λimm434/ura3::λimm434 his1::hisG/his1::hisG arg4::hisG/arg4::hisG</i>	Wilson et al., 1999
<b>DAY286</b>	DAY1	<i>ura3::λimm434/ura3::λimm434 his1::hisG/his1::hisG ARG4::URA3::arg4::hisG/arg4::hisG</i>	Wilson et al., 1999
<b>DAY185</b>	DAY286	<i>ura3::λimm434/ura3::λimm434 pHIS1::his1::hisG/his1::hisG ARG4::URA3::arg4::hisG/arg4::hisG</i>	Davis et al., 2000
<b>GK09</b>	BWP17	<i>ura3::λimm434/ura3::λimm434 his1::hisG/his1::hisG arg4::hisG/arg4::hisG mds3::Tn7::UAU1/mds3::Tn7::URA3</i>	Davis et al., 2002
<b>DAY417</b>	BWP17	<i>ura3::λimm434/ura3::λimm434 his1::hisG/his1::hisG arg4::hisG/arg4::hisG mds3::ARG4/mds3::URA3</i>	Davis et al., 2002
<b>DAY425 (VIC11)</b>	BWP17	<i>ura3::λimm434/ura3::λimm434 his1::hisG/his1::hisG arg4::hisG/arg4::hisG rim101::dpl200/rim101::dpl200 mds3::UAU1/mds3::URA3</i>	This study
<b>DAY439</b>	BWP17	<i>ura3::λimm434/ura3::λimm434 HIS1::his1::hisG/his1::hisG arg4::hisG/arg4::hisG mds3::Tn7::UAU1/mds3::Tn7::URA3</i>	Davis et al., 2002
<b>DAY435</b>	BWP17	<i>ura3::λimm434/ura3::λimm434 his1::hisG/his1::hisG arg4::hisG/arg4::hisG MDS3::HIS1::mds3::Tn7::UAU1/mds3::Tn7::URA3</i>	Davis et al., 2002
<b>DAY956</b>	BWP17	<i>ura3::λimm434/ura3::λimm434 his1::hisG/his1::hisG arg4::hisG/arg4::hisG mds3::ARG4/mds3::dpl200</i>	Zacchi et al., 2010a
<b>DAY972</b>	RM1000	<i>ura3::λimm434/ura3::λimm434 his1::hisG/his1::hisG sit4::HIS1/sit4::dpl200</i>	Lee et al., 2004
<b>DAY1046</b>	WO-1		Slutsky et al., 1987
<b>DAY1063 (DKCa127)</b>	SN76	<i>arg4/arg4 his1/his1 ura3::imm434/ura3::imm434 iro1::imm434/iro1::imm434 rad50Δ::CdHIS1/rad50Δ::CdARG4</i>	Legrand et al., 2007
<b>DAY1122</b>	DAY938	<i>ura3::λimm434/ura3::λimm434 his1::hisG/his1::hisG arg4::hisG/arg4::hisG mds3::ARG4/mds3::URA3-dpl200 TOR1/tor1::HIS1</i>	Zacchi et al., 2010a
<b>DAY1123</b>	DAY286	<i>ura3::λimm434/ura3::λimm434 his1::hisG/his1::hisG ARG4::URA3::arg4::hisG/arg4::hisG TOR1/tor1::HIS1</i>	Zacchi et al., 2010a
<b>DAY1124</b>	DAY1122	<i>ura3::λimm434/ura3::λimm434 his1::hisG/his1::hisG arg4::hisG/arg4::hisG mds3::ARG4/mds3::URA3-dpl200 TOR1-1/tor1::HIS1</i>	Zacchi et al., 2010a
<b>DAY1125</b>	DAY1123	<i>ura3::λimm434/ura3::λimm434 his1::hisG/his1::hisG ARG4::URA3::arg4::hisG/arg4::hisG TOR1-1/tor1::HIS1</i>	Zacchi et al., 2010a
<b>DAY1226 (GKO782)</b>	BWP17	<i>ura3::λimm434/ura3::λimm434 his1::hisG/his1::hisG arg4::hisG/arg4::hisG sch9::Tn7::UAU1/sch9::Tn7::URA3</i>	Davis et al., 2002
<b>DAY1224 (CJN6)</b>	GKO782	<i>ura3::λimm434/ura3::λimm434 SCH9::HIS1::his1::hisG/his1::hisG arg4::hisG/arg4::hisG sch9::Tn7::UAU1/sch9::Tn7::URA3</i>	Nobile et al., 2003
<b>LUZ111</b>	DAY417	<i>ura3::λimm434/ura3::λimm434 his1::hisG/his1::hisG arg4::hisG/arg4::hisG mds3::ARG4/mds3::URA3 MTLA/Δ</i>	This study
<b>LUZ124</b>	DAY286	<i>ura3::λimm434/ura3::λimm434 his1::hisG/his1::hisG ARG4::URA3::arg4::hisG/arg4::hisG MTLA/Δ</i>	This study
<b>LUZ127</b>	LUZ111	<i>ura3::λimm434/ura3::λimm434 his1::hisG/his1::hisG arg4::hisG/arg4::hisG mds3::ARG4/mds3::URA3 MTLA/a</i>	This study
<b>LUZ145</b>	LUZ124	<i>ura3::λimm434/ura3::λimm434 his1::hisG/his1::hisG ARG4::URA3::arg4::hisG/arg4::hisG MTLA/a</i>	This study
<b>LUZ166</b>	DAY956	<i>ura3::λimm434/ura3::λimm434 his1::hisG/his1::hisG arg4::hisG/arg4::hisG_mds3::ARG4/mds3::dpl200 cen5::URA3/CEN5</i>	This study
<b>LUZ225/6</b>	LUZ166	<i>ura3::λimm434/ura3::λimm434 HIS1::his1::hisG/his1::hisG arg4::hisG/arg4::hisG_mds3::ARG4/mds3::dpl200 cen5::URA3/CEN5</i>	This study

<b>LUZ227/8</b>	LUZ166	<i>ura3::λimm434/ura3::λimm434 HIS1::MDS3::his1::hisG/his1::hisG arg4::hisG/arg4::hisG mds3::ARG4/mds3::dp1200 cen5::URA3/CEN5</i>	This study
<b>LUZ796</b>	SSY194	<i>ura3::λimm434/ura3::λimm434 HIS1::his1::hisG/his1::hisG arg4::hisG/arg4::hisG mds3::Tn7::UAU1/mds3::Tn7::URA3</i>	This study
<b>LUZ797</b>	SSY194	<i>ura3::λimm434/ura3::λimm434 his1::hisG/his1::hisG arg4::hisG/arg4::hisG mds3::Tn7::UAU1/mds3::MDS3::HIS1::Tn7::URA3</i>	This study
<b>LUZ798</b>	SSY210	<i>ura3::λimm434/ura3::λimm434 HIS1::his1::hisG/his1::hisG arg4::hisG/arg4::hisG mds3::Tn7::UAU1/mds3::Tn7::URA3</i>	This study
<b>LUZ799</b>	SSY210	<i>ura3::λimm434/ura3::λimm434 his1::hisG/his1::hisG arg4::hisG/arg4::hisG mds3::Tn7::UAU1/mds3::MDS3::HIS1::Tn7::URA3</i>	This study

**Table 4.2.** Primers used in this study

<b>Primer</b>	<b>Sequence</b>	<b>Reference</b>
<b>a1-ORF-F</b>	TGGCATCTATACTGAGGACC	This study
<b>a1-ORF-R</b>	CACTAAATACCGCAACTAAGAT	This study
<b>MTL alpha2 5detect</b>	TCCTCATTGTTGGTAGAAAGAG	This study
<b>MTL alpha2 3detect</b>	TTGTGCGCTCAATGCCTGGG	This study
<b>944</b>	AGACCTATAGTGAGAGAGCA	Ketel et al., 2009
<b>945</b>	CAAACAATCCTCTACCAACA	Ketel et al., 2009
<b>1901</b>	GGGATGAAGACTATGATGTGC	Ketel et al., 2009
<b>1915</b>	CAGCCTTTGAGCCCTATT	Ketel et al., 2009
<b>1961</b>	TCTACTAAAATCAACGAAGC	Ketel et al., 2009
<b>2003</b>	CAGTCGGGCGATTATCT	Ketel et al., 2009
<b>2211</b>	CAATTGTAACACTACAAATTGTTACAGTTTTCAAATTCT ACTCAAACAAGCATTCCGAAGGACATTAATTAACGTT TTCCCAGTCACGACGTT	Ketel et al., 2009
<b>2212</b>	CTGACTCCTCTAATTAATCAATTCTACAACTTGAAT TCAAACCTTTTATTCCAGTATTCTGATTGATCTGTGG AATTGTGAGCGGATA	Ketel et al., 2009
<b>MDS3 5-detect</b>	AAGCGCCTGTTACAGTCTAC	Davis et al., 2002
<b>MDS3 3- detect</b>	AAATCAAATTCACATAAGTC	Davis et al., 2002

**Table 4.3.** Karyotypic rearrangements, aneuploidies, and resistance to rapamycin and DNA damage agents in switched *mds3A/A* strains.

Switched strain	<i>mds3A/A</i> parent	CHEF Results	CGH Results	Rap YPD	Rap Spider	TBHP	MMS	HU
SSY3	DAY425	Normal	ND	ND	ND	ND	ND	ND
SSY5	DAY425	Normal	ND	ND	ND	ND	ND	ND
SSY10	DAY425	Normal	ND	ND	ND	ND	ND	ND
SSY16	DAY425	Band between Chr 1-2, and Chr2-3	ND	= (S)	SS	ND	ND	ND
SSY18	DAY425	Normal	ND	ND	ND	ND	ND	ND
SSY20	DAY425	Normal	ND	ND	ND	ND	ND	ND
SSY22	DAY417	Normal	ND	ND	ND	ND	ND	ND
SSY24	DAY417	Normal	ND	ND	ND	ND	ND	ND
SSY26	DAY417	Normal	ND	ND	ND	ND	ND	ND
SSY28	DAY417	Normal	ND	ND	ND	ND	ND	ND
SSY30	DAY417	Normal	ND	ND	ND	ND	ND	ND
SSY32	DAY417	Band between Chr2-3	ND	ND	ND	ND	ND	ND
SSY34	DAY417	Normal	Normal	R+/-	SS	SS	SS	ND
SSY36	DAY417	Normal	ND	ND	ND	ND	ND	ND
SSY38	DAY417	Normal	ND	ND	ND	ND	ND	ND
SSY40	DAY417	Band between Chr2-3	ND	ND	ND	ND	ND	ND
SSY41	DAY425	Band between Chr2-3	ND	SS(S)	SS	ND	ND	ND
SSY45	DAY425	Normal	ND	ND	ND	ND	ND	ND
SSY47	DAY425	Normal	ND	ND	ND	ND	ND	ND
SSY49	DAY425	Normal	ND	ND	ND	ND	ND	ND
SSY51	DAY425	Normal	ND	ND	ND	ND	ND	ND
SSY53	DAY425	Normal	ND	ND	ND	ND	ND	ND
SSY55	DAY425	Band between Chr4-5	ND	SSS	SS	SS	S+/-	S
SSY57	DAY425	Normal	ND	ND	ND	ND	ND	ND
SSY59	DAY425	Normal	ND	ND	ND	ND	ND	ND
SSY61	DAY417	Normal	ND	ND	ND	ND	ND	ND
SSY63	DAY417	Band between Chr2-3	ND	S+/-	SS	SS	S+/-	ND
SSY65	DAY417	Band between Chr2-3	ND	S+/-	S+/-	SS	S+/-	S
SSY67	DAY417	Band between Chr2-3	ND	=	=	=	=	R
SSY69	DAY417	Normal	ND	ND	ND	ND	ND	ND
SSY71	DAY417	Normal	ND	ND	ND	ND	ND	ND
SSY73	DAY417	Band between Chr2-3	1/5 segm. mon. Chr 2	S+/-	SS	SS	SS	ND

<b>SSY75</b>	DAY417	Normal	4/5 segm. tris. Chr2	=	=	ND	ND	ND
<b>SSY77</b>	DAY417	Normal	ND	ND	ND	ND	ND	ND
<b>SSY79</b>	DAY417	Normal	ND	ND	ND	ND	ND	ND
<b>SSY117</b>	DAY439	ND	ND	SS	SSS	ND	ND	ND
<b>SSY137</b>	DAY439	ND	ND	S+/-	SSS	S+/-	S+/-	ND
<b>SSY147</b>	DAY439	ND	ND	S+/-	SS	SS	SS	ND
<b>SSY151</b>	DAY439	ND	ND	S+/-	S+/-	SSS	=	ND
<b>SSY155</b>	DAY439	ND	ND	=	=	SSS	=	=
<b>SSY159</b>	DAY439	ND	ND	S+/-	S+/-	SS	S+/-	ND
<b>SSY161</b>	DAY439	ND	ND	=	=	SS	S+/-	S+/-
<b>SSY171</b>	DAY439	ND	ND	S+/-	S+/-	SS	=	ND
<b>SSY185</b>	DAY439	ND	ND	R+/(S)	SSS(S)	SSS	= (S)	ND
<b>SSY194</b>	GKO9	ND	ND	ND	ND	ND	ND	ND
<b>SSY210</b>	GKO9	ND	Tris. Chr 6	=(R)	SS	SSS	SS	S+/-

ND= not determined, R= more resistant than parental, S= more sensitive than parental, (R) or (S) indicate that the parental already had a phenotype compared to the original *mds3Δ/Δ* strain. S+/-, SS, SSS indicate the different degrees of the phenotype.

Segm: segmental; Mon: monosomic; Tris: trisomic; Chr: chromosome

## **CHAPTER 5**

### ***MDS3*, AT THE CROSSROADS OF THE PATHWAYS TO PHENOTYPIC SWITCHING**

## SUMMARY

*Candida albicans* is one of the most important fungal pathogens of humans. As any other organism, *C. albicans* requires the ability to generate phenotypic variation for survival. One mechanism through which *C. albicans* obtains variation is through colony morphology phenotypic switching (CMPS). CMPS is defined as the stochastic formation of colonies with altered and heritable morphologies, and with low frequency reversibility. CMPS is associated with virulence in *C. albicans*. However, the mechanisms that lead to CMPS are not known. Mds3 is a negative regulator of CMPS, but the role of Mds3 in CMPS is unclear. Mds3 is also a regulator of the TOR pathway, which has led me to propose that the deregulation of the TOR pathway in the absence of *MDS3* predisposes *C. albicans* cells to undergo CMPS (Chapter 4). Here, I provide evidence that Mds3 is also a member of the Ras pathway in *C. albicans*, and I identify two new CMPS regulators: Ras1 and the TOR downstream effector kinase Sch9. The Ras and TOR pathways are critical regulators of cell growth in response to environmental nutrients, and they overlap in the regulation of many common downstream effectors, including those which are targets of Sch9. These results provide evidence that support the hypothesis that CMPS in *C. albicans* is a consequence of defects in the transmission of starvation and stress signals that are channeled through the TOR and Ras/cAMP signal transduction cascades.

## INTRODUCTION

*Candida albicans* is one of the leading causes of superficial and nosocomial systemic infections in the USA (Pfaller et al., 2001). One feature that makes this fungus such a successful commensal and opportunistic pathogen is its ability to undergo morphogenetic changes. One of the better understood *C. albicans* morphogenetic transitions is the switch from yeast morphology to pseudohyphal and hyphal morphologies (Biswas et al., 2007). The ability of *C. albicans* to transition between these cellular morphologies is critical for pathogenesis (Lo et al., 1997; Saville et al., 2003, 2008). *C. albicans* also forms chlamydo spores, which are thick-walled, spherical cells that appear at the tip of the hyphae during growth in certain nutrient poor media. Chlamydo spores have been found during infections and might be associated with *C. albicans* virulence (Staib and Morschhauser, 2007). Finally, *C. albicans* undergoes two types of phenotypic switching: white-opaque switching and colony morphology phenotypic switching (CMPS) (Soll, 1992; Lohse and Johnson, 2009). Both types of phenotypic switch involve the formation of colonies with an altered morphology, and these morphological alterations are also associated with changes in the expression of virulence traits and pathogenesis *in vitro* and *in vivo* (Gallagher et al., 1992; Kennedy et al., 1998; Kolotila and Diamond, 1990; Vargas et al., 1994, 2004; Kvaal et al., 1997, 1999; Anderson et al., 1989; Lan et al., 2002). White-opaque switching is a well studied bistable switch between two colonial and cellular morphologies (Soll et al., 2009; Lohse and Johnson, 2009; Morschhauser, 2010). On the contrary, very little is known about CMPS, perhaps because the larger number of interconvertible and stochastically reversible colony morphologies involved in CMPS has hindered the efforts to understand the mechanisms that regulate this phenomenon in *C. albicans* (Slutsky et al., 1985; Soll, 1992). The fact that morphogenetic transitions are required for *C. albicans* ability to colonize, survive in the host, and cause infection underscores the importance in understanding their regulation.

*C. albicans* morphogenetic transitions occur in response to the environment. The yeast-hyphal transition is controlled by several environmental signals, including temperature, serum, alkaline pH, starvation, and CO<sub>2</sub> concentration (Biswas et al., 2007; Cottier and Muhlschlegel, 2009). Chlamydospore formation is influenced by temperature and nutrients, but also by O<sub>2</sub> concentration, light, and moisture (Staib and Morschhauser, 2007). White-opaque phenotypic switching is affected by temperature, CO<sub>2</sub> concentration, and nutrients (Ramirez-Zavala et al., 2008; Huang et al., 2010). Finally, CMPS responds to glucose, glutamine, alkaline pH, and zinc (Chapter 4; L.F.Z. unpublished observations; Bedell and Soll, 1979). Alterations in the environment have a direct impact on morphogenesis in *C. albicans*.

Many signaling pathways are associated with specific responses to environmental signals (Bahn et al., 2007). For example, the response to glucose and CO<sub>2</sub> concentration occurs through the cAMP/protein kinase A (PKA) pathway (Cottier and Muhlschlegel, 2009). The TOR pathway responds to nitrogen sources and, to a lesser extent, to carbon source availability (Rohde et al., 2001, Wullschlegel et al., 2006). The Rim101, calcineurin, and PKA pathways respond to alkaline pH (Davis, 2009; O'Meara et al., 2010; Kullas et al., 2007). Finally, changes in temperature are likely controlled by the function of heat shock proteins and the PKA pathway (Shapiro et al., 2009). Thus, morphogenetic processes in *C. albicans* are regulated by several signal transduction pathways, and some of them, such as the cAMP/PKA pathway, appear to have a more extensive role in morphogenesis than others (Hogan and Sundstrom, 2009).

The two major cellular growth controlling pathways that respond to environmental nutrients in *C. albicans* are the PKA and the TOR pathway. In *C. albicans*, PKA is composed of two catalytic subunits, Tpk1 and Tpk2, and the regulatory subunit Bcy1 (Figures 5.1, 1.2; Souto et al., 2006; Giacometti et al., 2006, 2009; Bockmuhl et al., 2001; Thevelein and de Winde, 1999). During active growth, cAMP produced by the adenylate cyclase Cdc35 binds Bcy1 allowing PKA activation. Adenylate cyclase is activated by Ras1 and the Gpr1-Gpa2 parallel

circuit (Figure 5.1). Ras1 is active while bound to GTP, and inactive in its GDP bound state. The Ras guanine nucleotide exchange factor, Cdc25, and the activator of Ras GTPase, Ira2, function upstream of Ras1 and activate or inactivate Ras1 function, respectively (Thevelein and de Winde, 1999). Ras1 also lies upstream of the MAPK cascade, which is composed of Cst20, Ste11, Cek1, and Hst7. Known downstream effectors of PKA and MAPK are the transcription factors Efg1 and Cph1, respectively (Leberer et al., 2001; Maidan et al., 2005; Zaman et al., 2008; Monge et al., 2006). PKA is a positive regulator of transcription, translation, and glucose metabolism, and a repressor of glycogen accumulation and stress responses (Zaman et al., 2008). The Ras/PKA signaling cascade translates nutrient and stress environmental signals into changes of an array of cellular and metabolic responses in *C. albicans*, including protein synthesis and degradation, cell division and starvation responses.

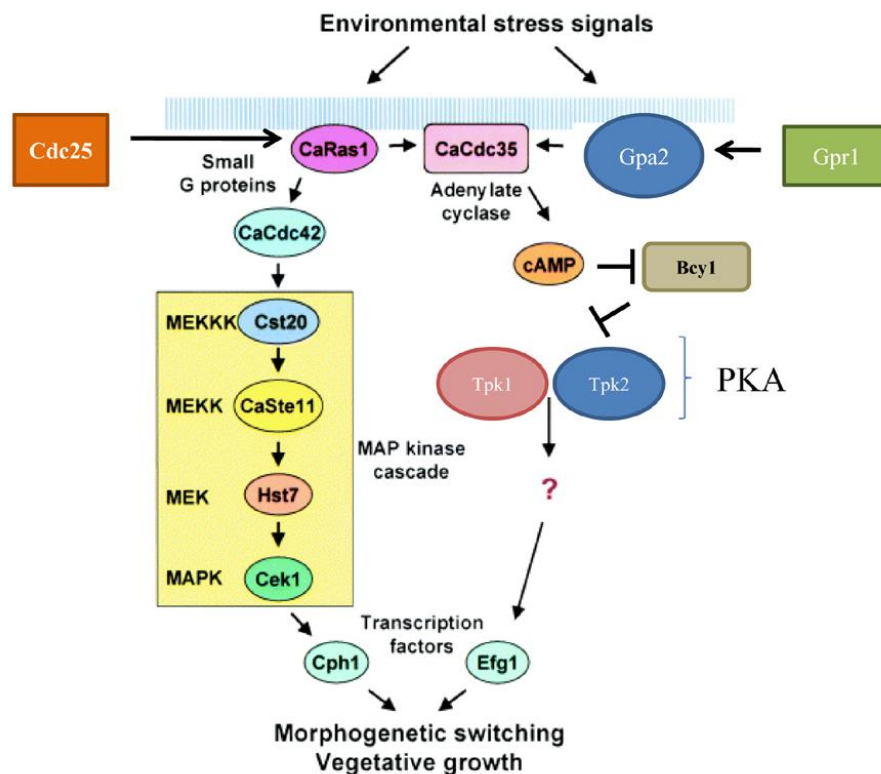


**Figure 5.1:** The Ras1 pathway in *C. albicans*. Figure adapted from Leberer et al (2001).

The second major growth controlling signal transduction pathway in yeast is the TOR pathway. Most of what is currently known about the fungal TOR pathway comes from studies in *S. cerevisiae* (Figure 1.3). In this yeast, the TOR pathway is composed of several upstream factors including Tsc1, Tsc2, and Rhb1. Tsc1/2 are negative regulators of Rhb1, which is a positive regulator of TOR (Wullscheleger et al., 2006; Rohde et al., 2008). TOR, which is a kinase, exists in two different multiprotein complexes, only one of which is sensitive to the TOR inhibitor rapamycin (Loewith et al., 2002; Heitman et al., 1991). One direct target of TOR activity is Tap42 (Duvel et al., 2003). During TOR activation, Tap42 remains bound to the downstream TOR effectors: the PP2A and PP2A-like phosphatases, inhibiting them (Duvel and Broach, 2004; Wang et al., 2003). These phosphatases control the response to stress and starvation in cells, and are activated upon TOR inhibition (Jacinto, 2007; Duvel and Broach, 2004). One PP2A-like phosphatase that is critical for TOR-dependent regulation of nitrogen responses and protein degradation is Sit4, also associated with morphogenetic regulation in *C. albicans* (Lee et al., 2004; Zacchi et al., 2010a; Rohde et al., 2004). TOR also directly phosphorylates effectors involved in transcription, protein synthesis regulation, and glycolysis, such as the kinase Sch9 (Urban et al., 2007). Similar to the PKA pathway, the TOR pathway controls cellular processes such as cellular growth and division and starvation responses. However, TOR also regulates the nitrogen catabolite repression response (Lee et al., 2004; Cutler et al., 2001; Nobile et al., 2003; Zacchi et al., 2010a; Bastidas et al., 2009). Therefore, both the TOR and PKA pathway are major regulators of growth in response to environmental nutrients.

The PKA and TOR pathways control several similar processes, either by regulating similar downstream effectors or by crosstalk in the pathways (Schmelzle et al., 2004; Zurita-Martinez and Cardenas, 2005; Martin et al., 2004; Zaman et al., 2008; Soulard et al., 2010). In mammals, Ras is a positive regulator of TOR, and functions upstream the TOR kinase (Shaw and Cantley, 2006). In *S. cerevisiae*, however, the interaction between the TOR and Ras pathways is

less clear. It has been proposed that TOR controls PP2A-independent functions through the Ras/PKA pathway, while others suggest that TOR and PKA function in parallel (Schmelzle et al., 2004; Zurita-Martinez and Cardenas, 2005; Martin et al., 2004; Soulard et al., 2010). Given their relevant role in cellular growth, it comes as no surprise that both the PKA and TOR pathways are strongly associated with the regulation of several morphogenetic processes in *C. albicans*, including yeast-hyphal transitions and chlamyospore formation (Lee et al., 2004; Cutler et al., 2001; Nobile et al., 2003; Zacchi et al., 2010; Bastidas et al., 2009; Hogan and Sundstrom, 2009; Biswas et al., 2007; Leberer et al., 2001). The TOR pathway also plays a role in the regulation of CMPS in *C. albicans* (Chapter 4). In agreement with their often overlapping functions, here I show that the Ras pathway is also involved in CMPS regulation in this fungus.

Only two genetic regulators of CMPS in *C. albicans* have been identified: the transcriptional co-repressor Ssn6 and the TOR pathway member Mds3. Ssn6 forms a co-repressor complex with Tup1, and is involved in the regulation of morphogenetic processes in *C. albicans* (Garcia-Sanchez et al., 2005; Hwang et al., 2003). Deletion of *SSN6* leads to the formation of colonies with altered, unstable morphology that are reminiscent of CMPS (Garcia-Sanchez et al., 2005). The mechanism through which *SSN6* regulates CMPS is unclear, but it is likely through its direct, reversible effects on gene transcription.

Mds3 is a large, cytoplasmic protein with N-terminal Kelch domains that is involved in the regulation of pH responses, chlamyospore formation, and yeast-hyphal transitions (Chapter 2; Davis et al., 2002; Nobile et al., 2003). Mds3 is also a regulator of the TOR pathway in *C. albicans*. However, Mds3 displays phenotypes that are Sit4-independent and potentially TOR-independent (Zacchi et al., 2010a). In *S. cerevisiae*, Mds3 has been associated with the Ras pathway. For example, Mds3 physically interacts with Cdc25, an *mds3Δ pmd1Δ* double mutant shares similar phenotypes with a *cdc25Δ* mutant [*PMD1* is a paralog of *MDS3* in *S. cerevisiae* (Benni and Neigeborn, 1997)], and an overactive *RAS<sup>V17</sup>* allele rescues the early sporulation

defect of the *mds3Δ pmd1Δ* mutant (Benni and Neigeborn, 1997; McDonald et al., 2009, Krogan et al., 2006; Tonikian et al., 2009; Gavin et al., 2006; Collins et al., 2007). Thus, Mds3 could function in both the Ras and TOR pathways.

Intrigued by the fact that Mds3 was associated with the Ras/PKA pathway in *S. cerevisiae* and that Mds3 appears to have Sit4-independent functions, I wished to determine the genetic interaction between Mds3, TOR, and Ras/PKA pathways in *C. albicans*. To this end, I tested mutants in the Ras/PKA, MAPK, Gpr1-Gpa2, and TOR pathways for phenotypes similar to an *mds3Δ/Δ* mutant. I also determined the genetic interaction between *MDS3*, *SIT4*, and *RAS1* using double mutants in these genes, and determined the ability of a *RAS1*<sup>V13</sup> overactive allele to rescue the *mds3Δ/Δ* and *sit4Δ/Δ* mutations. I found that Mds3 appears to function upstream of Ras1 in *C. albicans*, probably acting on Cdc25 function. Mutants in *CDC25* and *RAS1* shared similar phenotypes with a mutant in *MDS3*, including growth and transcriptional responses to the TOR inhibitor rapamycin, and phenotypic switching. Further, I showed that CMPS is not mediated by the MAPK pathway, and I identified a third regulator of CMPS in *C. albicans*, the Sch9 kinase, a critical downstream effector of the TOR pathway. Therefore, Mds3 appears to function in both the TOR and Ras/cAMP pathways, and both of these pathways are negative regulators of CMPS in *C. albicans*.

## MATERIALS AND METHODS

### *C. albicans* strains and plasmids

All yeast strains used in this study are listed in Table 5.1. The *ras1Δ/Δ sit4Δ/Δ* mutant LUZ613 was constructed by sequentially deleting both *RAS1* alleles from the *sit4Δ/Δ* strain DAY972, using the *ras1::URA3-dpl200* disruption cassette PCR amplified from pDDB57 with primers RAS1 5DR and RAS1 3DR (Table 5.3). All deletions are from the start to the stop codon and were generated by chemical transformation (Wilson et al., 1999). Correct integration of the disruption cassettes was verified by the PCR using the RAS1 5' detect, RAS1 3' detect, and URA3 internal detect primers (Table 5.3). The *URA3-dpl200* marker was recycled by growing the cells in SC medium supplemented with 5-fluoroorotic acid (5-FOA).

The *RAS1/ras1Δ mds3Δ/Δ* mutant (LUZ692) was constructed by sequentially deleting one copy of *RAS1* and one copy of *MDS3* from strain DAY415 using the *ras1::URA3-dpl200* disruption cassette described above, and the *mds3::URA3dpl200* cassette amplified with primers MDS3 5 DR and MDS3 3 DR from pDDB57 (Tables 5.1 and 5.3). The *URA3-dpl200* marker was recycled by growing the cells in SC medium supplemented with 5-fluoroorotic acid (5-FOA). To eliminate the remaining *RAS1* copy from LUZ692 I used the regular *ras1::URA3-dpl200* disruption cassette described above, and a *ras1int::URA3-dpl200* cassette with regions of homology within *RAS1* open reading frame (ORF), amplified with primers RAS1 int 5DR and RAS1 int 3 DR (Table 5.3). A total of 89 transformants (20 of which were made with the *ras1int::URA3-dpl200* cassette) were screened: 77 had ectopic integrations that retained the *RAS1* copy [70 mutants also retained the *ras1::dpl200* copy (including 1 strain with a triplication), and 6 strains only had the *RAS1* allele]; 10 lost the *ras1::dpl200* allele and retained the *RAS1* wild-type copy (5 of these were verified by PCR to be *RAS1/ras1::URA3dpl200*, indicating a marker replacement); and 2 appeared to have lost the *RAS1* wild-type copy but the *ras1::URA3-dpl200*

allele did not give the expected band size by PCR [one of these strains was saved as LUZ754]. Nevertheless, I was not able to generate a *ras1* $\Delta/\Delta$  *mds3* $\Delta/\Delta$  double mutant.

The complemented *sit4* $\Delta/\Delta$  *mds3* $\Delta/\Delta$ +*MDS3* mutant LUZ621 was generated as follows. Strain DAY1233 was plated on 5-FOA to generate LUZ616. Loss of the *mds3::URA3dpl200* allele was verified by genomic PCR using primers MDS3 null detect 5' and MDS3 null detect 3' (Table 5.3). LUZ616 was transformed with BseRI digested pLZ169, to generate LUZ621. Integration of a wild-type *MDS3* copy was verified by genomic DNA PCR using primers MDS3 null detect 5', MDS3 null detect 3', and MDS3 NruI Seq (Table 5.3).

The *RAS1* and *RAS1*<sup>G13V</sup> vectors pLZ172 and pLZ173 were constructed as follows. Wild-type *RAS1* ORF sequence with flanking promoter and terminator sequences was amplified in one high fidelity PCR (Pfu Turbo DNA polymerase, Stratagene) using primers RAS1 5' comp and RAS1 3' comp from strain BWP17 genomic DNA (Table 5.3). The PCR product was transformed with BamHI/XhoI-double digested pDDB76 into *S. cerevisiae* strain L40 to produce plasmid pLZ172 through *in vivo* recombination. Using pLZ172 as template, *RAS1* was amplified in two high fidelity PCRs (Pfu Turbo DNA polymerase, Stratagene) using primers pairs RAS1 5' comp and RAS1G13V 3', and RAS1 3' comp and RAS1G13V 5' that carry the GGT to GTT non-synonymous mutation that causes the G13V amino acid change (Table 5.3). The PCR products and BamHI/XhoI-double digested pDDB76 were *in vivo* recombined in *S. cerevisiae* strain L40 to produce plasmid pLZ173. The complete ORF of *RAS1* in pLZ172 and pLZ173 was verified by sequencing using primers RAS1 5' detect, and RAS1 5' seq-2. During the construction of these plasmids, we noticed that while the CGD database ([www.candidagenome.org](http://www.candidagenome.org)) indicates that the ORF of both alleles of *RAS1* are identical, *C. albicans* strains SC5314 (DAY963) and BWP17 actually carry two different *RAS1* alleles. Several independently constructed *RAS1* plasmids and PCR amplified *RAS1* from SC5314 and BWP17 genomic DNA were sequenced to corroborate the presence of two alleles. To sequence *RAS1* from SC5314/BWP17 strains, *RAS1* was amplified

in high fidelity PCRs (Pfu Turbo, Stratagene) from genomic DNA of *C. albicans* strains SC5314 and BWP17, using primers Ras1 3' comp and Ras1 5' seq, purified (Qiagen) and sequenced using RAS1 5' detect and RAS1 3' detect. Sequence runs showed overlapping peaks at three positions from the START codon of *RAS1*: nt 113 (G→A), nt 225 (C→T), and nt 388 (C→G), and the lack of sequence homology after the N227, the 5<sup>th</sup> asparagine residue (Figure 5.2), indicating the presence of two *RAS1* alleles. This methodology does not allow me to distinguish the exact nucleotide sequence of each allele. However, I suggest that the sequence of one *RAS1* allele is the one described in CGD, while the sequence of the second allele corresponds to the *RAS1* allele from *C. albicans* strain 1006 [Pubmed reference AF177670] (Feng et al., 1999). The plasmids I used here contain the CGD *RAS1* allele sequence. However, plasmids made in the second allele background show similar results (data not shown).

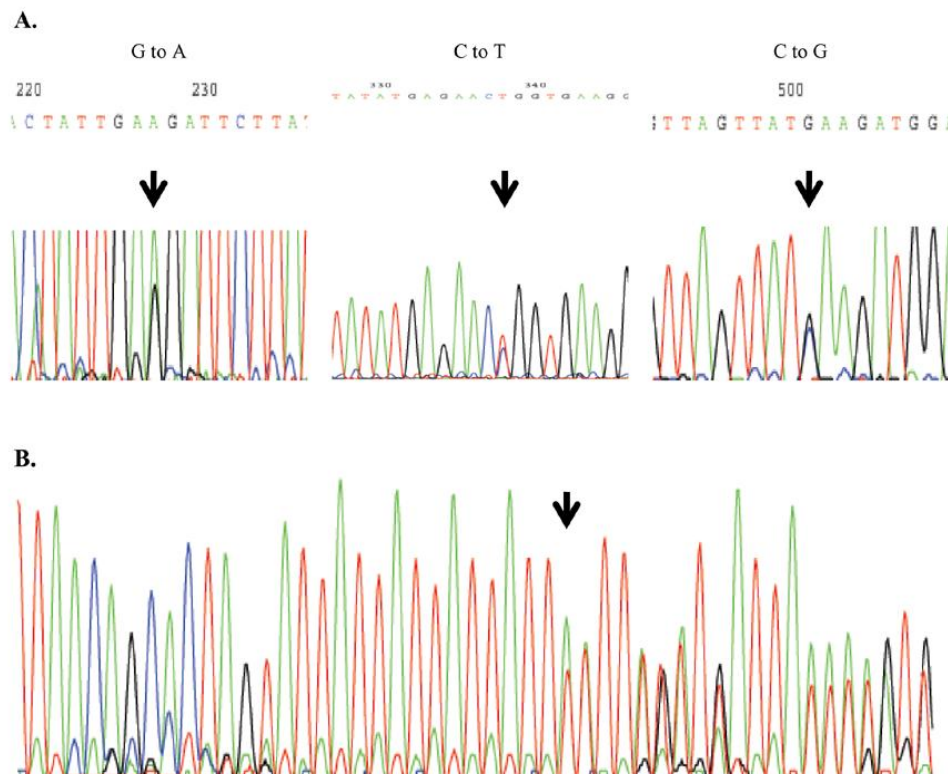


**Figure 5.2:** *C. albicans* SC5314 has two *RAS1* alleles. Sequence runs showing the overlapping peaks corresponding to the two alleles: A) the three point mutations, and B) the absence of an entire asparagine codon.

The *MDS3* complementation vector pLZ169 was generated as follows. An *AdhI/NheI* double digestion of pDDB353 was *in vivo* recombined with a *XhoI/BamHI* double digestion of pDDB76 in *S. cerevisiae* strain L40 to give plasmid pLZ169.

### **Media and growth conditions**

*C. albicans* was routinely grown at 30°C in YPD (2% Bacto-peptone, 2% dextrose, 1% yeast extract). For selection of Ura<sup>+</sup> or Trp<sup>+</sup> transformants, synthetic medium without uridine or tryptophan was used (0.17% yeast nitrogen base without ammonium sulfate (Q-BioGene), 0.5% ammonium sulfate, 2% dextrose, and supplemented with a dropout mix containing amino and nucleic acids except those necessary for the selection (Adams et al., 1997)). Media were buffered at the indicated pH using 150mM HEPES. Rapamycin (LC Laboratories) was added to the media at the indicated concentrations from a stock solution in 90% ethanol-10% Tween-20. For liquid assays of filamentation in the presence of rapamycin, strains were pre-grown in liquid YPD at 30°C, pelleted, resuspended in an equal volume of PBS and diluted 1:100 in M199 pH 8 supplemented with rapamycin or solvent alone. Samples were incubated for 6 hrs at 37°C. For growth assays in the presence of rapamycin, strains were pre-grown in liquid YPD at 30°C, diluted in PBS to an OD 600nm of 1.6, then serially diluted 5-fold in PBS, spotted on YPD or Spider medium (1% mannitol, 1% nutrient broth, 0.2% K<sub>2</sub>HPO<sub>4</sub>, pH 7.2 before autoclaving (Liu et al., 1994)) supplemented with rapamycin or solvent alone and incubated at 30°C for 2 or 3 days. For DNA damage experiments, methyl methanesulfonate (MMS, Sigma), hydroxyurea (HU, Sigma), and tert-butyl hydroxyperoxide (TBHP, Sigma) were added to YPD media at ~45-50°C; plates were incubated at 30°C in a plastic bag. All media except that for selection of Ura<sup>+</sup> transformants were supplemented with 80 µg/ml uridine. For solid media, 2% Bacto-agar was added, except for Spider medium which used 1.35% Bacto-agar.

### **Glycogen accumulation**

Cells were grown overnight in YPD, 5  $\mu$ l were spotted on YPD plates, grown at 30°C for 48 hrs, and exposed to iodine vapors for ~1 min. Pictures of plates were taken immediately, using a Canon Powershot A560 digital camera. Images were processed with Adobe Photoshop 7.0 software.

### **Northern blot analysis**

For RNA extraction, cells were grown as described by Bastidas et al (2009) and Zacchi et al (2010a). Briefly, strains were pre-grown in YPD, diluted to an OD<sub>600nm</sub> ~ 0.1, incubated at 30°C for 5 hrs, followed by 1 hr incubation at 30°C after addition of 20nM rapamycin. RNA extraction and Northern blot procedures were previously described (Zacchi et al., 2010a).

### **Phenotypic switching assay**

Strains were grown overnight (>16 hrs) in YPD at 30°C, diluted to 10<sup>-6</sup> in PBS, and 100  $\mu$ l plated on YP plates with 2% or 0.2% glucose, or YPD plates buffered at pH 6 or pH 8. Plates were incubated at 30°C for 48 hrs, and then at room temperature (~23-25°C) for three weeks, wrapped in parafilm to prevent agar desiccation. The % of colonies showing papilli on the colony surface was scored every 2-3 days beginning at day 6 of incubation.

### **Microscopy**

Images of liquid cultures were captured using a Zeiss Axio camera, Axiovision 4.6.3 software (Zeiss), and a Zeiss AxioImager fluorescence microscope. All images were processed with Adobe Photoshop 7.0 software.

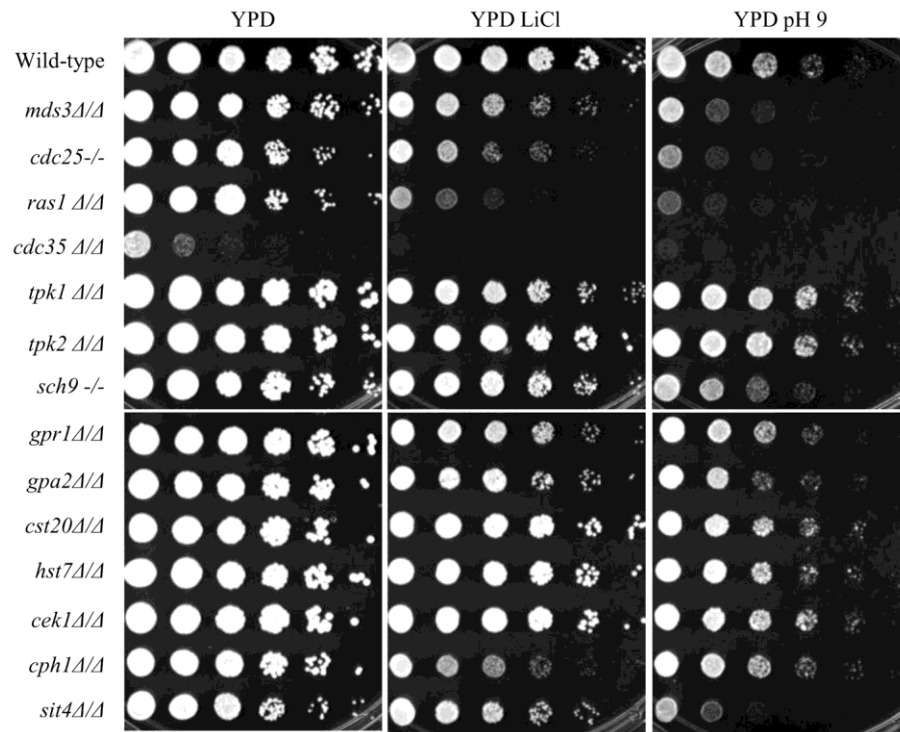
## RESULTS

### Mds3 and upstream PKA pathway members share similar functions

Mds3 was initially associated with the Ras pathway in *S. cerevisiae* (Benni and Neigeborn, 1997; McDonald et al., 2009, Krogan et al., 2006; Tonikian et al., 2009; Gavin et al., 2006; Collins et al., 2007). Since Mds3 has Sit4- and possibly TOR-independent functions in *C. albicans*, I hypothesized that these functions were Ras-dependent (Zacchi et al., 2010a). In *C. albicans*, Ras1 functions upstream of the PKA pathway, in parallel to Gpr1 and Gpa2, and upstream of the MAPK pathway (Figure 5.1; Maidan et al., 2005; Leberer et al., 2001). Therefore, I screened mutants in the PKA and MAPK pathways for *mds3Δ* related phenotypes, including growth in rich medium, LiCl, and alkaline pH, filamentation, and rapamycin resistance (Figure 5.3). In *S. cerevisiae*, the *mds3Δ pmd1Δ* mutant defects are rescued by an overactive *RAS1<sup>V17</sup>* allele, suggesting that Mds3 may act as a positive regulator of Ras1 (Benni and Neigeborn, 1997). If Mds3 indeed functions as a positive regulator of Ras1, then we should see similar phenotypes in the *mds3Δ/Δ* mutant and mutants in the Ras/MAPK and/or in the Ras/PKA pathways. Further, since *SCH9*, a downstream effector of the TOR pathway, is required for similar morphogenetic processes as *MDS3* [chlamydospore formation and filamentation], I reasoned that they may also share other functions (Nobile et al., 2003; Liu et al., 2010; Urban et al., 2007). Thus, I also included the *sch9-/-* mutant in this screen. Finally, Sit4, a second downstream effector of TOR that physically interacts with Mds3 and has some similar functions as Mds3 was also included as a control in the experiments (Rohde et al., 2004; Zacchi et al., 2010, Lee et al, 2004).

**Figure 5.3A:** Looking for *MDS3*-dependent phenotypes in mutants in the MAPK, PKA and TOR pathways. Overnights of the different strains (Table 1) were diluted in PBS and spotted on YPD, YPD supplemented with 150mM LiCl, YPD pH 9. Plates were incubated at 30°C and photographed after 48 or 72 hrs.

A.



*MDS3* is required for wild-type growth in rich medium, in the presence of LiCl, and at alkaline pH (Figure 5.3; Davis et al., 2002; Zacchi et al., 2010a (Chapter 3)). Thus, I tested the Ras/MAPK, PKA, and *sch9-/-* mutants for growth on YPD, LiCl, and pH9 media. The *sit4Δ/Δ* mutant has a growth defect on YPD and pH 9 media, but not on LiCl (Figure 5.3A; Zacchi et al., 2010a). However, *SIT4* is required for growth in LiCl in the presence of rapamycin, which indicates that Sit4 plays a role in LiCl resistance during TOR inactivation (data not shown). All the mutants in upstream members of the Ras-PKA pathway, including *CDC25*, *RAS1*, and *CDC35* showed a growth defect on YPD, LiCl, and pH 9 media (Figure 5.3A). On YPD and LiCl, the *cdc35Δ/Δ* mutant showed the strongest defect. I did not detect any defect in growth on YPD, LiCl, or pH 9 media of the single *tpk1Δ/Δ* and *tpk2Δ/Δ* mutants, which are mutants in the PKA catalytic subunits, perhaps because in *C. albicans* Tpk1 and Tpk2 often have redundant roles (Figure 5.3A; Bockmuehl et al., 2001). Mutants in *GPR1*, *GPA2*, and in the MAPK pathway also did not show a growth defect on YPD, LiCl, and pH 9 media. It is to note however, that the

downstream effector of the MAPK pathway, the transcription factor Cph1, showed a growth defect on LiCl (Figure 3A; Liu et al., 1994; Huang et al., 2008). The *sch9*<sup>-/-</sup> mutant showed a slight growth defect on YPD, but not on LiCl or pH 9 media. Therefore, the Ras-cAMP pathway, but not the Gpr1-Gpa2 or MAPK pathways, is required for growth on LiCl and pH 9. Further, the TOR downstream effectors Sit4, but not Sch9, is required for growth at alkaline pH, and neither is required for growth on LiCl.

Another phenotype of the *mds3* $\Delta/\Delta$  mutant is resistance to rapamycin in nutrient poor Spider medium but not in rich YPD medium. Thus, I determined the response to rapamycin in YPD and Spider media of the PKA, MAPK, and *sch9*<sup>-/-</sup> mutants (Figure 5.3B). As previously observed, the *sit4* $\Delta/\Delta$  mutant is more resistant to rapamycin in both YPD and Spider media (Zacchi et al., 2010a (Chapter 3)). Mutants in *CDC25* and *RAS1* were more resistant to rapamycin than the wild-type strain in both YPD and Spider media (Figure 5.3B). Due to the severe growth defect of the *cdc35* $\Delta/\Delta$  mutant it was not possible to determine whether it was more or less sensitive to rapamycin than the wild-type strain in YPD medium, but it appears slightly more resistant to rapamycin than wild-type strain in Spider medium (Figure 5.3B). While the *tpk1* $\Delta/\Delta$  mutant behaved similarly to wild-type in both YPD and Spider media, the *tpk2* $\Delta/\Delta$  mutant was more sensitive to rapamycin in both media (Figure 5.3B). The *gpr1* $\Delta/\Delta$  and *gpa2* $\Delta/\Delta$  mutants were more sensitive than wild-type to rapamycin on YPD medium, but more resistant to rapamycin on Spider medium. The *cst20* $\Delta/\Delta$ , *hst7* $\Delta/\Delta$ , and *cek1* $\Delta/\Delta$  MAPK mutants were more sensitive to rapamycin than wild-type in YPD medium, but only the *cst20* $\Delta/\Delta$  mutant was also more sensitive than wild-type in Spider medium (Figure 5.3B). The *cst20* $\Delta/\Delta$  mutant, the first in the MAPK cascade, was the most sensitive to rapamycin in YPD of all the mutants in the MAPK pathway (Figure 5.1 and 5.3B). Again, contrary to the phenotype of the upstream MAPK mutants, the *cph1* $\Delta/\Delta$  mutant showed a weak resistance to rapamycin compared to the wild-type strain in both YPD and Spider media (Figure 5.3B). Finally, the *sch9*<sup>-/-</sup> mutant was highly sensitive to

rapamycin in both YPD and Spider media (Figure 5.3B). Thus, all the mutants in the different signal transduction cascades showed a growth defect in the presence of rapamycin, although disparate responses to rapamycin were observed in mutants belonging to the same pathway or that share the same downstream effectors. None of the mutants screened were resistant to rapamycin only in Spider medium, the phenotype of the *mds3Δ/Δ* mutant.

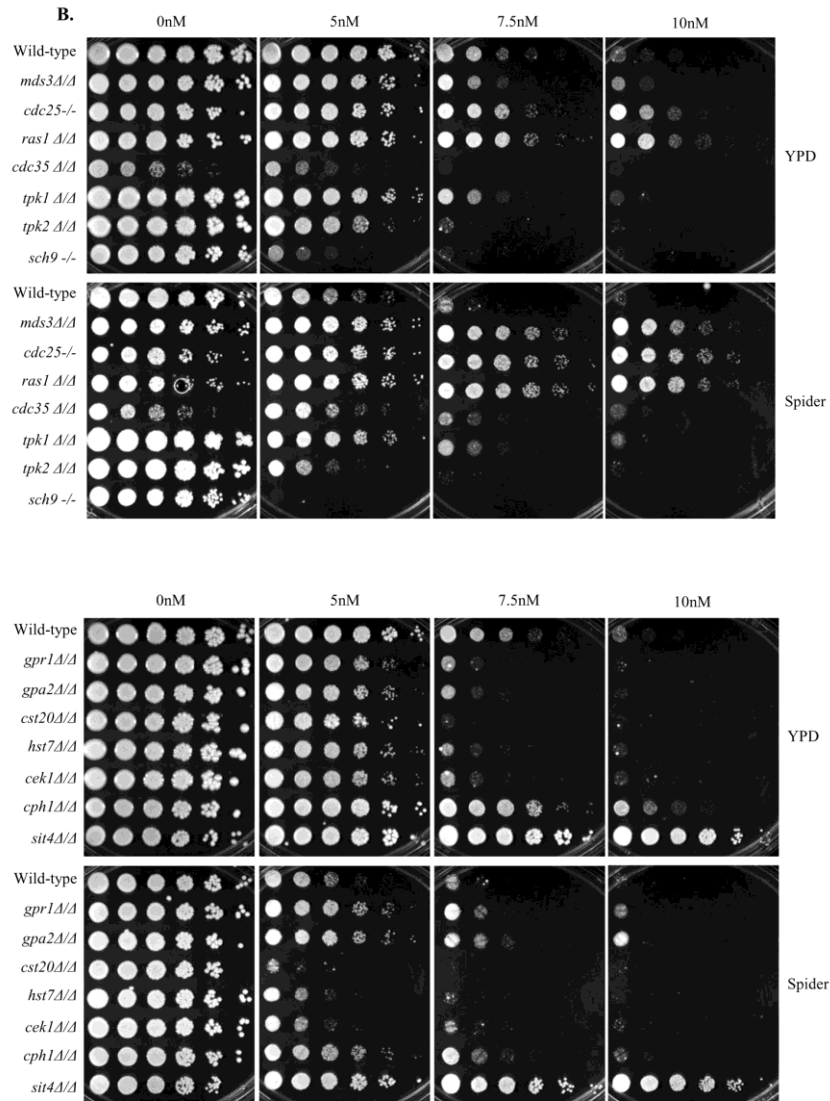


**Figure 5.3B:** Looking for *MDS3*-dependent phenotypes in mutants in the MAPK, PKA and TOR pathways. Overnights of the different strains (Table 1) were diluted in PBS and spotted on YPD and Spider media supplemented with solvent or rapamycin. Plates were incubated at 30°C and photographed after 48 or 72 hrs.

*MDS3* is required for filamentation in M199 medium buffered at pH 8 (Davis et al., 2002). Thus, I tested the ability of the Ras/cAMP, PKA, MAPK, and TOR mutants to filament in M199 pH 8 (Figure 5.3C). The *sit4Δ/Δ* mutant did not filament on M199 pH 8 media, as previously observed (Figure 5.3C; Zacchi et al., 2010a). Mutants in *CDC25*, *RAS1*, and *CDC35* also failed to filament, while mutants in *GPA2* and *CPH1* showed uneven filamentation around the perimeter of the colony. I noted that even though the mutant in *SCH9* did not filament into the agar, it showed a wrinkly surface, indicative of filamentation within the colony (Figure 5.3C). Mutants in *TPK1*, *TPK2*, *GPR1*, *HST7*, and *CEK1* filamented like the wild-type strain, while the mutant in *CST20* showed a slightly enhanced filamentation compared to wild-type (Figure 5.3C). Thus, the Ras/cAMP pathway is clearly required for filamentation at alkaline pH, while the MAPKs, the Gpr1-Gpa2 circuit, and *SCH9* have a more limited role, and the PKA subunits likely have redundant roles.

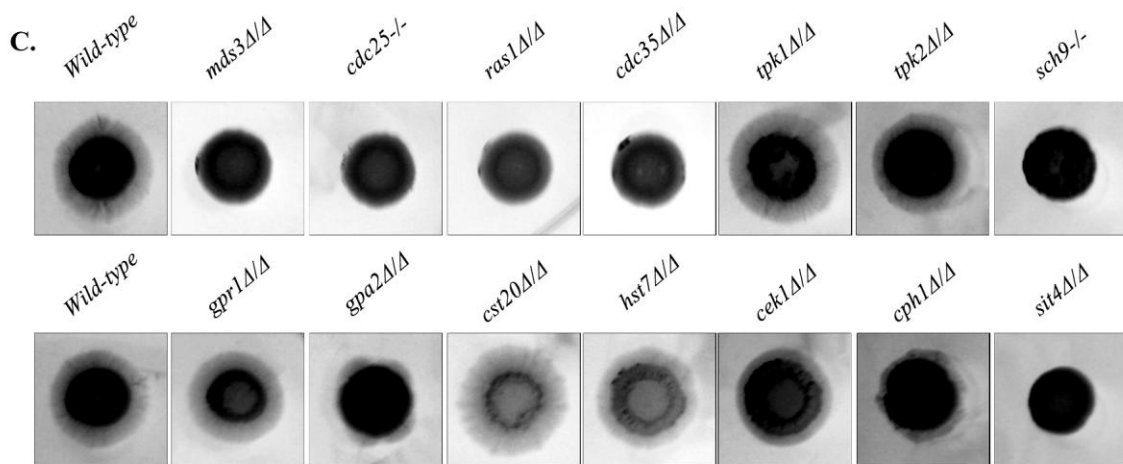


**Figure 5.3C:** Looking for *MDS3*-dependent phenotypes in mutants in the MAPK, PKA and TOR pathways. Overnights of the different strains (Table 1) were spotted on M199 pH 8 and incubated at 37°C for 6 days.

In sum, these results indicate that the upstream members of the Ras/cAMP pathway have a similar function as *Mds3*. It is difficult to assess the role of adenylate cyclase and PKA on *MDS3*-dependent phenotypes due to the severe growth defect of the *cdc35Δ/Δ* mutant and the

putative redundant function of the Tpk1/2 catalytic subunits. However, the MAPK pathway, which also functions downstream of Ras1 in *C. albicans*, did not show similar phenotypes as Mds3, suggesting that Mds3 does not function through the MAPK pathway. I noted that the MAPK effector Cph1 generally showed a different phenotype than the upstream MAPK members, indicating that the MAPK pathway is signaling through different effectors for the phenotypes tested, and that Cph1 is likely responding to other signaling pathways as well (Huang et al., 2008). Collectively, these results support the idea that, besides the TOR pathway, Mds3 also functions through the Ras pathway.

### **Genetic interaction between *MDS3*, *SIT4*, and *RAS1***

My results suggested that Mds3 also functions in the Ras pathway in *C. albicans*. One way to test this idea is to determine the genetic interaction among *MDS3*, *SIT4* and *RAS1*. To do this, I generated *mds3Δ/Δ sit4Δ/Δ* and *ras1Δ/Δ sit4Δ/Δ* double mutants, and tested them in the same growth assays described above. I was unable to construct an *mds3Δ/Δ ras1Δ/Δ* mutant, potentially because the double mutant has a severe growth defect (see Materials and Methods). As described previously, the *mds3Δ/Δ sit4Δ/Δ* double mutant showed an additive growth defect on rich medium and alkaline pH (reduced colony size), but not on LiCl as expected since only the *mds3Δ/Δ* mutant has a phenotype in this medium (Figure 5.4A; Zacchi et al., 2010a). The *ras1Δ/Δ sit4Δ/Δ* double mutant showed a more severe growth defect than the *mds3Δ/Δ sit4Δ/Δ* double mutant on rich medium, and an additive growth defect at alkaline pH, but not on LiCl, as expected since only the *ras1Δ/Δ* mutant has a phenotype in this medium (Figure 5.4A). Thus, both double mutants show additive growth defects in YPD and alkaline pH, but not on LiCl. These qualitative results suggest that Ras1 and Mds3 function in parallel pathways to Sit4 for growth on rich medium and at alkaline pH.

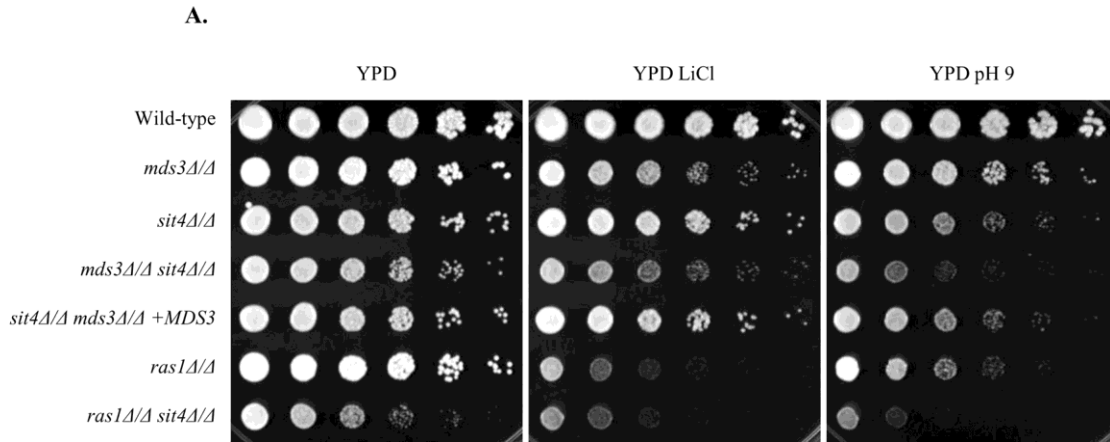


**Figure 5.4A:** Genetic interaction between *MDS3*, *SIT4*, and *RAS1*. Overnights of the wild-type (DAY185), *mds3Δ/Δ* (DAY1118), *sit4Δ/Δ* (DAY972), *mds3Δ/Δ sit4Δ/Δ* (DAY1233), *mds3Δ/Δ+MDS3 sit4Δ/Δ* (LUZ622), *ras1Δ/Δ* (DAY1109), *ras1Δ/Δ+RAS1* (DAY1228) and *ras1Δ/Δ sit4Δ/Δ* (LUZ613) strains were diluted in PBS and plated on YPD, YPD+150mM LiCl, YPD pH 9. Plates were incubated at 30°C for 48-72 hrs.

Another phenotype of interest is rapamycin resistance. Both the *sit4Δ/Δ* and *ras1Δ/Δ* mutants are more resistant to rapamycin in YPD and Spider media, while the *mds3Δ/Δ* mutant is only more resistant to rapamycin on Spider medium (Figure 5.3B, and Zacchi et al., 2010a). As previously shown, in YPD medium supplemented with rapamycin, the *mds3Δ/Δ sit4Δ/Δ* double mutant behaved similar to the *sit4Δ/Δ* mutant, as expected since only the *sit4Δ/Δ* mutant has a phenotype in this medium (Figure 5.4B; Zacchi et al., 2010a). In Spider medium supplemented with rapamycin, the *mds3Δ/Δ sit4Δ/Δ* double mutant grew similar to the *sit4Δ/Δ* mutant, and did not show an additive effect of both mutations (Figure 5.4B; Zacchi et al., 2010a). In YPD medium supplemented with rapamycin, the *ras1Δ/Δ sit4Δ/Δ* double mutant grew better than the *ras1Δ/Δ* single mutant but worse than the *sit4Δ/Δ* single mutant (Figure 5.4B). In Spider medium supplemented with rapamycin, the *ras1Δ/Δ sit4Δ/Δ* double mutant grew similar to the *ras1Δ/Δ* single mutant (Figure 5.4B). I must note that it is difficult to separate the growth defect of the *ras1Δ/Δ sit4Δ/Δ* mutant from the effect of rapamycin and through this methodology I cannot distinguish conclusively if both genes are contributing to rapamycin resistance completely

independently or through a shared pathway. However, it appears that Sit4 and Ras1 may be contributing to rapamycin sensitivity through dependent and independent pathways.

**B.**

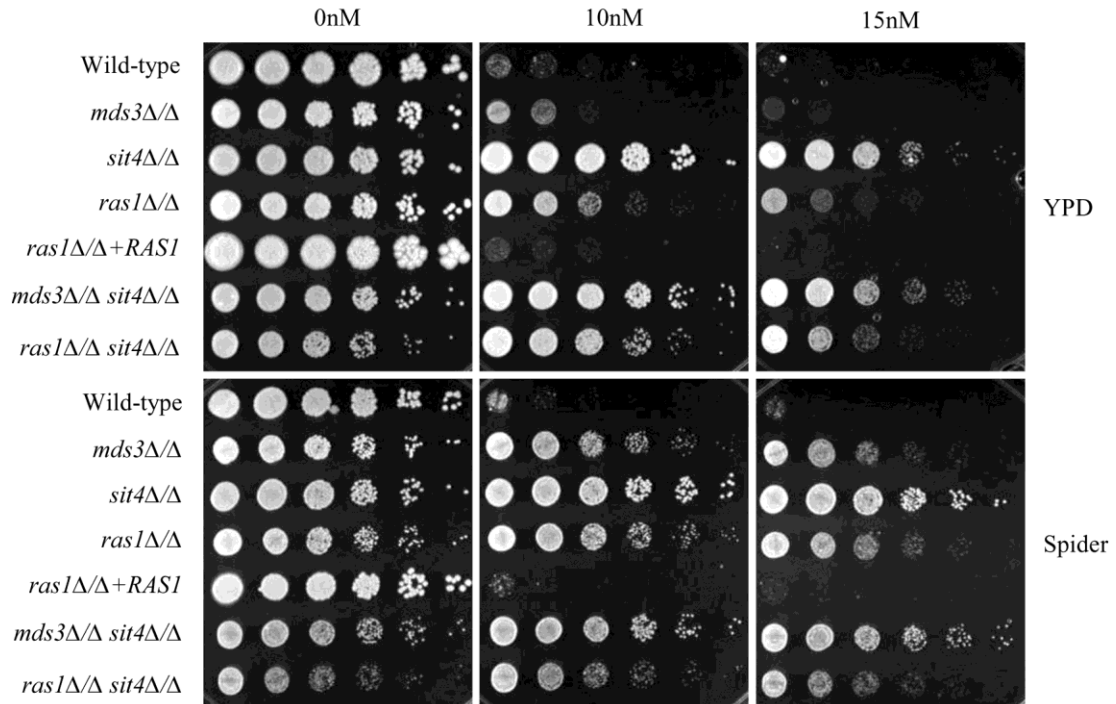


**Figure 5.4B:** Genetic interaction between *MDS3*, *SIT4*, and *RAS1*. Overnights of the wild-type (DAY185), *mds3Δ/Δ* (DAY1118), *sit4Δ/Δ* (DAY972), *mds3Δ/Δ sit4Δ/Δ* (DAY1233), *mds3Δ/Δ+MDS3 sit4Δ/Δ* (LUZ622), *ras1Δ/Δ* (DAY1109), *ras1Δ/Δ+RAS1* (DAY1228) and *ras1Δ/Δ sit4Δ/Δ* (LUZ613) strains were diluted in PBS and plated on YPD and Spider media supplemented with solvent or rapamycin. Plates were incubated at 30°C for 48-72 hrs.

The *mds3Δ/Δ* and *sit4Δ/Δ* mutants do not filament on solid M199 pH 8 medium, and have a defect in liquid M199 pH 8 medium that is partially rescued by rapamycin. However, Sit4 and Mds3 contribute independently to the filamentation response to rapamycin because the *mds3Δ/Δ sit4Δ/Δ* mutant does not filament with or without rapamycin in this medium (Figures 5.3C, 5.4C; Zacchi et al., 2010a). Thus, I wanted to test the effect of rapamycin on the *ras1Δ/Δ* mutant filamentation defect, and the effect of *RAS1* deletion on the response of the *sit4Δ/Δ* mutant. To do this, I assessed the ability of the double mutants to filament on M199 pH 8 medium in the

presence or absence of rapamycin. In M199 pH 8 solid and liquid media with solvent neither the *mds3Δ/Δ sit4Δ/Δ* or *ras1Δ/Δ sit4Δ/Δ* double mutants filamented, as expected since the single mutants do not filament in this media either (except for the *sit4Δ/Δ* mutant which shows a reduced filamentation in liquid M199 pH 8) (Figure 5.4C; Zacchi et al., 2010a). Addition of rapamycin to liquid M199 pH 8 partially rescued the filamentation defect of the *mds3Δ/Δ* and *sit4Δ/Δ* mutants, as previously observed, but did not rescue the *ras1Δ/Δ* or the *mds3Δ/Δ sit4Δ/Δ* and *ras1Δ/Δ sit4Δ/Δ* mutants filamentation defect (Figure 5.4C; Zacchi et al., 2010a). These results indicate that the ability of the *sit4Δ/Δ* mutant to filament in response to rapamycin requires *RAS1* and *MDS3*, and suggest that for this phenotype, *SIT4* functions in parallel to *MDS3*. No strong conclusion can be drawn about the relationship between *RAS1* and *SIT4* from this assay.

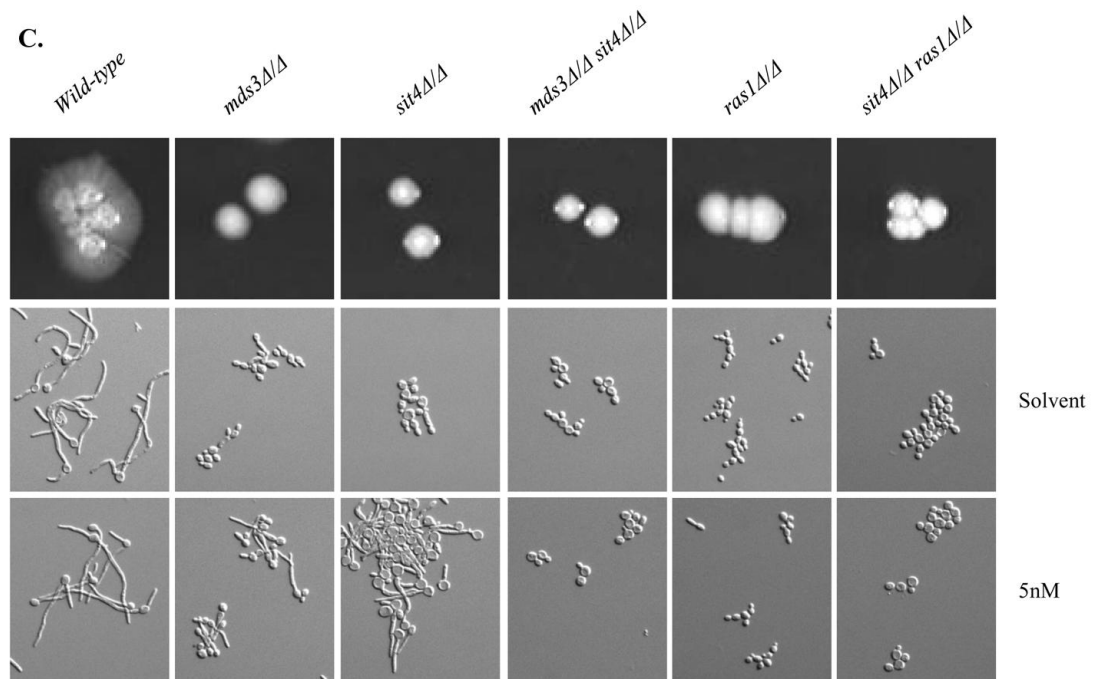


**Figure 5.4C:** Genetic interaction between *MDS3*, *SIT4*, and *RAS1*. Overnights of the wild-type (DAY185), *mds3Δ/Δ* (DAY1118), *sit4Δ/Δ* (DAY972), *mds3Δ/Δ sit4Δ/Δ* (DAY1233), *mds3Δ/Δ+MDS3 sit4Δ/Δ* (LUZ622), *ras1Δ/Δ* (DAY1109), *ras1Δ/Δ+RAS1* (DAY1228) and *ras1Δ/Δ sit4Δ/Δ* (LUZ613) strains were spotted on M199 pH 8 solid medium and plates were incubated at 37°C for 5-6 days; or were diluted 1:100 in M199 pH 8 supplemented with solvent or 5nM rapamycin and incubated 6 hrs at 37°C.

Although these epistasis analyses should be performed quantitatively, overall these results indicate that *MDS3* and *SIT4* share common functions regarding growth in the presence of rapamycin, while they also contribute independently to growth on rich medium and alkaline pH, and to filamentation. Further, these results suggest that *RAS1* and *SIT4* have independent contributions to most phenotypes tested, including growth in rich medium, alkaline pH, and rapamycin, and that the rapamycin induced filamentation in the *sit4Δ/Δ* mutant is *RAS1* dependent. Collectively, these results suggest that while Sit4 functions with Mds3 in the same pathway for certain phenotypes, Sit4 and Ras1 function in different pathways.

To continue to dissect the genetic interaction between *MDS3*, *SIT4*, and *RAS1*, I determined the expression of TOR-dependent genes in the single and double mutants grown in YPD medium supplemented with solvent or 20nM rapamycin (Zacchi et al., 2010a). The TOR pathway positively regulates the expression of genes involved in glycolysis, transcription, and translation such as *CDC19*, *RPS26A*, and *TEF1* (Bastidas et al., 2009; Cardenas et al., 1999). In YPD with solvent alone, the *mds3Δ/Δ*, *ras1Δ/Δ*, and *sit4Δ/Δ ras1Δ/Δ* mutants showed increased expression of the glycolytic enzyme *CDC19* compared to the wild-type strain, while the *sit4Δ/Δ* and *mds3Δ/Δ sit4Δ/Δ* mutants expressed *CDC19* at similar levels than wild-type (Figure 5.5). Results for *RPS26A* were not as clear, although in the presence of solvent alone there appeared to be a reduction in *RPS26A* expression compared to wild-type in all single and double mutants that had a *SIT4* deletion (Figure 5.5). *TEF1* expression in solvent alone remained unchanged in all strains except in the *sit4Δ/Δ* mutant in which *TEF1* expression is slightly lower than the rest of the strains (Figure 5.5). Addition of rapamycin to the medium reduced expression of *CDC19*, *RPS26A*, and *TEF1* in all strains compared to solvent alone (Figure 5.5). However, the expression of *CDC19* and *TEF1* in the *sit4Δ/Δ ras1Δ/Δ* mutant remained above the level of all other strains. Thus, while I did not observe major transcriptional differences in the expression of *TEF1* and *RPS26A* among the strains, these results suggest that Mds3, Sit4, and Ras1 regulate the

expression of glycolytic enzymes in YPD. In rich medium, Mds3 and Ras1 appear to function as negative regulators of *CDC19* expression, and Mds3 negative regulation of *CDC19* requires Sit4.

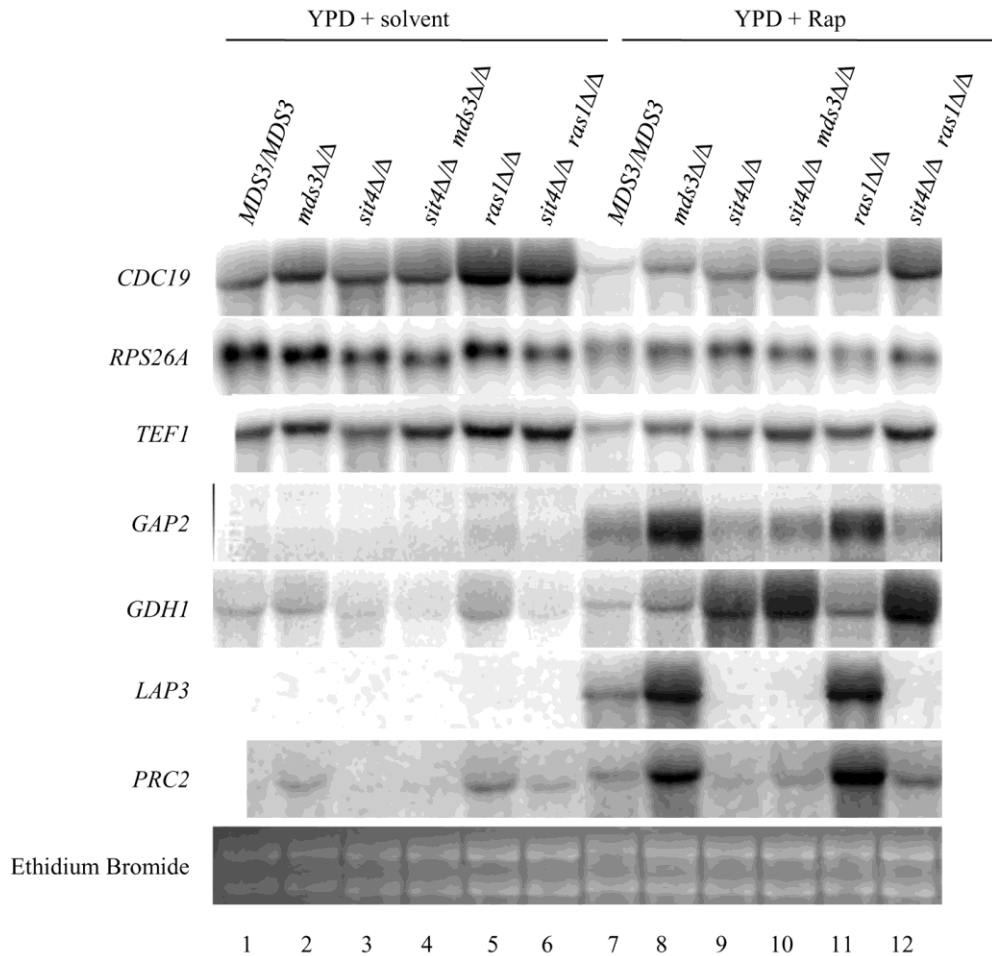


**Figure 5.5:** The *mds3Δ/Δ* and *ras1Δ/Δ* mutant have a similar gene expression profile, and *sit4Δ/Δ* mutation is dominant to both *mds3Δ/Δ* and *ras1Δ/Δ* mutations. Overnights of the wild-type (DAY185), *mds3Δ/Δ* (DAY1118), *sit4Δ/Δ* (DAY972), *mds3Δ/Δ sit4Δ/Δ* (DAY1233), *ras1Δ/Δ* (DAY1109), and *ras1Δ/Δ sit4Δ/Δ* (LUZ613) strains were diluted 0.125:40 in YPD medium and incubated at 30°C for 4 hrs, followed by 1 hr after addition of solvent or 20nM rapamycin.

The TOR pathway negatively regulates the expression of genes involved in the uptake and metabolism of alternative nitrogen sources (Bastidas et al., 2009; Cardenas et al., 1999). One gene whose regulation is TOR dependent and that is commonly used to determine TOR pathway function is *GAP2*, which encodes an amino acid permease. In the presence of solvent alone,

*GAP2* was not expressed in any strain. Addition of rapamycin induced *GAP2* expression in all strains (Figure 5.5). The *mds3Δ/Δ* and *ras1Δ/Δ* strains showed a higher expression of *GAP2* compared to the wild-type strain and the *sit4Δ/Δ* mutant, but the *mds3Δ/Δ sit4Δ/Δ* and *ras1Δ/Δ sit4Δ/Δ* mutants expressed *GAP2* similar to the *sit4Δ/Δ* mutant. This indicates that *GAP2* overexpression in the *mds3Δ/Δ* and *ras1Δ/Δ* mutants in the presence of rapamycin is *SIT4*-dependent (Figure 5.5; Zacchi et al., 2010a). *GDH1* encodes a glutamate dehydrogenase and its expression is also regulated by the TOR pathway (Bastidas et al., 2009). In the presence of solvent alone, the wild-type, *mds3Δ/Δ*, and *ras1Δ/Δ* strains expressed *GDH1* at similar levels. This expression was *SIT4*-dependent, because all the strains with a *sit4Δ/Δ* mutation showed reduced expression of *GDH1* compared to the wild-type (Figure 5.5). Addition of rapamycin did not affect *GDH1* expression in the wild-type, *mds3Δ/Δ*, and *ras1Δ/Δ* strains, but it markedly increased *GDH1* expression in all strains carrying a *SIT4* deletion (Figure 5.5). These results suggest that for genes involved in nitrogen metabolism, *MDS3* and *RAS1* have a similar function, and the *sit4Δ/Δ* mutation has a dominant effect (Figure 5.5). Further, these results support a model in which *SIT4* functions downstream *MDS3* and *RAS1* for the regulation of genes involved in nitrogen metabolism.

The TOR pathway also negatively regulates the expression of genes involved in protein degradation, such as *LAP3* and *PRC2* (Bastidas et al., 2009; Cardenas et al., 1999). In the presence of solvent alone the aminopeptidase *LAP3* was not expressed in any strain (Figure 5.5). Addition of rapamycin induced expression of *LAP3* in the wild-type, *mds3Δ/Δ*, and *ras1Δ/Δ* strains, but not in any strain with a *SIT4* deletion. The expression of *LAP3* was markedly higher in the *mds3Δ/Δ* and *ras1Δ/Δ* strains compared to the wild-type strain. Similar results were observed for *CPI1*, another vacuolar carboxypeptidase (data not shown). In the presence of solvent alone, the vacuolar carboxypeptidase *PRC2* was expressed more in the *mds3Δ/Δ*, *ras1Δ/Δ*, and *ras1Δ/Δ sit4Δ/Δ* mutants compared to the wild-type, *sit4Δ/Δ*, and *mds3Δ/Δ sit4Δ/Δ*

strains (Figure 5.5). Addition of rapamycin induced expression of *PRC2* in the wild-type, *mds3Δ/Δ*, and *ras1Δ/Δ* strains, but not in the *sit4Δ/Δ* mutant (Figure 5.5). The expression of *PRC2* was again markedly higher in the *mds3Δ/Δ* and *ras1Δ/Δ* strains compared to the wild-type strain. Again, *PRC2* overexpression in the *mds3Δ/Δ* mutant was *SIT4*-dependent, as evidenced by the similar low levels of *PRC2* expression in the *sit4Δ/Δ* and *mds3Δ/Δ sit4Δ/Δ* mutants. *PRC2* overexpression in the *ras1Δ/Δ* mutant was partially *SIT4*-dependent, since the *ras1Δ/Δ sit4Δ/Δ* strain showed lower *PRC2* expression than the *ras1Δ/Δ* single mutant but higher expression than the *sit4Δ/Δ* alone (Figure 5.5). These results support a model in which *SIT4* functions downstream *MDS3* and *RAS1* for the regulation of genes involved in protein degradation.

Overall, the results show that besides contributing to the regulation of glycolytic enzymes, both Mds3 and Ras1 also contribute to the regulation of genes involved in nitrogen metabolism and protein degradation, which are TOR regulated processes (Figure 5.5; Zacchi et al., 2010a). Further, the function of Mds3 and Ras1 on gene expression is opposite to the function of Sit4 (Figure 5.5.). The physical interaction between Mds3 and Sit4, the genetic and physical evidence that Mds3 functions upstream of Ras1, and the fact that *sit4Δ* deletion is dominant to *mds3Δ* deletion and semi-dominant to *ras1Δ* deletion in the presence or absence of rapamycin support a model in which Mds3 acts as a positive regulator of Ras1 and as a negative regulator of Sit4 (through Ras1 dependent and independent mechanisms) (Figure 5.3-5; Zacchi et al., 2010a; Krogan et al., 2006; Tonikian et al., 2009; Gavin et al., 2006; Collins et al., 2007; Benni and Neugeborn, 1997; McDonald et al., 2009). In other words, these results support a model in which the TOR pathway member Sit4 functions downstream of the Mds3-Ras1 signal transduction pathway.

It is critical to include in this analysis the *mds3Δ/Δ ras1Δ/Δ* double mutant. Since I was unable to construct this mutant through the regular knock-out strategy, alternative strategies to determine whether these two genes are synthetic lethal should be pursued. These include the use

of conditional knock-outs, the insertion of a third *RAS1* copy elsewhere in the genome and deletion of the second *RAS1* allele in locus, and the elimination of the last *RAS1* copy by introducing Cre/loxP sites surrounding *RAS1*. If viable, the *ras1Δ/Δ mds3Δ/Δ* double mutant will likely have a significant growth defect, which makes the process of finding this mutant more difficult.

The *mds3Δ/Δ* mutant has a different transcriptional phenotype on rich vs. poor nutrient media (Zacchi et al., 2010a). Thus, I wanted to test if the *ras1Δ/Δ* mutant also shared the *mds3Δ/Δ* transcriptional defects in M199 pH 8 medium. After 4 hrs of incubation in M199 pH 8 with solvent alone the wild-type strain expressed *GAP2*, while the *mds3Δ/Δ* or *ras1Δ/Δ* strains did not (Figure 5.6A). Addition of rapamycin rescued *GAP2* expression in both mutants to similar levels, indicating that the *ras1Δ/Δ* and *mds3Δ/Δ* mutants share similar phenotypes in poor nutrient medium as well (Figure 5.6A). Interestingly, I noted that in the *mds3Δ/Δ* mutant *GAP2* was overexpressed compared to the wild-type strain after an overnight incubation in YPD medium (Figure 5.6A, time 0 hr). The *ras1Δ/Δ* mutant also expressed more *GAP2* than the wild-type strain, but less than the *mds3Δ/Δ* mutant. These results suggest that absence of *MDS3*, and of *RAS1* to a lesser extent, lead to an earlier activation of starvation responses compared to the wild-type strain. Accordingly, I observed that the *mds3Δ/Δ* mutant accumulated more glycogen than the wild-type or *mds3Δ/Δ+MDS3* complemented strains (Figure 5.6B). Therefore, Mds3 and Ras1 also share functions in nutrient poor medium. Importantly, these results support a previously formulated idea that in rich medium *MDS3* is required to prevent the precocious induction of starvation responses (Benni and Neigeborn, 1997).

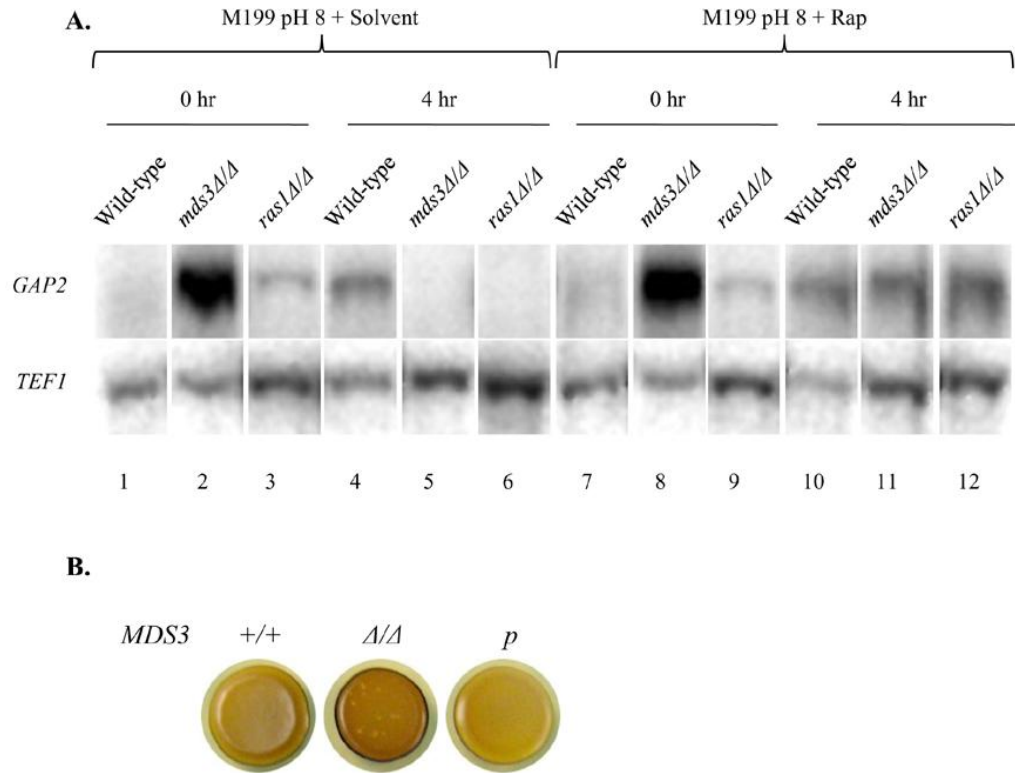


**Figure 5.6:** In the absence of *MDS3*, starvation responses are upregulated. (A) YPD overnights from the wild-type (DAY185), *mds3Δ/Δ* (DAY1118), and *ras1Δ/Δ* (DAY1109) were washed in PBS, diluted in pre-warmed M199 pH 8, and incubated at 37°C with or without 5nM Rapamycin. Samples for Northern Blot analysis were taken at time 0 and 4 hrs. (Similar results were observed for *sit4Δ/Δ* (DAY972)) B) Glycogen storage, the wild-type (+/+) (DAY185), *mds3Δ/Δ* (*Δ/Δ*) (DAY1118), and *mds3Δ/Δ+MDS3* (*p*) (DAY1119) were grown overnight in YPD, spotted on YPD and exposed to iodine vapors after 48 hrs of incubation at 30°C. Pictures show iodine-stained colonies.

### An overactive *RAS1* allele rescues the *mds3Δ/Δ* mutant, but not the *sit4Δ/Δ* mutant

Studies in *S. cerevisiae* suggest that Ras1 functions downstream or in parallel to *MDS3* and *TOR1* (Benni and Neigeborn, 1997; McDonald et al., 2009; Schmelze et al., 2004; Zurita-Martinez et al., 2004; Krogan et al., 2006; Tonikian et al., 2009; Gavin et al., 2006; Collins et al., 2007). My results suggest that Ras1 functions downstream of Mds3, but upstream or in parallel to the TOR effector Sit4 (Figures 5.3, 5.4, and 5.5). If indeed *RAS1* is downstream of *MDS3* in *C. albicans*, then expression of an overactive *RAS1* allele should rescue *mds3Δ/Δ* phenotypes; if *RAS1* functions upstream or in parallel to *MDS3* and *SIT4*, then the overactive allele will fail to

rescue some or all *mds3Δ* and *sit4Δ* mutants defects. In order to test these ideas I constructed a vector carrying an overactive *RASI*<sup>G13V</sup> allele under the control of its own promoter, and integrated this plasmid into the *RASI* locus of the wild-type, *mds3Δ/Δ* and *sit4Δ/Δ* mutants.

Introduction of an overactive *RASI*<sup>G13V</sup> allele into the wild-type strain did not affect growth on rich medium, LiCl or pH 9, but enhanced filamentation on M199 pH 8 (Figure 5.7A and C). Since the *ras1Δ/Δ* mutant is resistant to rapamycin in YPD and Spider media (Figure 5.4B), I predicted that the overactive allele would cause an enhanced sensitivity to the drug in the wild-type strain. However, introduction of the overactive *RASI*<sup>G13V</sup> allele (or of a third copy of *RASI*) into wild-type cells had no effect on growth on YPD or Spider media supplemented with rapamycin (Figure 5.7B).

Introduction of an overactive *RASI*<sup>G13V</sup> allele into the *mds3Δ/Δ* mutant rescued the growth phenotypes on rich medium, LiCl and pH 9, and induced filamentation on M199 pH 8 medium to the same extent as the wild-type strain with the *RASI*<sup>G13V</sup> allele (Figure 5.7A and C). The *RASI*<sup>G13V</sup> allele enhanced *mds3Δ/Δ* growth on YPD medium in the presence of rapamycin, similar to the wild-type strain (Figure 5.7B). The *RASI*<sup>G13V</sup> allele also abolished the rapamycin resistance of the *mds3Δ/Δ* strain on Spider medium (Figure 5.7B). Introduction of a third wild-type copy of *RASI* in the *mds3Δ/Δ* mutant did not have any phenotypic effect, indicating that the phenotypic rescue is a property of the *RASI*<sup>G13V</sup> mutation (Figure 5.7B). Therefore, the overactive *RASI*<sup>G13V</sup> allele rescued all phenotypes of the *mds3Δ/Δ* mutant.

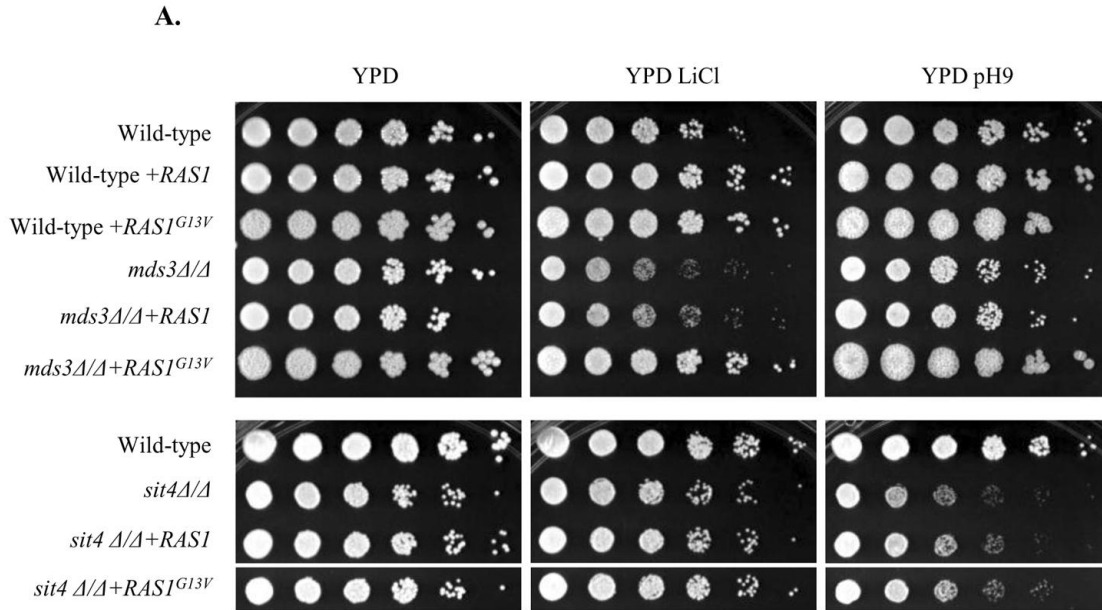


**Figure 5.7A:** An overactive *RAS1*<sup>G13V</sup> allele rescues *mds3Δ/Δ* defects, but not *sit4Δ/Δ* defects. Overnights of the wild-type (DAY286), wild-type + *RAS1* (LUZ756), wild-type + *RAS1*<sup>G13V</sup> (LUZ755), *mds3Δ/Δ* (DAY938), *mds3Δ/Δ* + *RAS1* (LUZ684), *mds3Δ/Δ* + *RAS1*<sup>G13V</sup> (LUZ686), *sit4Δ/Δ* (DAY972), *sit4Δ/Δ* + *RAS1* (LUZ688), and *sit4Δ/Δ* + *RAS1*<sup>G13V</sup> (LUZ690) strains were diluted in PBS and plated on (A) YPD, YPD+150mM LiCl, YPD pH 9. Plates were incubated at 30°C for 48-72 hrs.

Introduction of an overactive *RAS1*<sup>G13V</sup> allele into the *sit4Δ/Δ* mutant did not restore growth on rich medium or alkaline pH (Figure 5.7C). Further, the *RAS1*<sup>G13V</sup> allele did not induce peripheral filamentation into the agar in the M199 pH 8 in the *sit4Δ/Δ* mutant, although it caused the colony to become wrinkly on the surface (Figure 5.7B and C). However, the *RAS1*<sup>G13V</sup> allele did enhance the *sit4Δ/Δ* rapamycin resistance in both YPD and Spider media. A similar effect was also observed in *S. cerevisiae* (Figure 5.7C; Schmelzle et al., 2004). Therefore, an overactive *RAS1*<sup>G13V</sup> allele not only did not rescue *sit4Δ/Δ* defects, but actually enhanced the rapamycin resistance of this mutant independently of the nutrients in the media. Overall, these data support a model in which Mds3 functions upstream of Ras1, and Ras1 functions upstream of Sit4. Alternatively, Sit4 and Ras1 may function in parallel pathways, as shown in *S. cerevisiae* (Schmelzle et al., 2004), but they may govern a common set of downstream effectors.

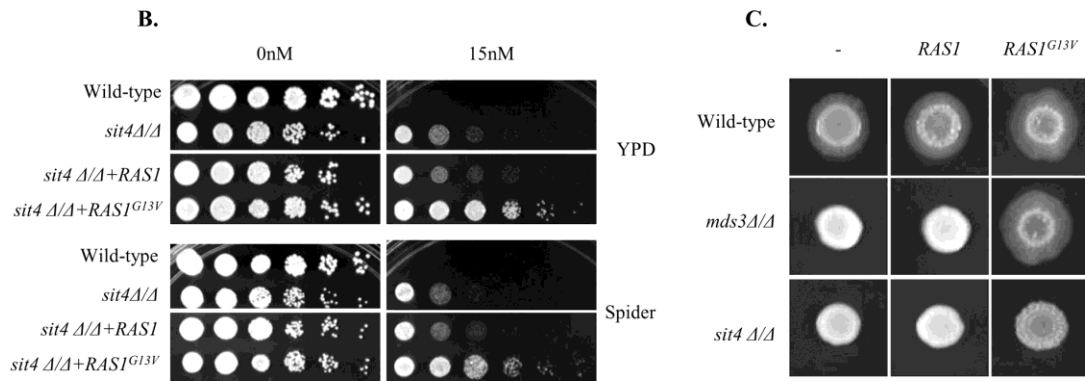
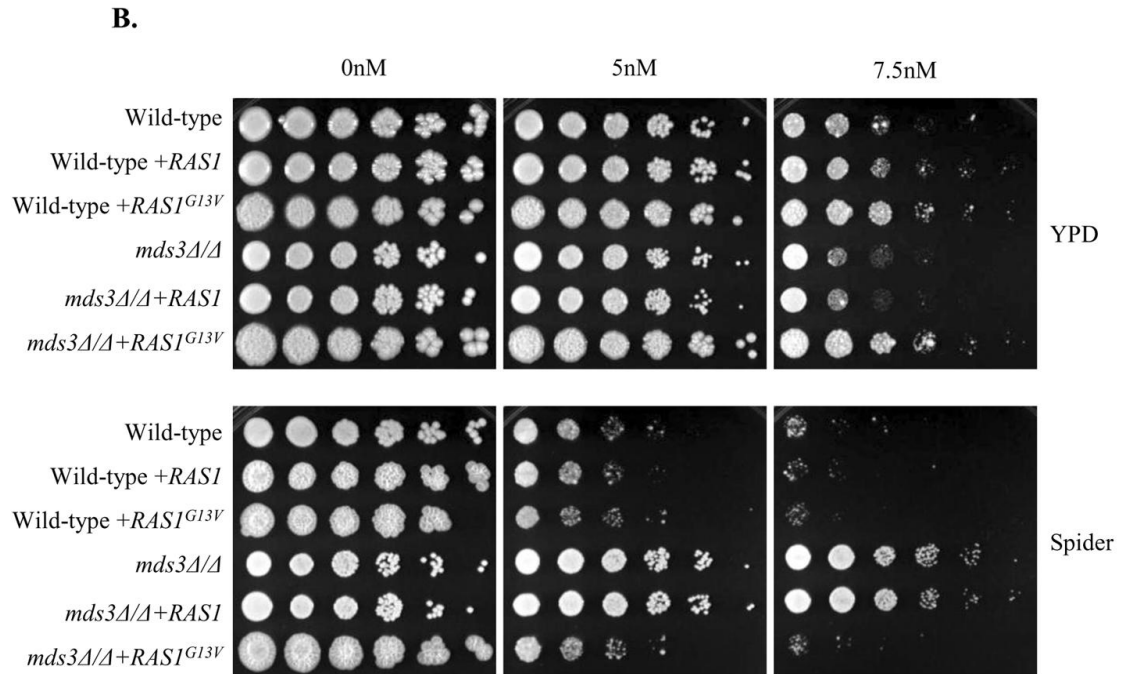


**Figure 5.7B, C:** An overactive *RAS1*<sup>G13V</sup> allele rescues *mds3Δ/Δ* defects, but not *sit4Δ/Δ* defects. Overnights of the wild-type (DAY286), wild-type + *RAS1* (LUZ756), wild-type + *RAS1*<sup>G13V</sup> (LUZ755), *mds3Δ/Δ* (DAY938), *mds3Δ/Δ* + *RAS1* (LUZ684), *mds3Δ/Δ* + *RAS1*<sup>G13V</sup> (LUZ686), *sit4Δ/Δ* (DAY972), *sit4Δ/Δ* + *RAS1* (LUZ688), and *sit4Δ/Δ* + *RAS1*<sup>G13V</sup> (LUZ690) strains were diluted in PBS and plated on (B) YPD and Spider media supplemented with solvent or rapamycin. Plates were incubated at 30°C for 48-72 hrs. (C) Overnights were spotted on M199 pH 8 solid medium and plates were incubated at 37°C for 5-6 days.

## Discovering new regulators of CMPS

Given the similarities observed between the phenotypes of the *mds3Δ/Δ*, *cdc25-/-*, and *ras1Δ/Δ* mutants (Figures 5.3-6), and the fact that Mds3 is predicted to interact with Cdc25, the upstream positive regulator of Ras1, I hypothesized that the Ras/cAMP pathway would be involved in the regulation of CMPS in *C. albicans* (Krogan et al., 2006; Tonikian et al., 2009; Gavin et al., 2006; Collins et al., 2007). Similarly, since Sit4 is a critical member of the TOR pathway, and since the *mds3Δ/Δ* and *sit4Δ/Δ* mutants share many phenotypes and interact physically, I hypothesized that the *sit4Δ/Δ* mutant would also form papilli (Figures 5.3 and 4; Zacchi et al. 2010a). Finally, since the *sch9-/-* mutant shares several phenotypes with the *mds3Δ/Δ* mutant (Figures 5.3), *SCH9* is a member of the TOR pathway, and is also a regulator of chlamydospore formation [an *MDS3*-dependent morphogenetic process in *C. albicans*], I hypothesized that *SCH9* is also involved in CMPS regulation (Urban et al., 2007; Nobile et al., 2003). Thus, I tested mutants involved in the Ras pathway (including the mutants in MAPK and PKA pathways), the Gpr1-Gpa2 parallel circuit, and the TOR pathway mutants in *SIT4* and *SCH9* for papilli formation (Figure 5.8A).

Overnights of all the strains were diluted in PBS, plated on YPD, and incubated 48 hrs at 30°C followed by room temperature incubation. The percentage of *mds3Δ/Δ* colonies showing papilli on the surface increased with time, while the wild-type strain did not produce any papilli after 18 days of incubation (Figure 5.8A, B). Indeed, the *cdc25-/-* and *ras1Δ/Δ* mutants showed progressive papilli formation, reaching a similar percentage of colonies with papilli as the *mds3Δ/Δ* mutant (Figure 5.8A, B). Interestingly, the *cdc35Δ/Δ* mutant also showed some papilli production, albeit at lower levels than the mutants in upstream Ras/cAMP pathway members Cdc25 and Ras1. This suggests that although papilli formation is influenced by low cAMP levels in the cell, this is not the main trigger of papilli formation in the *mds3Δ/Δ*, *cdc25-/-* and *ras1Δ/Δ* cells. One way to test if cAMP prevents papilli formation in the *mds3Δ/Δ*, *ras1Δ/Δ*, and *cdc35Δ/Δ*

mutant would be by supplementing the medium with dibutyryl-cAMP (a non metabolizable form of cAMP) and measuring papilli formation during time. Overall, these results confirm the hypothesis that the Ras/cAMP pathway contributes to the negative regulation of papilli formation in *C. albicans*. cAMP levels are positive regulators of PKA suggesting that the negative regulatory signal on CMPS is partially exerted by PKA (Figure 5.1). However, no papilli formation was observed in either of the single *tpk1* $\Delta/\Delta$  mutants, indicating that either the Tpk1/2 catalytic subunits share a redundant function in CMPS or that the signal is channeled through a different downstream effector of Ras1.

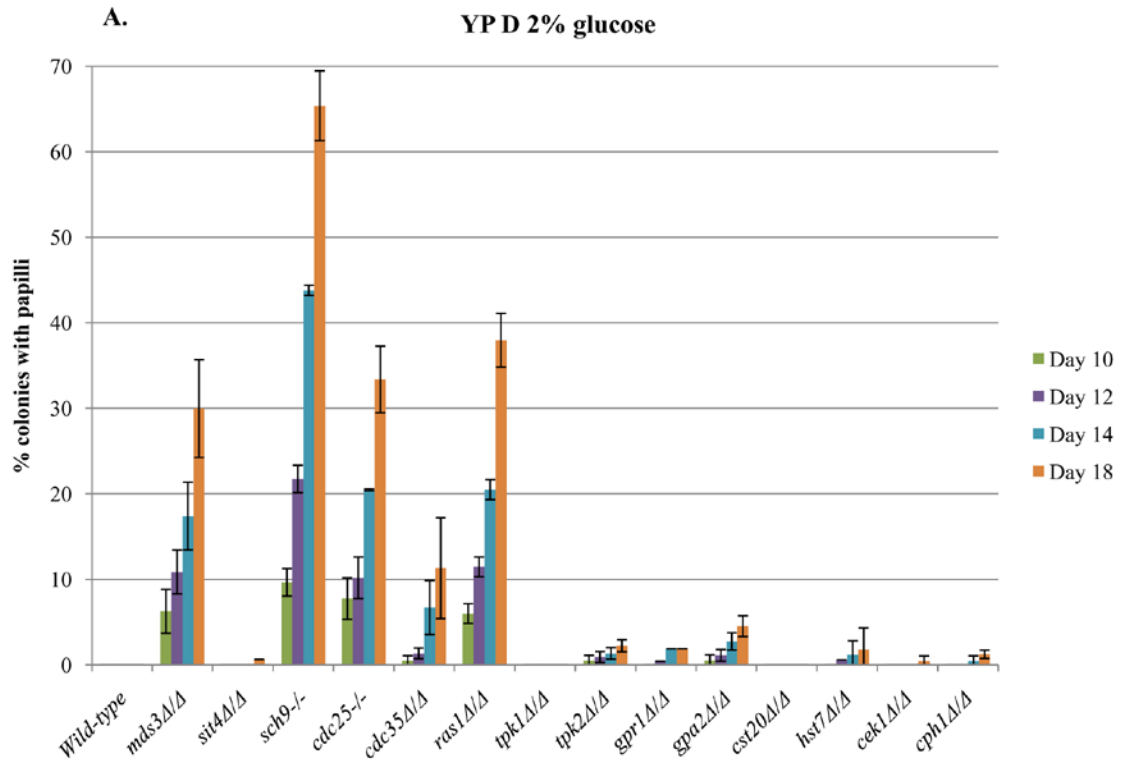


**Figure 5.8A:** *CDC25*, *RAS1*, and *SCH9* are also negative regulators of CMPS. YPD overnights from the different strains (Table 1) were diluted in PBS and plated in YPD with 2% or 0.2% glucose, or YPD buffered at pH 6 or pH 8. Plates were incubated 48 hrs at 30°C and then at room temperature for over two weeks. Papilli formation was scored in YPD plates every two days beginning at day 6.

None of the MAPK mutants, *gpr1Δ/Δ* or *gpa2Δ/Δ* mutants showed papilli formation, as expected since these mutants did not share *mds3Δ/Δ* phenotypes (Figures 5.3, 5.4, 5.8A). Unexpectedly, the *sit4Δ/Δ* mutant did not form papilli (Figure 5.8A, B). However, the *sch9-/-* mutant formed a significantly higher % of papilli compared to the *mds3Δ/Δ*, *cdc25-/-*, or *ras1Δ/Δ* mutants (Figure 5.8). Given that low glucose enhances papilli formation (Chapter 4), this assay was repeated in glucose starvation conditions. In YP + 0.2% glucose I observed an increase in papilli formation in the *mds3Δ/Δ*, *cdc25-/-*, *ras1Δ/Δ*, and *sch9-/-* strains, but glucose starvation did not induce papilli formation in the other mutants (Figure 5.8B and data not shown). Thus, I have identified several regulators of papilli formation in *C. albicans*: the Ras/cAMP pathway members Cdc25, Ras1, and Cdc35, and the TOR pathway member Sch9.

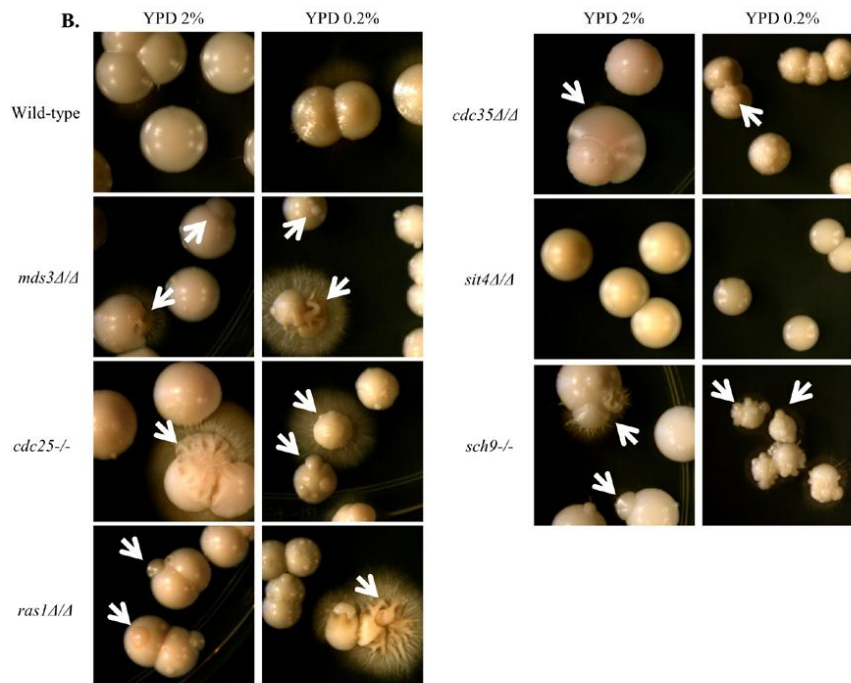


**Figure 5.8B:** *CDC25*, *RAS1*, and *SCH9* are also negative regulators of CMPS. Examples of papilli formation in the wild-type (DAY185), *mds3Δ/Δ* (DAY1118), *cdc25-/-* (DAY1326), *ras1Δ/Δ* (DAY1109), *cdc35Δ/Δ* (DAY1319), *sch9-/-* (DAY1226), and *sit4Δ/Δ* (DAY972) strains in YP with 2% or 0.2% glucose.

A critical requirement of CMPS is heritability of the morphological switch. Thus I verified that the papilli from the *cdc25*<sup>-/-</sup>, *ras1* $\Delta/\Delta$ , *cdc35* $\Delta/\Delta$ , and *sch9*<sup>-/-</sup> mutants indeed contained colonies with a heritable morphological alteration (data not shown). Further, I observed that cells from many of the switched isolates also had marked cellular morphological alterations, which included enlarged, elongated, and vacuolized cells (Figure 5.8C). The changes in cellular morphology of the switched strains are not surprising, they had been previously observed in *mds3* $\Delta/\Delta$  switched cells (data not shown), and they contribute to explain the changes in colony morphology (Dutton and Penn, 1989). Therefore *CDC25*, *RAS1*, *CDC35*, and *SCH9* constitute new CMPS regulators in *C. albicans*.

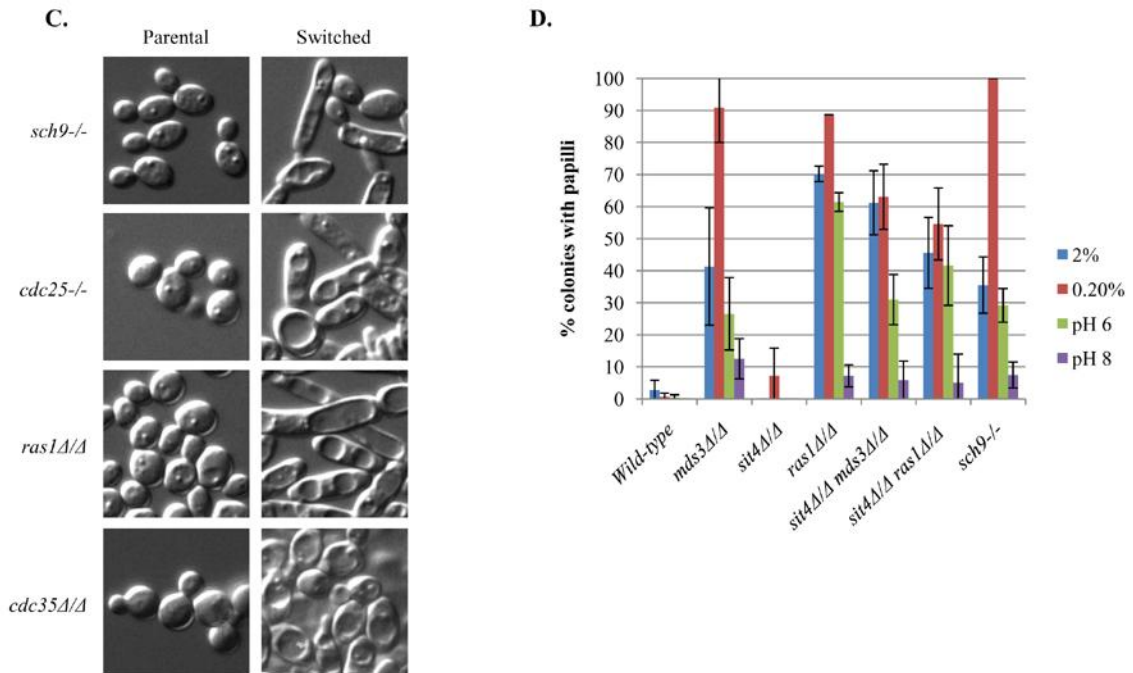


**Figure 5.8C,D:** *CDC25*, *RAS1*, and *SCH9* are also negative regulators of CMPS. (C) Examples of cellular morphology from papilli from *cdc25*<sup>-/-</sup> (DAY1326), *ras1* $\Delta/\Delta$  (DAY1109), *cdc35* $\Delta/\Delta$  (DAY1319), and *sch9*<sup>-/-</sup> (DAY1226) strains. (D) Papilli formation scored in YP with 2% or 0.2% glucose, or YPD buffered at pH 6 or pH 8 in the wild-type (DAY185), *mds3* $\Delta/\Delta$  (DAY1118), *sit4* $\Delta/\Delta$  (DAY972), *ras1* $\Delta/\Delta$  (DAY1109), *sch9*<sup>-/-</sup> (DAY1226), *mds3* $\Delta/\Delta$  *sit4* $\Delta/\Delta$  (DAY1233), and *ras1* $\Delta/\Delta$  *sit4* $\Delta/\Delta$  (LUZ613) strains. The graph represents the mean +/- standard deviation of three independent overnights/strain.

The unexpected result that *SIT4* does not inhibit papilli formation in *C. albicans* and the fact that *SIT4* appears to function downstream *MDS3* and *RAS1* prompted me to determine whether *SIT4* would be required for CMPS formation in the *mds3Δ/Δ* and *ras1Δ/Δ* mutants (Figures 5.5, 5.7 and 5.8). The *mds3Δ/Δ sit4Δ/Δ* and *ras1Δ/Δ sit4Δ/Δ* mutants formed papilli at the same rate as the single mutants in regular YPD medium. However, during glucose starvation, a condition that enhances papilli formation in the single *mds3Δ/Δ* and *ras1Δ/Δ* mutants (Figure 5.8B and D), the % of papilli formation of *mds3Δ/Δ sit4Δ/Δ* and *ras1Δ/Δ sit4Δ/Δ* double mutants was similar to the % of papilli formed by these mutants in regular YPD. This result indicates that absence of *SIT4* abolishes the effect of glucose starvation on papilli formation (Figure 5.8D).

Alkaline pH is an inhibitor of CMPS in the *mds3Δ/Δ* mutant (Chapter 4). Thus, I wished to determine if alkaline pH would inhibit CMPS in the *ras1Δ/Δ* and *sch9-/-* mutants (Figure 5.8D). Indeed, alkaline pH also inhibits papilli formation in the *ras1Δ/Δ* and *sch9-/-* mutants, suggesting that these mutants are contributing to CMPS through a similar mechanism. Alkaline pH still inhibited papilli formation in the double mutants, indicating that Sit4 is not required to transmit the alkaline pH signal (Figure 5.8D). Therefore, the environmental signals that regulate CMPS in the *mds3Δ/Δ* mutant also regulate CMPS in the *ras1Δ/Δ* and *sch9-/-* mutant; and while *SIT4* does not inhibit papilli formation in a wild-type background or in the presence of high levels of glucose, it appears to be required for the low glucose response observed in the *mds3Δ/Δ* and *ras1Δ/Δ* mutants.

### **Similar to Mds3, Ras1 and Sch9 also contribute to MMS sensitivity**

The *mds3Δ/Δ* mutant is more resistant to the DNA damage agent methyl methanesulfonate (MMS) than the wild-type strain. This feature of the *mds3Δ/Δ* mutant is relevant because defects in DNA damage response might lead to the phenotypic switch in the *mds3Δ/Δ* mutant (Chapter 4). Given the similar phenotypes on papilli formation of the *ras1Δ/Δ*

and *sch9*<sup>-/-</sup> mutants, I hypothesized that these mutants would also show enhanced MMS resistance. Thus, I grew the wild-type, *mds3Δ/Δ*, *ras1Δ/Δ*, *ras1Δ/Δ*+*RAS1*, and *sch9*<sup>-/-</sup> strains in the presence of MMS (Figure 5.9). I also tested a second DNA damaging agent, hydroxyurea (HU), which does not affect the growth of the *mds3Δ/Δ* mutant (Chapter 4). Indeed, the *ras1Δ/Δ* and *sch9*<sup>-/-</sup> mutants were also more resistant to MMS than the wild-type and *ras1Δ/Δ*+*RAS1* complemented strains, and there was no difference in growth in the presence of HU (Figure 5.9). These results support the idea that Mds3, Ras1, and Sch9 contribute to CMPS through similar mechanisms.

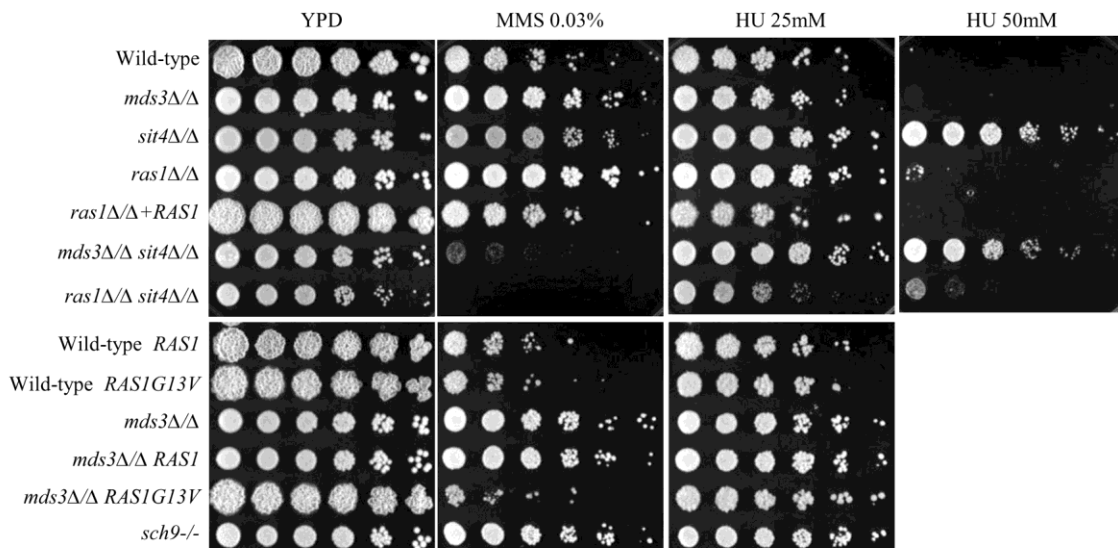


**Figure 5.9:** Genetic interaction between *MDS3*, *SIT4*, and *RAS1* in resistance to genotoxic stress. Overnights of the wild-type (DAY185), *mds3Δ/Δ* (DAY1118), *sit4Δ/Δ* (DAY972), *mds3Δ/Δ sit4Δ/Δ* (DAY1233), *ras1Δ/Δ* (DAY1109), *ras1Δ/Δ*+*RAS1* (DAY1228), *ras1Δ/Δ sit4Δ/Δ* (LUZ613), wild-type + *RAS1* (LUZ756), wild-type + *RAS1*<sup>G13V</sup> (LUZ755), *mds3Δ/Δ* (DAY956), *mds3Δ/Δ* + *RAS1* (LUZ684), *mds3Δ/Δ* + *RAS1*<sup>G13V</sup> (LUZ686), and *sch9*<sup>-/-</sup> (DAY1226) were diluted in PBS and plated on YPD medium supplemented with MMS and HU. Plates were incubated at 30°C for 48-72 hrs.

*SIT4* is required for enhanced papilli formation during glucose starvation (Figure 5.8D) and for the transcriptional response of the *mds3Δ/Δ* and *ras1Δ/Δ* mutants (Figure 5.5). Thus, I wanted to test if *SIT4* was also required for MMS and HU resistance in the wild-type, *mds3Δ/Δ*, and *ras1Δ/Δ* strains. Since the *sit4Δ/Δ* mutant grew more slowly than the *mds3Δ/Δ*, *ras1Δ/Δ*, and

*sch9*<sup>-/-</sup> mutants it is difficult to determine if this mutant is more or less sensitive to MMS than the wild-type strain (Figure 5.9). Interestingly, the *mds3Δ/Δ sit4Δ/Δ* and *ras1Δ/Δ sit4Δ/Δ* mutants were hypersensitive to MMS, suggesting that Mds3, Ras1, and Sit4 contribute to MMS resistance through independent mechanisms (Figure 5.9). I did not observe a difference in HU sensitivity in the wild-type, *mds3Δ/Δ*, *ras1Δ/Δ*, and *sch9*<sup>-/-</sup> strains. However, the *sit4Δ/Δ* mutant was markedly resistant to HU compared to the wild-type, *mds3Δ/Δ*, and *ras1Δ/Δ* strains (Figure 5.9). The *mds3Δ/Δ sit4Δ/Δ* double mutant was as HU resistant as the *sit4Δ/Δ* mutant, however the *ras1Δ/Δ sit4Δ/Δ* was only slightly more resistant to HU than the *ras1Δ/Δ* strain (Figure 5.9). The negative synergism between the *sit4Δ* and *ras1Δ* mutations on HU resistance suggests that Ras1 is required for the enhanced HU resistance of the *sit4Δ/Δ* mutant (Figure 5.9). Therefore, Mds3, Ras1, and Sch9 sensitize cells to MMS, and deletion of *SIT4* in an *mds3Δ/Δ* or *ras1Δ/Δ* background reduces the ability of these mutants to survive genotoxic stress.

Since the *ras1Δ/Δ* deletion affected growth in the presence of genotoxic agents and Mds3 appears to function upstream Ras1 (Figure 5.3-5, 5.7, 5.9), I hypothesized that an overactive *RAS1*<sup>G13V</sup> allele would rescue the *mds3Δ/Δ* mutant defects on MMS. Thus, I compared the growth on MMS of the wild-type and *mds3Δ/Δ* mutants containing an extra wild-type *RAS1* copy or an overactive *RAS1*<sup>G13V</sup> allele (Figure 5.9). While the *RAS1*<sup>G13V</sup> allele did not alter MMS sensitivity in the wild-type strain, it restored MMS sensitivity in the *mds3Δ/Δ* mutant (Figure 5.9). I also tested the effect of the *RAS1*<sup>G13V</sup> allele on HU resistance, and found that it had no effect on HU resistance in the wild-type or *mds3Δ/Δ* background (Figure 5.9). Addition of the extra *RAS1* copy had no effect on MMS or HU resistance, indicating that the phenotypes observed are a property of the overactive *RAS1*<sup>G13V</sup> allele. Thus, overactive *RAS1*<sup>G13V</sup> can induce MMS sensitivity but not HU sensitivity, in the *mds3Δ/Δ* mutant.

Taken together, the results presented here suggest that Mds3 also functions through the Ras/cAMP pathway in *C. albicans*. Mds3 and Ras1 share many similar functions, including LiCl,

alkaline pH, and rapamycin tolerance, MMS sensitivity, and the regulation of genes involved in the nitrogen catabolite response and protein degradation in a *SIT4* dependent manner. Importantly, I found that Ras1 and the TOR pathway member Sch9 are also CMPS regulators, and that they appear to respond to the same CMPS environmental stimuli as Mds3. The TOR pathway effector Sit4, which appears to function downstream of Mds3 and Ras1, not only does not inhibit papilli formation but it actually appears to be required for papilli formation during glucose starvation in the absence of *MDS3* or *RAS1*. These results indicate that there is a strong association between nutrient sensing through the TOR and Ras/cAMP pathways and CMPS during prolonged incubation and stationary phase. Given the extensive knowledge on Ras1 and Sch9 function compared to Mds3 function, associating CMPS with the Ras/cAMP and Sch9/Sit4/TOR pathways will significantly contribute to understanding the mechanism of the switch.

## DISCUSSION

Colony morphology phenotypic switching (CMPS) in *C. albicans* is poorly understood. Only two regulators of CMPS have been described, Ssn6 and Mds3, and they appear to affect CMPS through different mechanisms (Chapter 4; Garcia-Sanchez et al., 2005). Here, I describe two additional CMPS regulators: Ras1 and Sch9, which are members of the cAMP/MAPK and TOR pathways, respectively. Further, I provide evidence that indicates that, besides regulating the TOR pathway, Mds3 is also an upstream member of the Ras/cAMP pathway in *C. albicans*. These results place Mds3 in a critical position to regulate two major signal transduction pathways that sense environmental nutrients in fungi and support a model in which CMPS arises due to defective starvation responses (Chapter 4).

### **Regulation of CMPS occurs via two major signal transduction pathways**

The first CMPS regulator identified in this work is Ras1. In *S. cerevisiae*, Mds3 is associated with the Ras pathway (Benni and Neigeborn, 1997; McDonald et al., 2008, Krogan et al., 2006; Tonikian et al., 2009; Gavin et al., 2006; Collins et al., 2007). Similarly, my data suggests that in *C. albicans* Mds3 also functions upstream of Ras1, probably as a positive regulator of Cdc25 (Figure 5.10). For example, mutants in *MDS3* and *RAS1* (and *CDC25*, for those phenotypes in which it was tested) shared most phenotypes, including sensitivity to LiCl and alkaline pH, filamentation defects, rapamycin and MMS resistance, and enhanced expression of genes involved in starvation responses in a *SIT4*-dependent manner (Figures 5.3-5.6). Importantly, similar to Mds3, Ras1 is also a negative regulator of CMPS (Figure 5.8). Colonies from the *mds3Δ/Δ* and *ras1Δ/Δ* mutants produced papilli during prolonged incubation, and this papilli formation was inhibited by alkaline pH and enhanced by glucose starvation in a *SIT4*-dependent manner in both mutants (Figure 5.8, Chapter 4). Finally, a *RAS1* overactive allele rescued all phenotypes of the *mds3Δ/Δ* mutant [it was not possible to test for rescue of papilli

formation because colonies with a *RAS1* overactive allele became large and wrinkly making the papilli difficult to distinguish] (Figure 5.7, 5.9). Thus, CMPS is also regulated by the Ras pathway, and Mds3 is an upstream member of this pathway.

However, there were also phenotypic differences between the *ras1Δ/Δ* mutant and the *mds3Δ/Δ* mutant which suggests a complex interaction between these genes. First, the *ras1Δ/Δ* mutant was resistant to rapamycin in YPD, while the *mds3Δ/Δ* mutant was not; and while Mds3 and Sit4 contributed to rapamycin resistance through the same pathway, Ras1 and Sit4 appeared to contribute to rapamycin resistance through dependent and independent pathways (Figures 5.3, 5.4; Zacchi et al., 2010a). Second, the gene expression defects in the *ras1Δ/Δ* mutant were only partially *SIT4*-dependent (Figure 5.5). Finally, *GAP2* expression after an overnight incubation was markedly higher in the *mds3Δ/Δ* mutant compared to levels of the *ras1Δ/Δ* mutant (Figure 5.6). Therefore, while these data indicate that Mds3 and Ras1 function through the same pathway, Mds3 and Ras1 differ in their interactions with the TOR downstream effector Sit4. Importantly, an overactive Ras1 allele was unable to rescue *sit4Δ/Δ* defects, supporting a model in which Sit4 functions downstream of Ras1 (Figure 5.7). Alternatively, Sit4 could function independently of Ras1. Testing the phenotypes of the *mds3Δ/Δ ras1Δ/Δ* double mutant is critical to more definitely establish the association between Mds3 and Ras1. Overall, the data presented here indicate that Ras1 is a negative regulator of CMPS in *C. albicans*, and suggest that Ras1 regulates CMPS through similar mechanisms as Mds3.

The second CMPS regulator identified is the Sch9 kinase. Sch9 is a downstream effector of the TOR pathway, and proposed to be the ortholog for the mammalian S6K1 kinase, which is involved in protein synthesis (Urban et al., 2007; Huber et al., 2009). In *C. albicans* Sch9 is required for proper yeast-hyphal and chlamydospore morphogenetic transitions, similar to Mds3 (Nobile et al., 2003; Liu et al, 2010; Davis et al., 2002). Importantly, the *sch9-/-* mutant makes papilli after prolonged incubation at a higher proportion than the *mds3Δ/Δ* mutant (Figure

5.8). Similar to the *mds3Δ/Δ* mutant, the *sch9-/-* papilli formation is inhibited by alkaline pH and exacerbated by glucose starvation (Figure 5.8). Interestingly, we had previously shown that the combination of the *TOR1-1* allele with an *mds3Δ* mutation caused a marked increase in papilli formation (Chapter 4). The *TOR1-1* mutation has been shown to affect the ability of the TOR kinase to phosphorylate and thus, regulate some of its downstream effectors, including S6K1 in mammals, the human ortholog of Sch9 (McMahon et al., 2002; Urban et al., 2007). Thus, it is possible that the enhanced papilli formation in the *TOR1-1Δ mds3Δ/Δ* mutant is due to a defect in Sch9 function. It would be interesting to determine if there is an alteration in the phosphorylation pattern of Sch9 in the absence of *MDS3* and if altering the TOR-dependent phosphorylation sites in Sch9 would rescue the *mds3Δ/Δ* mutant defects (Urban et al., 2007). Finally, similar to *MDS3*, *SCH9* deletion confers MMS resistance (Figure 5.9). Overall, our data indicate that the downstream TOR pathway effector Sch9 is a negative regulator of CMPS in *C. albicans*, and suggest that Sch9 regulates CMPS through similar mechanisms as Mds3. However, there were several phenotypic differences between the *mds3Δ/Δ* and *sch9-/-* mutants, which include growth on LiCl and at pH 9, sensitivity to rapamycin, and filamentation on solid M199 pH 8 (Figure 5.3; Liu et al., 2010). Considering the current model of Mds3 and Sch9 function in the TOR pathway (Figure 5.10; Chapter 3, Figure 3.9; Chapter 1, Figure 1.3; Huber et al., 2009), these results suggest that Sch9 would only mediate some of Mds3's TOR-dependent functions.

The results presented here suggest that Mds3 has a dual-function on the TOR pathway (Figure 5.10). During growth in nutrient- poor M199 pH 8 medium, Mds3 functions as a negative regulator of TOR (Zacchi et al., 2010a). However, in nutrient-rich medium like YPD, Mds3 appeared to function as a positive regulator of TOR. For example, absence of *MDS3* led to enhanced starvation responses, including increased expression of *GAP2* and genes encoding protein degradation enzymes, and enhanced glycogen storage (Figures 5.5, 5.6). I noticed that the *ras1Δ/Δ* mutant did not induce *GAP2* expression to the levels of the *mds3Δ/Δ* mutant during an

overnight incubation, suggesting that these responses in the *mds3Δ/Δ* mutant could only be partially mediated by a defective Ras pathway (Figure 5.6). By being able to alter its effects on the regulation of the TOR pathway in the presence of different environmental signals, Mds3 would be contributing to fine-tune the activity of this major signal transduction pathway.

Taking all the data together, I propose the following model to explain CMPS regulation in *C. albicans* (Figure 5.10). CMPS is negatively regulated by the Ras/cAMP and TOR signal transduction pathways in response to environmental cues. Under conditions of nutrient depletion and in the absence of Mds3, Ras1, or Sch9, the Ras/cAMP and TOR pathways cannot transmit nutrient starvation signals efficiently, which leads to uncoordinated growth arrest, compromises entry into stationary phase, and induces replication stress. Replication stress is associated with increased DNA damage and genome instability (Weinberger et al., 2007; Burhans and Weinberger, 2007). Stress and DNA damage could accumulate during stationary phase and eventually trigger a suppressive response that induces unrestricted cellular growth and hence allows for papilli formation (Chapter 4). In support of this idea, the similar effect of *MDS3*, *RAS1*, and *SCH9* deletion on resistance to the genotoxic agent MMS suggests that these mutants do not respond properly to DNA damage-induced growth arrest, and continue to replicate under suboptimal conditions. Thus, defective DNA damage responses and cell cycle checkpoints in these mutants are possible common mechanisms of CMPS (see Chapter 4, discussion). Ras and Sch9 are associated with DNA damage, genomic instability, and the generation of variability in yeast and mammals (Madia et al., 2009; Weinberger et al., 2007; Bitterman et al., 2003; Fabrizio et al., 2005), which supports a role for these proteins and their signaling cascades in phenotypic switching in *C. albicans*.

It would be interesting to deep-sequence several switched strains and their non-switched counterparts, including not only the *mds3Δ/Δ*, *ras1Δ/Δ*, and *sch9-/-* mutants, but also environmental isolates. This would allow us to determine the following: 1) Which type/s of

genomic rearrangements happen in the switched strains?; 2) is there an increased overall mutation rate associated with the switch?; and importantly: 3) are there any particular mutations/rearrangements/aneuploidies, LOHs, etc associated with the switch and/or that correlate with any particular phenotype?

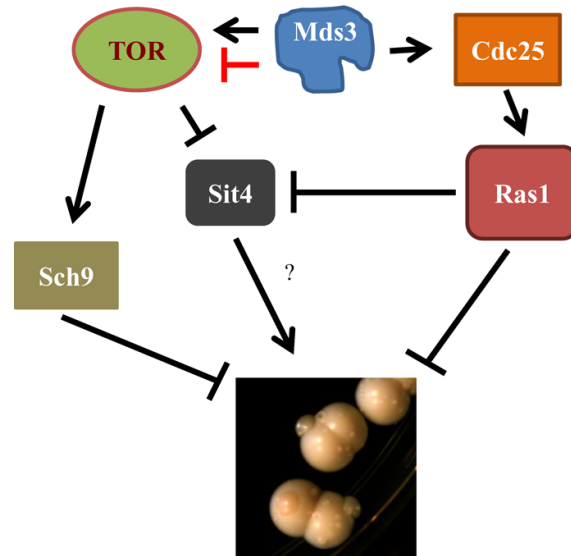


**Figure 5.10:** Model of Mds3, Ras1, and Sch9 regulation of CMPS in *C. albicans*.

### The connection between TOR and Ras

What is the relationship between the TOR and Ras pathways in *C. albicans*? Since the Ras/PKA pathway regulates similar downstream effectors as the TOR pathway, we would expect some level of redundancy in their function. In this scenario, mutants in the PKA pathway should show hypersensitivity to TOR inhibition by rapamycin. Indeed, the *tpk2Δ/Δ* mutant was more sensitive to rapamycin (Figure 5.3B). However, deletion of the upstream members of the PKA pathway, including *CDC25*, *RAS1*, and the *GPRI/GPA2* circuit showed rapamycin resistance (Figure 5.3B). The increased rapamycin resistance in the *cdc25Δ/Δ* and *ras1Δ/Δ* mutants was not due to a defect in MAPK signaling, since all MAPKs showed enhanced sensitivity to rapamycin (Figure 5.3B). Therefore, rapamycin resistance appears to be a property of Cdc35, the adenylate

cyclase, which lies downstream of both Ras1 and Gpr1/Gpa2 (Maidan et al., 2005; Wilson et al., 2010). Given the above result, it was no surprise that introduction of an overactive Ras1 allele induced rapamycin sensitivity in the *mds3Δ/Δ* mutant. However, this result is still counterintuitive: why would the overactivation of a pathway enhance dependence on a parallel pathway? One possibility is that the product of Cdc35 activity: cAMP acts on other signaling pathways independently of PKA, as it has been shown to occur in mammals (Busca et al., 2000; Cass et al., 1999; Tsygankova et al., 2000). In this model, *tpk2Δ/Δ* deletion might induce rapamycin sensitivity by increasing cAMP levels due to the relief of Tpk negative feedback on Cdc35 (Nikawa et al., 1987; Ma et al., 1999; Thevelein and De Winde, 1999). Alternatively, the difference between the Ras1 and PKA phenotypes might lie downstream of Ras1 but independently of cAMP and MAPK. For example, it is possible that Ras1 also regulates the function of the TOR pathway or of TOR downstream effectors, an idea supported by the results that suggest that Sit4 functions downstream of Ras1 (Figures 5.5, 5.7). Such a molecular arrangement is already established in mammalian organisms, in which Ras functions upstream of the TOR kinase (Wullschleger et al., 2006). Finally, there could be a regulatory feedback between the Ras and TOR pathways. Such an arrangement would ensure that both pathways act in concert to regulate growth and metabolism. Feedback regulatory mechanisms are common within the Ras/PKA and within the TOR pathways (Lempiainen et al., 2009, Thevelein and de Winde, 1999; Kockel et al., 2010).

The generation of phenotypic variability is critical for the perpetuation of any organism in its environment. The almost clonal reproductive style of *C. albicans* forces this organism to exploit alternative mechanisms to produce phenotypic variation in their populations. One such phenomenon is colony morphology phenotypic switching. Here, I show that CMPS is regulated by the Ras/cAMP and the TOR signal transduction pathways. I suggest that mutations in these

pathways cause uncoordinated growth arrest during stationary phase, leading to the accumulation of DNA damage and genomic instability. These processes eventually trigger the formation of variant strains that outgrow the colonies forming the papilli. The results shown here indicate that, similar to what is observed in mammals, flies, and *S. cerevisiae*, there is an intricate connection between signal transduction networks in *C. albicans*. It would be interesting to dissect the interaction between these signaling cascades in order to understand how *C. albicans* cells use these pathways to control several morphogenetic and virulence attributes in response to diverse environmental cues.

## TABLES

**Table 5.1.** *C. albicans* strains used in this study

Strain	Parent	Genotype	Reference
<b>DAY1 (BPW17)</b>	SC5314	<i>ura3::λimm434/ura3::λimm434 his1::hisG/his1::hisG arg4::hisG/arg4::hisG</i>	Wilson et al., 1999
<b>DAY185</b>	DAY286	<i>ura3::λimm434/ura3::λimm434 pHIS1::his1::hisG/his1::hisG ARG4::URA3::arg4::hisG/arg4::hisG</i>	Davis et al., 2000
<b>DAY415</b>	BWP17	<i>ura3::λimm434/ura3::λimm434 his1::hisG/his1::hisG arg4::hisG/arg4::hisG_mds3::ARG4/MDS3</i>	Zacchi et al., 2010
<b>DAY938</b>	BWP17	<i>ura3::λimm434/ura3::λimm434 his1::hisG/his1::hisG arg4::hisG/arg4::hisG_mds3::ARG4/mds3::URA3dpl200</i>	Zacchi et al., 2010a
<b>DAY956</b>	BWP17	<i>ura3::λimm434/ura3::λimm434 his1::hisG/his1::hisG arg4::hisG/arg4::hisG_mds3::ARG4/mds3::dpl200</i>	Zacchi et al., 2010a
<b>DAY1118</b>	DAY938	<i>ura3::λimm434/ura3::λimm434 HIS1::his1::hisG / his1::hisG arg4::hisG/ arg4::hisG_mds3::ARG4/mds3::URA3-dpl200</i>	Zacchi et al., 2010a
<b>DAY1119</b>	DAY938	<i>ura3::λimm434/ura3::λimm434 HIS1::MDS3::his1::hisG/ his1::hisG arg4::hisG/ arg4::hisG_mds3::ARG4/mds3::URA3-dpl200</i>	Zacchi et al., 2010a
<b>DAY1109 (CDH107)</b>	CAI4	<i>ura3/ura3 ras1::hisG-URA3-hisG/ras1::hisG</i>	Leberer et al., 2001.
<b>DAY972 (CM20)</b>	RM1000	<i>ura3::λimm434/ura3::λimm434 his1::hisG/ his1::hisG sit4::HIS1/sit4::dpl200</i>	Lee et al., 2004.
<b>LUZ599</b>	DAY972	<i>ura3::λimm434/ura3::λimm434 his1::hisG/ his1::hisG sit4::HIS1/sit4::dpl200 RAS1/ras1::ura3-dpl200</i>	This study
<b>LUZ602</b>	LUZ599	<i>ura3::λimm434/ura3::λimm434 his1::hisG/ his1::hisG sit4::HIS1/sit4::dpl200 RAS1/ras1::dpl200</i>	This study
<b>LUZ613</b>	LUZ602	<i>ura3::λimm434/ura3::λimm434 his1::hisG/ his1::hisG sit4::HIS1/sit4::dpl200 ras1::ura3-dpl200/ras1::dpl200</i>	This study
<b>LUZ616</b>	DAY1233	<i>ura3::λimm434/ura3::λimm434 his1::hisG/his1::hisG sit4::HIS1/sit4::dpl200 mds3::dpl200/mds3::dpl200</i>	This study
<b>LUZ622</b>	LUZ616	<i>ura3::λimm434/ura3::λimm434 his1::hisG/his1::hisG sit4::HIS1/sit4::dpl200 MDS3::URA3::mds3::dpl200/mds3::dpl200</i>	This study
<b>LUZ640</b>	DAY415	<i>ura3::λimm434/ura3::λimm434 his1::hisG/his1::hisG arg4::hisG/arg4::hisG_mds3::ARG4/MDS3 RAS1/ras1::URA3-dpl200</i>	This study
<b>LUZ651</b>	LUZ640	<i>ura3::λimm434/ura3::λimm434 his1::hisG/his1::hisG arg4::hisG/arg4::hisG_mds3::ARG4/MDS3 RAS1/ras1::dpl200</i>	This study
<b>LUZ682</b>	LUZ651	<i>ura3::λimm434/ura3::λimm434 his1::hisG/his1::hisG arg4::hisG/arg4::hisG_mds3::ARG4/mds3::URA3-dpl200 RAS1/ras1::dpl200</i>	This study
<b>LUZ692</b>	LUZ682	<i>ura3::λimm434/ura3::λimm434 his1::hisG/his1::hisG arg4::hisG/arg4::hisG_mds3::ARG4/mds3::dpl200 RAS1/ras1::dpl200</i>	This study
<b>LUZ684</b>	DAY956	<i>ura3::λimm434/ura3::λimm434 his1::hisG/his1::hisG arg4::hisG/arg4::hisG_mds3::ARG4/mds3::dpl200 RAS1/RAS1::RAS1::URA3</i>	This study
<b>LUZ686</b>	DAY956	<i>ura3::λimm434/ura3::λimm434 his1::hisG/his1::hisG arg4::hisG/arg4::hisG_mds3::ARG4/mds3::dpl200 RAS1/RAS1::RAS1<sup>G13V</sup>::URA3</i>	This study
<b>LUZ688</b>	DAY972	<i>ura3::λimm434/ura3::λimm434 his1::hisG/his1::hisG sit4::HIS1/sit4::dpl200 RAS1/RAS1::RAS1::URA3</i>	This study
<b>LUZ690</b>	DAY972	<i>ura3::λimm434/ura3::λimm434 his1::hisG/his1::hisG sit4::HIS1/sit4::dpl200 RAS1/RAS1::RAS1<sup>G13V</sup>::URA3</i>	This study
<b>LUZ756</b>	DAY1	<i>ura3::λimm434/ura3::λimm434 his1::hisG/his1::hisG arg4::hisG/arg4::hisG RAS1/RAS1::RAS1::URA3</i>	This study
<b>LUZ755</b>	DAY1	<i>ura3::λimm434/ura3::λimm434 his1::hisG/his1::hisG arg4::hisG/arg4::hisG RAS1/RAS1::RAS1<sup>G13V</sup>::URA3</i>	This study
<b>DAY1224 (CJN6)</b>	BWP17	<i>ura3::λimm434/ura3::λimm434 SCH9::HIS1::his1::hisG/his1::hisG arg4::hisG/arg4::hisG sch9::Tn7::UAU1/sch9::Tn7::URA3</i>	Nobile et al., 2003

<b>DAY1226</b> (GKO782)	BWP17	<i>ura3::λimm434/ura3::λimm434 his1::hisG/his1::hisG</i>	Davis et al., 2002
<b>DAY1227</b> (CDH108)	CAI4	<i>arg4::hisG/arg4::hisG sch9::Tn7::UAU1/sch9::Tn7::URA3</i>	Leberer et al., 2001
<b>DAY1228</b> (CDH110)	CAI4	<i>ura3Δ/Δ ras1Δ::hisG/ras1Δ::hisG pVEC [RAS1]</i>	Leberer et al., 2001
<b>DAY1233</b>	DAY972	<i>ura3::λimm434/ura3::λimm434 his1::hisG/his1::hisG</i>	Zacchi et al., 2010a
<b>DAY1305</b> (HPY300U)	SC5314	<i>sit4::HIS1/sit4::dpl200 mds3::URA3-dpl200/mds3::dpl200</i>	Parker et al., 2004
<b>DAY1307</b> (HPY400U)	SC5314	<i>tpk1Δ::hisG/tpk1Δ::hisG ura3Δ/ura3::URA3</i>	Parker et al., 2004
<b>DAY1309</b> (LDR8)	CAI4	<i>tpk2Δ::hisG/tpk2Δ::hisG ura3Δ/ura3::URA3</i>	Maidan et al., 2005
<b>DAY1311</b> (NM6)	CAI4	<i>ura3Δ/Δ grp1Δ::hisG/gpr1Δ::hisG-URA3-hisG</i>	Maidan et al., 2005
<b>DAY1314</b> (CK43B-16)	CAI4	<i>ura3Δ/Δ gpa2Δ::hisG/gpa2Δ::hisG-URA3-hisG</i>	Csank et al., 1998
<b>DAY1316</b> (CDH22)	CAI4	<i>ura3Δ/Δ cek1Δ::hisG/cek1Δ::hisG-URA3-hisG</i>	Leberer et al., 1996
<b>DAY1317</b> (CDH9)	CAI4	<i>ura3Δ/Δ cst20Δ::hisG/cst20Δ::hisG-URA3-hisG</i>	Leberer et al., 1996
<b>DAY1318</b> (CDH72)	CAI4	<i>ura3Δ/Δ hst7Δ::hisG/hst7Δ::hisG-URA3-hisG</i>	Leberer et al., 1996
<b>DAY1319</b> (CR216)	CAI4	<i>ura3Δ/Δ cph1Δ::hisG/cph1Δ::hisG-URA3-hisG</i>	Harcus et al., 2004
<b>DAY1326</b> (BMY15)	BWP17	<i>ura3::λimm434/ura3::λimm434 his1::hisG/his1::hisG</i>	Enloe et al., 2000
<b>L40</b>	<i>S. cerevisiae</i>	<i>arg4::hisG/arg4::hisG cdc25::Tn7::URA3/cdc25::Tn7::UAU1</i> <i>MATa, his3Δ200, trp1-901, leu2-3, 112, ade2, LYS2::(lexAop)<sub>4</sub>-HIS3,</i> <i>URA3::(lexAop)<sub>8</sub>-lacZ, GAL4</i>	Vojtek et al., 1993.

**Table 5.2.** Plasmids used in this study

Plasmid	Description	Reference
pDDB57	<i>URA3-dpl200</i> cassette for gene disruption	
pDDB78	<i>HIS1</i> vector	
pDDB295	<i>ARG4-URA3</i> vector	
pLZ169	<i>MDS3</i> in pDDB76 complementation vector	This study
pLZ172	<i>RAS1</i> in pDDB76	This study
pLZ173	<i>RAS1<sup>G13V</sup></i> in pDDB76	This study

**Table 5.3.** Primers used in this study

<b>Primer</b>	<b>Sequence</b>	<b>Reference</b>
<b>MDS3 5DR</b>	TCTTAAGGCACAAGTTATTGGCTTGACGTAGAAAGTTTGCA AAGATTTTCACAATATCATGTTTCCCAGTCACGACGTT	Davis et al., 2002
<b>MDS3 3DR</b>	ACCAATATAACGTGAATATACACCCCTATATTATTATCTTT TAATCCTGTAAACAATCCGTGGAATTGTGAGCGGATA	Davis et al., 2002
<b>MDS3null 5-detect</b>	GTGTCCCAATTTTGTCTAGC	This study
<b>MDS3null 3-detect</b>	TGCGGAAGAACTGTAAACCC	This study
<b>RAS1 5DR</b>	CAAAAAATCAAAAAGAAACCCCGGGCAAACACAAATTC ATATCCACACATATACATACCTTTCCCAGTCACGACGTT	This study
<b>RAS1 3DR</b>	AACAATCAATTGGATAGTAAATAGATAGATAAAAAATACG AGAACTTTTTAGTTAGCTCAGTGAATTGTGAGCGGATA	This study
<b>RAS1 5' detect</b>	TGATTAATTGGACATTGACC	This study
<b>RAS1 3' detect</b>	TGAATTGTTTCATCTTCTCCC	This study
<b>RAS1 5' seq</b>	AATCCCTCCCTAACCCAGC	This study
<b>RAS1 5'seq-2</b>	CAAGATGGATTAGCATTGGC	This study
<b>URA3 internal detect</b>	GTATGGGGTTGTTGCTCAGG	This study
<b>RAS1 5' comp</b>	AAGCTCGGAATTAACCCTCACTAAAGGGAACAAAAGCTGG TATGTATCATTGCCACACAC	This study
<b>RAS1 3' comp</b>	ACGACGGCCAGTGAATTGTAATACGACTCACTATAGGGCG AATGGAACAACCTGGTGGTGG	This study
<b>RAS1G13V 5'</b>	GTTGTTGGAGGTGTTGGTGTGGTAAATCCG	This study
<b>RAS1G13V 3' 3'detect</b>	CGGATTTACCAACACCAACACCTCCAACAAC TGTGGAATTGTGAGCGGATAACAATTCAC	This study
<b>RAS1 3' out</b>	ACTATATCAGCTCAACCTCG	This study
<b>MDS3 NruI Seq</b>	TTATGATGAGATTGCCATGC	This study
<b>LAP3 5'</b>	ACGAAATCAACCCAATCTCC	This study
<b>LAP3 3'</b>	ACCATCATTAACCTGGGTTGC	This study
<b>PRC2 5'</b>	TTGGCATTAGAGTTGGGTCC	This study
<b>PRC2 3'</b>	CAAATCACCTGTGTCTGGAG	This study
<b>RPS26A 5'</b>	CAAGAAAAGGTAGAGGTCACG	Zacchi et al., 2010a
<b>RPS26A 3'</b>	TTTAGCAGCATCTTGTGGAG	Zacchi et al., 2010a
<b>GDH1 5'</b>	TTGGCCAGATACATTGGTCC	This study
<b>GDH1 3'</b>	TCACCTGGTCAAACATGGC	This study
<b>GAP2 5'</b>	TTATTGTACAGTTATGTCCC	Zacchi et al., 2010a
<b>GAP2 3'</b>	CCAGCGAAAGCAAAGGCAGC	Zacchi et al., 2010a
<b>CDC19 5' a</b>	CTTCAATGTTGAAACTGTTCC	Zacchi et al., 2010a
<b>CDC19 3' b</b>	AACAGTGTTAGAGTGACCAG	Zacchi et al., 2010a
<b>TEF1-5'</b>	ATAGTCATAATCAATCATGGGT	Davis et al., 2000
<b>TEF1-3'</b>	CTTACATAATATTCAACTAGC	Davis et al., 2000

## **CHAPTER 6**

### **CONCLUDING REMARKS**

*Candida albicans*, one of the most frequent fungal pathogens for humans, is an obligate commensal yeast that colonizes highly diverse anatomical locations in the human body (Calderone, 2002). *C. albicans* appears to reproduce clonally, with a low mating frequency and a non-meiotic, parasexual cycle (Heitman, 2006; Johnson, 2003). Thus, *C. albicans* requires additional mechanisms to those involved in its reproduction in order to generate the variation it needs to survive a constantly changing environment. It has been proposed that *C. albicans* can achieve phenotypic variation through a process called colony morphology phenotypic switching (CMPS) (Soll, 1992). CMPS is the stochastic, low frequency emergence of colonies that have a heritable, but reversible alteration in morphology (Slutsky et al., 1985). CMPS has been associated with *C. albicans* commensal and pathogenic lifestyles (Soll, 1992). Genetically similar, but not identical *C. albicans* commensal strains were isolated from different anatomical locations in humans, and these genetic differences, presumably involved in niche specialization, were suggested to be an output of CMPS (Soll, 1992; Soll et al., 1991; Scherer and Stephens, 1988). Similarly, morphologically variant, but genetically similar colonies can be isolated from sites of infection in humans, and they usually display altered expression of virulence traits (Soll et al., 1988, 1989; Jones et al., 1994; Vargas et al., 2000, 2004). CMPS generates phenotypic diversity in *C. albicans* and is thus important to ensure the survival of this fungus in the host.

### **The regulation of CMPS**

CMPS was originally defined as a stochastic process (Slutsky et al., 1985; Soll, 1992). Here, I show that CMPS in *C. albicans* is not stochastic. In fact, CMPS is regulated by environmental cues such as glucose starvation, amino acids, and alkaline pH, and is under the control of two major signal transduction pathways: the Ras/cAMP and the TOR pathways (Figure 6.1, Chapters 4, 5). Both pathways regulate cellular growth in response to environmental nutrients, and control several critical processes including protein synthesis, protein degradation,

and carbohydrate metabolism (Wullschleger et al., 2006; Thevelein and de Winde, 1999). Through a combination of bioinformatic, biochemical, and genetic approaches, we determined that the negative regulator of CMPS, Mds3, was a member of the TOR pathway, and obtained evidence that Mds3 is also a member of the Ras/cAMP pathways in *C. albicans* (Chapters 3, 5; Zacchi et al., 2010a; Benni and Neigeborn, 1997; McDonald et al., 2009). Based on this information, I was able to identify the upstream Ras/cAMP members Cdc25, Ras1, and Cdc35 and the downstream TOR effector Sch9 as additional negative regulators of CMPS (Chapter 5; Zacchi et al., 2010a; Benni and Neigeborn, 1997; McDonald et al., 2009). Further, the TOR downstream effector Sit4, which is required for TOR-dependent induction of starvation responses (Duvet and Broach, 2004), appears to be required for CMPS induction during glucose starvation (Chapter 5). Even though the TOR pathway has traditionally been associated with the response to nitrogen sources, the fact that Sit4 function is effected by carbon sources had been previously shown (Di Como and Arndt, 1996). Thus, the data presented here supports the conclusion that CMPS in *C. albicans* is a process regulated by distinct environmental cues and by the TOR and Ras signal transduction pathways.

The TOR and Ras/cAMP pathways are associated with morphogenetic processes and phenotypic variation in very different organisms. For example, cAMP and the TOR pathway are involved in phenotypic variation in metazoans, and cAMP is also associated with morphogenesis, virulence, and phenotypic variation in diverse microbes (Mennon and Manning, 2009; Bjornsti and Houghton, 2004; Prasad et al., 2003; Taddei et al., 1995; Weeks, 2000; Fuchs et al., 2010; Horinouchi et al., 2001; Janion et al., 2002). In *C. albicans*, these pathways regulate white-opaque switching, the yeast-hyphal transition, and chlamyospore formation (Huang et al., 2010; Cutler et al., 2001; Bastidas et al., 2009; Zacchi et al., 2010a; Lee et al., 2004; Nobile et al., 2003; Biswas et al., 2007). Therefore, signal transduction pathways (or second messengers, cAMP) that are involved in phenotypic variation in diverse organisms also regulate CMPS in *C. albicans*.

This suggests that there is certain level of conservation in the networks that regulate phenotypic variation throughout evolution that is maintained among distantly related organisms.

### **The mechanisms of CMPS: lessons from the mutants**

One common characteristic of the *mds3Δ/Δ*, *cdc25-/-*, *ras1Δ/Δ*, and *sch9-/-* *C. albicans* mutants is that they all manifest CMPS by producing papilli on their colony surface after prolonged incubation (Chapters 4, 5). But how does papilli form in these mutants? One possibility is that the absence of the Ras and TOR pathways components Mds3, Cdc25, Ras1, or Sch9 leads to defects in signal transduction. Defects in the Ras and/or TOR pathways cause defective stress responses and lead to increased DNA damage and genomic instability. This generates mutations and genomic rearrangements which may accumulate during stationary phase (Figure 6.1) (Madia et al., 2009; Lee et al., 2001; Searle and Sanchez, 2004; Searle et al, 2004; Douville et al., 2004; Yarosh et al., 2000; Budanov and Karin, 2008). The accumulation of genetic (and epigenetic) alterations would then allow for the release from stationary phase cell-growth controlling signals and, thus, overgrowth with the consequent formation of papilli that contain phenotypic variants. In sum, I propose a model in which the phenotypic switch in *C. albicans* is caused by the progressive acquisition of random genetic/epigenetic alterations, especially during stationary phase growth, due to inappropriate responses to environmental, nutritional, and stress signals (Figure 6.1).

The model I propose for CMPS is similar to the bacterial mechanisms for phenotypic variation called stationary-phase mutation and stress-induced mutagenesis (Rosenberg, 2001; Galhardo et al., 2007; Foster, 2007). Stress-induced mutagenesis is a process in which mutations accumulate in a population of cells that are growth-limited and under stress, for example due to nutrient limitation, and which eventually may lead to growth-control escape (McKenzie et al., 2000). Further, in non-growing bacterial populations, the induction of the SOS response, which

prevents the accumulation of DNA damage, is cAMP dependent, which further links the cAMP pathway with phenotypic switching (Taddei et al., 1995). In agreement with this idea, the TOR pathway, including Sch9, and the Ras/cAMP pathway are also involved in the regulation of DNA damage responses in eukaryotes (Chapter 5; Madia et al., 2009; Lee et al., 2001; Searle and Sanchez, 2004; Searle et al, 2004; Douville et al., 2004; Yarosh et al., 2000; Budanov and Karin, 2008). Our model also contributes to explain why CMPS in *C. albicans* is observed after exposure to UV light, a potent inducer of DNA damage (Slutsky et al., 1985; Pomes et al., 1985). The CMPS model proposed here has an intriguing resemblance to the stepwise acquisition of mutations that are hallmarks of cancer in mammals (Hanahan and Weinberg, 2000), and poses the (perhaps naïve) question if CMPS formation in *C. albicans* could eventually become a model to study tumor formation and progression.

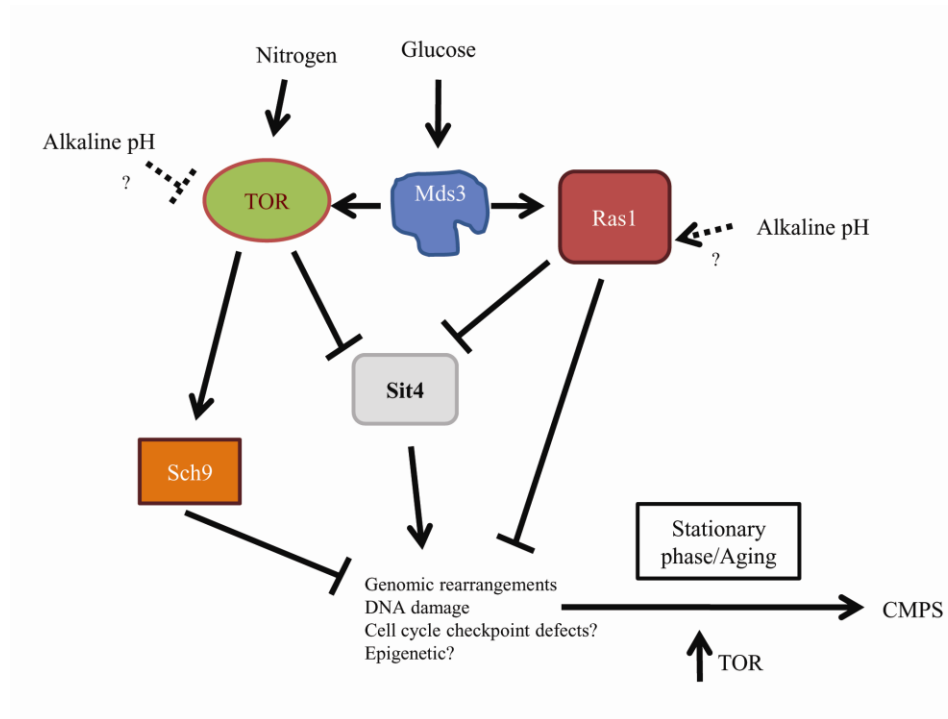


**Figure 6.1:** Model of CMPS regulation in *C. albicans*

Due to the apparently unpredictable nature of the transcriptional and genetic events that cause CMPS in *C. albicans*, each switched isolate displays a different array of phenotypes. Switched *mds3Δ/Δ* strains vary in their colony morphology, in their antifungal drug sensitivity, and in their ability to secrete proteinases or adhere to cells (our unpublished results). However, despite this inherent noise in the system of study, there appear to be two common responses that unify the switched strains: the increased susceptibility to rapamycin and to DNA damaging agents (Chapter 4). An increased susceptibility to rapamycin suggests an increased dependence on TOR function and points to an alteration in the function of this pathway. The increased sensitivity to DNA damage agents in the switched strains could also be associated with the defects in the TOR and Ras signal transduction pathways, and supports the model in which the accumulation of DNA damage contributes to the switch. However, we must keep in mind that an increased sensitivity to rapamycin or DNA damage may also be an output of the switch, not an indication of the cause. Thus, a better understanding of the interaction between the TOR and Ras pathways in *C. albicans*, and of the pathways and mechanisms controlling DNA damage responses and genomic instability in this organism should shed light on the mechanisms of the switch.

### **What is the role of CMPS in *C. albicans*?**

One classical example that illustrates the importance of phenotypic variation is the ability of different pathogens to evade the immune system by altering the expression of their surface antigens. This property is shared by highly diverse microorganisms, including the protozoan *Trypanosoma brucei*, the fungus *Pneumocystis carinii*, the bacteria *Neisseria gonorrhoea*, and the virus HIV (Morrison et al, 2009; Borst, 2002; Stringer, 2007; Klenerman et al., 2002; Mumford et al., 2007; Hills and Davies et al., 2009). Organisms able to maintain a low frequency of phenotypic variation in their population have higher chances of survival after unpredicted environmental changes (Avery et al., 2006; Dubnau and Losick, 2006; Zieg et al., 1977; Moxon

et al., 1994; Acar et al., 2008). In bacterial population genetics, this phenomenon is called bet-hedging (Veening et al., 2008). In the case of *C. albicans*, phenotypic variation likely has additional functions than being an adaptive bet-hedging strategy against potential environmental challenges, as previously suggested (Soll, 2002). There are at least two reasons for this. First, *C. albicans* is an obligate commensal of humans and has evolved remarkably efficient signal transduction pathways that allow it to respond to constantly changing microenvironments (Bahn et al., 2007; Biswas et al., 2007; Davis, 2009). Second, neither during the commensal state nor during infection have the morphologically switched variants ever been the isolated majority, indicating that they do not overtake a *C. albicans* population (Odds, 1997; Jones et al., 1994; Vargas et al., 2000; Soll et al., 1987, 1988, 1989). An exception to this argument is the acquisition of antifungal drug resistance, but in this case there is a very clear selective pressure for the variant phenotype. Therefore, CMPS in *C. albicans* is likely a way to generate *in situ* diversity with altruistic characteristics, and/or a mechanism to accelerate evolution in a clonal population, a concept related to stress-induced mutagenesis in bacteria (Rosenberg, 2001, Galhardo et al., 2007; Foster, 2007).

One possible role of CMPS in *C. albicans* is the generation of variants with an altruistic or cooperative role, a phenomenon observed in other organisms including bacteria, slime mold, and yeast (Boyd and Richerson, 1980; Ackermann et al., 2008; Smukalla et al., 2008; Brown and Buckling, 2008; Gardner and Kumerli, 2008, Diggle et al., 2007). For example, *Salmonella typhimurium* can induce an inflammatory response in the gut to eliminate competing microflora by having a few individuals upregulate the expression of specific virulence factors (Ackermann et al., 2008). *C. albicans* phenotypic variants may grow to form “micropopulations” within a colonized surface/tissue, whose function is to provide the community with a survival advantage. For example, the ability of certain “micropopulations” to secrete more hydrolytic enzymes might allow for enhanced tissue invasion. Further, variants may arise which are able to produce

different levels of quorum sensing signals or biofilm matrix, that can divide faster, that can interact with bacteria differently, that can induce or repress a particular immune response, that can adhere better to surfaces, and/or that can scavenge nutrients more efficiently. For instance, opaque *C. albicans* cells induce biofilm formation in white cells through pheromone signaling (Daniels et al., 2006). Biofilm formation is advantageous for *C. albicans* because it increases resistance to antifungal drugs and constitutes a source of inoculums to facilitate dissemination, colonization, and infection (d'Enfert et al., 2006; Hawser and Douglas, 1995). In other words, *C. albicans* variants may arise due to its altruistic, cooperative function in the community. If the variations are not detrimental, they are maintained in the population and may eventually contribute to the evolution of the pathogen (see below).

Alternatively, CMPS might be a mechanism to accelerate adaptation (Rosenberg et al., 2001). In this situation, acceleration of evolution could only happen in a restricted number of individuals, which would enter a high frequency switching mode compared to the rest of the population. This idea is supported by the fact that most of the switched strains that have been isolated *in vivo* are in a high frequency switching mode (Soll et al., 1987; Vargas et al., 2000). These “switchers” would generate random variability that may get fixed in the population. However, under a “switcher” condition, the fixation of the variation can only occur if it is successfully transferred to a non-switcher strain (Elena and Lenski, 2003). This might happen in *C. albicans* through mating, followed by a parasexual cycle (Forche et al., 2008). It would be interesting to determine if the strains that are in high CMPS frequency mode are also in a “high frequency mating” mode, similar to the WO-1 strain (Slutsky et al., 1987; Miller et al., 2002). Although mating in *C. albicans* was thought to inevitably require mating type locus homozygosis, it has recently been shown that it can happen in strains with a heterozygous mating locus (Alby and Bennett, 2009; Pendrak et al., 2004; Lohse and Johnson, 2009). This indicates that alternative means exist to induce *C. albicans* to mate, many of them unexplored, such as epigenetic silencing

of the mating locus, and CMPS or the mechanisms that lead to CMPS might be some of them. Alternatively, the formation of “switchers” might be transient and environmentally regulated (Giraud et al., 2001; Aersten and Michiels, 2005). Formation of “switchers” strains *in vivo* has been reported in other systems (Giraud et al., 2002; Oliver et al., 2000). Therefore, I propose that the primordial role of CMPS and other mechanisms to generate variation in *C. albicans* is to generate *in situ* phenotypic variation and/or to accelerate evolution (with the consequent generation of strains pre-adapted to future environmental challenges as a by-product).

### **CMPS in the host**

Much remains to be learned about the role and mechanisms of CMPS in *C. albicans* commensal/opportunistic pathogen lifestyle. For instance, although CMPS has been shown to occur *in vivo*, the factors that trigger CMPS and the frequency at which it happens is not known. Colonies with an altered morphology have been found more frequently during infections than during a commensal state, which suggest that there is a selective advantage for the formation or persistence of phenotypic variants during infection. Given the often significant increase in population size associated with an infection, it is possible that CMPS is a population-density dependent effect associated with, for example, quorum sensing (D.D.; Forche et al., 2009; Dutton and Penn, 1989; Soll et al., 1988, 2002; Kruppa et al., 2009). Further, it is important to keep in mind that not all phenotypic variation will lead to alterations in colony morphology, as demonstrated by ours and others results (Chapter 4; Anderson and Odds, 1985). Thus, by simply monitoring colony morphology we are likely underestimating the actual level of phenotypic variation in the *C. albicans* population. This indicates that, despite the available data, we still do not have a clear picture of the levels of phenotypic variation of *C. albicans in vivo*, nor of the effects of this variation on *C. albicans* survival in the host.

How could CMPS be triggered in the host? While in the host, *C. albicans* is subject to many different stress signals and to nutrient limitation. One possibility to explain CMPS involves a combination of environmental stress with transcriptional noise (Freed et al., 2008, Sriram et al., 2009). The transcriptional noise may affect the expression of a key CMPS regulator. This idea implies the existence of a master CMPS regulatory locus, similar to the *Wor1* regulation of the white-opaque phenotypic switching in *C. albicans* (Zordan et al., 2006, 2007; Lohse and Johnson, 2009). In other words, CMPS might be the consequence of the bi-stable formation of “switchers”. Alternatively, transcriptional noise may affect the expression of a member or a common downstream effector of the TOR and Ras pathways, and would induce a transient defect in TOR or Ras signaling causing the formation of phenotypic variants. A second possibility is that members or effectors of the TOR or Ras pathways can be reversibly functionally limited (e.g. by sequestration in subcellular compartments), leading to a transient “switcher” state. One example of such mechanism leading to increased mutation rates is the functional limitation of the DNA mismatch repair system in bacteria (Galhardo et al., 2007). The advantage of transcriptional noise coupled to an epigenetic regulatory feedback circuit or to the functional limitation of specific effectors is that the change from non-“switcher” to “switcher” would be reversible.

Another possibility to explain CMPS regulation is that stress and nutrient limitation may increase the chances that a specific but reversible mutation occurs in one of the members of the TOR or Ras pathways. This system is similar to the formation of wrinkly colonies in *S. cerevisiae* due to expression of *FLO10* that is caused by the mutagenic inactivation of the upstream Ras pathway members *IRA1* and *IRA2* (Halme et al., 2004). Intriguingly, these mutations in *IRA1* and *IRA2* appear to happen at a higher frequency than random mutation (Halme et al., 2004). If *C. albicans* had a similar mechanism, the “switcher” effect would not be transient and the “switcher” would remain locked in that state, unless, for example, a system similar to phase variation in bacteria existed that would ensure the reversibility of the switcher phenotype.

Finally, it is possible that CMPS in *C. albicans* is linked to the age of the cell. Aging is associated with genomic instability and DNA damage, and is regulated by signal transduction pathways including TOR, Sch9, and Ras (Bitterman et al., 2003; Wei et al., 2008). Thus, aged cells might be the source of CMPS *in vivo*. This idea is supported by the result that alkaline pH, which in *S. cerevisiae* inhibits age-dependent cell death, can also inhibit papilli formation in the *mds3Δ/Δ*, *ras1Δ/Δ*, and *sch9-/-* *C. albicans* mutants (Chapters 4, 5; Fabrizio et al., 2004). One way to test this would be by preventing *mds3Δ/Δ* cells from entering the aging program either by genetic or environmental mechanisms, and determining whether the *mds3Δ/Δ* colonies still form papilli. Another possibility that is directly related with the idea of aging is that papilli formation could be associated with the adaptive re-growth phenomenon observed in *S. cerevisiae*. During adaptive re-growth, a small subpopulation of cells can grow by utilizing nutrients released by the bulk of a population dying from starvation (Longo et al., 2005; Fabrizio et al., 2004). This idea is supported by my results that switched strains have increased sensitivity to oxidative agents (Chapter 4), which is a condition that enhances adaptive re-growth frequency in *S. cerevisiae* (Fabrizio et al., 2004). Further, adaptive re-growth is associated with an increased mutation rate, which is in agreement with my model of CMPS formation (see above). It would be interesting to compare the mutation rates of the *mds3Δ/Δ* mutant with the wild-type during logarithmic and stationary growth phase, and during glucose limitation and growth at acidic vs. alkaline pH (which are environmental conditions that affect CMPS rates (Chapter 4, 5)).

Thus, there are multiple possibilities that may account for the occurrence of CMPS in the host, and I have only mentioned here a few of them. A deeper understanding of the mechanisms that lead to CMPS *in vitro*, together with a more careful study of the frequency of CMPS *in vivo*, of the phenotypes of the switched strains, of the environments from where the switched strains were isolated, and of the genetic alterations associated with the switch will certainly shed light on the biological role of this phenomenon in *C. albicans*. In particular, dissecting the genetic and

genomic alterations associated with the switch –through a combination of deep-sequencing, comparative genomic hybridization, loss of heterozygosity assays, flow cytometry, and contour-clamped homogeneous electric field electrophoresis- might show common mutations or genomic aberrations that are associated with the phenotypic switch itself, or with particular phenotypic variants.

### **The importance of being Mds3**

The data I present here indicates that Mds3 plays an important role in the regulation of both the Ras and TOR pathways (Figure 6.1). But what is the function of Mds3 on these pathways? In the Ras pathway, Mds3 appears to function as an upstream positive regulator of Ras. First, mutants in *MDS3*, *CDC25*, and *RAS1* share similar phenotypes, both in *C. albicans* and in *S. cerevisiae* (Chapter 5, McDonald et al., 2009). Second, the *RAS1*<sup>V13</sup> and *RAS2*<sup>V17</sup> alleles can rescue *mds3Δ/Δ* phenotypes in *C. albicans* and *S. cerevisiae*, respectively (Chapter 5, Benni and Neigeborn, 1997). Third, Mds3 and Cdc25 physically interact in *S. cerevisiae* (Krogan et al., 2006; Tonikian et al., 2009; Gavin et al., 2006; Collins et al., 2007). Thus, Mds3 appears to function as a positive upstream regulator of Ras1, possibly effecting Cdc25 function/localization. It would be interesting to determine whether Mds3 and Cdc25 also interact in *C. albicans*, what genetic and environmental factors effect this interaction, and what role Mds3 plays on Cdc25 function.

The role of Mds3 on the TOR pathway appears to be more difficult to dissect. Our initial studies suggested that Mds3 acts as a negative regulator of TOR function (Chapter 3). However, subsequent analysis indicated that Mds3 could also function on the TOR pathway as a positive regulator (Chapter 5). For example, the *mds3Δ/Δ* mutant appears to induce starvation responses more rapidly than the wild-type strain (Chapter 5), implying that the TOR pathway is more readily inactivated in the absence of Mds3. Further, the *mds3Δ/Δ* mutant appears to survive

longer during starvation conditions than the wild-type strain (data not shown), a phenomenon associated with the downregulation of growth activating pathways like TOR and Ras. In fact, TOR downregulation in worms, flies, and mammals leads to life span extension; and the *tor1Δ/Δ*, *ras2Δ/Δ*, and *sch9Δ/Δ* *S. cerevisiae* mutants show extended life spans compared to the wild-type strain (Fabrizio et al., 2001; Longo, 1999; Bonawitz et al., 2007; Wei et al., 2008; Kapahi et al., 2004; Harrison et al., 2009; Hansen et al., 2007). Together, these results do not support a model in which Mds3 functions as a negative regulator of TOR. Rather, Mds3 might function as a modulator, acting positively or negatively on the pathway according to specific environmental cues. Such a dual-function protein, Raptor, has already been described for the mTOR pathway in mammals (Kim et al., 2002, 2003). The homolog of Raptor in *S. cerevisiae* and *C. albicans* is Kog1. Kog1 interaction with TOR is not effected by nutrients, suggesting that alternative factors, such as Mds3, might fulfill this role in these fungi (Loewith et al., 2002). Further, a model in which loss of *MDS3* leads to reduced TOR signaling is in agreement with the effect of loss of *SCH9*, the downstream TOR effector, on papilli formation. Alternatively, our results might also be explained if the increased starvation responses observed in the *mds3Δ/Δ* mutant are mediated by a reduced function of the Ras pathway, while the TOR pathway remains overactive. The effect of the *sch9Δ/Δ* mutant on papilli might then be explained by a feedback regulatory loop that causes TOR hyperactivation, already observed in *S. cerevisiae* (Lempiainen et al., 2009). However, in the simpler model Mds3 would act as a positive regulator of TOR during stationary phase (Figure 6.1).

The studies presented here suggest that there is a crosstalk between the TOR and Ras pathways in *C. albicans*, in which the TOR downstream effector Sit4 is also a downstream effector of Ras1 (Figure 6.1, Chapter 5). This arrangement is more similar to the mammalian Ras and mTOR pathways than to the *S. cerevisiae* Ras and TOR pathways (Schmelzle et al., 2004; Zurita-Martinez and Cardenas, 2005; Shaw and Cantley, 2006; Soulard et al., 2010). Regulatory

feedbacks between TOR and other signaling pathways exist in other systems and are critical for fine-tuning the function of these pathways (Carracedo et al., 2008, Kockel et al., 2010). The discovery that Mds3 is a member of the fungal TOR and Ras pathways opened up interesting possibilities of regulatory feedbacks between these networks mediated by Mds3. In fact, the molecular structure and subcellular localization of Mds3 are ideal for a protein that works as a (dual-function) regulator of several signal transduction pathways (Chapter 2). First, Mds3 is a large, modular protein containing only protein-protein interaction domains: a well defined six-bladed Kelch  $\beta$ -propeller at the N-terminus, and a putative BTB/POZ domain at the C-terminus (Chapter 2). Mds3 is separated into a minimum of two modules by the flexible serine-rich bridge located at the middle of the protein. This arrangement suggests that Mds3 is able to alter its conformation in response to posttranslational modifications or upon binding to different targets. By altering its conformation, Mds3 would modify its ability to bind specific substrates (Dyson and Wright, 2005). Further, stringent evolutionary bioinformatics studies predict that Mds3 has a PKA phosphorylation site after the N-terminal Kelch domains (Budovskaya et al., 2005). It is interesting to speculate that PKA phosphorylation might lead to alterations in Mds3's conformation and/or in its binding ability, orchestrating a feedback regulatory loop involving Mds3, Ras/PKA, and the TOR pathway.

Recent studies support the potential Mds3-mediated crosstalk between TOR and Ras. Mds3 and the TORC1 complex member Tco89 were independently pulled down in a high-throughput screen for proteins that interact with the enzyme *FBPI* in *S. cerevisiae*, supporting a possible role of Mds3 as an upstream regulator of TOR and as a member of the TORC complex (Figure 6.1; Brown et al., 2010; Reinke et al., 2004). Further, Bcy1, the regulatory subunit of PKA, is a target of TOR in *S. cerevisiae* (Soulard et al., 2010). Thus, PKA may indirectly affect TOR function by phosphorylating and potentially altering the function of Mds3 (potentially a TORC complex member); while TOR can directly alter PKA function through Bcy1

phosphorylation. In this way, Mds3 would contribute to close the feedback regulatory loop between both pathways. Further, Mds3 interacts with the Sit4 phosphatase, a TOR downstream effector, suggesting that Mds3 is a Sit4 substrate, and providing a second instance for regulatory crosstalk between the TOR and Ras pathways (Zacchi et al. 2010a). Alternatively, Mds3 conformational changes could also affect the ability of Sit4 to bind to different substrates or regulatory proteins, which also provides an instance for regulatory crosstalk between the TOR and the Ras/PKA pathways. Finally, the localization of Mds3 on cytoplasmic spots that resemble endocytic vesicles or membrane microdomains supports a role for Mds3 in the regulation of signaling pathways that converge at these locations, which include both the TOR and Ras pathways (Mitchell, 2008; Hancock, 2003; Zurita-Martinez et al., 2007; Sturgill et al., 2008; Aronova et al., 2007; Slessareva et al., 2006; Puria et al., 2008; Xu et al., 2004; Hancock and Parton, 2005; Tian et al., 2007). Therefore, the modular characteristics and cytoplasmic localization of Mds3 support the model in which this protein functions as a scaffold coordinating several signal transduction pathways and is involved in a crosstalk regulation between them.

It would be interesting to explore this connection further, not only to better understand the complexity of regulatory pathways in eukaryotic organisms, but also because of the critical role these two pathways play in *C. albicans* growth and pathogenesis.

What is the relevance of Mds3 in other systems? All searches for homology to Mds3 returned only proteins from fungal species, indicating that Mds3 appears to be a fungal specific protein. However, the putative Kelch/BTB domain combination in Mds3 is common in mammalian proteins (Prags and Adams, 2003). Thus, although there is no human homolog of Mds3 identified through amino acid sequence identity, the role of this potential Kelch/BTB scaffold might be fulfilled by other yet undiscovered human proteins with similar structures. Indeed, the TOR pathway is highly conserved throughout evolution, and elements from the Ras/cAMP pathways are also conserved in distantly related organisms. Regardless of whether or

not there is a human functional homolog of Mds3, this protein is an interesting target of study as it represents, to the best of my knowledge, the first fungal protein to be associated to the crosstalk regulation of two of the major highly conserved signal transduction pathways in eukaryotes.

For a long time CMPS was known to occur in *C. albicans* both *in vivo* in the human host and *in vitro*. Several mechanisms and environmental signals have been suggested to effect CMPS in this fungus, but it was unclear how they led to the switch. As it often happens in science, our discovery that Mds3 was involved in CMPS was completely serendipitous; but it sparked our interest in understanding the mechanisms that control this phenomenon. I have now found that CMPS in *C. albicans* is regulated by two major signal transduction cascades: the TOR and the Ras pathways. These pathways are also associated with phenotypic variation in many other highly diverse organisms. Mds3 appears to function at the crossroads between these two major growth controlling signal transduction cascades and may be critical in orchestrating a feedback regulatory crosstalk between and/or within these networks. The data collected here allows me to propose a model of CMPS in *C. albicans* that is based on the bacterial stress-induced mutagenesis model. In this model, random phenotypic variation in CMPS is achieved through the stepwise accumulation of genetic (and perhaps epigenetic) alterations during growth under stress and nutrient-limited conditions – which should be easily found by *C. albicans* while thriving in the host- due to defective signaling through the TOR and/or Ras pathways. Therefore, the studies described in this dissertation have begun to uncover the mechanisms of regulation of colony morphology phenotypic switching, a complex phenomenon directly associated with the pathogenesis of one of the most important human pathogens, the fungus *Candida albicans*.

## REFERENCES

- ACKERMANN, MARTIN, STECHER, BÄRBEL, FREED, NIKKI E, SONGHET, PASCAL, HARDT, WOLF-DIETRICH, & DOEBELI, MICHAEL. 2008. Self-destructive cooperation mediated by phenotypic noise. *Nature*, **454**(7207), 987–990.
- ACOSTA-RODRIGUEZ, EVA V, RIVINO, LAURA, GEGINAT, JENS, JARROSSAY, DAVID, GATTORNO, MARCO, LANZAVECCHIA, ANTONIO, SALLUSTO, FEDERICA, & NAPOLITANI, GIORGIO. 2007. Surface phenotype and antigenic specificity of human interleukin 17-producing T helper memory cells. *Nat Immunol*, **8**(6), 639–646.
- ADAMI, ALESSANDRA, GARCÍA-ALVAREZ, BEGOÑA, ARIAS-PALOMO, ERNESTO, BARFORD, DAVID, & LLORCA, OSCAR. 2007. Structure of TOR and its complex with KOG1. *Mol Cell*, **27**(3), 509–516.
- ADAMS, A., GOTSCHLING, D.E., KAISER, C.A., & STEARNS, T. 1997. *Methods in Yeast Genetics*. Cold Spring Harbor Press.
- ADAMS, J., KELSO, R., & COOLEY, L. 2000. The kelch repeat superfamily of proteins: propellers of cell function. *Trends Cell Biol*, **10**(1), 17–24.
- AERTSEN, ABRAM, & MICHIELS, CHRIS W. 2005. Diversify or die: generation of diversity in response to stress. *Crit Rev Microbiol*, **31**(2), 69–78.
- AGUILERA, ANDRÉS, & GÓMEZ-GONZÁLEZ, BELÉN. 2008. Genome instability: a mechanistic view of its causes and consequences. *Nat Rev Genet*, **9**(3), 204–217.
- AHMAD, KAMI, & HENIKOFF, STEVEN. 2002a. Histone H3 variants specify modes of chromatin assembly. *Proc Natl Acad Sci U S A*, **99 Suppl 4**(Dec), 16477–16484.
- AHMAD, KAMI, & HENIKOFF, STEVEN. 2002b. The histone variant H3.3 marks active chromatin by replication-independent nucleosome assembly. *Mol Cell*, **9**(6), 1191–1200.
- ALARCON, C. M., HEITMAN, J., & CARDENAS, M. E. 1999. Protein kinase activity and identification of a toxic effector domain of the target of rapamycin TOR proteins in yeast. *Mol Biol Cell*, **10**(8), 2531–2546.
- ALBY, KEVIN, & BENNETT, RICHARD J. 2009. Stress-induced phenotypic switching in *Candida albicans*. *Mol Biol Cell*, **20**(14), 3178–3191.
- ALBY, KEVIN, SCHAEFER, DANA, & BENNETT, RICHARD J. 2009. Homothallic and heterothallic mating in the opportunistic pathogen *Candida albicans*. *Nature*, **460**(7257), 890–893.
- ALLEGRUCCI, MAGEE, & SAUER, KARIN. 2007. Characterization of colony morphology variants isolated from *Streptococcus pneumoniae* biofilms. *J Bacteriol*, **189**(5), 2030–2038.
- ANDERSON, J., CUNDIFF, L., SCHNARS, B., GAO, M. X., MACKENZIE, I., & SOLL, D. R. 1989. Hypha formation in the white-opaque transition of *Candida albicans*. *Infect Immun*, **57**(2), 458–467.
- ANDERSON, J., MIHALIK, R., & SOLL, D. R. 1990. Ultrastructure and antigenicity of the unique cell wall pimple of the *Candida* opaque phenotype. *J Bacteriol*, **172**(1), 224–235.
- ANDERSON, JAMES B. 2005. Evolution of antifungal-drug resistance: mechanisms and pathogen fitness. *Nat Rev Microbiol*, **3**(7), 547–556.
- ANDERSON, M. L., & ODDS, F. C. 1985. Adherence of *Candida albicans* to vaginal epithelia: significance of morphological form and effect of ketoconazole. *Mykosen*, **28**(11), 531–540.
- ARBOUR, MÉLANIE, EPP, ELIAS, HOGUES, HERVÉ, SELLAM, ADNANE, LACROIX, CELINE, RAUCEO, JASON, MITCHELL, AARON, WHITEWAY, MALCOLM, & NANTEL, ANDRÉ. 2009. Widespread occurrence of chromosomal aneuploidy following the routine production of *Candida albicans* mutants. *FEMS Yeast Res*, **9**(7), 1070–1077.
- ARGIMÓN, SILVIA, WISHART, JILL A, LENG, ROGER, MACASKILL, SUSAN, MAVOR, ABIGAIL, ALEXANDRIS, THOMAS, NICHOLLS, SUSAN, KNIGHT, ANDREW W, ENJALBERT, BRICE, WALMSLEY, RICHARD, ODDS, FRANK C, GOW, NEIL A R, & BROWN, ALISTAIR J P. 2007. Developmental regulation of an adhesin gene during cellular morphogenesis in the fungal pathogen *Candida albicans*. *Eukaryot Cell*, **6**(4), 682–692.

- ARLT, MARTIN F, DURKIN, SANDRA G, RAGLAND, RYAN L, & GLOVER, THOMAS W. 2006. Common fragile sites as targets for chromosome rearrangements. *DNA Repair (Amst)*, **5**(9-10), 1126–1135.
- ARONOVA, SOFIA, WEDAMAN, KAREN, ANDERSON, SCOTT, YATES, JOHN, & POWERS, TED. 2007. Probing the membrane environment of the TOR kinases reveals functional interactions between TORC1, actin, and membrane trafficking in *Saccharomyces cerevisiae*. *Mol Biol Cell*, **18**(8), 2779–2794.
- ASAKURA, K., IWAGUCHI, S., HOMMA, M., SUKAI, T., HIGASHIDE, K., & TANAKA, K. 1991. Electrophoretic karyotypes of clinically isolated yeasts of *Candida albicans* and *C. glabrata*. *J Gen Microbiol*, **137**(11), 2531–2538.
- AU, WEI-CHUN, CRISP, MATTHEW J, DELUCA, STEVEN Z, RANDO, OLIVER J, & BASRAI, MUNIRA A. 2008. Altered dosage and mislocalization of histone H3 and Cse4p lead to chromosome loss in *Saccharomyces cerevisiae*. *Genetics*, **179**(1), 263–275.
- AUSIÓ, J., ABBOTT, D. W., WANG, X., & MOORE, S. C. 2001. Histone variants and histone modifications: a structural perspective. *Biochem Cell Biol*, **79**(6), 693–708.
- AUSIÓ, JUAN. 2006. Histone variants—the structure behind the function. *Brief Funct Genomic Proteomic*, **5**(3), 228–243.
- BAHN, Y. S., & SUNDSTROM, P. 2001. CAPI, an adenylate cyclase-associated protein gene, regulates bud-hypha transitions, filamentous growth, and cyclic AMP levels and is required for virulence of *Candida albicans*. *J Bacteriol*, **183**(10), 3211–3223.
- BAHN, YONG-SUN, XUE, CHAOYANG, IDNURM, ALEXANDER, RUTHERFORD, JULIAN C, HEITMAN, JOSEPH, & CARDENAS, MARIA E. 2007. Sensing the environment: lessons from fungi. *Nat Rev Microbiol*, **5**(1), 57–69.
- BAI, XIAOCHUN, MA, DONGZHU, LIU, ANLING, SHEN, XIAOYUN, WANG, QIMING J, LIU, YONGJIAN, & JIANG, YU. 2007. Rheb activates mTOR by antagonizing its endogenous inhibitor, FKBP38. *Science*, **318**(5852), 977–980.
- BAILLIE, G. S., & DOUGLAS, L. J. 1999. Role of dimorphism in the development of *Candida albicans* biofilms. *J Med Microbiol*, **48**(7), 671–679.
- BALABAN, NATHALIE Q, MERRIN, JACK, CHAIT, REMY, KOWALIK, LUKASZ, & LEIBLER, STANISLAS. 2004. Bacterial persistence as a phenotypic switch. *Science*, **305**(5690), 1622–1625.
- BAMBACH, ADRIENNE, FERNANDES, MARIANA P, GHOSH, ANUP, KRUPPA, MICHAEL, ALEX, DEEPU, LI, DONGMEI, FONZI, WILLIAM A, CHAUHAN, NEERAJ, SUN, NUO, AGRELLOS, ORLANDO A, VERCESI, ANIBAL E, ROLFES, RONDA J, & CALDERONE, RICHARD. 2009. Gho1p of *Candida albicans* localizes to the mitochondria during stress and is required for mitochondrial function and virulence. *Eukaryot Cell*, **8**(11), 1706–1720.
- BARBET, N. C., SCHNEIDER, U., HELLIWELL, S. B., STANSFIELD, I., TUIE, M. F., & HALL, M. N. 1996. TOR controls translation initiation and early G1 progression in yeast. *Mol Biol Cell*, **7**(1), 25–42.
- BARBOUR, A. G., & RESTREPO, B. I. 2000. Antigenic variation in vector-borne pathogens. *Emerg Infect Dis*, **6**(5), 449–457.
- BARCHIESI, F., NAJVAR, L. K., LUTHER, M. F., SCALISE, G., RINALDI, M. G., & GRAYBILL, J. R. 1996. Variation in fluconazole efficacy for *Candida albicans* strains sequentially isolated from oral cavities of patients with AIDS in an experimental murine candidiasis model. *Antimicrob Agents Chemother*, **40**(5), 1317–1320.
- BARRY, J. D., GINGER, M. L., BURTON, P., & MCCULLOCH, R. 2003. Why are parasite contingency genes often associated with telomeres? *Int J Parasitol*, **33**(1), 29–45.
- BARTON, R. C., & GULL, K. 1992. Isolation, characterization, and genetic analysis of monosomic, aneuploid mutants of *Candida albicans*. *Mol Microbiol*, **6**(2), 171–177.
- BARTON, R. C., & SCHERER, S. 1994. Induced chromosome rearrangements and morphologic variation in *Candida albicans*. *J Bacteriol*, **176**(3), 756–763.

- BARUCH, D. I., PASLOSKE, B. L., SINGH, H. B., BI, X., MA, X. C., FELDMAN, M., TARASCHI, T. F., & HOWARD, R. J. 1995. Cloning the *P. falciparum* gene encoding PfEMP1, a malarial variant antigen and adherence receptor on the surface of parasitized human erythrocytes. *Cell*, **82**(1), 77–87.
- BASTIDAS, ROBERT J, & HEITMAN, JOSEPH. 2009. Trimorphic stepping stones pave the way to fungal virulence. *Proc Natl Acad Sci U S A*, Jan.
- BASTIDAS, ROBERT J, REEDY, JENNIFER L, MORALES-JOHANSSON, HELENA, HEITMAN, JOSEPH, & CARDENAS, MARIA E. 2008. Signaling cascades as drug targets in model and pathogenic fungi. *Curr Opin Investig Drugs*, **9**(8), 856–864.
- BASTIDAS, ROBERT J, HEITMAN, JOSEPH, & CARDENAS, MARIA E. 2009. The protein kinase Tor1 regulates adhesin gene expression in *Candida albicans*. *PLoS Pathog*, **5**(2), e1000294.
- BATLLE, MONTSERRAT, LU, AILAN, GREEN, DAVID A, XUE, YONG, & HIRSCH, JEANNE P. 2003. Krh1p and Krh2p act downstream of the Gpa2p G(alpha) subunit to negatively regulate haploid invasive growth. *J Cell Sci*, **116**(Pt 4), 701–710.
- BAUER, JANINE, & WENDLAND, JÜRGEN. 2007. *Candida albicans* Sfl1 suppresses flocculation and filamentation. *Eukaryot Cell*, **6**(10), 1736–1744.
- BAUM, MARY, SANYAL, KAUSTUV, MISHRA, PRASHANT K, THALER, NATHANIEL, & CARBON, JOHN. 2006. Formation of functional centromeric chromatin is specified epigenetically in *Candida albicans*. *Proc Natl Acad Sci U S A*, **103**(40), 14877–14882.
- BAYLISS, C. D., FIELD, D., & MOXON, E. R. 2001. The simple sequence contingency loci of *Haemophilus influenzae* and *Neisseria meningitidis*. *J Clin Invest*, **107**(6), 657–662.
- BECK, T., & HALL, M. N. 1999. The TOR signalling pathway controls nuclear localization of nutrient-regulated transcription factors. *Nature*, **402**(6762), 689–692.
- BECK, T., SCHMIDT, A., & HALL, M. N. 1999. Starvation induces vacuolar targeting and degradation of the tryptophan permease in yeast. *J Cell Biol*, **146**(6), 1227–1238.
- BEDELL, G. W., & SOLL, D. R. 1979. Effects of low concentrations of zinc on the growth and dimorphism of *Candida albicans*: evidence for zinc-resistant and -sensitive pathways for mycelium formation. *Infect Immun*, **26**(1), 348–354.
- BELIZARIO, JOSÉ E, ALVES, JULIANO, GARAY-MALPARTIDA, MIGUEL, & OCCHIUCCI, JOÃO MARCELO. 2008. Coupling caspase cleavage and proteasomal degradation of proteins carrying PEST motif. *Curr Protein Pept Sci*, **9**(3), 210–220.
- BENNI, M. L., & NEIGEBORN, L. 1997. Identification of a new class of negative regulators affecting sporulation-specific gene expression in yeast. *Genetics*, **147**(3), 1351–1366.
- BENSEN, ERIC S, MARTIN, SAMUEL J, LI, MINGCHUN, BERMAN, JUDITH, & DAVIS, DANA A. 2004. Transcriptional profiling in *Candida albicans* reveals new adaptive responses to extracellular pH and functions for Rim101p. *Mol Microbiol*, **54**(5), 1335–1351.
- BERNARDIS, F. DE, CHIARI, P., CICCOTZI, M., PELLEGRINI, G., CEDDIA, T., D'OFFIZZI, G., QUINTI, I., SULLIVAN, P. A., & CASSONE, A. 1996. Elevated aspartic proteinase secretion and experimental pathogenicity of *Candida albicans* isolates from oral cavities of subjects infected with human immunodeficiency virus. *Infect Immun*, **64**(2), 466–471.
- BERNARDIS, F. DE, SULLIVAN, P. A., & CASSONE, A. 2001. Aspartyl proteinases of *Candida albicans* and their role in pathogenicity. *Med Mycol*, **39**(4), 303–313.
- BERNSTEIN, BRADLEY E, LIU, CHIH LONG, HUMPHREY, EMILY L, PERLSTEIN, ETHAN O, & SCHREIBER, STUART L. 2004. Global nucleosome occupancy in yeast. *Genome Biol*, **5**(9), R62.
- BERTRAM, PAULA G, CHOI, JAE H, CARVALHO, JOHN, CHAN, TING-FUNG, AI, WANDONG, & ZHENG, X. F STEVEN. 2002. Convergence of TOR-nitrogen and Snf1-glucose signaling pathways onto Gln3. *Mol Cell Biol*, **22**(4), 1246–1252.

- BIGGER, J. 1944. Treatment of staphylococcal infections with penicillin. *Lancet*, **ii**, 497–500.
- BISWAS, SUBHRAJIT, ROY, MONIDEEPA, & DATTA, ASIS. 2003. N-acetylglucosamine-inducible CaGAP1 encodes a general amino acid permease which co-ordinates external nitrogen source response and morphogenesis in *Candida albicans*. *Microbiology*, **149**(Pt 9), 2597–2608.
- BISWAS, SUBHRAJIT, DIJCK, PATRICK VAN, & DATTA, ASIS. 2007. Environmental sensing and signal transduction pathways regulating morphopathogenic determinants of *Candida albicans*. *Microbiol Mol Biol Rev*, **71**(2), 348–376.
- BITTERMAN, KEVIN J, MEDVEDIK, OLIVER, & SINCLAIR, DAVID A. 2003. Longevity regulation in *Saccharomyces cerevisiae*: linking metabolism, genome stability, and heterochromatin. *Microbiol Mol Biol Rev*, **67**(3), 376–99, table of contents.
- BJORNSTI, MARY-ANN, & HOUGHTON, PETER J. 2004. The TOR pathway: a target for cancer therapy. *Nat Rev Cancer*, **4**(5), 335–348.
- BLAGOSKLONNY, MIKHAIL V. 2009. TOR-driven aging: speeding car without brakes. *Cell Cycle*, **8**(24), 4055–4059.
- BLINKHORN, R. J., ADELSTEIN, D., & SPAGNUOLO, P. J. 1989. Emergence of a new opportunistic pathogen, *Candida lusitanae*. *J Clin Microbiol*, **27**(2), 236–240.
- BONAWITZ, NICHOLAS D, CHATENAY-LAPOINTE, MARC, PAN, YONG, & SHADEL, GERALD S. 2007. Reduced TOR signaling extends chronological life span via increased respiration and upregulation of mitochondrial gene expression. *Cell Metab*, **5**(4), 265–277.
- BORST, PIET. 2002. Antigenic variation and allelic exclusion. *Cell*, **109**(1), 5–8.
- DEN BOSSCHE, H. VAN, WILLEMSSENS, G., COOLS, W., CORNELISSEN, F., LAUWERS, W. F., & VAN CUTSEM, J. M. 1980. In vitro and in vivo effects of the antimycotic drug ketoconazole on sterol synthesis. *Antimicrob Agents Chemother*, **17**(6), 922–928.
- BOUCHONVILLE, KELLY, FORCHE, ANJA, TANG, KAREN E S, SELMECKI, ANNA, & BERMAN, JUDITH. 2009. Aneuploid chromosomes are highly unstable during DNA transformation of *Candida albicans*. *Eukaryot Cell*, **8**(10), 1554–1566.
- BOYD, ROBERT, & RICHERSON, PETER J. 1980. Effect of phenotypic variation on kin selection. *Proc Natl Acad Sci U S A*, **77**(12), 7506–7509.
- BRAUN, B. R., HEAD, W. S., WANG, M. X., & JOHNSON, A. D. 2000. Identification and characterization of TUP1-regulated genes in *Candida albicans*. *Genetics*, **156**(1), 31–44.
- BRAUN, B. R., KADOSH, D., & JOHNSON, A. D. 2001. NRG1, a repressor of filamentous growth in *C. albicans*, is down-regulated during filament induction. *EMBO J*, **20**(17), 4753–4761.
- BROACH, J. R. 1991. RAS genes in *Saccharomyces cerevisiae*: signal transduction in search of a pathway. *Trends Genet*, **7**(1), 28–33.
- BROCKERT, PAULA J, LACHKE, SALIL A, SRIKANTHA, THYAGARAJAN, PUJOL, CLAUDE, GALASK, RUDOLPH, & SOLL, DAVID R. 2003. Phenotypic switching and mating type switching of *Candida glabrata* at sites of colonization. *Infect Immun*, **71**(12), 7109–7118.
- BROEK, D., TODA, T., MICHAELI, T., LEVIN, L., BIRCHMEIER, C., ZOLLER, M., POWERS, S., & WIGLER, M. 1987. The *S. cerevisiae* CDC25 gene product regulates the RAS/adenylate cyclase pathway. *Cell*, **48**(5), 789–799.
- BROWN, CHARLES RANDELL, HUNG, GUO-CHIUAN, DUNTUN, DANIELLE, & CHIANG, HUI-LING. 2010. The TOR complex 1 is distributed in endosomes and in retrograde vesicles that form from the vacuole membrane and plays an important role in the vacuole import and degradation pathway. *J Biol Chem*, May.

- BROWN, D. H., GIUSANI, A. D., CHEN, X., & KUMAMOTO, C. A. 1999. Filamentous growth of *Candida albicans* in response to physical environmental cues and its regulation by the unique CZF1 gene. *Mol Microbiol*, **34**(4), 651–662.
- BROWN, SAM P, & BUCKLING, ANGUS. 2008. A social life for discerning microbes. *Cell*, **135**(4), 600–603.
- BUDANOV, ANDREI V, & KARIN, MICHAEL. 2008. p53 target genes *sestrin1* and *sestrin2* connect genotoxic stress and mTOR signaling. *Cell*, **134**(3), 451–460.
- BUDOVSKAYA, YELENA V, STEPHAN, JOSEPH S, DEMINOFF, STEPHEN J, & HERMAN, PAUL K. 2005. An evolutionary proteomics approach identifies substrates of the cAMP-dependent protein kinase. *Proc Natl Acad Sci U S A*, **102**(39), 13933–13938.
- BURHANS, WILLIAM C, & WEINBERGER, MARTIN. 2007. DNA replication stress, genome instability and aging. *Nucleic Acids Res*, **35**(22), 7545–7556.
- BURTNER, CHRISTOPHER R, MURAKAMI, CHRISTOPHER J, KENNEDY, BRIAN K, & KAEBERLEIN, MATT. 2009. A molecular mechanism of chronological aging in yeast. *Cell Cycle*, **8**(8), 1256–1270.
- CAFFERKEY, R., YOUNG, P. R., MCLAUGHLIN, M. M., BERGSMA, D. J., KOLTIN, Y., SATHE, G. M., FAUCETTE, L., ENG, W. K., JOHNSON, R. K., & LIVI, G. P. 1993. Dominant missense mutations in a novel yeast protein related to mammalian phosphatidylinositol 3-kinase and VPS34 abrogate rapamycin cytotoxicity. *Mol Cell Biol*, **13**(10), 6012–6023.
- CALDERONE, R. 2002. *Candida and Candidiasis*. ASM Press.
- CANNON, RICHARD D, LAMPING, ERWIN, HOLMES, ANN R, NIIMI, KYOKO, TANABE, KOICHI, NIIMI, MASAKAZU, & MONK, BRIAN C. 2007. *Candida albicans* drug resistance another way to cope with stress. *Microbiology*, **153**(Pt 10), 3211–3217.
- CARDENAS, M. E., & HEITMAN, J. 1995. FKBP12-rapamycin target TOR2 is a vacuolar protein with an associated phosphatidylinositol-4 kinase activity. *EMBO J*, **14**(23), 5892–5907.
- CARDENAS, M. E., CUTLER, N. S., LORENZ, M. C., COMO, C. J. DI, & HEITMAN, J. 1999. The TOR signaling cascade regulates gene expression in response to nutrients. *Genes Dev*, **13**(24), 3271–3279.
- CARLISLE, PATRICIA L, BANERJEE, MOHUA, LAZZELL, ANNA, MONTEAGUDO, CARLOS, LÓPEZ-RIBOT, JOSÉ L, & KADOSH, DAVID. 2009. Expression levels of a filament-specific transcriptional regulator are sufficient to determine *Candida albicans* morphology and virulence. *Proc Natl Acad Sci U S A*, **106**(2), 599–604.
- CARRACEDO, ARKAITZ, BASELGA, JOSE, & PANDOLFI, PIER PAOLO. 2008. Deconstructing feedback-signaling networks to improve anticancer therapy with mTORC1 inhibitors. *Cell Cycle*, **7**(24), 3805–3809.
- CASS, L. A., SUMMERS, S. A., PRENDERGAST, G. V., BACKER, J. M., BIRNBAUM, M. J., & MEINKOTH, J. L. 1999. Protein kinase A-dependent and -independent signaling pathways contribute to cyclic AMP-stimulated proliferation. *Mol Cell Biol*, **19**(9), 5882–5891.
- CASSONE, A., BERNARDIS, F. DE, MONDELLO, F., CEDDIA, T., & AGATENSI, L. 1987. Evidence for a correlation between proteinase secretion and vulvovaginal candidosis. *J Infect Dis*, **156**(5), 777–783.
- CASTAÑO, IRENE, PAN, SHIH-JUNG, ZUPANCIC, MARGARET, HENNEQUIN, CHRISTOPHE, DUJON, BERNARD, & CORMACK, BRENDAN P. 2005. Telomere length control and transcriptional regulation of subtelomeric adhesins in *Candida glabrata*. *Mol Microbiol*, **55**(4), 1246–1258.
- CASTILLO, ARACELI G, MELLONE, BARBARA G, PARTRIDGE, JANET F, RICHARDSON, WILLIAM, HAMILTON, GEORGINA L, ALLSHIRE, ROBIN C, & PIDOUX, ALISON L. 2007. Plasticity of fission yeast CENP-A chromatin driven by relative levels of histone H3 and H4. *PLoS Genet*, **3**(7), e121.
- CAUDA, R., TACCONELLI, E., TUMBARELLO, M., MORACE, G., BERNARDIS, F. DE, TOROSANTUCCI, A., & CASSONE, A. 1999. Role of protease inhibitors in preventing recurrent oral candidosis in patients with HIV infection: a prospective case-control study. *J Acquir Immune Defic Syndr*, **21**(1), 20–25.

- CAUSTON, H. C., REN, B., KOH, S. S., HARBISON, C. T., KANIN, E., JENNINGS, E. G., LEE, T. I., TRUE, H. L., LANDER, E. S., & YOUNG, R. A. 2001. Remodeling of yeast genome expression in response to environmental changes. *Mol Biol Cell*, **12**(2), 323–337.
- CHANG, C. H., & LUSE, D. S. 1997. The H3/H4 tetramer blocks transcript elongation by RNA polymerase II in vitro. *J Biol Chem*, **272**(37), 23427–23434.
- CHEN, ESTHER J, & KAISER, CHRIS A. 2003. LST8 negatively regulates amino acid biosynthesis as a component of the TOR pathway. *J Cell Biol*, **161**(2), 333–347.
- CHEN, XI, MAGEE, B. B., DAWSON, DEAN, MAGEE, P. T., & KUMAMOTO, CAROL A. 2004. Chromosome 1 trisomy compromises the virulence of *Candida albicans*. *Mol Microbiol*, **51**(2), 551–565.
- CHENG, GEORGINA, WOZNIAK, KAREN, WALLIG, MATTHEW A, FIDEL, PAUL L, TRUPIN, SUZANNE R, & HOYER, LOIS L. 2005. Comparison between *Candida albicans* agglutinin-like sequence gene expression patterns in human clinical specimens and models of vaginal candidiasis. *Infect Immun*, **73**(3), 1656–1663.
- CHOE, J., SCHUSTER, T., & GRUNSTEIN, M. 1985. Organization, primary structure, and evolution of histone H2A and H2B genes of the fission yeast *Schizosaccharomyces pombe*. *Mol Cell Biol*, **5**(11), 3261–3269.
- CHU, W. S., MAGEE, B. B., & MAGEE, P. T. 1993. Construction of an SfiI macrorestriction map of the *Candida albicans* genome. *J Bacteriol*, **175**(20), 6637–6651.
- CLARK-ADAMS, C. D., NORRIS, D., OSLEY, M. A., FASSLER, J. S., & WINSTON, F. 1988. Changes in histone gene dosage alter transcription in yeast. *Genes Dev*, **2**(2), 150–159.
- CLAYTON, ALISON L, HAZZALIN, CATHERINE A, & MAHADEVAN, LOUIS C. 2006. Enhanced histone acetylation and transcription: a dynamic perspective. *Mol Cell*, **23**(3), 289–296.
- COLES, L.S., WELLS-J.R.E., & ROBINS, A.J. 1989. *Histone and other basic nuclear proteins*. CRC Press, Boca Raton, FL.
- COLLINS, SEAN R, KEMMEREN, PATRICK, ZHAO, XUE-CHU, GREENBLATT, JACK F, SPENCER, FORREST, HOLSTEGE, FRANK C P, WEISSMAN, JONATHAN S, & KROGAN, NEVAN J. 2007. Toward a comprehensive atlas of the physical interactome of *Saccharomyces cerevisiae*. *Mol Cell Proteomics*, **6**(3), 439–450.
- COLOMINA, NEUS, LIU, YUHUI, ALDEA, MARTÍ, & GARÍ, ELOI. 2003. TOR regulates the subcellular localization of Ime1, a transcriptional activator of meiotic development in budding yeast. *Mol Cell Biol*, **23**(20), 7415–7424.
- COMO, C. J. DI, & ARNDT, K. T. 1996. Nutrients, via the Tor proteins, stimulate the association of Tap42 with type 2A phosphatases. *Genes Dev*, **10**(15), 1904–1916.
- COMO, CHARLES J DI, & JIANG, YU. 2006. The association of Tap42 phosphatase complexes with TORC1: another level of regulation in Tor signaling. *Cell Cycle*, **5**(23), 2729–2732.
- COOPER, TERRANCE G. 2002. Transmitting the signal of excess nitrogen in *Saccharomyces cerevisiae* from the Tor proteins to the GATA factors: connecting the dots. *FEMS Microbiol Rev*, **26**(3), 223–238.
- DE BOER, M., NIELSEN, P. S., BEBELMAN, J. P., HEERIKHUIZEN, H., ANDERSEN, H. A., & PLANTA, R. J. 2000. Stp1p, Stp2p and Abf1p are involved in regulation of expression of the amino acid transporter gene BAP3 of *Saccharomyces cerevisiae*. *Nucleic Acids Res*, **28**(4), 974–981.
- DEHART, AMY K A, SCHNELL, JOSHUA D, ALLEN, DAMIAN A, TSAI, JU-YUN, & HICKE, LINDA. 2003. Receptor internalization in yeast requires the Tor2-Rho1 signaling pathway. *Mol Biol Cell*, **14**(11), 4676–4684.
- D'ENFERT, CHRISTOPHE. 2006. Biofilms and their role in the resistance of pathogenic *Candida* to antifungal agents. *Curr Drug Targets*, **7**(4), 465–470.
- VAN DEN BROEK, DAAN, BLOEMBERG, GUIDO V, & LUGTENBERG, BEN. 2005. The role of phenotypic variation in rhizosphere *Pseudomonas* bacteria. *Environ Microbiol*, **7**(11), 1686–1697.

- CORDÓN-PRECIADO, VIOLETA, UFANO, SANDRA, & BUENO, AVELINO. 2006. Limiting amounts of budding yeast Rad53 S-phase checkpoint activity results in increased resistance to DNA alkylation damage. *Nucleic Acids Res*, **34**(20), 5852–5862.
- COSTE, ALIX T, KARABABA, MAHIR, ISCHER, FRANÇOISE, BILLE, JACQUES, & SANGLARD, DOMINIQUE. 2004. TAC1, transcriptional activator of CDR genes, is a new transcription factor involved in the regulation of *Candida albicans* ABC transporters CDR1 and CDR2. *Eukaryot Cell*, **3**(6), 1639–1652.
- COSTIGAN, C., & SNYDER, M. 1994. SLK1, a yeast homolog of MAP kinase activators, has a RAS/cAMP-independent role in nutrient sensing. *Mol Gen Genet*, **243**(3), 286–296.
- COTTIER, FABIEN, & MÜHLSCHLEGEL, FRITZ A. 2009. Sensing the environment: response of *Candida albicans* to the X factor. *FEMS Microbiol Lett*, **295**(1), 1–9.
- COWEN, LEAH E. 2008. The evolution of fungal drug resistance: modulating the trajectory from genotype to phenotype. *Nat Rev Microbiol*, **6**(3), 187–198.
- COWEN, LEAH E, & LINDQUIST, SUSAN. 2005. Hsp90 potentiates the rapid evolution of new traits: drug resistance in diverse fungi. *Science*, **309**(5744), 2185–2189.
- COX, KATHLEEN H, KULKARNI, AJIT, TATE, JENNIFER J, & COOPER, TERRANCE G. 2004. Gln3 phosphorylation and intracellular localization in nutrient limitation and starvation differ from those generated by rapamycin inhibition of Tor1/2 in *Saccharomyces cerevisiae*. *J Biol Chem*, **279**(11), 10270–10278.
- CRESPO, J. L., DAICHO, K., USHIMARU, T., & HALL, M. N. 2001. The GATA transcription factors GLN3 and GAT1 link TOR to salt stress in *Saccharomyces cerevisiae*. *J Biol Chem*, **276**(37), 34441–34444.
- CRESPO, JOSÉ L, & HALL, MICHAEL N. 2002. Elucidating TOR signaling and rapamycin action: lessons from *Saccharomyces cerevisiae*. *Microbiol Mol Biol Rev*, **66**(4), 579–91, table of contents.
- CRESPO, JOSÉ L, POWERS, TED, FOWLER, BRIAN, & HALL, MICHAEL N. 2002. The TOR-controlled transcription activators GLN3, RTG1, and RTG3 are regulated in response to intracellular levels of glutamine. *Proc Natl Acad Sci U S A*, **99**(10), 6784–6789.
- CROSS, S. L., & SMITH, M. M. 1988. Comparison of the structure and cell cycle expression of mRNAs encoded by two histone H3-H4 loci in *Saccharomyces cerevisiae*. *Mol Cell Biol*, **8**(2), 945–954.
- CRUZ, M. C., GOLDSTEIN, A. L., BLANKENSHIP, J., POETA, M. DEL, PERFECT, J. R., MCCUSKER, J. H., BENNANI, Y. L., CARDENAS, M. E., & HEITMAN, J. 2001. Rapamycin and less immunosuppressive analogs are toxic to *Candida albicans* and *Cryptococcus neoformans* via FKBP12-dependent inhibition of TOR. *Antimicrob Agents Chemother*, **45**(11), 3162–3170.
- CURRIE, B., SANATI, H., IBRAHIM, A. S., EDWARDS, J. E., CASADEVALL, A., & GHANNOUM, M. A. 1995. Sterol compositions and susceptibilities to amphotericin B of environmental *Cryptococcus neoformans* isolates are changed by murine passage. *Antimicrob Agents Chemother*, **39**(9), 1934–1937.
- CUTLER, N. S., HEITMAN, J., & CARDENAS, M. E. 1999. TOR kinase homologs function in a signal transduction pathway that is conserved from yeast to mammals. *Mol Cell Endocrinol*, **155**(1-2), 135–142.
- CUTLER, N. S., PAN, X., HEITMAN, J., & CARDENAS, M. E. 2001. The TOR signal transduction cascade controls cellular differentiation in response to nutrients. *Mol Biol Cell*, **12**(12), 4103–4113.
- DANIELS, KARLA J, SRIKANTHA, THYAGARAJAN, LOCKHART, SHAWN R, PUJOL, CLAUDE, & SOLL, DAVID R. 2006. Opaque cells signal white cells to form biofilms in *Candida albicans*. *EMBO J*, **25**(10), 2240–2252.
- DANN, STEPHEN G, & THOMAS, GEORGE. 2006. The amino acid sensitive TOR pathway from yeast to mammals. *FEBS Lett*, **580**(12), 2821–2829.
- DAVIE, JUDITH K, EDMONDSON, DIANE G, COCO, CHERIE B, & DENT, SHARON Y R. 2003. Tup1-Ssn6 interacts with multiple class I histone deacetylases in vivo. *J Biol Chem*, **278**(50), 50158–50162.

- DAVIS, D., EDWARDS, J. E., MITCHELL, A. P., & IBRAHIM, A. S. 2000a. *Candida albicans* RIM101 pH response pathway is required for host-pathogen interactions. *Infect Immun*, **68**(10), 5953–5959.
- DAVIS, D., WILSON, R. B., & MITCHELL, A. P. 2000b. RIM101-dependent and-independent pathways govern pH responses in *Candida albicans*. *Mol Cell Biol*, **20**(3), 971–978.
- DAVIS, DANA. 2003. Adaptation to environmental pH in *Candida albicans* and its relation to pathogenesis. *Curr Genet*, **44**(1), 1–7.
- DAVIS, DANA A. 2009. How human pathogenic fungi sense and adapt to pH: the link to virulence. *Curr Opin Microbiol*, **12**(4), 365–370.
- DAVIS, DANA A, BRUNO, VINCENT M, LOZA, LUCIO, FILLER, SCOTT G, & MITCHELL, AARON P. 2002. *Candida albicans* Mds3p, a conserved regulator of pH responses and virulence identified through insertional mutagenesis. *Genetics*, **162**(4), 1573–1581.
- DECHANT, REINHARD, BINDA, MATTEO, LEE, SUNG SIK, PELET, SERGE, WINDERICKX, JORIS, & PETER, MATTHIAS. 2010. Cytosolic pH is a second messenger for glucose and regulates the PKA pathway through V-ATPase. *EMBO J*, **29**(15), 2515–2526.
- DEITSCH, K. W., MOXON, E. R., & WELLEMS, T. E. 1997. Shared themes of antigenic variation and virulence in bacterial, protozoal, and fungal infections. *Microbiol Mol Biol Rev*, **61**(3), 281–293.
- DEITSCH, KIRK W, LUKEHART, SHEILA A, & STRINGER, JAMES R. 2009. Common strategies for antigenic variation by bacterial, fungal and protozoan pathogens. *Nat Rev Microbiol*, **7**(7), 493–503.
- DELGOFFE, GREG M, KOLE, THOMAS P, COTTER, ROBERT J, & POWELL, JONATHAN D. 2009. Enhanced interaction between Hsp90 and raptor regulates mTOR signaling upon T cell activation. *Mol Immunol*, **46**(13), 2694–2698.
- DENG, XIN, EICKHOLT, JESSE, & CHENG, JIANLIN. 2009. PreDisorder: ab initio sequence-based prediction of protein disordered regions. *BMC Bioinformatics*, **10**, 436.
- DIGGLE, STEPHEN P, GRIFFIN, ASHLEIGH S, CAMPBELL, GENEVIEVE S, & WEST, STUART A. 2007. Cooperation and conflict in quorum-sensing bacterial populations. *Nature*, **450**(7168), 411–414.
- DIOGO, DOROTHÉE, BOUCHIER, CHRISTIANE, D'ENFERT, CHRISTOPHE, & BOUGNOUX, MARIE-ELISABETH. 2009. Loss of heterozygosity in commensal isolates of the asexual diploid yeast *Candida albicans*. *Fungal Genet Biol*, **46**(2), 159–168.
- DOMERGUE, RENEE, CASTAÑO, IRENE, PEÑAS, ALEJANDRO DE LAS, ZUPANCIC, MARGARET, LOCKATELL, VIRGINIA, HEBEL, J. RICHARD, JOHNSON, DAVID, & CORMACK, BRENDAN P. 2005. Nicotinic acid limitation regulates silencing of *Candida* adhesins during UTI. *Science*, **308**(5723), 866–870.
- DORIGO, BENEDETTA, SCHALCH, THOMAS, BYSTRICKY, KERSTIN, & RICHMOND, TIMOTHY J. 2003. Chromatin fiber folding: requirement for the histone H4 N-terminal tail. *J Mol Biol*, **327**(1), 85–96.
- DOUGLAS, L. JULIA. 2003. *Candida* biofilms and their role in infection. *Trends Microbiol*, **11**(1), 30–36.
- DOUVILLE, J., DAVID, J., FORTIER, P-K., & RAMOTAR, DINDIAL. 2004. The yeast phosphotyrosyl phosphatase activator protein, yPtp1/Rrd1, interacts with Sit4 phosphatase to mediate resistance to 4-nitroquinoline-1-oxide and UVA. *Curr Genet*, **46**(2), 72–81.
- DROTSCHMANN, K., SHCHERBAKOVA, P. V., & KUNKEL, T. A. 2000. Mutator phenotype due to loss of heterozygosity in diploid yeast strains with mutations in MSH2 and MLH1. *Toxicol Lett*, **112-113**(Mar), 239–244.
- DRUMMOND, D. ALLAN, & WILKE, CLAU O. 2009. The evolutionary consequences of erroneous protein synthesis. *Nat Rev Genet*, **10**(10), 715–724.
- D'SOUZA, C. A., & HEITMAN, J. 2001a. Conserved cAMP signaling cascades regulate fungal development and virulence. *FEMS Microbiol Rev*, **25**(3), 349–364.

- D'SOUZA, C. A., & HEITMAN, J. 2001b. It infects me, it infects me not: phenotypic switching in the fungal pathogen *Cryptococcus neoformans*. *J Clin Invest*, **108**(11), 1577–1578.
- DUBNAU, DAVID, & LOSICK, RICHARD. 2006. Bistability in bacteria. *Mol Microbiol*, **61**(3), 564–572.
- DUNKEL, NICO, BLASS, JULIA, ROGERS, P. DAVID, & MORSCHHÄUSER, JOACHIM. 2008. Mutations in the multi-drug resistance regulator MRR1, followed by loss of heterozygosity, are the main cause of MDR1 overexpression in fluconazole-resistant *Candida albicans* strains. *Mol Microbiol*, **69**(4), 827–840.
- DURASINGH, MANOJ T, VOSS, TILL S, MARTY, ALLISON J, DUFFY, MICHAEL F, GOOD, ROBERT T, THOMPSON, JENNIFER K, FREITAS-JUNIOR, LUCIO H, SCHERF, ARTUR, CRABB, BRENDAN S, & COWMAN, ALAN F. 2005. Heterochromatin silencing and locus repositioning linked to regulation of virulence genes in *Plasmodium falciparum*. *Cell*, **121**(1), 13–24.
- DURRIN, L. K., MANN, R. K., & GRUNSTEIN, M. 1992. Nucleosome loss activates CUP1 and HIS3 promoters to fully induced levels in the yeast *Saccharomyces cerevisiae*. *Mol Cell Biol*, **12**(4), 1621–1629.
- DUTTON, S., & PENN, C. W. 1989. Biological attributes of colony-type variants of *Candida albicans*. *J Gen Microbiol*, **135**(12), 3363–3372.
- DÜVEL, K., & BROACH, J. R. 2004. The role of phosphatases in TOR signaling in yeast. *Curr Top Microbiol Immunol*, **279**, 19–38.
- DÜVEL, KATRIN, SANTHANAM, ARTI, GARRETT, STEPHEN, SCHNEPER, LISA, & BROACH, JAMES R. 2003. Multiple roles of Tap42 in mediating rapamycin-induced transcriptional changes in yeast. *Mol Cell*, **11**(6), 1467–1478.
- DYSON, H. JANE, & WRIGHT, PETER E. 2005. Intrinsically unstructured proteins and their functions. *Nat Rev Mol Cell Biol*, **6**(3), 197–208.
- ECROYD, HEATH, & CARVER, JOHN A. 2008. Unraveling the mysteries of protein folding and misfolding. *IUBMB Life*, **60**(12), 769–774.
- EISMAN, B., ALONSO-MONGE, R., ROMÁN, E., ARANA, D., NOMBELA, C., & PLA, J. 2006. The Cek1 and Hog1 mitogen-activated protein kinases play complementary roles in cell wall biogenesis and chlamydospore formation in the fungal pathogen *Candida albicans*. *Eukaryot Cell*, **5**(2), 347–358.
- EISSENBERG, L. G., POIRIER, S., & GOLDMAN, W. E. 1996. Phenotypic variation and persistence of *Histoplasma capsulatum* yeasts in host cells. *Infect Immun*, **64**(12), 5310–5314.
- ELENA, SANTIAGO F, & LENSKI, RICHARD E. 2003. Evolution experiments with microorganisms: the dynamics and genetic bases of adaptation. *Nat Rev Genet*, **4**(6), 457–469.
- ELOWITZ, MICHAEL B, LEVINE, ARNOLD J, SIGGIA, ERIC D, & SWAIN, PETER S. 2002. Stochastic gene expression in a single cell. *Science*, **297**(5584), 1183–1186.
- ENE, IULIANA V, & BENNETT, RICHARD J. 2009. Hwp1 and related adhesins contribute to both mating and biofilm formation in *Candida albicans*. *Eukaryot Cell*, **8**(12), 1909–1913.
- ENGELBERG-KULKA, H., DEKEL, L., ISRAELI-RECHES, M., & BELFORT, M. 1979. The requirement of nonsense suppression for the development of several phages. *Mol Gen Genet*, **170**(2), 155–159.
- ENLOE, B., DIAMOND, A., & MITCHELL, A. P. 2000. A single-transformation gene function test in diploid *Candida albicans*. *J Bacteriol*, **182**(20), 5730–5736.
- ERNST, J. F. 2000. Transcription factors in *Candida albicans* - environmental control of morphogenesis. *Microbiology*, **146** ( Pt 8)(Aug), 1763–1774.
- FABRIZIO, P., POZZA, F., PLETCHER, S. D., GENDRON, C. M., & LONGO, V. D. 2001. Regulation of longevity and stress resistance by Sch9 in yeast. *Science*, **292**(5515), 288–290.
- FABRIZIO, PAOLA, LIU, LEE-LOUNG, MOY, VANESSA N, DIASPRO, ALBERTO, VALENTINE, JOAN SELVERSTONE, GRALLA, EDITH BUTLER, & LONGO, VALTER D. 2003. SOD2 functions downstream of Sch9 to extend longevity in yeast. *Genetics*, **163**(1), 35–46.

- FABRIZIO, PAOLA, BATTISTELLA, LUISA, VARDAVAS, RAFFAELLO, GATTAZZO, CRISTINA, LIU, LEE-LOUNG, DIASPRO, ALBERTO, DOSSEN, JANIS W, GRALLA, EDITH BUTLER, & LONGO, VALTER D. 2004. Superoxide is a mediator of an altruistic aging program in *Saccharomyces cerevisiae*. *J Cell Biol*, **166**(7), 1055–1067.
- FARABAUGH, P. J. 1996. Programmed translational frameshifting. *Microbiol Rev*, **60**(1), 103–134.
- FEDOR-CHAIKEN, M., DESCHENES, R. J., & BROACH, J. R. 1990. SRV2, a gene required for RAS activation of adenylate cyclase in yeast. *Cell*, **61**(2), 329–340.
- FENG, Q., SUMMERS, E., GUO, B., & FINK, G. 1999. Ras signaling is required for serum-induced hyphal differentiation in *Candida albicans*. *J Bacteriol*, **181**(20), 6339–6346.
- FERRELL, JAMES E. 2002. Self-perpetuating states in signal transduction: positive feedback, double-negative feedback and bistability. *Curr Opin Cell Biol*, **14**(2), 140–148.
- FIGUEIREDO, LUISA M, CROSS, GEORGE A M, & JANZEN, CHRISTIAN J. 2009. Epigenetic regulation in African trypanosomes: a new kid on the block. *Nat Rev Microbiol*, **7**(7), 504–513.
- FILLER, S. G., IBE, B. O., LUCKETT, P. M., RAJ, J. U., & EDWARDS, J. E. 1991. *Candida albicans* stimulates endothelial cell eicosanoid production. *J Infect Dis*, **164**(5), 928–935.
- FILLER, S.G., SHEPPARD D.C. EDWARDS J.E. JR. 2006. *Molecular principles of fungal pathogenesis*. ASM Press.
- FLINN, RORY J, & BACKER, JONATHAN M. 2010. mTORC1 signals from late endosomes: Taking a TOR of the endocytic system. *Cell Cycle*, **9**(10).
- FORCHE, ANJA, MAY, GEORGIANA, & MAGEE, P. T. 2005. Demonstration of loss of heterozygosity by single-nucleotide polymorphism microarray analysis and alterations in strain morphology in *Candida albicans* strains during infection. *Eukaryot Cell*, **4**(1), 156–165.
- FORCHE, ANJA, ALBY, KEVIN, SCHAEFER, DANA, JOHNSON, ALEXANDER D, BERMAN, JUDITH, & BENNETT, RICHARD J. 2008. The parasexual cycle in *Candida albicans* provides an alternative pathway to meiosis for the formation of recombinant strains. *PLoS Biol*, **6**(5), e110.
- FORCHE, ANJA, MAGEE, P. T., SELMECKI, ANNA, BERMAN, JUDITH, & MAY, GEORGIANA. 2009. Evolution in *Candida albicans* populations during a single passage through a mouse host. *Genetics*, **182**(3), 799–811.
- FRAGA, MARIO F, BALLESTAR, ESTEBAN, VILLAR-GAREA, ANA, BOIX-CHORNET, MANUEL, ESPADA, JESUS, SCHOTTA, GUNNAR, BONALDI, TIZIANA, HAYDON, CLAIRE, ROPERO, SANTIAGO, PETRIE, KEVIN, IYER, N. GOPALAKRISHNA, PÉREZ-ROSADO, ALBERTO, CALVO, ENRIQUE, LOPEZ, JUAN A, CANO, AMPARO, CALASANZ, MARIA J, COLOMER, DOLORS, PIRIS, MIGUEL ANGEL, AHN, NATALIE, IMHOF, AXEL, CALDAS, CARLOS, JENUWEIN, THOMAS, & ESTELLER, MANEL. 2005. Loss of acetylation at Lys16 and trimethylation at Lys20 of histone H4 is a common hallmark of human cancer. *Nat Genet*, **37**(4), 391–400.
- FRANZOT, S. P., MUKHERJEE, J., CHERNIAK, R., CHEN, L. C., HAMDAN, J. S., & CASADEVALL, A. 1998. Microevolution of a standard strain of *Cryptococcus neoformans* resulting in differences in virulence and other phenotypes. *Infect Immun*, **66**(1), 89–97.
- FRASER, DAWN, & KAERN, MADS. 2009. A chance at survival: gene expression noise and phenotypic diversification strategies. *Mol Microbiol*, **71**(6), 1333–1340.
- FREED, NIKKI E, SILANDER, OLIN K, STECHER, BÄRBEL, BÖHM, ALEX, HARDT, WOLF-DIETRICH, & ACKERMANN, MARTIN. 2008. A simple screen to identify promoters conferring high levels of phenotypic noise. *PLoS Genet*, **4**(12), e1000307.
- FREITAS-JUNIOR, L. H., BOTTIUS, E., PIRIT, L. A., DEITSCH, K. W., SCHEIDIG, C., GUINET, F., NEHRBASS, U., WELLEMS, T. E., & SCHERF, A. 2000. Frequent ectopic recombination of virulence factor genes in telomeric chromosome clusters of *P. falciparum*. *Nature*, **407**(6807), 1018–1022.
- FRETZIN, S., ALLAN, B. D., VAN DAAL, A., & ELGIN, S. C. 1991. A *Drosophila melanogaster* H3.3 cDNA encodes a histone variant identical with the vertebrate H3.3. *Gene*, **107**(2), 341–342.

- FRIES, B. C., & CASADEVALL, A. 1998. Serial isolates of *Cryptococcus neoformans* from patients with AIDS differ in virulence for mice. *J Infect Dis*, **178**(6), 1761–1766.
- FRIES, B. C., CHEN, F., CURRIE, B. P., & CASADEVALL, A. 1996. Karyotype instability in *Cryptococcus neoformans* infection. *J Clin Microbiol*, **34**(6), 1531–1534.
- FRIES, B. C., GOLDMAN, D. L., CHERNIAK, R., JU, R., & CASADEVALL, A. 1999. Phenotypic switching in *Cryptococcus neoformans* results in changes in cellular morphology and glucuronoxylomannan structure. *Infect Immun*, **67**(11), 6076–6083.
- FRIES, B. C., TABORDA, C. P., SERFASS, E., & CASADEVALL, A. 2001. Phenotypic switching of *Cryptococcus neoformans* occurs in vivo and influences the outcome of infection. *J Clin Invest*, **108**(11), 1639–1648.
- FRIES, B. C., LEE, S. C., KENNAN, R., ZHAO, W., CASADEVALL, A., & GOLDMAN, D. L. 2005. Phenotypic switching of *Cryptococcus neoformans* can produce variants that elicit increased intracranial pressure in a rat model of cryptococcal meningoencephalitis. *Infect Immun*, **73**(3), 1779–1787.
- FRIES, BETTINA C, GOLDMAN, DAVID L, & CASADEVALL, ARTURO. 2002. Phenotypic switching in *Cryptococcus neoformans*. *Microbes Infect*, **4**(13), 1345–1352.
- FUCHS, ERIN L, BRUTINEL, EVAN D, KLEM, ERICH R, FEHR, ANTHONY R, YAHR, TIMOTHY L, & WOLFGANG, MATTHEW C. 2010. In vitro and in vivo characterization of the *Pseudomonas aeruginosa* cyclic AMP (cAMP) phosphodiesterase CpdA, required for cAMP homeostasis and virulence factor regulation. *J Bacteriol*, **192**(11), 2779–2790.
- FUKUI, Y., MIYAKE, S., SATOH, M., & YAMAMOTO, M. 1989. Characterization of the *Schizosaccharomyces pombe* *ral2* gene implicated in activation of the *ras1* gene product. *Mol Cell Biol*, **9**(12), 5617–5622.
- FUNCHAIN, P., YEUNG, A., STEWART, J. L., LIN, R., SLUPSKA, M. M., & MILLER, J. H. 2000. The consequences of growth of a mutator strain of *Escherichia coli* as measured by loss of function among multiple gene targets and loss of fitness. *Genetics*, **154**(3), 959–970.
- GALHARDO, RODRIGO S, HASTINGS, P. J., & ROSENBERG, SUSAN M. 2007. Mutation as a stress response and the regulation of evolvability. *Crit Rev Biochem Mol Biol*, **42**(5), 399–435.
- GALLAGHER, P. J., BENNETT, D. E., HENMAN, M. C., RUSSELL, R. J., FLINT, S. R., SHANLEY, D. B., & COLEMAN, D. C. 1992. Reduced azole susceptibility of oral isolates of *Candida albicans* from HIV-positive patients and a derivative exhibiting colony morphology variation. *J Gen Microbiol*, **138**(9), 1901–1911.
- GANLEY, AUSTEN R D, IDE, SATORU, SAKA, KIMIKO, & KOBAYASHI, TAKEHIKO. 2009. The effect of replication initiation on gene amplification in the rDNA and its relationship to aging. *Mol Cell*, **35**(5), 683–693.
- GARAY-MALPARTIDA, H. M., OCCHIUCCI, J. M., ALVES, J., & BELIZÁRIO, J. E. 2005. CaSPredictor: a new computer-based tool for caspase substrate prediction. *Bioinformatics*, **21 Suppl 1**(Jun), i169–i176.
- GARCÍA-SÁNCHEZ, SUSANA, MAVOR, ABIGAIL L, RUSSELL, CLAIRE L, ARGIMON, SILVIA, DENNISON, PAUL, ENJALBERT, BRICE, & BROWN, ALISTAIR J P. 2005. Global roles of *Ssn6* in *Tup1*- and *Nrg1*-dependent gene regulation in the fungal pathogen, *Candida albicans*. *Mol Biol Cell*, **16**(6), 2913–2925.
- GARDNER, ANDY, & KÜMMERLI, ROLF. 2008. Social evolution: this microbe will self-destruct. *Curr Biol*, **18**(21), R1021–R1023.
- GARDNER, MALCOLM J, HALL, NEIL, FUNG, EULA, WHITE, OWEN, BERRIMAN, MATTHEW, HYMAN, RICHARD W, CARLTON, JANE M, PAIN, ARNAB, NELSON, KAREN E, BOWMAN, SHAREN, PAULSEN, IAN T, JAMES, KEITH, EISEN, JONATHAN A, RUTHERFORD, KIM, SALZBERG, STEVEN L, CRAIG, ALISTER, KYES, SUE, CHAN, MAN-SUEN, NENE, VISHVANATH, SHALLOM, SHAMIRA J, SUH, BERNARD, PETERSON, JEREMY, ANGIUOLI, SAM, PERTEA, MIHAELA, ALLEN, JONATHAN, SELENGUT, JEREMY, HAFT, DANIEL, MATHER, MICHAEL W, VAIDYA, AKHIL B, MARTIN, DAVID M A, FAIRLAMB, ALAN H, FRAUNHOLZ, MARTIN J, ROOS, DAVID S, RALPH, STUART A, MCFADDEN, GEOFFREY I, CUMMINGS, LEDA M, SUBRAMANIAN, G. MANI, MUNGALL, CHRIS, VENTER, J. CRAIG, CARUCCI, DANIEL J, HOFFMAN, STEPHEN L, NEWBOLD, CHRIS,

- DAVIS, RONALD W, FRASER, CLAIRE M, & BARRELL, BART. 2002. Genome sequence of the human malaria parasite *Plasmodium falciparum*. *Nature*, **419**(6906), 498–511.
- GARZA, ANNA S, AHMAD, NIHAL, & KUMAR, RAJ. 2009. Role of intrinsically disordered protein regions/domains in transcriptional regulation. *Life Sci*, **84**(7-8), 189–193.
- GAVIN, ANNE-CLAUDE, BÖSCHE, MARKUS, KRAUSE, ROLAND, GRANDI, PAOLA, MARZIOCH, MARTINA, BAUER, ANDREAS, SCHULTZ, JÖRG, RICK, JENS M, MICHON, ANNE-MARIE, CRUCIAT, CRISTINA-MARIA, REMOR, MARITA, HÖFERT, CHRISTIAN, SCHELDER, MALGORZATA, BRAJENOVIC, MIRO, RUFFNER, HEINZ, MERINO, ALEJANDRO, KLEIN, KARIN, HUDAK, MANUELA, DICKSON, DAVID, RUDI, TATJANA, GNAU, VOLKER, BAUCH, ANGELA, BASTUCK, SONJA, HUHSE, BETTINA, LEUTWEIN, CHRISTINA, HEURTIER, MARIE-ANNE, COPLEY, RICHARD R, EDELMANN, ANGELA, QUERFURTH, ERICH, RYBIN, VLADIMIR, DREWES, GERARD, RAIDA, MANFRED, BOUWMEESTER, TEWIS, BORK, PEER, SERAPHIN, BERTRAND, KUSTER, BERNHARD, NEUBAUER, GITTE, & SUPERTI-FURGA, GIULIO. 2002. Functional organization of the yeast proteome by systematic analysis of protein complexes. *Nature*, **415**(6868), 141–147.
- GAVIN, ANNE-CLAUDE, ALOY, PATRICK, GRANDI, PAOLA, KRAUSE, ROLAND, BOESCHE, MARKUS, MARZIOCH, MARTINA, RAU, CHRISTINA, JENSEN, LARS JUHL, BASTUCK, SONJA, DÜMPELFELD, BIRGIT, EDELMANN, ANGELA, HEURTIER, MARIE-ANNE, HOFFMAN, VERENA, HOEFERT, CHRISTIAN, KLEIN, KARIN, HUDAK, MANUELA, MICHON, ANNE-MARIE, SCHELDER, MALGORZATA, SCHIRLE, MARKUS, REMOR, MARITA, RUDI, TATJANA, HOOPER, SEAN, BAUER, ANDREAS, BOUWMEESTER, TEWIS, CASARI, GEORG, DREWES, GERARD, NEUBAUER, GITTE, RICK, JENS M, KUSTER, BERNHARD, BORK, PEER, RUSSELL, ROBERT B, & SUPERTI-FURGA, GIULIO. 2006. Proteome survey reveals modularity of the yeast cell machinery. *Nature*, **440**(7084), 631–636.
- GEORIS, ISABELLE, TATE, JENNIFER J, COOPER, TERRANCE G, & DUBOIS, EVELYNE. 2008. Tor pathway control of the nitrogen-responsive DAL5 gene bifurcates at the level of Gln3 and Gat1 regulation in *Saccharomyces cerevisiae*. *J Biol Chem*, **283**(14), 8919–8929.
- GERAMI-NEJAD, MARYAM, DULMAGE, KEELY, & BERMAN, JUDITH. 2009. Additional cassettes for epitope and fluorescent fusion proteins in *Candida albicans*. *Yeast*, **26**(7), 399–406.
- GETTEMANS, JAN, MEERSCHAERT, KRIS, VANDEKERCKHOVE, JOEL, & CORTE, VEERLE DE. 2003. A kelch beta propeller featuring as a G beta structural mimic: reinventing the wheel? *Sci STKE*, **2003**(191), PE27.
- GIACOMETTI, ROMINA, SOUTO, GUADALUPE, SILBERSTEIN, SUSANA, GIASSON, LUC, CANTORE, MARÍA LEONOR, & PASSERON, SUSANA. 2006. Expression levels and subcellular localization of Bcy1p in *Candida albicans* mutant strains devoid of one BCY1 allele results in a defective morphogenetic behavior. *Biochim Biophys Acta*, **1763**(1), 64–72.
- GIACOMETTI, ROMINA, KRONBERG, FLORENCIA, BIONDI, RICARDO M, & PASSERON, SUSANA. 2009. Catalytic isoforms Tpk1 and Tpk2 of *Candida albicans* PKA have non-redundant roles in stress response and glycogen storage. *Yeast*, **26**(5), 273–285.
- GIRAUD, A., RADMAN, M., MATIC, I., & TADDEI, F. 2001. The rise and fall of mutator bacteria. *Curr Opin Microbiol*, **4**(5), 582–585.
- GIRAUD, ANTOINE, MATIC, IVAN, RADMAN, MIROSLAV, FONS, MICHEL, & TADDEI, FRANÇOIS. 2002. Mutator bacteria as a risk factor in treatment of infectious diseases. *Antimicrob Agents Chemother*, **46**(3), 863–865.
- GLOZAK, MICHELE A, SENGUPTA, NILANJAN, ZHANG, XIAOHONG, & SETO, EDWARD. 2005. Acetylation and deacetylation of non-histone proteins. *Gene*, **363**(Dec), 15–23.
- GOLDMAN, D. L., FRIES, B. C., FRANZOT, S. P., MONTELLA, L., & CASADEVALL, A. 1998. Phenotypic switching in the human pathogenic fungus *Cryptococcus neoformans* is associated with changes in virulence and pulmonary inflammatory response in rodents. *Proc Natl Acad Sci U S A*, **95**(25), 14967–14972.
- GONZALO, SUSANA. 2010. Epigenetic alterations in aging. *J Appl Physiol*, May.

- GOW, NEIL A R, BROWN, ALISTAIR J P, & ODDS, FRANK C. 2002. Fungal morphogenesis and host invasion. *Curr Opin Microbiol*, **5**(4), 366–371.
- GREEN, CLAYTON B, CHENG, GEORGINA, CHANDRA, JYOTSNA, MUKHERJEE, PRANAB, GHANNOUM, MAHMOUD A, & HOYER, LOIS L. 2004. RT-PCR detection of *Candida albicans* ALS gene expression in the reconstituted human epithelium (RHE) model of oral candidiasis and in model biofilms. *Microbiology*, **150**(Pt 2), 267–275.
- GREEN, CLAYTON B, MARRETTA, SANDRA MANFRA, CHENG, GEORGINA, FADDOUL, FADY F, EHRHART, E. J., & HOYER, LOIS L. 2006. RT-PCR analysis of *Candida albicans* ALS gene expression in a hyposalivatory rat model of oral candidiasis and in HIV-positive human patients. *Med Mycol*, **44**(2), 103–111.
- GREEN, SARAH R, & JOHNSON, ALEXANDER D. 2004. Promoter-dependent roles for the Srb10 cyclin-dependent kinase and the Hda1 deacetylase in Tup1-mediated repression in *Saccharomyces cerevisiae*. *Mol Biol Cell*, **15**(9), 4191–4202.
- GÖRNER, WOLFRAM, DURCHSCHLAG, ERICH, WOLF, JULIA, BROWN, ELIZABETH L, AMMERER, GUSTAV, RUIS, HELMUT, & SCHÜLLER, CHRISTOPH. 2002. Acute glucose starvation activates the nuclear localization signal of a stress-specific yeast transcription factor. *EMBO J*, **21**(1-2), 135–144.
- GROPP, KATHARINA, SCHILD, LYDIA, SCHINDLER, SUSANN, HUBE, BERNHARD, ZIPFEL, PETER F, & SKERKA, CHRISTINE. 2009. The yeast *Candida albicans* evades human complement attack by secretion of aspartic proteases. *Mol Immunol*, **47**(2-3), 465–475.
- GROZINGER, CHRISTINA M, & SCHREIBER, STUART L. 2002. Deacetylase enzymes: biological functions and the use of small-molecule inhibitors. *Chem Biol*, **9**(1), 3–16.
- GUERRERO, A., JAIN, N., GOLDMAN, D. L., & FRIES, B. C. 2006. Phenotypic switching in *Cryptococcus neoformans*. *Microbiology*, **152**(Pt 1), 3–9.
- GUERRERO, A., JAIN, N., WANG, X., & FRIES, B. C. 2010. *Cryptococcus neoformans* variants generated by phenotypic switching differ in virulence through effects on macrophage activation. *Infect Immun*, **78**(3), 1049–1057.
- GULLO, ANTONINO. 2009. Invasive fungal infections: the challenge continues. *Drugs*, **69 Suppl 1**, 65–73.
- HAKE, SANDRA B, GARCIA, BENJAMIN A, KAUER, MONIKA, BAKER, STEPHEN P, SHABANOWITZ, JEFFREY, HUNT, DONALD F, & ALLIS, C. DAVID. 2005. Serine 31 phosphorylation of histone variant H3.3 is specific to regions bordering centromeres in metaphase chromosomes. *Proc Natl Acad Sci U S A*, **102**(18), 6344–6349.
- HALKIDOU, KALIPSO, GAUGHAN, LUKE, COOK, SUSAN, LEUNG, HING Y, NEAL, DAVID E, & ROBSON, CRAIG N. 2004. Upregulation and nuclear recruitment of HDAC1 in hormone refractory prostate cancer. *Prostate*, **59**(2), 177–189.
- HALME, ADRIAN, BUMGARNER, STACIE, STYLES, CORA, & FINK, GERALD R. 2004. Genetic and epigenetic regulation of the FLO gene family generates cell-surface variation in yeast. *Cell*, **116**(3), 405–415.
- HAN, M., & GRUNSTEIN, M. 1988. Nucleosome loss activates yeast downstream promoters in vivo. *Cell*, **55**(6), 1137–1145.
- HAN, M., KIM, U. J., KAYNE, P., & GRUNSTEIN, M. 1988. Depletion of histone H4 and nucleosomes activates the PHO5 gene in *Saccharomyces cerevisiae*. *EMBO J*, **7**(7), 2221–2228.
- HANAHAH, D., & WEINBERG, R. A. 2000. The hallmarks of cancer. *Cell*, **100**(1), 57–70.
- HANCOCK, JOHN F. 2003. Ras proteins: different signals from different locations. *Nat Rev Mol Cell Biol*, **4**(5), 373–384.
- HANCOCK, JOHN F, & PARTON, ROBERT G. 2005. Ras plasma membrane signalling platforms. *Biochem J*, **389**(Pt 1), 1–11.

- HANLON, SEAN E, NORRIS, DAVID N, & VERSHON, ANDREW K. 2003. Depletion of H2A-H2B dimers in *Saccharomyces cerevisiae* triggers meiotic arrest by reducing IME1 expression and activating the BUB2-dependent branch of the spindle checkpoint. *Genetics*, **164**(4), 1333–1344.
- HANSEN, MALENE, TAUBERT, STEFAN, CRAWFORD, DOUGLAS, LIBINA, NATALIYA, LEE, SEUNG-JAE, & KENYON, CYNTHIA. 2007. Lifespan extension by conditions that inhibit translation in *Caenorhabditis elegans*. *Aging Cell*, **6**(1), 95–110.
- HARASHIMA, TOSHIAKI, & HEITMAN, JOSEPH. 2002. The Galpha protein Gpa2 controls yeast differentiation by interacting with kelch repeat proteins that mimic Gbeta subunits. *Mol Cell*, **10**(1), 163–173.
- HARASHIMA, TOSHIAKI, & HEITMAN, JOSEPH. 2005. Galpha subunit Gpa2 recruits kelch repeat subunits that inhibit receptor-G protein coupling during cAMP-induced dimorphic transitions in *Saccharomyces cerevisiae*. *Mol Biol Cell*, **16**(10), 4557–4571.
- HARASHIMA, TOSHIAKI, ANDERSON, SCOTT, YATES, JOHN R, & HEITMAN, JOSEPH. 2006. The kelch proteins Gpb1 and Gpb2 inhibit Ras activity via association with the yeast RasGAP neurofibromin homologs Ira1 and Ira2. *Mol Cell*, **22**(6), 819–830.
- HARCUS, DOREEN, NANTEL, ANDRÉ, MARCIL, ANNE, RIGBY, TRACEY, & WHITEWAY, MALCOLM. 2004. Transcription profiling of cyclic AMP signaling in *Candida albicans*. *Mol Biol Cell*, **15**(10), 4490–4499.
- HARDWICK, J. S., KURUVILLA, F. G., TONG, J. K., SHAMJI, A. F., & SCHREIBER, S. L. 1999. Rapamycin-modulated transcription defines the subset of nutrient-sensitive signaling pathways directly controlled by the Tor proteins. *Proc Natl Acad Sci U S A*, **96**(26), 14866–14870.
- HARRIS, R. S., KONG, Q., & MAIZELS, N. 1999. Somatic hypermutation and the three R's: repair, replication and recombination. *Mutat Res*, **436**(2), 157–178.
- HARRISON, DAVID E, STRONG, RANDY, SHARP, ZELTON DAVE, NELSON, JAMES F, ASTLE, CLINTON M, FLURKEY, KEVIN, NADON, NANCY L, WILKINSON, J. ERBY, FRENKEL, KRYSZYNA, CARTER, CHRISTY S, PAHOR, MARCO, JAVORS, MARTIN A, FERNANDEZ, ELIZABETH, & MILLER, RICHARD A. 2009. Rapamycin fed late in life extends lifespan in genetically heterogeneous mice. *Nature*, **460**(7253), 392–395.
- HASSA, PAUL O, & HOTTIGER, MICHAEL O. 2005. An epigenetic code for DNA damage repair pathways? *Biochem Cell Biol*, **83**(3), 270–285.
- HAUMAN, C. H., THOMPSON, I. O., THEUNISSEN, F., & WOLFAARDT, P. 1993. Oral carriage of *Candida* in healthy and HIV-seropositive persons. *Oral Surg Oral Med Oral Pathol*, **76**(5), 570–572.
- HAWSER, S. P., & DOUGLAS, L. J. 1995. Resistance of *Candida albicans* biofilms to antifungal agents in vitro. *Antimicrob Agents Chemother*, **39**(9), 2128–2131.
- HAZEN, K. C. 1995. New and emerging yeast pathogens. *Clin Microbiol Rev*, **8**(4), 462–478.
- HEALY, A. M., ZOLNIEROWICZ, S., STAPLETON, A. E., GOEBL, M., DEPAOLI-ROACH, A. A., & PRINGLE, J. R. 1991. CDC55, a *Saccharomyces cerevisiae* gene involved in cellular morphogenesis: identification, characterization, and homology to the B subunit of mammalian type 2A protein phosphatase. *Mol Cell Biol*, **11**(11), 5767–5780.
- HEGDE, RAMANUJAN S, & BERNSTEIN, HARRIS D. 2006. The surprising complexity of signal sequences. *Trends Biochem Sci*, **31**(10), 563–571.
- HEITMAN, J., MOVVA, N. R., & HALL, M. N. 1991. Targets for cell cycle arrest by the immunosuppressant rapamycin in yeast. *Science*, **253**(5022), 905–909.
- HEITMAN, JOSEPH. 2006. Sexual reproduction and the evolution of microbial pathogens. *Curr Biol*, **16**(17), R711–R725.
- HELLIWELL, S. B., WAGNER, P., KUNZ, J., DEUTER-REINHARD, M., HENRIQUEZ, R., & HALL, M. N. 1994. TOR1 and TOR2 are structurally and functionally similar but not identical phosphatidylinositol kinase homologues in yeast. *Mol Biol Cell*, **5**(1), 105–118.

- HELLSTEIN, J., VAWTER-HUGART, H., FOTOS, P., SCHMID, J., & SOLL, D. R. 1993. Genetic similarity and phenotypic diversity of commensal and pathogenic strains of *Candida albicans* isolated from the oral cavity. *J Clin Microbiol*, **31**(12), 3190–3199.
- HENNIG, KRISTA M, COLOMBANI, JULIEN, & NEUFELD, THOMAS P. 2006. TOR coordinates bulk and targeted endocytosis in the *Drosophila melanogaster* fat body to regulate cell growth. *J Cell Biol*, **173**(6), 963–974.
- HERNDAY, AARON, BRAATEN, BRUCE, & LOW, DAVID. 2004a. The intricate workings of a bacterial epigenetic switch. *Adv Exp Med Biol*, **547**, 83–89.
- HERNDAY, AARON D, BRAATEN, BRUCE A, BROITMAN-MADURO, GINA, ENGELBERTS, PATRICK, & LOW, DAVID A. 2004b. Regulation of the pap epigenetic switch by CpxAR: phosphorylated CpxR inhibits transition to the phase ON state by competition with Lrp. *Mol Cell*, **16**(4), 537–547.
- HILL, STUART A, & DAVIES, JOHN K. 2009. Pilin gene variation in *Neisseria gonorrhoeae*: reassessing the old paradigms. *FEMS Microbiol Rev*, **33**(3), 521–530.
- HNISZ, DENES, SCHWARZMÜLLER, TOBIAS, & KUCHLER, KARL. 2009. Transcriptional loops meet chromatin: a dual-layer network controls white-opaque switching in *Candida albicans*. *Mol Microbiol*, **74**(1), 1–15.
- HNISZ, DENES, MAJER, OLIVIA, FROHNER, INGRID E, KOMNENOVIC, VUKOSLAV, & KUCHLER, KARL. 2010. The Set3/Hos2 histone deacetylase complex attenuates cAMP/PKA signaling to regulate morphogenesis and virulence of *Candida albicans*. *PLoS Pathog*, **6**(5), e1000889.
- HOEGL, L., THOMA-GREBER, E., RÖCKEN, M., & KORTING, H. C. 1998. HIV protease inhibitors influence the prevalence of oral candidosis in HIV-infected patients: a 2-year study. *Mycoses*, **41**(7-8), 321–325.
- HOGAN, DEBORAH A, & SUNDSTROM, PAULA. 2009. The Ras/cAMP/PKA signaling pathway and virulence in *Candida albicans*. *Future Microbiol*, **4**(Dec), 1263–1270.
- HOGUES, HERVÉ, LAVOIE, HUGO, SELLAM, ADNANE, MANGOS, MARIA, ROEMER, TERRY, PURISIMA, ENRICO, NANTEL, ANDRÉ, & WHITEWAY, MALCOLM. 2008. Transcription factor substitution during the evolution of fungal ribosome regulation. *Mol Cell*, **29**(5), 552–562.
- HOLBROOK, ERIC D, & RAPPLEYE, CHAD A. 2008. *Histoplasma capsulatum* pathogenesis: making a lifestyle switch. *Curr Opin Microbiol*, **11**(4), 318–324.
- HORINOUCHI, S., OHNISHI, Y., & KANG, D. K. 2001. The A-factor regulatory cascade and cAMP in the regulation of physiological and morphological development in *Streptomyces griseus*. *J Ind Microbiol Biotechnol*, **27**(3), 177–182.
- HORTON, PAUL, PARK, KEUN-JOON, OBAYASHI, TAKESHI, FUJITA, NAOYA, HARADA, HAJIME, ADAMS-COLLIER, C. J., & NAKAI, KENTA. 2007. WoLF PSORT: protein localization predictor. *Nucleic Acids Res*, **35**(Web Server issue), W585–W587.
- HOYER, LOIS L, GREEN, CLAYTON B, OH, SOON-HWAN, & ZHAO, XIAOMIN. 2008. Discovering the secrets of the *Candida albicans* agglutinin-like sequence (ALS) gene family—a sticky pursuit. *Med Mycol*, **46**(1), 1–15.
- HUANG, GUANGHUA, WANG, HUAFENG, CHOU, SONG, NIE, XINYI, CHEN, JIANGYE, & LIU, HAOPING. 2006. Bistable expression of WOR1, a master regulator of white-opaque switching in *Candida albicans*. *Proc Natl Acad Sci U S A*, **103**(34), 12813–12818.
- HUANG, GUANGHUA, YI, SONG, SAHNI, NIDHI, DANIELS, KARLA J, SRIKANTHA, THYAGARAJAN, & SOLL, DAVID R. 2010. N-acetylglucosamine induces white to opaque switching, a mating prerequisite in *Candida albicans*. *PLoS Pathog*, **6**(3), e1000806.
- HUANG, HAO, HARCUS, DOREEN, & WHITEWAY, MALCOLM. 2008. Transcript profiling of a MAP kinase pathway in *C. albicans*. *Microbiol Res*, **163**(4), 380–393.

- HUBE, B., STEHR, F., BOSSENZ, M., MAZUR, A., KRETSCHMAR, M., & SCHÄFER, W. 2000. Secreted lipases of *Candida albicans*: cloning, characterisation and expression analysis of a new gene family with at least ten members. *Arch Microbiol*, **174**(5), 362–374.
- HUBER, ALEXANDRE, BODENMILLER, BERND, UOTILA, AINO, STAHL, MICHAEL, WANKA, STEFANIE, GERRITS, BERTRAN, AEBERSOLD, RUEDI, & LOEWITH, ROBBIE. 2009. Characterization of the rapamycin-sensitive phosphoproteome reveals that Sch9 is a central coordinator of protein synthesis. *Genes Dev*, **23**(16), 1929–1943.
- HUDSON, J. R., DAWSON, E. P., RUSHING, K. L., JACKSON, C. H., LOCKSHON, D., CONOVER, D., LANCIAULT, C., HARRIS, J. R., SIMMONS, S. J., ROTHSTEIN, R., & FIELDS, S. 1997. The complete set of predicted genes from *Saccharomyces cerevisiae* in a readily usable form. *Genome Res*, **7**(12), 1169–1173.
- HUGHES, T. R., ROBERTS, C. J., DAI, H., JONES, A. R., MEYER, M. R., SLADE, D., BURCHARD, J., DOW, S., WARD, T. R., KIDD, M. J., FRIEND, S. H., & MARTON, M. J. 2000. Widespread aneuploidy revealed by DNA microarray expression profiling. *Nat Genet*, **25**(3), 333–337.
- HUH, WON-KI, FALVO, JAMES V, GERKE, LUKE C, CARROLL, ADAM S, HOWSON, RUSSELL W, WEISSMAN, JONATHAN S, & O'SHEA, ERIN K. 2003. Global analysis of protein localization in budding yeast. *Nature*, **425**(6959), 686–691.
- HWANG, CHEOL-SANG, OH, JANG-HYUN, HUH, WON-KI, YIM, HYUNG-SOON, & KANG, SA-OUK. 2003. Ssn6, an important factor of morphological conversion and virulence in *Candida albicans*. *Mol Microbiol*, **47**(4), 1029–1043.
- HYLAND, EDEL M, COSGROVE, MICHAEL S, MOLINA, HENRIK, WANG, DONGXIA, PANDEY, AKHILESH, COTTEE, ROBERT J, & BOEKE, JEF D. 2005. Insights into the role of histone H3 and histone H4 core modifiable residues in *Saccharomyces cerevisiae*. *Mol Cell Biol*, **25**(22), 10060–10070.
- IAKOUCHEVA, LILIA M, BROWN, CELESTE J, LAWSON, J. DAVID, OBRADOVIC, ZORAN, & DUNKER, A. KEITH. 2002. Intrinsic disorder in cell-signaling and cancer-associated proteins. *J Mol Biol*, **323**(3), 573–584.
- ICHIKAWA, TOMOE, SUGITA, TAKASHI, WANG, LI, YOKOYAMA, KOJI, NISHIMURA, KAZUKO, & NISHIKAWA, AKEMI. 2004. Phenotypic switching and beta-N-acetylhexosaminidase activity of the pathogenic yeast *Trichosporon asahii*. *Microbiol Immunol*, **48**(4), 237–242.
- IHMELS, JAN, BERGMANN, SVEN, GERAMI-NEJAD, MARYAM, YANAI, ITAI, MCCLELLAN, MARK, BERMAN, JUDITH, & BARKAI, NAAMA. 2005. Rewiring of the yeast transcriptional network through the evolution of motif usage. *Science*, **309**(5736), 938–940.
- IWAGUCHI, S., HOMMA, M., & TANAKA, K. 1992. Clonal variation of chromosome size derived from the rDNA cluster region in *Candida albicans*. *J Gen Microbiol*, **138**(6), 1177–1184.
- JACINTO, E., GUO, B., ARNDT, K. T., SCHMELZLE, T., & HALL, M. N. 2001. TIP41 interacts with TAP42 and negatively regulates the TOR signaling pathway. *Mol Cell*, **8**(5), 1017–1026.
- JACINTO, ESTELA. 2007. Phosphatase targets in TOR signaling. *Methods Mol Biol*, **365**, 323–334.
- JACINTO, ESTELA. 2008. What controls TOR? *IUBMB Life*, **60**(8), 483–496.
- JAIN, N., LI, LI, MCFADDEN, D. C., BANARJEE, U., WANG, X., COOK, E., & FRIES, B. C. 2006. Phenotypic switching in a *Cryptococcus neoformans* variety *gattii* strain is associated with changes in virulence and promotes dissemination to the central nervous system. *Infect Immun*, **74**(2), 896–903.
- JAIN, NEENA, & FRIES, BETTINA C. 2009. Antigenic and phenotypic variations in fungi. *Cell Microbiol*, **11**(12), 1716–1723.
- JAMES, P., HALLADAY, J., & CRAIG, E. A. 1996. Genomic libraries and a host strain designed for highly efficient two-hybrid selection in yeast. *Genetics*, **144**(4), 1425–1436.

- JANBON, G., SHERMAN, F., & RUSTCHENKO, E. 1998. Monosomy of a specific chromosome determines L-sorbose utilization: a novel regulatory mechanism in *Candida albicans*. *Proc Natl Acad Sci U S A*, **95**(9), 5150–5155.
- JANION, CELINA, SIKORA, ANNA, NOWOSIELSKA, ANETTA, & GRZESIUK, ELZBIETA. 2002. Induction of the SOS response in starved *Escherichia coli*. *Environ Mol Mutagen*, **40**(2), 129–133.
- JENUWEIN, T., & ALLIS, C. D. 2001. Translating the histone code. *Science*, **293**(5532), 1074–1080.
- JIANG, Y., & BROACH, J. R. 1999. Tor proteins and protein phosphatase 2A reciprocally regulate Tap42 in controlling cell growth in yeast. *EMBO J*, **18**(10), 2782–2792.
- JOHNSON, ALEXANDER. 2003. The biology of mating in *Candida albicans*. *Nat Rev Microbiol*, **1**(2), 106–116.
- JONES, S., WHITE, G., & HUNTER, P. R. 1994. Increased phenotypic switching in strains of *Candida albicans* associated with invasive infections. *J Clin Microbiol*, **32**(11), 2869–2870.
- JUNG, WON HEE, & STATEVA, LUBOMIRA I. 2003. The cAMP phosphodiesterase encoded by CaPDE2 is required for hyphal development in *Candida albicans*. *Microbiology*, **149**(Pt 10), 2961–2976.
- KADOSH, D., & STRUHL, K. 1997. Repression by Ume6 involves recruitment of a complex containing Sin3 corepressor and Rpd3 histone deacetylase to target promoters. *Cell*, **89**(3), 365–371.
- KADOSH, D., & STRUHL, K. 1998. Targeted recruitment of the Sin3-Rpd3 histone deacetylase complex generates a highly localized domain of repressed chromatin in vivo. *Mol Cell Biol*, **18**(9), 5121–5127.
- KAERN, MADSEN, ELSTON, TIMOTHY C, BLAKE, WILLIAM J, & COLLINS, JAMES J. 2005. Stochasticity in gene expression: from theories to phenotypes. *Nat Rev Genet*, **6**(6), 451–464.
- KAPAHI, PANKAJ, ZID, BRIAN M, HARPER, TONY, KOSLOVER, DANIEL, SAPIN, VIVECA, & BENZER, SEYMOUR. 2004. Regulation of lifespan in *Drosophila* by modulation of genes in the TOR signaling pathway. *Curr Biol*, **14**(10), 885–890.
- KATAN-KHAYKOVICH, YAEL, & STRUHL, KEVIN. 2005. Heterochromatin formation involves changes in histone modifications over multiple cell generations. *EMBO J*, **24**(12), 2138–2149.
- KEARNS, DANIEL B, & LOSICK, RICHARD. 2005. Cell population heterogeneity during growth of *Bacillus subtilis*. *Genes Dev*, **19**(24), 3083–3094.
- KEELY, SCOTT P, CUSHION, MELANIE T, & STRINGER, JAMES R. 2003. Diversity at the locus associated with transcription of a variable surface antigen of *Pneumocystis carinii* as an index of population structure and dynamics in infected rats. *Infect Immun*, **71**(1), 47–60.
- KELLY, S. L., LAMB, D. C., KELLY, D. E., MANNING, N. J., LOEFFLER, J., HEBART, H., SCHUMACHER, U., & EINSELE, H. 1997. Resistance to fluconazole and cross-resistance to amphotericin B in *Candida albicans* from AIDS patients caused by defective sterol delta5,6-desaturation. *FEBS Lett*, **400**(1), 80–82.
- KELLY, MAIRE K, JAUERT, PETER A, JENSEN, LINNEA E, CHAN, CHRISTINE L, TRUONG, CHINH S, & KIRKPATRICK, DAVID T. 2007. Zinc regulates the stability of repetitive minisatellite DNA tracts during stationary phase. *Genetics*, **177**(4), 2469–2479.
- KENNEDY, M. J., ROGERS, A. L., HANSELMEN, L. R., SOLL, D. R., & YANCEY, R. J. 1988. Variation in adhesion and cell surface hydrophobicity in *Candida albicans* white and opaque phenotypes. *Mycopathologia*, **102**(3), 149–156.
- KEREN, IRIS, SHAH, DEVANG, SPOERING, AMY, KALDALU, NILO, & LEWIS, KIM. 2004. Specialized persister cells and the mechanism of multidrug tolerance in *Escherichia coli*. *J Bacteriol*, **186**(24), 8172–8180.
- KETEL, CARRIE, WANG, HELEN S W, MCCLELLAN, MARK, BOUCHONVILLE, KELLY, SELMECKI, ANNA, LAHAV, TAMAR, GERAMI-NEJAD, MARYAM, & BERMAN, JUDITH. 2009. Neocentromeres form efficiently at multiple possible loci in *Candida albicans*. *PLoS Genet*, **5**(3), e1000400.

- KHALAF, R. A., & ZITOMER, R. S. 2001. The DNA binding protein Rfg1 is a repressor of filamentation in *Candida albicans*. *Genetics*, **157**(4), 1503–1512.
- KIM, DO-HYUNG, SARBASSOV, D. D., ALI, SIRAJ M, KING, JESSIE E, LATEK, ROBERT R, ERDJUMENT-BROMAGE, HEDIYE, TEMPST, PAUL, & SABATINI, DAVID M. 2002. mTOR interacts with raptor to form a nutrient-sensitive complex that signals to the cell growth machinery. *Cell*, **110**(2), 163–175.
- KIM, DO-HYUNG, SARBASSOV, D. D., ALI, SIRAJ M, LATEK, ROBERT R, GUNTUR, KALYANI V P, ERDJUMENT-BROMAGE, HEDIYE, TEMPST, PAUL, & SABATINI, DAVID M. 2003. GbetaL, a positive regulator of the rapamycin-sensitive pathway required for the nutrient-sensitive interaction between raptor and mTOR. *Mol Cell*, **11**(4), 895–904.
- KIM, SAMIN, WOLYNIAK, MICHAEL J, STAAB, JANET F, & SUNDSTROM, PAULA. 2007. A 368-base-pair cis-acting HWP1 promoter region, HCR, of *Candida albicans* confers hypha-specific gene regulation and binds architectural transcription factors Nhp6 and Gcf1p. *Eukaryot Cell*, **6**(4), 693–709.
- KIM, U. J., HAN, M., KAYNE, P., & GRUNSTEIN, M. 1988. Effects of histone H4 depletion on the cell cycle and transcription of *Saccharomyces cerevisiae*. *EMBO J*, **7**(7), 2211–2219.
- KLAR, A. J., SRIKANTHA, T., & SOLL, D. R. 2001. A histone deacetylation inhibitor and mutant promote colony-type switching of the human pathogen *Candida albicans*. *Genetics*, **158**(2), 919–924.
- KLEIN, BRUCE S, & TEBBETS, BRAD. 2007. Dimorphism and virulence in fungi. *Curr Opin Microbiol*, **10**(4), 314–319.
- KLENERMAN, PAUL, WU, YING, & PHILLIPS, RODNEY. 2002. HIV: current opinion in escapology. *Curr Opin Microbiol*, **5**(4), 408–413.
- KLENGEL, TORSTEN, LIANG, WEI-JUN, CHALOUKKA, JAMES, RUOFF, CLAUDIA, SCHRÖPPEL, KLAUS, NAGLIK, JULIAN R, ECKERT, SABINE E, MOGENSEN, ESTELLE GEWISS, HAYNES, KEN, TUIITE, MICK F, LEVIN, LONNY R, BUCK, JOCHEN, & MÜHLSCHLEGEL, FRITZ A. 2005. Fungal adenylyl cyclase integrates CO<sub>2</sub> sensing with cAMP signaling and virulence. *Curr Biol*, **15**(22), 2021–2026.
- KLEPSE, MICHAEL E. 2006. *Candida* resistance and its clinical relevance. *Pharmacotherapy*, **26**(6 Pt 2), 68S–75S.
- KLIMPEL, K. R., & GOLDMAN, W. E. 1987. Isolation and characterization of spontaneous avirulent variants of *Histoplasma capsulatum*. *Infect Immun*, **55**(3), 528–533.
- KLIMPEL, K. R., & GOLDMAN, W. E. 1988. Cell walls from avirulent variants of *Histoplasma capsulatum* lack alpha-(1,3)-glucan. *Infect Immun*, **56**(11), 2997–3000.
- KOCH, K. A., ALLARD, S., SANTORO, N., CÔTÉ, J., & THIELE, D. J. 2001. The *Candida glabrata* Amt1 copper-sensing transcription factor requires Swi/Snf and Gcn5 at a critical step in copper detoxification. *Mol Microbiol*, **40**(5), 1165–1174.
- KOCKEL, LUTZ, KERR, KIMBERLY S, MELNICK, MICHAEL, BRÜCKNER, KATJA, HEBROK, MATTHIAS, & PERRIMON, NORBERT. 2010. Dynamic switch of negative feedback regulation in *Drosophila* Akt-TOR signaling. *PLoS Genet*, **6**(6), e1000990.
- KOLOTLA, M. P., & DIAMOND, R. D. 1990. Effects of neutrophils and in vitro oxidants on survival and phenotypic switching of *Candida albicans* WO-1. *Infect Immun*, **58**(5), 1174–1179.
- KROGAN, NEVAN J, CAGNEY, GERARD, YU, HAIYUAN, ZHONG, GOUQING, GUO, XINGHUA, IGNATCHENKO, ALEXANDR, LI, JOYCE, PU, SHUYE, DATTA, NIRAJ, TIKUISIS, AARON P, PUNNA, THANUJA, PEREGRÍN-ALVAREZ, JOSÉ M, SHALES, MICHAEL, ZHANG, XIN, DAVEY, MICHAEL, ROBINSON, MARK D, PACCANARO, ALBERTO, BRAY, JAMES E, SHEUNG, ANTHONY, BEATTIE, BRYAN, RICHARDS, DAWN P, CANADIEN, VERONICA, LALEV, ATANAS, MENA, FRANK, WONG, PETER, STAROSTINE, ANDREI, CANETE, MYRA M, VLASBLOM, JAMES, WU, SAMUEL, ORSI, CHRIS, COLLINS, SEAN R, CHANDRAN, SHAMANTA, HAW, ROBIN, RILSTONE, JENNIFER J, GANDI, KIRAN, THOMPSON, NATALIE J, MUSSO, GABE, ONGE, PETER ST, GHANNY, SHAUN, LAM, MANDY H Y, BUTLAND, GARETH, ALTAFA-UL, AMIN M, KANAYA, SHIGEHICO, SHILATIFARD, ALI, O'SHEA, ERIN, WEISSMAN, JONATHAN S, INGLES, C. JAMES, HUGHES, TIMOTHY R, PARKINSON, JOHN,

- GERSTEIN, MARK, WODAK, SHOSHANA J, EMILI, ANDREW, & GREENBLATT, JACK F. 2006. Global landscape of protein complexes in the yeast *Saccharomyces cerevisiae*. *Nature*, **440**(7084), 637–643.
- KRUPPA, MICHAEL. 2009. Quorum sensing and *Candida albicans*. *Mycoses*, **52**(1), 1–10.
- KÜGLER, S., SEBGHATI, T. SCHURTZ, EISSENBERG, L. GROPE, & GOLDMAN, W. E. 2000. Phenotypic variation and intracellular parasitism by *histoplasma Capsulatum*. *Proc Natl Acad Sci U S A*, **97**(16), 8794–8798.
- KULLAS, AMY L, MARTIN, SAMUEL J, & DAVIS, DANA. 2007. Adaptation to environmental pH: integrating the Rim101 and calcineurin signal transduction pathways. *Mol Microbiol*, **66**(4), 858–871.
- KUMAR, ANUJ, AGARWAL, SEEMA, HEYMAN, JOHN A, MATSON, SANDRA, HEIDTMAN, MATTHEW, PICCIRILLO, STACY, UMANSKY, LARA, DRAWID, AMAR, JANSEN, RONALD, LIU, YANG, CHEUNG, KEI-HOI, MILLER, PERRY, GERSTEIN, MARK, ROEDER, G. SHIRLEEN, & SNYDER, MICHAEL. 2002. Subcellular localization of the yeast proteome. *Genes Dev*, **16**(6), 707–719.
- KUNZ, J., SCHNEIDER, U., HOWALD, I., SCHMIDT, A., & HALL, M. N. 2000. HEAT repeats mediate plasma membrane localization of Tor2p in yeast. *J Biol Chem*, **275**(47), 37011–37020.
- KURDISTANI, SIAVASH K, & GRUNSTEIN, MICHAEL. 2003. Histone acetylation and deacetylation in yeast. *Nat Rev Mol Cell Biol*, **4**(4), 276–284.
- KURDISTANI, SIAVASH K, ROBYR, DANIEL, TAVAZOIE, SAEED, & GRUNSTEIN, MICHAEL. 2002. Genome-wide binding map of the histone deacetylase Rpd3 in yeast. *Nat Genet*, **31**(3), 248–254.
- KURTZ, M. B., ABRUZZO, G., FLATTERY, A., BARTIZAL, K., MARRINAN, J. A., LI, W., MILLIGAN, J., NOLLSTADT, K., & DOUGLAS, C. M. 1996. Characterization of echinocandin-resistant mutants of *Candida albicans*: genetic, biochemical, and virulence studies. *Infect Immun*, **64**(8), 3244–3251.
- KURUVILLA, F. G., SHAMJI, A. F., & SCHREIBER, S. L. 2001. Carbon- and nitrogen-quality signaling to translation are mediated by distinct GATA-type transcription factors. *Proc Natl Acad Sci U S A*, **98**(13), 7283–7288.
- KUSSELL, EDO, KISHONY, ROY, BALABAN, NATHALIE Q, & LEIBLER, STANISLAS. 2005. Bacterial persistence: a model of survival in changing environments. *Genetics*, **169**(4), 1807–1814.
- KVAAL, C., LACHKE, S. A., SRIKANTHA, T., DANIELS, K., MCCOY, J., & SOLL, D. R. 1999. Misexpression of the opaque-phase-specific gene PEP1 (SAP1) in the white phase of *Candida albicans* confers increased virulence in a mouse model of cutaneous infection. *Infect Immun*, **67**(12), 6652–6662.
- KVAAL, C. A., SRIKANTHA, T., & SOLL, D. R. 1997. Misexpression of the white-phase-specific gene WH11 in the opaque phase of *Candida albicans* affects switching and virulence. *Infect Immun*, **65**(11), 4468–4475.
- VAN HET HOOG, MARCO, RAST, TIMOTHY J, MARTCHENKO, MIKHAIL, GRINDLE, SUZANNE, DIGNARD, DANIEL, HOGUES, HERVÉ, CUOMO, CHRISTINE, BERRIMAN, MATTHEW, SCHERER, STEWART, MAGEE, B. B., WHITEWAY, MALCOLM, CHIBANA, HIROJI, NANTEL, ANDRÉ, & MAGEE, P. T. 2007. Assembly of the *Candida albicans* genome into sixteen supercontigs aligned on the eight chromosomes. *Genome Biol*, **8**(4), R52.
- LACHKE, S. A., SRIKANTHA, T., TSAI, L. K., DANIELS, K., & SOLL, D. R. 2000. Phenotypic switching in *Candida glabrata* involves phase-specific regulation of the metallothionein gene MT-II and the newly discovered hemolysin gene HLP. *Infect Immun*, **68**(2), 884–895.
- LACHKE, SALIL A, JOLY, SOPHIE, DANIELS, KARLA, & SOLL, DAVID R. 2002. Phenotypic switching and filamentation in *Candida glabrata*. *Microbiology*, **148**(Pt 9), 2661–2674.
- LAHIRI, MAYURIKA, GUSTAFSON, TANYA L, MAJORS, ELIZABETH R, & FREUDENREICH, CATHERINE H. 2004. Expanded CAG repeats activate the DNA damage checkpoint pathway. *Mol Cell*, **15**(2), 287–293.
- LAMB, T. M., XU, W., DIAMOND, A., & MITCHELL, A. P. 2001. Alkaline response genes of *Saccharomyces cerevisiae* and their relationship to the RIM101 pathway. *J Biol Chem*, **276**(3), 1850–1856.

- LAN, CHUNG-YU, NEWPORT, GEORGE, MURILLO, LUIS A, JONES, TED, SCHERER, STEWART, DAVIS, RONALD W, & AGABIAN, NINA. 2002. Metabolic specialization associated with phenotypic switching in *Candida albicans*. *Proc Natl Acad Sci U S A*, **99**(23), 14907–14912.
- LAW, D., MOORE, C. B., WARDLE, H. M., GANGULI, L. A., KEANEY, M. G., & DENNING, D. W. 1994. High prevalence of antifungal resistance in *Candida* spp. from patients with AIDS. *J Antimicrob Chemother*, **34**(5), 659–668.
- LEBERER, E., HARCUS, D., DIGNARD, D., JOHNSON, L., USHINSKY, S., THOMAS, D. Y., & SCHRÖPPEL, K. 2001. Ras links cellular morphogenesis to virulence by regulation of the MAP kinase and cAMP signalling pathways in the pathogenic fungus *Candida albicans*. *Mol Microbiol*, **42**(3), 673–687.
- LEE, C. H., SIDIK, K., & CHIN, K. V. 2001. Role of cAMP-dependent protein kinase in the regulation of DNA repair. *Cancer Lett*, **169**(1), 51–58.
- LEE, CHANG-MUK, NANTEL, ANDRÉ, JIANG, LINGHUO, WHITEWAY, MALCOLM, & SHEN, SHI-HSIANG. 2004a. The serine/threonine protein phosphatase SIT4 modulates yeast-to-hypha morphogenesis and virulence in *Candida albicans*. *Mol Microbiol*, **51**(3), 691–709.
- LEE, CHEOL-KOO, SHIBATA, YOICHIRO, RAO, BHARGAVI, STRAHL, BRIAN D, & LIEB, JASON D. 2004b. Evidence for nucleosome depletion at active regulatory regions genome-wide. *Nat Genet*, **36**(8), 900–905.
- LEGRAND, MELANIE, LEPHART, PAUL, FORCHE, ANJA, MUELLER, FRANK-MICHAEL C, WALSH, T., MAGEE, P. T., & MAGEE, BEATRICE B. 2004. Homozygosity at the MTL locus in clinical strains of *Candida albicans*: karyotypic rearrangements and tetraploid formation. *Mol Microbiol*, **52**(5), 1451–1462.
- LEGRAND, MELANIE, CHAN, CHRISTINE L, JAUERT, PETER A, & KIRKPATRICK, DAVID T. 2007. Role of DNA mismatch repair and double-strand break repair in genome stability and antifungal drug resistance in *Candida albicans*. *Eukaryot Cell*, **6**(12), 2194–2205.
- LEIDICH, S. D., IBRAHIM, A. S., FU, Y., KOUL, A., JESSUP, C., VITULLO, J., FONZI, W., MIRBOD, F., NAKASHIMA, S., NOZAWA, Y., & GHANNOUM, M. A. 1998. Cloning and disruption of caPLB1, a phospholipase B gene involved in the pathogenicity of *Candida albicans*. *J Biol Chem*, **273**(40), 26078–26086.
- LEMPIÄINEN, HARRI, UOTILA, AINO, URBAN, JÖRG, DOHNAL, ILSE, AMMERER, GUSTAV, LOEWITH, ROBBIE, & SHORE, DAVID. 2009. Sfp1 interaction with TORC1 and Mrs6 reveals feedback regulation on TOR signaling. *Mol Cell*, **33**(6), 704–716.
- LI, BING, CAREY, MICHAEL, & WORKMAN, JERRY L. 2007. The role of chromatin during transcription. *Cell*, **128**(4), 707–719.
- LI, YANDONG, SU, CHANG, MAO, XUMING, CAO, FANG, & CHEN, JIANGYE. 2007. Roles of *Candida albicans* Sfl1 in hyphal development. *Eukaryot Cell*, **6**(11), 2112–2121.
- LI, HONG, TSANG, CHI KWAN, WATKINS, MARCUS, BERTRAM, PAULA G, & ZHENG, X. F STEVEN. 2006. Nutrient regulates Tor1 nuclear localization and association with rDNA promoter. *Nature*, **442**(7106), 1058–1061.
- LIAO, WEI-LI, RAMÓN, ANA M, & FONZI, WILLIAM A. 2008. GLN3 encodes a global regulator of nitrogen metabolism and virulence of *C. albicans*. *Fungal Genet Biol*, **45**(4), 514–526.
- LIBUDA, DIANA E, & WINSTON, FRED. 2006. Amplification of histone genes by circular chromosome formation in *Saccharomyces cerevisiae*. *Nature*, **443**(7114), 1003–1007.
- LIFTON, R. P., GOLDBERG, M. L., KARP, R. W., & HOGNESS, D. S. 1978. The organization of the histone genes in *Drosophila melanogaster*: functional and evolutionary implications. *Cold Spring Harb Symp Quant Biol*, **42 Pt 2**, 1047–1051.
- LIN, LIN, IBRAHIM, ASHRAF S, XU, XIN, FARBER, JOSHUA M, AVANESIAN, VALENTINA, BAQUIR, BEVERLIE, FU, YUE, FRENCH, SAMUEL W, EDWARDS, JOHN E, & SPELLBERG, BRAD. 2009. Th1-Th17 cells mediate protective adaptive immunity against *Staphylococcus aureus* and *Candida albicans* infection in mice. *PLoS Pathog*, **5**(12), e1000703.

- LIU, H., KÖHLER, J., & FINK, G. R. 1994. Suppression of hyphal formation in *Candida albicans* by mutation of a STE12 homolog. *Science*, **266**(5191), 1723–1726.
- LIU, WEI, ZHAO, JINGWEN, LI, XICHUAN, LI, YUNXIANG, & JIANG, LINGHUO. 2010. The protein kinase CaSch9p is required for the cell growth, filamentation and virulence in the human fungal pathogen *Candida albicans*. *FEMS Yeast Res*, Mar.
- LO, H. J., KÖHLER, J. R., DIDOMENICO, B., LOEBENBERG, D., CACCIAPUOTI, A., & FINK, G. R. 1997. Nonfilamentous *C. albicans* mutants are avirulent. *Cell*, **90**(5), 939–949.
- LOEB, L. A. 2001. A mutator phenotype in cancer. *Cancer Res*, **61**(8), 3230–3239.
- LOEB, LAWRENCE A, BIELAS, JASON H, & BECKMAN, ROBERT A. 2008. Cancers exhibit a mutator phenotype: clinical implications. *Cancer Res*, **68**(10), 3551–7; discussion 3557.
- LOEWITH, ROBBIE, JACINTO, ESTELA, WULLSCHLEGER, STEPHAN, LORBERG, ANJA, CRESPO, JOSÉ L, BONENFANT, DÉBORA, OPPLIGER, WOLFGANG, JENOE, PAUL, & HALL, MICHAEL N. 2002. Two TOR complexes, only one of which is rapamycin sensitive, have distinct roles in cell growth control. *Mol Cell*, **10**(3), 457–468.
- LOHSE, MATTHEW B, & JOHNSON, ALEXANDER D. 2008. Differential phagocytosis of white versus opaque *Candida albicans* by *Drosophila* and mouse phagocytes. *PLoS One*, **3**(1), e1473.
- LOHSE, MATTHEW B, & JOHNSON, ALEXANDER D. 2009. White-opaque switching in *Candida albicans*. *Curr Opin Microbiol*, **12**(6), 650–654.
- LONGO, V. D. 1999. Mutations in signal transduction proteins increase stress resistance and longevity in yeast, nematodes, fruit flies, and mammalian neuronal cells. *Neurobiol Aging*, **20**(5), 479–486.
- LONGO, VALTER D, MITTELDORF, JOSHUA, & SKULACHEV, VLADIMIR P. 2005. Programmed and altruistic ageing. *Nat Rev Genet*, **6**(11), 866–872.
- LORENZ, M. C., & HEITMAN, J. 1995. TOR mutations confer rapamycin resistance by preventing interaction with FKBP12-rapamycin. *J Biol Chem*, **270**(46), 27531–27537.
- LORENZ, MICHAEL C, BENDER, JENNIFER A, & FINK, GERALD R. 2004. Transcriptional response of *Candida albicans* upon internalization by macrophages. *Eukaryot Cell*, **3**(5), 1076–1087.
- LÓPEZ-MIRABAL, H. REYNALDO, WINTHER, JAKOB R, & KIELLAND-BRANDT, MORTEN C. 2008. Oxidant resistance in a yeast mutant deficient in the Sit4 phosphatase. *Curr Genet*, **53**(5), 275–286.
- LU, YANG, SU, CHANG, MAO, XUMING, RANIGA, PRASHNA PALA, LIU, HAOPING, & CHEN, JIANGYE. 2008. Efg1-mediated recruitment of NuA4 to promoters is required for hypha-specific Swi/Snf binding and activation in *Candida albicans*. *Mol Biol Cell*, **19**(10), 4260–4272.
- LUKE, M. M., SETA, F. DELLA, COMO, C. J. DI, SUGIMOTO, H., KOBAYASHI, R., & ARNDT, K. T. 1996. The SAP, a new family of proteins, associate and function positively with the SIT4 phosphatase. *Mol Cell Biol*, **16**(6), 2744–2755.
- MA, BIAO, PAN, SHIH-JUNG, DOMERGUE, RENEE, RIGBY, TRACEY, WHITEWAY, MALCOLM, JOHNSON, DAVID, & CORMACK, BRENDAN P. 2009. High-affinity transporters for NAD<sup>+</sup> precursors in *Candida glabrata* are regulated by Hst1 and induced in response to niacin limitation. *Mol Cell Biol*, **29**(15), 4067–4079.
- MA, P., WERA, S., DIJCK, P. VAN, & THEVELEIN, J. M. 1999. The PDE1-encoded low-affinity phosphodiesterase in the yeast *Saccharomyces cerevisiae* has a specific function in controlling agonist-induced cAMP signaling. *Mol Biol Cell*, **10**(1), 91–104.
- MACORIS, S. A G, SUGIZAKI, M. F., PERAÇOLI, M. T S, BOSCO, S. M G, HEBELER-BARBOSA, F., SIMÕES, L. B., THEODORO, R. C., TRINCA, L. A., & BAGAGLI, E. 2006. Virulence attenuation and phenotypic variation of *Paracoccidioides brasiliensis* isolates obtained from armadillos and patients. *Mem Inst Oswaldo Cruz*, **101**(3), 331–334.

- MACPHERSON, SARAH, AKACHE, BASSEL, WEBER, SANDRA, DEKEN, XAVIER DE, RAYMOND, MARTINE, & TURCOTTE, BERNARD. 2005. *Candida albicans* zinc cluster protein Upc2p confers resistance to antifungal drugs and is an activator of ergosterol biosynthetic genes. *Antimicrob Agents Chemother*, **49**(5), 1745–1752.
- MADIA, FEDERICA, WEI, MIN, YUAN, VALERIE, HU, JIA, GATTAZZO, CRISTINA, PHAM, PHUONG, GOODMAN, MYRON F, & LONGO, VALTER D. 2009. Oncogene homologue Sch9 promotes age-dependent mutations by a superoxide and Rev1/Polzeta-dependent mechanism. *J Cell Biol*, **186**(4), 509–523.
- MAGASANIK, BORIS, & KAISER, CHRIS A. 2002. Nitrogen regulation in *Saccharomyces cerevisiae*. *Gene*, **290**(1-2), 1–18.
- MAGEE, P. T., BOWDIN, L., & STAUDINGER, J. 1992. Comparison of molecular typing methods for *Candida albicans*. *J Clin Microbiol*, **30**(10), 2674–2679.
- MAI, ANTONELLO, ROTILI, DANTE, MASSA, SILVIO, BROSCH, GERALD, SIMONETTI, GIOVANNA, PASSARIELLO, CLAUDIO, & PALAMARA, ANNA TERESA. 2007. Discovery of uracil-based histone deacetylase inhibitors able to reduce acquired antifungal resistance and trailing growth in *Candida albicans*. *Bioorg Med Chem Lett*, **17**(5), 1221–1225.
- MAIDAN, MYKOLA M, ROP, LARISSA DE, SERNEELS, JOKE, EXLER, SIMONE, RUPP, STEFFEN, TOURNU, HÉLÈNE, THEVELEIN, JOHAN M, & DIJCK, PATRICK VAN. 2005. The G protein-coupled receptor Gpr1 and the Galpha protein Gpa2 act through the cAMP-protein kinase A pathway to induce morphogenesis in *Candida albicans*. *Mol Biol Cell*, **16**(4), 1971–1986.
- MANLANDRO, CARA MARIE A, HAYDON, DEVON H, & ROSENWALD, ANNE G. 2005. Ability of Sit4p to promote K<sup>+</sup> efflux via Nha1p is modulated by Sap155p and Sap185p. *Eukaryot Cell*, **4**(6), 1041–1049.
- MAO, XUMING, CAO, FANG, NIE, XINYI, LIU, HAOPING, & CHEN, JIANGYE. 2006. The Swi/Snf chromatin remodeling complex is essential for hyphal development in *Candida albicans*. *FEBS Lett*, **580**(11), 2615–2622.
- MAO, XUMING, NIE, XINYI, CAO, FANG, & CHEN, JIANGYE. 2009. Functional analysis of ScSwi1 and CaSwi1 in invasive and pseudohyphal growth of *Saccharomyces cerevisiae*. *Acta Biochim Biophys Sin (Shanghai)*, **41**(7), 594–602.
- MARCELLO, LUCIO, & BARRY, J. DAVID. 2007. Analysis of the VSG gene silent archive in *Trypanosoma brucei* reveals that mosaic gene expression is prominent in antigenic variation and is favored by archive substructure. *Genome Res*, **17**(9), 1344–1352.
- MARTCHENKO, MIKHAIL, LEVITIN, ANASTASIA, HOGUES, HERVE, NANTEL, ANDRE, & WHITEWAY, MALCOLM. 2007. Transcriptional rewiring of fungal galactose-metabolism circuitry. *Curr Biol*, **17**(12), 1007–1013.
- MARTIN, DIETMAR E, & HALL, MICHAEL N. 2005. The expanding TOR signaling network. *Curr Opin Cell Biol*, **17**(2), 158–166.
- MARTIN, DIETMAR E, SOULARD, ALEXANDRE, & HALL, MICHAEL N. 2004. TOR regulates ribosomal protein gene expression via PKA and the Forkhead transcription factor FHL1. *Cell*, **119**(7), 969–979.
- MARTIN, DIETMAR E, POWERS, TED, & HALL, MICHAEL N. 2006. Regulation of ribosome biogenesis: where is TOR? *Cell Metab*, **4**(4), 259–260.
- MARTÍNEZ, PAULA, & LJUNGDAHL, PER O. 2005. Divergence of Stp1 and Stp2 transcription factors in *Candida albicans* places virulence factors required for proper nutrient acquisition under amino acid control. *Mol Cell Biol*, **25**(21), 9435–9446.
- MARTOGLIO, B., & DOBBERSTEIN, B. 1998. Signal sequences: more than just greasy peptides. *Trends Cell Biol*, **8**(10), 410–415.
- MARZLUF, G. A. 1997. Genetic regulation of nitrogen metabolism in the fungi. *Microbiol Mol Biol Rev*, **61**(1), 17–32.

- MASUDA, C. A., RAMÍREZ, J., PEÑA, A., & MONTERO-LOMELÍ, M. 2000. Regulation of monovalent ion homeostasis and pH by the Ser-Thr protein phosphatase SIT4 in *Saccharomyces cerevisiae*. *J Biol Chem*, **275**(40), 30957–30961.
- MATSUMOTO, S., & YANAGIDA, M. 1985. Histone gene organization of fission yeast: a common upstream sequence. *EMBO J*, **4**(13A), 3531–3538.
- MCDONALD, CHRISTINE M, WAGNER, MARISA, DUNHAM, MAITREYA J, SHIN, MARCUS E, AHMED, NOREEN T, & WINTER, EDWARD. 2009. The Ras/cAMP pathway and the CDK-like kinase Ime2 regulate the MAPK Smk1 and spore morphogenesis in *Saccharomyces cerevisiae*. *Genetics*, **181**(2), 511–523.
- MCKENZIE, G. J., & ROSENBERG, S. M. 2001. Adaptive mutations, mutator DNA polymerases and genetic change strategies of pathogens. *Curr Opin Microbiol*, **4**(5), 586–594.
- MCMAHON, LLOYD P, CHOI, KIN M, LIN, TAI-AN, ABRAHAM, ROBERT T, & LAWRENCE, JOHN C. 2002. The rapamycin-binding domain governs substrate selectivity by the mammalian target of rapamycin. *Mol Cell Biol*, **22**(21), 7428–7438.
- MEEKS-WAGNER, D., & HARTWELL, L. H. 1986. Normal stoichiometry of histone dimer sets is necessary for high fidelity of mitotic chromosome transmission. *Cell*, **44**(1), 43–52.
- MENON, S., & MANNING, B. D. 2008. Common corruption of the mTOR signaling network in human tumors. *Oncogene*, **27 Suppl 2**(Dec), S43–S51.
- MILLER, L. G., HAJJEH, R. A., & EDWARDS, J. E. 2001. Estimating the cost of nosocomial candidemia in the united states. *Clin Infect Dis*, **32**(7), 1110.
- MILLER, MATHEW G, & JOHNSON, ALEXANDER D. 2002. White-opaque switching in *Candida albicans* is controlled by mating-type locus homeodomain proteins and allows efficient mating. *Cell*, **110**(3), 293–302.
- MILLER, NANCY S, DICK, JAMES D, & MERZ, WILLIAM G. 2006. Phenotypic switching in *Candida lusitanae* on copper sulfate indicator agar: association with amphotericin B resistance and filamentation. *J Clin Microbiol*, **44**(4), 1536–1539.
- MIRANDA, ISABEL, ROCHA, RITA, SANTOS, MARIA C, MATEUS, DENISA D, MOURA, GABRIELA R, CARRETO, LAURA, & SANTOS, MANUEL A S. 2007. A genetic code alteration is a phenotype diversity generator in the human pathogen *Candida albicans*. *PLoS One*, **2**(10), e996.
- MITCHELL, A. P. 1998. Dimorphism and virulence in *Candida albicans*. *Curr Opin Microbiol*, **1**(6), 687–692.
- MITCHELL, AARON P. 2008. A VAST staging area for regulatory proteins. *Proc Natl Acad Sci U S A*, **105**(20), 7111–7112.
- MIWA, TAKUYA, TAKAGI, YUKINOBU, SHINOZAKI, MAKIKO, YUN, CHEOL-WON, SCHELL, WILEY A, PERFECT, JOHN R, KUMAGAI, HIDEHIKO, & TAMAKI, HISANORI. 2004. Gpr1, a putative G-protein-coupled receptor, regulates morphogenesis and hypha formation in the pathogenic fungus *Candida albicans*. *Eukaryot Cell*, **3**(4), 919–931.
- MONGE, R. ALONSO, ROMÁN, E., NOMBELA, C., & PLA, J. 2006. The MAP kinase signal transduction network in *Candida albicans*. *Microbiology*, **152**(Pt 4), 905–912.
- MONOD, M., TOGNI, G., HUBE, B., & SANGLARD, D. 1994. Multiplicity of genes encoding secreted aspartic proteinases in *Candida* species. *Mol Microbiol*, **13**(2), 357–368.
- MONOD, M., HUBE, B., HESS, D., & SANGLARD, D. 1998. Differential regulation of SAP8 and SAP9, which encode two new members of the secreted aspartic proteinase family in *Candida albicans*. *Microbiology*, **144** ( Pt 10)(Oct), 2731–2737.
- MOORE, GERALD D, SINCLAIR, DONALD A, & GRIGLIATTI, THOMAS A. 1983. Histone Gene Multiplicity and Position Effect Variegation in *DROSOPHILA MELANOGASTER*. *Genetics*, **105**(2), 327–344.

- MORAN, L., NORRIS, D., & OSLEY, M. A. 1990. A yeast H2A-H2B promoter can be regulated by changes in histone gene copy number. *Genes Dev*, **4**(5), 752–763.
- MORENO, C. S., PARK, S., NELSON, K., ASHBY, D., HUBALEK, F., LANE, W. S., & PALLAS, D. C. 2000. WD40 repeat proteins striatin and S/G(2) nuclear autoantigen are members of a novel family of calmodulin-binding proteins that associate with protein phosphatase 2A. *J Biol Chem*, **275**(8), 5257–5263.
- MORRISON, LIAM J, MARCELLO, LUCIO, & MCCULLOCH, RICHARD. 2009. Antigenic variation in the African trypanosome: molecular mechanisms and phenotypic complexity. *Cell Microbiol*, **11**(12), 1724–1734.
- MORROW, B., SRIKANTHA, T., & SOLL, D. R. 1992. Transcription of the gene for a pepsinogen, PEP1, is regulated by white-opaque switching in *Candida albicans*. *Mol Cell Biol*, **12**(7), 2997–3005.
- MORSCHHÄUSER, JOACHIM. 2010. Regulation of white-opaque switching in *Candida albicans*. *Med Microbiol Immunol*, Apr.
- MOURA, GABRIELA R, PAREDES, JOÃO A, & SANTOS, MANUEL A S. 2010. Development of the genetic code: insights from a fungal codon reassignment. *FEBS Lett*, **584**(2), 334–341.
- MOXON, E. R., RAINEY, P. B., NOWAK, M. A., & LENSKI, R. E. 1994. Adaptive evolution of highly mutable loci in pathogenic bacteria. *Curr Biol*, **4**(1), 24–33.
- MUMFORD, J. A. 2007. Vaccines and viral antigenic diversity. *Rev Sci Tech*, **26**(1), 69–90.
- MURAD, A. M., LENG, P., STRAFFON, M., WISHART, J., MACASKILL, S., MACCALLUM, D., SCHNELL, N., TALIBI, D., MARECHAL, D., TEKAIA, F., D'ENFERT, C., GAILLARDIN, C., ODDS, F. C., & BROWN, A. J. 2001. NRG1 represses yeast-hypha morphogenesis and hypha-specific gene expression in *Candida albicans*. *EMBO J*, **20**(17), 4742–4752.
- MÉTIVIER, RAPHAËL, PENOT, GRAZIELLA, HÜBNER, MICHAEL R, REID, GEORGE, BRAND, HEIKE, KOS, MARTIN, & GANNON, FRANK. 2003. Estrogen receptor-alpha directs ordered, cyclical, and combinatorial recruitment of cofactors on a natural target promoter. *Cell*, **115**(6), 751–763.
- NADAL, EULÀLIA DE, ZAPATER, MERITXELL, ALEPUZ, PAULA M, SUMOY, LAURO, MAS, GLÒRIA, & POSAS, FRANCESC. 2004. The MAPK Hog1 recruits Rpd3 histone deacetylase to activate osmoresponsive genes. *Nature*, **427**(6972), 370–374.
- NAGLIK, J. R., NEWPORT, G., WHITE, T. C., FERNANDES-NAGLIK, L. L., GREENSPAN, J. S., GREENSPAN, D., SWEET, S. P., CHALLACOMBE, S. J., & AGABIAN, N. 1999. In vivo analysis of secreted aspartyl proteinase expression in human oral candidiasis. *Infect Immun*, **67**(5), 2482–2490.
- NAGLIK, JULIAN R, CHALLACOMBE, STEPHEN J, & HUBE, BERNHARD. 2003. *Candida albicans* secreted aspartyl proteinases in virulence and pathogenesis. *Microbiol Mol Biol Rev*, **67**(3), 400–28, table of contents.
- PRINGLES ET AL., 1989. *Methods in Molecular Biology. Chapter 19: Fluorescence microscopy methods for yeast*. Academic Press.
- NANTEL, ANDRÉ, DIGNARD, DANIEL, BACHEWICH, CATHERINE, HARCUS, DOREEN, MARCIL, ANNE, BOUIN, ANNE-PASCALE, SENSEN, CHRISTOPH W, HOGUES, HERVÉ, VAN HET HOOG, MARCO, GORDON, PAUL, RIGBY, TRACEY, BENOIT, FRANÇOIS, TESSIER, DANIEL C, THOMAS, DAVID Y, & WHITEWAY, MALCOLM. 2002. Transcription profiling of *Candida albicans* cells undergoing the yeast-to-hyphal transition. *Mol Biol Cell*, **13**(10), 3452–3465.
- NAVARRO, M., & GULL, K. 2001. A pol I transcriptional body associated with VSG mono-allelic expression in *Trypanosoma brucei*. *Nature*, **414**(6865), 759–763.
- NEGRINI, SIMONA, GORGOLIS, VASSILIS G, & HALAZONETIS, THANOS D. 2010. Genomic instability—an evolving hallmark of cancer. *Nat Rev Mol Cell Biol*, **11**(3), 220–228.
- NEGRONI, P. 1935. Variacion hacia el tipo R de *Mycotorula albicans*. *Rev. Soc. Argent. Biol.*, **11**, 449–453.

- NETT, JENIEL E, SANCHEZ, HIRAM, CAIN, MICHAEL T, & ANDES, DAVID R. 2010. Genetic basis of *Candida* biofilm resistance due to drug-sequestering matrix glucan. *J Infect Dis*, **202**(1), 171–175.
- NIIMI, MASAKAZU, FIRTH, NORMAN A, & CANNON, RICHARD D. 2010. Antifungal drug resistance of oral fungi. *Odontology*, **98**(1), 15–25.
- NIKAWA, J., CAMERON, S., TODA, T., FERGUSON, K. M., & WIGLER, M. 1987. Rigorous feedback control of cAMP levels in *Saccharomyces cerevisiae*. *Genes Dev*, **1**(9), 931–937.
- NOBILE, CLARISSA J, & MITCHELL, AARON P. 2006. Genetics and genomics of *Candida albicans* biofilm formation. *Cell Microbiol*, **8**(9), 1382–1391.
- NOBILE, CLARISSA J, BRUNO, VINCENT M, RICHARD, MATHIAS L, DAVIS, DANA A, & MITCHELL, AARON P. 2003. Genetic control of chlamydospore formation in *Candida albicans*. *Microbiology*, **149**(Pt 12), 3629–3637.
- NOBILE, CLARISSA J, SCHNEIDER, HEATHER A, NETT, JENIEL E, SHEPPARD, DONALD C, FILLER, SCOTT G, ANDES, DAVID R, & MITCHELL, AARON P. 2008. Complementary adhesin function in *C. albicans* biofilm formation. *Curr Biol*, **18**(14), 1017–1024.
- NORRIS, D., & OSLEY, M. A. 1987. The two gene pairs encoding H2A and H2B play different roles in the *Saccharomyces cerevisiae* life cycle. *Mol Cell Biol*, **7**(10), 3473–3481.
- ODDS, E. C. 1997. Switch of phenotype as an escape mechanism of the intruder. *Mycoses*, **40 Suppl 2**, 9–12.
- ODDS, F.C. 1988. *Candida and candidosis: a review and bibliography*. Balliere and Tindcell.
- ODDS, FRANK C, BROWN, ALISTAIR J P, & GOW, NEIL A R. 2003. Antifungal agents: mechanisms of action. *Trends Microbiol*, **11**(6), 272–279.
- OGLE, JAMES M, & RAMAKRISHNAN, V. 2005. Structural insights into translational fidelity. *Annu Rev Biochem*, **74**, 129–177.
- OLIVER, A., CANTÓN, R., CAMPO, P., BAQUERO, F., & BLÁZQUEZ, J. 2000. High frequency of hypermutable *Pseudomonas aeruginosa* in cystic fibrosis lung infection. *Science*, **288**(5469), 1251–1254.
- OLLERT, M. W., WENDE, C., GÖRLICH, M., McMULLAN-VOGEL, C. G., VON ZEPELIN, M. BORG, VOGEL, C. W., & KORTING, H. C. 1995. Increased expression of *Candida albicans* secretory proteinase, a putative virulence factor, in isolates from human immunodeficiency virus-positive patients. *J Clin Microbiol*, **33**(10), 2543–2549.
- O'MEARA, TERESA R, NORTON, DIANA, PRICE, MICHAEL S, HAY, CHRISTIE, CLEMENTS, MEREDITH F, NICHOLS, CONNIE B, & ALSPAUGH, J. ANDREW. 2010. Interaction of *Cryptococcus neoformans* Rim101 and protein kinase A regulates capsule. *PLoS Pathog*, **6**(2), e1000776.
- OSLEY, M. A. 1991. The regulation of histone synthesis in the cell cycle. *Annu Rev Biochem*, **60**, 827–861.
- OZBUDAK, ERTUGRUL M, THATTAI, MUKUND, KURTSEY, IREN, GROSSMAN, ALAN D, & VAN OUDENAARDEN, ALEXANDER. 2002. Regulation of noise in the expression of a single gene. *Nat Genet*, **31**(1), 69–73.
- PARKER, J. 1989. Errors and alternatives in reading the universal genetic code. *Microbiol Rev*, **53**(3), 273–298.
- PAYS, E., GUYAUX, M., AERTS, D., MEIRVENNE, N. VAN, & STEINERT, M. 1985. Telomeric reciprocal recombination as a possible mechanism for antigenic variation in trypanosomes. *Nature*, **316**(6028), 562–564.
- PEÑAS, ALEJANDRO DE LAS, PAN, SHIH-JUNG, CASTAÑO, IRENE, ALDER, JONATHAN, CREGG, ROBERT, & CORMACK, BRENDAN P. 2003. Virulence-related surface glycoproteins in the yeast pathogen *Candida glabrata* are encoded in subtelomeric clusters and subject to RAP1- and SIR-dependent transcriptional silencing. *Genes Dev*, **17**(18), 2245–2258.

- PEETERS, TOM, VERSELE, MATTHIAS, & THEVELEIN, JOHAN M. 2007. Directly from Galpha to protein kinase A: the kelch repeat protein bypass of adenylate cyclase. *Trends Biochem Sci*, **32**(12), 547–554.
- PELKMANS, LUCAS, FAVA, EUGENIO, GRABNER, HANNES, HANNUS, MICHAEL, HABERMANN, BIANCA, KRAUSZ, EBERHARD, & ZERIAL, MARINO. 2005. Genome-wide analysis of human kinases in clathrin- and caveolae/raft-mediated endocytosis. *Nature*, **436**(7047), 78–86.
- PENDRAK, MICHAEL L, YAN, S. STEVE, & ROBERTS, DAVID D. 2004. Hemoglobin regulates expression of an activator of mating-type locus alpha genes in *Candida albicans*. *Eukaryot Cell*, **3**(3), 764–775.
- PEREPNIKHATKA, V., FISCHER, F. J., NIIMI, M., BAKER, R. A., CANNON, R. D., WANG, Y. K., SHERMAN, F., & RUSTCHENKO, E. 1999. Specific chromosome alterations in fluconazole-resistant mutants of *Candida albicans*. *J Bacteriol*, **181**(13), 4041–4049.
- PEREZ-TORRADO, ROBERTO, YAMADA, DAISUKE, & DEFOSSEZ, PIERRE-ANTOINE. 2006. Born to bind: the BTB protein-protein interaction domain. *Bioessays*, **28**(12), 1194–1202.
- PFALLER, M., & WENZEL, R. 1992. Impact of the changing epidemiology of fungal infections in the 1990s. *Eur J Clin Microbiol Infect Dis*, **11**(4), 287–291.
- PFALLER, M. A., RHINE-CHALBERG, J., REDDING, S. W., SMITH, J., FARINACCI, G., FOTHERGILL, A. W., & RINALDI, M. G. 1994. Variations in fluconazole susceptibility and electrophoretic karyotype among oral isolates of *Candida albicans* from patients with AIDS and oral candidiasis. *J Clin Microbiol*, **32**(1), 59–64.
- PFALLER, M. A., JONES, R. N., DOERN, G. V., FLUIT, A. C., VERHOEF, J., SADER, H. S., MESSER, S. A., HOUSTON, A., COFFMAN, S., & HOLLIS, R. J. 1999. International surveillance of blood stream infections due to *Candida* species in the European SENTRY Program: species distribution and antifungal susceptibility including the investigational triazole and echinocandin agents. SENTRY Participant Group (Europe). *Diagn Microbiol Infect Dis*, **35**(1), 19–25.
- PFALLER, M. A., DIEKEMA, D. J., JONES, R. N., SADER, H. S., FLUIT, A. C., HOLLIS, R. J., MESSER, S. A., & GROUP, S. E. N. T. R. Y. PARTICIPANT. 2001. International surveillance of bloodstream infections due to *Candida* species: frequency of occurrence and in vitro susceptibilities to fluconazole, ravuconazole, and voriconazole of isolates collected from 1997 through 1999 in the SENTRY antimicrobial surveillance program. *J Clin Microbiol*, **39**(9), 3254–3259.
- PFALLER, M. A. 1996. Nosocomial candidiasis: emerging species, reservoirs, and modes of transmission. *Clin Infect Dis*, **22 Suppl 2**(May), S89–S94.
- PFALLER, M. A., MESSER, S. A., HOUSTON, A., RANGEL-FRAUSTO, M. S., WIBLIN, T., BLUMBERG, H. M., EDWARDS, J. E., JARVIS, W., MARTIN, M. A., NEU, H. C., SAIMAN, L., PATTERSON, J. E., DIBB, J. C., ROLDAN, C. M., RINALDI, M. G., & WENZEL, R. P. 1998. National epidemiology of mycoses survey: a multicenter study of strain variation and antifungal susceptibility among isolates of *Candida* species. *Diagn Microbiol Infect Dis*, **31**(1), 289–296.
- PFALLER, M. A., MESSER, S. A., GEORGOPAPADAKOU, N., MARTELL, L. A., BESTERMAN, J. M., & DIEKEMA, D. J. 2009. Combination Testing of MGCD290, a Hos2 Histone Deacetylase Inhibitor, with Azole Antifungals against Opportunistic Fungal Pathogens. *J Clin Microbiol*, Sep.
- PHAN, QUYNH T, MYERS, CARTER L, FU, YUE, SHEPPARD, DONALD C, YEAMAN, MICHAEL R, WELCH, WILLIAM H, IBRAHIM, ASHRAF S, EDWARDS, JOHN E, & FILLER, SCOTT G. 2007. Als3 is a *Candida albicans* invasin that binds to cadherins and induces endocytosis by host cells. *PLoS Biol*, **5**(3), e64.
- PLEISS, JEFFREY A, WHITWORTH, GREGG B, BERGKESSEL, MEGAN, & GUTHRIE, CHRISTINE. 2007. Rapid, transcript-specific changes in splicing in response to environmental stress. *Mol Cell*, **27**(6), 928–937.
- POMÉS, R., GIL, C., & NOMBELA, C. 1985. Genetic analysis of *Candida albicans* morphological mutants. *J Gen Microbiol*, **131**(8), 2107–2113.
- POWERS, T., & WALTER, P. 1999. Regulation of ribosome biogenesis by the rapamycin-sensitive TOR-signaling pathway in *Saccharomyces cerevisiae*. *Mol Biol Cell*, **10**(4), 987–1000.

- POWERS, R. WILSON, KAEBERLEIN, MATT, CALDWELL, SETH D, KENNEDY, BRIAN K, & FIELDS, STANLEY. 2006. Extension of chronological life span in yeast by decreased TOR pathway signaling. *Genes Dev*, **20**(2), 174–184.
- PRADO, FÉLIX, & AGUILERA, ANDRÉS. 2005. Partial depletion of histone H4 increases homologous recombination-mediated genetic instability. *Mol Cell Biol*, **25**(4), 1526–1536.
- PRAG, SOREN, & ADAMS, JOSEPHINE C. 2003. Molecular phylogeny of the kelch-repeat superfamily reveals an expansion of BTB/kelch proteins in animals. *BMC Bioinformatics*, **4**(Sep), 42.
- PRASAD, K. N., COLE, W. C., YAN, X-D., NAHREINI, P., KUMAR, B., HANSON, A., & PRASAD, J. E. 2003. Defects in cAMP-pathway may initiate carcinogenesis in dividing nerve cells: a review. *Apoptosis*, **8**(6), 579–586.
- PRUSS, D., HAYES, J. J., & WOLFFE, A. P. 1995. Nucleosomal anatomy—where are the histones? *Bioessays*, **17**(2), 161–170.
- PUGH, D., & CAWSON, R. A. 1977. The cytochemical localization of phospholipase in *Candida albicans* infecting the chick chorio-allantoic membrane. *Sabouraudia*, **15**(1), 29–35.
- PURIA, REKHA, ZURITA-MARTINEZ, SARA A, & CARDENAS, MARIA E. 2008. Nuclear translocation of Gln3 in response to nutrient signals requires Golgi-to-endosome trafficking in *Saccharomyces cerevisiae*. *Proc Natl Acad Sci U S A*, **105**(20), 7194–7199.
- QUEITSCH, CHRISTINE, SANGSTER, TODD A, & LINDQUIST, SUSAN. 2002. Hsp90 as a capacitor of phenotypic variation. *Nature*, **417**(6889), 618–624.
- RADFORD, D. R., CHALLACOMBE, S. J., & WALTER, J. D. 1994. A scanning electronmicroscopy investigation of the structure of colonies of different morphologies produced by phenotypic switching of *Candida albicans*. *J Med Microbiol*, **40**(6), 416–423.
- RALPH, STUART A, & SCHERF, ARTUR. 2005. The epigenetic control of antigenic variation in *Plasmodium falciparum*. *Curr Opin Microbiol*, **8**(4), 434–440.
- RAMAN, SURESH BABU, NGUYEN, M. HONG, ZHANG, ZONGDE, CHENG, SHAOJI, JIA, HONG YAN, WEISNER, NGHE, ICZKOWSKI, KENNETH, & CLANCY, CORNELIUS J. 2006. *Candida albicans* SET1 encodes a histone 3 lysine 4 methyltransferase that contributes to the pathogenesis of invasive candidiasis. *Mol Microbiol*, **60**(3), 697–709.
- RAMÍREZ-ZAVALA, BERNARDO, REUSS, OLIVER, PARK, YANG-NIM, OHLSEN, KNUT, & MORSCHHÄUSER, JOACHIM. 2008. Environmental induction of white-opaque switching in *Candida albicans*. *PLoS Pathog*, **4**(6), e1000089.
- RAMSEY, H., MORROW, B., & SOLL, D. R. 1994. An increase in switching frequency correlates with an increase in recombination of the ribosomal chromosomes of *Candida albicans* strain 3153A. *Microbiology*, **140** ( Pt 7)(Jul), 1525–1531.
- RASER, JONATHAN M, & O'SHEA, ERIN K. 2005. Noise in gene expression: origins, consequences, and control. *Science*, **309**(5743), 2010–2013.
- RECHSTEINER, M., & ROGERS, S. W. 1996. PEST sequences and regulation by proteolysis. *Trends Biochem Sci*, **21**(7), 267–271.
- REID, GEORGE, GALLAIS, ROZENN, & MÉTIVIER, RAPHAËL. 2009. Marking time: the dynamic role of chromatin and covalent modification in transcription. *Int J Biochem Cell Biol*, **41**(1), 155–163.
- REINDERS, JOERG, ZAHEDI, RENÉ P, PFANNER, NIKOLAUS, MEISINGER, CHRIS, & SICKMANN, ALBERT. 2006. Toward the complete yeast mitochondrial proteome: multidimensional separation techniques for mitochondrial proteomics. *J Proteome Res*, **5**(7), 1543–1554.
- REINKE, AARON, ANDERSON, SCOTT, MCCAFFERY, J. MICHAEL, YATES, JOHN, ARONOVA, SOFIA, CHU, STEPHANIE, FAIRCLOUGH, STEPHEN, IVERSON, CORY, WEDAMAN, KAREN P, & POWERS, TED. 2004. TOR

- complex 1 includes a novel component, Tco89p (YPL180w), and cooperates with Ssd1p to maintain cellular integrity in *Saccharomyces cerevisiae*. *J Biol Chem*, **279**(15), 14752–14762.
- VAN DER REST, M. E., KAMMINGA, A. H., NAKANO, A., ANRAKU, Y., POOLMAN, B., & KONINGS, W. N. 1995. The plasma membrane of *Saccharomyces cerevisiae*: structure, function, and biogenesis. *Microbiol Rev*, **59**(2), 304–322.
- RICHARD, MATHIAS L, NOBILE, CLARISSA J, BRUNO, VINCENT M, & MITCHELL, AARON P. 2005. *Candida albicans* biofilm-defective mutants. *Eukaryot Cell*, **4**(8), 1493–1502.
- RIKKERINK, E. H., MAGEE, B. B., & MAGEE, P. T. 1988. Opaque-white phenotype transition: a programmed morphological transition in *Candida albicans*. *J Bacteriol*, **170**(2), 895–899.
- ROBERT, FRANÇOIS, POKHOLOK, DMITRY K, HANNETT, NANCY M, RINALDI, NICOLA J, CHANDY, MARK, ROLFE, ALEX, WORKMAN, JERRY L, GIFFORD, DAVID K, & YOUNG, RICHARD A. 2004. Global position and recruitment of HATs and HDACs in the yeast genome. *Mol Cell*, **16**(2), 199–209.
- ROBYR, DANIEL, SUKA, YUKO, XENARIOS, IOANNIS, KURDISTANI, SIAVASH K, WANG, AMY, SUKA, NORIYUKI, & GRUNSTEIN, MICHAEL. 2002. Microarray deacetylation maps determine genome-wide functions for yeast histone deacetylases. *Cell*, **109**(4), 437–446.
- ROGERS, S., WELLS, R., & RECHSTEINER, M. 1986. Amino acid sequences common to rapidly degraded proteins: the PEST hypothesis. *Science*, **234**(4774), 364–368.
- ROHDE, J., HEITMAN, J., & CARDENAS, M. E. 2001. The TOR kinases link nutrient sensing to cell growth. *J Biol Chem*, **276**(13), 9583–9586.
- ROHDE, J. R., & CARDENAS, M. E. 2004. Nutrient signaling through TOR kinases controls gene expression and cellular differentiation in fungi. *Curr Top Microbiol Immunol*, **279**, 53–72.
- ROHDE, JOHN R, & CARDENAS, MARIA E. 2003. The tor pathway regulates gene expression by linking nutrient sensing to histone acetylation. *Mol Cell Biol*, **23**(2), 629–635.
- ROHDE, JOHN R, CAMPBELL, SUSAN, ZURITA-MARTINEZ, SARA A, CUTLER, N. SHANE, ASHE, MARK, & CARDENAS, MARIA E. 2004. TOR controls transcriptional and translational programs via Sap-Sit4 protein phosphatase signaling effectors. *Mol Cell Biol*, **24**(19), 8332–8341.
- ROHDE, JOHN R, BASTIDAS, ROBERT, PURIA, REKHA, & CARDENAS, MARIA E. 2008. Nutritional control via Tor signaling in *Saccharomyces cerevisiae*. *Curr Opin Microbiol*, **11**(2), 153–160.
- ROMANI, LUIGINA. 2004. Immunity to fungal infections. *Nat Rev Immunol*, **4**(1), 1–23.
- ROMANI, LUIGINA, BISTONI, FRANCESCO, & PUCETTI, PAOLO. 2003. Adaptation of *Candida albicans* to the host environment: the role of morphogenesis in virulence and survival in mammalian hosts. *Curr Opin Microbiol*, **6**(4), 338–343.
- DA ROSA, JESSICA LOPES, BOYARTCHUK, VICTOR L, ZHU, LIHUA JULIE, & KAUFMAN, PAUL D. 2010. Histone acetyltransferase Rtt109 is required for *Candida albicans* pathogenesis. *Proc Natl Acad Sci U S A*, **107**(4), 1594–1599.
- ROSENBERG, S. M. 2001. Evolving responsively: adaptive mutation. *Nat Rev Genet*, **2**(7), 504–515.
- RUSTCHENKO, E. P., CURRAN, T. M., & SHERMAN, F. 1993. Variations in the number of ribosomal DNA units in morphological mutants and normal strains of *Candida albicans* and in normal strains of *Saccharomyces cerevisiae*. *J Bacteriol*, **175**(22), 7189–7199.
- RUSTCHENKO, E. P., HOWARD, D. H., & SHERMAN, F. 1994. Chromosomal alterations of *Candida albicans* are associated with the gain and loss of assimilating functions. *J Bacteriol*, **176**(11), 3231–3241.
- RUSTCHENKO, ELENA. 2007. Chromosome instability in *Candida albicans*. *FEMS Yeast Res*, **7**(1), 2–11.
- RUSTCHENKO-BULGAC, E. P., & HOWARD, D. H. 1993. Multiple chromosomal and phenotypic changes in spontaneous mutants of *Candida albicans*. *J Gen Microbiol*, **139 Pt 6**(Jun), 1195–1207.

- RUTHERFORD, JULIAN C, CHUA, GORDON, HUGHES, TIMOTHY, CARDENAS, MARIA E, & HEITMAN, JOSEPH. 2008. A Mep2-dependent transcriptional profile links permease function to gene expression during pseudohyphal growth in *Saccharomyces cerevisiae*. *Mol Biol Cell*, **19**(7), 3028–3039.
- RUTHERFORD, S. L., & LINDQUIST, S. 1998. Hsp90 as a capacitor for morphological evolution. *Nature*, **396**(6709), 336–342.
- SAMONIS, G., & BAFALOUKOS, D. 1992. Fungal infections in cancer patients: an escalating problem. *In Vivo*, **6**(2), 183–193.
- SANGLARD, DOMINIQUE, COSTE, ALIX, & FERRARI, SÉLÈNE. 2009. Antifungal drug resistance mechanisms in fungal pathogens from the perspective of transcriptional gene regulation. *FEMS Yeast Res*, **9**(7), 1029–1050.
- SANTHANAM, ARTI, HARTLEY, ALAN, DÜVEL, KATRIN, BROACH, JAMES R, & GARRETT, STEPHEN. 2004. PP2A phosphatase activity is required for stress and Tor kinase regulation of yeast stress response factor Msn2p. *Eukaryot Cell*, **3**(5), 1261–1271.
- SANTOS, M. A., & TUIITE, M. F. 1995. The CUG codon is decoded in vivo as serine and not leucine in *Candida albicans*. *Nucleic Acids Res*, **23**(9), 1481–1486.
- SAUNDERS, M. J., YEH, E., GRUNSTEIN, M., & BLOOM, K. 1990. Nucleosome depletion alters the chromatin structure of *Saccharomyces cerevisiae* centromeres. *Mol Cell Biol*, **10**(11), 5721–5727.
- SAVILLE, STEPHEN P, LAZZELL, ANNA L, MONTEAGUDO, CARLOS, & LOPEZ-RIBOT, JOSE L. 2003. Engineered control of cell morphology in vivo reveals distinct roles for yeast and filamentous forms of *Candida albicans* during infection. *Eukaryot Cell*, **2**(5), 1053–1060.
- SAVILLE, STEPHEN P, LAZZELL, ANNA L, CHATURVEDI, ASHOK K, MONTEAGUDO, CARLOS, & LOPEZ-RIBOT, JOSE L. 2008. Use of a genetically engineered strain to evaluate the pathogenic potential of yeast cell and filamentous forms during *Candida albicans* systemic infection in immunodeficient mice. *Infect Immun*, **76**(1), 97–102.
- SCHALLER, MARTIN, BORELLI, CLAUDIA, KORTING, HANS C, & HUBE, BERNHARD. 2005. Hydrolytic enzymes as virulence factors of *Candida albicans*. *Mycoses*, **48**(6), 365–377.
- SCHERER, S., & STEVENS, D. A. 1988. A *Candida albicans* dispersed, repeated gene family and its epidemiologic applications. *Proc Natl Acad Sci U S A*, **85**(5), 1452–1456.
- SCIASCIA, QUENTIN L, SULLIVAN, PATRICK A, & FARLEY, PETER C. 2004. Deletion of the *Candida albicans* G-protein-coupled receptor, encoded by orf19.1944 and its allele orf19.9499, produces mutants defective in filamentous growth. *Can J Microbiol*, **50**(12), 1081–1085.
- SCHMELZLE, T., & HALL, M. N. 2000. TOR, a central controller of cell growth. *Cell*, **103**(2), 253–262.
- SCHMELZLE, TOBIAS, BECK, THOMAS, MARTIN, DIETMAR E, & HALL, MICHAEL N. 2004. Activation of the RAS/cyclic AMP pathway suppresses a TOR deficiency in yeast. *Mol Cell Biol*, **24**(1), 338–351.
- SCHMIDT, A., BECK, T., KOLLER, A., KUNZ, J., & HALL, M. N. 1998. The TOR nutrient signalling pathway phosphorylates NPR1 and inhibits turnover of the tryptophan permease. *EMBO J*, **17**(23), 6924–6931.
- SEARLE, JENNIFER S, & SANCHEZ, YOLANDA. 2004. Stopped for repairs: a new role for nutrient sensing pathways? *Cell Cycle*, **3**(7), 865–868.
- SEARLE, JENNIFER S, SCHOLLAERT, KAILA L, WILKINS, BENJAMIN J, & SANCHEZ, YOLANDA. 2004. The DNA damage checkpoint and PKA pathways converge on APC substrates and Cdc20 to regulate mitotic progression. *Nat Cell Biol*, **6**(2), 138–145.
- SELLAM, ADNANE, ASKEW, CHRISTOPHER, EPP, ELIAS, LAVOIE, HUGO, WHITEWAY, MALCOLM, & NANTEL, ANDRÉ. 2009. Genome-wide mapping of the coactivator Ada2p yields insight into the functional roles of SAGA/ADA complex in *Candida albicans*. *Mol Biol Cell*, **20**(9), 2389–2400.

- SELMECKI, ANNA, BERGMANN, SVEN, & BERMAN, JUDITH. 2005. Comparative genome hybridization reveals widespread aneuploidy in *Candida albicans* laboratory strains. *Mol Microbiol*, **55**(5), 1553–1565.
- SELMECKI, ANNA, FORCHE, ANJA, & BERMAN, JUDITH. 2006. Aneuploidy and isochromosome formation in drug-resistant *Candida albicans*. *Science*, **313**(5785), 367–370.
- SELMECKI, ANNA, GERAMI-NEJAD, MARYAM, PAULSON, CARSTEN, FORCHE, ANJA, & BERMAN, JUDITH. 2008. An isochromosome confers drug resistance in vivo by amplification of two genes, ERG11 and TAC1. *Mol Microbiol*, **68**(3), 624–641.
- SELMECKI, ANNA M, DULMAGE, KEELY, COWEN, LEAH E, ANDERSON, JAMES B, & BERMAN, JUDITH. 2009. Acquisition of aneuploidy provides increased fitness during the evolution of antifungal drug resistance. *PLoS Genet*, **5**(10), e1000705.
- SHAMJI, A. F., KURUVILLA, F. G., & SCHREIBER, S. L. 2000. Partitioning the transcriptional program induced by rapamycin among the effectors of the Tor proteins. *Curr Biol*, **10**(24), 1574–1581.
- SHAPIRO, REBECCA S, UPPULURI, PRIYA, ZAAS, AIMEE K, COLLINS, CATHY, SENN, HEATHER, PERFECT, JOHN R, HEITMAN, JOSEPH, & COWEN, LEAH E. 2009. Hsp90 orchestrates temperature-dependent *Candida albicans* morphogenesis via Ras1-PKA signaling. *Curr Biol*, **19**(8), 621–629.
- SHAW, REUBEN J, & CANTLEY, LEWIS C. 2006. Ras, PI(3)K and mTOR signalling controls tumour cell growth. *Nature*, **441**(7092), 424–430.
- SHEN, CHANGXIAN, LANCASTER, CYNTHIA S, SHI, BIN, GUO, HONG, THIMMAIAH, PADMA, & BJORNSTI, MARY-ANN. 2007. TOR signaling is a determinant of cell survival in response to DNA damage. *Mol Cell Biol*, **27**(20), 7007–7017.
- SICKMANN, ALBERT, REINDERS, JÖRG, WAGNER, YVONNE, JOPPICH, CORNELIA, ZAHEDI, RENÉ, MEYER, HELMUT E, SCHÖNFISCH, BIRGIT, PERSCHIL, INGE, CHACINSKA, AGNIESZKA, GUIARD, BERNARD, REHLING, PETER, PFANNER, NIKOLAUS, & MEISINGER, CHRIS. 2003. The proteome of *Saccharomyces cerevisiae* mitochondria. *Proc Natl Acad Sci U S A*, **100**(23), 13207–13212.
- SILVERMAN, M., ZIEG, J., HILMEN, M., & SIMON, M. 1979. Phase variation in *Salmonella*: genetic analysis of a recombinational switch. *Proc Natl Acad Sci U S A*, **76**(1), 391–395.
- SIMONETTI, GIOVANNA, PASSARIELLO, CLAUDIO, ROTILI, DANTE, MAI, ANTONELLO, GARACI, ENRICO, & PALAMARA, ANNA TERESA. 2007. Histone deacetylase inhibitors may reduce pathogenicity and virulence in *Candida albicans*. *FEMS Yeast Res*, **7**(8), 1371–1380.
- SKERKER, JEFFREY M, & LAUB, MICHAEL T. 2004. Cell-cycle progression and the generation of asymmetry in *Caulobacter crescentus*. *Nat Rev Microbiol*, **2**(4), 325–337.
- SLESSAREVA, JANNA E, ROUTH, SHERI M, TEMPLE, BRENDA, BANKAITIS, VYTAS A, & DOHLMAN, HENRIK G. 2006. Activation of the phosphatidylinositol 3-kinase Vps34 by a G protein alpha subunit at the endosome. *Cell*, **126**(1), 191–203.
- SLUTSKY, B., BUFFO, J., & SOLL, D. R. 1985. High-frequency switching of colony morphology in *Candida albicans*. *Science*, **230**(4726), 666–669.
- SLUTSKY, B., STAEBELL, M., ANDERSON, J., RISEN, L., PFALLER, M., & SOLL, D. R. 1987. "White-opaque transition": a second high-frequency switching system in *Candida albicans*. *J Bacteriol*, **169**(1), 189–197.
- SMITH, J. D., CHITNIS, C. E., CRAIG, A. G., ROBERTS, D. J., HUDSON-TAYLOR, D. E., PETERSON, D. S., PINCHES, R., NEWBOLD, C. I., & MILLER, L. H. 1995. Switches in expression of *Plasmodium falciparum* var genes correlate with changes in antigenic and cytoadherent phenotypes of infected erythrocytes. *Cell*, **82**(1), 101–110.
- SMITH, M. M., & ANDRÉSSON, O. S. 1983. DNA sequences of yeast H3 and H4 histone genes from two non-allelic gene sets encode identical H3 and H4 proteins. *J Mol Biol*, **169**(3), 663–690.
- SMITH, M. M., & STIRLING, V. B. 1988. Histone H3 and H4 gene deletions in *Saccharomyces cerevisiae*. *J Cell Biol*, **106**(3), 557–566.

- SMITH, M. M., YANG, P., SANTISTEBAN, M. S., BOONE, P. W., GOLDSTEIN, A. T., & MEGEE, P. C. 1996. A novel histone H4 mutant defective in nuclear division and mitotic chromosome transmission. *Mol Cell Biol*, **16**(3), 1017–1026.
- SMITH, W. LAMAR, & EDLIND, THOMAS D. 2002. Histone deacetylase inhibitors enhance *Candida albicans* sensitivity to azoles and related antifungals: correlation with reduction in CDR and ERG upregulation. *Antimicrob Agents Chemother*, **46**(11), 3532–3539.
- SMUKALLA, SCOTT, CALDARA, MARINA, POCHE, NATHALIE, BEAUVAIS, ANNE, GUADAGNINI, STEPHANIE, YAN, CHEN, VINCES, MARCELO D, JANSEN, AN, PREVOST, MARIE CHRISTINE, LATGÉ, JEAN-PAUL, FINK, GERALD R, FOSTER, KEVIN R, & VERSTREPEN, KEVIN J. 2008. FLO1 is a variable green beard gene that drives biofilm-like cooperation in budding yeast. *Cell*, **135**(4), 726–737.
- SOBEL, J. D. 1992. Pathogenesis and treatment of recurrent vulvovaginal candidiasis. *Clin Infect Dis*, **14** Suppl 1(Mar), S148–S153.
- SOLL, D. R. 1992. High-frequency switching in *Candida albicans*. *Clin Microbiol Rev*, **5**(2), 183–203.
- SOLL, D. R., LANGTIMM, C. J., MCDOWELL, J., HICKS, J., & GALASK, R. 1987. High-frequency switching in *Candida* strains isolated from vaginitis patients. *J Clin Microbiol*, **25**(9), 1611–1622.
- SOLL, D. R., STAEBELL, M., LANGTIMM, C., PFALLER, M., HICKS, J., & RAO, T. V. 1988. Multiple *Candida* strains in the course of a single systemic infection. *J Clin Microbiol*, **26**(8), 1448–1459.
- SOLL, D. R., GALASK, R., ISLEY, S., RAO, T. V., STONE, D., HICKS, J., SCHMID, J., MAC, K., & HANNA, C. 1989. Switching of *Candida albicans* during successive episodes of recurrent vaginitis. *J Clin Microbiol*, **27**(4), 681–690.
- SOLL, DAVID R. 2002. *Candida* commensalism and virulence: the evolution of phenotypic plasticity. *Acta Trop*, **81**(2), 101–110.
- SOLLARS, VINCENT, LU, XIANGYI, XIAO, LI, WANG, XIAOYAN, GARFINKEL, MARK D, & RUDEN, DOUGLAS M. 2003. Evidence for an epigenetic mechanism by which Hsp90 acts as a capacitor for morphological evolution. *Nat Genet*, **33**(1), 70–74.
- SONNEBORN, A., BOCKMÜHL, D. P., GERADS, M., KURPANEK, K., SANGLARD, D., & ERNST, J. F. 2000. Protein kinase A encoded by TPK2 regulates dimorphism of *Candida albicans*. *Mol Microbiol*, **35**(2), 386–396.
- SOULARD, ALEXANDRE, CREMONESI, ALESSIO, MOES, SUZETTE, SCHÜTZ, FRÉDÉRIC, JENÖ, PAUL, & HALL, MICHAEL N. 2010. The Rapamycin-sensitive Phosphoproteome Reveals That TOR Controls PKA Toward Some but Not All Substrates. *Mol Biol Cell*, Aug.
- SOUTO, GUADALUPE, GIACOMETTI, ROMINA, SILBERSTEIN, SUSANA, GIASSON, LUC, CANTORE, MARÍA LEONOR, & PASSERON, SUSANA. 2006. Expression of TPK1 and TPK2 genes encoding PKA catalytic subunits during growth and morphogenesis in *Candida albicans*. *Yeast*, **23**(8), 591–603.
- SRIKANTHA, T., TSAI, L., DANIELS, K., KLAR, A. J., & SOLL, D. R. 2001. The histone deacetylase genes HDA1 and RPD3 play distinct roles in regulation of high-frequency phenotypic switching in *Candida albicans*. *J Bacteriol*, **183**(15), 4614–4625.
- SRIKANTHA, THYAGARAJAN, DANIELS, KARLA J, WU, WEI, LOCKHART, SHAWN R, YI, SONG, SAHNI, NIDHI, MA, NING, & SOLL, DAVID R. 2008. Dark brown is the more virulent of the switch phenotypes of *Candida glabrata*. *Microbiology*, **154**(Pt 11), 3309–3318.
- SRIRAM, K., SOLIMAN, SYLVAIN, & FAGES, FRANÇOIS. 2009. Dynamics of the interlocked positive feedback loops explaining the robust epigenetic switching in *Candida albicans*. *J Theor Biol*, **258**(1), 71–88.
- STAIB, PETER, & MORSCHHÄUSER, JOACHIM. 2005. Differential expression of the NRG1 repressor controls species-specific regulation of chlamyospore development in *Candida albicans* and *Candida dubliniensis*. *Mol Microbiol*, **55**(2), 637–652.

- STAIB, PETER, & MORSCHHÄUSER, JOACHIM. 2007. Chlamydospore formation in *Candida albicans* and *Candida dubliniensis*—an enigmatic developmental programme. *Mycoses*, **50**(1), 1–12.
- STAN, R., MCLAUGHLIN, M. M., CAFFERKEY, R., JOHNSON, R. K., ROSENBERG, M., & LIVI, G. P. 1994. Interaction between FKBP12-rapamycin and TOR involves a conserved serine residue. *J Biol Chem*, **269**(51), 32027–32030.
- STEHR, FRANK, FELK, ANGELIKA, GÁCSEK, ATTILA, KRETSCHMAR, MARIANNE, MÄHNSS, BIRGIT, NEUBER, KARSTEN, HUBE, BERNHARD, & SCHÄFER, WILHELM. 2004. Expression analysis of the *Candida albicans* lipase gene family during experimental infections and in patient samples. *FEMS Yeast Res*, **4**(4-5), 401–408.
- STEIN, G. S., STEIN, J. L., VAN WIJNEN, A. J., & LIAN, J. B. 1992. Regulation of histone gene expression. *Curr Opin Cell Biol*, **4**(2), 166–173.
- STERLING, T. R., & MERZ, W. G. 1998. Resistance to amphotericin B: emerging clinical and microbiological patterns. *Drug Resist Updat*, **1**(3), 161–165.
- STOLER, S., KEITH, K. C., CURNICK, K. E., & FITZGERALD-HAYES, M. 1995. A mutation in CSE4, an essential gene encoding a novel chromatin-associated protein in yeast, causes chromosome nondisjunction and cell cycle arrest at mitosis. *Genes Dev*, **9**(5), 573–586.
- STRIMPAKOS, ALEX S, KARAPANAGIOTOU, ELENI M, SAIF, M. WASIF, & SYRIGOS, KOSTAS N. 2009. The role of mTOR in the management of solid tumors: an overview. *Cancer Treat Rev*, **35**(2), 148–159.
- STRINGER, JAMES R. 2007. Antigenic variation in pneumocystis. *J Eukaryot Microbiol*, **54**(1), 8–13.
- STURGILL, THOMAS W, & HALL, MICHAEL N. 2007. Holding back TOR advances mitosis. *Nat Cell Biol*, **9**(11), 1221–1222.
- STURGILL, THOMAS W, COHEN, ADIEL, DIEFENBACHER, MELANIE, TRAUTWEIN, MARK, MARTIN, DIETMAR E, & HALL, MICHAEL N. 2008. TOR1 and TOR2 have distinct locations in live cells. *Eukaryot Cell*, **7**(10), 1819–1830.
- SU, X. Z., HEATWOLE, V. M., WERTHEIMER, S. P., GUINET, F., HERRFELDT, J. A., PETERSON, D. S., RAVETCH, J. A., & WELLEMS, T. E. 1995. The large diverse gene family var encodes proteins involved in cytoadherence and antigenic variation of *Plasmodium falciparum*-infected erythrocytes. *Cell*, **82**(1), 89–100.
- SUDBERY, PETER, GOW, NEIL, & BERMAN, JUDITH. 2004. The distinct morphogenic states of *Candida albicans*. *Trends Microbiol*, **12**(7), 317–324.
- SUKROONGREUNG, S., LIM, S., TANTIMAVANICH, S., EAMPOKALAP, B., CARTER, D., NILAKUL, C., KULKERATIYUT, S., & TANSUPHASWADIKUL, S. 2001. Phenotypic switching and genetic diversity of *Cryptococcus neoformans*. *J Clin Microbiol*, **39**(6), 2060–2064.
- SULLIVAN, K. F., HECHENBERGER, M., & MASRI, K. 1994. Human CENP-A contains a histone H3 related histone fold domain that is required for targeting to the centromere. *J Cell Biol*, **127**(3), 581–592.
- SUNDSTROM, PAULA. 2002. Adhesion in *Candida* spp. *Cell Microbiol*, **4**(8), 461–469.
- SUZUKI, T., KOBAYASHI, I., KANBE, T., & TANAKA, K. 1989. High frequency variation of colony morphology and chromosome reorganization in the pathogenic yeast *Candida albicans*. *J Gen Microbiol*, **135**(Pt 2), 425–434.
- SUZUKI, T., MIYAMAE, Y., & ISHIDA, I. 1991. Variation of colony morphology and chromosomal rearrangement in *Candida tropicalis* pK233. *J Gen Microbiol*, **137**(1), 161–167.
- SUZUKI, T., UEDA, T., & WATANABE, K. 1997. The 'polysemous' codon—a codon with multiple amino acid assignment caused by dual specificity of tRNA identity. *EMBO J*, **16**(5), 1122–1134.
- SVAREN, J., & HÖRZ, W. 1993. Histones, nucleosomes and transcription. *Curr Opin Genet Dev*, **3**(2), 219–225.

- SWAIN, PETER S, ELOWITZ, MICHAEL B, & SIGGIA, ERIC D. 2002. Intrinsic and extrinsic contributions to stochasticity in gene expression. *Proc Natl Acad Sci U S A*, **99**(20), 12795–12800.
- SWEET, S. P., COOKSON, S., & CHALLACOMBE, S. J. 1995. *Candida albicans* isolates from HIV-infected and AIDS patients exhibit enhanced adherence to epithelial cells. *J Med Microbiol*, **43**(6), 452–457.
- TADDEI, F., MATIC, I., & RADMAN, M. 1995. cAMP-dependent SOS induction and mutagenesis in resting bacterial populations. *Proc Natl Acad Sci U S A*, **92**(25), 11736–11740.
- TAIPALE, MIKKO, JAROSZ, DANIEL F, & LINDQUIST, SUSAN. 2010. HSP90 at the hub of protein homeostasis: emerging mechanistic insights. *Nat Rev Mol Cell Biol*, **11**(7), 515–528.
- TAKAYAMA, YUKO, & TAKAHASHI, KOHTA. 2007. Differential regulation of repeated histone genes during the fission yeast cell cycle. *Nucleic Acids Res*, **35**(10), 3223–3237.
- TAMAKI, HISANORI. 2007. Glucose-stimulated cAMP-protein kinase A pathway in yeast *Saccharomyces cerevisiae*. *J Biosci Bioeng*, **104**(4), 245–250.
- TATE, JENNIFER J, GEORIS, ISABELLE, FELLER, ANDRE, DUBOIS, EVELYNE, & COOPER, TERRANCE G. 2008. Rapamycin-induced Gln3 dephosphorylation is insufficient for nuclear localization: Sit4 and PP2A phosphatases are regulated and function differently. *J Biol Chem*, **284**(Nov), 2522–2534.
- TAVERNA, SEAN D, LI, HAITAO, RUTHENBURG, ALEXANDER J, ALLIS, C. DAVID, & PATEL, DINSHAW J. 2007. How chromatin-binding modules interpret histone modifications: lessons from professional pocket pickers. *Nat Struct Mol Biol*, **14**(11), 1025–1040.
- TEBARTH, BERND, DOEDT, THOMAS, KRISHNAMURTHY, SHANKARLING, WEIDE, MIRKO, MONTEROLA, FREIDA, DOMINGUEZ, ANGEL, & ERNST, JOACHIM F. 2003. Adaptation of the Efg1p morphogenetic pathway in *Candida albicans* by negative autoregulation and PKA-dependent repression of the EFG1 gene. *J Mol Biol*, **329**(5), 949–962.
- THATCHER, T. H., & GOROVSKY, M. A. 1994. Phylogenetic analysis of the core histones H2A, H2B, H3, and H4. *Nucleic Acids Res*, **22**(2), 174–179.
- THEVELEIN, J. M., & DE WINDE, J. H. 1999. Novel sensing mechanisms and targets for the cAMP-protein kinase A pathway in the yeast *Saccharomyces cerevisiae*. *Mol Microbiol*, **33**(5), 904–918.
- THOMAS, CHARLES F, & LIMPER, ANDREW H. 2004. Pneumocystis pneumonia. *N Engl J Med*, **350**(24), 2487–2498.
- THON, G., BALTZ, T., GIROUD, C., & EISEN, H. 1990. Trypanosome variable surface glycoproteins: composite genes and order of expression. *Genes Dev*, **4**(8), 1374–1383.
- TIAN, TIANHAI, HARDING, ANGUS, INDER, KERRY, PLOWMAN, SARAH, PARTON, ROBERT G, & HANCOCK, JOHN F. 2007. Plasma membrane nanoswitches generate high-fidelity Ras signal transduction. *Nat Cell Biol*, **9**(8), 905–914.
- TILBURN, J., SARKAR, S., WIDDICK, D. A., ESPESO, E. A., OREJAS, M., MUNGROO, J., PEÑALVA, M. A., & ARST, H. N. 1995. The *Aspergillus* PacC zinc finger transcription factor mediates regulation of both acid- and alkaline-expressed genes by ambient pH. *EMBO J*, **14**(4), 779–790.
- TODA, T., CAMERON, S., SASS, P., ZOLLER, M., SCOTT, J. D., MCMULLEN, B., HURWITZ, M., KREBS, E. G., & WIGLER, M. 1987a. Cloning and characterization of BCY1, a locus encoding a regulatory subunit of the cyclic AMP-dependent protein kinase in *Saccharomyces cerevisiae*. *Mol Cell Biol*, **7**(4), 1371–1377.
- TODA, T., CAMERON, S., SASS, P., ZOLLER, M., & WIGLER, M. 1987b. Three different genes in *S. cerevisiae* encode the catalytic subunits of the cAMP-dependent protein kinase. *Cell*, **50**(2), 277–287.
- TOMPA, PETER, BUZDER-LANTOS, PETER, TANTOS, AGNES, FARKAS, ATTILA, SZILÁGYI, ANDRÁS, BÁNÓCZI, ZOLTÁN, HUDECZ, FERENC, & FRIEDRICH, PETER. 2004. On the sequential determinants of calpain cleavage. *J Biol Chem*, **279**(20), 20775–20785.

- TONIKIAN, RAFFI, XIN, XIAOFENG, TORET, CHRISTOPHER P, GFELLER, DAVID, LANDGRAF, CHRISTIANE, PANNI, SIMONA, PAOLUZI, SERENA, CASTAGNOLI, LUISA, CURRELL, BRIDGET, SESHAGIRI, SOMASEKAR, YU, HAIYUAN, WINSOR, BARBARA, VIDAL, MARC, GERSTEIN, MARK B, BADER, GARY D, VOLKMER, RUDOLF, CESARENI, GIANNI, DRUBIN, DAVID G, KIM, PHILIP M, SIDHU, SACHDEV S, & BOONE, CHARLES. 2009. Bayesian modeling of the yeast SH3 domain interactome predicts spatiotemporal dynamics of endocytosis proteins. *PLoS Biol*, **7**(10), e1000218.
- TSAO, CHANG-CHIH, CHEN, YU-TING, & LAN, CHUNG-YU. 2008. A small G protein Rhb1 and a GTPase-activating protein Tsc2 involved in nitrogen starvation-induced morphogenesis and cell wall integrity of *Candida albicans*. *Fungal Genet Biol*, Dec.
- TSAO, CHANG-CHIH, CHEN, YU-TING, & LAN, CHUNG-YU. 2009. A small G protein Rhb1 and a GTPase-activating protein Tsc2 involved in nitrogen starvation-induced morphogenesis and cell wall integrity of *Candida albicans*. *Fungal Genet Biol*, **46**(2), 126–136.
- TSONG, ANNIE E, TUCH, BRIAN B, LI, HAO, & JOHNSON, ALEXANDER D. 2006. Evolution of alternative transcriptional circuits with identical logic. *Nature*, **443**(7110), 415–420.
- TSUBOI, R., KOMATSUZAKI, H., & OGAWA, H. 1996. Induction of an extracellular esterase from *Candida albicans* and some of its properties. *Infect Immun*, **64**(8), 2936–2940.
- TSUI, K., SIMON, L., & NORRIS, D. 1997. Progression into the first meiotic division is sensitive to histone H2A-H2B dimer concentration in *Saccharomyces cerevisiae*. *Genetics*, **145**(3), 647–659.
- TSYGANKOVA, O. M., KUPPERMAN, E., WEN, W., & MEINKOTH, J. L. 2000. Cyclic AMP activates Ras. *Oncogene*, **19**(32), 3609–3615.
- VAN SLEGTENHORST, MARJON, CARR, ERIKKA, STOYANOVA, RADKA, KRUGER, WARREN D, & HENSKEL, ELIZABETH PETRI. 2004. Tsc1+ and tsc2+ regulate arginine uptake and metabolism in *Schizosaccharomyces pombe*. *J Biol Chem*, **279**(13), 12706–12713.
- UETZ, P., GIOT, L., CAGNEY, G., MANSFIELD, T. A., JUDSON, R. S., KNIGHT, J. R., LOCKSHON, D., NARAYAN, V., SRINIVASAN, M., POCHART, P., QURESHI-EMILI, A., LI, Y., GODWIN, B., CONOVER, D., KALBFLEISCH, T., VIJAYADAMODAR, G., YANG, M., JOHNSTON, M., FIELDS, S., & ROTHBERG, J. M. 2000. A comprehensive analysis of protein-protein interactions in *Saccharomyces cerevisiae*. *Nature*, **403**(6770), 623–627.
- UHL, M. ANDREW, BIERY, MATT, CRAIG, NANCY, & JOHNSON, ALEXANDER D. 2003. Haploinsufficiency-based large-scale forward genetic analysis of filamentous growth in the diploid human fungal pathogen *C. albicans*. *EMBO J*, **22**(11), 2668–2678.
- URANO, J., TABANCA, A. P., YANG, W., & TAMANOI, F. 2000. The *Saccharomyces cerevisiae* Rheb G-protein is involved in regulating canavanine resistance and arginine uptake. *J Biol Chem*, **275**(15), 11198–11206.
- URBAN, JÖRG, SOULARD, ALEXANDRE, HUBER, ALEXANDRE, LIPPMAN, SOYEON, MUKHOPADHYAY, DEBDYUTI, DELOCHE, OLIVIER, WANKE, VALERIA, ANRATHER, DOROTHEA, AMMERER, GUSTAV, RIEZMAN, HOWARD, BROACH, JAMES R, VIRGILIO, CLAUDIO DE, HALL, MICHAEL N, & LOEWITH, ROBBIE. 2007. Sch9 is a major target of TORC1 in *Saccharomyces cerevisiae*. *Mol Cell*, **26**(5), 663–674.
- VARGAS, K., WERTZ, P. W., DRAKE, D., MORROW, B., & SOLL, D. R. 1994. Differences in adhesion of *Candida albicans* 3153A cells exhibiting switch phenotypes to buccal epithelium and stratum corneum. *Infect Immun*, **62**(4), 1328–1335.
- VARGAS, K., MESSER, S. A., PFALLER, M., LOCKHART, S. R., STAPLETON, J. T., HELLSTEIN, J., & SOLL, D. R. 2000. Elevated phenotypic switching and drug resistance of *Candida albicans* from human immunodeficiency virus-positive individuals prior to first thrush episode. *J Clin Microbiol*, **38**(10), 3595–3607.
- VARGAS, KEEREN, SRIKANTHA, RUPASREE, HOLKE, ANAMIKA, SIFRI, TAMIM, MORRIS, RYAN, & JOLY, SOPHIE. 2004. *Candida albicans* switch phenotypes display differential levels of fitness. *Med Sci Monit*, **10**(7), BR198–BR206.

- VEENING, JAN-WILLEM, SMITS, WIEP KLAAS, & KUIPERS, OSCAR P. 2008. Bistability, epigenetics, and bet-hedging in bacteria. *Annu Rev Microbiol*, **62**, 193–210.
- VENDITTI, S., VEGA-PALAS, M. A., STEFANO, G. DI, & MAURO, E. DI. 1999. Imbalance in dosage of the genes for the heterochromatin components Sir3p and histone H4 results in changes in the length and sequence organization of yeast telomeres. *Mol Gen Genet*, **262**(2), 367–377.
- VERSTREPEN, KEVIN J., & FINK, GERALD R. 2009. Genetic and epigenetic mechanisms underlying cell-surface variability in protozoa and fungi. *Annu Rev Genet*, **43**, 1–24.
- VILELLA-BACH, M., NUZZI, P., FANG, Y., & CHEN, J. 1999. The FKBP12-rapamycin-binding domain is required for FKBP12-rapamycin-associated protein kinase activity and G1 progression. *J Biol Chem*, **274**(7), 4266–4272.
- VOJTEK, A. B., HOLLENBERG, S. M., & COOPER, J. A. 1993. Mammalian Ras interacts directly with the serine/threonine kinase Raf. *Cell*, **74**(1), 205–214.
- VÉZINA, C., KUDELSKI, A., & SEHGAL, S. N. 1975. Rapamycin (AY-22,989), a new antifungal antibiotic. I. Taxonomy of the producing streptomycete and isolation of the active principle. *J Antibiot (Tokyo)*, **28**(10), 721–726.
- WADA, M., SUNKIN, S. M., STRINGER, J. R., & NAKAMURA, Y. 1995. Antigenic variation by positional control of major surface glycoprotein gene expression in *Pneumocystis carinii*. *J Infect Dis*, **171**(6), 1563–1568.
- WALL, M. A., COLEMAN, D. E., LEE, E., IÑIGUEZ-LLUHI, J. A., POSNER, B. A., GILMAN, A. G., & SPRANG, S. R. 1995. The structure of the G protein heterotrimer Gi alpha 1 beta 1 gamma 2. *Cell*, **83**(6), 1047–1058.
- WALSH, T. J., & GROLL, A. H. 1999. Emerging fungal pathogens: evolving challenges to immunocompromised patients for the twenty-first century. *Transpl Infect Dis*, **1**(4), 247–261.
- WANG, AMY, KURDISTANI, SIAVASH K., & GRUNSTEIN, MICHAEL. 2002. Requirement of Hos2 histone deacetylase for gene activity in yeast. *Science*, **298**(5597), 1412–1414.
- WANG, HUAMIN, WANG, XIAODONG, & JIANG, YU. 2003. Interaction with Tap42 is required for the essential function of Sit4 and type 2A phosphatases. *Mol Biol Cell*, **14**(11), 4342–4351.
- WARNER, J. R. 1999. The economics of ribosome biosynthesis in yeast. *Trends Biochem Sci*, **24**(11), 437–440.
- WATSON, A. D., EDMONDSON, D. G., BONE, J. R., MUKAI, Y., YU, Y., DU, W., STILLMAN, D. J., & ROTH, S. Y. 2000. Ssn6-Tup1 interacts with class I histone deacetylases required for repression. *Genes Dev*, **14**(21), 2737–2744.
- WEEKS, G. 2000. Signalling molecules involved in cellular differentiation during *Dictyostelium* morphogenesis. *Curr Opin Microbiol*, **3**(6), 625–630.
- WEI, MIN, FABRIZIO, PAOLA, HU, JIA, GE, HUANYING, CHENG, CHAO, LI, LEI, & LONGO, VALTER D. 2008. Life span extension by calorie restriction depends on Rim15 and transcription factors downstream of Ras/PKA, Tor, and Sch9. *PLoS Genet*, **4**(1), e13.
- WEINBERGER, MARTIN, FENG, LI, PAUL, ANITA, SMITH, DANIEL L, HONTZ, ROBERT D, SMITH, JEFFREY S, VUJICIC, MARIJA, SINGH, KESHAV K, HUBERMAN, JOEL A, & BURHANS, WILLIAM C. 2007. DNA replication stress is a determinant of chronological lifespan in budding yeast. *PLoS One*, **2**(1), e748.
- WEINSTEIN, I. BERNARD. 2002. Cancer. Addiction to oncogenes—the Achilles heel of cancer. *Science*, **297**(5578), 63–64.
- WEISMAN, R., & CHODER, M. 2001. The fission yeast TOR homolog, tor1+, is required for the response to starvation and other stresses via a conserved serine. *J Biol Chem*, **276**(10), 7027–7032.
- WEISSMAN, ZIVA, SHEMER, REVITAL, CONIBEAR, ELIZABETH, & KORNITZER, DANIEL. 2008. An endocytic mechanism for haemoglobin-iron acquisition in *Candida albicans*. *Mol Microbiol*, **69**(1), 201–217.

- WHEAT, L. JOSEPH. 2006. Histoplasmosis: a review for clinicians from non-endemic areas. *Mycoses*, **49**(4), 274–282.
- WHITE, T. C., MARR, K. A., & BOWDEN, R. A. 1998. Clinical, cellular, and molecular factors that contribute to antifungal drug resistance. *Clin Microbiol Rev*, **11**(2), 382–402.
- WHITE, THEODORE C, HOLLEMAN, SCOTT, DY, FRANCIS, MIRELS, LAURENCE F, & STEVENS, DAVID A. 2002. Resistance mechanisms in clinical isolates of *Candida albicans*. *Antimicrob Agents Chemother*, **46**(6), 1704–1713.
- WHITEWAY, MALCOLM, & OBERHOLZER, URSULA. 2004. *Candida* morphogenesis and host-pathogen interactions. *Curr Opin Microbiol*, **7**(4), 350–357.
- WICKES, B., STAUDINGER, J., MAGEE, B. B., KWON-CHUNG, K. J., MAGEE, P. T., & SCHERER, S. 1991. Physical and genetic mapping of *Candida albicans*: several genes previously assigned to chromosome 1 map to chromosome R, the rDNA-containing linkage group. *Infect Immun*, **59**(7), 2480–2484.
- WICKSTEAD, BILL, ERSFELD, KLAUS, & GULL, KEITH. 2004. The small chromosomes of *Trypanosoma brucei* involved in antigenic variation are constructed around repetitive palindromes. *Genome Res*, **14**(6), 1014–1024.
- WILSON, LESLIE S, REYES, CAROLINA M, STOLPMAN, MICHELLE, SPECKMAN, JULIE, ALLEN, KAROLINE, & BENEY, JOHNNY. 2002. The direct cost and incidence of systemic fungal infections. *Value Health*, **5**(1), 26–34.
- WILSON, R. B., DAVIS, D., & MITCHELL, A. P. 1999. Rapid hypothesis testing with *Candida albicans* through gene disruption with short homology regions. *J Bacteriol*, **181**(6), 1868–1874.
- WILSON, DUNCAN, FIORI, ALESSANDRO, BRUCKER, KATRIJN DE, DIJCK, PATRICK VAN, & STATEVA, LUBOMIRA. 2010. *Candida albicans* Pde1p and Gpa2p comprise a regulatory module mediating agonist-induced cAMP signalling and environmental adaptation. *Fungal Genet Biol*, **47**(9), 742–752.
- WONG, LEE H, REN, HUA, WILLIAMS, EVAN, MCGHIE, JAMES, AHN, SOYEON, SIM, MARCUS, TAM, ANGELA, EARLE, ELIZABETH, ANDERSON, MELISSA A, MANN, JEFFREY, & CHOO, K. H ANDY. 2009. Histone H3.3 incorporation provides a unique and functionally essential telomeric chromatin in embryonic stem cells. *Genome Res*, **19**(3), 404–414.
- WORKMAN, JERRY L. 2006. Nucleosome displacement in transcription. *Genes Dev*, **20**(15), 2009–2017.
- WU, WEI, PUJOL, CLAUDE, LOCKHART, SHAWN R, & SOLL, DAVID R. 2005. Chromosome loss followed by duplication is the major mechanism of spontaneous mating-type locus homozygosity in *Candida albicans*. *Genetics*, **169**(3), 1311–1327.
- WULLSCHLEGER, STEPHAN, LOEWITH, ROBBIE, & HALL, MICHAEL N. 2006. TOR signaling in growth and metabolism. *Cell*, **124**(3), 471–484.
- WYRICK, J. J., HOLSTEGE, F. C., JENNINGS, E. G., CAUSTON, H. C., SHORE, D., GRUNSTEIN, M., LANDER, E. S., & YOUNG, R. A. 1999. Chromosomal landscape of nucleosome-dependent gene expression and silencing in yeast. *Nature*, **402**(6760), 418–421.
- XU, WENJIE, SMITH, FRANK J, SUBARAN, RYAN, & MITCHELL, AARON P. 2004. Multivesicular body-ESCRT components function in pH response regulation in *Saccharomyces cerevisiae* and *Candida albicans*. *Mol Biol Cell*, **15**(12), 5528–5537.
- XU, EUGENIA Y, ZAWADZKI, KARL A, & BROACH, JAMES R. 2006. Single-cell observations reveal intermediate transcriptional silencing states. *Mol Cell*, **23**(2), 219–229.
- XUE, CHAOYANG, HSUEH, YEN-PING, & HEITMAN, JOSEPH. 2008. Magnificent seven: roles of G protein-coupled receptors in extracellular sensing in fungi. *FEMS Microbiol Rev*, **32**(6), 1010–1032.
- XUE, Y., BATLLE, M., & HIRSCH, J. P. 1998. GPR1 encodes a putative G protein-coupled receptor that associates with the Gpa2p Galpha subunit and functions in a Ras-independent pathway. *EMBO J*, **17**(7), 1996–2007.

- YAHARA, I. 1999. The role of HSP90 in evolution. *Genes Cells*, **4**(7), 375–379.
- YAMAMOTO, SHOUJI, & KUTSUKAKE, KAZUHIRO. 2006. FljA-mediated posttranscriptional control of phase I flagellin expression in flagellar phase variation of *Salmonella enterica* serovar Typhimurium. *J Bacteriol*, **188**(3), 958–967.
- YAN, GONGHONG, SHEN, XIAOYUN, & JIANG, YU. 2006. Rapamycin activates Tap42-associated phosphatases by abrogating their association with Tor complex 1. *EMBO J*, **25**(15), 3546–3555.
- YANG, XIANG-JIAO, & GRÉGOIRE, SERGE. 2005. Class II histone deacetylases: from sequence to function, regulation, and clinical implication. *Mol Cell Biol*, **25**(8), 2873–2884.
- YANG, XIANG-JIAO, & SETO, EDWARD. 2003. Collaborative spirit of histone deacetylases in regulating chromatin structure and gene expression. *Curr Opin Genet Dev*, **13**(2), 143–153.
- YARDEN, Y., & SLIWKOWSKI, M. X. 2001. Untangling the ErbB signalling network. *Nat Rev Mol Cell Biol*, **2**(2), 127–137.
- YAROSH, D. B., CRUZ, P. D., DOUGHERTY, I., BIZIOS, N., KIBITEL, J., GOODTZOVA, K., BOTH, D., GOLDFARB, S., GREEN, B., & BROWN, D. 2000. FRAP DNA-dependent protein kinase mediates a late signal transduced from ultraviolet-induced DNA damage. *J Invest Dermatol*, **114**(5), 1005–1010.
- YOON, S. A., VAZQUEZ, J. A., STEFFAN, P. E., SOBEL, J. D., & AKINS, R. A. 1999. High-frequency, in vitro reversible switching of *Candida lusitanae* clinical isolates from amphotericin B susceptibility to resistance. *Antimicrob Agents Chemother*, **43**(4), 836–845.
- ZACCHI, LUCIA F, GOMEZ-RAJA, JONATAN, & DAVIS, DANA A. 2010a. Mds3 regulates morphogenesis in *Candida albicans* through the TOR pathway. *Mol Cell Biol*, **30**(14), 3695–3710.
- ZACCHI, LUCIA F, SCHULZ, WADE L, & DAVIS, DANA A. 2010b. HOS2 and HDA1 encode histone deacetylases with opposing roles in *Candida albicans* morphogenesis. *PLoS One*, **5**(8), e12171.
- ZACCHI, LUCIA F, SELMECKI, ANNA M, BERMAN, JUDITH, & DAVIS, DANA A. 2010. Low dosage of histone H4 leads to growth defects and morphological changes in *Candida albicans*. *PLoS One*, **5**(5), e10629.
- ZAMAN, SHADIA, LIPPMAN, SOYEON IM, ZHAO, XIN, & BROACH, JAMES R. 2008. How *Saccharomyces* responds to nutrients. *Annu Rev Genet*, **42**, 27–81.
- ZHANG, LIWEN, EUGENI, ERICKA E, PARTHUN, MARK R, & FREITAS, MICHAEL A. 2003. Identification of novel histone post-translational modifications by peptide mass fingerprinting. *Chromosoma*, **112**(2), 77–86.
- ZHAO, Y., BOGUSLAWSKI, G., ZITOMER, R. S., & DEPAOLI-ROACH, A. A. 1997. *Saccharomyces cerevisiae* homologs of mammalian B and B' subunits of protein phosphatase 2A direct the enzyme to distinct cellular functions. *J Biol Chem*, **272**(13), 8256–8262.
- ZHENG, X. F., & SCHREIBER, S. L. 1997. Target of rapamycin proteins and their kinase activities are required for meiosis. *Proc Natl Acad Sci U S A*, **94**(7), 3070–3075.
- ZHU, YONG, FANG, HAO-MING, WANG, YAN-MING, ZENG, GUI-SHENG, ZHENG, XIN-DE, & WANG, YUE. 2009. Ras1 and Ras2 play antagonistic roles in regulating cellular cAMP level, stationary-phase entry and stress response in *Candida albicans*. *Mol Microbiol*, **74**(4), 862–875.
- ZHU, WEIDONG, & FILLER, SCOTT G. 2010. Interactions of *Candida albicans* with epithelial cells. *Cell Microbiol*, **12**(3), 273–282.
- ZIEG, J., SILVERMAN, M., HILMEN, M., & SIMON, M. 1977. Recombinational switch for gene expression. *Science*, **196**(4286), 170–172.
- ZINZALLA, VITTORIA, & HALL, MICHAEL N. 2008. Signal transduction: Linking nutrients to growth. *Nature*, **454**(7202), 287–288.
- ZORDAN, REBECCA E, GALGOCZY, DAVID J, & JOHNSON, ALEXANDER D. 2006. Epigenetic properties of white-opaque switching in *Candida albicans* are based on a self-sustaining transcriptional feedback loop. *Proc Natl Acad Sci U S A*, **103**(34), 12807–12812.

ZORDAN, REBECCA E, MILLER, MATHEW G, GALGOCZY, DAVID J, TUCH, BRIAN B, & JOHNSON, ALEXANDER D. 2007. Interlocking transcriptional feedback loops control white-opaque switching in *Candida albicans*. *PLoS Biol*, **5**(10), e256.

ZURITA-MARTINEZ, SARA A, & CARDENAS, MARIA E. 2005. Tor and cyclic AMP-protein kinase A: two parallel pathways regulating expression of genes required for cell growth. *Eukaryot Cell*, **4**(1), 63–71.

ZURITA-MARTINEZ, SARA A, PURIA, REKHA, PAN, XUEWEN, BOEKE, JEF D, & CARDENAS, MARIA E. 2007. Efficient Tor signaling requires a functional class C Vps protein complex in *Saccharomyces cerevisiae*. *Genetics*, **176**(4), 2139–2150.

## APPENDIX A

### ***HOS2* AND *HDA1* ENCODE HISTONE DEACETYLASES WITH OPPOSING ROLES IN *CANDIDA ALBICANS* MORPHOGENESIS**

**Zacchi, L.F.**, Schulz, W. L., Davis, D.A. (2010). *HOS2* and *HDA1* encode histone deacetylases with opposing roles in *Candida albicans* morphogenesis. *PLoS ONE*. 5(8): e12171

## SUMMARY

Epigenetic mechanisms regulate the expression of virulence traits in diverse pathogens, including protozoan and fungi. In the human fungal pathogen *Candida albicans* virulence traits such as antifungal resistance, white-opaque switching, and adhesion to lung cells are regulated by histone deacetylases (HDACs). However, the role of HDACs in the regulation of the yeast-hyphal morphogenetic transitions, a critical virulence attribute of *C. albicans*, remains poorly explored. In this study, we wished to determine the relevance of other HDACs on *C. albicans* morphogenesis. We generated mutants in the HDACs *HOS1*, *HOS2*, *RPD31*, and *HDA1*, and determined their ability to filament in response to different environmental stimuli. We found that while *HOS1* and *RPD31* have no or a more limited role in morphogenesis, the HDACs *HOS2* and *HDA1* have opposite roles in the regulation of hyphal formation. Our results demonstrate an important role for HDACs on the regulation of yeast-hyphal transitions in the human pathogen *C. albicans*.

## INTRODUCTION

*Candida albicans* is the most common fungal pathogen of humans and is the fourth most common cause of nosocomial bloodstream infections (Pfaller et al., 2001). *C. albicans* pathogenesis depends on its ability to transition between the yeast, pseudohyphal, and hyphal cellular morphologies (Sudbery et al., 2004), and these transitions are triggered by diverse environmental cues, including temperature, serum, pH, and starvation (Biswas et al., 2007). Both the yeast and hyphal morphologies are required for pathogenesis in animal models of infection (Lo et al., 1997; Saville et al., 2003, 2008), and are required for the formation of normal biofilms (Baillie and Douglas, 1999; Richard et al., 2005), a structure that increases antifungal drug resistance and constitutes a source of inoculum for disseminated and recurrent infections (Hawser and Douglas, 1995). The different cellular morphologies can also trigger immune tolerance or activation against *C. albicans* (Acosta-Rodriguez et al., 2007; Romani et al., 2003, 2004). Therefore, the ability to switch between morphologies has pleiotropic effects on *C. albicans* interaction with the host and on its ability to cause infection.

As epigenetic regulators of gene expression, chromatin modifying enzymes regulate diverse aspects of *C. albicans* biology. For example, histone modifying enzymes are required for the regulation of virulence traits and for pathogenesis in *C. albicans* (Klar et al., 2001; Smith and Edlind, 2001; Hnisz et al., 2009; Lu et al., 2008; Mai et al., 2007; Simonetti et al., 2007; Srikantha et al., 2001; Pfaller et al., 2009; Raman et al., 2006; Tebarth et al., 2003; Sellam et al., 2009). Since the yeast-hyphal switch is critical for pathogenesis, we investigated the role of histone deacetylases (HDACs) in the regulation of this virulence trait. Here, we screened mutants in *HOS1*, *HOS2*, *RPD31*, and *HDA1* for a role in *C. albicans* morphogenesis. We found that *HOS1* and *RPD31* have little to no role in morphogenesis, and that *HOS2* and *HDA1* encode proteins with opposing roles in morphogenesis: Hos2 functions as a repressor, while Hda1 functions as an inducer of filamentation.

## MATERIALS AND METHODS

### Strains and plasmids

All *C. albicans* strains used in this study derive from *C. albicans* strain BWP17 (Table A.3). The *hos1/hos1*, *hos2/hos2*, and *rpd31/rpd31* strains were generated using the Tn7::*UAU1* insertional mutagenesis system (Davis et al., 2002) using clones obtained from TIGR. Mutagenesis and selection of Tn7::*UAU1* transformants was performed using primers in Table A.4 as previously described (Davis et al., 2002). The *hda1Δ/Δ* mutant DAY694 was constructed by sequentially deleting both *HDA1* alleles from the start to the stop codon from BWP17 strain, using *hda1::ARG4* and *hda1::URA3-dpl200* disruption cassettes PCR amplified with primers HDA1 5DR and HDA1 3DR (Table A.4). The complemented and prototrophic strains (Table A.3) were constructed by transformation with *NruI* digested plasmids pDDB503 for *HOS2* complementation, pDDB504 for *HDA1* complementation, and empty vector pDDB78.

The *HOS2* and *HDA1* complementation vectors pDDB503 and pDDB504 were constructed as follows. Wild-type *HOS2* and *HDA1* open reading frames (ORF), together with ~1kb upstream and 0.5kb downstream of the *HOS2* and *HDA1* ORF, were amplified in high fidelity PCRs (Pfu Turbo DNA polymerase, Stratagene) from BWP17 DNA using primers HOS2 DDB78 comp 5' and HOS2 DDB78 comp 3', and HDA1 5' comp, HDA1 5-1 comp, HDA1 3-1 comp and HDA1 3' comp (Table A.4). The resulting PCR products were *in vivo* recombined in *S. cerevisiae* strain L40 into a *NotI/EcoRI*-digested pDDB78 to generate plasmids pDDB503 and pDDB504.

### Media and growth conditions

*C. albicans* was routinely grown at 30°C in YPD (2% Bacto-peptone, 2% dextrose, 1% yeast extract). For selection of Ura<sup>+</sup>, Arg<sup>+</sup>, His<sup>+</sup> or Trp<sup>+</sup> transformants, synthetic medium without uridine, arginine, histidine or tryptophan was used (0.17% yeast nitrogen base without ammonium sulfate (Q-BioGene), 0.5% ammonium sulfate, 2% dextrose, and supplemented with a dropout mix containing amino and nucleic acids except those necessary for the selection (Adams et al., 1997)). M199 medium (Gibco BRL) was buffered at the indicated pH using 150mM HEPES. The filamentation assays in solid media were performed in M199 medium buffered at pH 8, SLAD (0.17% yeast nitrogen base without ammonium sulfate (Q-BioGene), 50μM ammonium sulfate, 2% dextrose), Spider medium (1% mannitol, 1% nutrient broth, 0.2% K<sub>2</sub>HPO<sub>4</sub>, pH 7.2 before autoclaving) (Liu et al., 1994), embedded agar (2% Bacto-peptone, 2% sucrose, 1% yeast extract) (Brown et al., 1999), and synthetic medium supplemented with 4% bovine calf serum (BCS). The filamentation assays in liquid media were performed in M199 pH 8, Spider, YP + 0.5% N-acetyl glucosamine (GlcNAc), and YP + 10% fetal bovine serum (FBS) (Gibco). Filamentation assays were conducted at 37°C except for embedded agar which was incubated at 23°C. The liquid assays for filamentation were performed as follows. Strains were grown overnight in liquid YPD at 30°C, pelleted, resuspended in an equal volume of PBS and diluted 1:100 in M199 pH 8, Spider, YP+GlcNAc or YP+FBS. Samples were incubated at 37°C. The samples from Spider medium were gently sonicated to disrupt clumping. The percentage of cells forming germ tubes in M199 pH 8 medium at 60 min or in Spider medium at 45 min was determined by counting 300 cells/sample, in triplicate. All media except that for selection of Ura<sup>+</sup> transformants were supplemented with 80 μg/ml uridine. For solid media, 2% Bacto-agar was

added, except for Spider medium and embedded agar which required 1.35% and 1% Bacto-agar, respectively.

### **Microscopy**

Pictures of colonies were taken using a Canon Powershot A560 digital camera on a Zeiss Opton microscope. Images of liquid cultures were captured using a Zeiss Axio camera, Axiovision 4.6.3 software (Zeiss), and a Zeiss AxioImager fluorescence microscope. All images were processed with Adobe Photoshop 7.0 software.

## RESULTS

Chromatin remodeling proteins effect diverse aspects of *C. albicans* biology. Several histone modifying enzymes in *C. albicans*, including the histone methyltransferase Set1 and the histone acetyl transferase complex NuA4, are required for the expression of virulence factors and for pathogenesis *in vivo* (Lu et al., 2008; Raman et al., 2006). The yeast-to-hyphal transition is one biological property of *C. albicans* required for pathogenesis, and it is governed at least in part by epigenetic processes (Lu et al., 2008; Tebarth et al., 2003). To further address the role of chromatin remodeling proteins and epigenetic regulation on pathogenesis, we investigated the role of HDACs in the yeast-to-hyphal transition.

We identified Tn7::*UAU1* insertion clones located close to the START codon of *HOS1* (orf19.4411), *HOS2* (orf19.5377), and *RPD31* (orf19.6801) (Table A.1). When available, two clones were used to disrupt the same gene to enhance the robustness of the approach. (Tn7::*UAU1* insertions were identified within additional HDACs, but these plasmids had complex or incomplete inserts (data not shown)). We generated *hos1/hos1*, *hos2/hos2*, and *rpd31/rpd31* mutants using the Tn7::*UAU1* insertional mutagenesis system (Davis et al., 2002). The *hda1Δ/Δ* mutant was generated by sequential gene deletion using auxotrophic markers (Table A.1). All mutants were tested for filamentation in solid and liquid media (Figures A.1 and A.2 and Table A.2). Since *HOS1* and *RPD31* had little effect on filamentation (data not shown), we only describe the results for the *hos2/hos2* and *hda1Δ/Δ* mutants.

Several different environmental conditions induce the hyphal morphology in *C. albicans*. Incubation at body temperature (37°C), alkaline pH, starvation, and serum are some of the signals that trigger hyphal morphogenesis in this fungus (Biswas et al., 2007). Further, incubation on solid surfaces, liquid media, or embedment in a matrix also impact *C. albicans* morphogenetic responses (Brown et al., 1999; Ernst, 2000). Thus, we tested the ability of the HDACs mutants to filament in several different environmental conditions, including solid and liquid M199 pH 8, serum, and Spider media, solid SLAD medium, embedded agar, and liquid media supplemented with GlcNAc. The *hos2/hos2* mutants consistently showed enhanced filamentation compared to the wild-type strain on most solid media tested (Figure A.1). On M199 pH 8, the *hos2/hos2* mutants filamented robustly, and showed a homogeneous peripheral halo of filamentation after 48 hrs of incubation, ~24 hrs earlier than the wild-type strain (Figure A.1 and data not shown). Similar results were observed on Spider medium, in embedded agar, and on serum (Figure A.1). On SLAD, however, the *hos2/hos2* mutants showed either no filamentation or irregular filamentation around some colonies (Figure A.1 and data not shown). Complementation of the *hos2/hos2* mutation restored filamentation to wild-type levels in all media except SLAD. Lack of complementation on SLAD medium may indicate haploinsufficiency of *HOS2*, as reported previously for other mutants grown on SLAD, such as *gap1Δ/Δ* and *gpr1Δ/Δ* (Biswas et al., 2003; Sciascia et al., 2004). An independent *hos2Δ/Δ* start-to-stop deletion mutant also showed enhanced filamentation, corroborating the results of the insertional mutations (data not shown). Thus, Hos2 functions as an inhibitor of filamentation, except in conditions of nitrogen starvation (SLAD) in which Hos2 function is required for morphogenesis.

The *hda1Δ/Δ* mutant showed poor filamentation compared to the wild-type strain on most solid media tested (Figure A.1). On M199 pH 8 and SLAD, the *hda1Δ/Δ* mutant did not filament. On Spider medium, the *hda1Δ/Δ* mutant showed a slight but reproducible smoother

surface than the wild-type strain. In embedded agar, the *hda1Δ/Δ* mutant showed poor filamentation. On serum, the *hda1Δ/Δ* mutant showed a slight defect in hyphal formation. Complementation of the *hda1Δ/Δ* mutation restored filamentation to wild-type on M199 pH 8, Spider, embedded, and serum media, and partially rescued the defects on SLAD. Thus, Hda1 functions as an inducer of filamentation.

In liquid media, the *hos2/hos2* strain filamented similarly to wild-type in all media tested (Figure A.2 and Table A.2). The *hda1Δ/Δ* mutant also filamented in all media tested, but the filaments of the *hda1Δ/Δ* mutant appeared shorter than wild-type. Accordingly, we detected a delay in *hda1Δ/Δ* mutant germ tube formation in M199 pH 8 and Spider media compared to the wild-type, *hos2/hos2*, and *hda1Δ/Δ+HDA1* strains (Table A.2). We noted that the results obtained in liquid media were more variable compared to solid media. Since changes in gene silencing occurs over several generations (Xu et al., 2006; Katan-Khaykovich and Struhl, 2005), the rapid induction of filamentation in liquid medium may be more susceptible to variations than in solid media because of the differences in incubation time (<1 hr vs >24 hrs, respectively). This difference between liquid and solid medium filamentation may also be due to the fact that liquid filamentation is assessed at the single cell level while solid filamentation is assessed at the population (colony) level (Xu et al., 2006). While the requirement for several generations in order for silencing to be altered may explain the disparate results for the *hda1Δ/Δ* mutant in solid vs. liquid media, it is also possible that Hda1 might be associated with regulators of filamentation that play a more prominent role in solid compared to liquid media. Differences in the function of regulators of hyphal formation in *C. albicans* when cells are incubated in solid, semi-solid, or liquid media have been previously described (Brown et al., 1999; Ernst, 2000; Bockmuehl et al., 2001; Bastidas et al., 2009). Overall, our results demonstrate that the HDACs *HOS2* and *HDA1* have opposing roles in the regulation of hyphal formation in *C. albicans*.

## DISCUSSION

Epigenetic mechanisms regulate virulence traits of diverse microbes, including *Trypanosoma brucei* and *Candida glabrata* (Figueiredo et al., 2008; Domergue et al., 2005). Epigenetic mechanisms also regulate aspects of *C. albicans* pathogenesis. Set1, a histone methyltransferase, the chromatin remodeling complex Swi/Snf, the histone acetyltransferase NuA4 complex, and the HDAC Sin3 regulate morphogenesis, adherence to epithelial cells, and/or are required for pathogenesis in animal models (Lu et al., 2008; Raman et al., 2006; Mao et al., 2006). Furthermore, histone acetylation, regulated by the SAGA/ADA coactivator complex is required for the proper response to oxidative stress and antifungals (Sellam et al., 2009). White-opaque switching is regulated by transcriptional feedback loops and HDACs (Klar et al., 2001; Hnisz et al., 2009; Srikantha et al., 2001; Zordan et al., 2007). HDACs function is also required for antifungal resistance and adhesion to human pneumocytes (Smith and Edlind, 2002; Mai et al., 2007; Simonetti et al., 2007; Pfaller et al., 2009). Therefore, epigenetic mechanisms play an important role in the pathogenesis of *C. albicans*.

Here, we show that Hos2 and Hda1 regulate the yeast-to-hyphal transition in opposing ways. Previously, Hos2 and Hda1 were reported to have opposing effects on white-opaque switching (Hnisz et al., 2009; Srikantha et al., 2001). This suggests that Hos2 and Hda1 may inversely govern a common set of genes. Histone deacetylation is usually associated with transcriptional repression (Grozinger and Schreiber, 2002; Yang and Seto, 2003). However, HDACs are also required for gene expression, and it has been proposed that acetylation and deacetylation cycles are responsible for maintaining promoter activity (De Nadal et al., 2004; Wang et al., 2002; Clayton et al., 2006). HDACs can deacetylate histones globally (non-targeted deacetylation) or at specific promoters to which they are tethered in complex with specific transcription factor and other DNA binding proteins (targeted deacetylation) (Kadosh and Struhl, 1998; Kurdistani et al., 2002). Thus, one possible mechanisms of Hos2 and Hda1 function on filamentation in *C. albicans* is through the association with transcriptional regulators of hyphal formation, including the positive regulators Cph1, Cph2, Efg1, Tec1, Bcr1, Czf1, and/or Rim101, and the negative regulators Nrg1, Tup1, Rfg1, and/or Sfl1 (Biswas et al., 2007; Brown et al., 1999; Bauer and Wendland, 2007; Braun et al., 2001; Davis et al., 2000; Khalaf and Zitomer, 2001). For example, Hos2 and Hda1 have been associated with Tup1 and Efg1 function in *S. cerevisiae* and *C. albicans*, respectively (Davie et al., 2003; Green and Johnson, 2004; Hnisz et al., 2010). HDACs could also impact filamentation by affecting the expression of the regulators themselves (Srikantha et al., 2001; Tebarth et al., 2003) or by deacetylating transcription factors and other non-histone proteins that have a direct or indirect role in morphogenesis (Wang et al., 2002; Kurdistani et al., 2002; Glozak et al., 2005; Yang and Gregoire, 2005; Kadosh and Struhl, 1997; Watson et al., 2000; Robyr et al., 2002). Thus, Hos2 and Hda1 might impact hyphal formation through a diverse array of mechanisms.

Why is *HOS2* required for filamentation in SLAD but acts as an inhibitor of hyphal formation in all other conditions tested? In *C. albicans*, hyphal formation on SLAD is modulated by transcription factors, some of which function specifically during nitrogen starvation, such as Gln3. It is possible that Hos2 is required for the function of these specific transcription factors. Alternatively, loss of Hos2 may promote expression of genes that inhibit morphogenesis during nitrogen starvation. Thus, the *hos2Δ/Δ* effect on morphogenesis in *C. albicans* varies with the

environmental conditions, a phenomenon that has also been observed for the histone deacetylase Set3 (Hnisz et al., 2010).

HDAC inhibitors have been proposed as antifungal adjuvants, due to their effect on preventing antifungal resistance *in vitro* (Smith and Edlind, 2002; Mai et al., 2007; Pfaller et al., 2009). However, no studies have shown the efficacy of HDAC inhibitors as antifungals *in vivo*. These types of experiments become even more critical in lieu of our and others findings that HDACs have differential effects on hyphal formation. Previous reports show conflicting *in vitro* results on the effect of different HDAC inhibitors on germ tube formation in liquid serum (Smith and Edlind, 2002; Simonetti et al., 2007). However, inhibiting HDAC function could enhance filamentation in semi-solid surfaces (Figure A.1) (such as mucosae), possibly leading to enhanced tissue invasion and biofilm formation, with the potential to cause more damage and increase antifungal resistance (Niimi et al., 2010). On the contrary, the use of specific HDAC inhibitors might enhance antifungal effectiveness by limiting hyphal development (e.g. against Hda1 (Figure A.1)), or by limiting yeast development (e.g. against Hos2 (Figure A.1) and (Hnisz et al., 2010)). The critical role of HDACs in *C. albicans* pathogenesis and survival to antifungal treatment underscores the necessity to study HDAC function in this organism. A combination of *in vitro* and *in vivo* studies that assess the role of HDACs in biofilm development, genomic instability, colonization, survival, and pathogenesis could determine the potential of HDAC inhibitors as antifungal drugs. Overall, our results contribute to demonstrate the importance of epigenetic regulators in governing virulence traits in *C. albicans*, and support the potential of HDAC inhibitors to prevent and/or treat candidal infections.

**Table A.1.** List of mutants in histone deacetylases, the mutagenesis strategies, and corresponding TIGR CAG clones

ORF19	Gene	Clone ID	Mutagenesis strategy	pDDB#	Strain
orf19.4411	<i>HOS1</i>	36246	Tn7 insertion clone CAGLH56	362	DAY1249
orf19.5377	<i>HOS2</i>	51640	Tn7 insertion clone CAGN203	363	DAY1242
orf19.5377	<i>HOS2</i>	17390	Tn7 insertion clone CAGFC21	357	DAY1243
orf19.2772	<i>HOS3</i>	65221	Tn7 insertion clone CAGR472	365	DAY1248
orf19.6801	<i>RPD31</i>	38517	Tn7 insertion clone CAGJX54	361	DAY1247
orf19.6801	<i>RPD31</i>	32377	Tn7 insertion clone CAGH755	358	DAY1246
orf19.2606	<i>HDA1</i>	-	Start-to-stop deletion		DAY694

**Table A.2.** Germ tube formation delay of the *hda1Δ/Δ* mutant in M199 pH 8 and Spider media

Strain	% germ tube ± SE		
	M199 pH 8	Spider	
DAY185	Wild-type	62.5 ± 2.4	71.2 ± 4.3
DAY1252	<i>hos2/hos2</i>	69.8 ± 2.8	71.0 ± 4.2
DAY1250	<i>hos2/hos2 + HOS2</i>	66.1 ± 3.4	77.5 ± 3.2
DAY1240	<i>hda1Δ/Δ</i>	27.3 ± 2.8**	55.2 ± 3.8*
DAY1241	<i>hda1Δ/Δ + HDA1</i>	67.2 ± 2.2	72.7 ± 2.5

Mean (% germ tubes) ± SE (Standard Error) of two independent experiments (n=6). \* p<0.03, \*\* p<0.003. Statistical analysis was performed using two tailed, paired T-Test.

**Table A.3.** *C. albicans* strains

Strain	Parent	Genotype	Reference
<b>DAY1</b> <b>(BPW17)</b>	SC5314	<i>ura3::λimm434/ura3::λimm434 his1::hisG/his1::hisG</i> <i>arg4::hisG/arg4::hisG</i>	(Wilson et al., 1999)
<b>DAY185</b>	DAY286	<i>ura3::λimm434/ura3::λimm434 pHIS1::his1::hisG/his1::hisG</i> <i>ARG4::URA3::arg4::hisG/arg4::hisG</i>	(Davis et al., 2002)
<b>DAY1242</b>	DAY1	<i>ura3::λimm434/ura3::λimm434 his1::hisG/his1::hisG</i> <i>arg4::hisG/arg4::hisG hos2::Tn7::ARG4/hos2::Tn7::URA3</i>	This study
<b>DAY1243</b>	DAY1	<i>ura3::λimm434/ura3::λimm434 his1::hisG/his1::hisG</i> <i>arg4::hisG/arg4::hisG hos2::Tn7::ARG4/hos2::Tn7::URA3</i>	This study
<b>DAY1246</b>	DAY1	<i>ura3::λimm434/ura3::λimm434 his1::hisG/his1::hisG</i> <i>arg4::hisG/arg4::hisG rpd31::Tn7::ARG4/ rpd31::Tn7::URA3</i>	This study
<b>DAY1247</b>	DAY1	<i>ura3::λimm434/ura3::λimm434 his1::hisG/his1::hisG</i> <i>arg4::hisG/arg4::hisG rpd31::Tn7::ARG4/ rpd31::Tn7::URA3</i>	This study
<b>DAY1249</b>	DAY1	<i>ura3::λimm434/ura3::λimm434 his1::hisG/his1::hisG</i> <i>arg4::hisG/arg4::hisG hos1::Tn7::ARG4/hos1::Tn7::URA3</i>	This study
<b>DAY694</b>	DAY1	<i>ura3::λimm434/ura3::λimm434 his1::hisG/his1::hisG</i> <i>arg4::hisG/arg4::hisG hda1::ARG4/hda1::URA3-dpl200</i>	This study
<b>DAY1250</b>	DAY1242	<i>ura3::λimm434/ura3::λimm434</i> <i>pHIS1::HOS2::his1::hisG/his1::hisG arg4::hisG/arg4::hisG</i> <i>hos2::Tn7::ARG4/hos2::Tn7::URA3</i>	This study
<b>DAY1251</b>	DAY1243	<i>ura3::λimm434/ura3::λimm434</i> <i>pHIS1::HOS2::his1::hisG/his1::hisG arg4::hisG/arg4::hisG</i> <i>hos2::Tn7::ARG4/hos2::Tn7::URA3</i>	This study
<b>DAY1252</b>	DAY1242	<i>ura3::λimm434/ura3::λimm434 pHIS1::his1::hisG/his1::hisG</i> <i>arg4::hisG/arg4::hisG hos2::Tn7::ARG4/hos2::Tn7::URA3</i>	This study
<b>DAY1253</b>	DAY1243	<i>ura3::λimm434/ura3::λimm434 pHIS1::his1::hisG/his1::hisG</i> <i>arg4::hisG/arg4::hisG hos2::Tn7::ARG4/hos2::Tn7::URA3</i>	This study
<b>DAY1241</b>	DAY694	<i>ura3::λimm434/ura3::λimm434</i> <i>pHIS1::HDA1::his1::hisG/his1::hisG arg4::hisG/arg4::hisG</i> <i>hda1::ARG4/hda1::URA3-dpl200</i>	This study
<b>DAY1240</b>	DAY694	<i>ura3::λimm434/ura3::λimm434 pHIS1::his1::hisG/his1::hisG</i> <i>arg4::hisG/arg4::hisG hda1::ARG4/hda1::URA3-dpl200</i>	This study
<b>DAY1305</b>	DAY1249	<i>ura3::λimm434/ura3::λimm434 pHIS1::his1::hisG/his1::hisG</i> <i>arg4::hisG/arg4::hisG hos1::Tn7::ARG4/hos1::Tn7::URA3</i>	This study
<b>DAY1306</b>	DAY1246	<i>ura3::λimm434/ura3::λimm434 pHIS1::his1::hisG/his1::hisG</i> <i>arg4::hisG/arg4::hisG rpd31::Tn7::ARG4/ rpd31::Tn7::URA3</i>	This study
<b>DAY1307</b>	DAY1247	<i>ura3::λimm434/ura3::λimm434 pHIS1::his1::hisG/his1::hisG</i> <i>arg4::hisG/arg4::hisG rpd31::Tn7::ARG4/ rpd31::Tn7::URA3</i>	This study
<b>DAY414</b> <b>(L40)</b>	<i>S. cerevisiae</i>	<i>MATα his3Δ200 trp1-901 leu2-3,-112 ade2 LYS2::(lexAop)<sub>4</sub>-</i> <i>HIS3 URA3::(lexAop)<sub>8</sub>-lacZ GAL4</i>	(Vojtek et al., 1993)

**Table A.4.** Primers used in this study

Name	Sequence (5' to 3')	Reference
<b>HOS2 DDB78 comp 5'</b>	ACGACGGCCAGTGAATTGTAATACGACTCACTATAGGGCGCCAATCACAGAACTCAAGGC	This study
<b>HOS2 DDB78 comp 3'</b>	AAGCTCGGAATTAACCCTCACTAAAAGGGAACAAAAGCTGGCTATCTTGTTAATTGATGGG	This study
<b>HDA1 5' comp</b>	AAGCTCGGAATTAACCCTCACTAAAAGGGAACAAAAGCTGGTCATCTGCTCTCCATTGACG	This study
<b>HDA1 3' comp</b>	ACGACGGCCAGTGAATTGTAATACGACTCACTATAGGGCGGAATTTAATGAACCCGATGG	This study
<b>HDA1 5-1 comp</b>	ATATATCCATATCCGGCTGG	This study
<b>HDA1 3-1 comp</b>	TTCTGGTATGCACGACGGTG	This study
<b>ARG4-detect</b>	GGAATTGATCAATTATCTTTTGAAC	This study
<b>FC21 5detect</b>	TTTTTACAATCGATAACTCC	This study
<b>FC21 3detect</b>	ACGTTGGTTGAAATTTTCGTG	This study
<b>N203 5detect</b>	CCAATATATAACCATAGGAG	This study
<b>N203 3detect</b>	GGCAATATCTGACATTCCTG	This study
<b>H755 5detect</b>	GCTGATATTGGGAATTATGC	This study
<b>H755 3detect</b>	GCTTCTTCAACACCATCACC	This study
<b>JX54 5detect</b>	GCCGCCAGATTGAATCGTGG	This study
<b>JX54 3detect</b>	CCACCAACTACCATCATTGG	This study
<b>R472 5detect</b>	GCATTTGAAACAACATTGAC	This study
<b>R472 3detect</b>	GCCAATAATCGTTGTGGACG	This study
<b>LH56 5detect</b>	CCCGTCCAATAAGGGAAGAC	This study
<b>LH56 3detect</b>	CAACCCCATCCCCATGATGC	This study
<b>HDA1 3DR</b>	CAATCTTCGGAAGAGGAGTAGTCTTCAATTGAATCTAATATGAAATCTACTCCTTCATCGTGGAATTGTGAGCGGATA	This study
<b>HDA1 5DR</b>	ATGTCGACTGGTCAAGAAGAACATCTAGATTCTAAGCTAGAAAATCAAATCTCAGAGGATTTCCAGTCACGACGTT	This study
<b>HDA1 5-detect</b>	ATAGAAGCTACCATTTTCAC	This study
<b>HDA1 3-detect</b>	AGAGATTTCTAGTTATGTG	This study

## FIGURES

**Figure A.1:** HDACs regulate filamentation on solid media. Overnight cultures of *C. albicans* wild-type (DAY185), *hos2/hos2* (DAY1252), *hos2/hos2 +HOS2* (DAY1250), *hda1Δ/Δ* (DAY1240), and *hda1Δ/Δ +HDA1* (DAY1241) strains grown in YPD at 30°C were: spotted onto M199 buffered to pH 8; serially diluted in PBS up to ~100 CFU and plated on Spider and SLAD media; diluted 1:1000 in 2 ml fresh YPD, incubated 4 hrs at 30°C and 8μl were plated in embedded agar; streaked in synthetic complete medium supplemented with 4% bovine calf serum (BCS). All plates were incubated at 37°C, except for embedded agar which was incubated at 23°C. A minimum of three independent repetitions for each filamentation assay was performed.

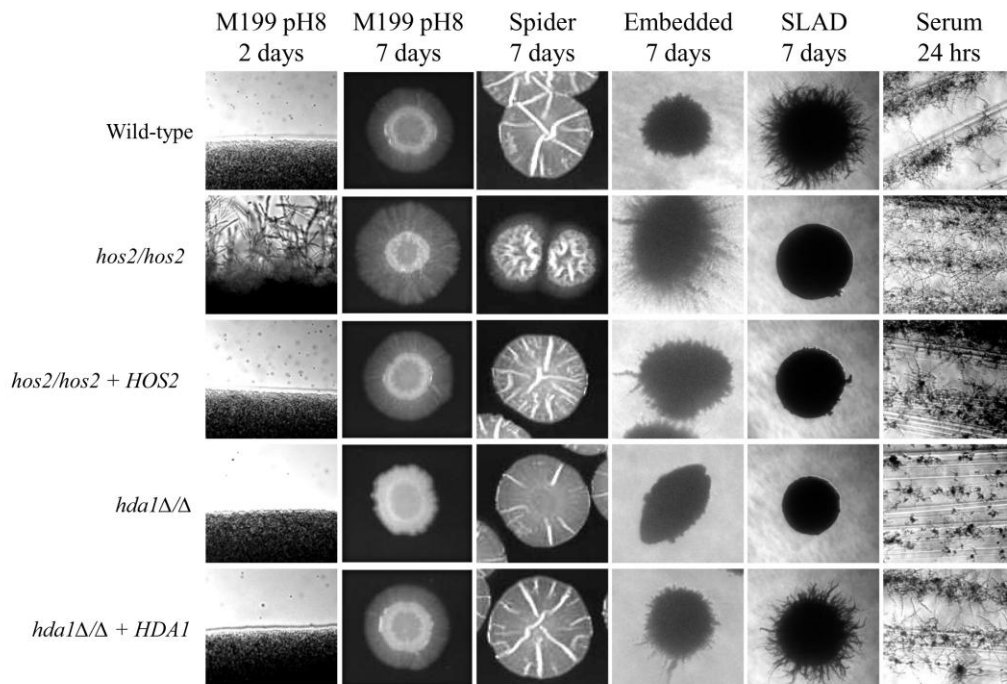
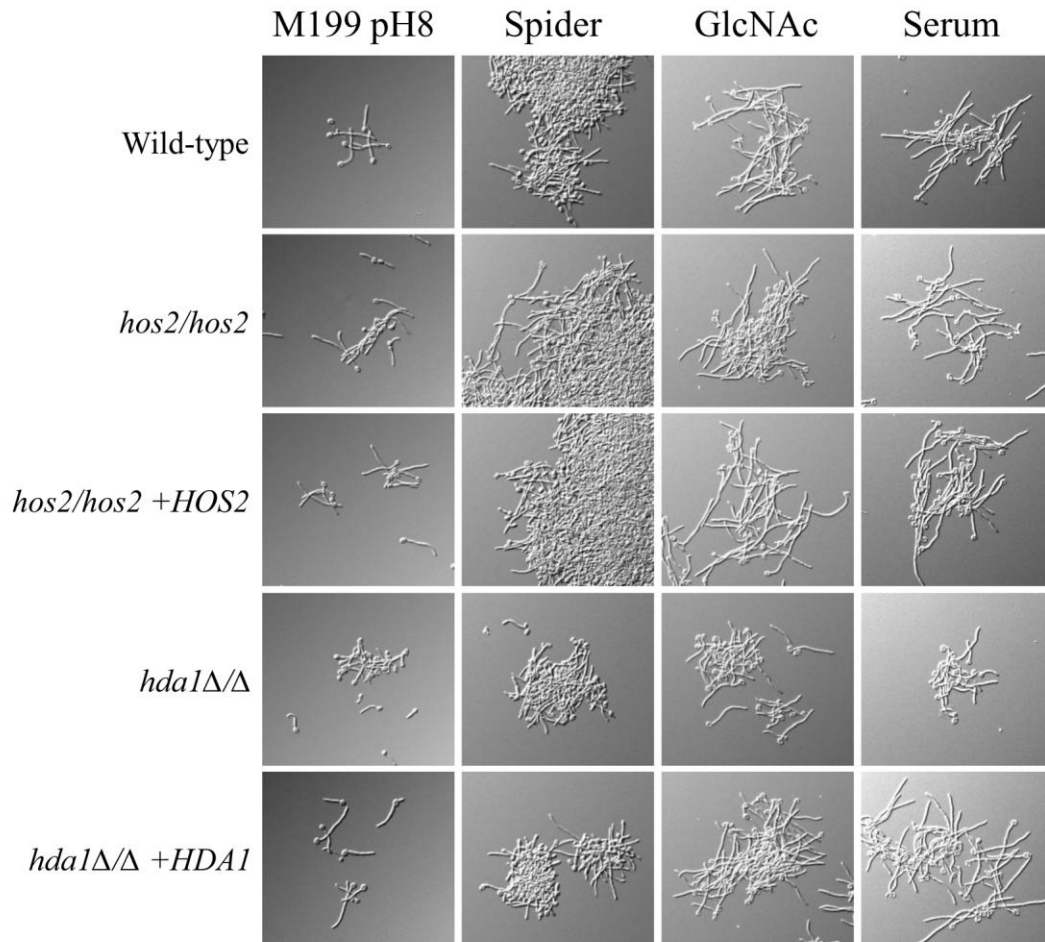


**Figure A.2:** HDACs regulate filamentation in liquid media. Overnight YPD cultures of *C. albicans* wild-type (DAY185), *hos2/hos2* (DAY1252), *hos2/hos2 +HOS2* (DAY1250), *hda1Δ/Δ* (DAY1240), and *hda1Δ/Δ +HDA1* (DAY1241) strains were washed in PBS, diluted 1:100 in M199 pH 8, Spider, YP+10% BCS, and YP+0.5% GlcNAc media and incubated 3 hrs at 37°C.



## **APPENDIX B**

### **LOW DOSAGE OF HISTONE H4 LEADS TO GROWTH DEFECTS AND MORPHOLOGICAL CHANGES IN *CANDIDA ALBICANS***

**Zacchi, L.F.**, Selmecki, A.M., Berman, J., Davis, D.A. (2010). Low dosage of histone H4 leads to growth defects and morphological changes in *Candida albicans*. *PLoS ONE*. 5(5):e10629

## SUMMARY

Chromatin function depends on adequate histone stoichiometry. Alterations in histone dosage affect transcription and chromosome segregation, leading to growth defects and aneuploidies. In the fungal pathogen *Candida albicans*, aneuploidy formation is associated with antifungal resistance and pathogenesis. Histone modifying enzymes and chromatin remodeling proteins are also required for pathogenesis. However, little is known about the mechanisms that generate aneuploidies or about the epigenetic mechanisms that shape the response of *C. albicans* to the host environment. Here, we determined the impact of histone H4 deficit in the growth and colony morphology of *C. albicans*. We found that *C. albicans* requires at least two of the four alleles that code for histone H4 (*HHF1* and *HHF22*) to grow normally. Strains with only one histone H4 allele show a severe growth defect and unstable colony morphology, and produce faster-growing, morphologically stable suppressors. Segmental or whole chromosomal trisomies that increased wild-type histone H4 copy number were the preferred mechanism of suppression. This is the first study of a core nucleosomal histone in *C. albicans*, and constitutes the prelude to future, more detailed research on the function of histone H4 in this important fungal pathogen.

## INTRODUCTION

*Candida albicans* is a major human fungal pathogen and is the fourth most common cause of nosocomial bloodstream infections (Pfaller et al., 2001). *C. albicans* is a common commensal of the skin and mucosa, and often causes superficial, non-life threatening infections at these sites (Calderone, 2002). However, in immune-compromised individuals *C. albicans* can cause systemic infections, which have a mortality rate of > 30% even in patients undergoing antifungal therapy (Pfaller et al., 1998). The steady increase in the population of immune-compromised individuals due to modern medical practices such as chemotherapy and organ transplantation, as well as because of the AIDS epidemic continues to provide niches for the development of *C. albicans* systemic and mucosal infections.

*C. albicans* pathogenesis has been increasingly linked to alterations in chromosome structure and dynamics. *C. albicans* strains with altered karyotypes are frequently isolated from clinical samples, from passage through mammalian hosts, and by growth in specific carbon sources or antifungals *in vitro* (Forche et al., 2009; Rustchenko, 2007). *C. albicans* has a high tolerance to aneuploidies, perhaps because they provide a source for phenotypic variation, critical for survival and pathogenesis (Rustchenko-Bulgac et al., 1990). Aneuploidies are associated with antifungal resistance, metabolic changes, and mating (Perepnikhatka et al., 1999; Janbon et al., 1998; Rustchenko et al., 1994; Selmecki et al., 2006; Wu et al., 2005; Magee and Magee, 2000; Coste et al., 2007). Altered karyotypes have also been associated with variations in colony morphology (Forche et al., 2005, 2009; Rustchenko-Bulgac et al., 1990; Suzuki et al., 1989). However, the mechanisms that promote ploidy changes and genomic rearrangements are not well understood.

Histone modifying enzymes and chromatin remodeling proteins also contribute to the regulation of pathogenesis traits. For example, mutants in histone deacetylases, methylases, acetyltransferases, and members of chromatin remodeling complexes show defects in yeast-hyphal transitions, white-opaque switching, adhesion to epithelial cells, and/or antifungal and stress resistance (Hnisz et al., 2009; Klar et al., 2001; Lu et al., 2008; Mao et al., 2006; Raman et al., 2006; Srikantha et al., 2001; Smith and Edling, 2002; Sellam et al., 2009). Therefore, changes in the structure and function of the chromatin leads to epigenetic defects and potentially to karyotypic variations that have a direct impact on *C. albicans* virulence.

Chromatin is a dynamic structure composed of DNA and DNA binding proteins that allows for an efficient storage and usage of the genetic information. The basic unit of chromatin architecture is the nucleosome, which is composed of the evolutionary conserved histones H2A, H2B, H3 and H4 assembled in a hetero-octamer of two H2A/H2B dimers and one H3/H4 tetramer. The DNA is wrapped around the nucleosome, constituting the first level of chromatin compaction. Due to this intimate relationship with the DNA, histones are involved in all processes associated with chromatin structure and function, including transcription, replication, DNA repair, recombination, and chromosome segregation. Histones participate in the regulation of these processes by providing a platform to transmit information to other proteins (e.g. DNA and RNA polymerases) through posttranslational modifications in their residues (Jenuwein and Allis, 2001; Taverna et al., 2007) and through nucleosomal occupancy of regulatory regions in the DNA (Workman, 2006; Li et al., 2007). Thus, histones constitute the primary regulators of chromatin activity.

Alterations in histone availability have profound effects on the cell. Unbalanced histone dimer stoichiometry causes defects in the segregation of mitotic chromosomes, increases recombination and genetic instability, and leads to sporulation defects in *S. cerevisiae* (Kim et al., 1988; Meeks-Wagner and Hartwell, 1986; Smith et al., 1996; Au et al., 2008; Tsui et al., 1997; Hanlon et al., 2003; Norris and Osley, 1987; Saunders et al., 1990; Venditti et al., 1999; Prado and Aguilera, 2005). Furthermore, incomplete nucleosomal occupancy due to histone dosage defects directly impacts transcriptional regulation (Han and Grunstein, 1988; Han et al., 1988; Wyrick et al., 1999; Clark-Adams et al., 1988; Durrin et al., 1992; Lee et al., 2004; Svaren and Horz, 1993). Therefore, alterations in histone stoichiometry have pleiotropic effects in cells.

In this study we performed serial deletions of *C. albicans* histone H4 genes and determined the effect of a deficit in histone H4 on growth. We found that reduced histone H4 dosage caused a severe growth defect and the formation of colony morphology variants. *C. albicans* primarily counterbalanced the low dosage of histone H4 by increasing histone H4 gene copy number through the formation of aneuploidies. Suppression of the growth defect associated with low histone H4 dosage also restored colony morphology to the wild-type morphology. This is the first study on core histones in *C. albicans*, which provides background genetic information for future experiments that address the role of chromatin structure and function in *C. albicans* biology and pathogenesis.

## MATERIALS AND METHODS

### Strains and plasmids

All strains used in this study are listed in Table B.1. Strain DAY1069 was generated as follows. BWP17 was transformed with a *hht2-hhf22::URA3-dpl200* disruption cassette amplified in a PCR using primers HHT2-HHF22 5DR and 3DR new (Table B.2) to give strain DAY1067. DAY1067 was then transformed with a *hht2-hhf22::ARG4* disruption cassette amplified as above. The *hht2-hhf22* disruption cassettes delete the region from nucleotide +329 of *HHT2* to the stop codon of *HHF22* (Figure B.1). The *URA3-dpl200* marker from strain DAY1069 was recycled by plating the cells in synthetic medium supplemented with 5-fluoroorotic acid (5-FOA) to obtain strain DAY1071. Strain DAY1072 was generated by replacing nucleotide +114 to the stop codon of one *HHF1* alleles in DAY1071 using the *hhf1::URA3* disruption cassette, which was amplified in a PCR using primers HHF1 5DR 100 in and HHF1 3DR new (Figure B.1 and Table B.2).

DAY1068 was generated by transforming strain BWP17 with the *hhf1::URA3-dpl200* disruption cassette (Figure B.1) to generate strain DAY1066, followed by transformation with the *hht2-hhf22::ARG4* disruption cassette (Table B.2). Strain DAY1070 was obtained by plating DAY1068 in synthetic medium supplemented with 5-FOA to recycle the *URA3-dpl200* marker. Strains DAY1074, DAY1076 and DAY1078 were generated by partially deleting the last *HHF1* copy from DAY1070 using an *hhf1::URA3* disruption cassette amplified from plasmid DDB383 with primers HHF1 5' fragm DDB78 and HHF1 3' fragm DDB78. Plasmid DDB383 contains the disruption cassette bordered by additional *HHF1* flanking regions in order to increase the efficiency of integration into the *HHF1* locus. Strains DAY1075 and DAY1079 are large colony revertants of strains DAY1074 and 1078, respectively. The genotypes of the strains and the correct integration of the disruption cassettes were verified by the PCR using primers HHF1 5 detect, HHF1 3 detect, HHT2-HHF22 5 detect and HHT2-HHF22 3'detect-new that flank the integration site (Table B.2), and by Southern blot.

Plasmid DDB383 was generated by *in vivo* recombination as follows. An *hhf1::URA3* disruption cassette was amplified in a PCR from DDB245 (Wilson et al., 1999) using primers HHF1 5' 100 in for DDB78 and HHF1 3' for DDB78 (Table B.2). The two flanking *HHF1* regions of 570 bp and 523 bp with homology upstream (including the first 113 nucleotides of *HHF1*) and downstream of *HHF1*, respectively, were amplified in two high fidelity PCRs (Pfu Turbo DNA polymerase, Stratagene) from BWP17 genomic DNA using the primer pairs HHF1 5' fragm DDB78 and HHF1 5' fragm 3', and HHF1 3' fragm DDB78 and HHF1 3' fragm 5', respectively. The three PCR products were co-transformed with a NotI/EcoRI double digestion of DDB78 into *trp<sup>-</sup> Saccharomyces cerevisiae* L40 strain to generate DDB383.

### Media and growth conditions

*C. albicans* was routinely grown at 30°C in YPD supplemented with uridine (2% bacto-peptone, 1% yeast extract, 2% dextrose, and 80 µg ml<sup>-1</sup> of uridine). Mutants were selected on synthetic medium (0.17% yeast nitrogen base without ammonium sulfate (Q-BioGene), 0.5% ammonium sulfate, 2% dextrose, and supplemented with a dropout mix containing amino and nucleic acids except those necessary for the selection (Adams et al., 1997). Solid media were prepared by addition of 2% Bacto-agar.

### **Southern blot and comparative genomic hybridizations**

For the *HHF1* and *HHF22* dosage experiments, genomic DNA was digested with HindIII or NcoI, respectively (Figure B.1), separated in a 1.2% agarose gel by electrophoresis, and transferred by capillary action to a nylon membrane. Probes D (for *HHF1*) and G (for *HHF22*) were PCR amplified from *C. albicans* BWP17 genomic DNA using primer pairs HHF1 5' fragm 5' and HHF1 5' fragm 3', and HHF22 5' SB and HHF22 3' detect, respectively (Figure B.1 and Table B.2). The probes were radiolabelled with [ $\alpha$ -<sup>32</sup>P]-dCTP using the Prime-a-Gene labeling system (Promega). Blots were developed with a phosphoimager (STORM system). Densitometry analysis of the images was performed using ImageJ 1.30v (Wayne Rasband, NIH, USA). For comparative genomic hybridizations (CGH), genomic DNA was prepared from *C. albicans* strains grown overnight to saturation in 5 ml YPAD medium using phenol/chloroform as described (Hoffman and Winston, 1987). 3  $\mu$ g of DNA was digested with HaeIII (Invitrogen), labeled with Cy3 (experimental strains) or Cy5 (reference strain, SC5314), and hybridized to microarrays as described previously (Selmecki et al., 2005). The microarrays were printed in-house and contain 14,688 total spots, representing 6175 ORFs, designed using Assembly six *C. albicans* ORFs (Bensen et al., 2004) and updated with Assembly 19 ORFs. Arrays were scanned (ScanArray 5000) using QuantArray v.2.01 software (GSI Lumonics, Watertown, MA). Data were analyzed using GenePixPro 5.1 and GeneTraffic 3.1. The average mean log<sub>2</sub> ratio average of two duplicate spots per microarray slide was calculated and plotted as a function of chromosome position using Chromosome\_Map (Selmecki et al., 2005).

## RESULTS AND DISCUSSION

### Histone H3 and H4 genes in *Candida albicans*

Several characteristics of histones H3 and H4 prompted us to focus on them for the purpose of this study. First, histones H3 and H4 show greater conservation than histones H2A and H2B (Thatcher and Gorovsky, 1994). Second, the H3/H4 tetramer has a more critical role in nucleosome assembly and chromatin condensation, as the H3/H4 tetramer interacts more strongly with the central portion of the nucleosomal DNA than the H2A/H2B dimers (Pruss et al., 1995; Dorigo et al., 2003), and it has the ability to block transcriptional elongation *in vitro* (Chang and Luse, 1997). Third, the effect of histones H3 and H4 posttranslational modifications is better understood and includes modifications in both the amino terminal tail and globular core domains (Zhang et al., 2003; Hyland et al., 2005). Based on the higher conservation, the prominent role in chromatin structure, and the extensive knowledge on histone H3 and H4 posttranslational modifications, we focused on the histone H3-H4 cluster and, in particular, on histone H4, for reasons discussed below.

Most eukaryotes, including *C. albicans*, contain multiple copies of histone H3 and H4 genes, which are generally organized in clusters (Osley, 1991). The *S. cerevisiae* genome contains two genes, *HHT1* and *HHT2*, which encode identical proteins for the canonical histone H3 isoform. The *C. albicans* genome contains three genes that encode histone H3: *HHT1* (orf19.6791), *HHT2* (orf19.1853), and *HHT21* (orf19.1061). *HHT2* and *HHT21* encode identical histone H3 isoforms, whereas *HHT1* encodes a histone H3 with three differences when compared to *HHT2/21*: a non-conserved S32V change, and two conserved S33T and S81T changes (Figure B.2A). When compared to *S. cerevisiae* *HHT1/2*, there are five amino acid differences, which are found in all three *C. albicans* histone H3 genes and are located in the C terminal half of the protein (Figure B.2A).

Similar to *S. cerevisiae* and *Schizosaccharomyces pombe* (Matsumoto and Yanagida, 1985; Smith and Andresson, 1983), *C. albicans* *HHT2* and *HHT21* are divergently transcribed from the histone H4 genes *HHF22* (orf19.1059) and *HHF1* (orf19.1854), respectively. *HHT2-HHF22* is on chromosome R; *HHT21-HHF1* is on chromosome 1 (Figure B.1). *HHT1*, on chromosome 3, is unique in that it is not paired with a histone H4 gene. Unpaired histone genes are also observed in other fungi, including *S. pombe*, which has an unpaired histone H2A (Matsumoto and Yanagida, 1985; Smith and Andresson, 1983; Choe et al., 1985). *HHT2* and *HHT21* are located 900-1000 bp from their cognate histone H4 gene and likely share the same promoter. However, we noted a potential open reading frame (ORF), orf19.1060, within the *HHT21-HHF1* intergenic region (Figure 1). This ORF can encode a protein of 169 residues. However, this predicted protein has no significant homology to other proteins or identifiable motifs, suggesting that orf19.1060 is a spurious ORF. Therefore, the genomic arrangement of the H3/H4 cluster in *C. albicans* is similar to *S. cerevisiae*, except for the presence in *C. albicans* of a single unpaired, divergent third histone H3 gene.

Since Hht1 has a divergent amino acid sequence compared to Hht2/21 and is expressed independent of a histone H4, we propose that Hht1 is a histone H3 variant. Histone variants are usually replication-independent, diverge from the canonical histone sequences, and have a different function (Ausio et al., 2001; Stein et al., 1992). For example, *Drosophila melanogaster* and vertebrates express histone H3.3, a canonical histone H3 variant that differs in four amino

acids, three of which are clustered in the histone fold domain (Fretzin et al., 1991; Wells et al., 1989; Ahmad and Henikoff, 2002a, b). Although all three *C. albicans* histone H3s are of the H3.3 class and the amino acid differences in Hht1 are not within the histone fold domain, Hht1 might still constitute a histone H3 variant. In particular, the S32V change in Hht1 could affect epigenetic regulatory events as it eliminates a potential phosphorylation site in the N-terminus tail of Hht1 (Hake et al., 2005; Wong et al., 2009). Thus, *HHT1* may encode a histone H3 homomorphic variant.

The *C. albicans* genome contains two genes, *HHF1* and *HHF22*, that encode identical histone H4 proteins. The *S. cerevisiae* genome also encodes two identical histone H4 proteins. Comparison of *C. albicans* Hhf1/22 to *S. cerevisiae* Hhf1/2, revealed seven amino acid differences (Figure B.2B). Therefore, the genomic arrangement of histone H4 genes in *C. albicans* is similar to *S. cerevisiae*. Since *C. albicans* contains three non-allelic histone H3 genes as well as a heteromorphic histone H3 variant Cse4, which replaces histone H3 in centromeric chromatin (Ketel et al., 2009; Sanyal and Carbon, 2002), we focused our studies on histone H4, which is encoded by two genes and is present in all nucleosomes.

### **Reduced histone H4 dosage impairs *C. albicans* growth.**

Previous work in *S. cerevisiae*, *S. pombe*, and *D. melanogaster* showed that alterations in the dosage of the core nucleosomal histones can lead to pleiotropic phenotypes, including growth and cell cycle defects, chromosomal and telomere instability and gene expression deregulation (Kim et al., 1988; Meeks-Wagner and Hartwell, 1986; Norris and Osley, 1987; Venditti et al., 1999; Han and Grunstein, 1988; Han et al., 1988; Clark-Adams et al., 1988; Smith and Stirling, 1988; Castillo et al., 2007; Moore et al., 1983). In order to understand the effects of altering histone H4 dosage in *C. albicans*, sequential deletions of three of the four histone H4 alleles were performed.

First, we generated a deletion of the *HHF22-HHT2* region, which lacks additional ORFs (Figure B.1). *HHF22* and *HHT2* were simultaneously deleted in order to reduce any potentially harmful effects of changing the histone H3/histone H4 ratio (Venditti et al., 1999; Clark-Adams et al., 1988; Castillo et al., 2007; Moran et al., 1990). The entire *HHF22* ORF, 80% of the *HHT2* ORF, and the intergenic region were replaced by an auxotrophic marker cassette (Figure B.1). We were able to generate both *HHF22-HHT2/hhf22-hht2Δ* heterozygous and *hhf22-hht2Δ/Δ* homozygous strains, and these strains had no overt growth or morphological phenotypes (Figure B.3A). This suggests that Hhf22 and Hht2 are not essential for growth.

*S. cerevisiae* diploids containing a single H3-H4 locus have a longer generation time and a more prolonged G1 phase than wild-type cells (Smith and Stirling, 1988). Further, deletion of *HHT2-HHF2* in *S. cerevisiae*, but not *HHT1-HHF1*, causes greater minichromosome loss compared to wild-type (Smith and Stirling, 1988), indicating that, although both H3-H4 loci are generally functionally redundant, there are differences between both loci. To determine if *C. albicans* has a different requirement for *HHF1* or *HHF22* for growth, we constructed a strain in which both copies of *HHF1* were deleted. We were readily able to generate *HHF1/hhf1Δ* and *hhf1Δ/Δ* strains, and these strains did not show growth or morphological defects (Figure B.3B and data not shown), indicating that Hhf1 is also not essential for growth in *C. albicans*. Therefore,

unlike in *S. cerevisiae*, in *C. albicans* the presence of either one of the histone H4 gene is sufficient to ensure normal growth and colony morphology.

When we attempted to mutate one copy of *HHF1* in the *hhf22-hht2Δ/Δ* background, we only recovered a single homologous recombinant (1 homologous recombinant/395 transformants screened). Similarly, when we attempted to mutate the remaining copy of *HHF22-HHT2* copy from a *HHF22-HHT2/hhf22-hht2Δ HHF1/hhf1Δ* double heterozygote, we only recovered homologous recombinants 7% of the time (32 homologous recombinants/437 transformants screened). However, all of these recombinants retained a wild-type *HHF22-HHT2* copy and arose by a marker exchange (29/32) or a by a increased *HHF22-HHT2* copy number (3/32). To increase the rate of homologous recombination, we generated an *hhf1::URA3* disruption cassette containing regions of homology ~9x larger than the original cassettes (Table B.2). Using this extended disruption cassette we increased homologous recombination in the *hhf22-hht2Δ/Δ* strain to 50% (11/22). All *hhf22-hht2Δ/Δ HHF1/hhf1Δ* transformants had a pronounced growth defect (Figure 3A) and gave rise to both smooth and wrinkly colonies of heterogeneous size (Figure B.4A and B). The difficulty in eliminating a third histone H4 gene and the severe growth defects observed in the mutant with only one *HHF1* copy suggested that *C. albicans* might require at least two copies of histone H4 for normal growth. Alternatively, *HHF22* might be the primary histone H4 gene in *C. albicans*.

If *HHF22* is indeed the primary histone H4 gene in *C. albicans*, we predicted that we could construct an *HHF22/hhf22Δ hhf1Δ/Δ* mutant without impacting growth. To construct this mutant, we eliminated the last *HHF1* copy from a *HHF22-HHT2/hhf22-hht2Δ HHF1/hhf1Δ* double heterozygous strain. As before, the use of longer regions of homology increased the rate of homologous recombinants (44/45). However, in most cases (40/44) the wild-type *HHF1* copy was retained. While the *HHF22-HHT2/hhf22-hht2Δ HHF1/hhf1Δ* strain had no overt growth defects compared to wild-type colonies, the four *HHF22-HHT2/hhf22-hht2Δ hhf1Δ/Δ* mutants obtained had severe growth defects (Figure B.3B). *HHF22-HHT2/hhf22-hht2Δ hhf1Δ/Δ* strains also gave rise to heterogeneous colony sizes with both smooth and wrinkly morphologies (Figure B.4 and B.5). The similar growth defects in the *HHF22-HHT2/hhf22-hht2Δ hhf1Δ/Δ* and *hhf22-hht2Δ/Δ HHF1/hhf1Δ* strains suggest that *HHF22* is not the primary histone H4 gene. Rather, *C. albicans* growth is dependent on the presence of at least two copies of histone H4.

We noticed that both *hhf22-hht2Δ/Δ HHF1/hhf1Δ* and *HHF22-HHT2/hhf22-hht2Δ hhf1Δ/Δ* strains gave rise to larger colonies at a low frequency (Figure B.3 and B.4). We considered the possibility that the larger colonies contained stable suppressor mutations. To address this, we re-isolated small and large colonies on fresh medium. When re-isolated, *hhf22-hht2Δ/Δ HHF1/hhf1Δ* small colonies gave rise to primarily small colonies with distinct morphologies (Figure B.5), and a few large and always smooth colonies (Figure B.4C). However, *hhf22-hht2Δ/Δ HHF1/hhf1Δ* large colonies gave rise to uniformly large and smooth colonies (Figure B.4C). Re-isolation of small colonies from the *HHF22-HHT2/hhf22-hht2Δ hhf1/hhf1Δ* strain also gave rise to small colonies with distinct morphologies, and to large colonies (Figure B.4D and B.5). In contrast to the *hhf22-hht2Δ/Δ HHF1/hhf1Δ* strain (Figure B.4E), re-isolation of large colonies from the *HHF22-HHT2/hhf22-hht2Δ hhf1Δ/Δ* strain gave rise to primarily large colonies, but also occasionally to small colonies (Figure B.4F). When re-isolated, these small colonies behaved like the parental *HHF22-HHT2/hhf22-hht2Δ hhf1Δ/Δ* small colonies (data not

shown), indicating that the suppressor phenotype may be reversible. These results suggest that the severe growth defect caused by the low dosage of both *HHF1* and *HHF22* confers a strong selective pressure for the generation of secondary suppressor, reversible mutations, which restore growth. Further, the differences observed in the emergence of small colonies during re-isolation of large colonies in both type of mutants is likely a consequence of how the stability of the suppressors that arose in the mutants.

### **Aneuploidy as a mechanism for H4 dosage compensation in *C. albicans***

Two copies of histone H4 are necessary and sufficient for wild-type growth. Thus, we reasoned that the increased colony size and phenotypic stability observed in the large suppressor colonies reflected an increase in histone H4 copy number. Since aneuploidies are common in *C. albicans* strains (Rustchenko, 2007; Perepnikhatka et al., 1999; Janbon et al., 1998; Selmecki et al., 2005, 2006; Wu et al., 2005; Coste et al., 2007; Chen et al., 2004; Magee et al., 1992; Arbour et al., 2009; Diogo et al., 2009; Legrand et al., 2004), we hypothesized that the large suppressor colonies had duplicated the remaining histone H4 gene, thereby restoring the number of histone H4 alleles to two, which supports normal and phenotypically stable growth (Figure B.3). The duplication of large DNA fragments, including whole chromosomes, as a mechanism to suppress a slow growth defect has also been described in *S. cerevisiae* (Hughes et al., 2000).

In order to determine if the large colonies of the *hhf22-hht2Δ/Δ HHF1/hhf1Δ* and *HHF22-HHT2/hhf22-hht2Δ hhf1Δ/Δ* mutants had increased the number of wild-type H4 allele copies, we performed quantitative Southern blot analysis. Two probes, Probe D and Probe G, were designed to anneal equally to both the wild-type and the mutated versions of *HHF1* or *HHF22*, respectively (Figure B.1). Densitometry analysis was performed on Southern blots of small and large colonies isolated from the mutants to determine the ratio of mutated to wild-type histone H4 allele (Figure B.6). We included the *HHF22-HHT2/hhf22-hht2Δ HHF1/hhf1Δ* heterozygous strain DAY1070 as a control, which had a 1:1.1 *hhf22Δ/HHF22* ratio by quantitative Southern blot (Figure B.6B). Indeed, the small colonies of the histone mutants retained a 1:0.9-1.1 ratio of mutated to wild-type H4 alleles while the large colonies presented a 1:1.5-2.6 ratio of mutated to wild-type H4 alleles (Figure B.6A and B.6B). Thus, the large colonies of the *hhf22-hht2Δ/Δ HHF1/hhf1Δ* and *HHF22-HHT2/hhf22-hht2Δ hhf1Δ/Δ* mutants analyzed showed an increase in DNA associated with the wild-type histone H4 compared to the small colonies. Thus, the suppressor colonies arise by increasing the genomic dosage of histone H4.

We reasoned that an increase in histone H4 copy number could involve either a segmental aneuploidy or a trisomy. Using comparative genome hybridization (CGH) arrays, we found that, as expected, a small colony of *hhf22-hht2Δ/Δ HHF1/hhf1Δ* had a diploid content of chromosome 1 (Figure B.7). However, CGH analysis of a large suppressor colony derived from the *hhf22-hht2Δ/Δ HHF1/hhf1Δ* small colony revealed a trisomy of chromosome 1. Thus, a reduction in histone H4 dosage causes a severe growth defect that can be overcome through whole chromosome aneuploidy to increase histone H4 copy number. While we cannot rule out segmental aneuploidy as a mechanism to restore histone H4 dosage, whole chromosome aneuploidy is clearly one mechanism that can restore histone H4 dosage.

We noted two additional aneuploidies in our CGH analysis. First, a segmental monosomy of one end of chromosome 5 in both the small and large colony (Figure B.7). This is an attribute of the RM1000 background from which these strains are descended which is known to have a stable deletion in one arm of chromosome 5 (Magee and Magee, 2000; Selmecki et al., 2005). Second, a whole chromosome monosomy in chromosome 3 was observed in the *hhf22-hht2Δ/Δ HHF1/hhf1Δ* small colony, but not the large suppressor colony derivative. Defects on histone dosage have been implicated in the generation of aneuploidies and chromosome instability, and this may reflect evidence of that phenomenon in *C. albicans*. However, it is also possible that reduced chromosome 3 dosage provides some advantage to cells containing one histone H4 locus.

It is noteworthy that not all large colonies gave the expected 1:~2 ratio of mutant to wild-type histone H4 by quantitative Southern blot (Figure B.6C). We found a 0:1 ratio (arbitrarily set to 1 as there was no mutant allele to normalize to), which lost the mutant histone H4 allele, a 1:1 ratio, which maintained the ratio of the starting strain, and a ~2:1 ratio, which duplicated the mutant histone H4 allele. The 0:1 ratio found in large colonies indicates that the mutated version of the histone H4 was replaced with the wild-type histone H4 by mitotic recombination or by loss of the chromosome carrying the mutant allele followed by duplication of the remaining chromosome containing the wild type allele. The 1:1 ratio found in large colonies indicates that either the strain became tetrasomic for both loci or that there exist alternative suppressor mechanisms. The ~2:1 ratio found in large colonies indicates that the mutated version of the histone H4 was duplicated, perhaps causing a trisomy of part or all of chromosome R. This type of aneuploidy may restore growth, however we cannot rule out the possibility that chromosome R is found in a 4:2 mutant to wild-type ratio in these cells. In fact this latter possibility seems to be supported by the increased *hhf22Δ* and *HHF22* signals observed in this sample (Figure B.6C). We noted that the large colonies carrying a 0:1, 1:1, and 1:2 ratio of mutant to wild-type histone H4 had the typical smooth morphology, but the colonies carrying a 2:1 ratio showed a wrinkly top and were more heterogeneous in size (Figure B.6D). These differences in colony morphology are in agreement with the formation of alternative karyotypes (see below). The 0:1, 1:1, and 2:1 ratio for large colonies arose from the *HHF22-HHT2/hhf22-hht2Δ hhf1Δ/Δ* mutant but not from the *hhf22-hht2Δ/Δ HHF1/hhf1Δ* mutant, which suggests that Chromosome R is less stable than Chromosome 1.

Since maintenance of genomic integrity is critical for survival, cells have different mechanisms to compensate for histone dosage defects, including genomic rearrangements and, more commonly, transcriptional alterations. Genomic rearrangements have been observed in *S. cerevisiae*, which can increase histone H2A-H2B copy number by forming a small circular chromosome (Libuda and Winston, 2006). Dosage compensation through transcriptional up-regulation of histone gene expression has been observed both in *S. cerevisiae*, where the expression of one of the H2A-H2B loci (*HTA1-HTB1*) is regulated by the availability of histones H2A-H2B in the cell (Moran et al., 1990), as well as in *S. pombe* (Takayama and Takahashi, 2007). Thus, while we observed an increase in gene copy number in the large colonies screened, we cannot rule out the possibility that *C. albicans* can increase histone H4 availability by transcriptional mechanisms.

We observed that while the large colonies of the *hhf22-hht2Δ/Δ HHF1/hhf1Δ* strain were phenotypically stable, the large colonies isolated from the *HHF22-HHT2/hhf22-hht2Δ hhf1Δ/Δ*

strain often gave rise to small colonies. This observation suggests that a Chromosome R trisomy (*HHF22*) is less stable than a Chromosome 1 trisomy (*HHF1*). Chromosome R has a variable electrophoretic mobility. These variations are found in natural isolates, in spontaneous morphological mutants, and in randomly selected colonies from a clonal population of a reference strain (Wickes et al., 1991; Asakura et al., 1991; Rustchenko et al., 1993). However, chromosome R variations are attributed to changes in the number of rDNA repeats, and not to ploidy changes (Rustchenko et al., 1993; Iwaguchi et al., 1992). A random gain and subsequent loss of an extra copy of Chromosome R might explain the slightly unstable phenotype of the large colonies with only *HHF22*. Acquiring a third Chromosome R copy would provide a selective growth advantage because it increases histone H4 copy number. However, excess of rDNA synthesis, or other chromosome R associated locus, could be deleterious for cells growing at suboptimal conditions (Rustchenko et al., 1993; Ganley et al., 2009; Warner, 1999). Thus, some suppressor cells might randomly lose the extra Chromosome R copy and revert to a slow growth small colony phenotype. Trisomy in Chromosome 1 might not have as negative an effect on growth, explaining the more stable colony morphology of the suppressors from strains with only a single allele of *HHF1*. In fact, some stocks of the routinely used laboratory strain CAI-4 are stably trisomic for Chromosome 1 under non-stress conditions with no obvious effects on growth or colony morphology (Chen et al., 2004). Therefore, the alterations in colony size observed in both histone H4 mutants could be attributed to the gain and loss of a segment or an entire copy of Chromosome R or Chromosome 1.

### **Histone H4 deficit causes colony morphology changes**

When growing on agar plates at 30°C, *C. albicans* normally forms smooth, round, cream-colored colonies composed of yeast cells. Wrinkly colonies are generally composed of a higher percentage of cells that are filamenting, a fact that explains why it is possible to exacerbate some colony morphology phenotypic differences at 37°C. Altered *C. albicans* colony morphologies have been detected in strains isolated from infected patients, from studies in mouse models, and can also be induced in the laboratory through UV irradiation and genetic manipulation (Forche et al., 2005, 2009; Soll et al., 1987, 1988, 1989; Garcia-Sanchez et al., 2005; Slutsky et al., 1985; Barton and Scherer, 1994). The changes in colony morphology are a manifestation of underlying genomic changes that can involve a group of genes (like in the white-opaque switching) or major karyotypic rearrangements (Rustchenko et al., 1994). Thus, alterations in diverse factors can lead to changes in colony morphology.

When small, smooth colonies that carry only one H4 allele are sub-cultured onto a rich medium plate they give rise to colonies that have different morphologies (Figure B.5A). The change in colony morphologies of small colonies was generally penetrant, although they also gave rise to colonies with other types of morphologies (Figure B.5B). On the contrary, the large and smooth suppressor colonies did not produce colonies with altered morphology when they were sub-cultured, indicating that their colony morphology phenotype is stable (Figure B.5C). One exception to this statement is the already mentioned formation of small colonies from re-streaking of the large colonies, which most likely arise by the loss of the duplicated chromosome R.

One explanation for the formation of semi-penetrant morphological variants in the histone mutants is karyotypic rearrangements. As previously mentioned, altered colony morphologies have been associated with altered karyotypes or with loss of heterozygosity (Rustchenko et al., 1994; Forche et al., 2009; Uhl et al., 2003). Imbalances in histone dosage can lead to chromosome missegregation (Kim et al., 1988; Meeks-Wagner and Hartwell, 1986; Smith et al., 1996; Au et al., 2008). Further, the histone mutants grow slowly, a condition that might be more permissive to the accumulation and tolerance of aneuploidies (Forche et al., 2009). This latter idea is supported by the presence of a monosomic chromosome 3 in a *hhf22-hht2Δ/Δ HHF1/hhf1Δ* small colony (Figure B.7). Thus, karyotypic rearrangements favored by the combination of the slow growth and the nucleosomal deficit of the histone H4 mutants might be one mechanism behind the formation of colony variants.

*Candida albicans* is the most important human fungal pathogen, causing serious infections in immunosuppressed individuals. *C. albicans* has a diploid genome with an unexpectedly high level of heterozygosity, given the primarily clonal reproductive style of this organism (Jones et al., 2004). The genome of *C. albicans* has a remarkably high tolerance for genomic rearrangements. The ability to thrive with an altered karyotype may provide a profound advantage to this organism, because it represents a potential source of genetic variation (Rustchenko, 2007). Karyotypic rearrangements and aneuploidies in *C. albicans* are associated with pathogenesis: they affect cellular and colonial morphology, increase metabolic diversity, are required for mating, and, importantly, constitute a mechanism of antifungal resistance. Histone modifying enzymes and chromatin remodeling proteins are also required for pathogenesis in *C. albicans* (Hnisz et al., 2009; Klar et al., 2001; Lu et al., 2008; Mao et al., 2006; Raman et al., 2006; Srikantha et al., 2001; Smith and Edling, 2002; Sellam et al., 2005). The study of chromatin dynamics and structure in this fungus therefore is critical for understanding the nature of *C. albicans* pathogenicity and, furthermore, it may uncover potential targets for antifungal therapies. In this study, we have generated and characterized strains that can be used for future analysis of specific histone H4 mutant alleles, in order to begin to dissect the function and impact of epigenetic regulation in *C. albicans* lifestyle and pathogenesis.

**Table B.1.** Strains used in this study

Strain	Parent	Genotype	Reference
<b>DAY1</b>	BWP17	<i>ura3::λimm434/ura3::λimm434 his1::hisG/his1::hisG arg4::hisG/arg4::hisG</i>	Wilson et al., 1999
<b>DAY286</b>	DAY1	<i>ura3::λimm434/ura3::λimm434 his1::hisG/his1::hisG ARG4::URA3::arg4::hisG/arg4::hisG</i>	Davis et al., 2002
<b>DAY963</b>	SC5314	Prototrophic clinical isolate	Davis et al., 2002
<b>DAY1066</b>	DAY1	<i>ura3::λimm434/ura3::λimm434 his1::hisG/his1::hisG arg4::hisG/arg4::hisG HHF1/hhf1::URA3-dpl200</i>	This study
<b>DAY1067</b>	DAY1	<i>ura3::λimm434/ura3::λimm434 his1::hisG/his1::hisG arg4::hisG/arg4::hisG HHT2-HHF22/hht2-hhf22::URA3-dpl200</i>	This study
<b>DAY1068</b>	DAY1066	<i>ura3::λimm434/ura3::λimm434 his1::hisG/his1::hisG arg4::hisG/arg4::hisG HHF1/hhf1::URA3-dpl200 HHT2-HHF22/hht2-hhf22::ARG4</i>	This study
<b>DAY1069</b>	DAY1067	<i>ura3::λimm434/ura3::λimm434 his1::hisG/his1::hisG arg4::hisG/arg4::hisG hht2-hhf22::ARG4/hht2-hhf22::URA3-dpl200</i>	This study
<b>DAY1070</b>	DAY1068	<i>ura3::λimm434/ura3::λimm434 his1::hisG/his1::hisG arg4::hisG/arg4::hisG HHF1/hhf1::dpl200 HHT2-HHF22/hht2-hhf22::ARG4</i>	This study
<b>DAY1071</b>	DAY1069	<i>ura3::λimm434/ura3::λimm434 his1::hisG/his1::hisG arg4::hisG/arg4::hisG hht2-hhf22::ARG4/hht2-hhf22::dpl200</i>	This study
<b>DAY1072</b>	DAY1071	<i>ura3::λimm434/ura3::λimm434 his1::hisG/his1::hisG arg4::hisG/arg4::hisG HHF1/hhf1::URA3 hht2-hhf22::ARG4/hht2-hhf22::dpl200</i>	This study
<b>DAY1074</b>	DAY1070	<i>ura3::λimm434/ura3::λimm434 his1::hisG/his1::hisG arg4::hisG/arg4::hisG hhf1::URA3/hhf1::dpl200 HHT2-HHF22/hht2-hhf22::ARG4</i>	This study
<b>DAY1075</b>	DAY1074	<i>ura3::λimm434/ura3::λimm434 his1::hisG/his1::hisG arg4::hisG/arg4::hisG hhf1::URA3/hhf1::dpl200 HHT2-HHF22/hht2-hhf22::ARG4</i>	This study
<b>DAY1076</b>	DAY1070	<i>ura3::λimm434/ura3::λimm434 his1::hisG/his1::hisG arg4::hisG/arg4::hisG hhf1::URA3/hhf1::dpl200 HHT2-HHF22/hht2-hhf22::ARG4</i>	This study
<b>DAY1078</b>	DAY1070	<i>ura3::λimm434/ura3::λimm434 his1::hisG/his1::hisG arg4::hisG/arg4::hisG hhf1::URA3/hhf1::dpl200 HHT2-HHF22/hht2-hhf22::ARG4</i>	This study
<b>DAY1079</b>	DAY1078	<i>ura3::λimm434/ura3::λimm434 his1::hisG/his1::hisG arg4::hisG/arg4::hisG hhf1::URA3/hhf1::dpl200 HHT2-HHF22/hht2-hhf22::ARG4</i>	This study
<b>DAY414 (L40)</b>	<i>S. cerevisiae</i>	<i>MATα his3Δ200 trp1-901 leu2-3, 112 ade2 LYS2::(lexAop)<sub>4</sub>-HIS3 URA3::(lexAop)<sub>8</sub>-lacZ GAL4</i>	Vojtek et al., 1993

**Table B.2.** Primers used in this study

<b>Name</b>	<b>Sequence (5' to 3')</b>	<b>Reference</b>
<b>HHF1 5 DR 100 in</b>	TAAACGTCACAGAAAGATTTTAAAGAGATAACATTCAAGGTATTACAAAACCAGCTATCAGTTTCCC AGTCACGACGTT	This study
<b>HHF1 3 DR new</b>	TTAATACTATAACAATAAAGAAAACGAACTAAAAAGACAATTAGAAATACAACCCAGTTTGTGGA ATTGTGAGCGGATA	This study
<b>HHT2-HHF22 5 DR</b>	CTTCTAGCTAATTGCATATCTTTCTTTTGAATGGTAACTCTCTTAGCATGGATAGCACACTTTCCCA GTCACGACGTT	This study
<b>HHT2-HHF22 3 DR new</b>	TAATCTAAAAATACAGTTATCATGAATCGAAAAACATAAAGAAAAGAAGATATTTCTTTAGTGGGA ATTGTGAGCGGATA	This study
<b>HHF1 5 detect</b>	TCTTAGTGTAAGGAACCTCC	This study
<b>HHF1 3 detect</b>	ACGATTATAAAGGAGAAGGTG	This study
<b>HHT2-HHF22 5 detect</b>	AAATGTCCAATACCAGCACC	This study
<b>HHT2-HHF22 3'detect-new</b>	CCGAAAATAATTTGCTTGCCCTTGCC	This study
<b>HHF1 5' fragm DDB78</b>	ACGACGGCCAGTGAATTGTAATACGACTCACTATAGGGCGGCTCACTCTTAGTGTAAGGAACCTCC	This study
<b>HHF1 5'fragm 3'</b>	CTGATAGCTGGTTTTGTAAATACC	This study
<b>HHF1 3'fragm 5'</b>	ACTGGGTTGTATTTCTAATTGTC	This study
<b>HHF1 3' fragm DDB78</b>	AAGCTCGGAATTAACCTCACTAAAGGGAACAAAAGCTGGTCTCAGTGAGCTGTTACGAGGC	This study
<b>HHF1 5'fragm 5</b>	CTCACTCTTAGTGTAAGGAACCTCC	This study
<b>HHF1 5'fragm 3'</b>	CTCAGTGAGCTGTTACGAGGC	This study
<b>HHF1 5' 100 in for DDB78</b>	TAAACGTCACAGAAAGATTTTAAAGAGATAACATTCAAGGTATTACAAAACCAGCTATCAGGGGCG AATTGGGGAGCTCCC	This study
<b>HHF1 3' for DDB78</b>	TTAATACTATAACAATAAAGAAAACGAACTAAAAAGACAATTAGAAATACAACCCAGTTTACGATA AGCTTCATCTAGAAGG	This study
<b>HHF22 5 SB</b>	ACCTTGTATGGTTTCGGTGG	This study
<b>HHF22 3 detect</b>	GTTATTCGGTTAGAAAGCGG	This study

## FIGURES

**Figure B.1:** Genomic organization of the histone H3 and H4 loci in *Candida albicans*. The black boxes indicate the extent of the deleted regions in the mutants, which are replaced by the auxotrophic markers *ARG4*, *URA3*, *URA3-dpl200* or the *dpl200* loop-out. *HHF1* is deleted from nucleotide +114 to the STOP codon (65% of the gene) and the *HHF22-HHT2* cluster is deleted from the STOP codon of *HHF22* to nucleotide +329 of *HHT2* (80% of the *HHT2* gene). Orf19.1060 is a possible spurious ORF. In red, the regions recognized by the probes D and G used for determining *HHF1* or *HHF22* copy dosage by Southern Blot are shown. H: HindIII; N: NcoI.

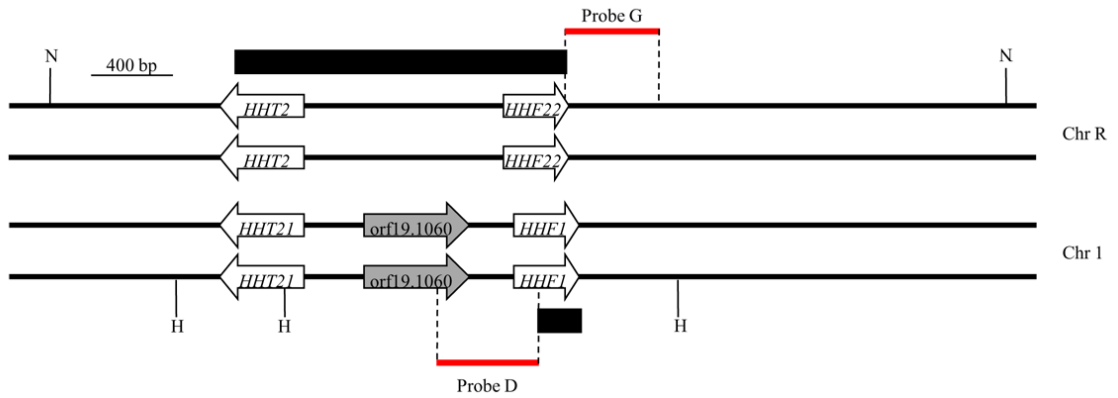


**Figure B.2:** Amino acid sequence alignment of histone H3 and H4 genes. Comparison of the amino acid sequences of histone H3 (A) and histone H4 (B) alleles from *C. albicans* and *S. cerevisiae* using ClustalW.

**A**

```

CaHHT1      MARTKQTARKSTGGKAPRKQLASKAARKSAPVSGGVKKPHRYKPGTVALREIRRFQKSTE 60
CaHHT2/21   MARTKQTARKSTGGKAPRKQLASKAARKSAPSTGGVKKPHRYKPGTVALREIRRFQKSTE 60
ScHHT1/2    MARTKQTARKSTGGKAPRKQLASKAARKSAPSTGGVKKPHRYKPGTVALREIRRFQKSTE 60
*****:*****

CaHHT1      LLIRKLPFQRLVREIAQDFKSDLRFQSSAIGALQEAVEAYLVGLFEDTNLCAIHAKRVTI 120
CaHHT2/21   LLIRKLPFQRLVREIAQDFKTDLRFQSSAIGALQEAVEAYLVGLFEDTNLCAIHAKRVTI 120
ScHHT1/2    LLIRKLPFQRLVREIAQDFKTDLRFQSSAIGALQESVEAYLVSLFEDTNLAAIHAKRVTI 120
*****:*****:*****.*****.*****

CaHHT1      QKKDMQLARRLRGERS- 136
CaHHT2/21   QKKDMQLARRLRGERS- 136
ScHHT1/2    QKKDIKLARRLRGERS- 136
****:*****

```

**B**

```

CaHHF1/22   MSGTGRGKGGKGLGKGGAKRHRKILRDNIQGITKPAIRRLARRGGVKKRISALIYEEVRV 60
ScHHF1/2    MS--GRGKGGKGLGKGGAKRHRKILRDNIQGITKPAIRRLARRGGVKKRISGLIYEEVR 58
** *****.*****.*

CaHHF1/22   LKQFLENVIRDAVITYTEHAKRKTVTSLDVVYALKRQGRTLYGFGG 105
ScHHF1/2    LKSFLESVIRDSVITYTEHAKRKTVTSLDVVYALKRQGRTLYGFGG 103
**.***.***.******

```

**Figure B.3:** Growth of (A) wild-type (DAY286), *HHF22-HHT2/hhf22-hht2Δ* (DAY1067), *hhf22-hht2Δ/hhf22-hht2Δ* (DAY1069), and *hhf22-hht2Δ/hhf22-hht2Δ* *HHF1/hhf1Δ* (DAY1072) or (B) wild-type (DAY286), *HHF1/hhf1Δ* (DAY1066), *HHF1/hhf1Δ* *HHF22-HHT2/hhf22-hht2Δ* (DAY1068), and *hhf1Δ/hhf1Δ* *HHF22-HHT2/hhf22-hht2Δ* (DAY1074) histone H4 mutants in rich medium. All strains were grown overnight at 30°C in liquid YPD, streaked on YPD, and incubated at 30°C for 48 hrs.

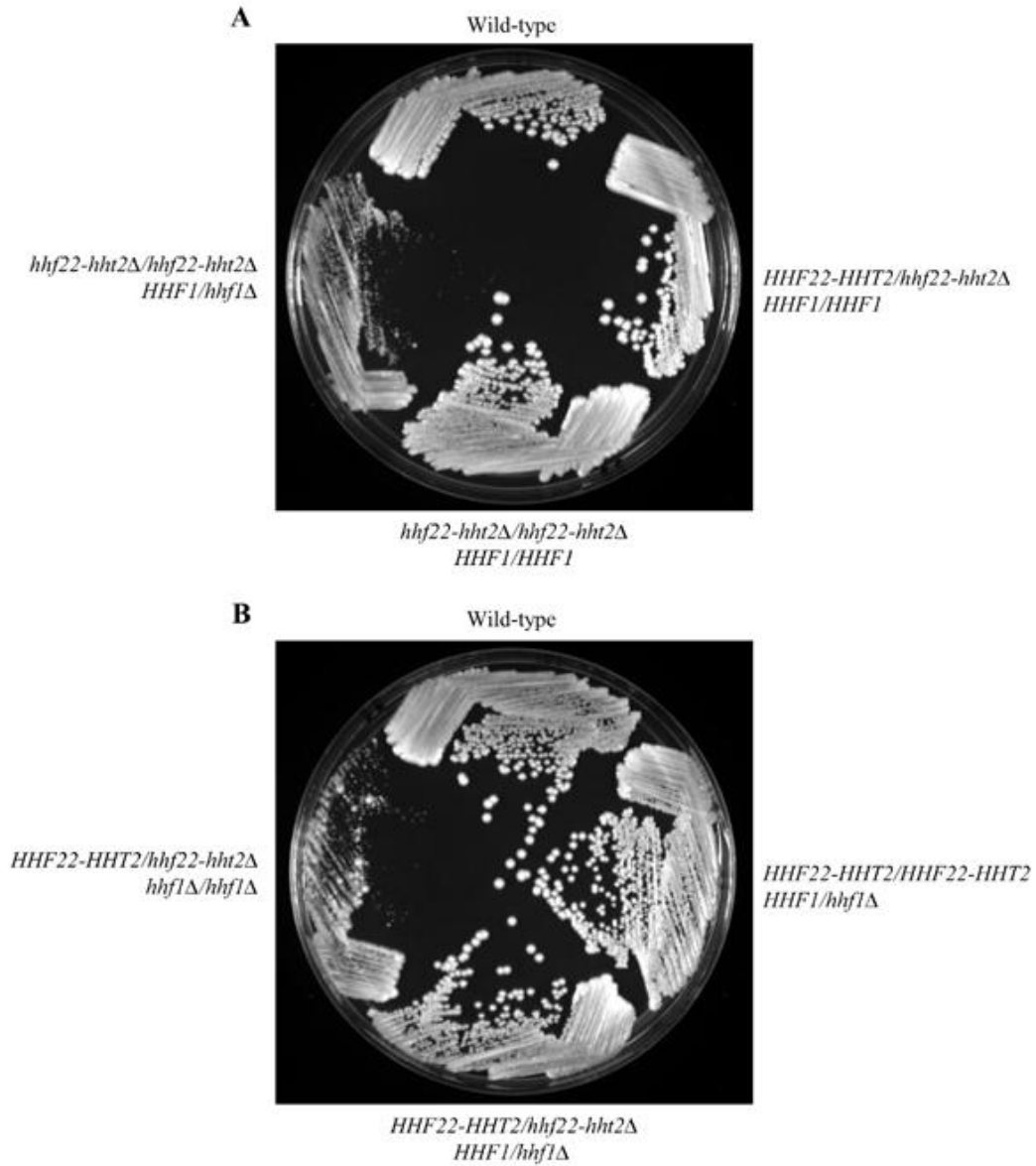


**Figure B.4:** Growth defect and phenotypic instability of mutants containing a single allele of histone H4. A small colony of a histone H4 mutant (DAY1072) was re-streaked on YPD medium and incubated 4 days at 30°C (A), close-up picture (B). Re-isolated small (C) and large (C, E) colonies of *hhf22-hht2Δ/Δ HHF1/hhf1Δ* (DAY1072), and small (D) and large (D, F) colonies of *HHF22-HHT2/hhf22-hht2Δ hhf1Δ/Δ* (DAY1074 and DAY1079) incubated on YPD for 48 hrs at 30°C.

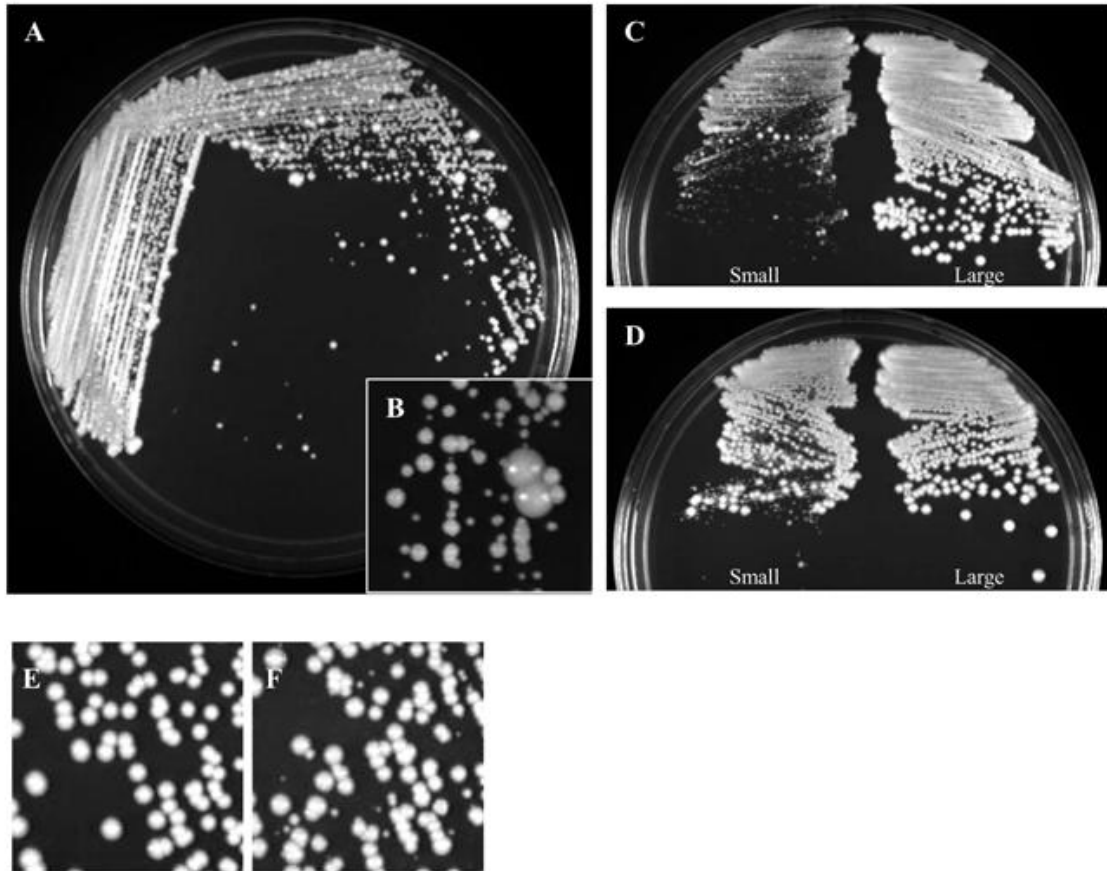


**Figure B.5:** Histone deficit causes alterations in colony morphology. Examples of morphologically altered colonies that arise in mutants with only one *HHF1* (DAY1072) or one *HHF22* (DAY1079) allele after overnight incubation at 30°C on YPD (A). Partial penetrance of the morphological change in the small colonies (B). Stable morphology of the large smooth suppressor colonies after subculturing (C).

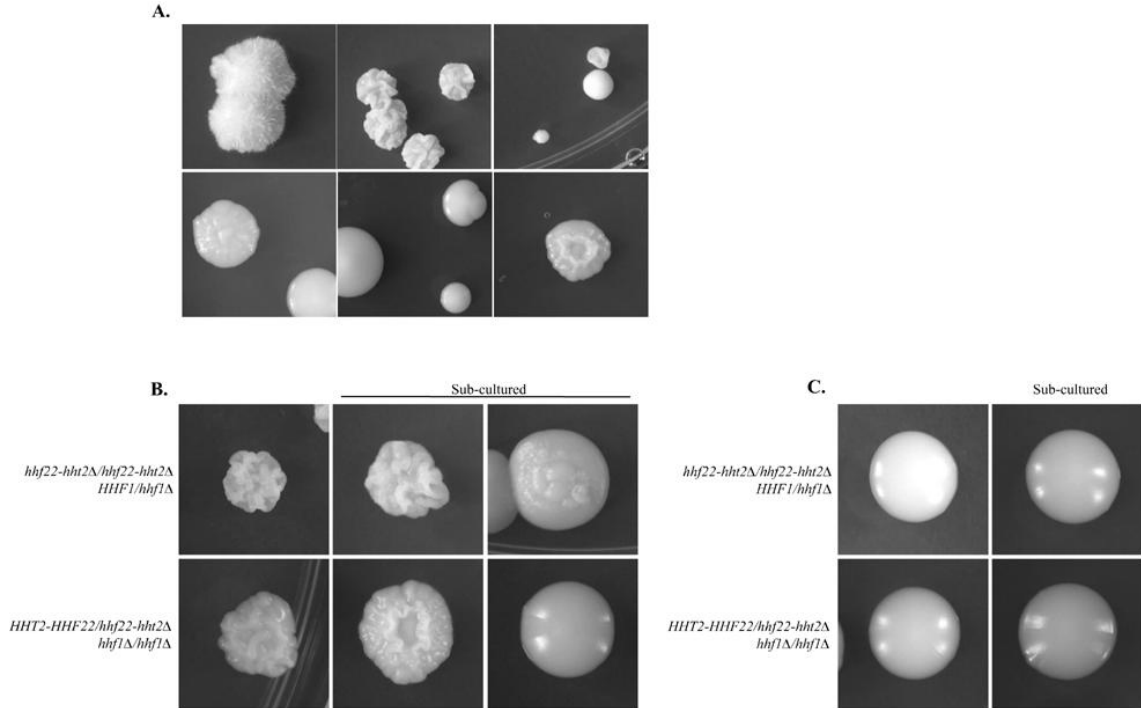


**Figure B.6:** Quantitative Southern blot of histone H4 alleles. DNA samples were obtained from 30°C overnight cultures of small and large colonies isolated from (A) *hhf22-hht2Δ/Δ HHF1/hhf1Δ* (DAY1072) and (B and C) *HHF22-HHT2/hhf22-hht2Δ hhf1Δ/Δ* (DAY1074, DAY1075, DAY1076, DAY1078 and DAY1079). Due to the formation of suppressors, the proportion of small to large colonies was verified for each overnight culture by colony count on YPD to ensure that the DNA extraction was representative of a small or a large colony population. Overnight cultures from small colonies with a minimum of 80% of small colonies were used to prepare DNA for the Southern blot. Representative colonies from these plates corresponding to different ratios of mutated to wild-type histone H4 ratio are shown (D). Probes D and G were used to detect the alleles: *hhf1::URA3* and *HHF1*, and *hhf22::ARG4* and *HHF22*, respectively. *HHF22-HHT2/hhf22-hht2Δ HHF1/Δ* (DAY1070) was used in (B) as a control for a 1:1 mutated to wild-type *HHF22* ratio.

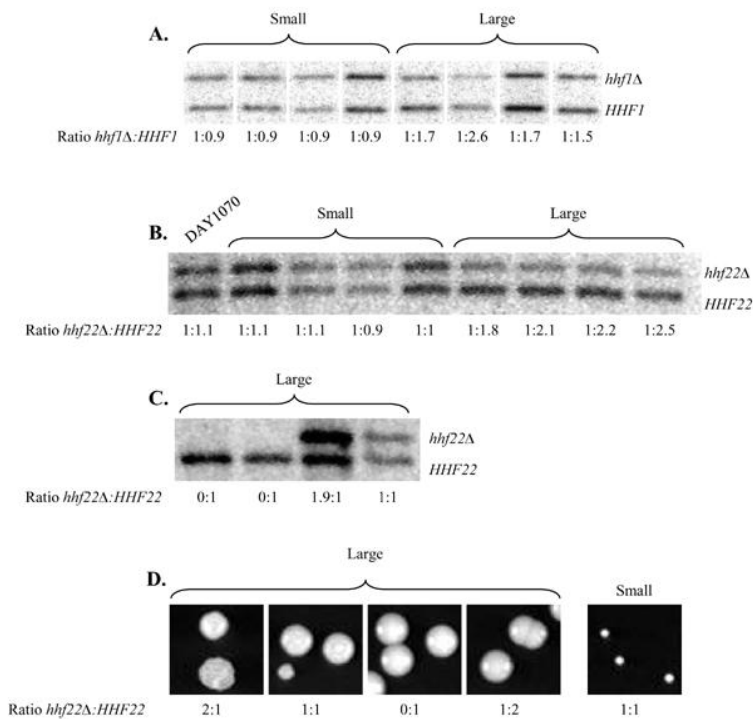
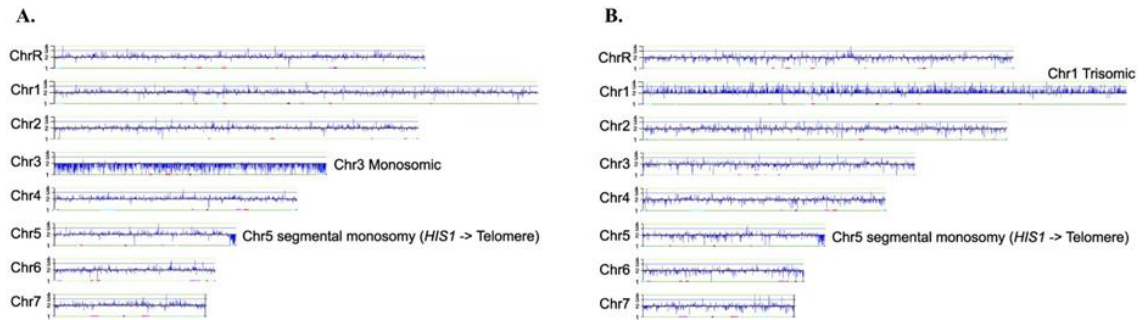


**Figure B.7:** CGH analysis of a *hhf22-hht2Δ/Δ HHF1/hhf1Δ* (DAY1072) small colony (A) and a spontaneous large colony suppressor (B). Genomic DNA was purified from both a DAY1072 small colony and large colony and compared to genomic DNA from SC5314. The DAY1072 small colony is monosomic for Chromosome 3 while the DAY1072 large colony is trisomic for Chromosome 1. Both isolates have a short segmental aneuploidy on Chromosome 5R, which is present in the strain background (Magee and Magee, 2000; Selmecki et al., 2005).



## **APPENDIX C**

### **OPEN QUESTIONS AND SHORT PROJECTS**

## OPEN QUESTIONS

The work presented in this dissertation originates many open questions. Below I provide some of them:

- 1) Does the deregulation of the TOR and Ras/cAMP pathways lead to increased DNA damage, genomic instability, LOH, and epigenetic or cell cycle checkpoints defects?
  - a. If yes, what is the mechanism through which they do that? Is there a defect in Rad53 function in switched isolates? Do the original mutants or the switched strains have cell cycle defects?
  - b. What is the level of LOH and genomic rearrangements in the switched strains? Deep sequencing, together with CGHs, CHEFs, SNP RFLP analysis, and microarray analyses of several switched strains would show if there are specific genomic or genetic alterations responsible for the switch or for particular phenotypes.
  - c. Do the switched strains in mutants in the Ras/cAMP and in the TOR pathways show similar defects in rapamycin and genotoxic agents resistance than the *mds3Δ/Δ* switched strains?
- 2) Is there crosstalk between the TOR and Ras/cAMP pathways in *C. albicans*?
- 3) Is the function of the TOR and Ras/cAMP pathways altered in the switch strains? If yes, How?
  - a. How do the downstream effectors of TOR and Ras/cAMP pathways behave in the switched strains compared to their parental counterparts? This analysis should include transcription factors commonly regulated by both pathways, like Msn2/4 and Maf1; and other (apparently) TOR-dependent effectors only such as Tap42, Rtg1/3, Gln3, Npr1, and Sch9.
- 4) Do switched papilli arise due to mutations that suppress defects in the TOR and Ras/cAMP pathways?
- 5) Is there any correlation between Chromosome 2 aneuploidies and the mechanism of suppression? If yes, is Rad53 function associated with Chromosome 2 aneuploidy formation?
- 6) Is there a fragile site in Chromosome 2, and can we exploit this to further understand genomic instability in eukaryotes?
- 7) How do glucose starvation, alkaline pH, zinc, and the amino acid composition in the media affect CMPS and the function of the TOR and Ras pathways?
  - a. Is there any other nutrient becoming limiting during glucose starvation?
- 8) Can we monitor alterations in TOR or Ras/cAMP signaling *in vivo*? And can we correlate these alterations with changes in CMPS frequency?
- 9) Does CMPS happen *in vivo* and does it affect the outcome of infection? (Dutton and Penn, 1989) (This question is vital to answer if we want to confirm a role for CMPS in pathogenesis in *C. albicans*).
- 10) Do the clinical *C. albicans* isolates that are in high frequency switching mode also have defects in TOR or Ras/cAMP signaling?

- 11) Is Mds3 localized in vesicles? Does it interact with Cdc25? What other proteins does Mds3 interact with? (since we are able to pull down Mds3, it would be interesting to pursue high-throughput immunoprecipitation studies coupled to mass spectrometry to detect potential interacting partners).
- 12) Is Mds3 a phosphoprotein? If yes:
  - a. Is Mds3 phosphorylation TOR- or PKA-dependent?
  - b. Is Mds3 a substrate of PKA or TOR?
  - c. How does the phosphorylation of Mds3 affect the ability of Mds3 to interact with its binding partners? And its localization?
  - d. Does an alteration in Mds3 phosphorylation change its ability to regulate CMPS? Is this caused by a defect on TOR or Ras/cAMP signaling?
- 13) Are the switching systems in other fungi also regulated by these signal transduction cascades and/or mechanisms?

### SHORT PROJECTS FOR UNDERGRADUATES

- 1) Is the phenotypic switch associated with changes in centromeric silencing?

Plate *mds3Δ/Δ CEN5/cen5::URA3* and *mds3Δ/Δ+MDS3 CEN5/cen5::URA3* strains in YPD. Isolate cells from papilli and from the colony where the papilli originated. Compare *URA3* silencing frequency of the *mds3Δ/Δ CEN5/cen5::URA3* switched with the non-switched counterparts, and with the original *mds3Δ/Δ CEN5/cen5::URA3* and the wild-type *CEN5/cen5::URA3* strains. Get silencing protocol and the wild-type *CEN5/cen5::URA3* strain from Berman lab.

- 2) Does Mds3 affect Rad53 function?

Tag Rad53 in the *mds3Δ/Δ* mutant with the construct obtained from Richard Bennett's lab (Alby and Bennett, 2009), and compare Rad53 phosphorylation with the wild-type control (also obtained from Alby and Bennett, 2009), in the presence of different concentrations of MMS and rapamycin. Also look at Rad53 in the *ras1Δ/Δ* mutant, the *sit4Δ/Δ* mutant, and the *TOR1-1* variant strains.

Isolate papilli from the *mds3Δ/Δ RAD53/RAD53::TAG* strain and test Rad53 phosphorylation in the same conditions as above. Compare with non-switched parental strains.

- 3) How common is Chromosome 2 aneuploidy in switched *mds3Δ/Δ* strains?

Obtain genomic DNA from different SSY strains and determine by SNP-RFLP whether there are Chromosome 2 aneuploidies or LOH events.

- 4) Is PKA deregulation associated with the switching in the *mds3Δ/Δ* mutant?

Get the *BCY1* complementation vector from Berman lab and transform SSY strains, test if there is a change in colony morphology or in switching frequency. Make sure to include in the transformation those strains that have a Chromosome 2 aneuploidy by CGH. Also, put *BCY1*

under the control of a promoter that activates in early or in late stationary phase. Transform the *mds3Δ/Δ* mutant. Verify proper expression of construct by Northern blot or RT-PCR and then determine the ability of these strains to form papilli.

- 5) Is the MTL loci associated with CMPS? And is Mds3 involved in white-opaque switching?

Determine white-opaque and CMPS switching frequencies of the wild-type *MTLa/alpha*, wild-type *MTLa/a*, *mds3Δ/Δ MTLa/alpha*, and *mds3Δ/Δ MTLa/a*. Construct an *mds3Δ/Δ* strain in the WO-1 background and determine white-opaque and CMPS switching frequency.

- 6) Is Mds3 associated with CMPS in other yeasts?

Look for Mds3 orthologs in *C. glabrata* and *C. neoformans* (among other fungi). Make deletion or insertion mutants and determine frequencies of phenotypic variation compared to the wild-type strains.

- 7) Is *MDS3* involved in entry in/progression through stationary phase? Does the switch affect the ability of cells to enter, survive, and/or exit stationary phase?
- 8) Does the nitrogen source in the medium affect CMPS? My preliminary data suggests that presence of glutamine (a TOR activator) enhances CMPS, while presence of proline (mimics TOR inactivation) represses it.

Plate the *mds3Δ/Δ* mutant in YNB media supplemented with specific nitrogen sources: ammonium, proline, glutamine, and glucose or glycerol as carbon sources. Measure papilli formation during time. Since the nitrogen source signal should feed through Gln3, determine what happens with Gln3 (and Npr1) phosphorylation in the switched strains in the different media.

- 9) Does zinc affect colony morphology?

Plate the *mds3Δ/Δ* mutant in YPD with different concentrations of zinc (this is to re-verify my preliminary data that high zinc concentration inhibit CMPS in the *mds3Δ/Δ* mutant). Make a strain that overexpresses *ZRT2* (or just add one more copy) and delete *ZRT2* in a wild-type and *mds3Δ/Δ* background, and determine papilli formation.

- 10) Does Mds3 physically interact with Cdc25?

Tag Cdc25 with V5 or Flag. Verify expression by Western Blot. Co-IP Mds3 with Cdc25. Use a positive control like a tagged Ras1, for example, to ensure that Cdc25 pull downs are working properly. If pull down is successful, determine whether rapamycin treatment, *sit4Δ*, or growth condition (log vs. stationary phase) affect this interaction.

- 11) Analyze if there is an increase in mutation rate in *mds3Δ/Δ* colonies as they progress through stationary phase, in low glucose, and at different pH.

Introduce different markers: *lacZ*, *NAT1*, *ADE2*, GFP, etc into an *mds3Δ/Δ* and wild-type strain. Plate strains and let colonies age on the plate. At different time points, take colonies and assay the cells in them for loss of function of the different markers, including gain of function in resistance to fluconazole. It would also be useful to analyze different LOH by RFLP. The fluorescent marker can aid in visualization by doing flow cytometry. The Berman lab has a high-throughput screening system set up (384 strains simultaneously) that could be very useful for an experiment like this.

12) Can we observe phenotypic switching in liquid media?

If YES, then we can use a 96 well system to try many different conditions simultaneously, including different mutants, environmental conditions, and supplementation of chemicals that inhibit or induce different signaling pathways.

13) Do the *mds3Δ/Δ*, *ras1Δ/Δ*, and *sch9Δ/Δ* mutants have a longer life span than the wild-type? Are these mutants able to survive longer condition of nutrient limitation? Do they produce adaptive regrowth mutants at higher frequency than the wild-type strain during liquid growth? How do the switched vs non-switch strains compare in these assays?

14) Do alkaline pH and glucose starvation affect life span in the wild-type and the *mds3Δ/Δ*, *ras1Δ/Δ*, *sit4Δ/Δ*, and *sch9<sup>-/-</sup>* strains?